The Impact of Climate Change on Wind Energy Generation in the UK

Lucy Catherine Cradden

Thesis submitted for the degree of Doctor of Philosophy
The University of Edinburgh
August 2009

Abstract

The release of carbon dioxide from the burning of fossil fuels for energy is thought to be one of the main contributors to increasing greenhouse gas concentrations in the atmosphere. This increase is reported to be causing irreversible changes to the earth's climate, giving rise to temperature increases and other consequent alterations in weather patterns.

Amid growing concern about climate change and its impact on the world, targets have been set through agreements such as the Kyoto Protocol and via European Union and government legislation to force countries to work towards decreasing their greenhouse gas emissions. Increasing the contribution that renewable sources make to energy production is a major part of most countries' strategies to meet these targets.

The UK has arguably the greatest potential for wind power generation in Europe and the government is seeking to build upon this strength by exploiting the resource further. The liberalised electricity market infers a requirement for private investment in order to develop the wind portfolio and this in turn requires financial and economic feasibility. Given the changes in weather patterns that are projected to occur over the course of the coming century, the possibility that this could change the UK's wind resource, and hence the financial viability of wind power developments, must be addressed. Other aspects of how changes in the wind resource could impact on the operation of the fragmented electricity system ought also to be considered in this context.

This thesis attempts to understand how the current generation of climate models project surface wind climate to change, and seeks to make the model information relevant at a site level by using statistical and physical modelling techniques. The projected changes indicated by the models are small, and it has been assessed that potential impacts on the electricity system, from project feasibility to the potential for inclusion of wind in the generation mix, will be limited.

Acknowledgements

My biggest debt of gratitude is owed to my supervisor, Dr Gareth Harrison, for the time and energy dedicated to this work, and for always having an open door and an open mind. I'm most grateful for his unfailing sense of humour.

A big thank you to my IES friends and colleagues, the camaraderie was – and is – invaluable. Special thanks for the impromptu Matlab lessons kindly provided by Ronan Costello, and assistance with GIS from Niall Duncan and Sam Hawkins.

To my family, I'm very thankful for having had so much support to get to the end of my thesis. Special thanks are due to Mum, for never doubting that I could do it, and to Dad, for patient editing and being the voice of academic experience. And massive thanks to Joan and Russell for providing holidays and respite shopping.

Finally, to my best friend and partner, Mat, I am more grateful than I can put into words. I hope I can return the many hours of patience and support you have given to me while I've been on this mental safari.

Financial support in the form of an ESPRC studentship is gratefully acknowledged.

The following trademarks are used within this thesis and are hereby acknowledged: MatLab (version 2008a) of Math Works, Inc.; WA^{S}P (version 9) of Risoe National Laboratory; RETScreen (version 4) of National Resources Canada; ArcGIS (version 9.2) of Environmental Systems Research Institute, Inc.

The GCM data was obtained from the World Climate Research Program's (WCRP's) Coupled Model Intercomparison Project phase 3 (CMIP3) multi-model dataset. We acknowledge the modelling groups for making their model output available for analysis, the Program for Climate Model Diagnosis and Intercomparison (PCMDI) for collecting and archiving this data, and the WCRP's Working Group on Coupled Modelling (WGCM) for organizing the model data analysis activity. The WCRP CMIP3 multi-model dataset is supported by the Office of Science, U.S. Department of Energy. Other data was supplied by: The British Atmospheric Data Centre; UK Climate Impacts Programme 2002; EDINA Digimap; European Environment Agency.

Declaration

I declare that this thesis has been written by myself. The research contained within is my own except where indicated to the contrary. The work has not been submitted for any other degree or professional qualification.

The work in section 4.4 was a collaboration between Dr. Gareth Harrison and myself and has been published in Harrison *et al* (2008).

Contents

Abbreviations

a.g.l	above ground level
AGCM	Atmosphere General Circulation Model
AOGCM	Atmosphere-Ocean General Circulation Model
AR4	IPCC Fourth Assessment Report
BADC	British Atmospheric Data Centre
BERR	Department for Business, Enterprise and Regulatory Reform
BIS	Department for Business, Innovation and Skills
BWEA	British Wind Energy Association
CCC	Canadian Climate Center
CDM	Clean Development Mechanism
CH_4	Methane
CMIP3	Coupled Model Intercomparison Project phase 3
CO_2	Carbon dioxide
DECC	Department for Energy and Climate Change
DEFRA	Department for Environment, Food and Rural Affairs
DG	Distributed Generation
DNO	Distribution Network Operator
DTI	Department of Trade and Industry
ECHAM5 (ECH5)	MPI-ECHAM5 General circulation climate model
ECMWF	European Centre for Medium-range Weather Forecasting
EIA	Energy Information Administration
EMEC	European Marine Energy Centre
ERA40	ECMWF 40-year reanalysis project
ETS	Emissions Trading Scheme
G8	Group of Eight
GCM	General Circulation Model
GHG	Greenhouse Gas
HCFC	Halofluorocarbon
IPCC	Intergovernmental Panel on Climate Change
IRR	Internal Rate of Return
LAM	Limited Area Model
LIDAR	Light Detection and Ranging
LLGHG	Long-lived Greenhouse Gas
LOLP	Loss of Load Probability
MAPE	Mean Absolute Percentage Error
MCP	Measure-Correlate-Predict
MCT	Marine Current Turbines

MIDAS	Met office Integrated Data Archive System
MMD	Multi-model dataset
MOS	Model Output Statistics
MPI	Max-Planck Institute
MSLP	Mean Sea-Level Pressure
N_2O	Nitrous oxide
NAO	North Atlantic Oscillation
NAP	National Allocation Plan
NCAR	National Center for Atmospheric Research
NCEP	National Centers for Environmental Prediction
NIPCC	Non-governmental International Panel on Climate Change
NOABL	Numerical Objective Analysis of Boundary Layer
NPV	Net Present Value
O&M	Operations and Maintenance
PBL	Planetary Boundary Layer
PP	Perfect Prognosis
RCM	Regional Climate Model
ROC	Renewables Obligation Certificates
SODAR	Sound Detection and Ranging
SRES	Special Report on Emissions Scenarios
TAR	IPCC Third Assessment Report
UKCIP02	UK Climate Impacts Programme 2002
UKMO	UK Meteorological Office
UNEP	United Nations Environment Programme
UNFCCC	United Nations Framework Convention on Climate Change
VEMAP	Vegetation Ecosystem Modelling and Analysis Project
WAsP	Wind Atlas Analysis and Application Program
WCRP	World Climate Research Programme
WMO	World Meteorological Organisation

Symbols

Symbol	Description	Units
ρ	air density	kg/m^3
A_x, A_d, A_∞, A_w	cross-sectional area of the streamtube (actuator disc model)	m^2
U, U_d U_∞, U_w	flow velocity (actuator disc model)	m/s
$\dot{m}$	mass flow rate	kg/s
a	axial flow induction factor	
g	acceleration due to gravity (constant ~9.81)	m/s^2
p	static pressure	Pa
KE	kinetic energy	J
P	power	W
C_p	power coefficient	
V_g	geostrophic wind	m/s
f	Coriolis parameter (frequency)	s^{-1}
$\frac{dp}{dn}$	pressure gradient in direction n	Pa/m
z_0	surface roughness	m
h	height of roughness element	m
S	cross-sectional area of the roughness element facing the wind	m^2
A_H	average horizontal area available to each element	m^2
u_*	friction velocity	m/s
z	height above ground level	m
L	characteristic length of hill	m
κ	von Karman constant (~0.4)	
R^2	r-squared correlation coefficient	
σ	standard deviation	
E'	Centred pattern root mean square (RMS) difference	
A	Weibull distribution scale parameter	
k	Weibull distribution shape parameter	
ω	angular velocity of the earth	rad/s
u_g	westerly (eastward) geostrophic wind	m/s
v_g	southerly (northward) geostrophic wind	m/s
ϕ	*latitude*	°

List of Figures and Tables

Figures

Tables

Chapter 1

Introduction

1.1 Thesis background

The challenge of mitigating climate change is a hotly debated matter, both within UK government circles and also, via the media, in the public domain. It is widely agreed that part of the mitigation strategy will involve changing from mainly fossil-fuel based power generation to renewable sources of energy. Regardless of what is done now, however, climate change will proceed throughout the coming century due to past human behaviour; and given the innate dependence of many renewable energy sources on the prevailing climate, it seems sensible to consider the impacts of predicted climate change on such sources.

The aim of this work, therefore, is to analyse the impacts of climate change on the wind resource in the UK on two different levels: first, as regards the possible impact on individual stakeholders within the wind industry and, second, in terms of the broader issue of the development of public policy on energy sources. Wind power is currently the fastest growing renewable energy source and is expected to fulfil a large part of the UK government's 20% 'renewables' target by 2020. In order to meet this, as well as those targets expected to be set in the longer-term, knowledge is required about future wind climate; indeed, is the current government plan aiming high enough, or could we place ourselves in a position to exploit the resource significantly more than presently anticipated? Do we need, for example, to look at alternatives and perhaps expand the mix of available energy sources?

As the lifetime of wind farms is generally in the region of twenty to thirty years, ongoing climate change over this period may impact on the financial viability of wind farm developments and thus their attractiveness to investors. The added uncertainty arising from anecdotal reports of apparently increasing climate change may increase in turn the 'perceived risk' and make such developments even less attractive. This project

is intended to address the question at both the levels already referred to, by seeking to understand the range of potential changes to energy output at individual sites across the UK, and by extrapolating this to an understanding of the aggregate affect on the country as a whole.

1.2 Project objectives and scope

The project objectives are as follows:

1. to understand the potential sensitivity of wind power to climate change and to examine the ways in which this could impact on the industry;
2. to determine the current state of knowledge on how climate change scenarios suggest changes in wind power, and to understand possible limitations in the applicability of the research to various industry stakeholders;
3. to develop a method of analysis for climate change impacts on wind power, at both a macro and a micro scale;
4. to apply the results of the analysis in an exploration of the scale of the impacts and how these could impinge on future electricity generation from wind in the UK.

1.3 Thesis contribution to knowledge

The fundamental proposition of the thesis is that:

> *climate change will impact on wind resources in the UK in such a way that the effects will require a change of strategy for the wind power industry.*

A thorough analysis of projected changes to the UK's wind climate is in itself a new piece of research. This kind of work has been carried out in the US and Scandinavia, but the techniques have yet to be applied in a UK context. Taking this wind climate analysis a step further so as to look at potential changes in wind energy output is something that the US and Scandinavian studies have undertaken; however, this has not been done in such a way as to comprehend the financial impact of such changes, or how the levels of projected change could affect the electricity industry at other levels.

A novel method has been developed for using data from models that project changes in the future climate. This attempts to enhance the wind climate information available from these models and make it more applicable to wind power analysis. The work has been completed in a format that will ensure that the methodology can be easily reapplied with alternative data. It has been designed to be simple enough to be used by non-climate experts, whilst not sacrificing anything in terms of the quality of results.

1.4 Thesis outline

The thesis consists of seven chapters, plus appendices:

Chapter 2 frames the work in the context of both changing climate and an emerging renewable energy industry. Future projections of global climate change are presented along with a discussion of the atmospheric modelling techniques involved in developing these scenarios. Also discussed is the development of a renewables sector in the electricity industry as a result of both climate change and predictions of depletion of oil and gas reserves.

Chapter 3 concentrates specifically on wind power, looking at its history, the physics of energy production and integration of wind into the electricity system. The chapter goes on to explore the sensitivity of wind power project finances to changes in the mean wind climate.

Chapter 4 first compares the output of climate model surface wind data (at 10m above ground level) to reanalysis wind data for a control period and, having established some degree of success, investigates what the model projects for future scenarios. The second part of the chapter uses projections of future scenarios from a higher resolution climate model to calculate potential changes in seasonal energy production.

Chapter 5 seeks to discover whether looking at changes in the larger-scale climate factors that ultimately drive surface wind speeds can assist with understanding potential changes at a surface level.

Chapter 6 develops a process for downscaling the larger-scale climate factors to calculate changes at a surface level at a higher resolution than the model itself.

Chapter 7 discusses the results of the analysis of climate model data, from the raw surface data to the downscaled geostrophic wind. It examines the potential impacts of the projected changes for various parts of the wind industry and for the electricity industry as a whole. Finally, the limitations of the analysis are detailed, along with suggestions for further work.

Appendix A contains some additional discussion on wind turbine power extraction, atmospheric stability and the Weibull distribution; *Appendix B* details the construction of Taylor Diagrams; *Appendices C and D* present detailed results from the work of Chapters 4 and 5; *Appendix E* consists of Ordnance Survey maps of the sites used in Chapter 6.

Chapter 2

Climate Change

Climate change represents one of the greatest scientific, socio-economic and political challenges for the world in the coming century. The consensus reached by the majority of scientific experts is that anthropogenic emissions of carbon dioxide (CO_2) and other greenhouse gases will cause global warming on a scale beyond that which would have been expected under natural variability; moreover, this has the potential to provoke change all around the globe. This chapter aims to examine the science behind the projections of climate change, and the actions of politicians and the general public in response to this knowledge.

2.1 The science behind climate

The Intergovernmental Panel on Climate Change (IPCC) was formed by the United Nations Environment Programme (UNEP) and the World Meteorological Organisation (WMO) in 1988. It aims to be a dissemination body, objectively assessing the latest scientific, technical and socio-economic information on climate change to make the most up-to-date evidence available for policy-makers. It does not conduct any research itself, nor does it make policy; and it endeavours to be unbiased and dispassionate in its approach to all scientific theory (IPCC, 2009). The organisation publishes reports, approximately every four to six years, containing what its panel of experts consider to be the most relevant scientific opinions on all aspects of climate change and its potential impacts, as well as proposing mitigation and adaptation strategies. The most recent report, published in 2007, is known as the Fourth Assessment Report (AR4); the previous report published in 2001 is referred to as the Third Assessment Report (TAR).

The IPCC is not untouched by controversy. Whilst its aims are entirely honourable, as a UN organisation it is influenced by its funding structure. Of particular note is the interference of the US government, allegedly under pressure from the oil and gas lobby, which prompted the resignation in 2002 of the IPCC chairman, the eminent British climate scientist Robert Watson. Watson was replaced

by Rajendra Pachauri from India, who was thought to be less hostile to the Bush Administration's policy of climate change scepticism (Pearce, 2002). Prior to the publication of the latest report in 2007, a document prepared by US government officials was leaked to the media, indicating how they wished some details of the forthcoming report to be altered to suit their particular viewpoints (Adam, 2007).

Policy-makers aside, many of the scientists who do not accept the current widely-held verdict on climate change and anthropogenic forcing are not enthusiastic about the IPCC either (Pearce, 2006). One group of sceptics go under the banner 'Nongovernmental International Panel on Climate Change (NIPCC). Some members of this organisation dispute the human contribution to temperature changes, whilst others debate the temperature change itself. Together they have produced a significant critique of the IPCC's fourth assessment (NIPCC 2009). A common theme is a belief that the IPCC is ignoring newer pieces of work in favour of the more established theories, and that it is too embroiled in political wrangling to be truly objective.

However, it is important to recognise that the IPCC's mandate is to take the balance of evidence into account. The organisation plainly cannot reject the findings of the majority of scientists in favour of those of a small minority who disagree. Rather, the expert panel members can only take the evidence that they are presented with, weigh up its scientific and/or technical merit and support the most likely theories in an unprejudiced manner. It is with this in mind that the rest of this thesis uses data and information from the IPCC AR4, on the basis that it is the most up-to-date and broadly accepted data available.

2.1.1 Definitions

2.1.1.1 Weather and Climate

The term 'weather' depicts the state of the Earth's atmosphere at a particular time (AMS, 2009), often in a specific location. The term 'climate' describes, usually in statistical terms, the long-term weather conditions in a particular area (Le Treut *et al.*, 2007). The energy balance of the Earth is driven externally by the inward and outward flux of radiation from the sun, and as such, any changes in the flux will have an effect on the state of the atmosphere, and thus on weather and climate.

2.1.1.2 Climate Change

The term ‘climate change’, or ‘climatic change’ as it is sometimes called, can be interpreted differently depending on the situation. The IPCC (2007a) define it as:

> …a change in the state of the climate that can be identified (e.g. using statistical tests) by changes in the mean and/or the variability of its properties, and that persists for an extended period, typically decades or longer. It refers to any change in climate over time, whether due to natural variability or as a result of human activity.

This differs from, for example, the definition given by the United Nations Framework Convention on Climate Change (UNFCCC, 2009b), which refers only to climate change as a direct result of human activity. The IPCC definition is clearly more pragmatic, because when considering impacts and adaptation or mitigation strategies, it is the compound effects of nature and humankind that will be felt and that need to be addressed.

2.1.2 Solar Flux

Changes can occur in both the inward and outward solar radiation flux to the earth, altering the energy balance. The tilt of the Earth’s axis and its orbital path could potentially change the amount of inward solar radiation incident upon its surface. There is some scientific evidence that this has previously affected the temperature of the earth (McGuffie & Henderson-Sellers, 1997) but the process is not precisely understood and modelling is still in progress. More commonly cited causes of changes in solar radiation incident upon the earth are sunspots. There is a cycle in solar activity which has been linked to past climatic fluctuations, such as the ‘Little Ice Age’ in the late seventeenth Century, but again, this link is still under scrutiny and the exact effects have not been absolutely quantified (McGuffie & Henderson-Sellers, 1997). It may be worth noting that numbers of sun spots are currently at a low (Phillips, 2009).

Changes to the outward flux of solar radiation, i.e. the amount reflected or scattered by the surface or atmosphere, and the changes in the amount of infrared heat radiated from the earth have been in recent years subject to more investigation than the changes in inward radiation. The causes of these changes are often divided into two kinds – anthropogenic, i.e. caused by human activity; and non-anthropogenic, or ‘natural’.

2.1.2.1 Non-anthropogenic effects

The so-called 'natural' effects include those due to volcanic activity and changes in the ocean circulations. Eruptions of volcanoes cause a mixture of particulates and gases - typically sulphur dioxide (SO_2) - to be released into the atmosphere where they change the reflectivity, or albedo, of the atmosphere. A large amount of aerosol matter in the atmosphere will deflect some of the sun's incoming radiation back out into space and thus result in a net cooling effect (McGuffie & Henderson-Sellers, 1997). There is also evidence that aerosol particles in the atmosphere can induce cloud formation, further increasing albedo (Dusek *et al.,* 2006).

Changes in oceanic circulation patterns are thought to occur naturally on scales of years, e.g. the El Niño phenomenon, and on much longer glacial time scales, such as the North Atlantic thermohaline circulation (McGuffie & Henderson-Sellers, 1997). These circulations change the way heat is distributed around the earth by large bodies of water. The changes in heat distribution cause differences in the path of atmospheric circulations, thereby altering the climate.

2.1.2.2 Anthropogenic effects

Anthropogenic effects - effects originating from the activity of humans - on climatic variability have been studied and modelled in great detail in recent years and there is consequently a large amount of scientific information available. It is considered by the majority of scientists in the field to be the most likely cause of substantial changes in climate in the coming century, with the IPCC (2007b) stating that

> The understanding of anthropogenic warming and cooling influences on climate has improved since the TAR, leading to *very high confidence* that the global average net effect of human activities since 1750 has been one of warming…

A significant part of the current research deals with the greenhouse effect, something which has been given a lot of attention by the media in the last ten years and the increase in which is generally accepted by the majority of the scientific community to be attributable to human activity.

2.1.3 The greenhouse effect

The phenomenon known as 'the greenhouse effect' is so-called because it describes how particular gases in the atmosphere trap radiation causing a heating effect, much like a greenhouse. These gases, known collectively as the greenhouse gases (GHGs),

trap the infrared part of the radiation and are, in fact, necessary to life as we know it on earth - for without them the surface would not be warm enough for survival. Water is a greenhouse gas, and obviously is a natural component of the atmosphere, along with other GHGs like carbon dioxide. However, especially since the industrial revolution, humankind has been generating increasing levels of some atmospheric gases beyond that which existed in the past. Through the use of modelling techniques, scientists are projecting that increasing these levels at our current rate will lead to irreversible and potentially devastating heating of the planet.

GHG	**Anthropogenic source**
Carbon dioxide (CO_2)	Fossil fuel combustion, deforestation
Nitrous oxide (N_2O)	Agriculture and fossil fuel combustion
Methane (CH_4)	Agriculture, landfill
Halocarbons (CFCs)	Industrial processes

Table 2-1: Primary greenhouse gases increasing due to anthropogenic activity
(Forster *et al.*, 2007)

2.1.4 Comparing the different GHGs

Each greenhouse gas in the atmosphere absorbs light at a particular wavelength in the infrared spectrum, preventing outgoing solar radiation from leaving the Earth. Probably the most widely recognised gas in connection with climate change is carbon dioxide (CO_2). A number of greenhouse gases have been described in the IPCC AR4 as 'LLGHGs', or long-lived greenhouse gases, due to their long-lasting effects in the atmosphere. These gases take the longest time to be removed from the atmosphere and their concentrations can remain high for long periods after their rates of emission have been reduced, e.g. haloflurocarbons (HCFCs).

2.1.4.1 Radiative Forcing (RF)

Generally, the incoming radiation is balanced approximately by the outgoing radiation around the globe as a whole. Anything causing a change in this balance, i.e. a net gain or loss of radiative energy, is termed a radiative forcing. The relative radiative forcing of various different greenhouse gases (and for cooling, aerosols) can be evaluated, although there remains some debate as to whether there is an

absolute link between radiative forcing and climate response to some of these substances (Forster *et al.*, 2007). Fig 2-1 shows the different radiative forcing effects of various greenhouse gases and other substances, with the thin error bar showing the range of uncertainty about the values. The biggest uncertainty bars appear to surround cloud albedo - the overall average reflection coefficient - and aerosols.

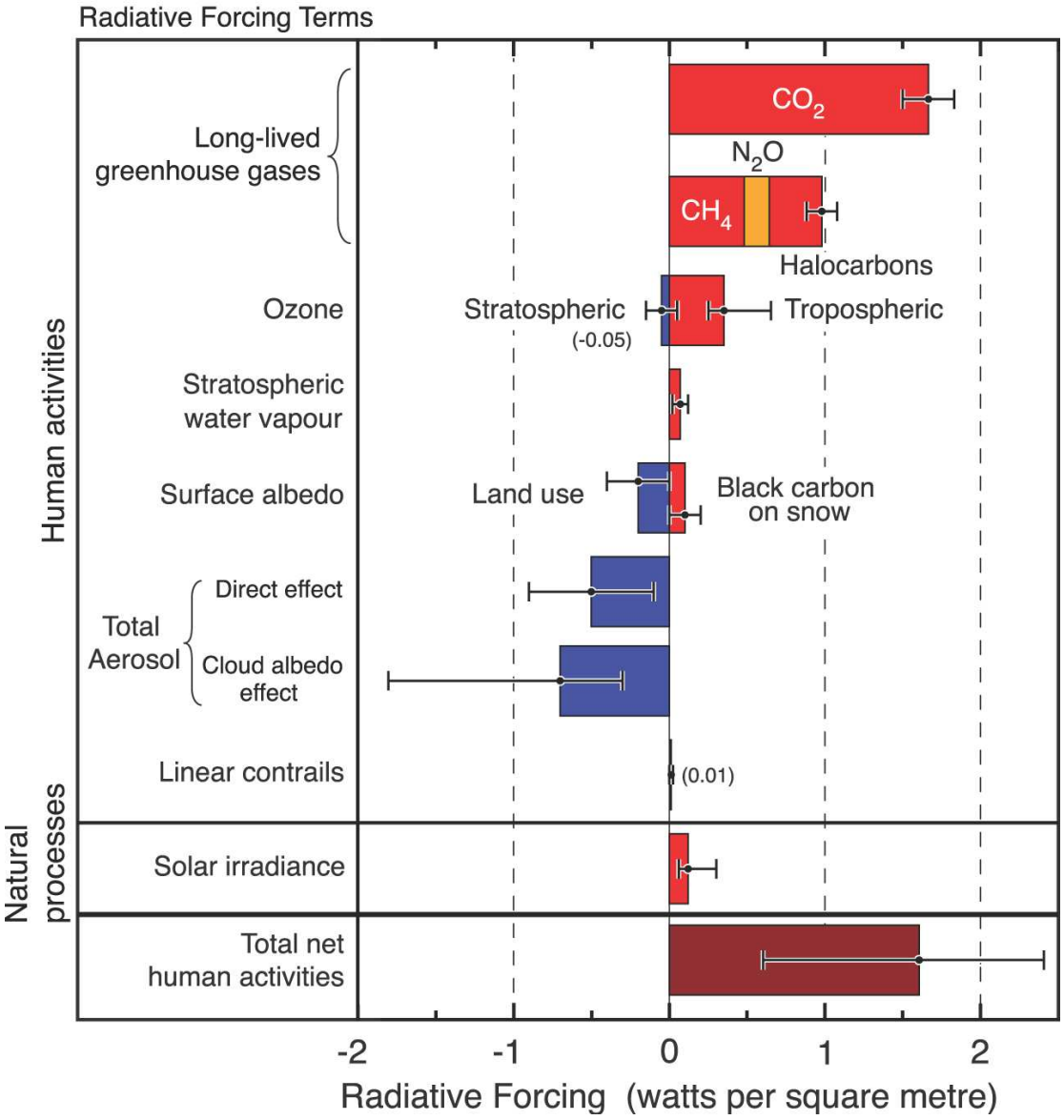

Fig. 2-1 Radiative forcing of climate between 1750 and 2005

(Forster *et al.*, 2007)

2.1.4.2 Global warming potential

Since CO_2 is the predominant GHG, it is used as a measurement base: the 'carbon dioxide equivalent' (CO_2-eq) of each gas is found by measuring its warming (or

radiative) effect relative to CO_2. Each gas is given a 'global warming potential' (GWP) relative to carbon dioxide, calculated from the radiative forcing effect of the gas over a given time period (often 100 years) (IPCC, 2007a). The CO_2-eq of the gas is then calculated by multiplying its concentration in the atmosphere by its GWP. For example, the GWP of methane over 100 years is 25; for nitrous oxide it is 298; and for sulphur hexafluoride it is 22,800 (Forster *et al.*, 2007). The total CO_2-eq of all the greenhouse gases can be found by summing together all the individual CO_2-eqs. The CO_2 equivalent is a useful measure for understanding the relative effects of different gases at different concentrations in the atmosphere and comparing them.

2.1.4.3 Carbon Dioxide

Given the evidence that CO_2 is probably the worst offender in terms of its radiative forcing potential (see Fig 2-1), it then has to be proven that its concentrations in the atmosphere are increasing at an unsustainable rate. From Fig 2-2 it can be seen that in the 20th Century, CO_2 concentrations have been overwhelmingly increased from their historical levels, as have those of methane and nitrous oxide, the next two highest offenders on the radiative forcing index.

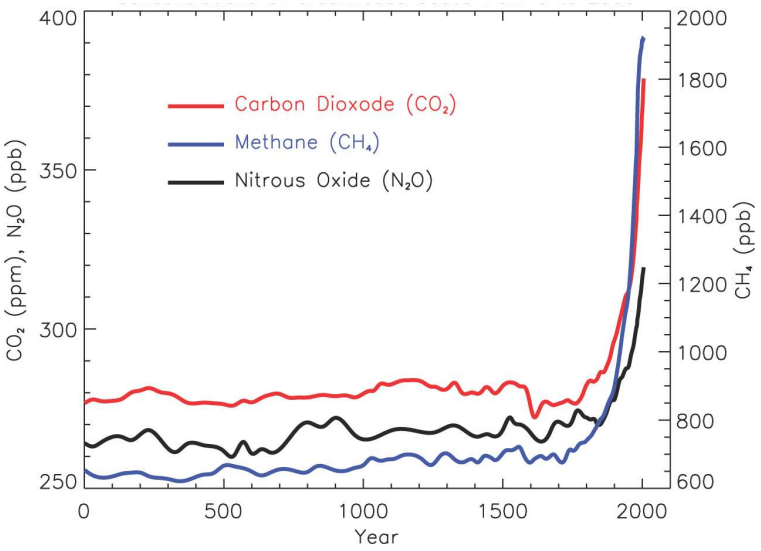

Fig. 2-2 Concentrations of atmospheric carbon dioxide

(Forster *et al.*, 2007)

Carbon dioxide is released into the atmosphere from natural processes, such as the decay of natural matter as part of the carbon cycle (Fig. 2-3). However, IPCC (2007b) affirms that,

> … most of the observed increase in global average temperatures since the mid-20th century is very likely due to the observed increase in anthropogenic greenhouse gas concentrations.

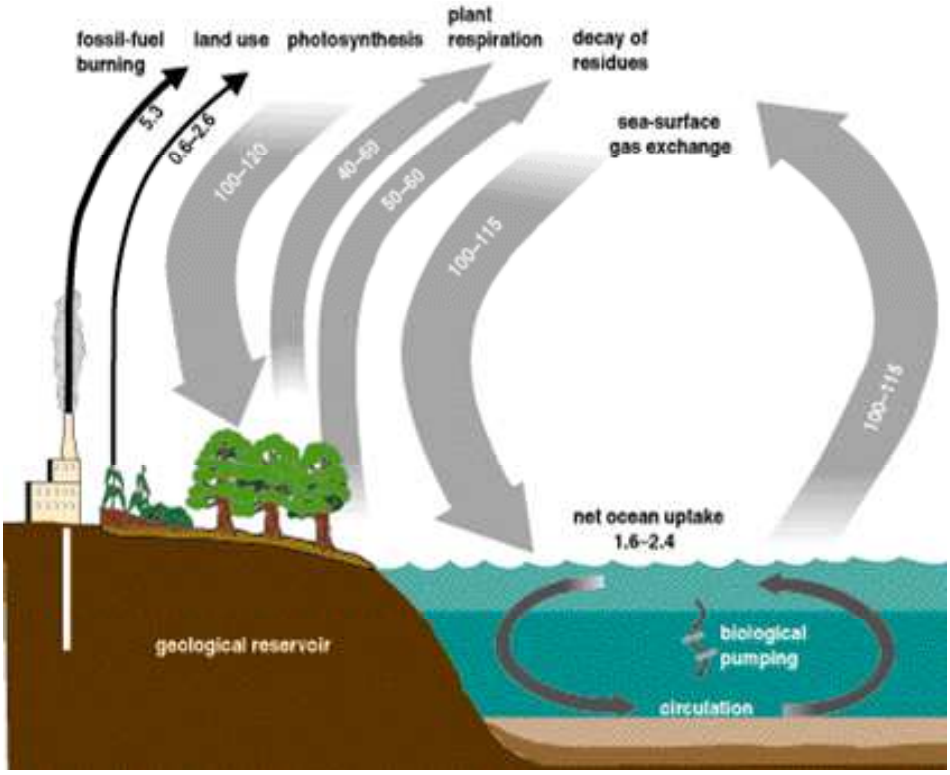

Fig. 2-3 The Global Carbon Cycle

(Post *et al.*, 1990)

Burning of fossil fuels to generate energy is stated as the primary source, along with deforestation - which results in less uptake of CO_2 by plants. Increases in methane and N_2O are both due to heavy industrialisation of agriculture, with fossil fuel use also contributing to methane increases. Anthropogenic cooling effects due to emission of aerosol particles - which also mean increased cloud formation causing a further cooling effect - are not enough to counteract the positive radiative forcing from the greenhouse gases (Forster *et al.*, 2007).

2.1.5 What is the evidence for warming?

2.1.5.1 Historical climate records

Investigations of past climate are important in order to understand how all the factors affecting the climate system link together. Historical records of climate variables provide insight into the degree of natural variation in the past, indicating what levels of greenhouse gases it may be possible for humankind to adapt to. Instrumental records of sufficient accuracy going back more than 150 years are very few. However, scientists have developed 'proxies' which may signify the state of the climate at a particular time in the past - such as tree ring density. These are useful but it is accepted that these reconstructions are not infallible.

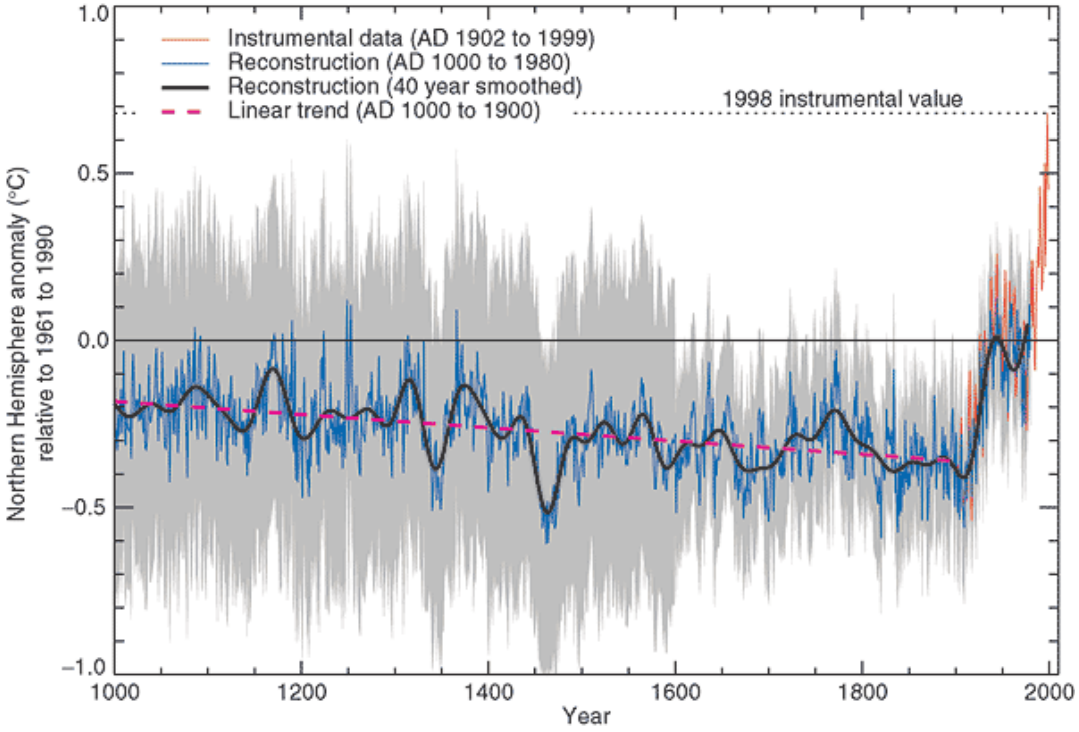

Fig. 2-4 Temperature reconstructions

(Folland *et al.*, 2001) [1]

The most famous and widely circulated image of historic temperature change is the 'hockey-stick graph' from Mann *et al.* (1999) cited in the IPCC TAR (Fig.2-4). It was used by a number of media sources, and also by former US Vice-President Al

[1] Millennial Northern Hemisphere (NH) temperature reconstruction (blue) and instrumental data (red) from AD 1000 to 1999, adapted from Mann et al. (1999). Smoother version of NH series (black), linear trend from AD 1000 to 1850 (purple-dashed) and two standard error limits (grey shaded) are shown.

Gore in his documentary *An Inconvenient Truth* (Guggenheim, 2006). The image was developed using a number of inputs - including ice-core analysis, tree ring analysis and documentary evidence - to reconstruct a northern hemisphere temperature time series for the last 1000 years. There has been much controversy concerning the validity of Mann's model and the methods used to obtain the data; a number of research groups have run similar studies and produced similar data whilst others have provided contradictory data in order to undermine it. The IPCC TAR reports that several "largely independent" studies have found similar results to Mann, showing that the 1990s were the warmest decade of the past 1000 years even though their results for historical periods varied somewhat due to different reconstruction methods (Folland *et al.*, 2001).

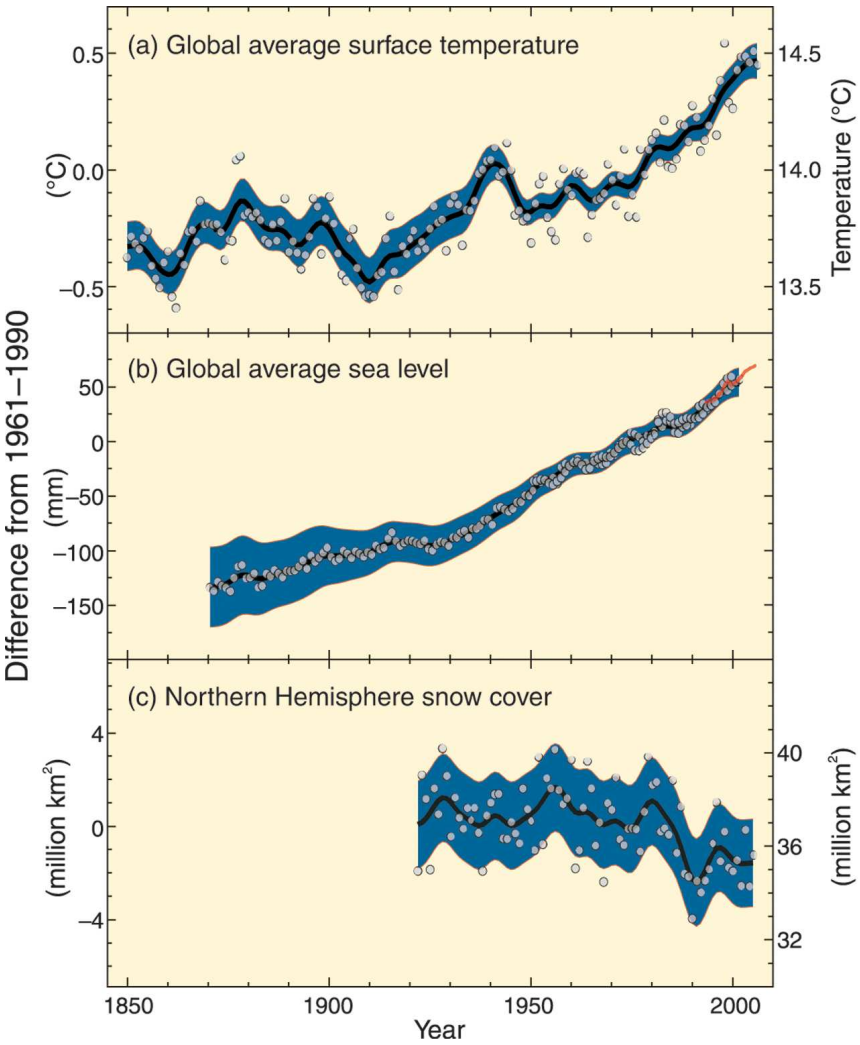

Fig. 2-5 Historic records of temperature, sea level and snow cover
(IPCC, 2007b)

The IPCC AR4 did not explicitly include the controversial graph (Fig. 2-4). Steffen (2008) believes this subsequent IPCC report deals with the 'hockey stick' issue in a "refreshingly open and honest way", by attempting to incorporate a range of scientific argument on the matter. The AR4 Summary for Policymakers (IPCC, 2007b) describes the observed trends over the last century and, in more detail, over the last 30-40 years - as shown in Fig. 2-5. The global average surface temperature has clearly shown an increase beyond that experienced in the last 150 years; the rate of this increase is also significant. There is a notable corresponding decrease over the last 10 to 15 years in northern hemisphere snow cover in the spring period - which might of course be expected given the temperature increase. The pattern of sea-level rise is of particular concern as it suggests ice-cap melting at the poles. A relatively modest increase in sea level could have potentially disastrous consequences for coastal areas.

2.1.6 Modelling the future

The best tools available for the analysis of future climate are General Circulation Models (GCMs), which are complex numerical models of the Earth's atmosphere and oceans. As well as evaluating investigations into historical climate patterns, the IPCC reports have provided a dissemination of the output of many of the most advanced climate modelling experiments, intended to make projections about what future climate will look like under projected levels of anthropogenic forcings.

The projected levels of, in particular, greenhouse gases, are chosen based on a number of different 'storylines'. The storylines are devised by experts who plot plausible evolutionary paths for the world, depicting a range of combinations of potential technological and socio-economic developments that may occur; each of these could produce different levels of GHG emissions. The various storylines were put together in the IPCC *Special Report on Emissions Scenarios* (Nakicenovic, 2000). The emissions levels corresponding to each of these storylines are used by climate modellers to compare different models with the same emissions levels. None of the scenarios is claimed to be any more or less likely than the others; and they are given equal weighting when considering the range of possible changes. Three of the original six scenarios - corresponding to 'low' (B1), 'medium' (A1B) and 'high'

(A2) emissions (Meehl *et al.*, 2007) - have been chosen to be used as part of a project in which numerous models will be run to the year 2100 under the same scenarios, and will then compare their output (World Climate Research Programme (WCRP) Coupled Model Intercomparison Project Phase 3 (CMIP3)). The results from this are referred to throughout the IPCC AR4 report as the 'multi-model data set', or MMD.

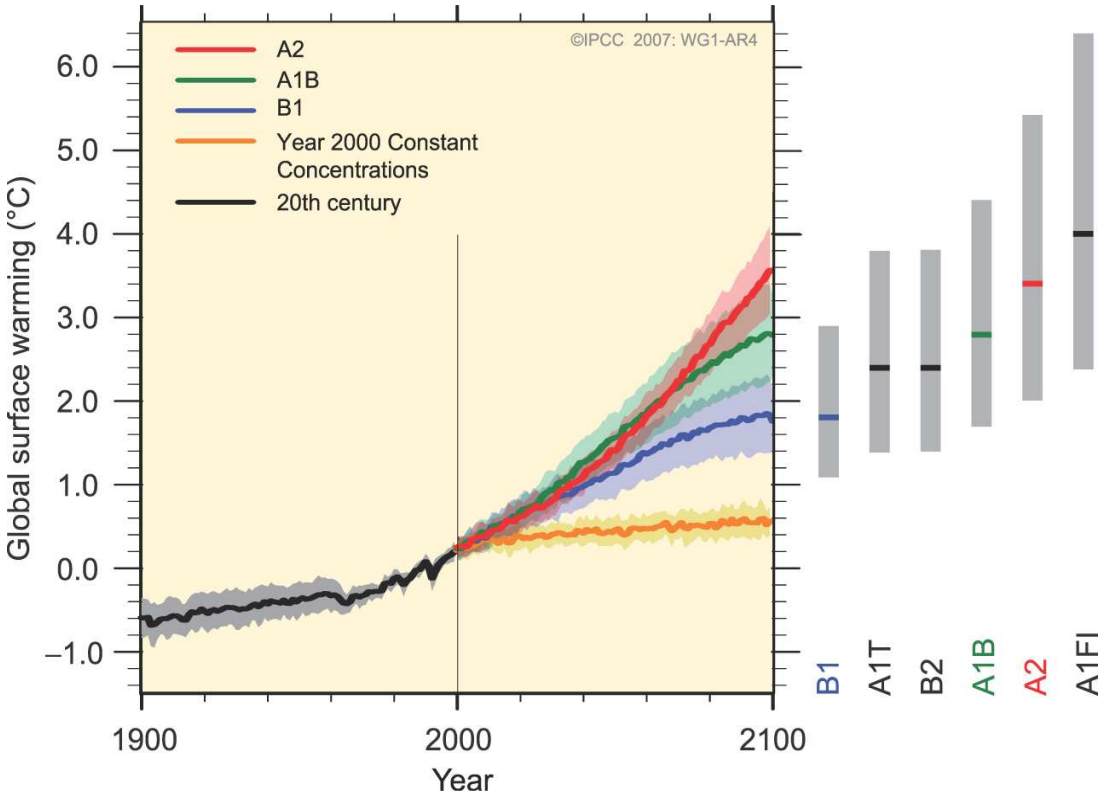

Fig. 2-6 Multi-model averages and assessed ranges for surface warming
(IPCC, 2007b)

The term 'Global Mean Warming' is used to describe the change projected in annual mean surface air temperature. Fig. 2-6 shows the projected trend in the global mean warming over the next one hundred years compared with simulations run for the twentieth century. Depending on the scenario, the models project a warming of between approximately 1.5 and 4˚C. The orange line depicts the scenario if concentrations of GHGs were held constant at the levels of the year 2000, showing a slow response time in the climate system, and suggesting that some degree of warming will still occur even if this concentration was somehow sustained (IPCC, 2007b).

There are a number of secondary climate factors suggested by the IPCC AR4 as being likely or very likely to undergo change. Heat waves and heavy precipitation events are very likely to occur more often; tropical cyclones are likely to involve higher peak wind speeds and heavier precipitation; the mid-latitude storm tracks will move towards the poles, changing their nature in terms of wind speeds, precipitation and temperature; precipitation is very likely to increase in high latitudes and decrease in subtropical regions; and it is very likely that the meridional overturning circulation in the Atlantic ocean will slow down - but it is very unlikely to change abruptly (IPCC, 2007b).

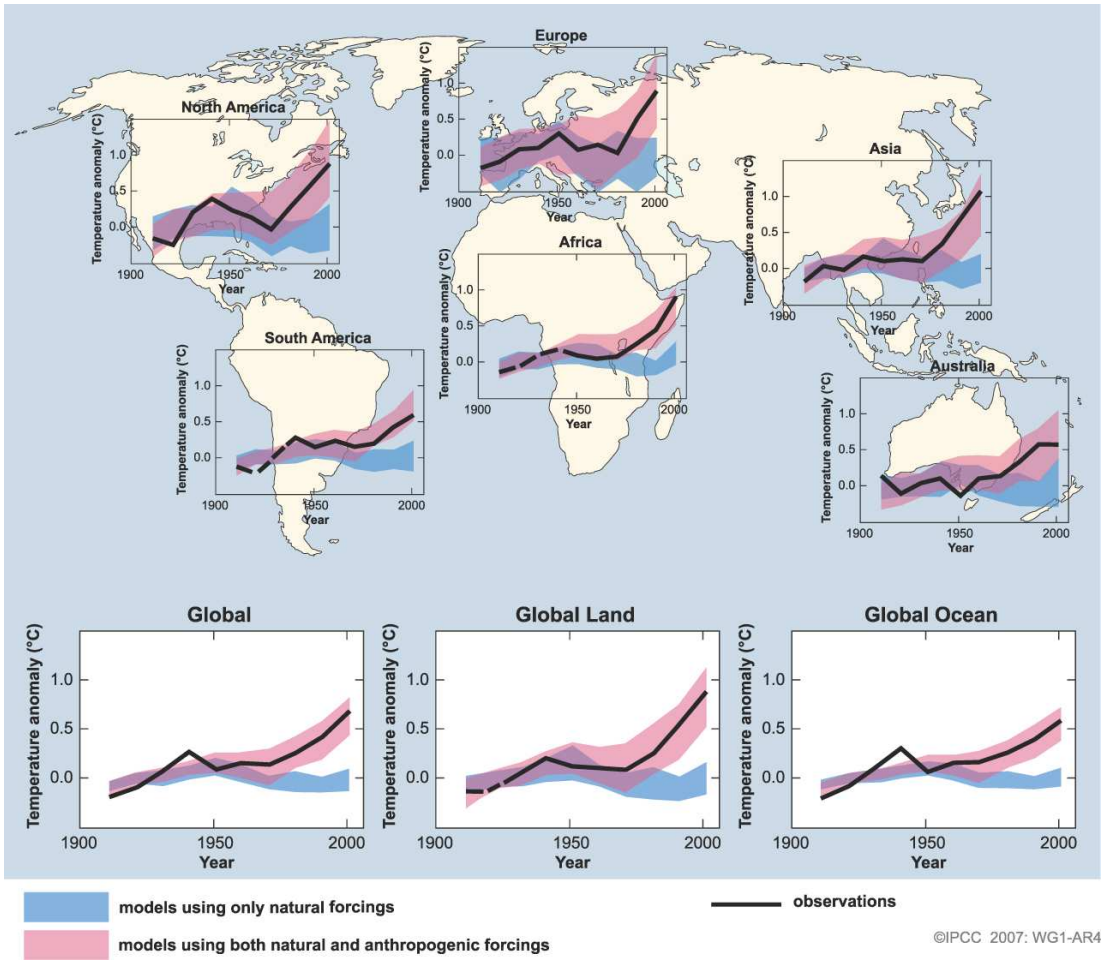

Fig. 2-7 Global and continental climate change

(IPCC, 2007b)

The models used to produce projections of future climate are often run for past climate, and then compared with the observed records in order to validate their results. IPCC (2007b) contains a graphic (Fig. 2-7) showing how the model output

looks when only natural forcings are included in the model calculations, and then run again including both natural and anthropogenic forcing. When the range of outputs is compared to the observed record, it is very clear that the results including anthropogenic forcings are much more similar to the observed data than those with only natural forcings. The IPCC AR4 used this to conclude that it is likely that an anthropogenic climate response is in progress already (IPCC, 2007b).

2.1.6.1 Uncertainty

There is uncertainty in both the observed historical and the projected future climates from models. Looking first at the observational uncertainties in Fig. 2-5, it can be seen that the uncertainty bounds on the records of temperature and sea level begin to converge with time, the more recent observations being much more reliable. Even within the range of uncertainty displayed on these graphs for data from 150 years ago, the witnessed change in the climate variables is still notably more than the difference in the upper and lower uncertainty bounds. Uncertainty within the model projections is less clear and less easy to define; and there are several levels of uncertainty which must be summed together.

SRES storylines inherently contain uncertainty. Whilst it is possible to understand the particular emissions levels likely to occur given a particular set of technological constraints and a particular type of economy, trying to put exact figures on this is not trivial. The storylines themselves are based on combinations of particular socio-economic circumstances and worldwide governmental choices which cannot be predicted with any certainty. The storylines each have equal likelihood, as it is not possible to put probabilities on the various scenarios, given the complexity of the inputs.

Each climate model, whilst based on the same physics, and often on the same dynamics, is slightly different. Different parameterisation schemes – for example, for cloud processes – resolutions, grids, and so forth contribute to their differences. The weight of scientific opinion may lie behind one model or another but in general, each has to be assumed to be equally accurate. Two models run under the same SRES scenario may give quite different future projections and their outcomes must be considered equally likely. If three models are run, and two produce similar results with one showing something different, the outcome from the two similar models is

believed to be more likely. As the models are producing data for future time periods, the intrinsic inability to validate their results against observed data means that whilst some verification and validation techniques attempt to deal with the problem, we cannot assume absolute certainty.

2.1.7 Climate impacts studies

The latest information from the IPCC cited above, such as global average temperature increase, is interesting and useful at a general level. However, in terms of gauging the effects of climate change on various regions throughout the world or on specific secondary systems such as crop growth, energy demand and so on, more detailed data is essential. In order to understand the full scale of data available about climate change, consideration must be given to the methods by which this data is generated.

2.1.8 The Atmosphere

2.1.8.1 The structure of the atmosphere

The gaseous composition of the earth's atmosphere is 78% nitrogen, 20% oxygen and small parts of argon, carbon dioxide and other gases - including other halogen gases, ozone and methane. Water makes up around 1% by volume of the atmosphere but this is a spatial and temporal average, and considerable variation occurs within this (Barry & Chorley, 1998).

The atmosphere is constructed of four layers: the troposphere, stratosphere, mesosphere and thermosphere. The dividing 'lines' between the layers are known as the tropopause, stratopause and mesopause. The troposphere refers to the section closest to the earth's surface and at the bottom of this layer is a boundary layer where it interacts with the surface. Fig. 2-8a shows the scales of the various layers and Fig. 2-8b the troposphere containing the boundary layer.

The troposphere is the layer of most interest to meteorologists, as this is where most of the weather-causing processes occur (Barry & Chorley, 1998). The boundary layer is of particular interest as the processes within it are those which, as observers perched on the surface, we feel directly. The boundary layer can vary in thickness but is generally around 1km deep and the transports within it are heavily

influenced by the earth's surface, reacting to the forcings within less than one hour, as opposed to the slow reaction of the rest of the atmosphere (Stull, 1993). The main feature of the boundary layer is its response to the absorption of solar energy by the surface - there is a diurnal temperature variation within the boundary layer that is not present anywhere else in the atmosphere (Stull, 1993).

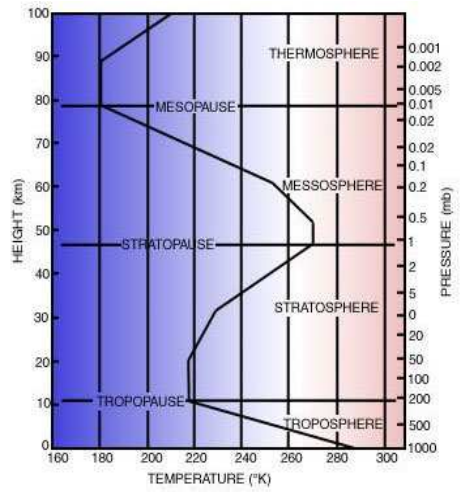

Fig. 2-8 Scale of Atmospheric Layers
Adapted from Met Office (2008)

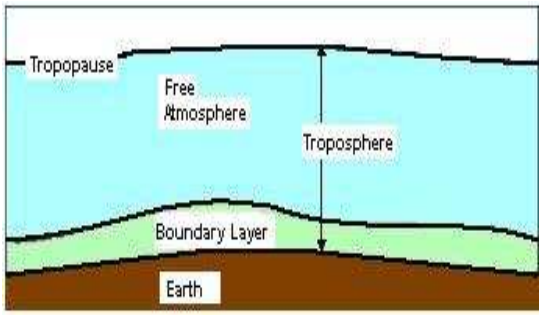

Fig. 2-9 The atmosphere
Adapted from Stull (1993)

The other key feature of the boundary layer is turbulence, which is responsible for the irregular perturbations of motion around the mean flow. Turbulence within the boundary layer is generated by a number of forcings, including wakes forming downwind from obstacles, friction with the ground and thermally-induced flows as hot air rises from the ground on a sunny day. Turbulent eddies can vary in size from millimetres to the full depth of the boundary layer (Stull, 1993).

2.1.8.2 Modelling the atmosphere

In order to understand weather and climate, it is necessary to understand the processes within the lower atmosphere and how various systems interact with each other. The use of models to aid this understanding is paramount, as experiments conducted with the atmosphere are beyond the current realms of science (Beniston, 1998).

The inward flux of solar radiation to the earth is the primary energy source for the atmosphere. Because the earth has a broadly spherical shape, the radiation is

not received equally across its surface; higher levels of heating occur at the equator and the heating decreases towards the poles. Heat is also radiated outwards from the earth, but this outward flux has an almost constant rate over all latitudes. Differing surface types distributed over the earth also contribute to the uneven heating patterns as different surfaces absorb and reflect different amounts of solar radiation (Beniston, 1998). The overall net heating at the equator and net cooling at the poles sets up a temperature gradient, inducing motion within the atmosphere as it strives towards an equilibrium (Dutton, 1976).

There are many levels of complex motion within the atmosphere, at a range of different scales, with little or no evidence of an overall basic north or southward flow of air, as intuition might suggest. One of the largest scale motions prevalent in the mid-latitudes in the northern hemisphere is a westerly flow – i.e. from the west – known as the polar jet stream. This is indeed the result of a pressure gradient, caused by the temperature difference between the high and low latitudes, but it is not the sole force acting on the air parcels (Dutton, 1976).

Acting alone, a pressure gradient like this would result in a poleward flow of air from high to low pressure areas. In addition, however, the turning force of the earth, the Coriolis force, turns the air to the right (in the northern hemisphere) as it moves away from the high pressure area. The air parcel is 'thrown outwards' by the centripetal acceleration of the planet. Because of this, observations show that within the large-scale circulation, air tends to move parallel to the isobars, with the low pressure on its left (in the northern hemisphere) (Dutton, 1976).

In many cases, especially in the past when computing power was very limited, mathematical models of the atmosphere investigating particular phenomenon tend to assume independence from different scales of motion, i.e. turbulence models would not consider the large scale circulation, and vice versa (Dutton, 1976). Beniston (1998) shows how models can be divided into temporal and spatial scales, which assume a 'diagonal' type relationship, i.e. phenomenon at large temporal scales tend to vary on large spatial scales, whereas small temporal scale variables tend to vary on small spatial scales. However, he also makes clear that interactions between scales must be included in all models in "a physically coherent and numerically efficient manner".

A complete atmospheric model must involve seven variables and their seven equations: pressure, temperature, moisture, density and the three orthogonal components of wind velocity. The equations are formulated by considering Newton's laws of motion, the laws of thermodynamics and the conservation of mass. They must first be applied to a parcel of air and then transformed to a fixed coordinate system where the parcels at all points are considered, giving a rate of change for the variables in space (Dutton, 1976). These laws arise from the study of fluid mechanics and, as such, are accurate and verified by experiment, and should enable prediction of fluid behaviour over infinite time. There are, however, atmospheric phenomena that appear to behave in a non-predictable manner and are often casually referred to as 'chaotic' – this is untrue in the strictest mathematical sense. These factors serve to limit the predictive abilities of atmospheric models to small time increments.

Many approximations are applied in atmospheric models, usually assumptions of particular states, such as zero acceleration within the flow. This produces surprisingly accurate answers at large scales. At smaller spatial scales, the approximations are no longer valid. The development of empirically derived or statistical relationships for sections of the problem is required here (Dutton, 1976). Whilst these relationships are useful in producing valid solutions, these often are only applicable in limited situations.

General circulation models of the kind used to investigate climate change, which operate at best on cell sizes of around 100-200 kilometres, are typical of large-scale atmospheric models in that they use the equations of motion with a number of approximations to resolve the large-scale flow; they then parameterise the smaller-scale variables in terms of the large-scale factors. This is the best achievable solution with current computing power. It does, however, limit the use of the small-scale information, and the reliance on the quality of the parameterisation schemes is not ideal.

2.1.8.3 General Circulation Models

General circulation models (GCMs) are the most complex 'earth system' models. They are three-dimensional models incorporating interactions between the land surface, the ocean and the atmosphere. The models aim to represent the dynamics,

physics and other processes within the atmosphere with a timestep of around 30 minutes. The dynamics involve all the different levels of transport within the atmosphere and oceans, whilst the physics represent the laws of conservation of momentum, mass and energy and the ideal gas law. Other processes involve, for example, heat fluxes and clouds. The earth is usually divided into grid squares over the surface, and these are developed into columns within the atmosphere and ocean, where vertical exchanges between grid squares take place. Horizontal exchanges can take place either between grid cells (fixed grid models) or are represented as waves in the frequency domain (spectral models) (McGuffie & Henderson-Sellers, 1998).

Modelling the boundary layer in a GCM is particularly difficult due to the very small scale of many of the processes, relative to the size of the GCM grid squares and columns. Processes such as cloud formation and surface winds are often poorly approximated by the low resolution models. Limits on computing power also restrict the ability to solve the most complex atmospheric models. The current European Centre for Medium-Range Weather Forecasting (ECMWF) integrated forecast modelling system runs on an IBM computer facility consisting of two parallel clusters, which have the power to carry out 33 trillion calculations per second (Lynch, 2008). The computational requirements of a model are scaled at $(1/\text{resolution})^4$, so, for example, doubling the resolution will require a sixteen-fold increase in computing power. General circulation climate models have increased their resolution since 1990 from around 500km to just over 100km, thus the computing power required is now extraordinarily high. However, the trend in supercomputer performance is that they double their computing power every 18-24 months in accordance with Moore's Law (Lynch, 2008), so models are able to exploit improved computing facilities as time progresses.

Direct results from GCMs are not always suitable for climate impacts research, due to the restrictions on their resolution. Many studies, for example Wilby *et al.* (1998), Mearns *et al.* (1999), mention how GCM data is of too low a spatial resolution for regional climate change impact investigation. Wilby *et al.* (1998) state that GCMs have "uncertain reliability…on timescales of months or less". Due to the local nature and the importance of high temporal frequency climate variations, this restricts the applicability of GCM results in regional climate change studies.

Running GCMs at higher spatial resolution is theoretically possible, but the processing time required under current conditions makes this impractical - except for very specific experiments. Thus, downscaling techniques have been developed that use the GCM output in some form and increase its resolution to make it applicable to smaller areas under analysis. A common technique used by impact researchers is the 'change factor method' (Wilby *et al.*, 2004) or 'perturbation method'. This involves applying lower resolution GCM anomaly data for a particular variable, i.e. the change field projected by the model, to a higher resolution observed dataset of this variable. For example, Breslow & Sailor (2002) have used the VEMAP (Vegetation Ecosystem Modelling and Analysis Project) dataset which contains historical observed surface wind climate data on a 10km grid, and have applied two sets of lower resolution GCM-predicted surface wind changes to it. This approach has been used because there is "more confidence in the predicted changes in wind fields than in the absolute prediction of these fields".

Although the output of their study is now on the same resolution as the original VEMAP data, the changes applied were of GCM resolution - so realistically the output data is not physically consistent with the original data. The method also assumes that range and variability remain unchanged (Wilby *et al.*, 2004) and thus does not really add any information over and above what the GCM supplies (Mearns *et al.*, 2003). Obviously being able to use this technique is dependent on having a reliable base climate dataset at a suitable resolution. For individual 'site-specific' information, the GCM output from the grid boxes nearest the site of interest can be interpolated to the site but this can give a false precision to the results (Wilby *et al.*, 2004).

A number of different climate downscaling projects have been carried out in the last ten years, in which researchers have taken the low resolution GCM output and attempted to make it useful for small-scale impact studies. Two techniques are prevalent in the literature, namely Statistical or (Semi)Empirical downscaling, and Regional Climate Models (RCMs), also referred to as Dynamical downscaling. Some studies show comparisons between the statistical and dynamical techniques and discuss the relative merits of both (Mearns *et al.*, 1999; Kidson & Thompson, 1998; Murphy, 2000). There have also been some evaluative studies, which have

collated information on several of the different methods that have been used and their evolution over time (Murphy, 1999). The majority of the information available is temperature or precipitation based; only limited research appears to have been carried out on wind climate.

Three techniques considered more effective than the change factor method, in that they actually enhance the regional information from the GCM, have been described in the IPCC Third Assessment (Giorgi *et al.*, 2001):

- High resolution/variable resolution Atmosphere GCMs (AGCMs),
- Regional Climate Models (RCMs)
- Statistical downscaling.

2.1.8.4 Atmospheric General Circulation Models

Giorgi *et al.* (2001) states that the idea behind Atmospheric General Circulation Models (AGCMs) is that the modeller will select a 'period of interest' from the full Atmosphere-Ocean GCM (AOGCM) solution and model it at a higher spatial resolution using the Sea Surface Temperatures (SSTs) and sea-ice distributions from the AOGCM as boundary conditions, using the same aerosol forcing as the AOGCM. This increases the resolution of results over a specific area of interest for a smaller 'time-slice'. The use of such models, however, has been limited due to cost and development times. Giorgi *et al.* (2001) suggest that they can be used as an 'intermediate step' between full AOGCMs and RCMs or statistical downscaling, whereby the higher resolution output from the AGCM is used in the downscaling methods as the AOGCM data would otherwise be. The UK Climate Impacts Programme 2002 (UKCIP02) used this technique in their analysis of climate change, using an AOGCM (HadCM3) to develop boundary conditions to run an AGCM (HadAM3H), and then taking boundary conditions from the AGCM to drive an RCM (HadRM3) (Hulme *et al.*, 2002).

2.1.8.5 Regional Climate Models

Regional Climate Models (RCMs), also commonly referred to in the literature as 'Dynamical Downscaling', are physical climate models run at higher spatial resolution than GCMs, but over a much smaller regional area. The driving conditions for the model – surface boundary conditions, initial time conditions – are

obtained from a GCM and they work on similar physical principles to GCMs, modelling the dynamic response of circulations and climate variables within a small area to the large scale forcings from the GCM data. The current published models do not feed into the GCM (two-way coupling) but this idea has been considered and is under development (Giorgi *et al.*, 2001).

There are many variations in regional climate models, and due to having been developed by many different organisations, they may produce dissimilar results even though they may model similar regions (Pan *et al.*, 2001). It has been found that using a single RCM with two different driving GCMs can also produce dissimilar output (Raisanen *et al.*, 2004; Pryor *et al.*, 2005d).

The advantage of using RCMs to downscale GCM data is that they are capable of producing physically consistent output at high enough resolution to be used in regional impacts studies. However, due to their complexity, they require large computational resources and time. They are also vulnerable to perpetuating systematic errors from the forcing GCM; and without two-way feedback, it is argued that neglecting to account for the effect of regional forcing on the large scale circulations will affect the accuracy of the output (Giorgi *et al.*, 2001).

2.1.8.6 Statistical Downscaling

The premise behind statistical downscaling techniques is that a finer-scale local climate variable (predictand) is linked by a consistent relationship over time to a large, global-scale circulation factor (predictor). Using historical data to derive this relationship, the local variable values can be extrapolated into the future using the GCM output for the larger scale factor.

The crucial linkage between the variables can be developed in any number of ways using some form of statistical analysis. The simplest form of statistical downscaling is to perform a straightforward linear regression, taking historical observations of two variables, one the predictor and one the predictand, and fitting a line of least squares. In some cases this gives an acceptable correlation for minimum effort. Enhancing the linear regression using multiple predictor variables can give better results (Solman & Nunez, 1999) and using more advanced methods on the data such as Principal Components Analysis (Huth & Pokorna, 2005) or Canonical Correlation Analysis (Busuioc *et al.*, 2001) can further increase confidence in the

output. Going further, some studies have attempted to define the predictor-predictand relationship using non-linear analyses such as neural networks (Sailor *et al.*, 2000; Trigo & Palutikof, 2001).

A technique referred to as the 'analog' method is described in Zorita & von Storch (1999). It requires historical large scale circulations to be classified and related to a particular local climate. The large scale circulations predicted by a GCM are then sorted into the classification groups (their 'analogs') and thus the local climate projections can be analysed. Mearns *et al.* (1999) developed another weather-typing method which they call "semi-empirical statistical". They used classified large scale circulation patterns as part of a regression function to obtain local climate projections with a GCM.

Weather generator methods are commonly applied in downscaling studies. They involve using a stochastic weather generator which is trained on large scale atmospheric variables. The weather generator is then perturbed by the changes projected in the GCM and the change in output for local variables such as rainfall can be analysed (Wilby *et al.*, 1998).

The advantages of using statistical downscaling techniques are mainly related to their simplicity. Provided there is sufficient historical observed data available, it will usually only require a fairly straightforward utilisation of statistical theory to obtain a good predictor-predictand relationship. GCM data from a number of different models is easily obtained and the relationship can be applied to it, although most studies up to now have only used one GCM (Wilby *et al.*, 2004). The other distinguishing advantage of this technique is that it can be applied on a site-specific basis, provided the historical data are available to derive a basic predictor-predictand relationship (Wilby *et al.*, 2004). The main disadvantage stems from the caveat that because a relationship has existed between the variables in the past, does not implicitly mean that an identical relationship will hold in the future. However, this issue also applies to Regional Climate Modelling (and also GCMs themselves) – parameterisations that have been assumed may not necessarily hold under conditions of climate change (Wilby *et al.*, 2004). Other problems with statistical downscaling are that models are not transferable between regions and that insufficient data can render them ineffective.

2.1.8.7 Model Output Statistics (MOS) vs. Perfect Prognosis (PP)

In the process of statistical downscaling, when establishing a transfer function between two variables, Model Output Statistics (MOS) techniques derive the relationship using the output of the model as the predictor and observed variables as their predictand. The advantage of the technique is that by deriving a relationship between model-generated predictors and observed predictands, any inherent biases in the model are accounted for in the relationship. Perfect Prognosis (PP), on the other hand, assumes that the model is 'perfect' and, once a relationship has been established between an observed predictor and an observed predictand, this relationship is directly applied to the model output for the predictor variable(s) (AMS, 2009). The 'change factor' method discussed in section 2.1.8.3 can also be applied in statistical downscaling, where the statistical relationship is derived between an observed predictor and observed predictand. The GCM is used to derive the future change in the predictor variable and this change then applied to the observed predictor dataset. Fig. 2-10 compares the processes involved in the MOS, PP and change factor methods.

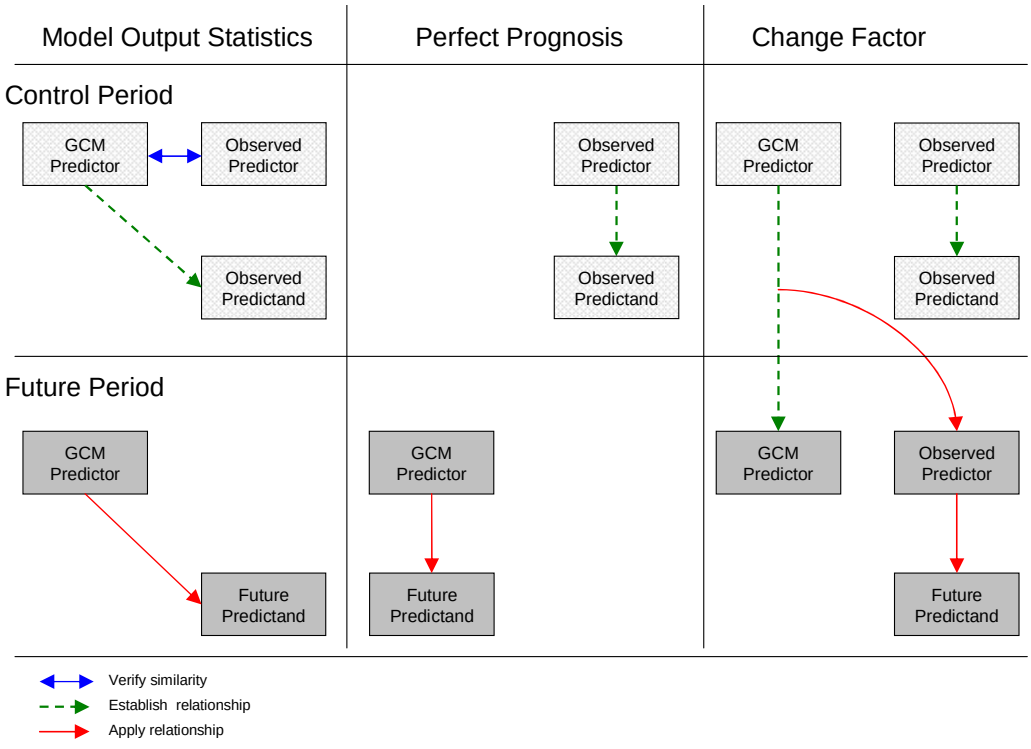

Fig. 2-10 Schematic diagram of MOS and PP techniques alongside the Change Factor method

In the case of other studies looking at wind and climate change, the MOS technique has been adopted (e.g. Pryor *et al.,* 2005b), mainly because there is such a large degree of doubt as to how well the GCMs represent the relationship between variables, especially with regard to surface winds.

2.1.8.8 Validation of Results

Validating the results of any kind of climate projection in order to show that they are reasonable forms a necessary part of the modelling process, and provides some level of confidence in the output. However, conventional validation procedures involve checking the results from a model against the actual physical values that the model is trying to simulate, and in a future climate projection scenario this is obviously impossible. There are two ways in which 'semi-validation' is carried out for these models in order to allow some analysis of their success.

The first is based on an assumption that if the model correctly simulates current climate, it will be similarly accurate in the future. For GCM data, the results of a model run for a control period, quite often the period 1961-90, are usually compared against the observed climate for this time; the more closely they reproduce the observational statistics, the better the model is considered to be. For RCMs, the methodology is analogous (Pryor *et al.*, 2005d), but for statistical downscaling the process is different, due to the observed climate dataset having been used to develop the relationship in the first place.

Many statistical downscaling researchers divide their observed climate dataset into two sections, a calibration period and a verification period (Solman & Nunez, 1999; Trigo & Palutikof, 2001; Mearns *et al.*, 1999), which ensures that the statistical relationship developed for a particular period of time is at least valid for one other period of time. This method is common when the dataset is large, i.e. more than 30 years long (Wilby *et al.*, 2004). Alternatives include cross-validating by removing a particular month, say, from the calibration dataset and comparing the output of the model with the actual observations for that month (Murphy, 1999).

The second method of 'semi-validation' of climate models is to compare their output with a different model. Because RCMs and statistical downscaling are evolving simultaneously, many studies have compared output from both methods with each other, or with a GCM (Murphy, 2000; Mearns *et al.*, 1999). Having

already assessed the skill of the RCM or GCM in replicating current climate, this is an alternative approach to validating against actual observations, with the caveat that there is no guarantee of the validity of either model in future projections.

In terms of the measures used to compare climate models, either with observations or with each other, the most obvious statistics to compare are the means and standard deviations of the sets of results. Correlation coefficients and the root mean square error can be used to gauge the success of a regression (Wilby & Wigley, 1998; Pryor *et al.*, 2005d). Pryor *et al.* (2005b) use Taylor diagrams (Taylor, 2001) to display simultaneously the correlation between the observed and simulated results and their root mean squared difference. Comparisons of the shapes of frequency distributions resulting from time series of observations with time series from the models can show qualitatively the detail of the differences in variance, mean, mode and so on (Pryor *et al.*, 2005b). Qualitative examination of the spatial patterns of climate developed by a model alongside those from observations or from other models provides insight into how the model success can vary over the region of interest (Raisanen *et al.*, 2004; Pryor *et al.*, 2005d).

2.2 The Policy Response to Climate Change

In light of the information and scientific consensus on the changing climate, it is the responsibility of the world's governments to take the lead on mitigation and adaptation strategies. This section assesses what has been done so far in the UK and Europe, and what is planned for the coming years.

2.2.1 Economics, Energy and Developing Renewables

There is a well established and inextricable link between energy and economic development. A ready supply of relatively cheap energy allowed those countries now classified as 'developed' to make rapid economic gains from the start of the industrial revolution until the late 20th century. This cheap energy was provided largely by coal, oil and later by gas. Growth in energy-intensive activity now means that the UK has one of the highest per-capita energy demands in the world. The Energy Information Administration (EIA) places the UK ninth in terms of overall energy consumption (EIA, 2006) - energy that comes primarily from the burning of fossil fuels directly for heat and transport, and for electricity generation. The same source places the UK eighth in terms of carbon dioxide emissions from this fossil fuel use. An overwhelming reliance on fossil fuel-based energy forges an inconvenient link between economic growth and carbon, a link that world leaders are putting their minds to breaking for a number of reasons, including climate change.

Energy security is generally defined as keeping up the supply of energy to a nation without disruption to its economy (Löschel *et al.*, 2009). Maintaining energy security has been a priority on the governmental agenda for many years, in recognition of the intrinsic link between energy and economic growth. It is vital that disruptions to supply are kept to a minimum to sustain the desired level of growth. Adopting climate change mitigation strategies often demands that we reduce our fossil-fuel-based energy dependence to limit carbon dioxide emissions and arrest global warming, but there are concerns about the effect of this on economic stability. Decoupling the economy from energy is unrealistic, some might say impossible, but the development of carbon-free energy sources provides an option to remove the carbon element of energy supply whilst maintaining desired levels of economic growth.

The climate change issue has arisen at a point when there is also question as to whether the earth's natural fossil-fuel resources are running low (Leggett, 2005). The exhaustion of these resources would prevent any further carbon dioxide being emitted, but could potentially bring the world to a halt if no other viable sources of energy were available. Other reasons for energy insecurity lie in the political tensions between big energy users and nations with areas rich in fossil fuel resources. If, for example, Russia were to shut down its main gas pipeline to Europe, the UK - without significant new storage facilities - would be very quickly short of power and heat for its domestic and industrial users - leading to all sorts of obvious difficulties. Some indication of the possible disruption has been given recently during disputes between Russia and the Ukraine in January 2009 (BBC News, 2009).

The DECC (2009d) define renewables as "energy that occurs naturally in the environment" and claim that the majority of these can be traced back to the sun's energy and are thus "inexhaustible". In the face of climate change and other pressing energy security threats, most countries, including the UK, have their eyes trained on technological developments in the field of renewable energy, hoping that with mass production and additional technical advances they could be made competitive with conventional energy sources. The development of indigenous renewable energy resources could provide a degree of energy independence for the UK and safeguard the economy from political instability elsewhere.

While fossil fuels remain cheap to extract and refine, their price will remain comfortably affordable, despite some price volatility. Meanwhile, alternative energy sources - with the uncertainties of a non-established supply chain, no proven economies of scale, and high risk investment strategies - may seem unaffordable and out-of-reach. Introducing these alternative energy sources requires either forcing mechanisms from government or for the price of fossil fuels to rise above the price of the alternatives - assuming these are readily available. Supply-side control of emissions through the use of renewables is obviously a key factor in the government's policy, but demand-side reductions may provide additional gains, i.e. improving end-use energy efficiency.

2.2.2 Climate Change energy policy internationally

There are a large number of projects throughout the world attempting to tackle the issue of emissions reduction, simply in order to prevent, or at least minimise, climate change. According to the DECC (2009b) the UK energy policy is influenced at an international level from three major sources: the EU, the G8 and the United Nations Framework Convention on Climate Change (UNFCCC).

2.2.2.1 G8 - The Group of Eight

The 'Group of Eight', or G8, was founded by an original six members in 1975; they were: USA, Japan, Germany, France, the UK and Italy. Canada joined them in 1976, making it the G7, and finally Russia also became a member in 1998. These are eight of the richest countries in the world; their leaders meet on a yearly basis at G8 summits but work also takes place in the background. They discuss and develop agreements mainly on economic issues such as trade and development, but also deal with security, environmental issues and energy. These agreements tend to be followed through fairly consistently: "compliance is particularly high in regard to agreements on international trade and energy" (G8 Information Centre, 2005).

The G8 presidency fell to the UK in 2005 and following a meeting in Gleneagles, Scotland in June 2005, the Gleneagles Plan of Action on climate change, clean energy and sustainable development was drawn up (G8, 2005). This ten-page document detailed a number of commitments to increase energy efficiency across a number of sectors including buildings and aviation, and increase development of renewable energy sources and cleaner fossil fuels. It also signalled interest in furthering and sharing research in various areas and, importantly, reinforced a belief in a market-led approach to investment in 'green' technology.

2.2.2.2 UNFCCC – The Kyoto Protocol

In response to the growing amounts of information coming from the scientific community regarding climate change and its link to our high rate of fossil fuel use, the United Nations Framework Convention on Climate Change (UNFCCC) was created in 1992; the aim was to establish informal or voluntary emissions reduction targets, ideally to reach pre-1990 levels. They followed up the voluntary targets with the creation of the Kyoto Protocol in 1997, which was designed to set legally binding

targets for emission reduction in each of the developed countries which ratified it (UNFCCC, 2009c). Due to what were clearly political considerations, two of the world's largest polluters - Australia and the USA - refused to ratify the protocol. Both were put under international pressure and later realised that political advantage could be had by reversing this decision. Australia finally ratified in December 2007 and it is expected that the USA will soon do likewise.

There is still an unresolved issue regarding the developing nations and their contribution to carbon dioxide levels. When the G8 presidency fell to the UK in 2005, the result of a meeting in Gleneagles, here in Scotland, was an informal offer to help the developing nations towards cleaner, greener energy sources. A UNFCCC meeting in Bali in December 2007 resulted in a roadmap of plans directed towards emissions reductions to pre-1990 levels globally, and an action plan for a new target negotiations process. However, there is still some debate about the contribution that developing nations ought to make, with many of the developed nations aggrieved that their developing counterparts do not have specific binding targets similar to their own. There is an argument to suggest that since the developed nations created the current problem, it is unfair to ask the developing nations to arrest their own economic development - which hinges on a cheap energy supply - in order to counteract damage done by economically better-off others.

It is essential that as cleaner, greener, more sustainable technology is developed, it is deployed to developing countries at the lowest possible cost. One particular measure devised to help this happen is the Clean Development Mechanism (CDM). This was built into the Kyoto Protocol and allows richer countries to carry out work in a developing country to reduce emissions yet be able to count this reduction towards their own target. Examples of such projects mentioned by the UNFCCC (2009a) are installation of solar panels in a rural area or installation of more energy efficient boilers. This is a good arrangement for the developing country, since it boosts the economy in a sustainable manner; but it also lets the originating developed country 'off the hook' for a chunk of its own emissions which may still need addressed. The mechanism has potential to be seen as a 'cheat', but the wealth transfer possibilities that the scheme opens up for the developing countries cannot be denied.

2.2.2.3 EU context

The Kyoto Protocol contains what is known as a 'Bubble arrangement', whereby the EU has taken on responsibility for a percentage reduction in emissions which is spread out in different proportions among its member states. The target for the EU as a whole is 8% below 1990 levels, with, for example, the UK committed to reducing by 12.5% whilst Portugal, for example, is allowed to increase its levels by 27% (DECC, 2009c). This arrangement allows the EU to assist nations who are on the border between developing and being developed - like some of the former communist-bloc countries -and allows them to 'catch up' with older member states in terms of economic development. The EU member states are privileged in that they have the structure already in place to spread the burden of reducing emissions whilst still pushing for economic development. Sadly, many developing countries outside of the EU are struggling to balance their dual mandate of pushing for economic growth whilst reducing emissions, and must compete for Clean Development Mechanism (CDM) investment.

2.2.2.4 Emissions Trading Scheme

The European Union Emissions Trading Scheme (ETS) began operation in 2005. It is a cap-and-trade scheme which requires each country to allocate a particular emissions level to its industrial CO_2 producers under what is known as a 'national allocation plan' (NAP). These industries must then either meet the allocation, or purchase allowances from other industries which have come in below their set allocation (DECC, 2009a). The members have the option of utilising the CDM to help reach their targets. The level of allowances set by each of the participating countries is a key factor in determining the market price; in the initial phase (2005-2007) there were more allowances available than were needed, forcing the price down to less than €1/tonne of CO_2 (Skjaerseth & Wettestad, 2008). There are issues regarding the differing levels of ambitiousness of different countries, with some, such as the UK, willing to cap emissions and allocate fewer permits than its current emissions level, whilst others handed out more permits than were required (Skjaerseth & Wettestad, 2008). It is hoped that the market in the second phase of implementation (2008-2012) will work more effectively with more ambitious emission reduction targets. Further modifications to the scheme are planned for the

2013-2020 period (EU Commission, 2009) with a still more ambitious emission reduction target being set.

2.2.3 UK-specific mechanisms

The electricity supply industry in the UK was broken up and sold to private investors by the government in the early 1990s. The action, part of a broader privatisation plan by the Conservative government, was intended to reduce the influence of trade unions, promote shareholding among the public and generate funding for tax cuts. In addition, it would allow the markets to determine the price and supply of energy; this was supposed to provide perfect competition with the price of energy being set at exactly the level of its economic worth. However, there is ongoing debate about how well the energy market actually operates, and whether the competition is actually imperfect. The other problem is that under conditions of required change, i.e. emissions reduction - which is likely to be costly - the market does not necessarily move in the direction of change without government intervention, as factors like climate change are externalities.

The UK has to meet targets for emissions reduction and renewable energy generation set through the EU and the Kyoto Protocol, along with the less formal G8 agreements. The system of government does not make the setting of long-term goals that require significant shifts in attitude particularly simple but after much deliberation, movement is being made towards building a suitable framework for a significant reduction in emissions.

2.2.3.1 The Stern report

Sir Nicholas Stern, a British government advisor, economist, and former Senior Vice-President of the World Bank, was commissioned by the government in 2006 to write a report on how climate change might impact on the economy, and about what could best be done to adapt to this (Stern, 2006). The report estimated that many of the effects of climate change would be felt most keenly in the poorer areas of the world, i.e. those least equipped to deal with it. The economic modelling strategy used in the report was long-range and attempted to take into account the results from the latest climate modelling scenarios. It came to the conclusion that although adaptation strategies may seem expensive in the short-term, it would be advisable to invest now,

as the cost of dealing with climate change later would be much greater. Stern argued that climate change could be tackled now in such a way as not to "cap the aspirations for growth of rich or poor countries" and reduce the likelihood of facing situations where it was too late to mitigate.

2.2.3.2 Energy White Paper 2007 and Energy Bill 2008

In 2007, the then department of Trade and Industry (DTI)[2] published an Energy White Paper: "Meeting the Energy Challenge" (DTI, 2007a). This was intended to bring together information on climate change and additional energy security issues and to set out plans for "meeting the challenge". The Paper displayed the government's dual intentions: first, to generally support the development of more competitive energy markets; but, second - by acknowledging that the privatised energy sector might not drive in the direction of renewable energy technology of its own accord - to develop support mechanisms to stimulate the instigation of successful renewable energy development. The document also stated that Britain would be aiming for at least a 60% reduction in emissions from a 1990 baseline and that there would be a parliamentary bill to ensure that this target was legally binding. There was a clear commitment in the document to a number of strategies to achieve this, including investment in carbon capture research, replacement of the aging nuclear power stations, energy efficiency measures and enhancement of the EU ETS.

Arising from a cabinet reshuffle in Autumn 2008, a new Department of Energy and Climate Change (DECC) was created. It assumed responsibility for climate change issues from the department of the Environment, Food and Rural Affairs (DEFRA), and energy issues from the then department of Business, Enterprise and Regulatory Reform (BERR). Binding targets from the EU and Kyoto means that significant changes are needed in the energy generation and transmission systems. The Energy Bill 2008 was passed in October 2008 as a follow-on from the Energy White Paper mentioned above. This bill increased the UK target of reducing its emissions from 60% to 80% by 2050; the target includes emissions from aviation and shipping - something which had been ignored in most of the preceding target-setting processes as it was unclear how these should be assigned to a particular

[2] The DTI subsequently became the department of Business, Enterprise and Regulatory Reform (BERR); in June 2009 it became the department of Business, Innovation and Skills (BIS)

country. Because of the late inclusion of the emissions of any ships or aeroplanes that refuel in the UK in the 80% target, it is unlikely that reductions in this area will feature prominently in the next few years. Focus instead will be on electricity generation, heating and possibly some domestic transport.

The UK has a current target to meet 15% of its energy needs with renewable sources by 2020 (DECC, 2009d), and with long waiting lists for grid connections for new wind farm developments, it looks unlikely to be met unless major action in terms of changes to planning legislation and funding incentives is taken by the new department.

2.2.3.3 Demand

Demand for electricity in the UK has been increasing since the 1970s, although it appears to have stabilised in the last 5 or so years (see Fig. 2-10), possibly due to energy efficiency strategies encouraged by government, combined with rising prices and the decline in heavy industry. Somewhat of a crisis is anticipated in the next 10-15 years if demand continues to increase - even if more slowly than in the last few decades - as much of the ageing nuclear plant is to be decommissioned without concrete plans for replacement; and many of the older (and more polluting) coal plants are also to be closed down. It is simply not clear at the moment where the capacity to meet expected demand is likely to come from.

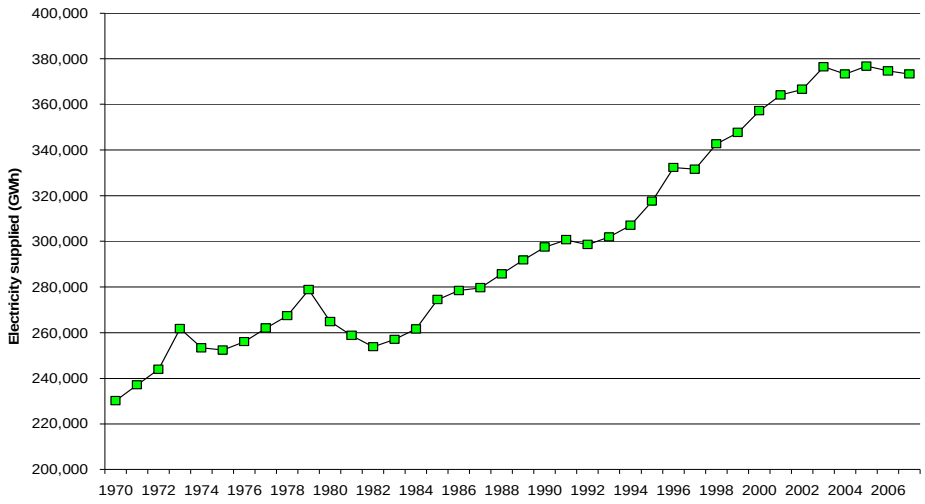

Fig. 2-10 Electricity supplied in the UK (incl. Isle of Man and Channel Islands) per annum 1970-2007

(BERR, 2008)

2.2.3.4 Current renewables in the UK and related targets

In the UK at the moment, on- and offshore wind, biomass and hydro are the most common renewable energy sources. Including hydro, renewables meet around 5% of electricity demand (DECC, 2009d). Looking at the details of the renewable energy contributors as shown in Fig. 2-11 and Fig. 2-12, over the last ten years wind has increased its energy yield six-fold, doubling its percentage contribution to renewables generation, whilst the total amount of hydro energy has stayed fairly constant. Biomass generation has tripled, increasing its percentage contribution further. Wave power is still very much in the development phase; there is just one wave power device, Limpet (Voith Hydro Wavegen, 2009), an oscillating water column, currently connected to the grid in the UK, but a small number of devices are being tested with a view to large-scale development and grid connection. The Pelamis wave power device (Pelamis, 2009), thought to be among the strongest contenders for potential large-scale development, was designed and built in Scotland. Some of its prototype testing was carried out in Orkney at the European Marine Energy Centre (EMEC) but the first grid connection of a commercial wave farm in Europe was in Portugal using three Pelamis devices. Further installations of Pelamis devices are planned for the Orkney coast in the near future (Pelamis, 2007).

Tidal power has also received attention recently in an attempt to harness a number of potential resources around the UK, but as yet remains largely in the research and development phase. A major testing centre has been established near the UK's greatest tidal current resource in the Pentland Firth, north of Scotland (EMEC, 2009), where many designs and devices are undergoing testing. A single tidal turbine developed by the company Marine Current Turbines (MCT) is in testing at a site in Northern Ireland (MCT, 2009) and some large power companies have expressed interest in developing this resource further. A tidal barrage scheme is also being considered across the estuary of the River Severn which would generate a relatively large and regular amount of power.

The UK hopes to meet 15% of its energy demand with renewable resources by 2020, as part of an EU directive related to meeting Kyoto targets, and the latest government report suggests up to 30% of electricity could come from renewables by

this time (DECC 2009d). The majority of this increase is currently expected to be met by massive expansion of both onshore and offshore wind power. Debate surrounds the feasibility of connecting so much distributed generation to the aging national grid in such a short period of time; some government investment is needed to expand the grid's capability and there is also question about the supply chain and logistics within the wind turbine industry itself (Aubrey, 2007). The large-scale tidal power project, the Severn Barrage, is being suggested as another major contributor; but the environmental impact of the Barrage is a matter of critical concern to several groups and it is currently not known whether the project will be approved through the planning stages.

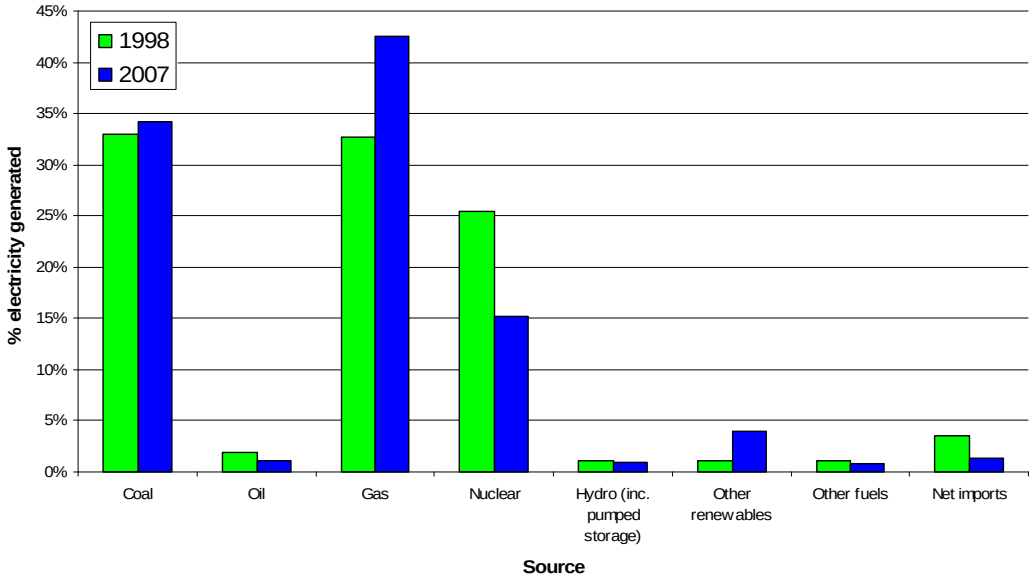

Fig. 2-11 Percentage of Electricity generated from various sources in the UK
(BERR, 2008)

Renewables Obligation Certificates (ROCs) are the primary support mechanism for generation of power from renewable sources in the UK. In the simplest terms, they are given to generators of renewable energy for a specific amount of electricity generated, who can then sell them to one of the designated electricity suppliers. The electricity suppliers must buy enough certificates to cover a certain percentage of their sold electricity, and the percentage has risen from the instigation of the system in 2002 - from 3% to a planned 15% by 2015 (BERR, 2009b). In this way, financial

support is provided for development of renewable energy directly. An appendix to the Energy White Paper 2007 covers some proposed amendments to the system, including providing different levels of support for different renewable sources to encourage success for newer technologies, and the option to increase the total obligation to 20% if required (BERR, 2009b).

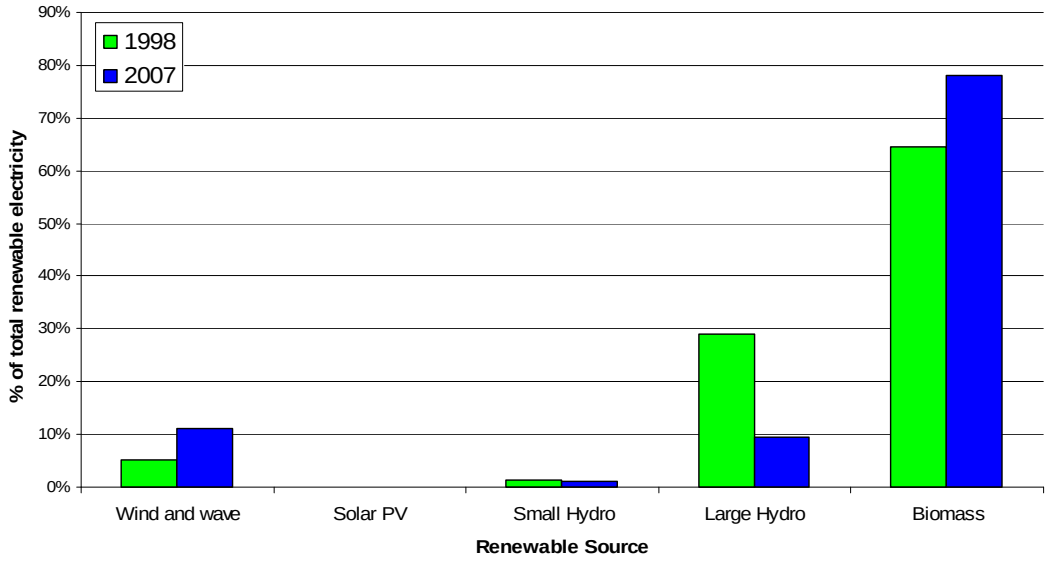

Fig. 2-12 Percentage of renewables from each source
(BERR, 2008)

2.3 Conclusion

The first part of this chapter discussed the latest scientific information available on climate change. Much of the information is disseminated and presented by the IPCC and from their publications it is apparent that the majority of scientists working in the field believe that climate change is likely due to a rise in anthropogenic emissions of greenhouse gases. The data for future climate projections is obtained through climate modelling, using numerical models of atmospheric dynamics and physics combined with scenarios of future emissions levels to calculate how climate will evolve under these scenarios. The models project warming to occur over the course of the next 50-100 years plus consequent changes in other climate factors like precipitation; the specific changes are often different in different regions of the world. For many

climate variables, the resolution of the GCMs is not sufficient to provide reliable localised estimates of future change, and so techniques have been developed to downscale these to provide higher resolution data over smaller areas.

In response to the expanding levels of scientific information, action has been taken governmentally, both globally via organisations like the UNFCCC and the G8, and at a national level. The UK has seen rapid growth in energy demand over the last thirty years, most of which has been met by fossil fuel-based sources which have contributed substantially to emissions of greenhouse gases. In the face of climate change concern, and also potentially dwindling oil and gas reserves, effort is being made to encourage a reduction in fossil-fuel dependence and move – at least partially – to more sustainable energy sources such as renewables. Many of the renewable technologies are in their infancy and not immediately deployable; wind energy currently presents the most mature and economically feasible option.

Chapter 3

Wind Power

Wind power has advanced particularly fast in the last twenty years to become an economically viable and clean alternative to fossil fuel-based electricity generation. Increasing wind generation is an essential part of the global drive to reduce carbon dioxide emissions but changing from a power system built on a foundation of large thermal generators to the more distributed nature of wind power generators is challenging. Knowledge of wind climatic conditions is important both at an investment level and to optimise development strategies, and it is clear that obtaining this kind of information is not straightforward. Compounding the complexity is the issue of climate change and its potential impacts on wind power generation - as already referred to in Chapter 2. In this chapter, the mechanics of wind turbines and their incorporation into electricity systems are examined. The available techniques and databases for analyses of wind climate are also investigated. Finally, a sensitivity analysis is carried out to show the potential impacts of wind speed variations on wind power project finances.

3.1 History of wind power

Wind turbines have been in existence in the world in some form for at least three thousand years (Burton *et al.*, 2001). They were probably first used in a similar way to water wheels, for grinding grain in mills, and some of these types of machine are still in existence in parts of Northern Europe. Windmills were designed to operate at relatively low altitude and their blades, normally four, began as simple flat structures; but they were developed over time into twisted structures with an aerofoil-type shape (Manwell *et al.*, 2002). Historically, wind power was also used as a means of pumping water from the ground, for direct consumption or as a farming irrigation tool. These kinds of turbines would have been typically high solidity, low altitude machines designed to run at relatively low speeds. Wind-driven farming irrigation pumps are still in use in rural areas of southern Europe and the USA, e.g. Texas.

The first evidence of electricity generation from wind power is from around the late 1800s in the USA; but due to the advance of large-scale electrification in the western world, this kind of isolated system became obsolete (Burton *et al.*, 2001). From the 1930s onwards there are examples of wind turbines for electricity being developed in the former USSR, the UK, Denmark, France and Germany but, due to the relatively low price and high availability of fossil fuels, serious interest was not shown until the 1970s (Burton *et al.*, 2001).

During the 'oil crisis' of the seventies, a rising price drove governments to invest in research into wind power as an alternative to fossil fuel-based power generation. A raft of developments led to the initial trials of wind power for grid-connected electricity generation. A number of designs were considered but have converged on a Danish design of a three-bladed horizontal axis machine - although vertical axis turbines made a short appearance in the U.S.A. The Californian state government initiated some of the most favourable financial support mechanisms for wind power development (Manwell *et al.*, 2002) which, in its technological infancy, was much more expensive than conventional power. Thus it was the first part of the world to use wind power on a relatively large scale in the late 1970s and early 1980s, albeit with quite small – in today's terms – 100kW machines (Burton *et al.*, 2001). The Reagan administration discarded the incentives in the early 1980s however, as the oil price stabilised, and the race for wind power generation faded (Manwell *et al.*, 2002).

During the 1990s with mounting concern about climate change and other energy security issues, wind became more attractive to nations keen to establish an indigenous, independent and clean energy source. Denmark is now considered to be the country at the forefront of wind technology development. It is home to both premier research facilities and a large proportion of the turbine manufacturing industry, and generates a large percentage of its electricity from wind power. By the end of 2008, the country with the largest installed wind power capacity was the USA with over 25GW; Germany was a close second with almost 24GW and the UK was ranked 8th with 3.2GW (Danish Wind Industry Association, 2009).

3.2 Turbine power extraction

A wind turbine extracts power from the wind by converting the kinetic energy of the air parcels moving towards it into kinetic energy in its blades. The simplest model for understanding the process is an actuator disc model as described in Burton *et al.* (2001). The full derivation of the key equations is given in appendix A.1.

In a situation with no wind turbine, the power available in the air can be found by considering the kinetic energy, where

$$KE = \frac{1}{2} m U^2 \tag{3.1}$$

Power can be expressed as kinetic energy per unit time, such that

$$P = \frac{1}{2} \dot{m} U^2 = \frac{1}{2} \rho A_x U^3 \tag{3.2}$$

It is found that the power, P, extracted by the turbine in the actuator disc model, is a function of density, ρ, the swept area of the blades, A_d, and the cubed velocity of the incoming air, U^3, such that,

$$P = F_d U_d = 2\rho A_d U_\infty^3 a(1-a) \tag{3.3}$$

where $\dot{m}$ is the mass flow rate and a is the 'axial flow induction factor'. We define a power coefficient, C_p, as the ratio of power extracted by the turbine to the power available in the air,

$$C_p = \frac{2\rho A_d U_\infty^3 a(1-a)}{\frac{1}{2}\rho U_\infty^3 A_d} = 4a(1-a)^2 \tag{3.4}$$

The maximum C_p occurs when $\frac{dC_p}{da} = 0 = 4(1-a)(1-3a)$ which gives $a = \frac{1}{3}$, thus

$$C_{p,\max} = \frac{16}{27} = 0.593 \tag{3.5}$$

This is known as the Betz limit, and infers that a maximum of 59% of the energy in the air can be extracted by a wind turbine.

The relationship between available power and the velocity of the incoming air to a turbine is cubic, as per equation 3.2. This implies that a small change in velocity will create a proportionately larger change in the power output from the turbine. It is this that makes the study of changes in wind so important, as the financial yield depends heavily on the power output over a given period of time.

3.2.1 Power Curve

Wind turbines are set up in such a way as to extract the highest possible amounts of energy from the wind with the minimum of risk of failure and an optimum level of maintenance. A typical wind turbine power curve is shown in Fig. 3-2a. They 'cut-in', i.e. begin operation as wind speed rises above 3-4m/s and the power output increases with wind speed until they reach their maximum power output at around 15m/s. The power output is limited to rated power between 15m/s and 25m/s. The turbine will shut down, known as 'cut-out', in high wind situations, usually above 25m/s and will not resume operation until the wind has dropped below a value of approximately 22m/s. This is referred to as 'high wind hysteresis' (Horváth *et al.*, 2007) and is designed to minimise potential damage to blades caused by the high wind forces. Some new turbine designs operate on a slightly different control system; for example, the Enercon E-70 (Enercon, 2009), does not shut down completely when the wind speed rises above the cut-out speed, but turns its blades out of the wind to keep its rotational speed lower and minimise damage risk - see Fig. 3-2b. The blades can then simply turn back in when the wind speed drops again, reducing the yield losses associated with the cut-out and restart of a standard turbine.

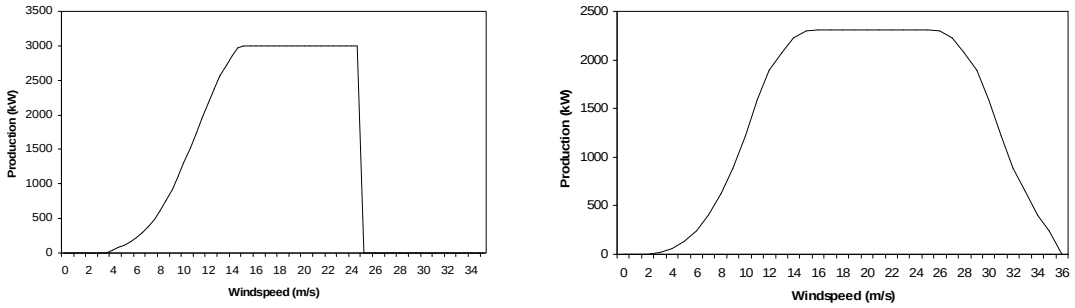

Fig. 3-1 Typical wind turbine power curves

(a) Vestas V90 3MW from Vestas (2004); (b) Enercon-type storm control power curve, adapted from Enercon (2009)

3.2.2 Wind energy production

Calculating the exact energy yield from a wind turbine to be installed at a particular location would require *a priori* knowledge of the wind conditions for its lifetime. This is an impossible task, and so estimates of the likely wind conditions, generally based on a period of past climate data, are used to estimate possible output by

combining them with the information from the proposed turbine power curve. There are a number of methods currently used, some of which are considered more accurate than others but there is a trade-off between accuracy and the difficulty involved in obtaining the information and/or the time required to do so. All methods are predicated on the underlying physics.

3.3 The physics of wind climate

Large-scale atmospheric circulation is driven by pressure gradients, set up by differing heating patterns across the surface of the earth (as described in Chapter 2). The wind climate at a given point on the surface is the result of a combination of these large-scale flows and the effects of the surrounding topography in the region (Troen & Petersen, 1989). Referring to Fig. 2-9 in Chapter 2, the planetary boundary layer is described as the region of the atmosphere within the troposphere between 0 and ~1000m above the Earth's surface. This is the layer which interacts with the surface and activity within the layer can be affected by the surface properties.

In the upper portion of the earth's surface boundary layer (600-1000m), the effects of surface friction on the flow are minimal, and the flow is said to be geostrophic. The geostrophic wind speed represents a balance between the pressure gradient, which pulls the air from an area of high pressure to an area of low pressure, and the turning force of the earth, the Coriolis force, as shown in Fig. 3-2a.
It can be calculated from these quantities by,

$$V_g = \frac{1}{f\rho} \cdot \frac{dp}{dn} \tag{3.6}$$

where V_g is geostrophic wind, f is the Coriolis parameter, ρ is the air density, and $\frac{dp}{dn}$ is the mean sea-level pressure gradient in the direction, n.

In the lower portion of the boundary layer (below approximately 600m), the topography of the surrounding surface influences the flow significantly by introducing a frictional force (Fig. 3-2b). Troen & Petersen (1989) classifies the three terrain characteristics that affect the wind climate as:

- the surface roughness class,
- the presence of obstacles,
- the orography, i.e. terrain height variations.

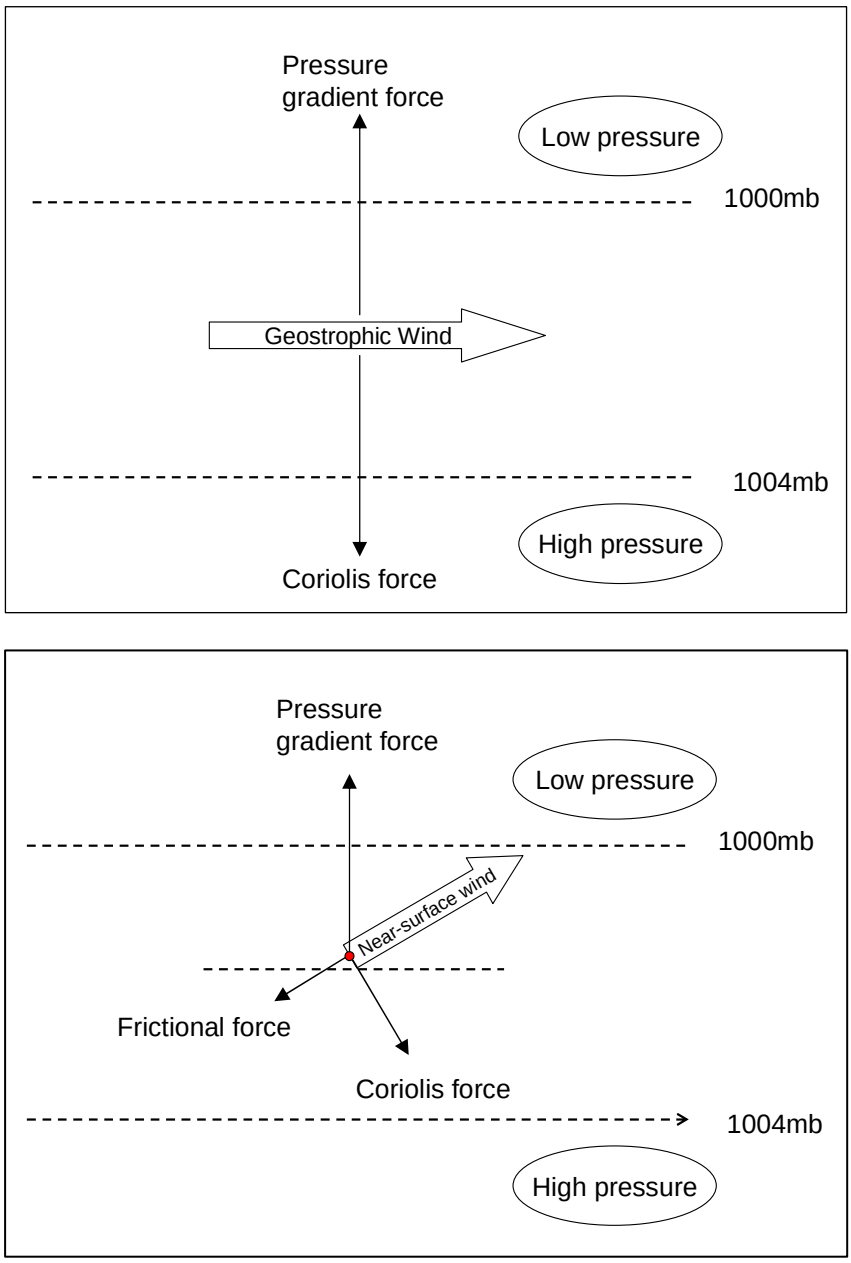

Fig. 3-2 Schematic diagram of wind under geostrophic and near-surface conditions

(a) Geostrophic wind; (b) Near-surface wind

3.3.1 Surface roughness

The roughness length of a surface, z_0, is found from an empirical formula for onshore applications where the surface contains roughness elements such as vegetation or buildings,

$$z_0 = 0.5 \cdot \frac{h \cdot S}{A_H} \tag{3.7}$$

where h is the height of the roughness element, S is the cross-sectional area of the roughness element facing the wind and A_H is the average horizontal area available to each element (Troen & Petersen, 1989). A higher surface roughness implies greater frictional resistance to air flow, caused by having an element with relatively large cross-sectional area in a relatively small horizontal area. For an area over water, the relation,

$$z_0 = b \cdot \frac{u_*^2}{g} \tag{3.8}$$

was obtained by Charnock, where $b \sim 0.014$, g is the gravitational acceleration and u_* is the friction velocity (Troen & Petersen, 1989). Friction over water tends to be lower than over a land-surface area.

Given a neutrally stable atmosphere (see appendix A.2), the wind shear profile, $U(z)$ (i.e. the variation in wind speed with height), is given by the relation,

$$\overline{U}(z) \propto \ln\left(\frac{z}{z_0}\right) \tag{3.9}$$

where z is the height above ground level and z_0 is the surface roughness length (Manwell *et al.*, 2002). It can be seen that as the surface roughness length increases, the parameter on the right hand side becomes smaller, so for a given height above ground level, the wind speed will be lower for terrain with greater surface roughness length.

3.3.2 Obstacles

An obstacle in the path of the wind will reduce the wind speed measured close by, and provide a sheltering effect. The degree of the sheltering effect will be determined by the distance from the obstacle to where the wind speed is being measured, the height at which the measurement is being taken, and the height, length and porosity of the obstacle itself. In addition, there will be an increase in the wind speed directly in front of and above the obstacle (Troen & Petersen, 1989).

3.3.3 Orography

Experimental work has shown that wind speed varies with changes in the surface orography, with winds at the top of a hill experiencing ‘speed-up’. There are also

small decreases in the speed directly in front of and behind the hill, although the experimental work given in Troen & Petersen (1989) has shown these decreases to be smaller relative to the increases at the hill peak. The value for the speed-up, ΔS, at the top of the hill relative to the free stream velocity, is given by,

$$\Delta S \approx 2\frac{h}{L} \tag{3.10}$$

This relates the speed-up to the height of the hill, h, and a characteristic length, L, where L is typically half the width of the hill. The calculation for an 'ideal' hill in an otherwise straightforward plane would therefore be fairly simple, but for complex orographic situations, modelling techniques are required (Troen & Petersen, 1989).

3.4 Data for energy production estimates

Wind climate is monitored throughout the UK by the UK Meteorological Office (UKMO) using a network of surface-based weather stations, data from which are available at the BADC (BADC, 2009c). The traditional cup anemometer is the most common instrument, usually placed on a mast approximately 10m above ground level (a.g.l). Records are often not complete for long time periods (greater than 30 years), especially pre-1970 records. Where there are gaps in an otherwise continuous dataset, it is possible to develop small algorithms, to interpolate the data and 'fill in' the missing data, for example in Boehme (2008). Nearby data can also be used as a proxy to fill in gaps.

From winds recorded at 10m a.g.l, the data must be scaled to the hub height of the proposed turbine in order to calculate energy yields. This can be done using either of two common relations:

1. The power law (Manwell *et al.*, 2002) relates U_H, the wind velocity at the desired height, to U_{10}, the velocity at 10m by

$$U_H = U_{10}\left(\frac{z_H}{z_{10}}\right)^n \tag{3.11}$$

where z_H and z_{10} are the hub and reference heights. The power exponent, n, is often taken to have a value of 1/7, particularly at sites where the local information is not known, but this can also be empirically derived from measurements.

2. The logarithmic wind profile (Manwell *et al.*, 2002) is more often used in situations where there is sufficient information about the site surface roughness characteristics. This states that *U(z)*, the velocity at the required height, *z*, is found by,

$$U(z) = \frac{u^*}{\kappa} \ln\left(\frac{z}{z_0}\right) \qquad (3.12)$$

where u^* is the friction velocity, κ is the von Karman constant with a value of 0.4 and z_0 is the surface roughness.

The UKMO anemometers are not, unfortunately, placed in a regular spacing throughout the country. They are often sited in places like airports, RAF bases, academic institutions and harbours. Obtaining detailed, accurate information on the met stations is also difficult; being so close to the ground the wind records are heavily influenced by the surface roughness around the mast - but this can only be subjectively assessed by a visit, something not always convenient or possible. Knowledge of obstacles which affect the flow is not readily available either, and again must be visually examined by the data user, often by a site visit. Google Earth (Google, 2009), MS Bing (Microsoft, 2009) and similar facilities make this somewhat easier than previously, but perfection is unobtainable - they cannot account for temporal variations in the local flow caused by, for example, the siting of a temporary building or the growth of a group of trees close to the mast.

Gathering of wind data in recent years has become more sophisticated than use of the simple cup anemometer. The UKMO, via the British Atmospheric Data Centre (BADC), provide data gathered from wind profilers, which use a swinging radar beam to create a profile of the wind in its locality throughout the whole boundary layer (BADC, 2009b). The earliest data available from one of these profilers via the BADC is from 1998; there are now data from seven sites but is limited to six years at most, which is unlikely to be sufficient in a long-term climate study. SODAR (Sound Detection And Ranging) and LIDAR (Light Detection And Ranging) devices use sound and light (often laser) wave scattering respectively to detect wind speeds over the boundary layer. They work on similar principles to radar devices but are newer technologies and still present some challenges (IEA, 2007).

Wind speed and direction data can also be calculated from the position over time of radiosondes, which ascend via a helium balloon and take measurements at set pressure levels throughout the atmosphere (BADC, 2009a). Data are available from 1997 to the present but the number of observing stations is relatively low.

3.4.1 Gridded data

Gridded data, that is, where the country has been divided up into a regularly spaced grid, will give an estimated mean wind speed – and possibly direction - for each grid square. The higher the resolution of the grid, the more likely it is that the wind climate in a given grid square will be representative of the climate at a particular location within the square. These kinds of datasets are useful for analysing systems involving the entire country, or a fairly large region within the country, but are not suitable for detailed individual site analyses unless the spatial resolution is very high. They may be employed in early feasibility studies for wind farm developments, or for wind power development companies planning long-term strategies, for example.

For applications where a lower resolution than tens of kilometres is acceptable, perhaps the most useable source of wind climate information comes from 'reanalysis' projects. There are a number of these, but the two most commonly cited in the literature are the NCEP-NCAR reanalysis (Kalnay *et al.*, 1996) and the ERA40 reanalysis from the ECMWF (Uppala *et al.*, 2005). The projects use a numerical weather prediction model with applied boundary conditions based on actual observations. They aim to develop a regular gridded, homogeneous dataset which removes potential errors due to changes in, for example, the calibration of the measuring equipment. The NCEP-NCAR output is available at 2.5˚ resolution, whilst the ERA40 data is on a 1˚ resolution grid.

To support the UK Climate Impacts Programme (UKCIP) project, the UKMO undertook an interpolation of the met station data in order to have regular and up-to-date gridded reference data for climate change impact studies (Perry & Hollis, 2005). The dataset was produced at 5km x 5km resolution and for wind, resulted in monthly mean values for the period 1969 onwards at this resolution for the whole country. Due to the low temporal resolution, using this data for resource assessment would

require assumptions about the wind speed distribution, which may or may not be accurate. Nevertheless, this is an interesting dataset for reference purposes.

Wind data from a mesoscale atmospheric model for the country ought to be ideal, especially since they are run at a relatively high resolution. However, these models rely on the quality of the information supplied and the quality of the physics and dynamics of the model. They thus need to be rigorously tested against good-quality observed data in order to be certain of their validity. Average mean wind speed data is available from one of this type of model, the Numerical Objective Analysis of Boundary Layer (NOABL) - which was run on behalf of the then Department of Trade and Industry (DTI) at 1km resolution, initialised with met station data from 1975-1984 (Burch *et al.*, 1992). The model was tested in 1995 as part of a DTI-funded project investigating different wind climate data analysis methods (Halliday *et al.*, 1995). The testing showed that the NOABL model generally underestimated the mean wind as compared to two other models, and suggested that this may be due to the lower resolution of the NOABL model data relative to that of the comparative models. Boehme (2006; 2008) developed another high resolution dataset for Scotland and found that when this was evaluated against the NOABL dataset, the NOABL results tended to be higher; although it should be emphasised that the dataset in Boehme (2006; 2008) was at a higher resolution than the NOABL data. The UK department of BIS still provides data from the NOABL model as a first-guess estimate for wind power siting, along with relevant warnings about its potential failings (BERR, 2009a). It is perhaps worth noting that there are a number of other atmospheric mesoscale models available but they require extensive levels of expertise and computing power to run, and are potentially very expensive.

3.4.2 Techniques for detailed analysis of potential wind farm sites

When considering siting a wind farm, often the first type of data consulted is time series data from a local weather station - recorded in a database such as the MIDAS dataset from the UKMO, which is available commercially (and is free for purposes of academic research). The data has been recorded (originally manually, but the process is now automated at most stations) at hourly or three-hourly intervals from an anemometer. This information is useful as an indicator of how ‘windy’ locations in

the vicinity are likely to be. However, as we have noted already, wind speeds are strongly influenced by their immediate surroundings, and unless the weather station is in very close proximity to the proposed wind turbine site, it is unlikely to have identical wind conditions. Ultimately, the best indication of the suitability of a local wind climate is obtained by analysis of long-term data from the particular site, but for obvious practical reasons this is usually unavailable.

The 'Measure-Correlate-Predict' (MCP) method of estimating wind conditions at a site uses long-term time series wind data, such as that from MIDAS, in combination with some data collected *in-situ*. Measurements are taken for a short period, at least six months but often a year, at the position of the proposed wind turbine site, and a relationship between this data and the data for the same period from a nearby met station is derived. The year's worth of data for the site then can be extrapolated to a much longer period by applying the long-term met station data. (Burton *et al.*, 2001). Because wind climate does display a large degree of inter-annual variability, this method is preferable to relying on the year's site data alone; but it assumes stationarity - a constant relationship between the wind climate at the two sites - and this cannot ultimately be proven to hold over extended periods. The relationship is subject to uncertainty due to physical changes over time at the site, for example, the growth of trees near to the measuring mast, or due to a change in the wind climate itself, such as the typical directional pattern.

An understanding of the three terrain effects that alter the geostrophic wind near the surface (see above) has allowed the development of a technique for taking near-surface wind measurements at one site and translating this information, by means of subtracting the three influences, to a so-called regional wind climate. This regional wind climate can then be re-applied to obtain near-surface wind climate at another point within the region, by adding back the three influences for the particular locality in question (Petersen *et al.*, 1998a). Known as the Wind Atlas Method, this has been the basis for the development of the Wind Atlas Analysis Software and Application Program (WA^SP); it takes a regional topographical map as input, plus wind speed and direction timeseries at a point within the map, and outputs the likely wind climate parameters at any other point in the map (Mortensen *et al.*, 2009). The

program has been used extensively by wind farm developers and is well-recognised within the wind energy community.

WA^{S}P does not attempt to produce time series data for the new site. Instead, it describes the wind climate in terms of the two-parameter Weibull distribution and a directional histogram, commonly known as a wind rose. It does, however, have the advantage over MCP techniques of being physically based and consistent, rather than relying on statistical connections.

3.5 Connecting wind to the electricity network

The electricity industry in the UK was privatised in the 1990s and the system split into three components: Generation, Transmission and Distribution. There are a large number of generating companies, ranging from those running small renewable devices to those running large nuclear plant. The transmission network is divided into four regional areas and owners: National Grid owns and manages the transmission network for England and Wales; Scottish Power owns the transmission network for the south of Scotland and Scottish and Southern Energy for the north of Scotland, but these are both operated by National Grid; Northern Ireland Electricity operates both the transmission and distribution networks for Northern Ireland as part of an Ireland-wide group. The distribution network in England, Scotland and Wales is split into a number of smaller regions and is owned and managed by eight companies in total.

Wind power typically falls into the category of generation known as ‘distributed’ or ‘embedded’ generation, meaning that due to the relatively low power capacity and likely rural location it is often connected not to the higher voltage transmission network like a conventional power plant, but instead is connected at medium or low voltage to a distribution network (BERR, 2001). (In some cases, it will be connected to the transmission network, particularly for larger wind farms.)

The connection of distributed generation sources (DG) to the distribution network entails various problems. In the simplest terms, the distribution network was created with the assumption that power would flow from the substation to the customer load, with decreasing capacity on the equipment as the line feeds out towards its most remote point. Connection of DG to a point towards the end of this

line, with a fairly high possibility that there will be more generation than demand, will result in a 'reverse' power flow back towards the substation. There is also increased potential for power flows higher than the rated capacity of the equipment. The priority for the distribution network operator (DNO) is to ensure quality of supply for the end users: that is, voltage within certain limits. Altering the power flows by adding distributed generation could result in violations of the statutory limits on the supply voltage; several scenarios for this are shown in Harrison *et al.* (2002). Maintaining power quality so as to minimise the transient variations in voltage experienced by customers is of paramount importance to the DNO. Connection and disconnection of DG can cause temporary current changes, and thus voltage changes, on the network. These problems can generally be addressed by generator design (Jenkins *et al.*, 2000). In the case of wind power, a problem known as 'flicker' can occur due to the phenomenon of 'tower shadow'. This causes a drop in power output as the turbine blade passes the tower and the torque on the rotor reduces temporarily - though it is more common in older wind turbine designs. Other periodic variations can be caused by turbine dynamics as particular vibrations and resonances are reflected in the power output (Burton *et al.*, 2001).

Another issue caused by a high level of DG on the distribution network is the increased current flowing in the case of a fault in the network; the protection equipment may need to be upgraded to withstand these higher currents (Jenkins *et al.*, 2000; Harrison *et al.*, 2002). Protection against this is expected to be provided by the DNO to ensure a secure and reliable supply of electricity for the customer. The provision of such protection is often based on traditional centrally planned schemes, and the potential for many different permutations of power flows and directions may lead to complications in the settings for this protection - with the ultimate possibility of reduced protection for the customer (Harrison *et al.*, 2002).

Solutions to all these problems need to be found before opening up the grid to the connection of more renewable power - most of which is likely to be from distributed generation. There are a number of grid management strategies intended to mitigate infringements of statutory voltage limits (Harrison *et al.*, 2002), and solutions to the power quality variations caused by wind turbines are detailed in Burton *et al.* (2001), including the use of a number of power electronic systems.

Careful choices regarding the location of wind farms and the available grid connections are also required. Researchers have proposed a number of 'intelligent' systems that may assist the DNOs in managing higher penetration of renewable energy sources, including a change in the control systems of generators to maintain local voltage limits when required (Wallace & Kiprakis, 2002). The wind turbine standards as drawn up by the IEC try to address the issue of transient voltage variations by forcing designers to consider power quality in the design stages (Burton *et al.*, 2001).

Much discussion surrounds the increasing amounts of planned offshore wind power and the possible development of wave and tidal power. Availability of connections to the grid on land from large offshore wind farms are sparse and generally expensive. They create a need for updating and expanding the network which, much like the planning issues with wind farms themselves, raise objections on grounds of spoilt aesthetics; there is, for example, the case of the Beauly-Denny upgrade plan which is currently undergoing a public inquiry (SSE, 2009). The 'least-cost solution' favoured by the privatised companies controlling industry obviously tends towards the rejection of the more expensive solutions - such as under-sea cabling - due to their relatively high cost (both in terms of initial investment and of ongoing maintenance costs) when compared with standard overhead cable networks.

Many objectors to high penetration of wind power in the UK cite the obstacle of 'intermittency' and the requirement for large amounts of backup generation for 'when the wind doesn't blow' and demand is peaking. The work of Sinden (2007) showed that whilst the variability of the wind resource is a valid concern when integrating large amounts of wind power into the grid, the probability of there being low or very high wind conditions – in which turbines produce no power – across the whole country is very low. The need for a geographically diverse portfolio of wind power generation is referred to in this work as key to successful operation. Sinden (2007) also showed that the daily and annual patterns of average electricity demand tend to show a positive relationship with the daily and annual patterns of wind variability, for example, peak winter demand coincides with peak winter wind power production.

The issue of wind industry 'capacity factor' is an important one. The measure is defined for conventional generators as the ratio of the amount of energy output to the maximum energy output if the generator was running at its rated capacity over the calculated time period. Generally, conventional thermal plant will be run at rated power whenever possible, but its capacity factor will be most affected by demand and reliability. For wind generators, the capacity factor is influenced most by the wind regime under which it operates. Since turbines only produce their maximum rated power at wind speeds of between about 15m/s and 25m/s, for most sites in the UK – based on the European Wind Atlas mean wind speed values (Troen & Petersen, 1989) – they will, on average, run at lower than rated power for most of the time. A typical average capacity factor for wind turbines in the UK is suggested by Sinden (2007) to be around 30% based on current operational developments.

3.6 Wind power development in the UK

In the UK in 2008, around 5% of the electricity demand was met by renewable power sources (DECC, 2009d). The target of '20% renewables by 2020' mentioned in the previous chapter is largely expected to be met by a combination of on- and offshore wind, biomass and potentially a small amount of wave and tidal, as mentioned in 2.2.3.4. Several issues stand in the way of further development of wind power. Some of these are political issues, such as obtaining planning consent, and some are physical constraints, mainly to do with the ageing electricity network. The most difficult issue in the whole planning process is the sheer amount of time that it takes to get an application from the initial point to being given consent - or otherwise. The British Wind Energy Association (BWEA) (BWEA, 2009a) has been vociferous in seeking to shorten the time scale and simplify the requirements, and is an important source of information on how the industry is progressing. For example, there are currently 274 wind farms in the planning stages, 138 consented, 42 under construction and 218 completed projects (BWEA, 2009b).

As of October 2008, Britain became the country with the highest offshore wind power capacity: 590MW in total (Jha, 2008). For offshore development, apart from the obvious difficulties in siting a large industrial plant in the ocean, one of the most problematic areas is getting a connection to the electricity network. As

mentioned previously, there have been suggestions mooted for large, undersea cables but in a liberalised electricity market, high-cost options like this are often the least favoured even if the long-term gain is great. Cooperation between potential wave and tidal operations and offshore wind is a possibility, where developments in close proximity would share connections, but these are much-talked-about with little in the way of tangible evidence of their happening.

3.7 Wind Sensitivity to Climate Change

Wind as a renewable power source is governed ultimately by the climate which, as mentioned in the previous chapter, is projected by climate scientists to undergo significant change in the coming century. There is a striking caveat to bear in mind when considering renewable energy in the context of climate change. Going back to the very first section of this chapter, it was noted that climate is driven primarily by the inward and outward flux of solar radiation. That there will be climate change relies on the premise that these fluxes will change. From the definition of renewable energy, it is understood that most of the renewable resources are governed by the sun. Consequently, it is likely that in a changing climate, renewable energy resources are themselves vulnerable to change.

Some studies have been carried out into how wind and hydro power may be particularly vulnerable to changes in climate. Harrison *et al.* (2003) found that climate change could have potentially adverse effects on river flows, making hydropower projects financially vulnerable. Results are available in the literature from several studies on wind power using empirical and dynamic downscaling of climate models. None of these involved the UK but, because of geographical proximity, results of studies conducted in the Baltic states could possibly be considered indicative of the kind of expected outcomes in the UK.

Pryor & Barthelmie (2005d) carried out a detailed investigation using RCM simulations to predict wind energy availability over Scandinavia and the Baltic states using RCM output from the Rossby Centre in Sweden. The authors conclude that there is a statistically significant increase indicated by the model in wind energy density between 1961-90 and the 2080s, and also some evidence to suggest that the increases are more substantial in winter. However, “the uncertainty of these

prognoses remains high". The same authors also conducted work using empirical downscaling methods. Pryor *et al.*. (2005b) finds a negative trend in wind speeds across the Baltic States using statistical downscaling of a GCM, with most stations showing a decrease in the 2071-2100 period in energy density; 90^{th} percentile wind speed; and mean wind speed. In comparing the parts of the two studies that concern the same driving GCM, it was found that the RCM predicted wind speeds tend to be lower than those from the empirical downscaling; but in terms of the future predictions they show a general increase in mean wind speeds in contrast to the decrease predicted by the empirical method.

Pryor *et al.*, (2005a) describes the results of an extension of the empirical downscaling method using multiple GCMs. The general findings are that "there is no significant difference between conditions during 2046-2065 and 1961-90 based on the ensemble of the model results" but that the period 2071-2100 shows - consistent with the initial empirical downscaling study - a slight decrease in mean wind speeds, 90^{th} percentile wind speeds and energy density.

Two studies covering the US again give a varying pattern of results. As in the Baltic, using different GCMs seems to result in very different answers. For example, Breslow & Sailor (2002) used the output of two different GCMs for future periods compared to an observational dataset for 1948-1978: the Hadley Centre model suggested insignificant changes in mean wind speed by the 2050s over much of the US, whilst the Canadian model showed a reduction of 10-15% for the same period. The authors speculate that this could result in a reduction of wind power generation of 30-40% by the 2050s. Segal *et al.*. (2001) undertook a study into wind power in the US under future atmospheric conditions with increased CO_2 (corresponding to projected levels for the 2040s) using an RCM driven by the Hadley Centre GCM. Their comparison was based on control simulations using CO_2 levels from the late twentieth Century, representing present climate conditions. From the results of the future predictions, they conclude that over most of the US, wind power would decrease by 0-30% on a seasonal basis under the future scenario, with a few small areas seeing increases of the same magnitude. Annually, the changes were shown to be around +/-10%. It is noted that due to the sensitivity of the results to the particular GCM used to drive the model, the results should be considered 'exploratory'.

The UK Government has shown an intention to invest heavily in wind generation capacity in the next twenty to fifty years, and it would seem highly likely that there will be a much higher percentage of the country's electricity generated by wind power in the future. Given these two facts, it would seem prudent to investigate any potential impacts that climate change may have on the wind climate in the UK, and if so, how serious these impacts might be.

Ultimately, it requires the analysis of climate model data to understand exactly what changes may occur and calculate their bearing on the wind industry, but a sensitivity analysis should also provide some insight into the magnitude of changes required to make a significant difference to the scope of wind development. It will also provide an understanding as to what parameters within an analysis of wind climate are particularly sensitive to levels of accuracy in their calculation. Since the use of climate model data is likely to introduce uncertainties, it may be helpful to know the bounds beyond which the uncertainties become more significant than those imposed by other factors in the analysis.

3.8 Wind power economics

Unravelling the complexities of the UK wind industry from an economic point of view is not easy. What would seem like a simple cost-benefit analysis becomes more convoluted when the context of the entire electricity generation and distribution system is considered, and when different environmental perspectives are adopted. Manwell *et al.* (2002) explains the economics of wind energy in the diagram in Fig. 3-3. Obviously, the costs on the left must be less than the market value of the energy sold in order that the industry should make a profit. The way in which the economic evaluation to determine the overall profitability is carried out is open to many variations. A simple payback analysis may give an indication of feasibility, but the level of detail can be increased up to a full life-cycle costing analysis.

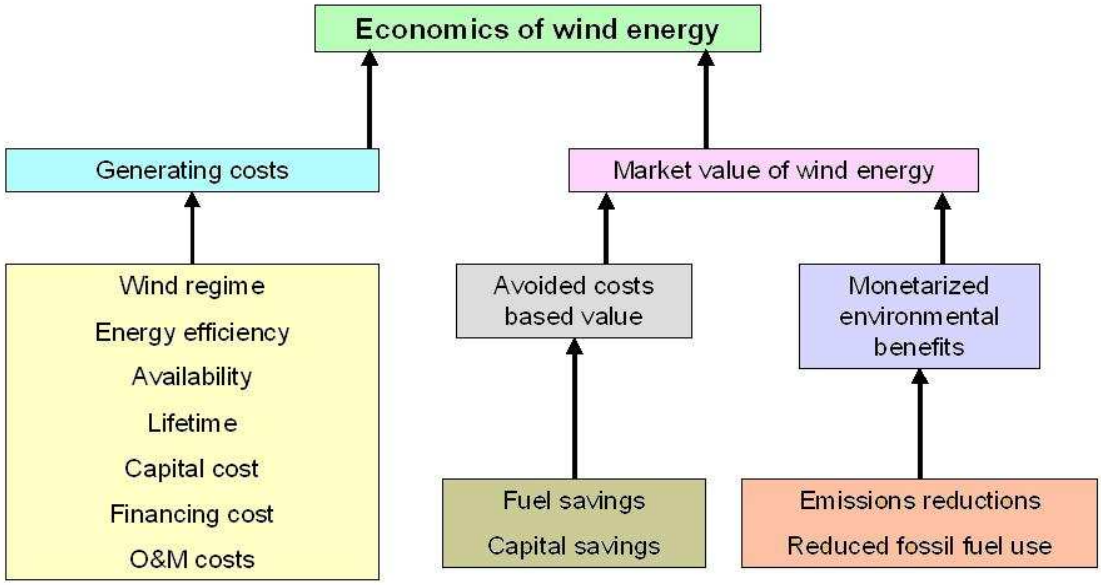

Fig. 3-3 The economics of wind energy

(Adapted from Manwell *et al.*, 2002)

Considering the cost dependencies listed in Fig. 3-3, the once-off capital costs for feasibility studies, site assessments, construction, machinery and so forth is probably the largest single outlay within a project. The capital cost of wind turbines has been falling in the last decade and this is predicted to continue, with 2020 costs likely to be between 55% and 70% of current cost for onshore developments (Strbac *et al.*, 2007). The financing costs depend on how the capital is being raised by the developer, whether through bank loans, current equity or from investors, and how much interest and loan fees will be charged over the lifetime of the development. These costs are very project-specific; large power companies would plainly have very different financing costs for a development than a community-owned project.

Operations and maintenance (O&M) costs tend to be expressed as a percentage of the original turbine cost, often 1.5-3% (Manwell *et al.*, 2002). For a turbine cost of £750 per kW, this would suggest a figure between £11/kW/yr and £23/kW/yr. This is in reasonable agreement with Strbac *et al.* (2007), which finds the O&M costs per kW per year as varying from £10/kW/yr to £20/kW/yr for onshore wind farms. The costs of O&M for offshore wind turbines is significantly more, thought to be £20 to £25/kW/yr (Strbac *et al.*, 2007), mainly due to the extra

difficulty in accessing the machines. The availability of a turbine represents the percentage of time that the turbine is 'available' to produce power. Planned downtime for O&M reduces availability, but there is a balance to be struck in keeping planned downtime at a sufficient level so as to avoid failures that cause unplanned downtime - which may involve a larger availability hit in the long term. The BWEA (2007) suggests that 98% is a reasonable figure for modern wind turbine availability.

The wind regime of the project site is clearly paramount as regards economic viability, as is choosing an effective turbine. At a site with a lower mean wind speed, the capacity factor of the wind turbine would tend to be lower than average, reducing the revenue generated by the turbine. It is economically beneficial for a country such as the UK to employ two particular strategies regarding geographic siting of wind power generation: firstly, to ensure geographic diversity within the system and thus increase the possibility of having good wind conditions in at least some of the sites; secondly, to locate wind farms at sites with the highest average wind speeds (Sinden, 2007).

Looking at the benefits stream in the diagram in Fig. 3.3, there are two influencing factors offered for establishing the market value of wind energy. The first of these, the value placed on the avoided costs, relates to how building wind plant can displace the need for conventional plant. Because the 'fuel' for wind energy is free, this can be seen as an avoided cost. However, the non-dispatchable nature of wind power means that its value to the grid is seen as a certain fraction of its rated power. Manwell *et al.* (2002) defines the term 'capacity value' (referred to in Strbac *et al.* (2007) as 'capacity credit') as the

> …amount of conventional capacity which must be installed to maintain the ability of the power system to meet the consumers' demand if the wind power installation is deleted.

Whilst introducing a wind turbine into the electricity supply system can displace an amount of *energy* that would otherwise be produced by a conventional thermal plant, it is not considered to displace its equivalent amount of rated capacity. The variability of the wind speeds, and the relative difficulty in forecasting these, means that a given power output at a particular time is not guaranteed, and so only a fraction of the installed capacity is counted as capacity credit. This, in effect, means that for each wind power installation, only a certain percentage of the capacity can be counted

towards meeting power requirements at peak demand - assuming there is no storage or demand management system.

The electricity system as it was pre-liberalisation, operated on the basis that there ought to be enough capacity to provide an extra 24% above the peak power demand, assuming that the generators had an availability of 85% and that there may be an increase in the predicted demand peak (Strbac *et al.*, 2007). This system of 'plant margin', designed with the vast majority of generation coming from conventional thermal plant, meant that there was a low probability of a power cut to consumers, hence a 'secure' supply. Maintaining this security was deemed an essential price to pay to avoid the detrimental costs of supply interruptions. Since privatisation, market forces rather than strict regulation are meant to ensure this security, but it is still considered to be important when investigating the integration of large amounts of renewable energy into the power system (Strbac *et al.*, 2007).

There are a number of methods for obtaining the 'capacity credit' for a wind farm, the standard being based on the Loss of Load Probability (LOLP) index - which is used to establish the probability of a power deficit (Jenkins *et al.*, 2000). The level of acceptable probability is generally regarded as 9% at peak demand for the Great Britain transmission system. Calculating a more realistic capacity value or credit for wind generation – and other variable power sources, is being considered but is somewhat difficult, given the need to comprehend co-incidence between the wind resource and peak demand levels.

The second contribution to the market value of wind energy comes in the form of its role in preventing emissions from fossil fuel generation. This environmental benefit is given a monetary value by many governments keen to encourage investment - for example, the Renewables Obligation Certificates (ROCs) in the UK, described in section 2.2.3.4. An alternative system used, for example, in Germany is the 'feed-in tariff'. This pays a guaranteed price for electricity generated from renewable sources, set at higher rates than the cost of generation. It reduces the investment risk involved in renewables by providing price certainty, and encourages growth in the sector, especially at micro-generation-scale, as the contracts are generally fixed for long-term periods. Stern (2006) mentions in his climate change

report that the feed-in tariff system is potentially more successful than tradable quota systems such as ROCs due to its mitigation of long-term price risks.

3.8.1 Financing Wind Development

Wind projects in the UK are mostly funded by private enterprise, often in the shape of large power companies. They gain an advantage in an unfavourable market by the use of ROCs. Many of the large power companies operating in the country since liberalisation have invested heavily in wind, presumably profitably. How much of the revenue can be attributed to the ROC system is unclear. Given the liberalised market situation and the commercial sensitivity of the information involved, it is impossible to obtain any information on the finances of an individual wind power project, particularly with regard to the margins required for feasibility.

The output of financial analyses are quantities such as 'net present value' (NPV) or 'internal rate of return' (IRR) which help to assess the level of risk associated with investment in a particular project. Companies will have pre-determined acceptable levels of risk and corresponding NPV or IRR levels below which they will not be prepared to go in proceeding with a project. Generally, if the IRR is greater than the discount rate (effectively the cost of borrowing) this infers that the rate of return on the project is greater than the opportunity cost of capital, and thus is a sound investment - although caution is obviously advisable. Moreover, the NPV must be greater than zero to ensure that the return on the investment is positive.

A tool developed by Natural Resources Canada called 'RETScreen'[1] (2009) enables a financial analysis to be carried out on a theoretical project so as to give an indication of its likely profitability. The RETScreen software also allows the analysis of various sensitivities in the project, that is, considering the impact of variations in inputs on an output parameter, such as the NPV.

3.8.2 Methodology

An analysis was carried out using the RETScreen software in respect of two particular cases: the first was a 'low' wind site in Wittering, Cambridgeshire, with a mean wind speed of 5m/s; the second was a 'high' wind site on the Scottish island of

[1] RETSCREEN is a registered trademark of Natural Resources Canada, © 1997-2009

Lewis, with a mean wind speed of 8m/s. For the base case in each instance, a Rayleigh distribution and a wind shear exponent of 1/7 was assumed as in eqn. 3.11. The projects each involved ten standard Vestas V90 3MW wind turbines, the assumed power curve being that embedded in the RETScreen software. (*This is slightly different to that developed in Harrison *et al.* (2008)). Assuming 98% availability of the turbines and 10% miscellaneous losses, the low wind site has a capacity factor of 24.5%; the high wind site has a capacity factor of 50.3%. An identical set of standard assumptions were chosen for the project cost variables:

- Feasibility costs £20,000
- Turbine cost £750 per kW
- Engineering and development works £550,000
- Road construction, transmission lines and substation £650,000
- Miscellaneous costs £35,000
- Contingencies of 10%, totalling £2,375,500
- Interest paid during construction £1,306,525
- Annual O&M costs of £20/kW plus 10%, £660,000
- Electricity export cost (i.e. sales price), £50/MWh with an escalation rate of 5% per annum – includes revenue from ROCs
- Inflation rate 4%, discount rate 10%, project life 20 years
- Debt ratio 60% @ 10% interest over 20 years

The first part of the analysis was to find how the energy output of each development would change with variation in assumptions about the wind climate. A ±10% and ±20% change in the mean wind speed was applied, with the distribution shape parameter and wind shear exponent held constant and the change in annual energy output recorded. The distribution shape parameter was then changed to 1.8 and 2.2 with the mean wind speed constant and the energy output recorded. Finally, the wind shear exponent was varied to 1/6 and 1/8 with the distribution shape parameter and the mean wind speed constant, again recording the energy output.

In the second part of the investigation, the sensitivity of the project NPV was analysed in relation to variation in mean wind speed. Again, the mean wind speed was varied by ±10% and ±20% and the new project NPV and the new cost of energy production recorded in each case.

Finally, the project was analysed for its sensitivity to variations in wind speed when compared to sensitivity in other project parameters: capital cost, O&M cost and the electricity export price. This is similar to the analysis carried out in Harrison & Wallace (2005).

3.8.3 Results

Fig. 3-4a indicates the impact of variation in energy output with variation in mean wind speed. It shows that the low wind site experiences approximately twice the percentage energy change for a given percentage change in wind speed. The high wind site is less sensitive, showing about the same percentage change in energy output for a given percentage change in wind speed. Intuition would suggest that given the combination of a Rayleigh distribution and a typical wind turbine power curve, the gradient of the relationship would be steeper at lower wind speeds, and gradually decrease as the wind speed increases. It would be expected that given the cut-out of the power curve above 25m/s, the increase in energy output would begin to tail off with increasing mean wind speed to a point where it starts to decrease. It is highly unlikely, however, that any wind site in the UK would undergo these kind of conditions. It should be noted that the simple model used in this analysis does not include any adjustments for the fact that when a turbine shuts down as the speed exceeds 25m/s, it does not restart until the speed decreases to below 22m/s. This would incur only a very small loss in energy output and is included in the general 10% losses calculated in the energy tool part of the model.

Comparing the change in energy output caused by a difference in mean wind speed with that which is incurred by assuming an incorrect wind shear exponent (Fig. 3-4c) or distribution shape parameter (Fig. 3-4b) shows that a 10% wind speed variation has a much larger impact. The Rayleigh distribution is often used to describe a wind speed probability distribution in cases where time series is unavailable, i.e., the shape parameter of the Weibull distribution cannot be independently calculated and is thus assumed to be equal to 2. Most wind sites will have a shape parameter between 1 and 3 (Natural Resources Canada, 2005), and a common variation for the UK is between 1.8 and 2.2. The Rayleigh assumption in

these situations is not hugely detrimental, giving only a ~3% variation in energy output in the high wind case, and less in the low wind case.

(a)

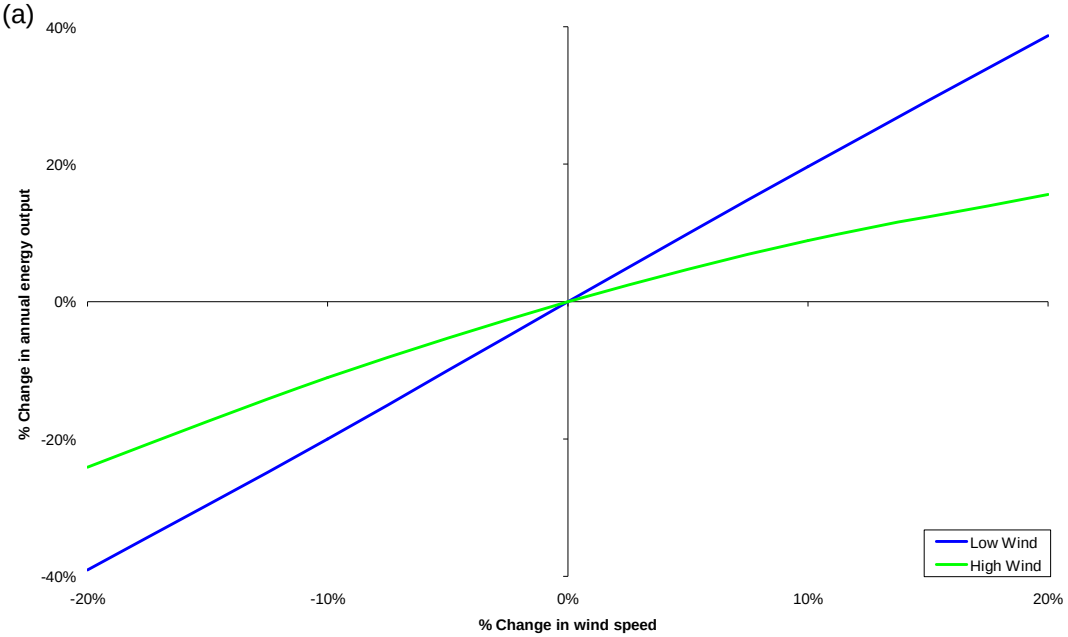

(b)

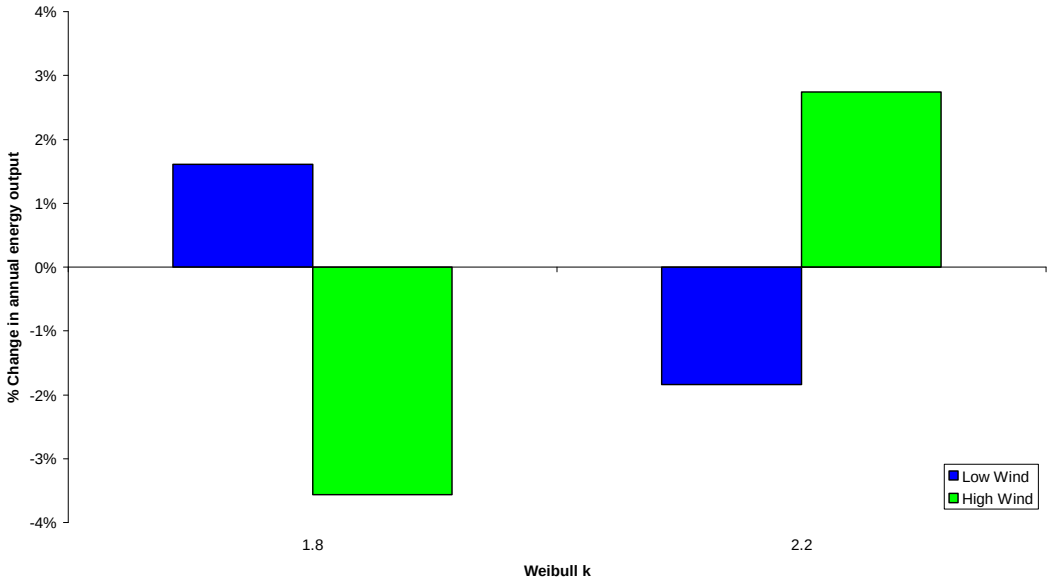

Fig. 3-4 Results of RETScreen analysis

Change in energy output with (a) mean wind speed; (b) Weibull k parameter

(c)

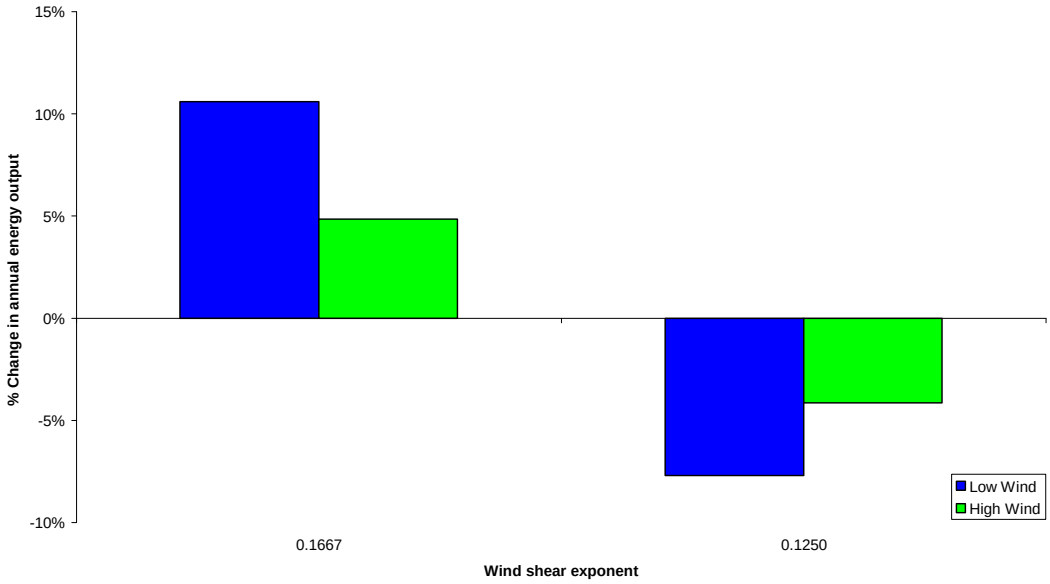

(d)

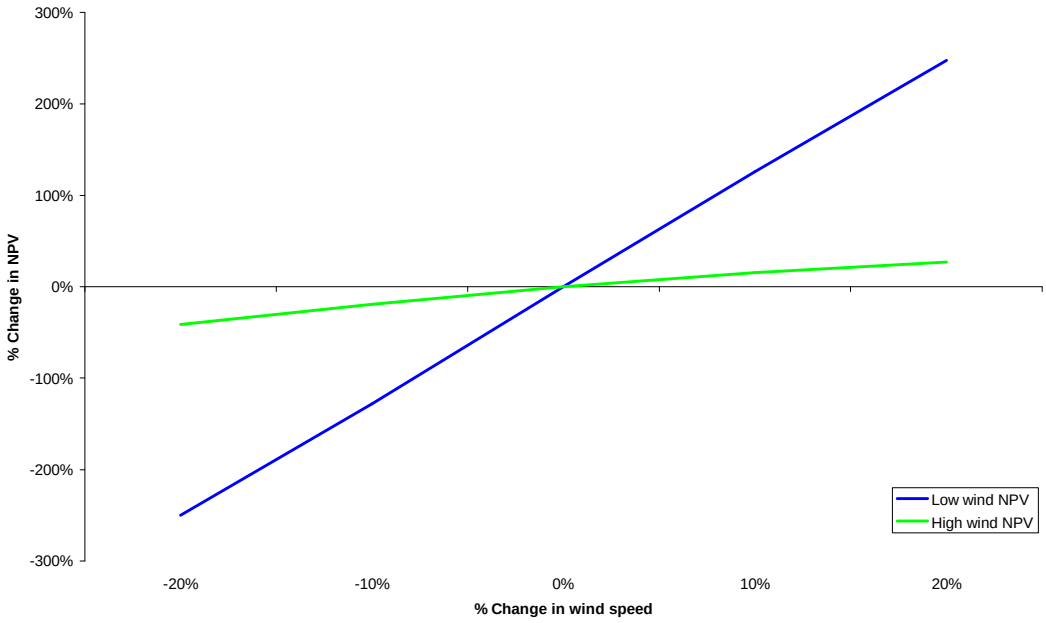

Fig. 3-4 cont. Results of RETScreen analysis

(c) Change in energy output with wind shear exponent; (d) Change in NPV with mean wind speed

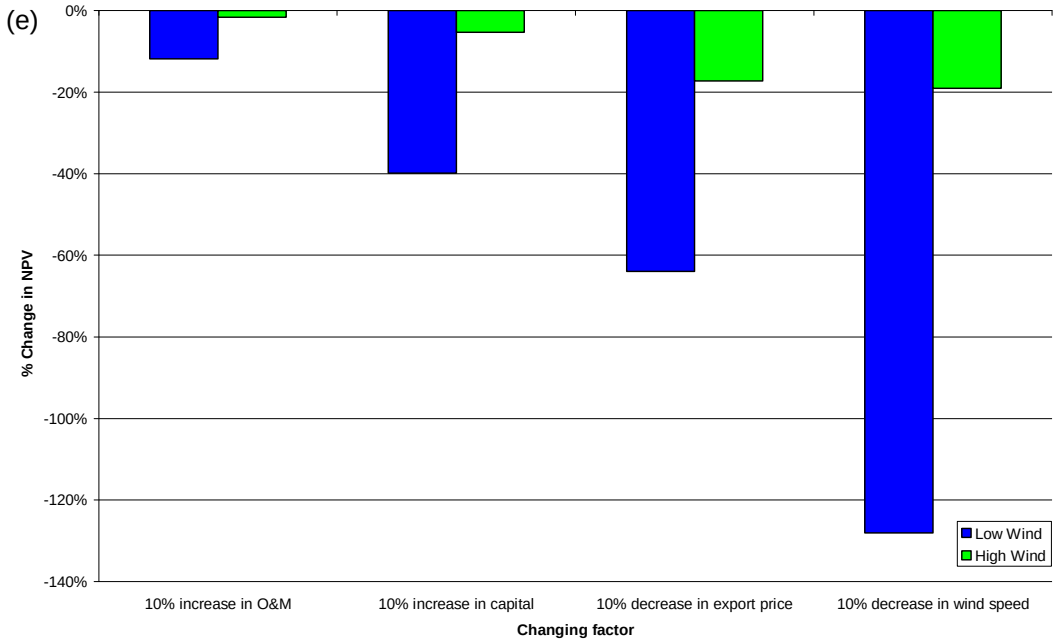

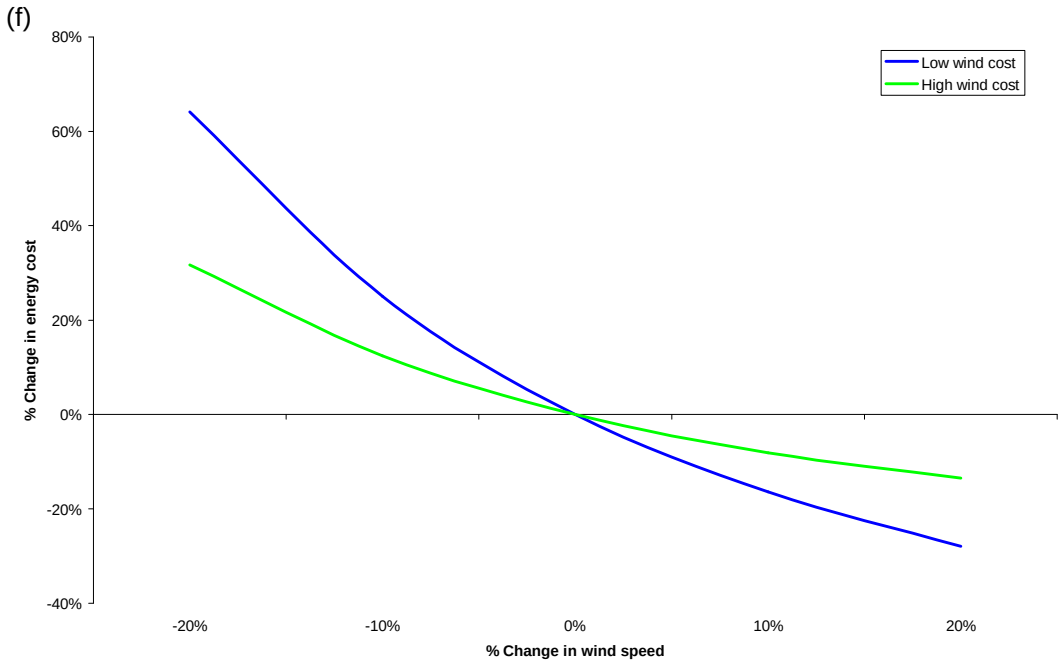

Fig. 3-4 cont. Results of RETScreen analysis

(e) Change in NPV with a10% change in other project parameters; (f) Change in energy cost with mean wind speed

The wind shear exponent is used in eqn. 3.11 to transpose a surface wind measurement to the height of the proposed wind turbine. The assumption of a 1/7 wind shear exponent is generally accepted in a situation where no information about

the site roughness is available (Manwell *et al.*, 2002). Changing this parameter from 1/7 to 1/6 creates a 10% increase in energy output from the low wind project, and decreasing it to 1/8 decreases the energy output by 8%. It is clearly important when carrying out an analysis such as this, therefore, to understand the terrain around which the measurements of surface wind have been taken and the particular wind shear exponent that applies.

Taking the ±10% and ±20% changes in wind speeds and their corresponding changes in energy output, calculations of how the NPV of a project would change under these circumstances were carried out; results are illustrated in Fig.3-4d. A negative NPV means that the project will cost the developers money rather than generating it: the bigger the NPV, the more profitable the investment. In the case of the low wind site, the project's feasibility is clearly highly sensitive to the wind speed. Indeed, looking at the actual values rather than the percentage changes, the NPV becomes negative in this case with a 10% drop in mean wind speed. The high wind case does not become negative, even with a 20% drop in mean wind speed; but it is clear that it suffers a profit drop. Looking at the cost of generating energy in Fig.3-4f, the non-linear relationship indicates that a drop in wind speed produces a greater increase in the cost of generation than the decrease in cost for a corresponding increase in wind speed. Again, the low wind site is more sensitive to both increases and decreases in wind speed.

The final part of the analysis, shown in Fig.3-4e, relates the change in NPV caused by wind speed variation to changes in NPV caused by similar percentage changes in other project parameters – capital cost, O&M cost and the electricity export price. As per the other parts of the analysis, the low wind site is more sensitive to changes in any of the parameters than the high wind site. The parameter which least affects the NPV is the O&M costs since they represent such a small part of the overall budget. The high wind site is relatively insensitive to changes in capital costs, whereas the low wind site, operating on a much lower profit margin, is much more sensitive, with a 10% increase in the capital cost reducing the NPV by 40% - although it still remains positive. Reductions in the electricity export price or wind speed of 10% both produce changes in NPV of just under 20% in the high wind case, so are similarly important. In the low wind case, a 10% drop in export price gives an

NPV reduction of 60%, whilst a 10% wind speed drop gives an NPV reduction of nearly 130% - in this case, rendering the NPV negative and the project no longer viable. Wind speed is thus the most important factor in both cases, but only marginally more than the export price in the high wind case.

3.8.4 Conclusion

From the above analysis, whilst it is clear that wind climate parameters such as wind shear exponent and choice of probability distribution are important and do contribute to the overall calculated energy output of a proposed development, mean wind speed is the most important factor to be considered.

In terms of financial considerations, when considering the viability of a project, it is again clear that variations in cost of capital and O&M costs are relatively unimportant as compared to the electricity export price and the site mean wind speed. In the case of the UK, a significant proportion of variation in electricity export price from a renewable energy source comes from ROCs. However, this is something that can be controlled if necessary, by government and government-enforced independent regulation. The climate is not amenable to control, certainly at a site level; nor is it easy to predict. As discussed here, it is thus self-evidently sensible to avail of the best techniques available to analyse its trends and project how it may alter in future.

Chapter 4

Analysis of surface winds from climate models

Projected changes in various climate variables under increasing greenhouse gas levels can be obtained from general circulation models (GCMs) and regional climate models. As described in Chapter 2, these model atmospheric physics and dynamics and combine many levels of expertise to produce estimates of future climates under various scenarios. The skill of climate models is generally measured as the ability to hindcast for an historical period for which there is a comprehensive set of observations to compare. Different climate variables are modelled by GCMs and RCMs with varying degrees of success, with surface wind among the more difficult parameters to reproduce dependably. In this chapter, surface wind climate results from one GCM and one RCM project are analysed, firstly to understand the shortcomings in their hindcasting ability, and secondly to assess their projections for future wind conditions. Their outcomes are discussed in the context of potential changes in wind energy production.

4.1 General circulation models and wind

GCMs are considered to be most successful at modelling climate on relatively large temporal and spatial scales, as validated with observed data for an historical period (Pryor et al, 2005c). McGuffie & Henderson-Sellers (1998) suggests that the boundary layer in general is not able to be fully modelled by GCMs due to the scale of the processes within the layer being smaller than the resolution of the model grid in both horizontal and vertical directions. Small scale processes still have an important bearing on climate, however, and methods must be built into the model to account for their effects and interactions with larger-scale processes (Beniston, 1998). Because of the limitations on resolution, GCMs use parameterisations to describe and relate the sub-grid scale processes and events, i.e. described in terms of other parameters, usually in a more simplistic way than would result from a full physical-dynamical representation (AMS, 2009). The quality of the parameterisations within the model is key to the output being realistic, but even so,

inputs to the parameterisation scheme are averaged typically over 2 to 3˚ latitude and longitude, which results in a similarly highly averaged output.

In the case of wind, the variability of surface wind climate tends to be well below the spatial grid scales of most GCMs. Surface wind parameterisations usually involve factors such as surface roughness and orography, which vary at scales of metres, rather than typical GCM grid cell size. Surface wind parameterisations using these kinds of parameters will generalise the wind climate for a grid cell so much that it may not necessarily reflect the wind conditions at any point within it. This is not necessarily very helpful for resource analysis, which is often dependent on localised wind information or regional variations. Despite this limitation, it is interesting to compare the output of a GCM with some higher resolution historical observations in order to understand the inherent problems, and identify whether or not their broad trend over the UK is accurate enough to allow the drawing of conclusions from their future projections.

A number of other studies have considered the direct use of GCM wind results for other parts of the world, with varying degrees of success. Pryor et al (2005c) found that the UKMO HadCM3 model showed good spatial correspondence with the NCEP-NCAR and ERA40 reanalyses but generally underestimated the wind speeds over Scandinavia and the Baltic States - possibly due to its low resolution or "*weakness in simulation of pressure gradients*", referring to the predominant driving factor for wind climate. In terms of projections of future wind climates, the authors use the method of wind indices, whereby the wind speeds are normalised by a long-term mean to eliminate the effects of any systematic bias. Despite this, the authors remain cautious about placing any confidence in the GCM output. Their analysis suggested a slight decrease in the annual wind index in the south west of the Baltic and an increase in the north east.

A study using the output of two GCMs for North America (Breslow & Sailor, 2002) found that both the Canadian Climate Center (CCC) and UK Met Office (UKMO) HadCM2 models showed some deficiencies in representing the historical seasonal means averaged over the whole region. This was assumed to be due to poor representation of local topography in the GCMs. Rather than look at the actual future projected wind fields generated by the GCMs, the authors chose to extract

information about the future anomalies versus the baseline climate and apply them to a high resolution observed dataset - known as a 'change factor' technique (IPCC, 2004), as discussed in 2.1.8.3. They used an interpolation method to map the baseline and future fields to a higher resolution grid, and then calculated the future anomalies on this grid. A dataset containing observed 10m wind data, also on this higher resolution grid, was substituted as the baseline climate and the anomalies applied to it. Their results for the HadCM2 model indicated very little in the way of significant change during the twenty-first century over the whole region. For the CCC model, however, results varied by region and season; but the broad trend was towards a decrease in wind speeds. The authors noted that the two models were more similar in their projections for the early part of the twenty-first century than they were for 2100. This highlights the potential differences in climate models depending on, among other things, boundary conditions, parameterisations and their representations of large-scale climate patterns, which tend to cause divergence in the model results over long time periods.

4.2 Comparing GCM hindcast and reanalysis data

4.2.1 Data

In this section, 10m wind data from a GCM are analysed against data from the ERA40 reanalysis developed by the European Centre for Medium-range Weather Forecasting (ECMWF) (Kalnay et al, 2005). Reanalysis projects, such as ERA40, use a numerical weather prediction (NWP) model to derive historical climatologies, with observations applied as initial boundary conditions and during the model run as a feedback system. This helps to remove any bias in the observed data due, for example, to changes in measurement techniques. The output is a coherent and homogeneous dataset on a regular grid. ERA40 10m wind climate data are available from the British Atmospheric Data Centre (BADC) on a 1˚ latitude x 1˚ longitude resolution (Fig. 4-1b) from 1958-2002 in 6-hourly time series (European Centre for Medium-range Weather Forecasting, 2006).

The GCM chosen was the ECHAM5 model (Roeckner, 2005) from the Max Planck Institute (MPI), which has a relatively high resolution at 1.865˚ latitude x 1.875˚ longitude (Fig. 4-1a). The data from this model will be referred to as ECH5

hereafter. The data are available at daily time steps from the World Climate Research Program's (WCRP's) Coupled Model Inter-comparison Project phase 3 (CMIP3) multi-model dataset via the IPCC data distribution centre (IPCC Data Distribution Centre, 2005a). Increasing interest in climate modelling, alongside the development of computer power over the last number of years, has led the modelling community to the point where it is now considered best practice to carry out several 'runs' of each climate model under slightly different conditions and group the outputs together in what is known as an ensemble (AMS, 2009). The IPCC make the results of each run of the climate model available for research purposes. For the ECH5 model, two runs are available at daily temporal resolution and two at monthly resolution; the analysis here is limited to the two daily runs.

A section of 10m wind data from the 1961-90 period has been obtained from a twentieth Century simulation of the ECH5 GCM for an area approximately covering the latitudes 49˚ to 61˚ north, and longitudes -12˚ to 2˚ east. 10m wind data from the ERA40 reanalysis project for the same period over a similar area on a 1˚ square grid has been interpolated by cubic splines (via a standard Matlab function) to the lower resolution ECH5 grid. Because the GCM is not expected to faithfully reproduce timeseries, but rather will output such that the distribution of the values represents the average wind climate (Pryor *et al*, 2005b), the daily values for each month were collected together and the monthly means, standard deviations and Weibull parameters compared for the entire 30-year period.

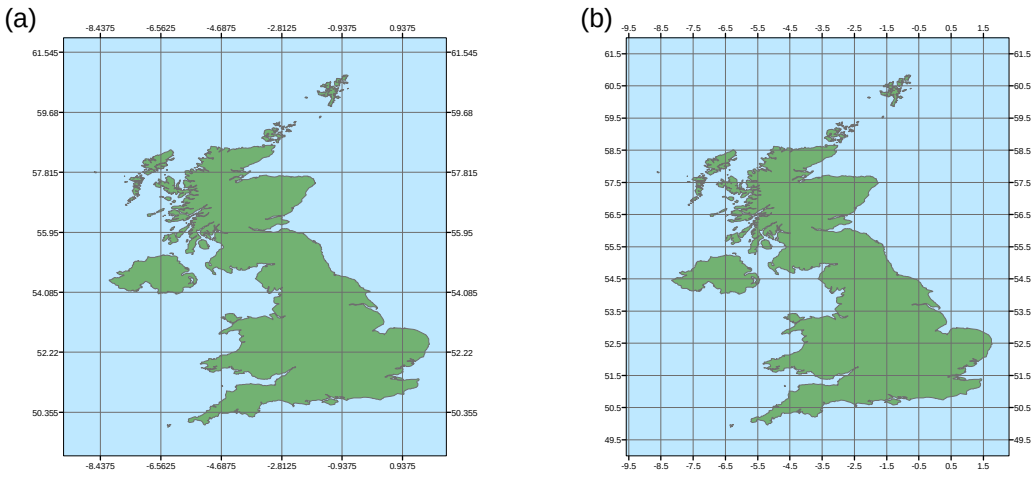

Fig. 4-1 Representation of the model grid sizes

(a) ECH5; (b) ERA40

4.2.2 Spatial average monthly means

Fig. 4-2 shows that in terms of the overall mean for the area, the general seasonal trend of minimum values in summer months and maximum values in winter months is well captured by the ECH5 GCM. The ERA40 mean wind speed for the region peaks at 8.03m/s in the month of December, with January having a very similar result of 8.02m/s. Run 1 of ECH5 also has a maximum value in December of 9.03m/s with January dropping slightly to 8.71m/s. Run 4 of ECH5 has a value of 8.60m/s in December but reaches its maximum value of 8.66m/s in January. ERA40 gives a minima of 5.22m/s in the month of July, and has a very similar value of 5.23m/s in June. Both runs of the GCM, reach a low in June, with values of 5.86m/s for Run 1 and 5.81m/s for Run 4.

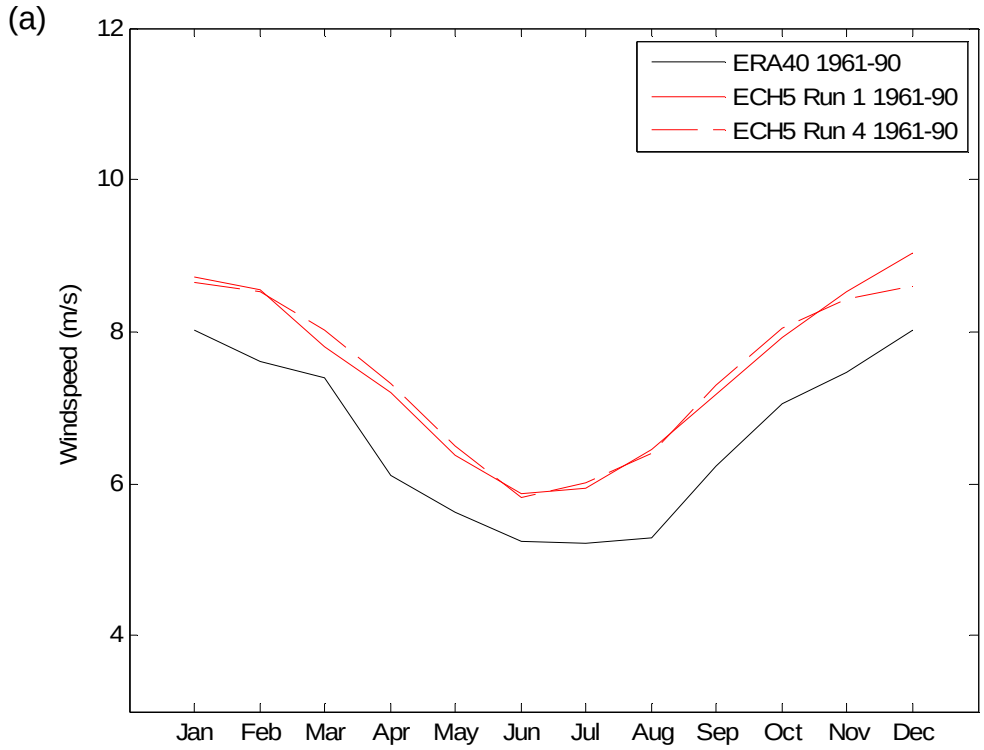

Fig. 4-2 Spatial average monthly means and boxplots

(a) ERA40 and ECH5 Run 1 and 4 monthly means

(b)

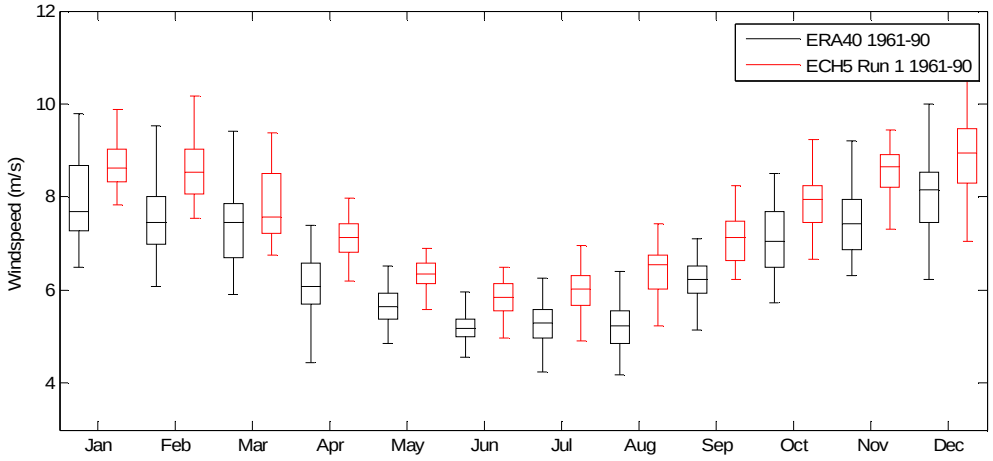

(c)

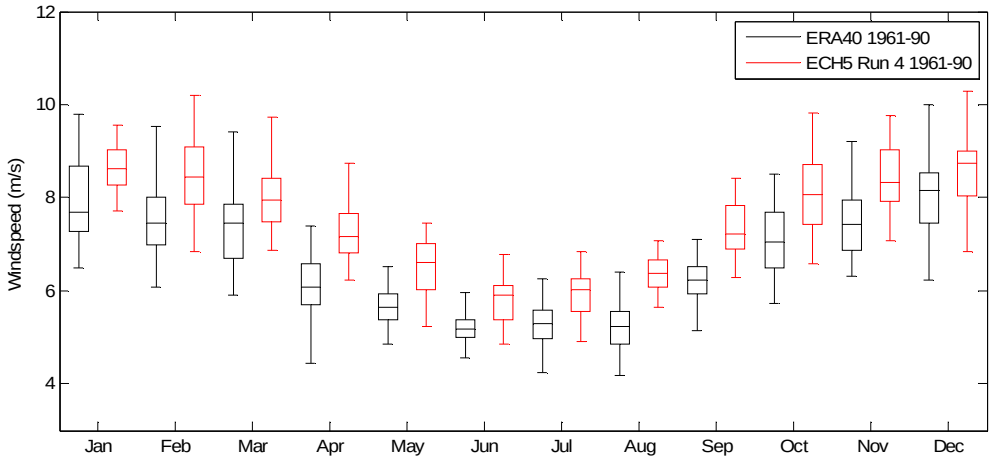

Fig. 4-2 cont. Spatial average monthly means and boxplots

(b) ERA40 and ECH5 Run 1 1961-90 boxplot; (c) ERA40 and ECH5 Run 4 1961-90 boxplot

The boxplots drawn in Fig. 4-2b and c give some indication of the interannual variability within the months for each of the datasets. The 75th and 25th quartile values mark the top and bottom boundaries of the box, and the median value is drawn as a line within the box. The "whiskers" extend to the highest and lowest values (up to a limit of 1.5 times the interquartile range). The interannual variability for individual months appears to vary quite substantially both between the two runs of ECH5 themselves, and between these results and the reanalysis data as can be seen in the boxplots. The variability of the monthly means is highest for the reanalysis data in the winter period, from December to March, particularly January and

February where the standard deviation peaks at around 1 m/s. The minimum standard deviation for ERA40 is 0.35 m/s in June. Run 1 of the GCM captures the June minimum and shows greater variability than the reanalysis in December, but has a much lower range in January and February, with a standard deviation of 0.6 m/s. Run 4 does not show a distinctly smaller range of variability in the summer months but does have its greatest range in a winter month, February, with a standard deviation of 0.86 m/s.

Fig. 4-3 shows the mean percentage differences between the ECH5 output and ERA40 data for each month for the two GCM runs. In both Run 1 and Run 4 there is a clear and consistent tendency to overestimate the mean wind speed in all months compared to the reanalysis data by between 5 and 25%. April and August are the months of maximum overestimation with percentage differences versus ERA40 of between 17 and 22%. The winter months of December to March show the lowest percentage differences, ranging from around 7 to 13%.

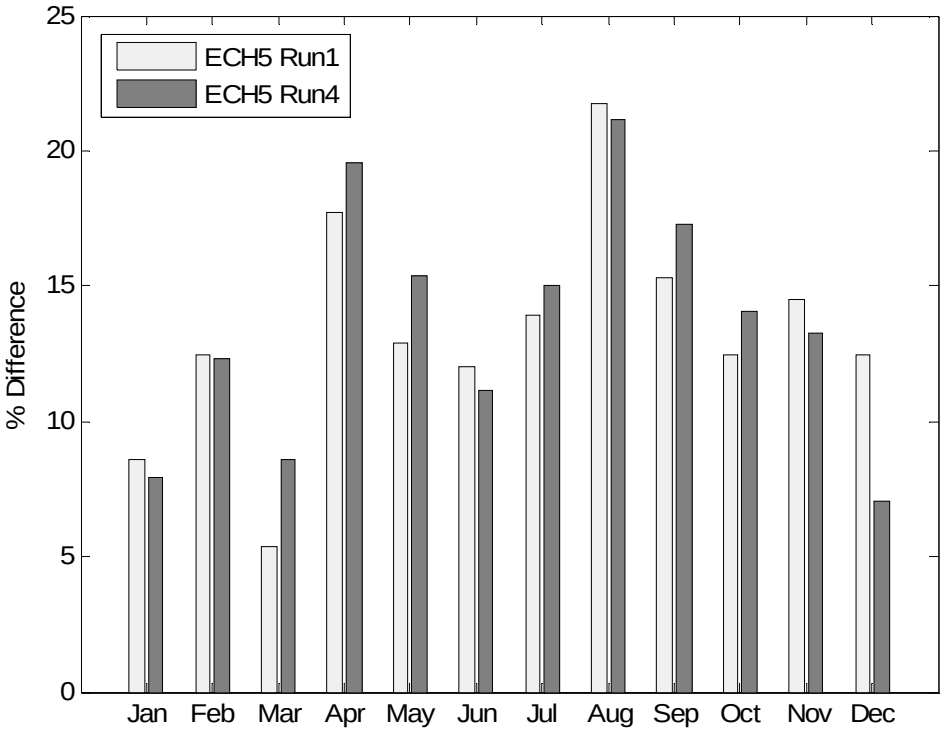

Fig. 4-3 Monthly mean percentage differences vs. ERA40 for ECH5 runs 1 and 4

4.2.3 Annual mean field

The spatial variance in the annual mean fields in each of the datasets is shown in Fig. 4-4. Even when mapped to a lower resolution grid, a contour diagram of the ERA40 data gives a better representation of the coastal effects on the wind speed pattern. Both the ECH5 fields are very similar in pattern and in mean values but the complex coastline of the British Isles is not ideally represented in the model and so Ireland is not captured as a separate body of land; similarly, the complexities of northern England and Scotland are not clearly characterised. The ECH5 values are, as seen above, slightly higher than the ERA40 values.

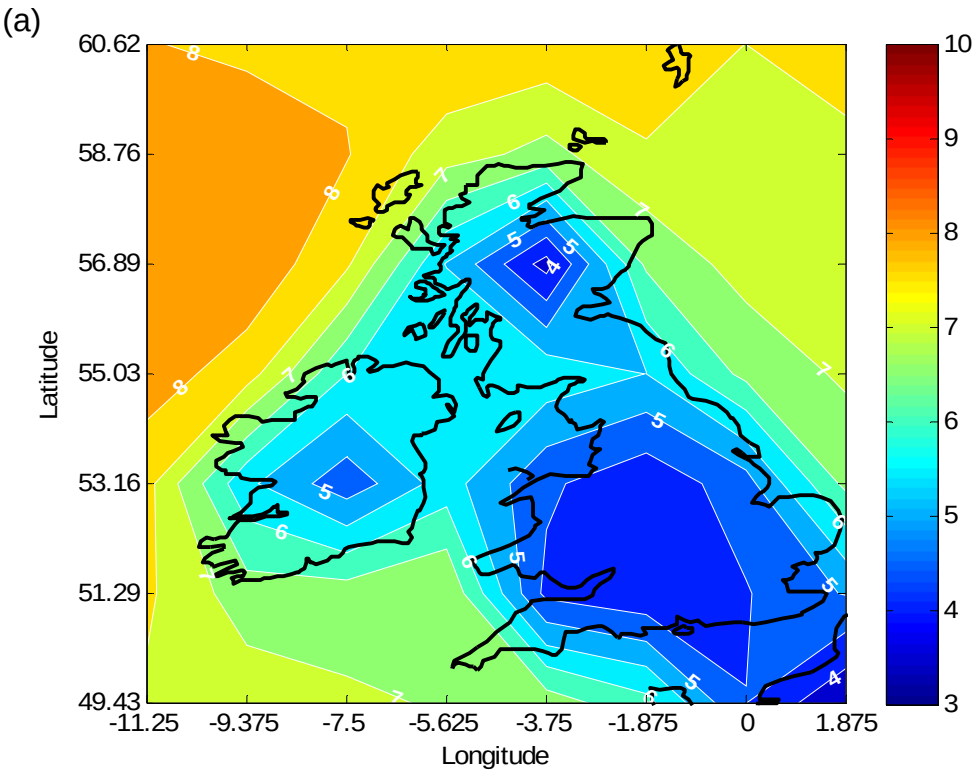

Fig. 4-4 Annual average mean wind speed 1961-90 (m/s)

(a) ERA40

(b)

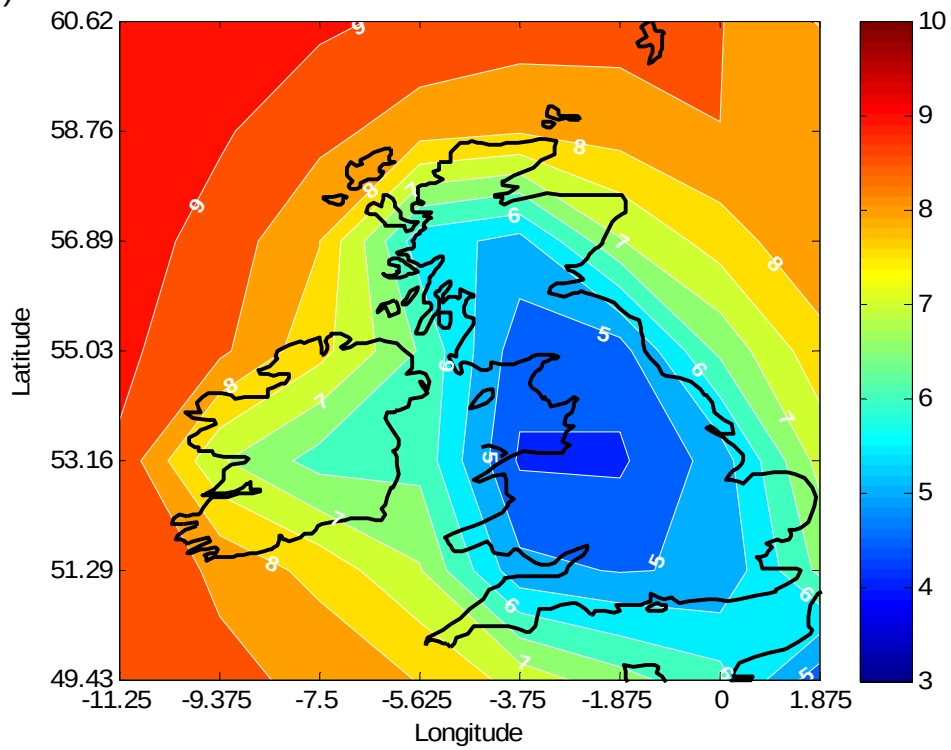

(c)

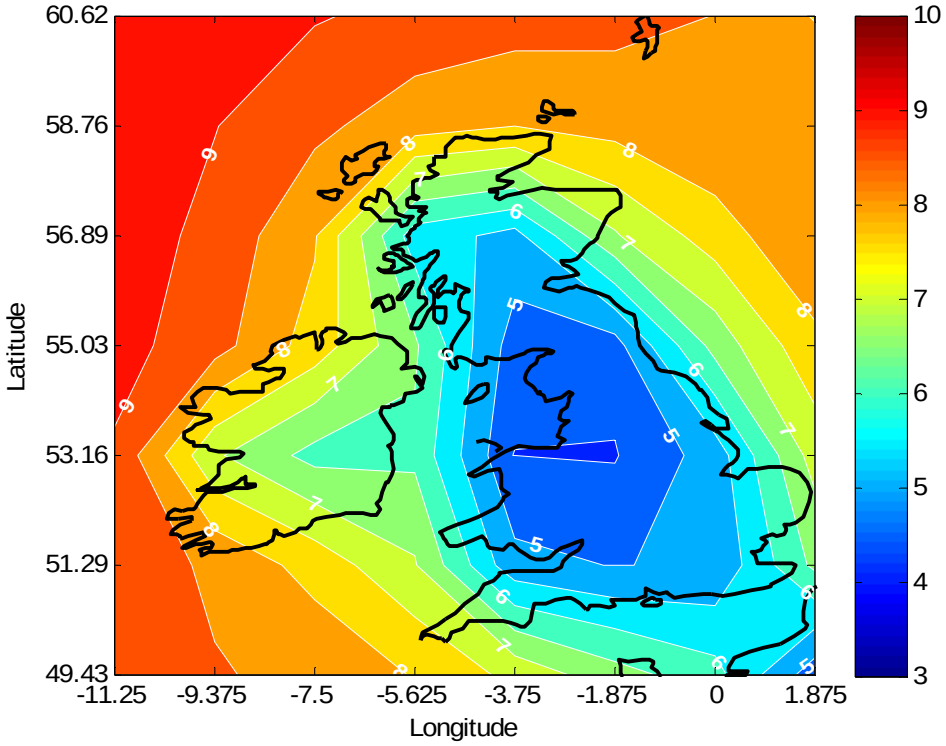

Fig. 4-4 cont. Annual average mean wind speed 1961-90 (m/s)

(b) ECH5 Run 1; (c) ECH5 Run 4

4.2.4 Taylor Diagrams and correlation fields

A method devised by Karl Taylor (Taylor, 2001) and used in the IPCC AR4 is a convenient method for visualisation of several statistics used to determine the success of a model in representing the pattern described by an observed field, namely root mean square error, correlation and normalised standard deviation. Pryor *et al* (2005b) used this method in their comparison of monthly mean pressure gradients and vorticity from several GCMs and a similar approach has been adopted here. An exact description of the metrics included in the diagram is given in appendix B.1. In brief, the x and y axes of the diagram describe the standard deviation of each mean monthly field calculated from the GCM relative to the standard deviation of the same field from ERA40. The radial axis defines the correlation between each monthly field from ECH5 and ERA40. The root mean square error of the GCM fields, i.e. the error in the pattern without reference to the mean value, compared to the ERA40 fields is described by the distance of the monthly point from the origin.

As in section 4.1.1.3, considering the twelve mean monthly values for the whole space, a Taylor Diagram was constructed for the region based on documentation in Taylor (2005) in order to assess if there was good correlation between the pattern of monthly means within the grid and whether or not the mean monthly fields had similar spatial standard deviations in an average month. Like the Taylor Diagrams of Pryor *et al* (2005b), each number 1 to 12 in the diagrams represents a month, where 1 is January, 2 is February etc. Figs. 4-5a and 4-6a show that for most months in both runs of the ECH5 model, the correlation is quite high, as indicated by the values also shown in the figure. The highest correlation for Run 1 is 0.932 in May, and for Run 2, 0.937 in September. In both runs, July has the lowest correlation, at 0.85 for Run 1 and 0.87 for Run 2. June and November also show correlations in the lower range in both runs.

In all months, the standard deviation over the region was higher in both runs of ECH5 than for the reanalysis data. Examining the data in Fig. 4-4, it seems the higher standard deviation in this GCM is caused not by greater variability within the data overall but by a high bias in offshore mean wind speeds in the GCM to the north west of the UK - whilst onshore they appear more similar to the reanalysis. This

increased difference between this offshore region and onshore results in a higher value for standard deviation in the GCM grid.

The Taylor diagram shows a fairly consistent normalised centred RMS error in all months, for both ECH5 runs, of approximately 0.5. This is difficult to interpret as the centred RMS error is solely representative of the pattern error rather than giving an actual indication of bias (Taylor, 2005). What can be said is that the pattern error is consistent in all months, and does not show a tendency to be higher in any one particular month.

In Fig. 4-5b and 4-6b a contour plot of the R-squared values superimposed on a coastal plot is shown below the appropriate Taylor diagrams to give some indication as to how the relationship between typical monthly means in the GCM and reanalysis data varies within the spatial field. The maximum R^2 values of around 0.96 are found in the North Sea area and the southern and western offshore region. Values are minimum in inland Scotland and Ireland, reaching lows of 0.84. It is clear that the match between the ECH5 and reanalysis datasets is worse in areas where the coastline and orography is more complex, such as in western and central Scotland. In offshore areas and over the large body of land in southern England, the data is better correlated than for Scotland and, in Run 1, for Ireland. A plausible reason for this is the failure of the GCM resolution to capture the changes in the surface in these areas. Looking at the mean fields back in Fig 4-3, averaged over all months in the 30 year period, it is clear that the GCM does not represent the land-sea changes fully, whereas the ERA40 dataset even interpolated from its originally high resolution to a lower resolution is more representative.

(a)

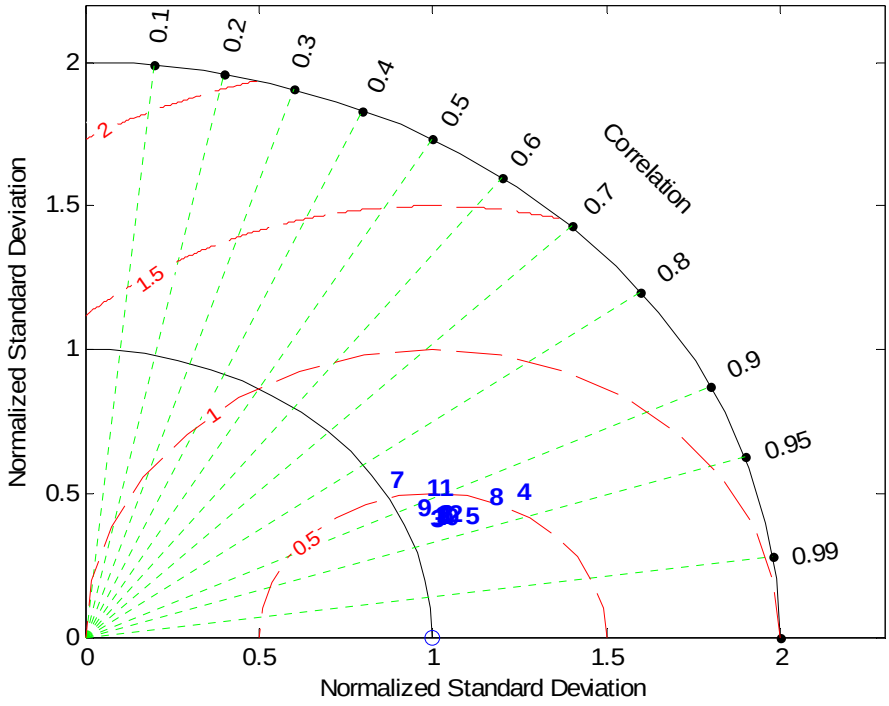

(b)

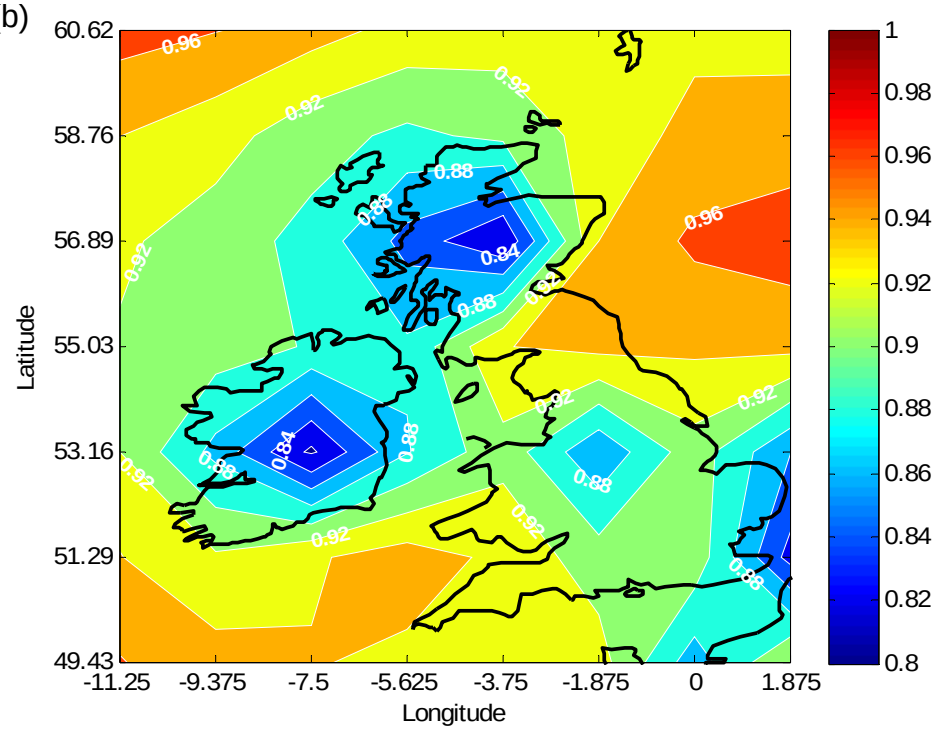

Fig. 4-5 Comparison of spatial pattern correlations between ERA40 and ECH5 Run 1 1961-90

(a) Taylor diagram for UK region for each of the 12 months; (b) R^2 coefficients of monthly mean wind speeds over the region

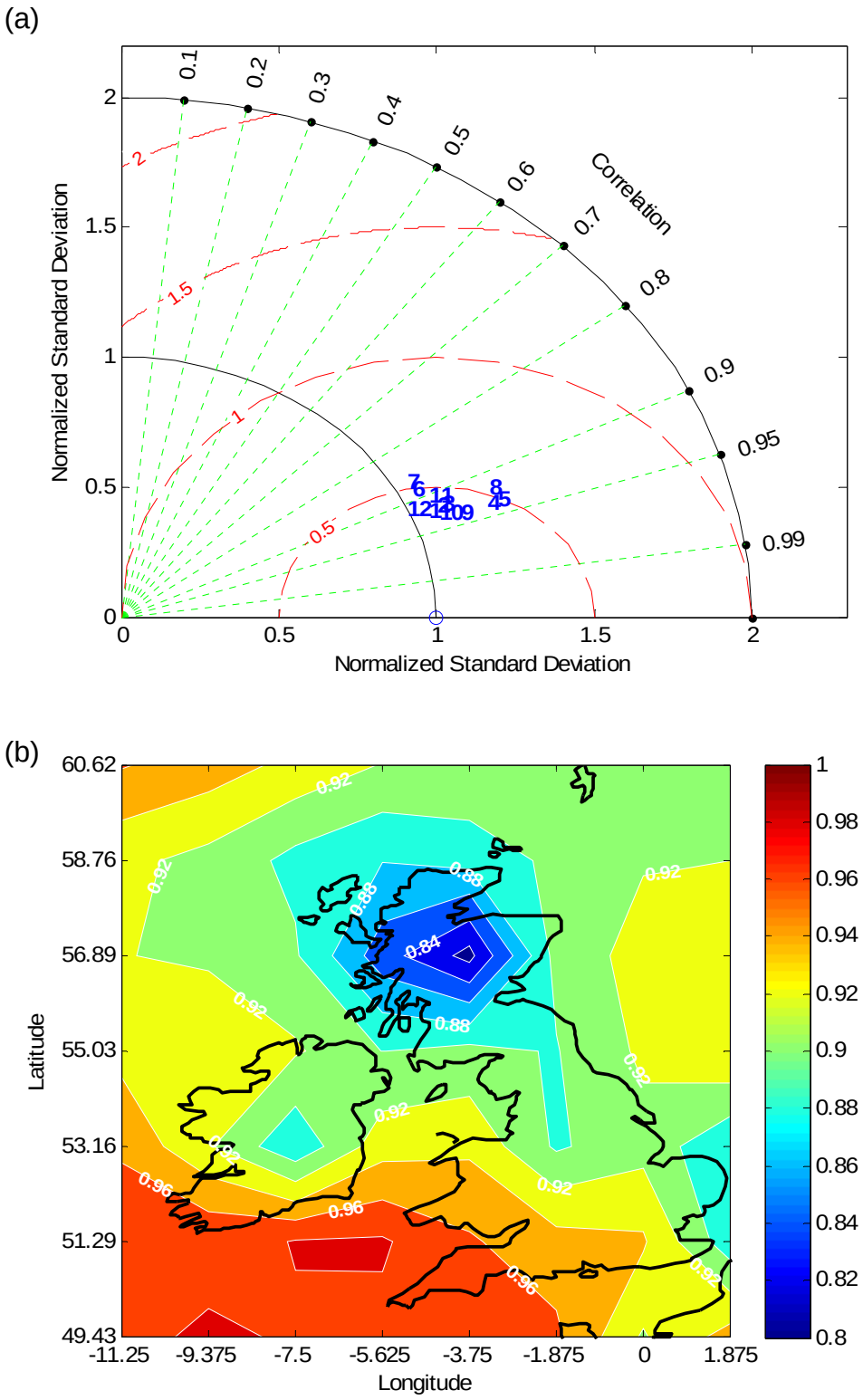

Fig. 4-6 Comparison of spatial pattern correlations between ERA40 and ECH5 Run 4 1961-90

(a) Taylor diagram for UK region for each of the 12 months; (b) R^2 coefficients of monthly mean wind speeds over the region

4.2.5 Comparison of monthly fields

Plots of the mean wind vectors over the whole field for each month comparing GCM output with the reanalysis data are presented for each of the ECH5 runs in appendix C.1. From Fig. 4-7, it is clear that some months are more successfully represented in the GCM than others, with both runs having large discrepancies versus the reanalysis data in March and April. These differences are mainly an issue of direction, with the vectors for both these months tending to be rotated in an anticlockwise direction away from the ERA40 vectors between 40˚ and 100˚. The rotation appears to be a maximum in March in the north west of the domain, with the angle between the vectors at approximately 90˚, but reducing both to the east and the south. For April, the angle between the vectors is at its greatest, over 90˚, in the North Sea region directly to the east of England, with the difference reducing towards the west of the grid in Run 1. In Run 4, the north west corner of the domain shows similarly large differences in the wind direction as in the North Sea region.

January shows similarly poor correspondence with the reanalysis output but only in the Run 4 data, with the GCM vector becoming more rotated anticlockwise away from the ERA40 vector towards the north, and reaching a maximum of 90˚ in the north west corner. Run 1 shows only a very small rotation of the GCM vector in the very north west grid point and a small number of points to the east of northern England and Scotland.

The UK, particularly in western coastal regions, experiences predominantly south westerly winds, and this seems to be well-captured by ECH5. The reanalysis, on the other hand, seems to suggest more of a westerly tendency. In the ERA40 results of both runs for April there is a ‘dividing line’ between northern and southern UK in April, where, in the west of the domain, winds to the south of this line are north-westerly and winds to the north appear south-westerly. This is possibly because of the location of a typical low centre to the north west and high centre to the south west. Their precise locations cause the apparent divergence of wind flow over the UK. It appears that a similar pattern is not captured by the ECH5 model, with the pressure centres perhaps in slightly different locations, so its winds are more consistent in direction across the domain for this month.

(a)

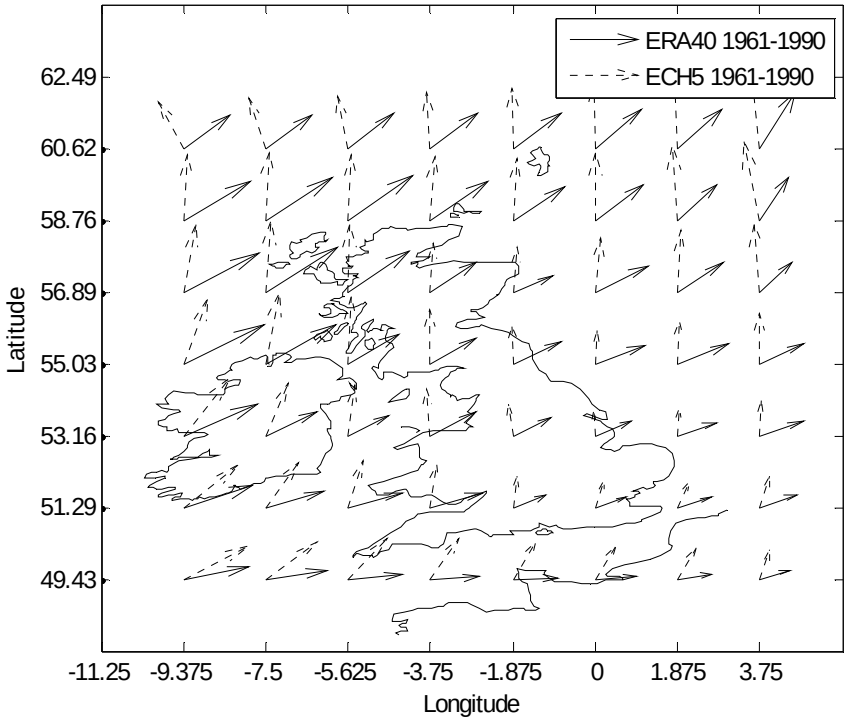

(b)

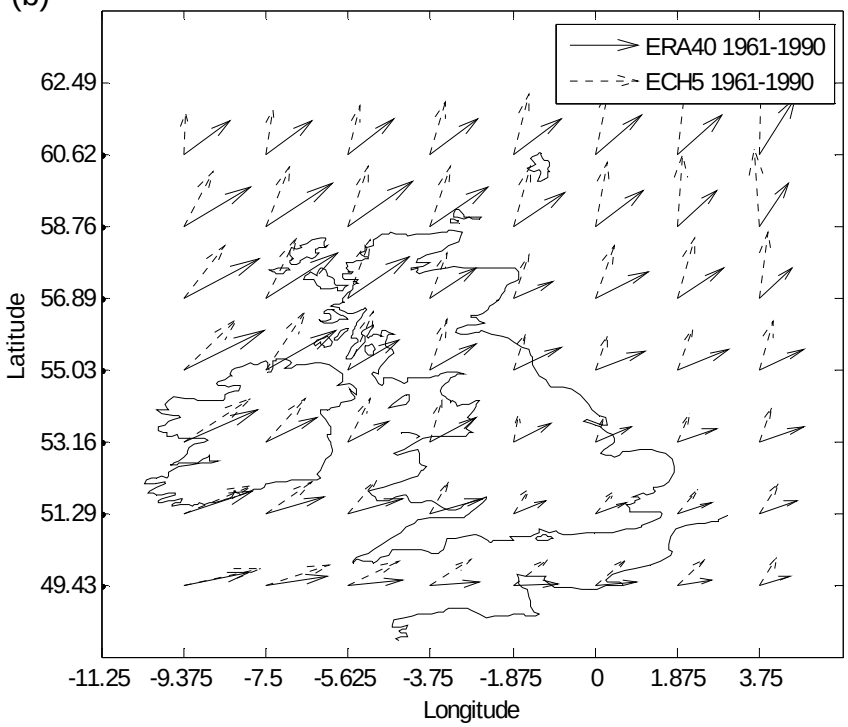

Fig. 4-7 ERA40 monthly mean vectors vs. ECH5 monthly mean vectors 1961-90

(a) March Run 1; (b) March Run 4

(c)

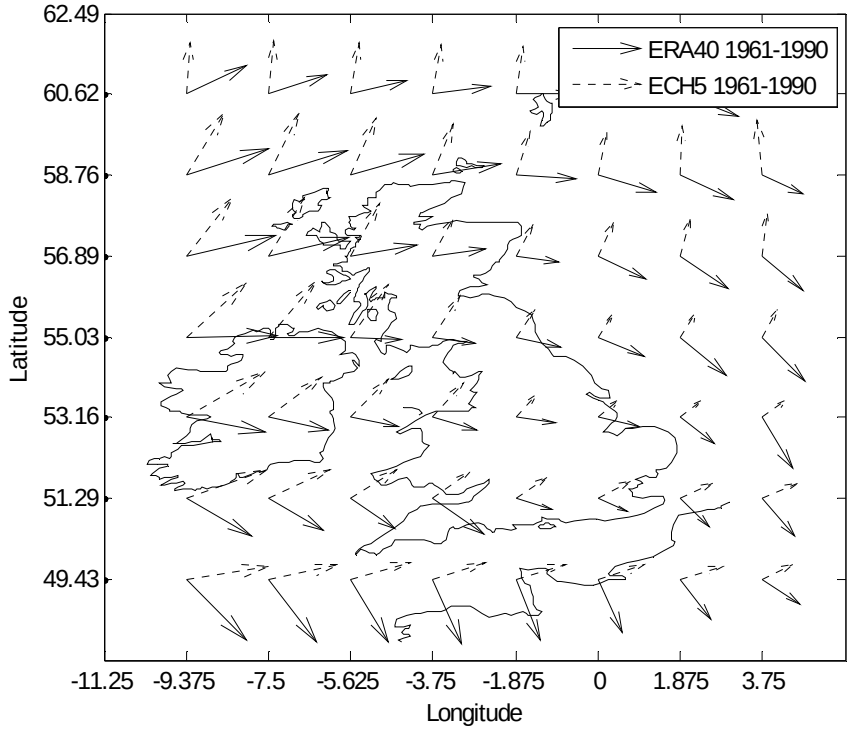

(d)

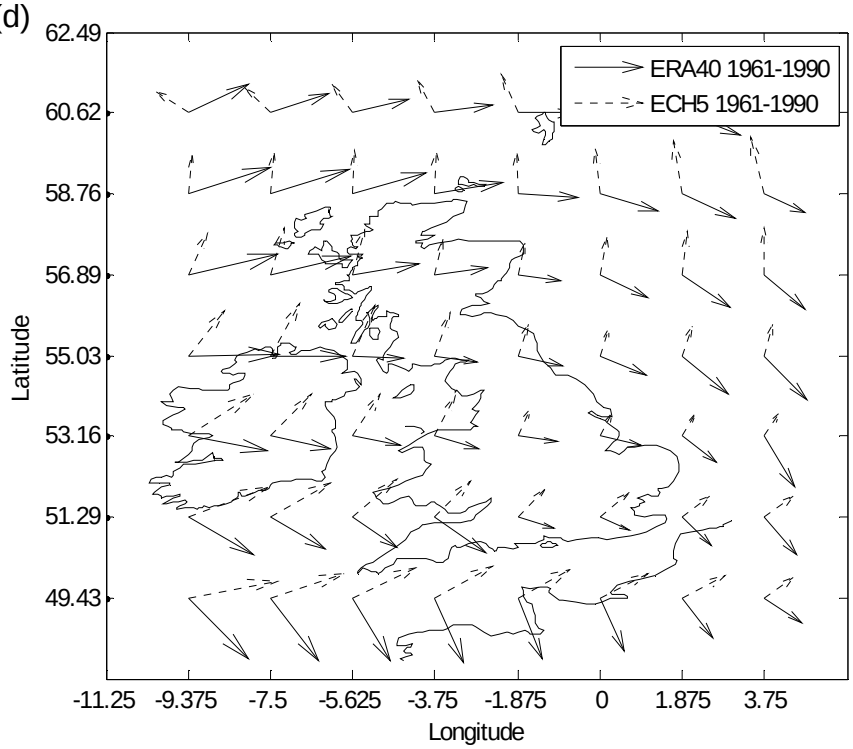

Fig. 4-7 cont. ERA40 monthly mean vectors vs. ECH5 monthly mean vectors 1961-90

(c) April Run 1; (d) April Run 4

(e)

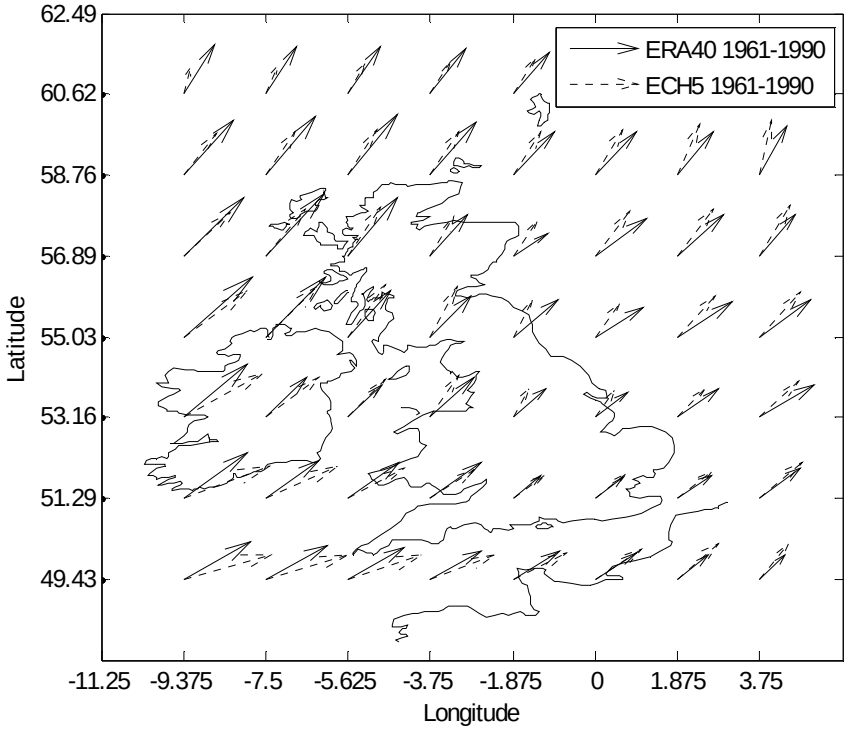

(f)

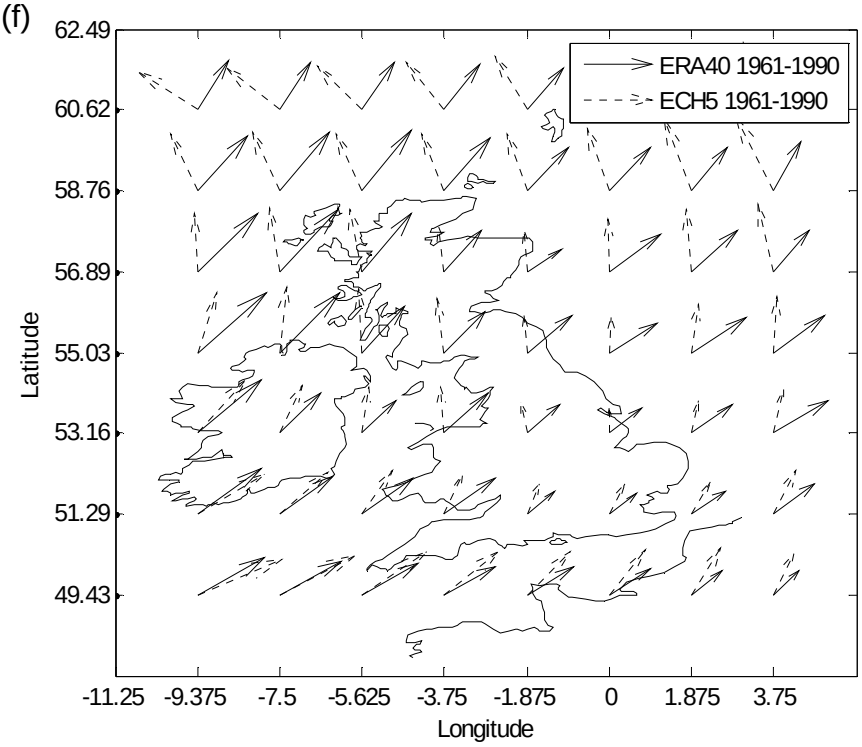

Fig. 4-7 cont. ERA40 monthly mean vectors vs. ECH5 monthly mean vectors 1961-90

(e) January Run 1; (f) January Run 4

Wind Roses have been drawn for three locations, shown in Fig. 4-8. One of the cells represents a region in Scotland, 'Scot'; one is located in the north east of England, 'NE Eng'; the third cell chosen is in the south of England, 'S Eng'.

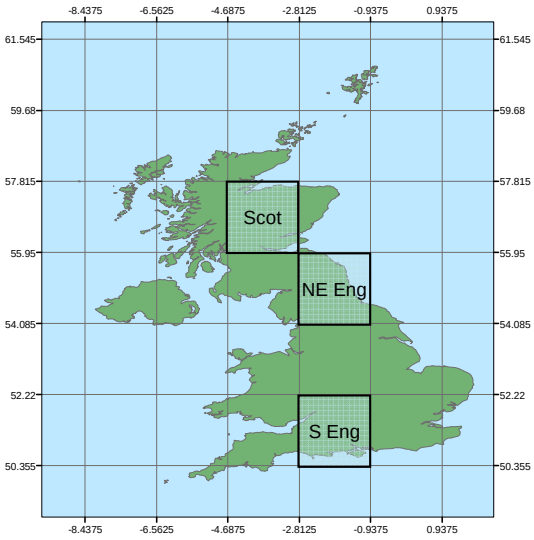

Fig. 4-8 Locations for wind rose analysis

Fig. 4-9 shows that the tendency in all of the cells from the ERA40 model is for the highest frequencies to occur in the quadrant 180˚-270˚, but the GCM provides similar representation of this only for the S Eng cell. The N Eng and Scot cells in ECH5 show the highest frequencies in directions around 20˚ anticlockwise away from the highest frequencies of the ERA40 data. The S Eng data from the GCM does not show high enough frequencies of winds in the north east quadrant compared to ERA40 but the other cells have closer patterns in this quadrant.

Two other differences are of note: the first relates to the Scot cell, which, in the ERA40 data shows a very strong pattern of west-south-westerly winds and limited frequencies in other directions. The ECH5 pattern for this cell has a greater occurrence of winds between 150˚ and 200˚. The second notable difference in the roses is regarding the frequencies of higher wind speeds, greater than 8 m/s. ECH5 gives greater frequencies of these winds in the S Eng and Scot cells, which is in accordance with the findings that ECH5 overestimates the average wind speeds as discussed in 4.2.2. However, in the N Eng cell, ERA40 shows more frequent occurrence of winds in the higher categories. Referring to 4.2.3, the annual mean in

this region is slightly higher in ERA40 than in ECH5 and so it may be attributed to the issue of grid resolution.

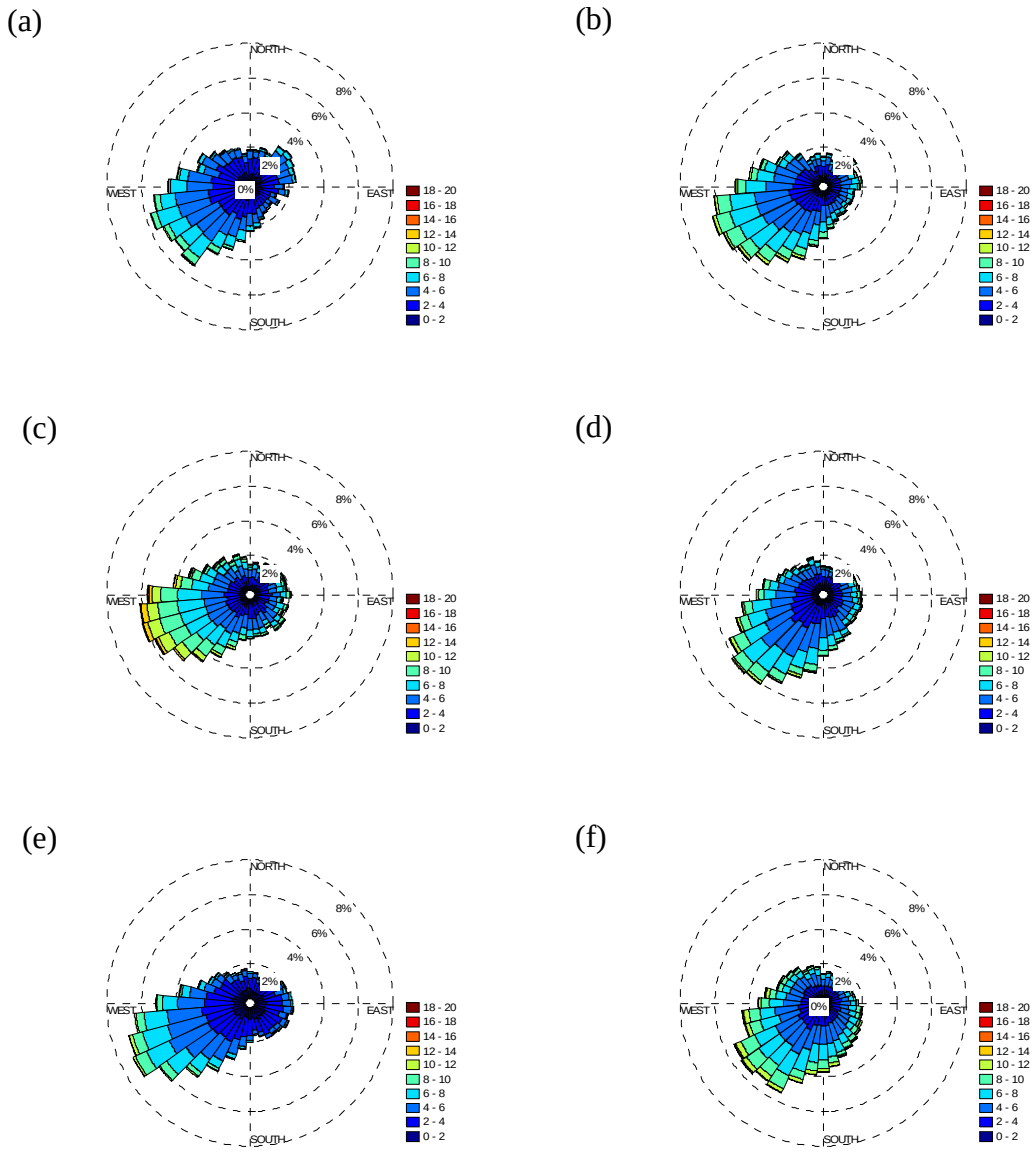

Fig. 4-9 S Eng (a) ERA40 and (b) ECHAM5; NE Eng (c) ERA40 and (d) ECHAM5; Scot (e) ERA40 and (f) ECHAM5

Considering just the mean 10m wind speed with no directional information, the percentage differences were calculated between the monthly mean data from the two GCM runs and the ERA40 data for each month. The pattern of percentage differences is firstly very consistent in all months for both runs, and secondly, very

distinctive. The image for each month is in appendix C.1, but shown in Fig: 4-10 are two sample months, January and April, from each run. There are typically three areas of overestimation by the GCM within the region, over northern Scotland, Ireland, and the south of England. In the midst of this is an area of underestimation over the north of England. The magnitude of the overestimates tends to be larger than that of the underestimated values, reaching a maximum of about 40% in northern Scotland. The largest value of underestimated wind speed is around -20%. This explains the regionally averaged wind speeds calculated in section 4.1.2.2 being in general, higher than the ERA40 averages, as the overestimates outweigh the underestimates.

a)

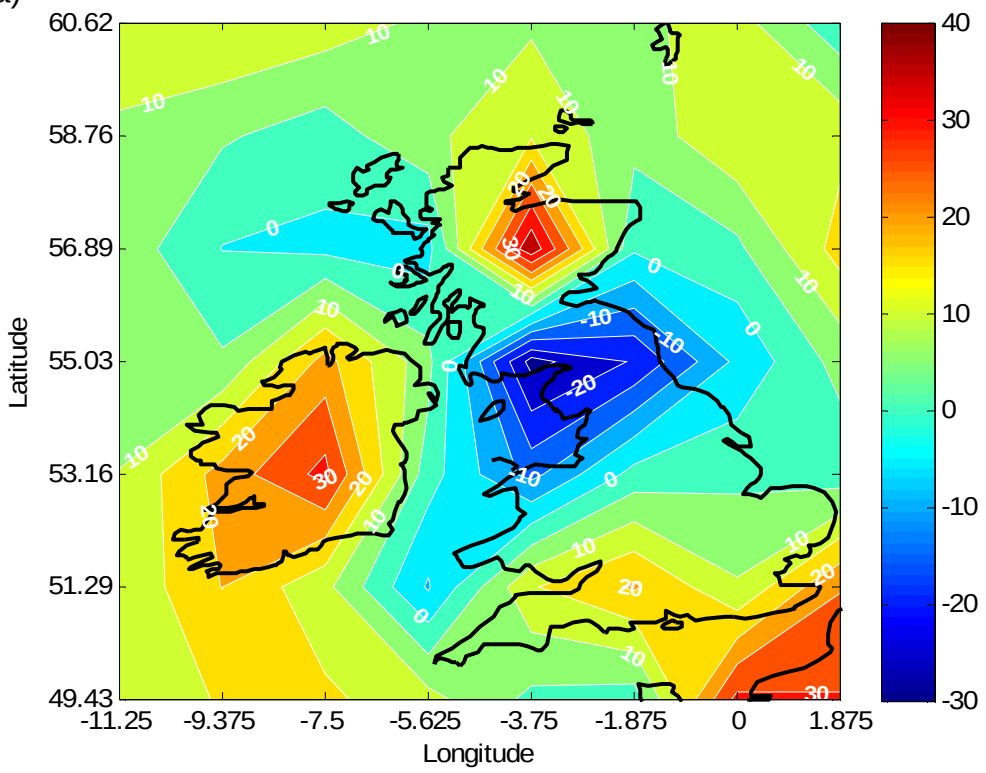

Fig. 4-10 Percentage differences between ECH5 and ERA40 1961-90

(a) January Run 1

(b)

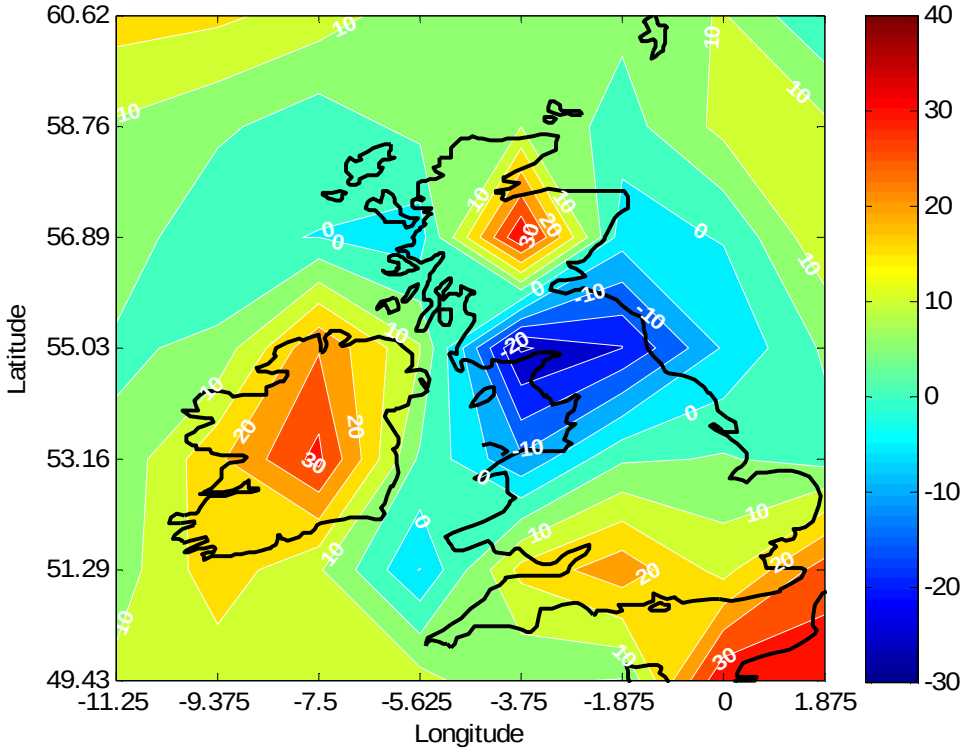

(c)

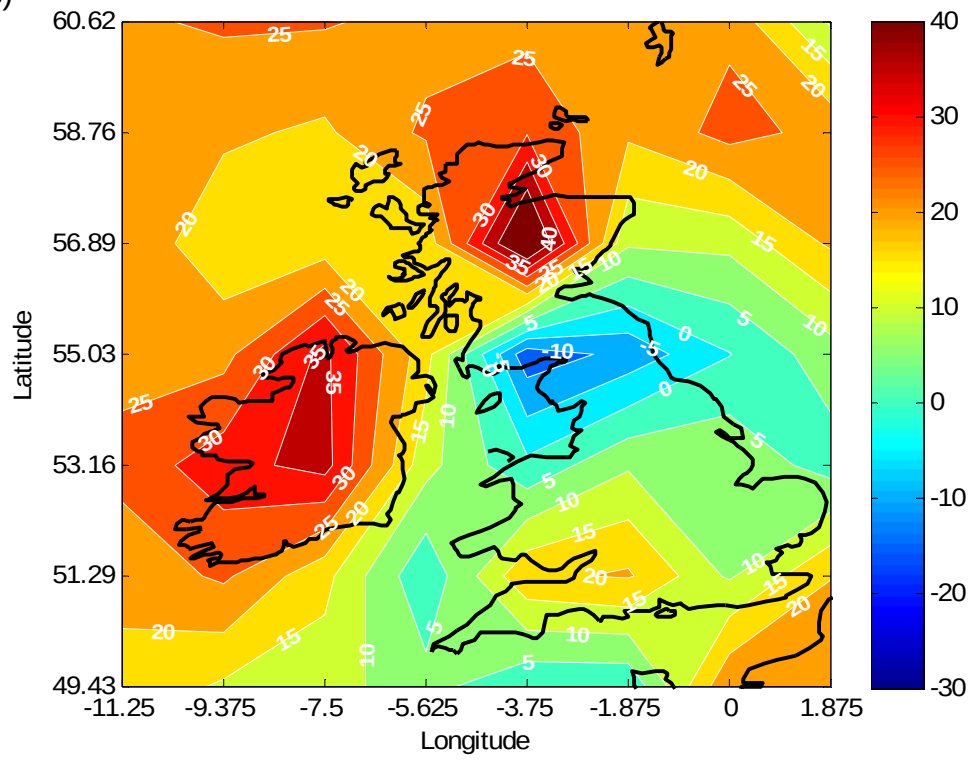

Fig. 4-10 cont. Percentage differences between ECH5 and ERA40 1961-90

(b) January Run 4; (c) April Run 1

(d)

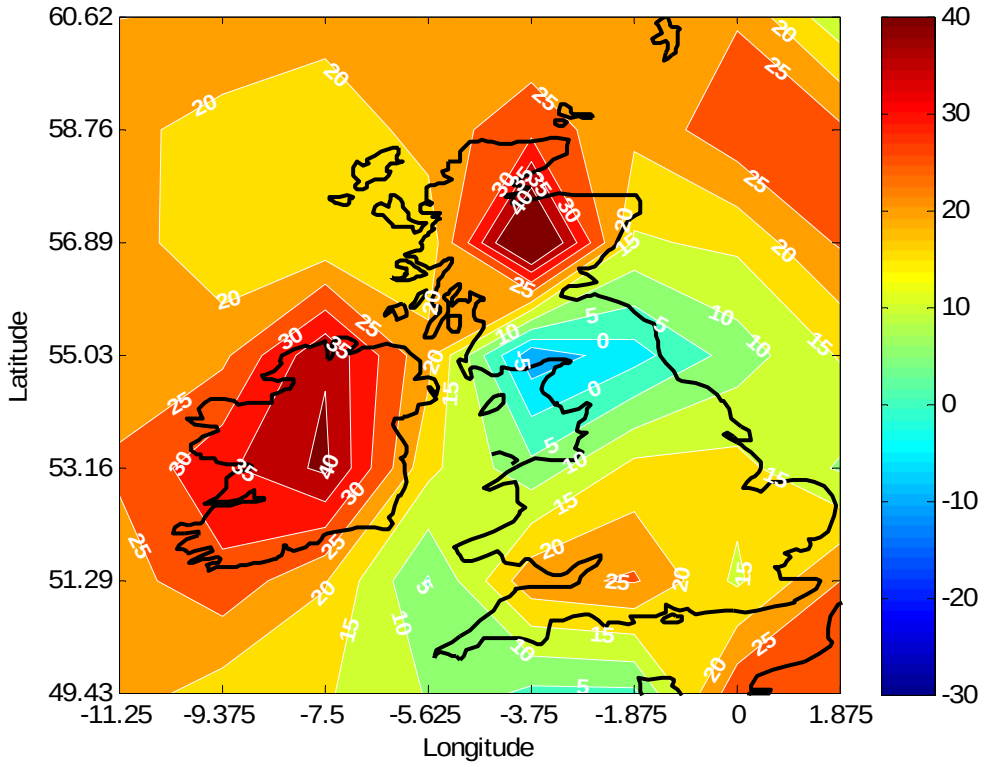

Fig. 4-10 cont. Percentage differences between ECH5 and ERA40 1961-90

(d) April Run 4

The most obvious explanation for this difference pattern is the grid resolution. Where ERA40 has a resolution of 1˚ latitude and longitude, the GCM has a resolution of almost half that, and struggles to resolve the complex heterogeneous terrain and coastline which is a dominant feature of the landscape - particularly in the northern half of the UK. This results in monthly wind speed output not resembling true wind speeds enough to be useful.

4.2.6 Weibull parameters

A different view on the climate data produced by the GCM can be taken: rather than considering the monthly mean fields, the parameters of the distribution of time series wind data can be used as an indication of the model's success. The particular distribution often used to describe wind speeds is the Weibull distribution.

The two-parameter Weibull distribution is described by a scale parameter, *A*, and a shape parameter, *k*, giving a probability density function *p(U)* of:

$$p(U) = \left(\frac{k}{A}\right)\left(\frac{U}{A}\right)^{k-1} \exp\left[-\left(\frac{U}{A}\right)^{k}\right] \tag{4.1}$$

The mean wind speed can be found from the distribution by

$$\overline{U} = A\Gamma\left(1+\frac{1}{k}\right) \tag{4.2}$$

where *Γ(x)* is the gamma function such that

$$\Gamma(x) = \int_0^\infty e^{-t} t^{x-1} dt \tag{4.3}$$

(Manwell *et al*, 2002)

Generally, a higher *k* value will result in a higher modal value of wind speed but lower frequencies of winds at very high speeds. Higher *A* values will tend to produce more 'spread' distributions that have larger ranges of wind speeds. The combined effects of various *A* and *k* parameters will result in permutations of the typical Weibull shape in terms of 'skewness' and 'spread'. Graphical representations of these combinations are shown in appendix A.3.

The Weibull distribution is reported to be representative of the hourly wind speed distribution at most wind sites (Petersen, 1998a) but a Weibull distribution fitted to daily wind speeds is potentially different in terms of the shape parameter as time-period averaging will reduce the variance in the data. For this reason, daily data such as the ECH5 data, could not be expected to have the same Weibull *k* parameter as, say, hourly data. The ERA40 data is provided at six hourly resolution so the daily mean for this data was calculated by averaging the four daily values. As with the mean data, the ERA40 data was interpolated to the lower resolution ECH5 grid covering the same area as above. Weibull parameters *A* and *k* were fitted to the daily values over 30 years for each grid cell; the results for *k* are presented in Fig. 4-11.

(a)

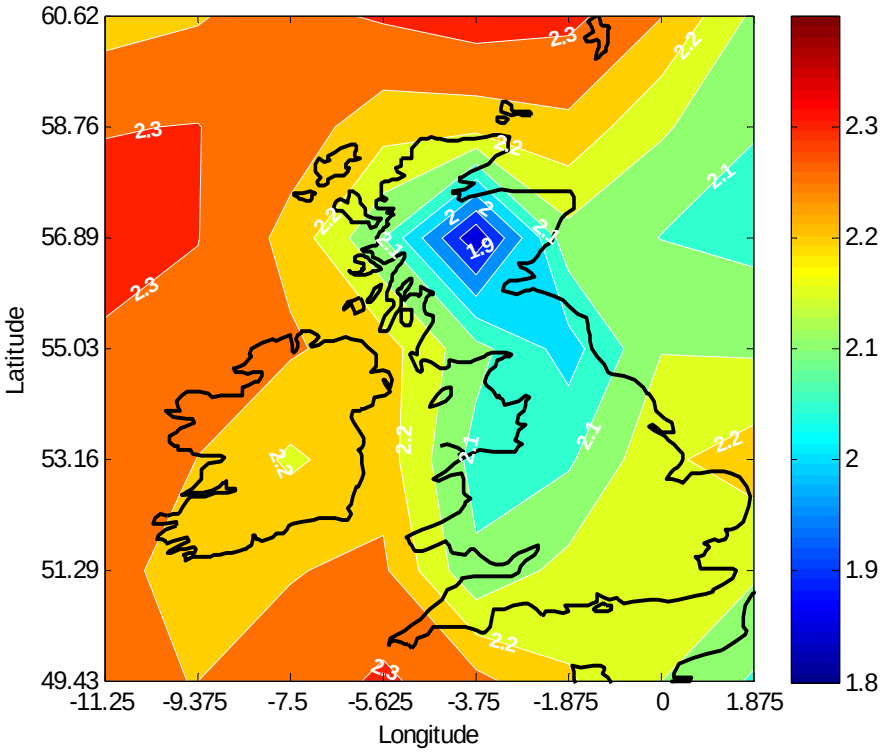

(b)

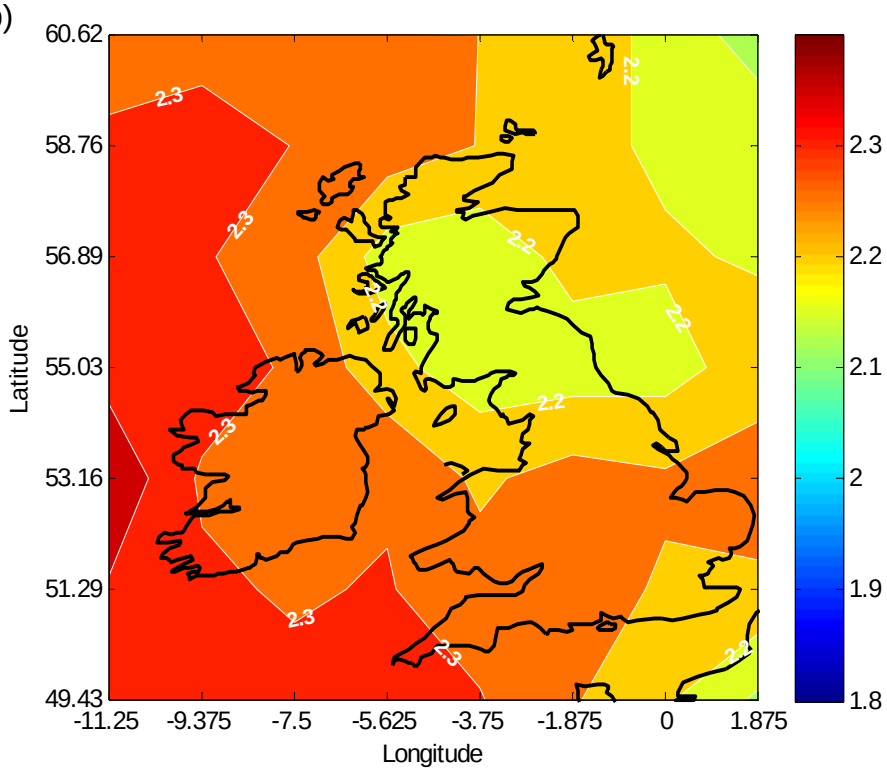

Fig. 4-11 Weibull *k* parameters 1961-90

(a) ERA40; (b) ECH5 Run 1

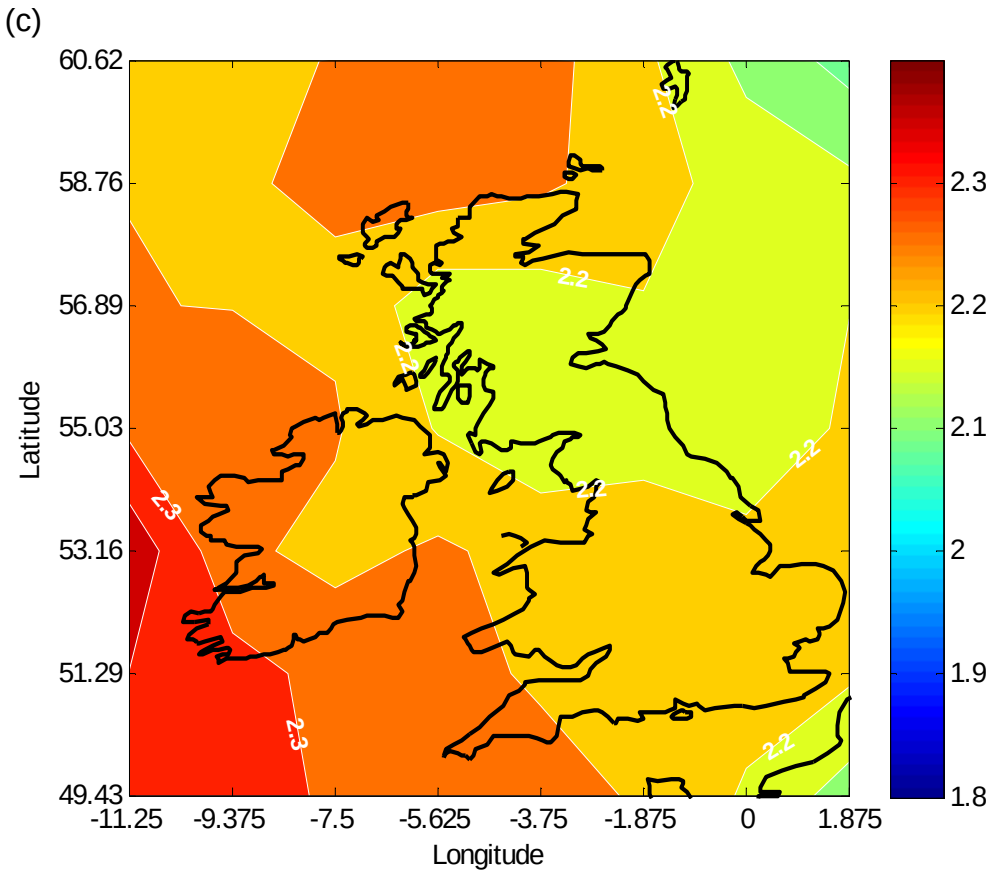

Fig. 4-11 cont. Weibull *k* parameters 1961-90

(c) ECH5 Run 4

Due to their close relationship, the Weibull *A* parameter shows a very similar pattern to that of the mean wind speed. As with the mean speed, it is obvious that the GCM representation of the land-sea boundary is poorer than in the ERA40 model, and that it fails to capture as much detail in the pattern as ERA40. However, the general pattern, although biased high in a similar way to mean wind speed, is quite similar between the two datasets.

With the Weibull *k* parameter, again, the GCM data does not show as much detail as the ERA40 results, but the pattern of lower *k* values over Scotland and northern England is somewhat alike in the two datasets. The lack of detail is especially obvious in the Scottish region where the ERA40 model shows a significant drop in the *k* parameter to 1.9 in the central Highlands. As can be seen from Fig. 4-11, a lower *k* parameter is indicative of a lower modal wind speed, accompanied by higher probability of very high wind speeds. Overall, the Weibull parameters are not

captured as well in the GCM in terms of the spatial resolution, but do show similar overall tendencies to the ERA40 model output.

4.2.7 Conclusions of hindcast analysis

For the area 49˚ to 61˚ north, and -12˚ to 2˚ east, a comparison between ECH5 GCM 10m wind data and ERA40 reanalysis 10m wind data for the 1961-90 period shows some deficiencies in the GCM. This could potentially render the direct use of the data for wind energy applications problematic.

Averaged over the whole area, the monthly mean wind speeds in both runs of the ECH5 GCM are between 5 and 25% higher than those from the ERA40 reanalysis, with the greatest percentage difference in summer and lowest in winter. The R^2 correlation coefficient varies in space, between the lowest value of 0.84 in Scotland and the highest of 0.96 in the North Sea area. The R^2 value also shows variation with season, with the best result in the winter and spring months and the poorest in the summer.

Looking at the mean monthly fields individually, there is quite a significant discrepancy in the vector direction in March and April from Run 1 of the GCM, and March, April and January for Run 4. The vectors in these months are rotated anticlockwise from the ERA40 vectors, to varying degrees over the whole area, but tending to be particularly different in the far north west of the domain. In terms of the percentage difference in the mean monthly resultant wind speeds, the pattern of change in all months is very similar, with the GCM data from both runs giving an overestimation of up to 40% in northern Scotland and Ireland, and a slightly less severe overestimate in the south west of England. The model then also shows an underestimation of the wind speed in northern England. It is clear there is an issue of resolution in this result, with the GCM unable to resolve the wind climate changes resulting from heavily variable terrain over the whole of the UK.

The Weibull parameter estimates from the GCM runs, compared to the reanalysis data show a similar spatial pattern for the scale parameter, A, but the lower resolution of the GCM data is obvious, as is its bias towards higher mean wind speeds. Similarly, the shape parameter, k, has an indication of lower values over the onshore region as with the reanalysis data, but the resolution is simply too low to

display the detail. The k parameters from the GCM runs tend to be higher in general than those of the reanalysis data, suggesting a lower range of wind speeds - perhaps an indication of its inability to model extreme conditions.

Given the large discrepancies in mean wind speed values and the fact that the daily wind speed distributions are not particularly well replicated by the GCM, it would not be prudent to use the GCM data directly to draw specific conclusions about future surface wind speeds, or indeed about the potential impact on wind energy resources. Examining change fields projected by the GCM, however, may give a qualitative indication as to how mean speeds and directions might change in the future. Care must be taken not to assume these projections are precise and absolute – for this reason they will not be used directly for energy calculations, given the large uncertainties involved.

4.3 Future projections for changes in wind speed

4.3.1 Data

Future wind climate data was obtained from a single run of the ECH5 GCM carried out under the conditions of the SRES A2 scenario (representing 'high' levels of emissions, see 2.1.6) for the twenty-year period 2081-2100 (IPCC Data Distribution Centre, 2005b). Both runs of the model for the 1961-90 period have been used as a baseline for comparison.

4.3.2 Spatial average monthly means

Taking the spatial average and looking at monthly mean values (Fig. 4-12a), the seasonal pattern remains very similar, with the lowest wind speeds in summer and the highest in winter. The percentage change in the future period was calculated using both a Run 1 and a Run 4 control period baseline and is shown in Fig. 4-13. The greatest changes common to both baselines are April and May with values of around -4% versus Run 1 and -6% versus Run 4. July and August also have fairly consistent results from both baselines, of around -2 to -3%. For the remaining months, the two different baseline datasets give varying future percentage changes but there is an apparent seasonal pattern, with most of the changes in the September

to February period being positive, and all of the March-August changes being negative.

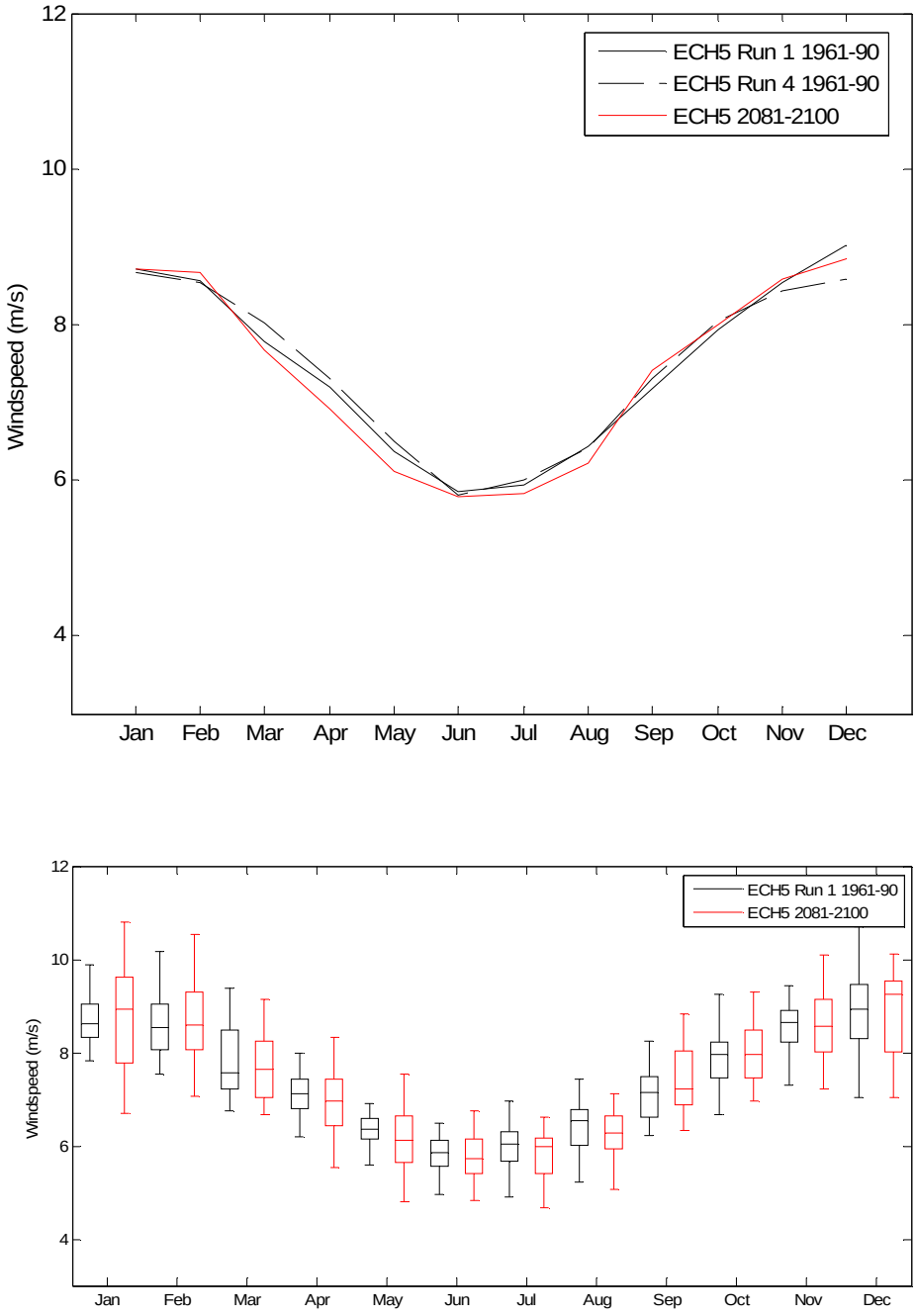

Fig. 4-12 Spatial average monthly means and boxplots

(a) ECH5 Run 1 and 4 1961-90 and ECH5 2081-2100 monthly means (b) ECH5 Run 1 1961-90 and ECH5 2081-2100 boxplot

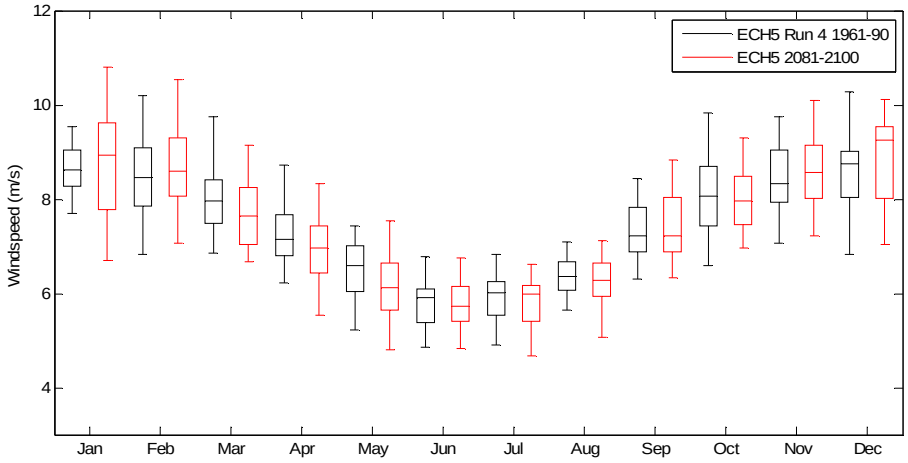

Fig. 4-12 cont. Spatial average monthly means and boxplots

(c) ECH5 Run 4 1961-90 and ECH5 2081-2100 boxplot

It is interesting to note that the future run of ECH5, as seen in Fig. 4-12 b and c, shows a maximum variability for January and February that comes closer to that of the ERA40 data for the control period, with a standard deviation of around 1 m/s. There is a small increase in the standard deviations for April, May and June compared with the ECH5 control period data for Run 1, but these are similar values to those seen in Run 4.

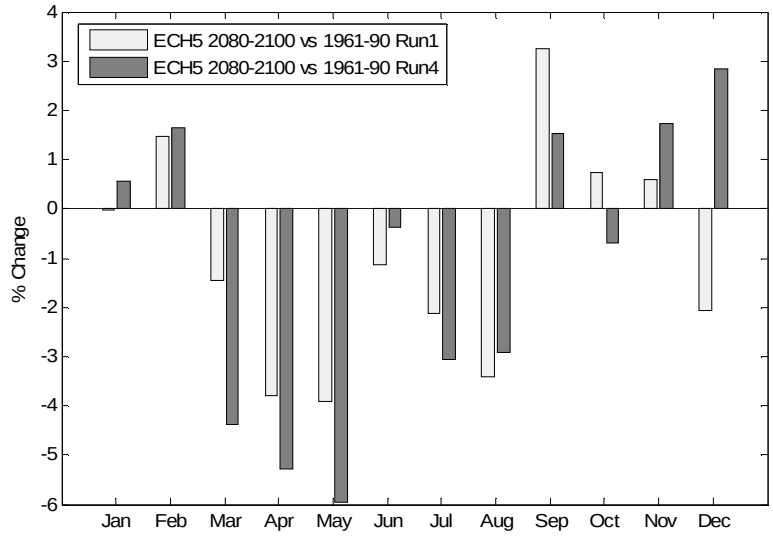

Fig. 4-13 Monthly mean percentage differences for ECH5 2081-2100 vs ECH5 runs 1 and 4 1961-90

4.3.3 Annual mean field

Looking at the results averaged over time in Fig. 4-14, the overall annual mean wind speeds for the 2081-2100 period under emissions scenario SRESA2 are very similar to the 1961-90 control period, and maintain a very similar spatial pattern. The lowest wind speeds are found in the inland UK region, increasing towards the coasts.

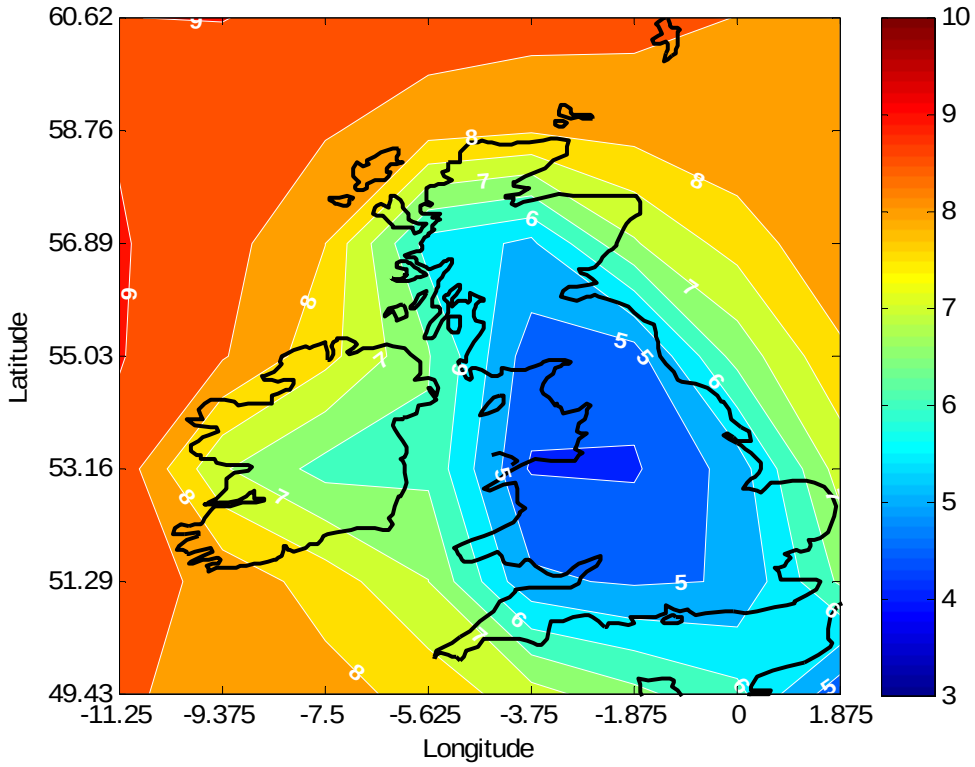

Fig. 4-14 Annual mean wind speed ECH5 2081-2100

4.3.4 Future change fields

A calculation of the annual percentage change for each point in the grid in the ECH5 model from the 1961-90 period to the 2080s gives quite similar change fields when Run 1 of the future model is compared with both control runs. As shown in Fig. 4-15, there is a slight rise in mean speed of perhaps 1% in or around the Scottish region using both Run 1 and Run 4 as a baseline. Against Run 1 the projection gives mainly a slightly positive change in the remaining onshore areas of between 0 and 0.5%, whilst against Run 4, a bigger area is affected by a small negative change of around -0.5%. There is some indication of a greater decrease offshore to the south and west of the region.

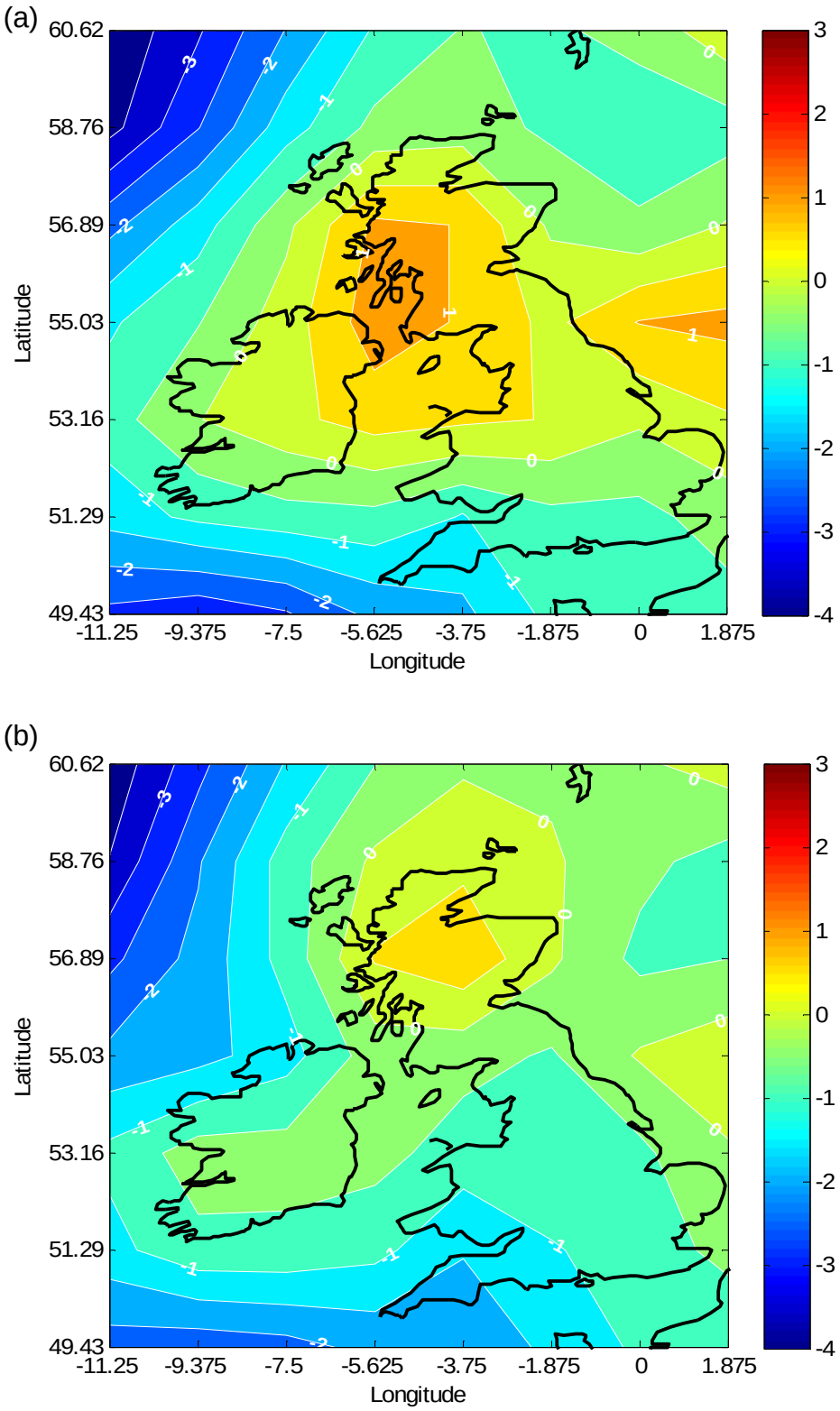

Fig. 4-15 ECH5 2080s annual percentage change field vs. ECH5 6190

(a) Run 1; (b) Run 4

The percentage change fields were also calculated on a month-by-month basis and are shown for each month in appendix C.2. The results show that the annual mean change has 'averaged out' a large degree of the projected seasonal variation, especially with regard to the offshore area to the north west of the UK. Several months displayed in Fig. 4-16 give particularly interesting results for onshore areas:

- April – the north of Scotland and to a lesser degree, the north coast of Ireland, show decreases in mean wind of up to 10%.

- July – the north of Scotland shows increases of up to 6% on the Run 1 baseline, but only around 2% on the Run 4 baseline, whilst the rest of the UK experiences decreases of up to 7% on both baselines.

- August – there is a notable decrease in mean wind speed in the south west of England of around 10% versus the Run 1 baseline, and around 7% versus the Run 4 baseline.

- September – compared to the Run 1 baseline, the future period results show increases of up to 9%, mainly concentrated in the north of England and Scotland. Against the Run 4 baseline, the increases are smaller and more widely consistent, with most of the onshore British Isles seeing an increase of between 3 and 5%.

- December – against both runs, the future results show an increase in the south east of England of around 4- 6%. From a Run 1 baseline, Scotland sees a decrease of up to 7%, whilst from a Run 4 baseline, Scotland experiences a similar level of increase as the rest of the UK, of around 4%.

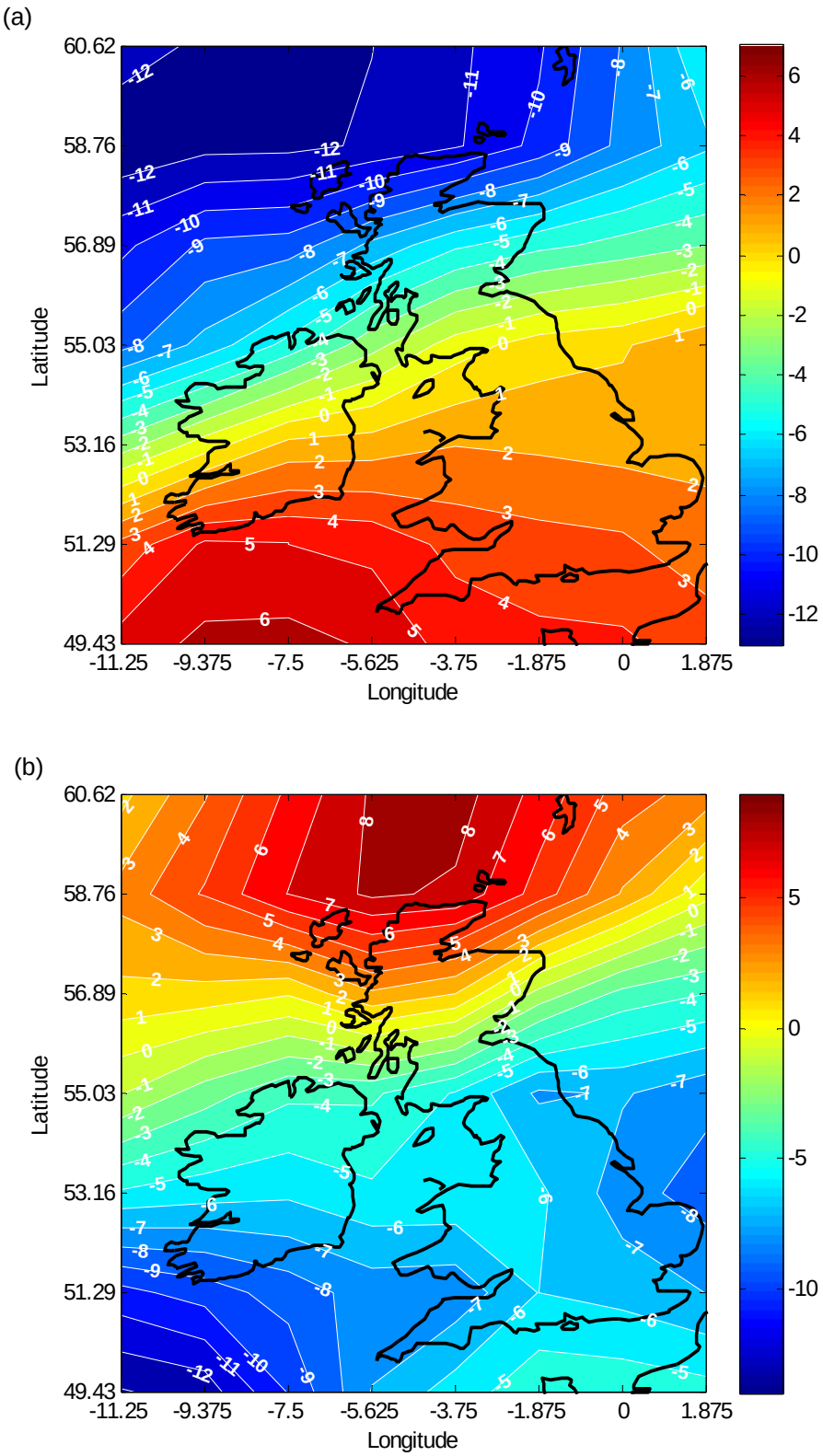

Fig. 4.16 Annual % Change in wind fields for ECH5 2081-2100 vs. ECH5 1961-90 Run 1 baseline

(a) April; (b) July

(c)

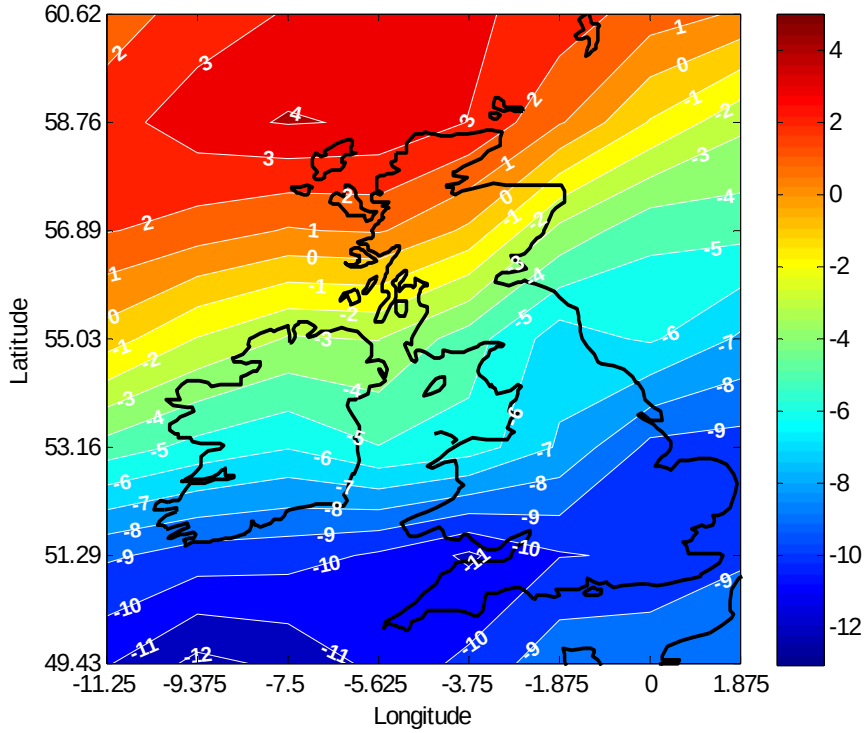

(d)

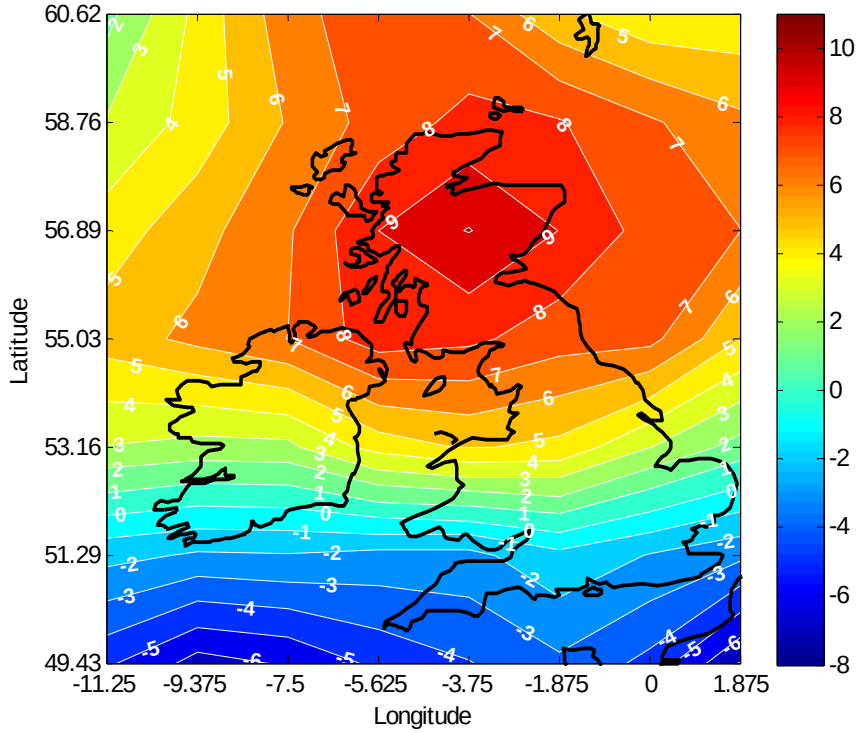

Fig. 4.16 cont. Annual % Change in wind fields for ECH5 2081-2100 vs. ECH5 1961-90 Run 1 baseline

(c) August; (d) September

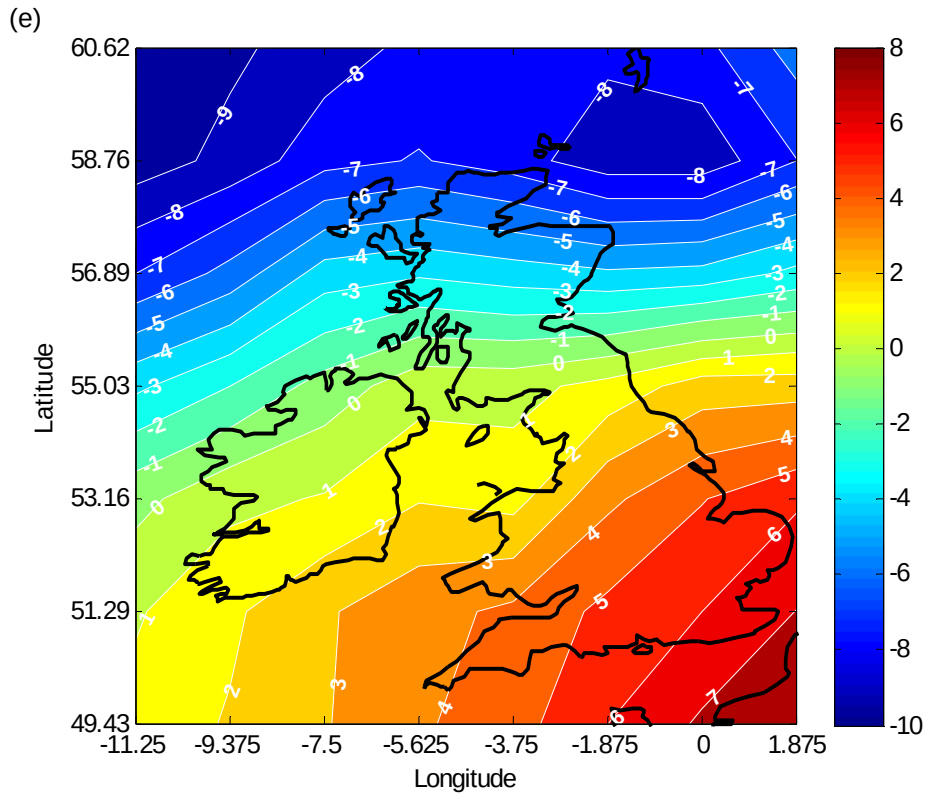

Fig. 4.16 cont. Annual % Change in wind fields for ECH5 2081-2100 vs. ECH5 1961-90 Run 1 baseline

(e) December

Because both sets of baseline data are fairly consistent, and only one dataset for the future period has been used, the patterns of future change are reasonably similar from both baselines. The onshore regions which appear to suffer the largest degree of change are the far north of Scotland and the south of England. This may relate to changes in the large-scale pressure oscillations that dominate in the region, such as the North Atlantic Oscillation (NAO) or the East Atlantic Pattern (EAP).

In terms of directional patterns, appendix C.2 shows how the ECH5 monthly patterns change in the future period relative to 1961-90 averages. The months that show the greatest differences against a Run 1 baseline are March and May, shown in Fig. 4-17, but it is interesting to note that these were some of the months in which both runs of ECH5 bore the least resemblance to ERA40 reanalysis for the control period. It is difficult to say, therefore, whether or not these changes should be taken seriously, given that the model showed an inability to hindcast them accurately.

(a)

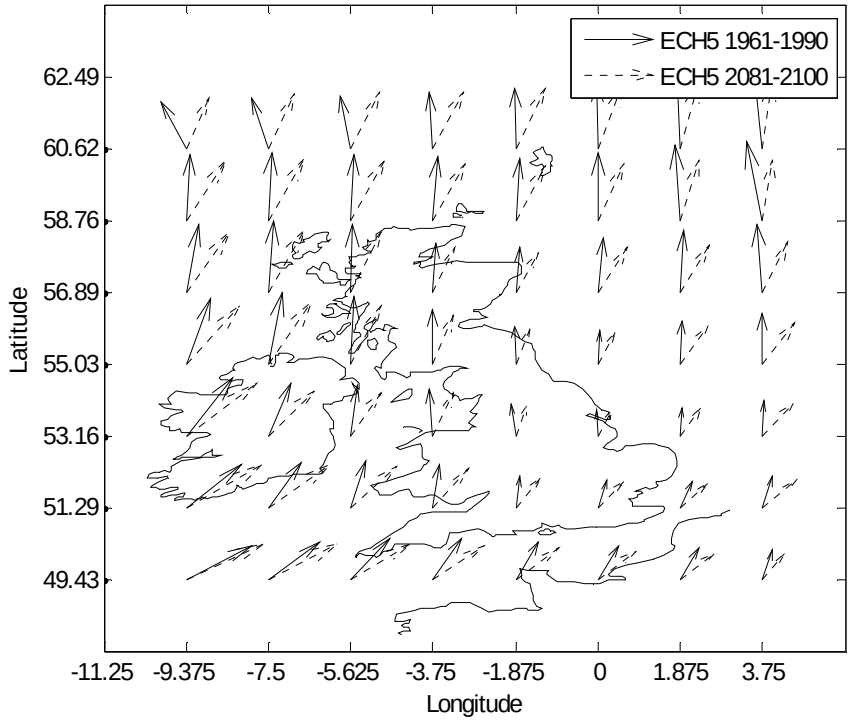

(b)

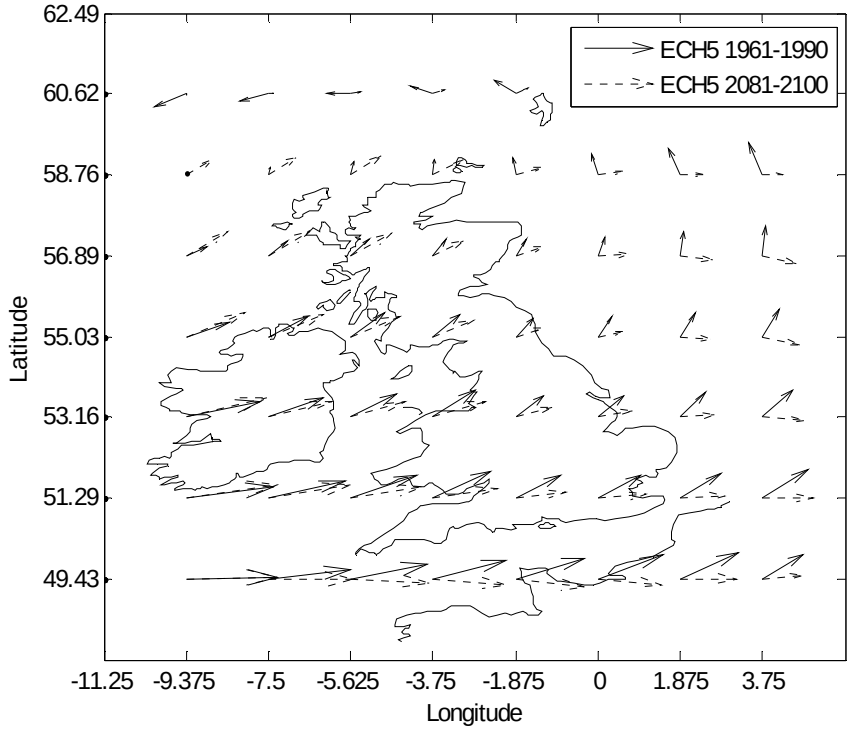

Fig. 4-17 ECH5 1961-90 monthly mean vectors vs. ECH5 2081-2100 monthly mean vectors

(a) March Run 1; (b) May Run 1

(c)

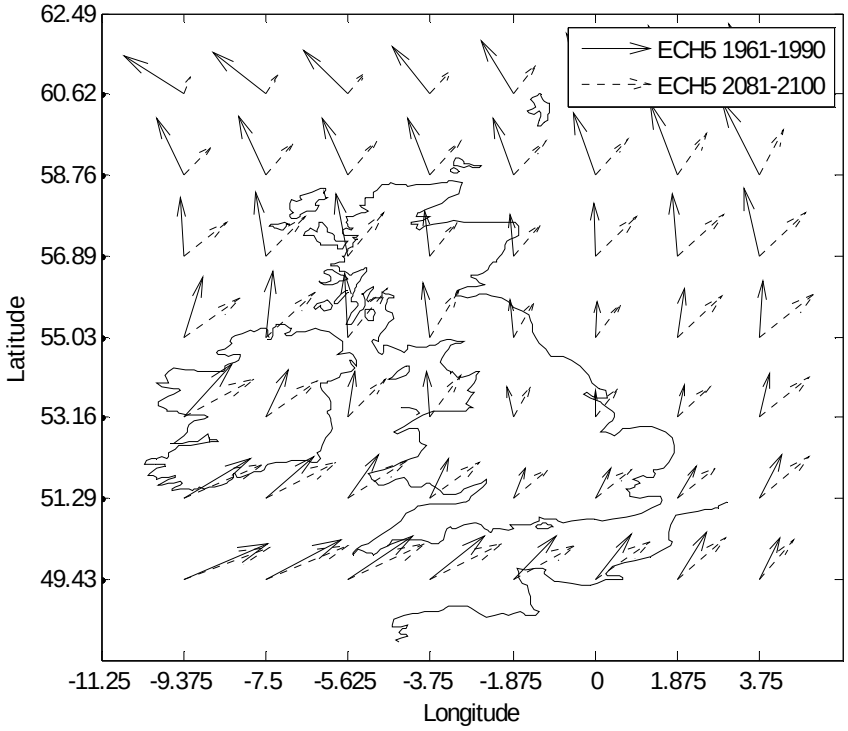

(d)

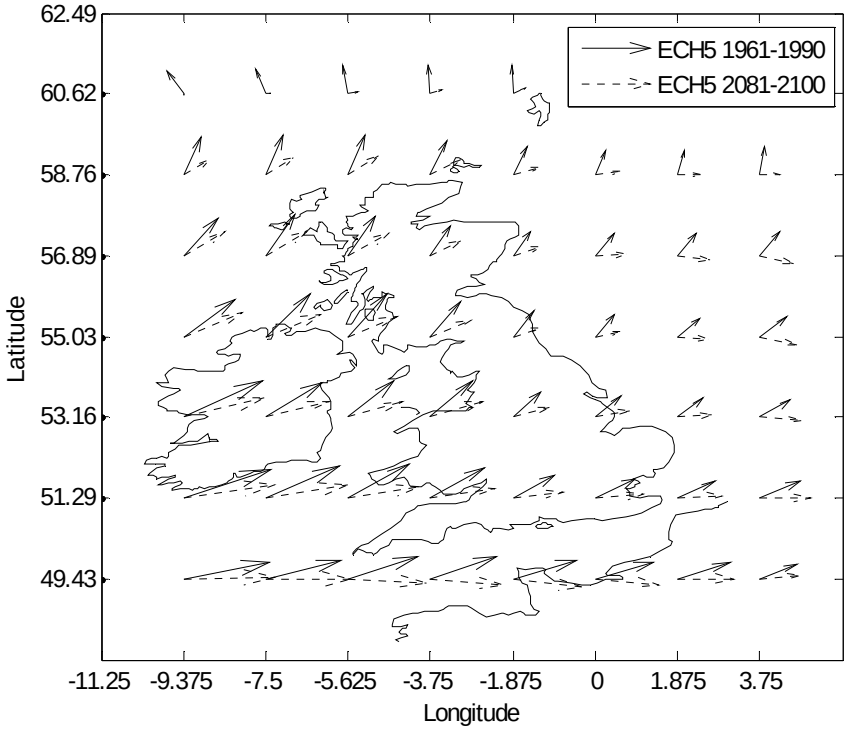

Fig. 4-17 cont. ECH5 1961-90 monthly mean vectors vs. ECH5 2081-2100 monthly mean vectors

(c) January Run 4; (d) May Run 4

Against a Run 4 baseline, those months which show the greatest changes are January and May, with April also showing quite a deviation in vector direction. Again, however, these were months that showed the least similarity with the ERA40 reanalysis - which suggests there is a high degree of uncertainty surrounding the baseline results in the first instance.

The vector plots also highlight that the area within the region of interest that shows the most propensity for change is the northern half of the region, and in particular the north-west Atlantic area. The size of the vectors, as well as their direction, is more divergent from the control period in this area than any other. This is suggestive of changes in the cyclonic activity which is so dominant in this region; but it is difficult to tell purely from surface wind data whether or not this is the case, or to identify particular modes of change. It is also pertinent to note that, as with the individual months which show the most change, this region was the least successfully hindcast when compared with the ERA40 reanalysis. It may be useful to consider large-scale pressure patterns, such as the NAO or the EAP in order to further understand the changes in this area.

Analysis of the wind roses for 1961-90 and 2081-2100 from ECH5 for the three locations discussed in 4.2.5 shows some minor changes in the directional distribution of winds (Fig. 4-18). In all cells there appears to be a 'broadening' of the distribution within the south western sector of the quadrant, with higher frequencies occurring in a wider range of directional sectors in this 90˚ range. There is drop in the frequencies of winds in the two eastern sectors as a consequence. The pattern is broadly similar over each of the three cells considered.

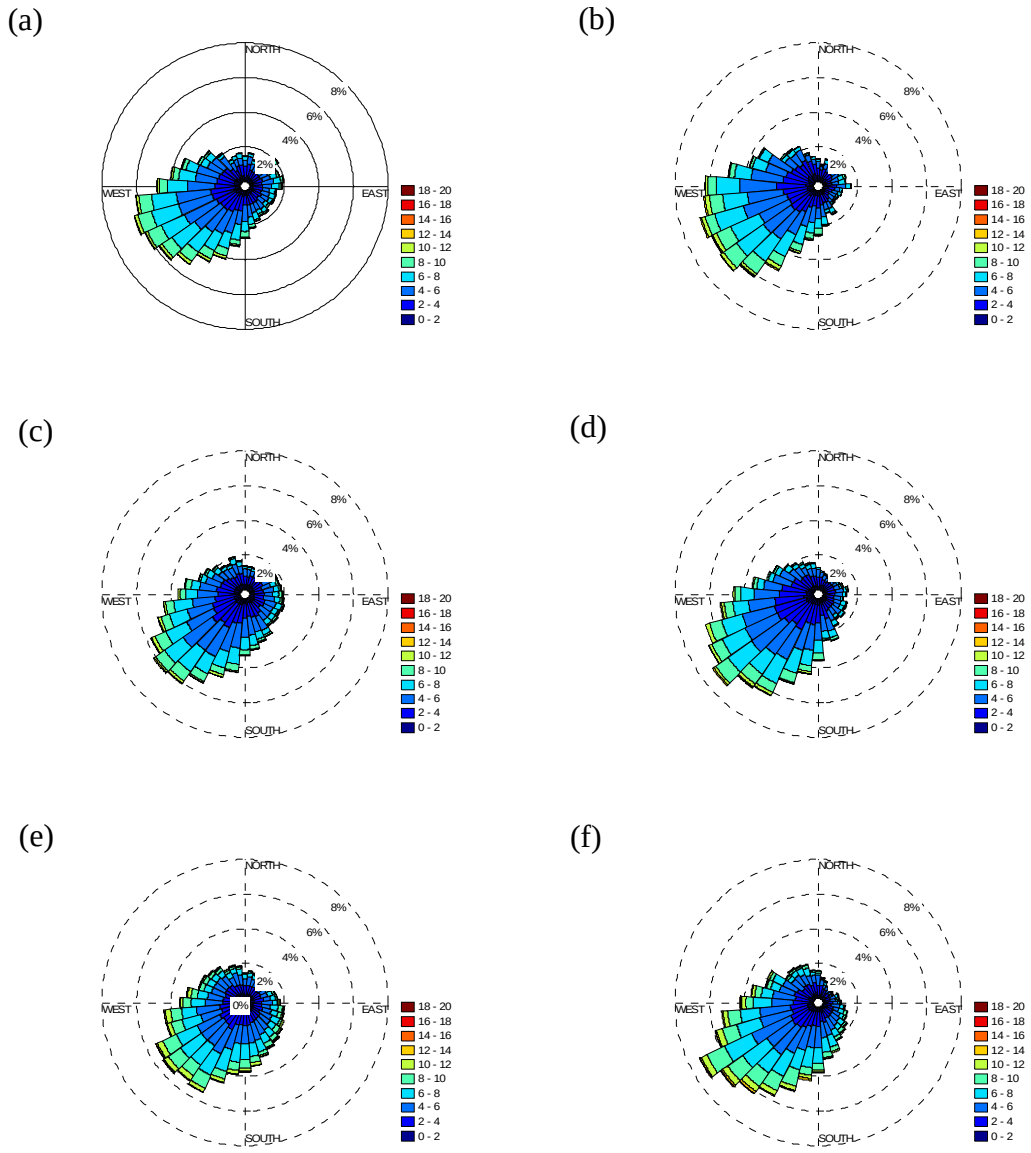

Fig. 4-18 S Eng (a) 1961-90 and (b) 2081-2100; NE Eng (c) 1961-90 and (d) 2081-2100; Scot (e) 1961-90 and (f) 2081-2100

4.3.5 Weibull parameters

As mentioned in section 4.1.6, rather than looking only at monthly mean results from the models, it is interesting to compare the frequency distribution of wind speed output from the models – assuming a good fit to the Weibull distribution..

The *A* parameter shows much the same pattern as the mean wind speed, as would be anticipated, with not much evidence of significant change. Fig. 4-19 shows the annual spatial pattern of the Weibull *k* parameters for ECH5 in the 2081-2100 period. The *k* parameter is also very similar over mainland Britain in the future projection, as in both the control period runs. This would suggest no remarkable change in the modal wind speed or in the range of wind speeds experienced - that is, no increase or decrease in the frequencies of occurrence of extreme winds. In the region to the south west of the domain, including a large part of Ireland, the contour showing a value of 2.25 for the *k* parameter seems to cover a larger area, compared to the same region in both Run 1 and Run 4 for the control period, where the value shows an increase to 2.3 and 2.35. The magnitude of change for the region is small, but a decreasing *k* value suggests an increase in frequencies of winds at high speeds, and a tendency for the distribution in this region to become more skewed towards lower wind speeds.

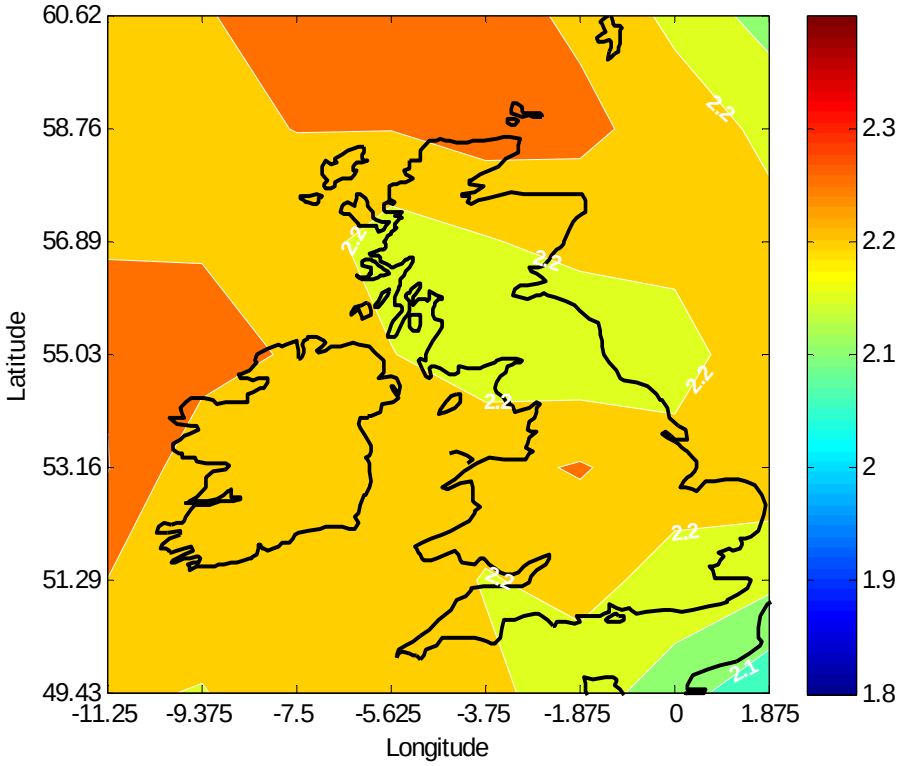

Fig. 4-19 Weibull *k* parameters ECH5 2081-2100

4.3.6 Conclusions on future changes

The conclusions from these future projections of wind speeds must be that there is no indication of a definite change signal in the model on an annual time scale. There is, however, rather more variation within individual months, with winter wind speeds, already typically high, showing a propensity to increase, whilst the lower spring and summer wind speeds are inclined to decrease further. The degree and tendency of monthly changes when averaged over the region varies from -6% in April and May to +4% in September and December. There is further variation within the region of study, with the northernmost and southernmost regions tending to experience the greatest changes.

Analysis of the frequency distributions from the control period and the future period shows little change in the Weibull parameters for the majority of the region, giving no indication of any tendency towards more or less extreme conditions. A small area in the south west of the region experiences a very slight decrease in the Weibull k parameter, which might suggest a greater occurrence of high wind speeds but the change is very small and its impact likely to be similarly minimal.

There is not sufficient confidence in the results to state whether or not this would have an impact on any wind power production facilities, certainly not on an annual basis. It is, however, worth noting that changes in the monthly or seasonal production, whilst not significantly impacting on the annual energy output of any particular facility, may affect how wind power is dealt with at a national level.

4.4 Dynamic downscaling – using a regional climate model

Referring back to the description of dynamic downscaling given in Chapter 2, regional climate models (RCM), also known as limited area models (LAM), are similar to GCMs, in that they are dynamic physical models of the atmosphere; but they are run over smaller (limited) areas at higher resolution. They are generally forced at their limits by boundary conditions imposed by a lower resolution climate model. Two studies using an RCM to provide projections of future wind speeds are referred to in chapter 2. Segal *et al* (2001) and Pryor *et al* (2005a) both stress that the results are preliminary and highly uncertain.

The results discussed in the remaining sections of this chapter have been published in Harrison *et al,* (2008). The wind speed data from a regional climate model designed to produce climate simulations for the UK region were obtained through the UK Climate Impacts Programme (UKCIP02) (Hulme *et al*, 2002). The modelling technique involved the nesting of the Hadley Centre HadRM3, a 50km resolution limited area model, within HadAM3, an atmosphere-only general circulation model (AGCM) with a resolution of approximately 120km. This in turn was nested within HadCM3, a full atmosphere-ocean GCM (AOGCM) which has a resolution of 2.5˚ latitude x 3.75˚ longitude – this translates to around 265km x 300km for the UK landmass. The nesting system was one-way only, which meant that feedbacks from the smaller models were not input to the larger models.

The UKCIP02 work produced projections for future climate based on four of the SRES emissions scenarios, corresponding to low, medium-low, medium-high and high levels of emissions. Outputs from the AOGCM corresponding to these emissions scenarios were fed into the higher resolution models. The models were run to provide simulations of the 1961-1990 control period, and then using the medium-low and medium-high emissions scenarios, for a thirty-year period corresponding to the end of the twenty-first century - referred to as the 2080s. Results were then derived by scaling techniques for two earlier time periods - the 2020s and the 2050s, and, by further scaling, for the low and high emissions scenarios for each of the time periods.

4.4.1 Qualitative comparison of RCM with ERA40

A qualitative comparison of the UKCIP02 model output for the control period with ERA40 reanalysis data (both scaled to 80m a.g.l) shows firstly, that the RCM has a slightly higher resolution and could thus be assumed to be better able to represent wind speed variation within the UK. The annual mean wind speed over the UK is shown in Fig. 4-20 for ERA40 and Fig. 4-21a for the RCM. Both show a similar mean speed for the body of land including most of England and Wales of between 5 and 7m/s and there is some indication in both datasets of a drop in the mean speed in inland Scotland. Coastal features are better captured in the RCM, and it does show some higher speeds in eastern coastal areas; mostly these are in excess of the speeds

in near-coastal grid squares in the reanalysis data. No directional information was available from the UKCIP02 wind results, and so this cannot be compared with the reanalysis data. The data is provided as monthly means, with no information on time series at a higher temporal resolution than this, so it is impossible to calculate frequency distribution parameters.

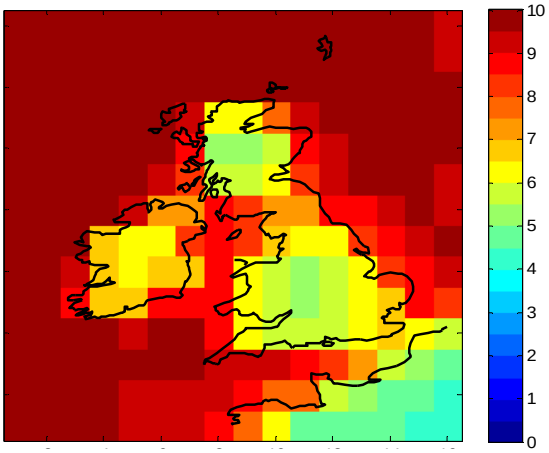

Fig. 4-20 ERA40 1961-90 Annual mean wind speeds (m/s)

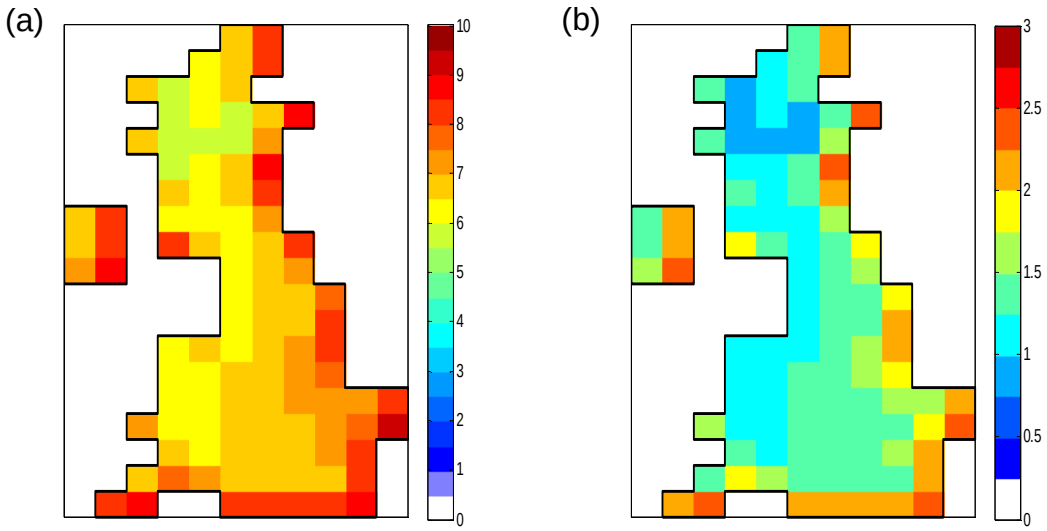

Fig. 4-21 Baseline (1961-90) annual RCM data

(a) wind speed (m/s); (b) energy production on UKCIP grid (annual GWh per single turbine)

4.4.2 RCM future projections for wind and energy

Given that it is of higher resolution than ERA40 reanalysis data and seems to include more detail in the representation of UK wind climate, in the following analysis of the UKCIP02 results for wind speed, the baseline climate for the period 1961-90 was taken directly from the RCM. The seasonal mean wind speed for each of the 'land' grid cells was scaled to 80m height using the $1/7^{th}$ power law, then used to generate an assumed Rayleigh distribution (a Weibull distribution with the shape parameter (k) set to 2). The binned wind speed distribution was then combined with the power curve of a single Vestas V90 3MW wind turbine (Vestas, 2004) (see Fig. 3-1a). For each speed in the distribution, therefore, there is an associated probability (frequency) from the binned distribution and an output power from a turbine, allowing a calculation of the energy output over a given period at each speed. The summation of these provides a baseline estimated annual energy output for a turbine in each of the grid cells. A second annual energy output was calculated using the projections for wind speeds for the three future periods, 2020s, 2050s and 2080s under each of the four emissions scenarios. The percentage changes versus baseline wind speeds and potential wind energy output for each season are discussed below for the high emissions scenario in the 2080s, given that this was the period and emissions scenario to show the most significant changes.

4.4.2.1 Annual changes

The overall changes in annual wind speed and the subsequent projected changes in annual wind energy output are relatively small when averaged over the entire UK. Seasonally, however, there are some more significant projected changes in wind speed leading to changes in annual energy output that would be quite serious for the industry.

4.4.2.2 Winter

In winter, as can be seen in Fig. 4-22, most of southern and midland England and Wales see an increase in the mean wind speed of 5-10%. Northern England, Northern Ireland and most of Scotland are less affected, with increases of around 5%. The most northerly parts of Scotland, however, see a slight decrease of up to 5% in

the mean wind speed. The consequent changes in annual energy output follow similar patterns but with greater magnitude than changes in wind speed. The southerly parts of the region see an increase in wind energy of up to 15%, reducing to 5-10% in northern England and Scotland. The north of Scotland sees a small decrease in energy production.

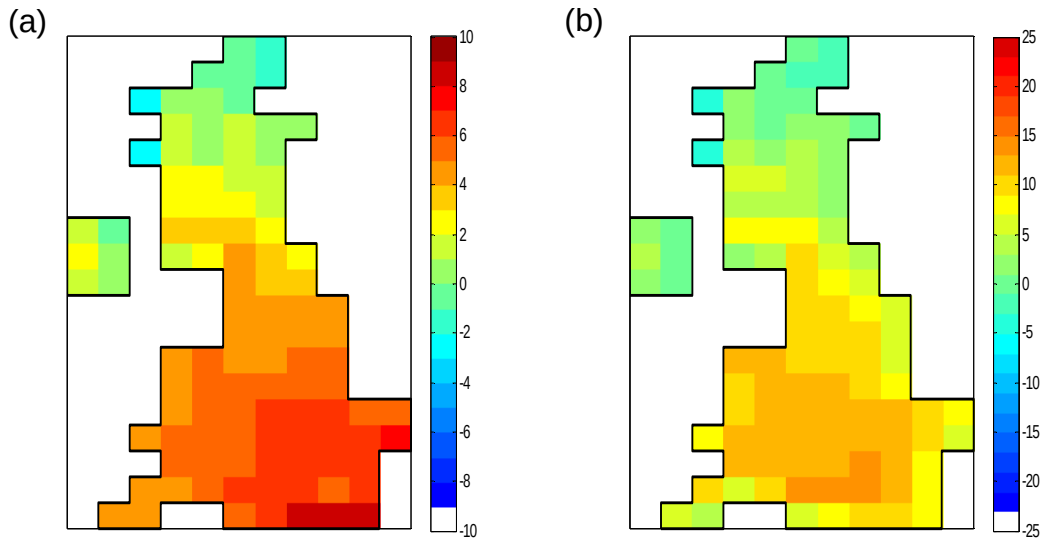

Fig. 4-22 Percentage changes in winter by 2080

(a) wind speed; (b) energy production

4.4.2.3 Summer

Referring to Fig. 4-23, summer projections show broadly the opposite trends to winter, with most of the UK seeing reductions in mean wind speed of 5-10%, with parts of western Scotland and Northern Ireland seeing decreases of up to 15%. Some isolated parts such as the north coast of Scotland and the south coast of England show increases in mean speed of up to 5%. In terms of energy production, the pattern is, again, obviously similar but more extreme. The projected decreases in annual energy output in parts of Northern Ireland and the west of Scotland reach 25%. Northern Scotland and parts of the south of England, conversely, see increases of 10-15%.

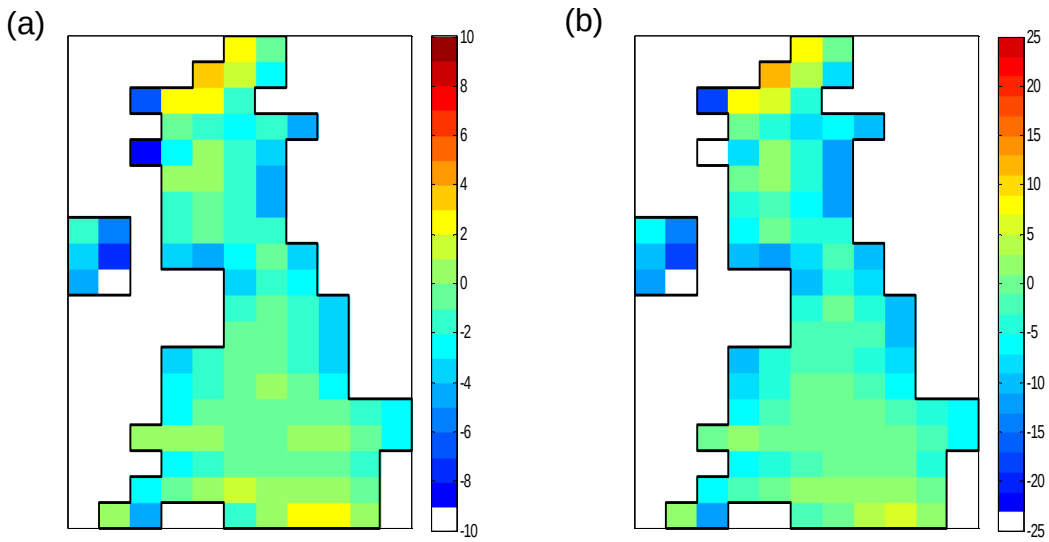

Fig. 4-23 Percentage changes in summer by 2080

(a) wind speed; (b) energy production

4.4.2.4 Autumn and Spring

Autumn and spring projections for wind speeds and corresponding energy outputs generally show smaller changes versus the baseline than for summer and winter. Fig. 4-24 demonstrates that much of the country sees a small decrease in wind speed of 5%, with a decrease in energy of 5-10%, in autumn. Parts of northern and western Scotland show speed increases of 5%, creating energy increases of up to 10%. The whole region is projected to see an increase of around 5% in wind speed in spring, as shown in Fig. 4-25, giving rise to energy increases of 5-10% in most parts.

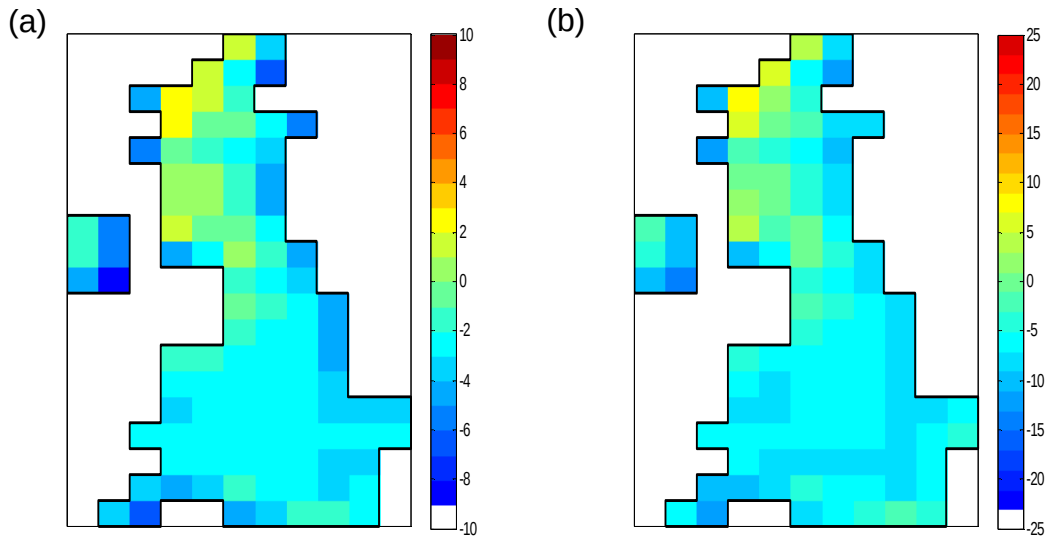

Fig. 4-24 Percentage changes in autumn by 2080

(a) wind speed; (b) energy production

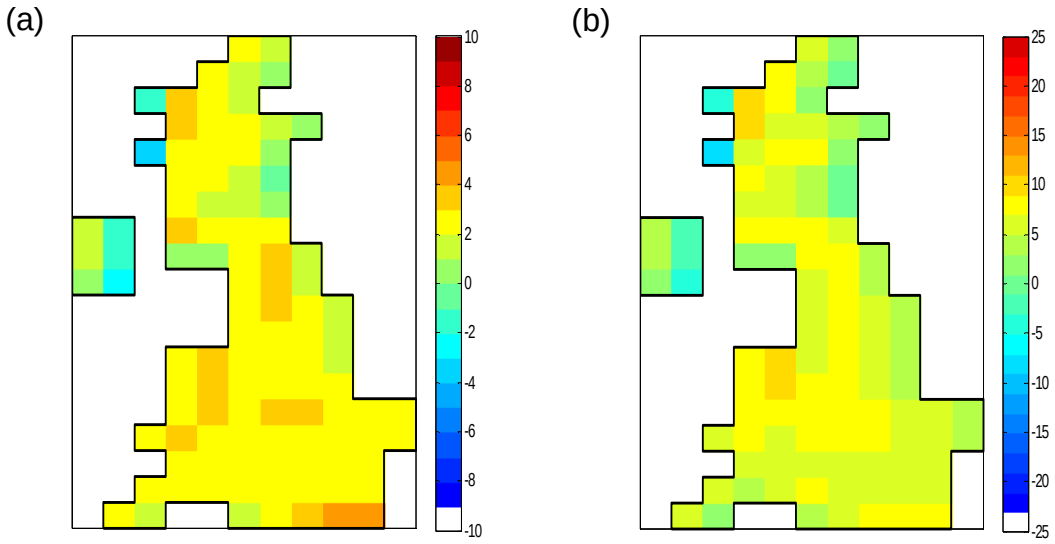

Fig. 4-25 Percentage changes in spring by 2080

(a) wind speed; (b) energy production

4.4.2.5 Specific locations in detail

In order to investigate further the different projected trends in different parts of the UK, five disparate locations (see Fig. 4-26) were chosen and their changes in mean wind speed and annual energy production for each month were plotted, shown in Fig. 4-27.

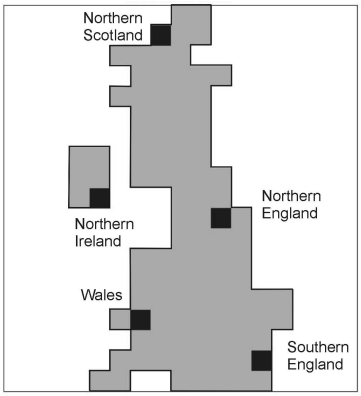

Fig. 4-26 Locations for monthly analyses

The changes in the cells located in England and Wales follow fairly similar patterns, with the increases in wind speed peaking at 5-7% in December and January, falling fairly steadily to an unchanged mean in July. August, September and October are projected to have decreased mean speeds of 3-5%, with November similar to July, experiencing no significant change. The energy production trends represent an amplified version of the wind speed trends, with a range of ±10%.

As noted in the analysis above, the grid cell representing the north of Scotland shows a somewhat different pattern to most of the rest of the region. The tendency is for the mean wind speed mainly to increase, with only very minor decreases in January and February. The maximum increase in wind speed of around 5% is projected to be in the months of May, June and July, with October and November showing increases of 2-3%. These translate to energy output increases of 20% in summer and 5% in the autumn.

The exceptional trend in this part of the UK may be linked to the high dependency of its wind speeds on the North Atlantic Oscillation. This teleconnection pattern, characterised by a low pressure centre over Iceland and a high pressure centre over the Azores, has a large effect on the winter wind climate in the UK. Its

effects are more dominant in northern and western Scotland (Corbel *et al*, 2007) than in other parts of the country; and there is some evidence that it will tend to be more positive in the future under increased greenhouse gas emissions than in previous years (Meehl *et al*, 2007).

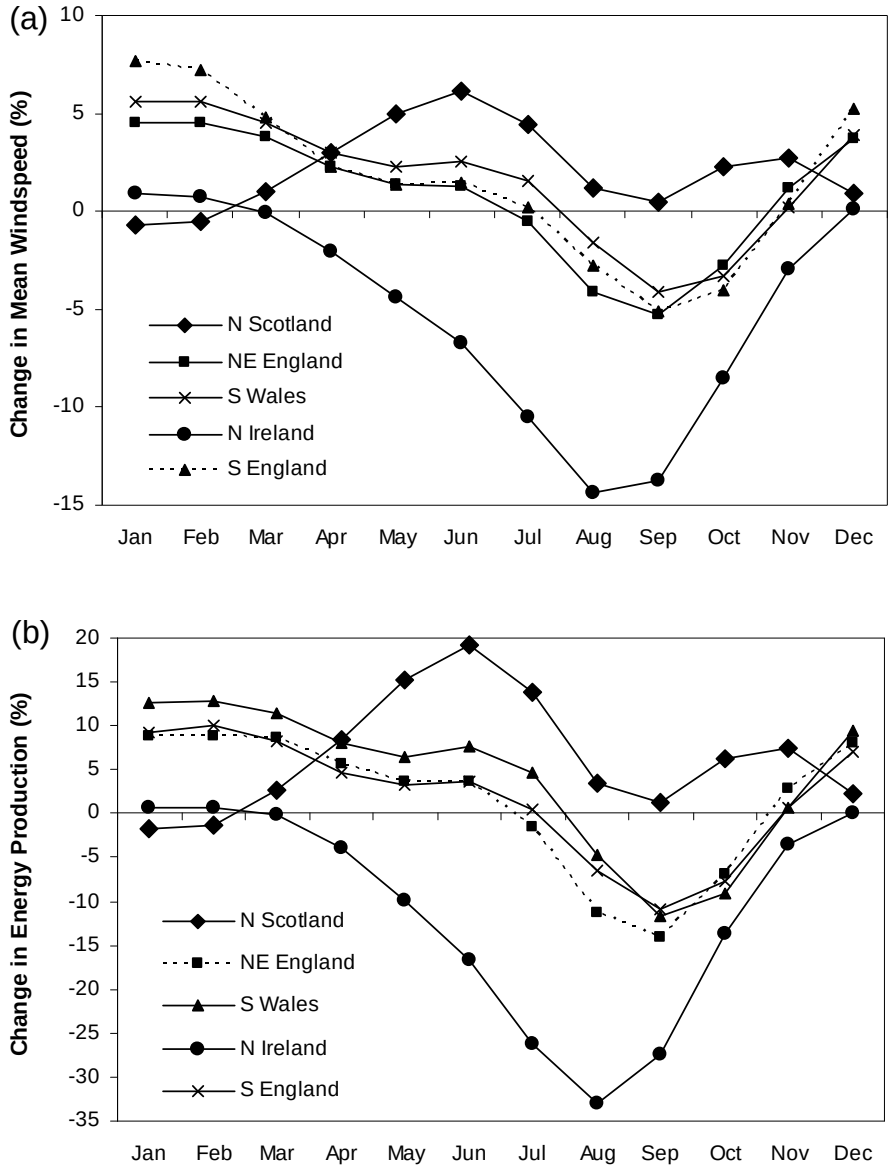

Fig. 4-27 Percentage change at five locations by 2080

(a) Mean wind speed; (b) Energy production

The cell located in Northern Ireland also bucks the general UK trend given by the model. It displays the opposite pattern to that of the northern Scottish grid cell, giving minor increases in wind speed in January and February with decreases in all other months. Of particular note are the decreases from May through to September, which peak at 15%, giving rise to a decrease in energy output of almost 35%. It is difficult to pinpoint why this may be the case, but there is a possibility that the poor resolution of the model and its failure to capture the coastline sufficiently well has resulted in an unrepresentative climate.

4.5 Conclusion

On the whole, it was found that the ECH5 GCM broadly captured the wind climate of the 1961-90 control period, showing similar mean wind speeds and directions in most months to that of the ERA40 reanalysis. Both Run 1 and Run 4 gave similar results and correlated about equally well with the reanalysis data. When averaged over the region, the monthly mean values were slightly overestimated in the GCM in both runs. The projections of change were, when averaged over the entire year, rather small and unlikely to be of significance to the energy output of a wind farm. However, changes in individual months were on a greater scale and if they were expected to occur, could influence strategies within the power industry.

The results of future projections from the HadCM3 model were examined indirectly through the analysis of a regional climate modelling project, which utilised HadCM3 to provide boundary conditions to a LAM. A qualitative look at the baseline climate from the LAM confirmed its general similarity to the ERA40 reanalysis data for the 1961-90 period. Future projections for the 2080s under a 'high' emissions scenario - similar conditions to those examined for the ECH5 GCM - showed that, like the GCM, on an annual basis the projected changes were relatively small, but that individual months show changes that may prove important. The investigation of results from specific grid squares also highlighted that the trends in all parts of the UK do not follow the same pattern.

Correspondence between the results from the ECH5 GCM and the RCM was closer than anticipated. There is fairly good agreement between both models with regard to the 'sign' of the seasonal trends, both suggesting that the majority of the

country will experience a reduction in summer wind speeds and an increase in winter mean speeds by the 2080-2100 period. Of particular interest is the difference in trend shown for the north of Scotland compared to the southern half of the mainland UK, which is captured somewhat in the GCM as well as the RCM, with the GCM showing a positive change in summer months in the far north of Scotland. Unlike the RCM, the GCM does not show a negative change in winter in this region – except against a Run 1 baseline in December – but does indicate negative trends in the offshore area to the north west of Scotland.

When considering these results and in particular their effects on wind power production in the UK, two problematic questions arise. Firstly, are the low resolution data representative enough of wind climate to be of use to the industry? Secondly, is the uncertainty involved in the underlying dynamics and physics of the climate models - especially when compounded with the uncertainty associated with the resolution issue - too great to allow any realistic conjecture to be made from their projections about the consequences for wind energy production? The answer to these questions is that there are probably too many uncertainties and the resolution is certainly not sufficient to enable the data to be used directly in, for example, a detailed resource assessment. However, they do provide information about the potential scale of projected changes, based on sensible assumptions about emissions scenarios, as well as in-depth knowledge of atmospheric physics and dynamics. This kind of awareness is useful from a strategic point of view and opens the door for further analysis as the models become more sophisticated.

Chapter 5

The relationship between pressure and wind climate

This chapter aims to use larger scale climate variables which are more successfully modelled by a GCM as a proxy for surface wind speed, in order to investigate the potential for wind speed change in a future undergoing climate change.

The North Atlantic Oscillation (NAO) is introduced and its possible link with surface wind speeds in northern Europe discussed. Analysis is carried out to show correlation between the NAO and UK wind speeds from reanalysis data. The future trends of the NAO as modelled by a GCM are presented, together with suggestions as to what this might infer for UK wind climate.

The relationship between regional mean sea-level pressure fields and the wind climate of the UK is discussed, and a method for the derivation of geostrophic wind from pressure gradients is presented. Geostrophic winds from a GCM are derived for an historical control period and their correspondence with geostrophic winds from a reanalysis dataset analysed. The trends modelled by the GCM for geostrophic winds in a future period are shown and their potential implications for surface winds considered.

5.1 Proxies

In Chapter 4, it was noted how GCMs use parameterisations to represent sub-grid scale processes, and how these parameterisations do not always produce adequate simulations of surface wind climate at GCM resolution - for the purposes of, for example, wind energy resource estimation. There is also some suggestion that dynamic downscaling of GCMs using regional climate models (RCMs or LAMs) with cell sizes of 25-50km, gives too low a resolution to capture the high spatial variation in wind climates (Pryor *et al.*, 2005d).

For the wind energy industry, the relevant time-scale for consideration of climate variability at individual sites is around 20-25 years - the expected lifespan of a wind turbine or wind farm. Attention is focussed particularly on the near-surface wind climatology - whether time series or projected distribution - as this can be

readily used to calculate expected energy production. It is understood that these kinds of localised wind analyses are highly particular to individual sites; the mean local wind climate being very strongly related to the regional topography, terrain and so forth. In terms of developing a broader view of the industry and devising a strategy for exploiting wind power as much as possible, time-scales considered can be anything from 20 to 100 years. Accurate site-specific wind climates are fairly irrelevant in this case; rather it is the regional climate, its spatial variability and temporal tendencies which are the focus. It may be interesting in light of this to consider using large-scale climate variability as a proxy for near-surface wind climate, in order to understand if climate models could be indicating broad changes in UK regional wind climate over the coming century, and if so, what can be done to best position the wind power industry to make optimum use of the resource.

AOGCMs have been shown to be better at describing historical climate characteristics on a macro scale, perhaps at hundreds of kilometres, rather than factors of the scale of surface winds (Wilby *et al.*, 2004). Pressure patterns, which vary on these larger scales, have been used to generate downscaled higher resolution surface wind climate from AOGCMs in a number of studies (e.g. Pryor *et al.*, 2005b; Sailor *et al.*, 2008). As such, they are known to be very closely related to wind climate. Before embarking on a downscaling process, two methods of analysis of pressure patterns and their relationships with wind climate have been given consideration in this section:

1. The NAO index – This is defined as the normalised difference between a low pressure centre over Iceland and a high pressure centre over the Azores (Osborn, 2000). The NAO is known to strongly influence the UK climate, particularly in the winter months, and its future evolution may provide evidence of long-term shifts in the climatology.
2. Geostrophic wind is a wind field derived from pressure gradients and is representative of frictionless balanced flow. It was reasoned that deriving the theoretical geostrophic winds from the pressure gradient information may give more useful information than pressure fields alone; this is because calculation of the geostrophic wind vector allows obvious analysis of both wind speed and direction changes.

5.1.1 Pressure patterns in the UK

The mean pressure field in the area over northern and western Europe is dominated in all seasons by a region of low pressure around Iceland - the 'Icelandic Low' - and a high pressure centre near the Azores - the 'Azores High'. These areas move and vary in intensity, but are normally present in all seasons (Barry & Chorley, 1998). Areas of low pressure, known as depressions or cyclones, tend to track eastwards over northern Europe. The presence of a fairly permanent anticyclone over Siberia in winter prevents direct eastward movement of the depressions, and they travel either over the Norwegian Sea, or the Mediterranean Sea. In summer the depressions, which tend to be less intense in these months, are able to track due east as there is a generally low pressure situated further east, over Asia (Barry & Chorley, 1998).

A peculiarity in the general zonal flow of depressions over northern Europe can be caused by an area of high pressure over Scandinavia, which results in the diversion of the depressions either north or south of its centre - an effect known as blocking. The presence of the Scandinavian anticyclone causes easterly winds over Britain as the air moves around it, bringing very cold air to the region (Barry & Chorley, 1998).

Lamb (1950; 1977) identified seven primary categories of airflow pattern associated with particular isobaric patterns over Britain, each relating to particular weather characteristics (Barry & Chorley, 1998). Frequencies of observation of the seven categories change throughout the year, with 'westerly' being the most common annually. The typical isobaric pattern for this type includes a fairly intense low pressure system over Iceland, and a high pressure area with a centre at around the same latitude as northern Portugal, but around 10 degrees west of its coast. The Lamb objective classification system has been further extended in Jenkinson & Collison (1977) to include a full range of directional types and a number of hybrid weather types, and can thus be applied to any region. Another weather classification system which extends to the whole of Europe is the 'Grosswetterlagen' system, literally meaning 'general weather situation'. The most recent version is attributed to Hess & Brezowsky (1977) and it defines 29 distinct airflow patterns each lasting at least 3 days (James, 2007). An objective classification system developed by James

(2007) to identify Grosswetterlagen types from ERA40 reanalysis data for the period 1952-2002 found that the three most prevalent types were westerly types: 'anti-cyclonic westerly'; 'cyclonic westerly'; and 'maritime westerly (block eastern Europe)'. These three types typically feature a dominating low pressure area centred upon Iceland and a high pressure area over or slightly to the west of the Iberian Peninsula, which together bring strong westerly winds to the UK region.

5.2 The North Atlantic Oscillation

As mentioned in 5.1.1, two of the most prevalent features of the north Atlantic mean pressure field are the Icelandic Low and the Azores High. These phenomena are present all year round, and together their variability is linked with and referred to as the North Atlantic Oscillation (NAO). The NAO index refers to the difference between the mean sea-level pressure measured at stations located somewhere near the two centres, often normalised by a long-term mean. The measuring stations most commonly employed are in the Azores and Iceland, but alternative cited sites for the high pressure point are Portugal and Gibraltar (Osborn, 2000). An NAO index can also be derived from the principal component time series of mean sea level pressure at these points - that is, the component within a regression of the two pressure series that explains the maximum amount of variance (Ulbrich & Christoph, 1999).

The NAO is, as mentioned previously, detected in all seasons of the year but is seen to be more related to climate in northern Europe in the boreal winter months of December, January and February (Osborn, 2000). Some studies refer to an 'extended winter' NAO index which also includes November and/or March (e.g Osborn *et al.*, 1999). The index typically oscillates between around -3 and +3; a negative NAO implies a weakening of the low and high pressures, whilst a positive NAO suggests a strengthening of the pressure centres (Hurrell *et al.*, 2001). Evidence suggests that the strength of the NAO may have an influence on the wind climate of the north Atlantic. A swing from the positive to the negative phase will produce changes in the mean speed and direction in the region, according to Hurrell *et al.* (2003). Pryor & Barthelmie (2003) indicate that positive phase NAO indices are associated with stronger westerly winds, whilst negative indices give rise to greater 'meridionality', i.e. in the south-north direction. This latter study found that

half of the variability of mean winter wind speeds in the Baltic Sea area could be explained by the NAO index. The effects of the NAO on regional wind speeds in the UK is not well defined. Siegismund & Schrum (2001) found a correlation of 0.69 between the NAO index and mean winter wind speeds in the North Sea area, which lies to the east of the UK, but due to the position of the UK landmass to the west and the Scandinavian peninsula to the east, this region might be expected to experience a different wind climate to that of the UK. One of the only studies concerned specifically with the UK is the work of Corbel *et al.* (2007) in which the authors found a strong correlation between the NAO and both the occurrence of 'gale days' and the occurrence and frequency of south-westerlies during winter in a westerly location in Scotland. Woolf *et al.* (2002) also identified a very strong relationship between the NAO and wave height in the north Atlantic to the west of the UK, which is interesting given the strength of the relationship between wind and wave climates.

Two of the studies mentioned above (Pryor & Barthelmie, 2003; Siegismund & Schrum, 2001) observe that the trend of the NAO index over the last number of decades has been increasing, whilst also noting that mean wind speeds in the regions under discussion have increased. Siegismund & Schrum (2001) define three distinct types of change in the wind field in the years 1958-1997 over the North Sea area: two involving increases in the occurrence and intensity of west-southwesterly wind directions; and one relating to an increase in mean speed for southerly winds. They hypothesise that each of these may be connected with the positive trend in the NAO index. Pryor & Barthelmie (2003) states that an increase in the annual mean wind speed over the Baltic region has been caused by an increase in cyclonic activity, resulting in higher pressure gradients which in turn are due to a higher frequency of positive-NAO winters.

The trend over the last 30-40 years for the NAO to increase is interesting in light of a possible connection to anthropogenic GHG emissions. Gillet *et al.* (2003) looked at a number of studies using statistical models to define whether or not the last 30 years of the winter NAO have been 'unusual'; and whilst some models do find significant trends in the data, others do not. Reconstructions of NAO indices that go back for several centuries show that the current upward trend is not, in fact, unusual; (e.g. Cook & D'Arrigo, 2002) but caution is strongly advised regarding the

inherent uncertainty of these reconstructions, and an awareness that there may have been possible external forcings on past climate.

5.2.1 Relationship between the NAO and wind speeds in the UK

Following on from the work of Corbel *et al.* (2007), Pryor & Barthelmie (2003) and Siegismund & Schrum (2001), it was postulated that, given a high degree of correlation between wind speeds in regions to the east of the UK with the NAO index - and in a particular location in western Scotland - there could be a similarly strong correlation between mean winter wind speeds in the whole of the UK area and the NAO index.

For the purposes of the analysis the wind data employed are the 10m u (eastwards) and v (northwards) wind speed vectors from the ERA40 reanalysis model (European Centre for Medium-range Weather Forecasting, 2006), obtained from the BADC. The NAO index obtained from Salmon (2004) has been derived from station data in Iceland and the Azores. Comparing model data with observed time series may be seen as contentious, but it is assumed here that the ERA40 data is reliable enough to be used as a substitute for observed data.

Considering firstly the whole UK area, the mean winter wind speed averaged over the area 48˚ to 61˚ north and -12˚ to 3˚ east was calculated from the u and v vectors for each year in the period 1961-90 and compared with the documented NAO index. A plot of the observed winter (December to February) NAO index alongside the mean ERA40 winter wind speed in Fig. 5-1 appears to show correspondence between many of the yearly values, and a very similarly increasing trend in each of the datasets. Fig. 5-2 shows a simple linear regression between the two datasets, which gives an R^2 correlation coefficient of just over 0.5, indicating that the UK mean winter wind speeds have a similar relationship with the NAO as those in the Baltic study region from Pryor & Barthelmie (2003).

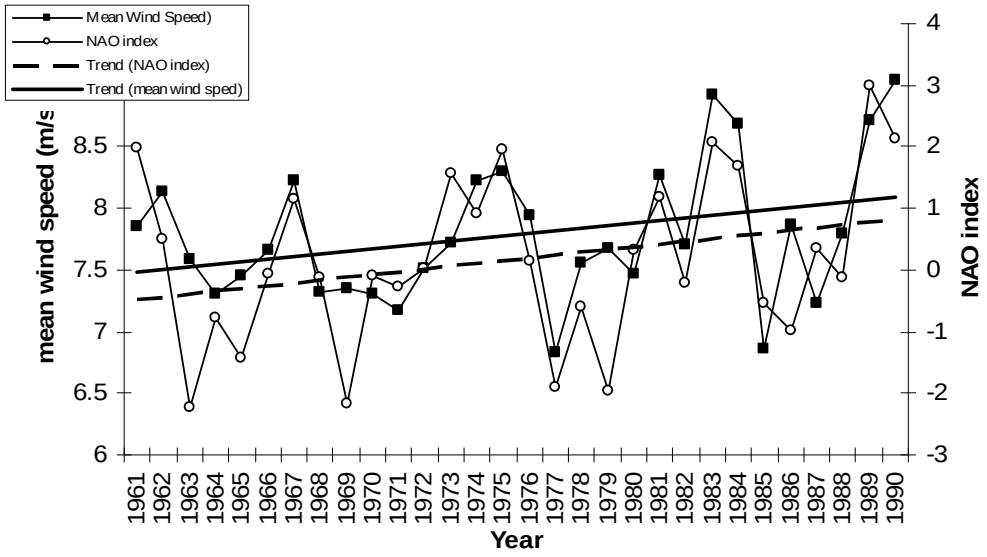

Fig. 5-1 Winter NAO index and mean UK wind speed 1961-90

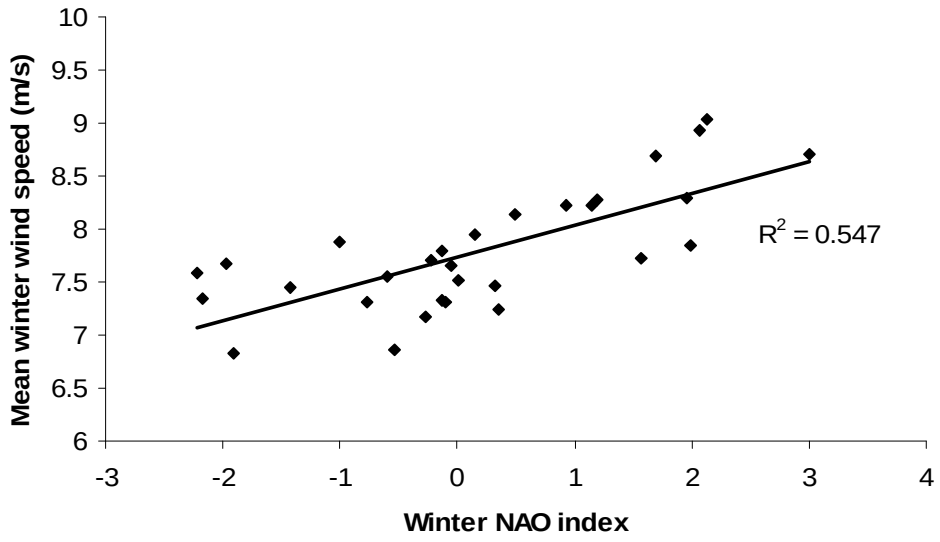

Fig. 5-2 Correlation between mean winter wind speed and the winter NAO 1961-1990

The ERA40 mean winter wind speeds for 1961-90 have also been analysed on a grid cell basis, comparing the results for each with the winter NAO index for this period. A pictorial representation of the R^2 correlation coefficients for the area is shown in Fig. 5-3, a to c.

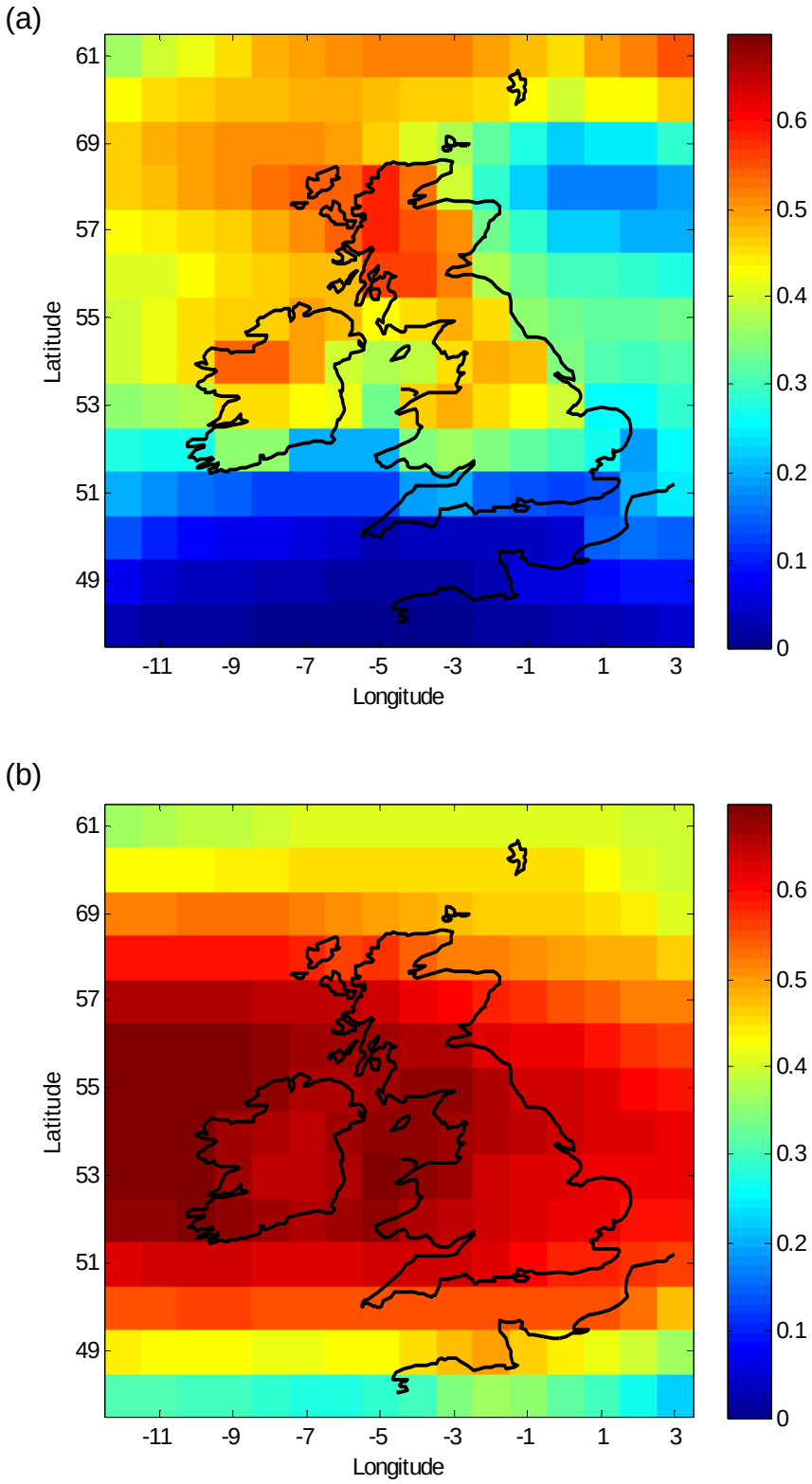

Fig. 5-3 R^2 correlation coefficients for mean UK winter wind speeds vs NAO Index

(a) mean resultant wind; (b) mean u wind

(c)

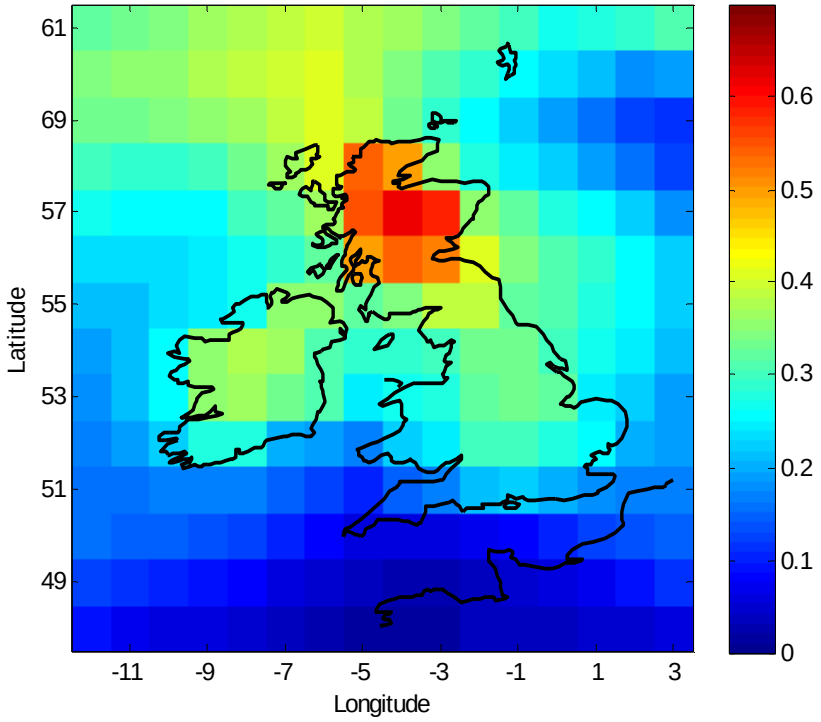

Fig. 5-3 cont. R^2 correlation coefficients for mean UK winter wind speeds vs NAO Index

(c) mean v wind

It is clear from this that the highest correlations with averaged winter wind speeds are to be found, perhaps unsurprisingly, on the north western coasts of the UK and Ireland. Similarly, Corbel *et al.* (2007) found that for three sites in Scotland, the one in the most westerly location had the strongest relationship with the NAO. Carrying out a grid cell analysis for u (westerly) and v (southerly) wind speeds separately, the correlations, as expected, are higher for u wind alone than for the mean speed but show a slightly different spatial pattern, with onshore mainland UK areas having more consistent R^2 values, of between 0.5 and 0.7. Once more, however, the western areas of the country tend to have slightly better correlations. For v winds, only a small area in the northern half of Scotland has a relatively high R^2 value of around 0.6, whilst the remaining area has values around 0.2-0.4, indicating a more tenuous correlation with this component of wind speed.

These results are in fairly good agreement with Corbel *et al.* (2007), which suggests that there is a strong correlation between winds occurring in the sector 180-

270˚ in western Scotland and the NAO index. In both the case of the mean overall wind speed and the u wind vector, the relationship with the NAO is positive, suggesting that as the index becomes increasingly positive, the mean wind speed, and in particular the westerly component, becomes stronger. This supports the theory of both Pryor & Barthelmie (2003) and Siegismund & Schrum (2001) that a more positive NAO index involves a strengthening of the westerlies. Siegismund & Schrum (2001) also suggest that the NAO is

> *…positively correlated to the number of nearly stationary cyclones centred south east of Greenland. This may be related to the increase in southerly wind directions for the northern North Sea*.

Together, the results suggest that an increase in the NAO index will lead to greater wind speeds in both the eastwards and northwards directions, something which may be of relevance to this research later on.

The correlations found in this exercise are not of sufficient value as to generate confidence in the use of the generated linear relation, in a quantitative manner, to project changes in wind climate under an overall climate change scenario. That said, the link is potentially useful in a qualitative sense, in enabling estimation of the possible magnitude of projected changes in wind speeds and directions affecting the whole of the UK area. Given that up to 50% of the variability in mean wind speed is explained by the NAO index, application of the derived relationship might allow for some insight into future changes - albeit that the factors influencing the other 50% might add to or indeed counteract these changes. However, it must first be ascertained whether or not the NAO can be successfully modelled by GCMs, and whether the future projections of the oscillation can be relied upon.

5.2.2 Modelling the NAO - past

Some debate surrounds the ability of GCMs to capture the variability of the NAO. According to Hurrell *et al.* (2001), it has been assumed in the past that the NAO results from a combination of internal atmospheric processes and is thus inherently difficult to predict. A number of studies have investigated the phenomenon's presence in various climate models. Osborn *et al.* (1999) examined how well the AOGCM HadCM2 was able to reproduce the historical variability of the NAO index. They found that using present-day radiative forcing conditions,

…in a temporal sense the simulation is compatible with the observations if the recent observed trend…in the winter NAO index is ignored.

The observed trend, from 1961-90, as shown in Fig. 5-1 was not found to be reproduced in the control run of the model, and the authors state that this could be due to either model deficiencies or external forcings not present in the model, i.e. increased anthropogenic emissions. Similarly, Ulbrich & Christoph (1999) found that for a control run of the ECH4 model, no trend in NAO index was present, suggesting that the last 30-40 years have been anomalous.

5.2.3 Modelling the NAO - future

The work of Osborn *et al.* (1999) states that different climate models appear to respond differently to anthropogenic forcings and, whilst their results using HadCM2 suggest a future forcing would lead to a decreasing winter NAO index, other studies using different GCMs find an increasing trend in the index. A study primarily concerned with the response of the Arctic Oscillation (AO) - which is closely related to the NAO - to increasing greenhouse gas concentrations (Gillet *et al.,* 2002) found that the successor to HadCM2, HadCM3 showed a positive relationship between increasing GHGs and the NAO index. They found similarly "unambiguous" positive relationships in three other GCMs: ECHAM3, ECHAM4 and GISS-S. In their paper, Gillet *et al.* (2003) summarise the findings on the response of the NAO to increasing anthropogenic greenhouse gas emissions from twelve GCMs. Three have a response which is either not significant or is dependent on the definition of the NAO index used; the remaining nine models all show the response of the NAO to the increasing GHG concentrations to be positive, i.e. increasing. Given the time lag in the climate system, it may be too strong to state that the NAO index has shown an increasing trend over the last 30 years due to increasing GHG emissions but these results are certainly interesting.

All of the above studies note the differences found when various definitions of the NAO index are used. When station-based indices are employed, i.e. mean sea-level pressure is computed at fixed points over time, there is an assumption that the centres of action are stationary over this time frame. It was noted in Ulbrich & Christoph (1999) that in the ECHAM4 model, the centres of action moved under the influence of increasing GHG concentrations, with the low pressure centre moving

eastwards. Pinto *et al.* (2009) also found a 'stretching' of the northern low pressure centre in the ECHAM5 model under SRESA1B, compared with its location in the twentieth Century.

5.2.4 Future NAO trends and wind speeds

Pryor & Barthelmie (2003) analysed the NAO representation in HadCM3, using surface pressure and temperature fields at two points, and compared the probability distribution of daily indices from 1990-1999 under SRES A2 with similar information from the NCEP-NCAR reanalysis dataset. Their results indicated good correspondence between the datasets, and suggest that HadCM3 does accurately describe the NAO for the period of analysis. In terms of future changes, they deduced from their results that for the future period 2000-2030, the winter wind climate in Denmark will be very similar to that of the 1990s.

In an investigation using the ECHAM4+OPYC3 AOGCM, Ulbrich & Christoph (1999) cite a number of studies that connect the NAO with the activity of the Atlantic storm track, and describe how a positive NAO index corresponds with a typically more intense and northerly storm track. They go on to suggest that the recent trend of increase in wind speeds in northern Europe as well as a tendency towards more westerly flow could be linked to a more frequently positive NAO via increased pressure gradients. Thus the increasing NAO index trend evident in their increased GHG simulation of the GCM is consistent with simulations of increasing storm activity and stronger zonal flow in the north Atlantic and over northern Europe.

Pinto *et al.* (2009) also refer to the link between north Atlantic cyclones and the NAO index, with a positive NAO associated with more frequent cyclones and a north-easterly movement of the storm track. In the regions near the UK, the authors find that regardless of the NAO index, the ECH5 model shows an increase in extreme cyclones.

5.2.5 Using ECHAM5 to investigate future changes in the NAO

Bearing in mind that an index derived from two points fixed in space may not be fully representative of the NAO when using GCM future projections, it was decided that a station-based index would allow straightforward like-for-like comparison with

that used in the analysis in section 5.2.1. The locations of the weather station at Ponta Delgada, Azores (37.7˚N, 25.7˚W) and Stykkisholmur, Iceland (65.0˚N, 22.8˚W) (Jones *et al.*, 1997) were used to identify the grid cells from the ECHAM5 (hereafter referred to as ECH5) GCM (IPCC Data Distribution Centre, 2005a) containing these points. The daily mean sea-level pressure time series data from 1961-2000 was extracted for each of the two grid cells and normalised by the monthly means and standard deviations from the whole period as in Jones *et al.* (1997). An NAO index was then calculated for the model by subtracting the Azores normalised pressure from the Iceland normalised pressure. The results are confirmed by Demuzere *et al.* (2008), who used a similar method to calculate their NAO index from the same GCM, and get very similar values.

For the period 1961-2000, the results of the time series are plotted in Fig. 5-4, alongside the observed index from section 5.2.1. The correspondence in terms of time series values is low, but in terms of the probability distribution of values, the two series show some similar properties. Interestingly, the minimum (-3.9) and maximum (+3.6) points in the ECH5 series fall outside of the range of the observed index used here, which has a minimum of -2.2 and a maximum of 3. They are, however, close to being within the range of another station-based NAO index (Hurrell, 1995), which has a minimum of -4.3 and a maximum of 3.4 and so it is supposed that these values are not impossible.

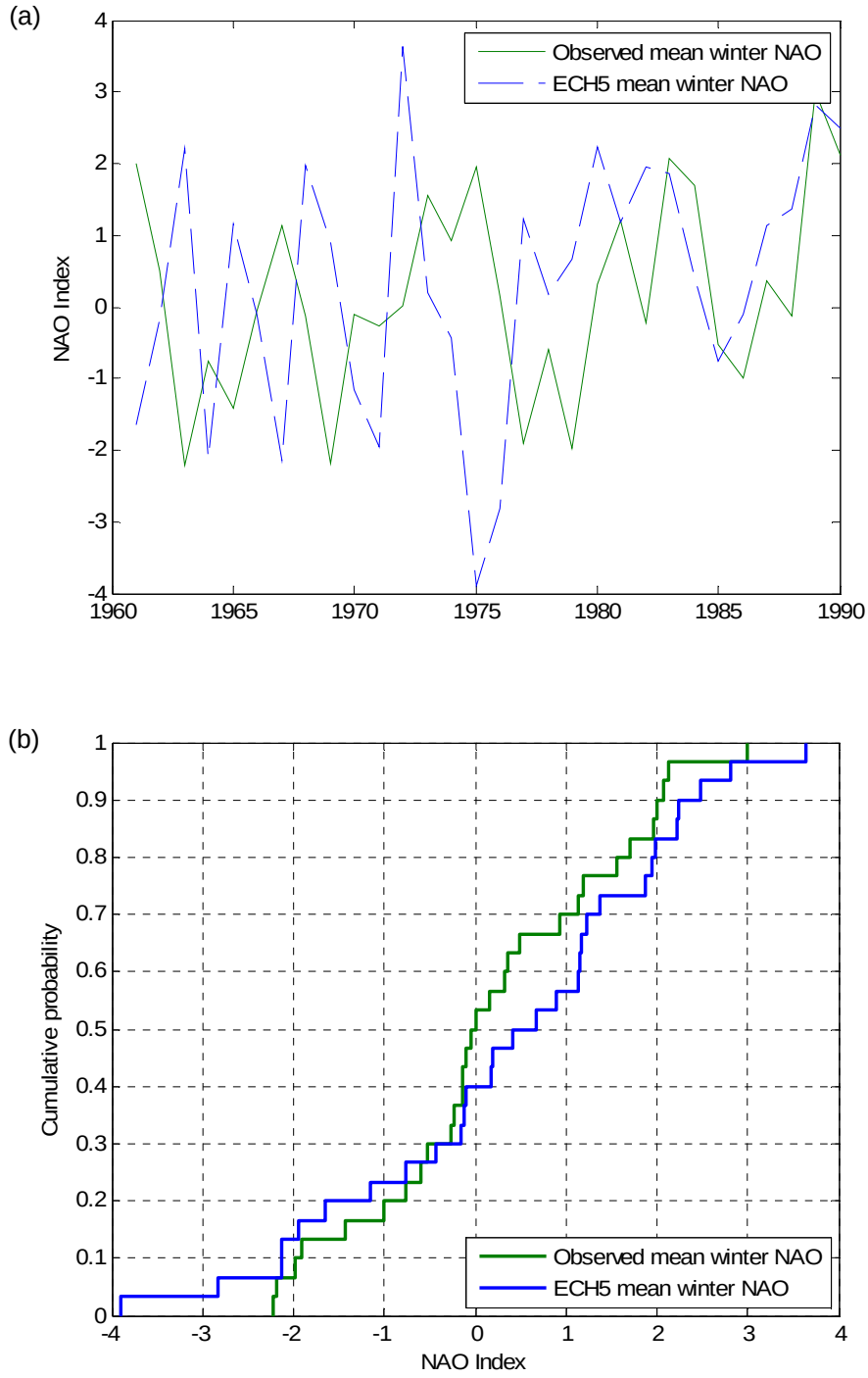

Fig. 5.4 Mean winter (DJF) NAO index

(a) Observed and ECH5 modelled 1961-90; (b) Cdf plot of observed and ECH5 modelled 1961-90

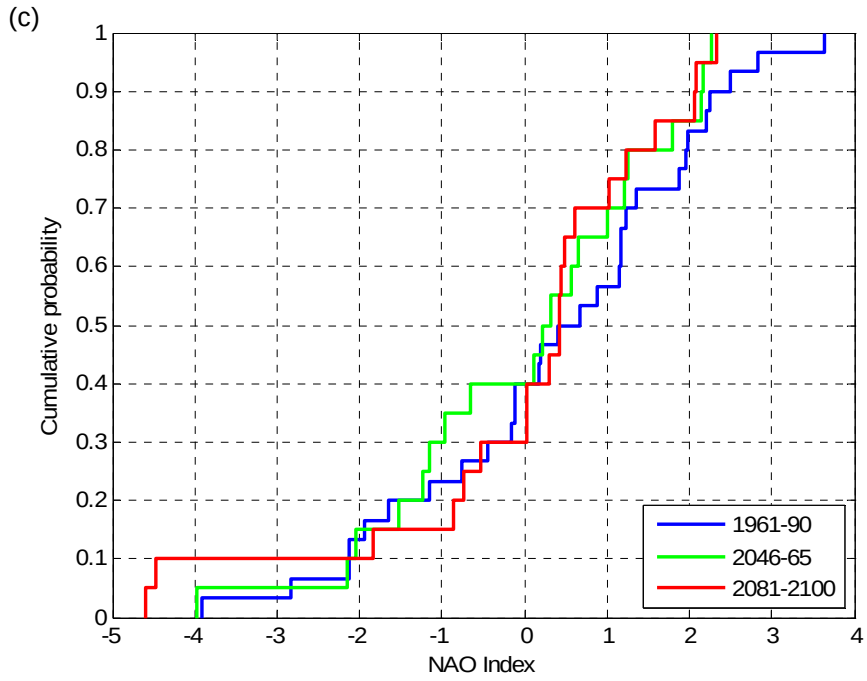

Fig. 5-4 cont. Mean winter (DJF) NAO index

(c) Cdf plot of ECH5 modelled 1961-90, 2046-65 and 2081-2100

Given that ECH5 does appear to produce values for the NAO index that are within a sensible range, an NAO index was derived from the model for two future periods: 2046-2065 and 2081-2100 (IPCC Data Distribution Centre, 2005b). The cumulative probability distribution (cdf) for these indices are shown superimposed on the 1961-90 distribution in Fig. 5-4c. It is here that the difficulties of using an index based on fixed points may arise. The cdf for the two future periods show a slight tendency to stretch out in the negative NAO direction, implying a weakening of the pressure gradient between the two centres of action. However, considering the results from the ECHAM4 model in Ulbrich & Christoph (1999) where it was found that the low pressure centre moved in future model projections, it could be that the weakening seen in the results here is a result of this movement. The pressure will naturally be slightly higher at some radius from the cyclone centre, and thus the gradient from here to the high pressure centre will be smaller and give a more negative NAO index.

5.2.6 What do these results imply for UK wind climate?

There are two distinct problems presented by the analysis above. The first is that because the observed NAO index explains only up to 50% of the variance in UK

mean wind speeds, the factors contributing to the remaining variance could either compound or counteract the effects of a change in the NAO regime. The other underlying influences need to be identified, quantified, and the results analysed simultaneously in order that all possibilities be examined. The level of uncertainty is too high to permit taking the derived relationship between mean wind speed and the NAO index and extrapolating it into the future using GCM NAO projections.

The second problem arises from the derivation of a station-based NAO index from the future GCM mean sea-level pressure projections. The literature suggests that whilst indices based on fixed points are potentially valid, there is some evidence that a change in the spatial location of the NAO pressure centres may occur under increasing GHG forcings. It is thus difficult to make even any qualitative suggestions based on the station-based indices as to what the future might entail for the UK wind climate. Suffice to say, the results from this analysis ought to be interpreted with a great deal of caution.

Ideally, further analysis, perhaps using principal component analysis of the sea-level pressure fields, would allow the development of a better-defined NAO index for the future. It is felt, however, that because the relationship between the NAO and UK mean wind speeds is not as strong as was initially hoped, there is more to be gained by investigating the relationship between regional pressure fields and wind climate in more detail instead.

5.3 Geostrophic Wind

The geostrophic wind is a theoretical idea representing a balance in atmospheric flow between the pressure gradient force and the acceleration of air due to the Coriolis effect as a result of the Earth's rotation. The horizontal pressure gradient force (*PGF*) drives the movement of air from areas of high pressure to those of lower pressure, and is expressed per unit mass,

$$PGF = -\frac{1}{\rho}\frac{\partial p}{\partial n} \tag{5.1}$$

where $\frac{\partial p}{\partial n}$ is the horizontal pressure gradient over a distance ∂n, and ρ the local air density (Barry & Chorley, 1998). The Coriolis acceleration, *a*, acts perpendicular to

the wind vector, and is proportional to the wind velocity, V_g, and dependent on latitude, ϕ , such that

$$a = -2\omega \sin \phi . V_g \tag{5.2}$$

where ω is the angular velocity of the Earth and $2\omega \sin \phi$ is commonly referred to as the Coriolis parameter, *f*. Referring to Fig. 5-5, the geostrophic approximation equates these two factors, thereby neglecting the influence of surface friction, such that the geostrophic wind, V_g is expressed by,

$$V_g = \frac{1}{\rho f} \frac{\partial p}{\partial n} \tag{5.3}$$

where $\frac{\partial p}{\partial n}$ is the pressure gradient perpendicular to the wind flow (Gordon *et al.*, 1998).

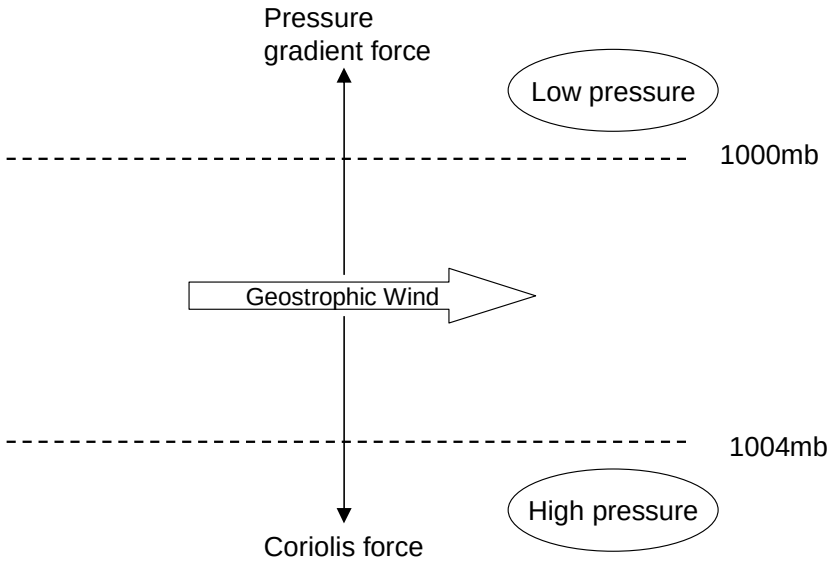

Fig. 5-5 Schematic diagram of geostrophic wind conditions

The geostrophic wind is approximated by the winds above the planetary boundary layer (PBL) where friction has little influence on the flow of air (see section 3.3), and so can be estimated from observed wind climate data at 500-1000m above ground level (Watson *et al.*, 2001; McQueen & Watson, 2006). As well as neglecting the effects of friction, the geostrophic approximation assumes linear, parallel isobars. In

the case of curved isobars, for example due to a cyclone where air is circulating anticlockwise around the low pressure centre, an extra component in the balance is required to take account of the inward centripetal acceleration of the air as it travels in a circular path. The wind in this case is referred to as the 'gradient wind'. The climatology of the UK is such that anticyclones and particularly cyclones are a common feature, and at these times the wind will not be geostrophic. (Barry & Chorley, 1998). It is considered, however, that the magnitude of the centripetal acceleration will be small except in the case of very high velocity winds caused by extreme cyclones. Barry & Chorley (1998) state that these are only of "meteorological significance" when they occur near the equator where the Coriolis force is low - or in the case of tornados.

5.3.1 How well do the GCMs model geostrophic wind?

Before using geostrophic winds as a proxy for surface wind climate, it is of benefit to investigate whether the ECH5 GCM (IPCC Data Distribution Centre, 2005a) reproduces the geostrophic wind climate with reasonable accuracy for an historical control period. The process of determining the skill of ECH5 in reproducing historical geostrophic wind fields for the UK requires comparison of the GCM output with climate records for a typical 30-year period, often taken in the IPCC assessments to be 1961-90. Rather than use data from the small irregular network of observation stations directly for the comparisons in this case, it has been decided that ERA40 reanalysis data (European Centre for Medium Range Weather Forecasting, 2006) would be more suitable - as with the analyses carried out in chapter 4. By interpolating the higher resolution ERA40 data to the lower resolution GCM grid, results for each of the GCM grid squares covering the UK can be analysed, giving consideration to the entire spatial area as opposed to individual sites. Watson *et al.* (2001) demonstrated a good degree of similarity between the NCEP-NCAR reanalysis and observed geostrophic wind data, and it is assumed here that ERA40 reanalysis will show similar success.

5.3.1.1 Calculating geostrophic wind from gridded data

Using gridded mean sea-level pressure data, the components of geostrophic wind in the x (westerly) and y (southerly) direction, labelled u_g and v_g respectively, can be found by considering the geostrophic wind equation in directional form, such that:

$$u_g = -\frac{1}{f\rho} \cdot \frac{\partial p}{\partial y} \tag{5.4}$$

$$v_g = +\frac{1}{f\rho} \cdot \frac{\partial p}{\partial x} \tag{5.5}$$

where, $\frac{\partial p}{\partial y}$ is the mean sea level pressure gradient in the y direction (northward), $\frac{\partial p}{\partial x}$ in the x direction (eastward), u_g is the westerly (eastward) and v_g the southerly (northward) geostrophic wind, and f is the Coriolis parameter (McQueen & Watson, 2006; Gordon *et al.*, 1998).

The value of f varies with latitude, and is calculated from eqn. 5.2 to give,

$$f = 2\ \omega\ sin\phi \tag{5.6}$$

where ω is the angular velocity of the earth and ϕ is the latitude. As the earth rotates $2\pi^{rad}$ in 24 hours, this gives

$$\omega = \frac{2\pi}{24*60*60} = 7.27\times10^{-5}\, rad \cdot s^{-1} \tag{5.7}$$

For simplicity, a latitude of 50˚N has been taken giving constant f = 1.146 x 10^{-4} s^{-1}.

For an area approximately 43 to 66˚ north in latitude and -23 to 24˚ east in longitude, shown in Fig. 5-6b, the reanalysis pressure data were interpolated using cubic splines (via a standard Matlab function) to the lower resolution GCM grid.

(a) (b)

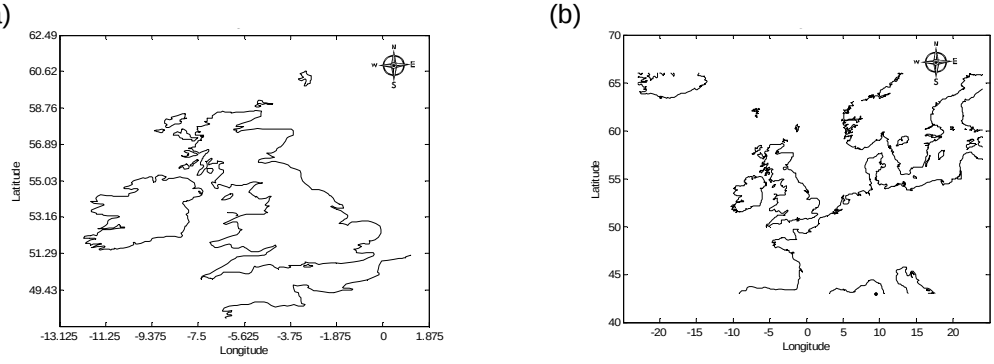

Fig. 5-6 Regions of interest selected

(a) Small region, 48˚ to 61˚ N, -12˚ to 3˚ E; (b) Large region, 43 to 66˚ N, -23 to 24˚ E

The pressure gradients at each point in the grid for both the GCM and reanalysis datasets were then calculated over distances of ±1 grid boxes in the north-south direction and ±2 grid boxes in the east-west direction, which keeps the spacing relatively similar in both directions in terms of metric measurements. (One degree of latitude is approximately 111km, while one degree of longitude in the UK region is approximately 70km.) From the pressure gradients, the u and v geostrophic wind vectors were calculated as per equations 5.4 and 5.5.

5.3.1.2 Spatial average results

A spatial average of the monthly geostrophic wind speeds for the period 1961-90 was calculated over the area approximately 48˚ to 61˚ north and -12˚ to 3˚ east, i.e. that directly covering the onshore UK area, as shown in Fig. 5-6a. Fig. 5-7a compares the results for ERA40 data and ECH5 data showing the individual values for each month in the period.

(a)

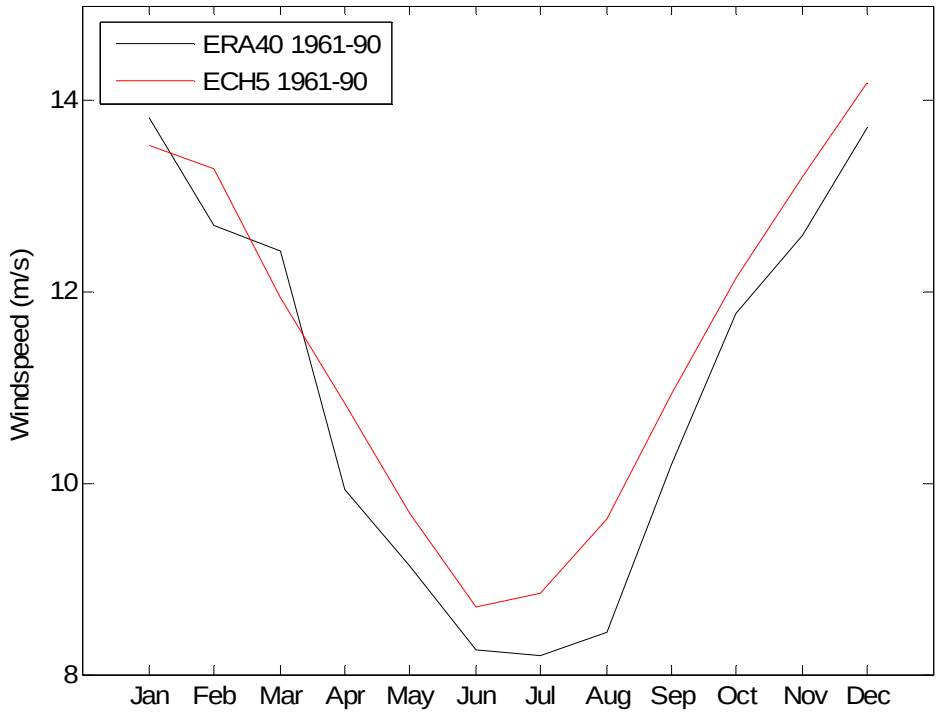

Fig. 5-7 Comparison of ERA40 and ECH5 spatial average monthly means 1961-90

(a) ERA40 and ECH5 monthly means

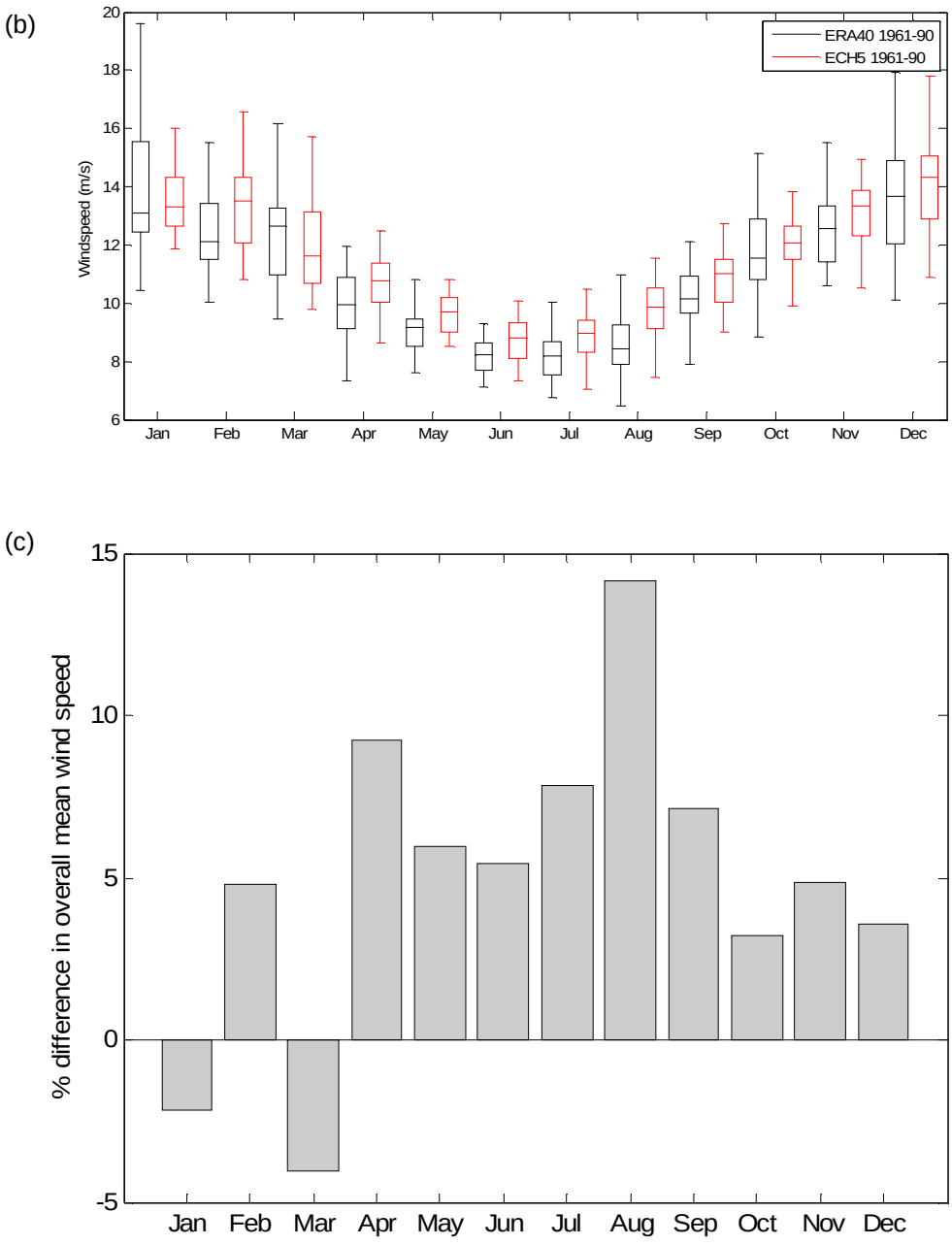

Fig. 5-7 cont. Comparison of ERA40 and ECH5 spatial average monthly means 1961-90
(b) Boxplot of distributions (c) Percentage differences in overall monthly means between ERA40 and ECH5

The typical monthly mean averaged over the entire area is fairly well represented in the GCM compared to the ERA40 dataset, with the recognised seasonal pattern - of highest wind speeds in the winter months and lowest in the summer - being adequately reproduced. The ERA40 model has peaks of 13.43 m/s in December and

13.55 m/s in January, whilst the ECH5 model peaks at 14.20 m/s in December and falls to 13.53 m/s in January. The lowest months for both models are June and July; ERA40 gives values of 7.96 and 7.91 m/s for the June and July respectively, and ECH5 gives higher minima of 8.72 m/s for June and 8.84 m/s for July. Looking at Fig. 5-7c, there is some indication of a high bias in the ECH5 results, which, excluding January and March, are all between 3 and 15% higher than the ERA40 results, with an average percentage difference of around 7% for these months. A possible explanation for this, given in Demuzere *et al.* (2008), is that ECH5 tends to underestimate the MSLP to the north of the British Isles and overestimate it in the Mediterranean Sea area - leading to a larger north-south pressure gradient, which results in a higher magnitude of westerly geostrophic flow.

The range of mean monthly wind climate variability within the two datasets appears to be different, as can be seen in the boxplot of Fig. 5-7c, with the ECH5 model appearing not to capture as broad a range of variability in the mean monthly geostrophic wind speed as the ERA40 model, particularly in winter months. Looking at the range of values for each month, the reanalysis data has particularly high interannual variability in the months of December to March with an average standard deviation of 1.95 m/s; ECH5 has an average standard deviation of 1.52m/s for these months, and is particularly low relative to ERA40 in December and January. This may be simply an issue of resolution, with the GCM unable to resolve some of the extremes either in space or time, but it may also point to a more systematic failure such as the location of cyclone tracks. Further investigation of the spatial characteristics of the two datasets is required.

5.3.1.3 Temporal average results

A map image of the squared correlation coefficients (R^2) between the GCM and the ERA40 data monthly means for the period 1961-1990 (Fig. 5-8) shows that, while the R^2 values are very high in general, the two datasets show better similarity in some areas of the UK than others.

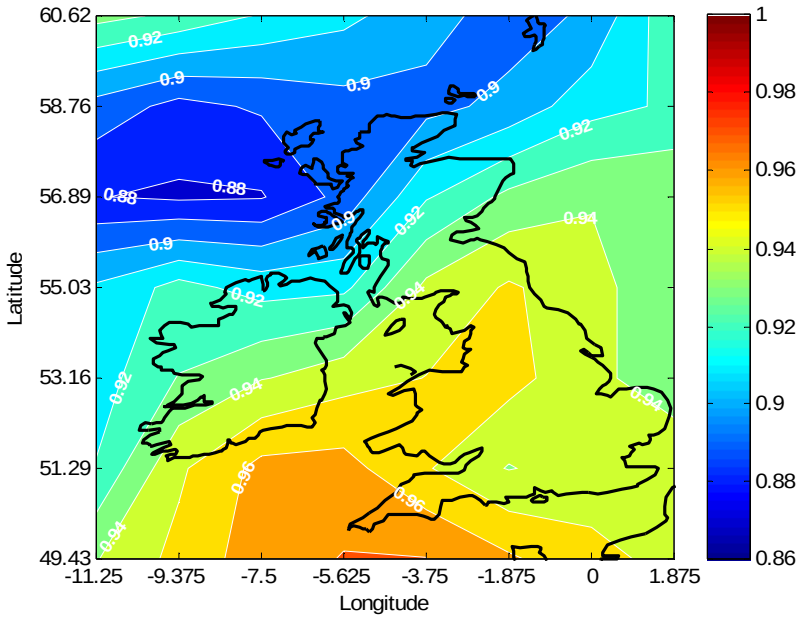

Fig. 5-8 Map of R^2 correlation coefficients between ECH5 and ERA40 monthly means 1961-90

One feature of the pattern appears to be that the GCM is less well correlated to ERA40 in the area to the north and west of the country. This is possibly due to the location of depressions which regularly track eastwards over this region. Their precise track may not be represented identically in the GCM as compared with the reanalysis model.

Taylor Diagrams have been used to asses the success of the ECH5 GCM in replicating the geostrophic wind patterns as defined by the ERA40 reanalysis model. The features described by the graph are discussed in brief 4.2.4 and in further detail in Appendix B. Fig. 5-9a shows that the correlation coefficients for the relationship between the GCM for the larger spatial region and the reference data are between 0.82 and 0.96 for the ECH5 model, a fairly acceptable range of correlation. July and November were the months with the lowest correlation coefficient, and the months of September, October and May had the highest. The standard deviation is similar to reanalysis for some months in this region, with normalised standard deviations for July, August, September, November and December close to a value of 1. June has the lowest value, at 0.58, and April has a value slightly higher than one, 1.10.

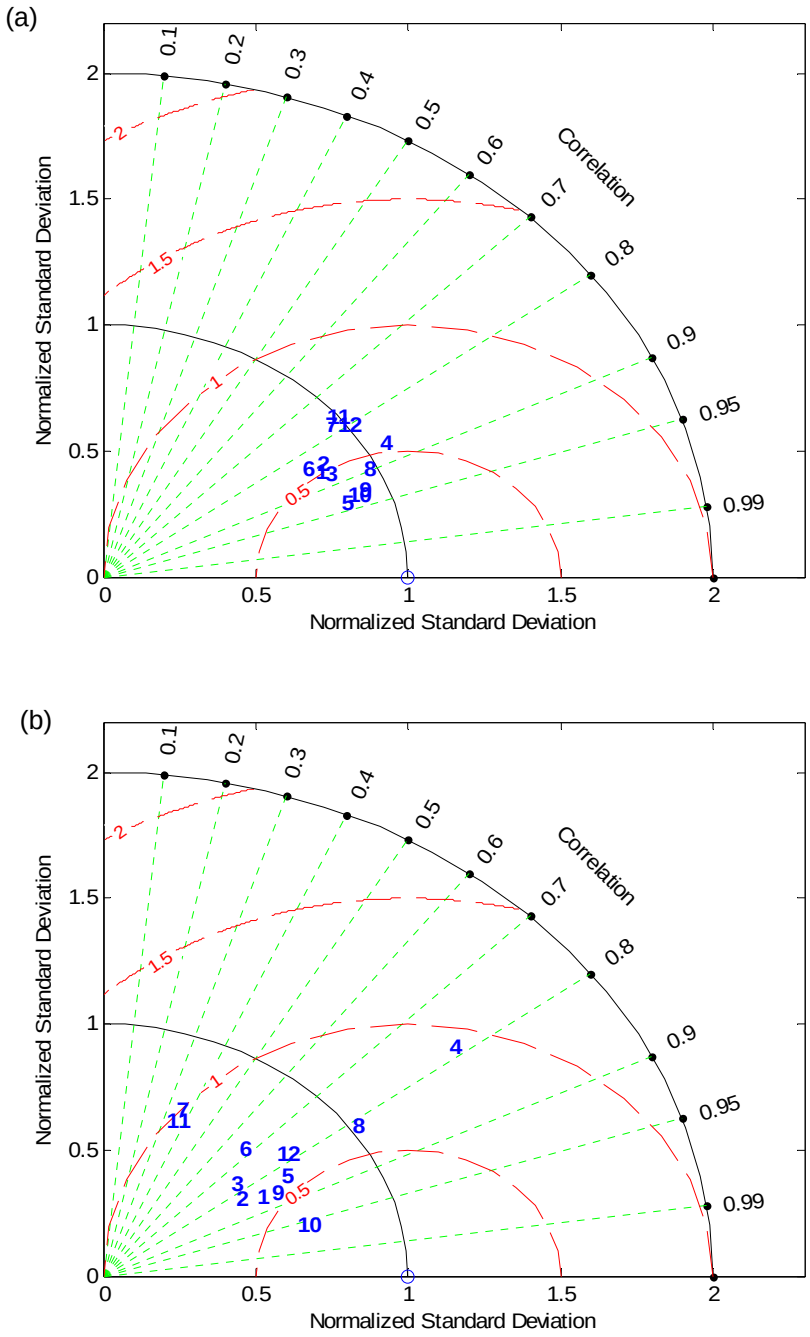

Fig. 5-9 Taylor Diagrams for ECH5 vs. ERA40 geostrophic wind 1961-90

(a) Larger spatial domain; (b) Smaller spatial domain

Fig. 5-9b is a Taylor Diagram drawn for the smaller region, that is, directly over the UK onshore area. It is perhaps intuitive that it shows that there is less similarity between the two datasets for this small section - since the pressure pattern varies on large scales, reducing the region of comparison increases the possibility that the

patterns are different. In terms of correlations, the two months of lowest correlation for this smaller region are July and November, with values of 0.38 and 0.35 respectively. August and April also stand out in the diagram for the smaller region, both having normalised standard deviations of 1.10 and 2.26 - suggesting higher variability within the region in these months than in ERA40.

5.3.1.4 Monthly mean whole field results for ECH5

Given the differences in the datasets when averaged in space and time as discussed above, more detailed analysis of the mean monthly fields for the area above is required. Taking solely the mean resultant geostrophic wind speed first of all, Fig. 5-10, a and b, shows the worst performing months, July and August, in terms of percentage difference relative to ERA40.

Both months show areas where ECH5 has significantly over-estimated wind speeds over north western Scotland by up to 30%. The images for the remaining months are in appendix D.1. They show that for the winter months, ECH5 typically produces geostrophic wind speeds within ±10% of ERA40 values. The tendency in most months is towards over-prediction in the immediate onshore UK region, with January and March predominantly under-predicted, as was manifest in the spatial average statistics in section 5.3.1.2.

In terms of regionality, the GCM appears to show closer correspondence to ERA40 in the Midlands and South than the North. This might perhaps be because the western seaboard region, particularly in the northern half of the country, is very sensitive to the location of cyclones in the north Atlantic region, whilst the Midlands and south are less affected by their precise location. Seasonally, averaged over all cells, the GCM does much better in the winter months. One possible explanation for this is that the wind climate tends to be driven by larger-scale forcings in these months, such as the NAO, and which are well-represented by the GCM.

Because it is both wind speed and direction that are of direct concern in this work, observed fields are compared with those modelled by the GCMs in terms of their u and v vector components. The mean monthly field of the geostrophic wind vectors for the 1961-90 period was calculated from the daily averages for each month. For most months of the year, the GCM fields look broadly similar in both magnitude and direction to those from the ERA40 reanalysis dataset. For example,

in Fig. 5-11 are two examples of two months with fairly similar fields - January and November, and two with obvious differences - March and April: (graphics of the remainder are provided in appendix D.1).

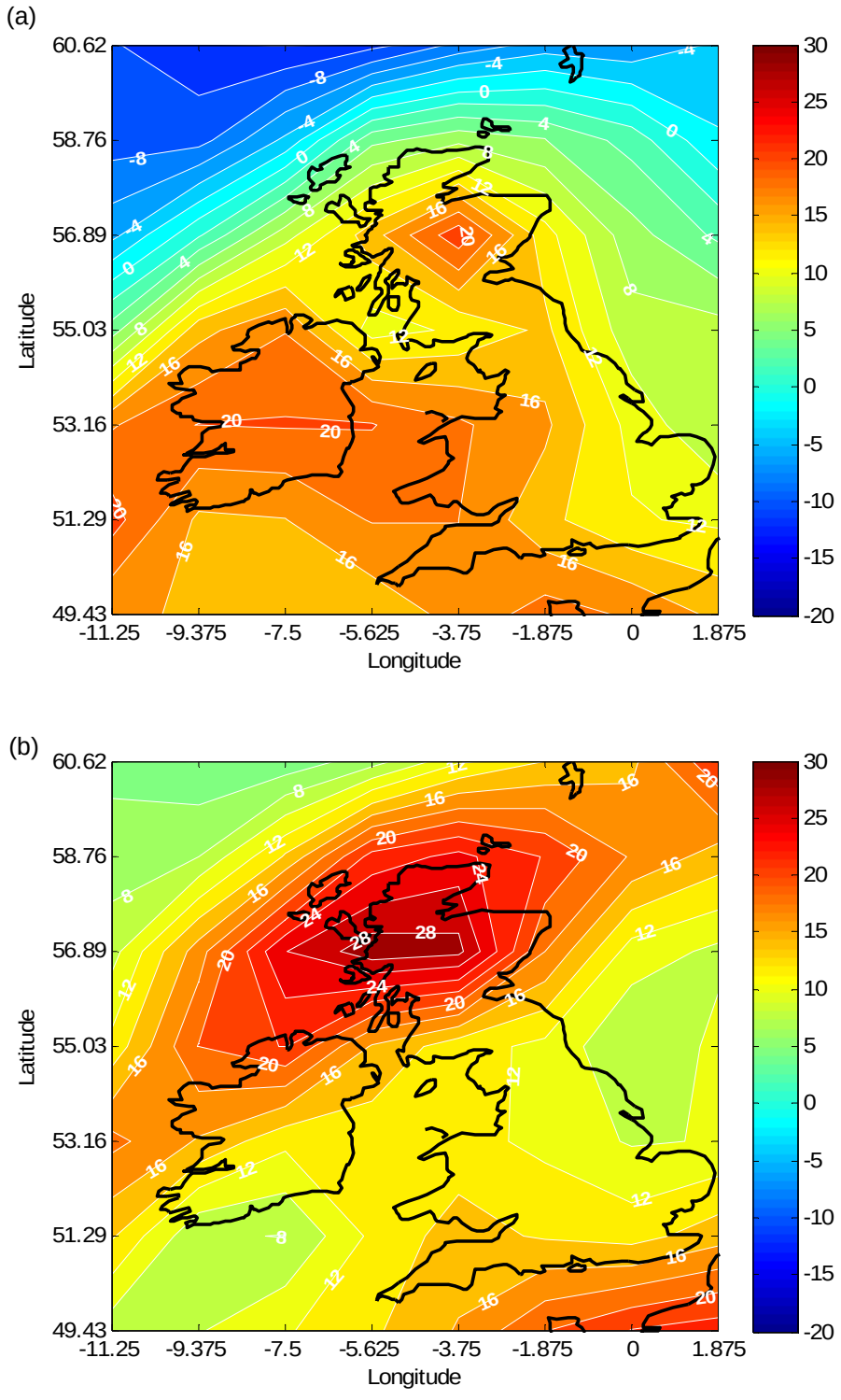

Fig. 5-10 Monthly mean percentage differences ECH5 vs. ERA40 1961-90

(a) July; (b) August

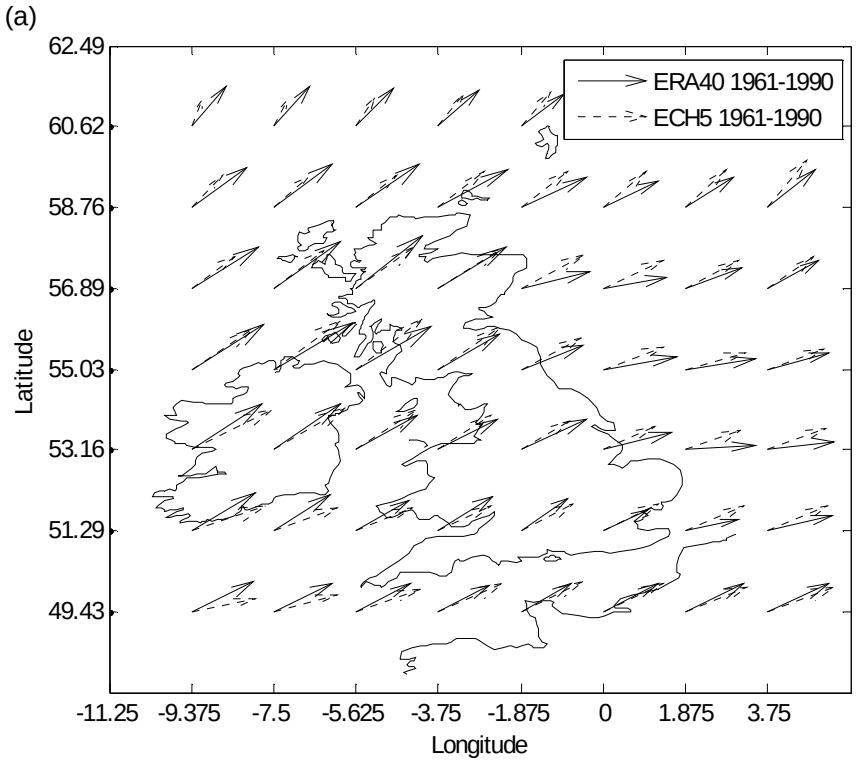

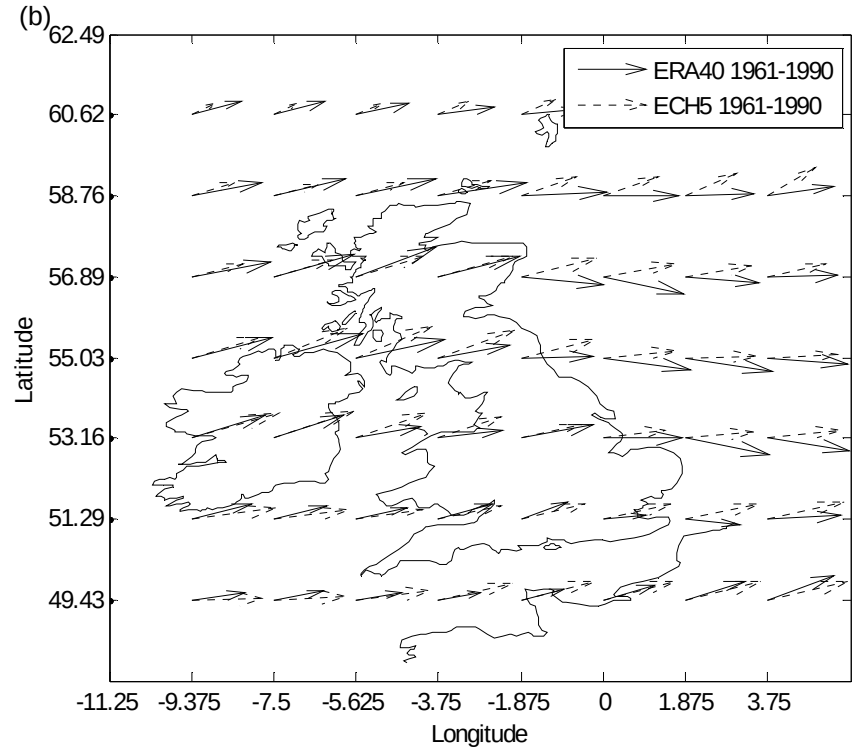

Fig. 5-11 Geostrophic wind vectors ERA40 and ECH5 1961-90

(a) January; (b) November

(c)

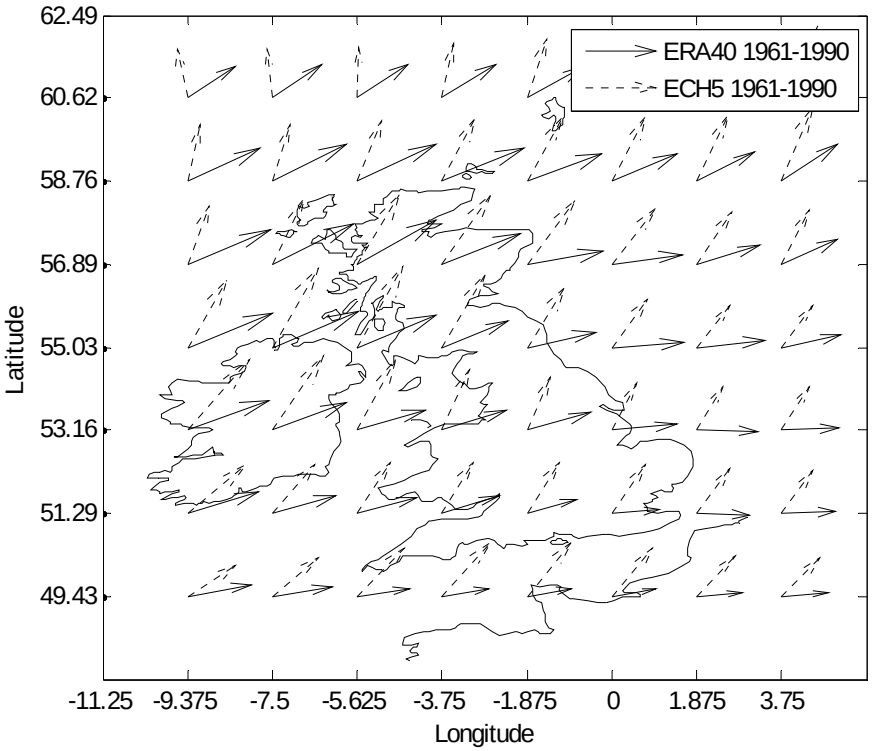

(d)

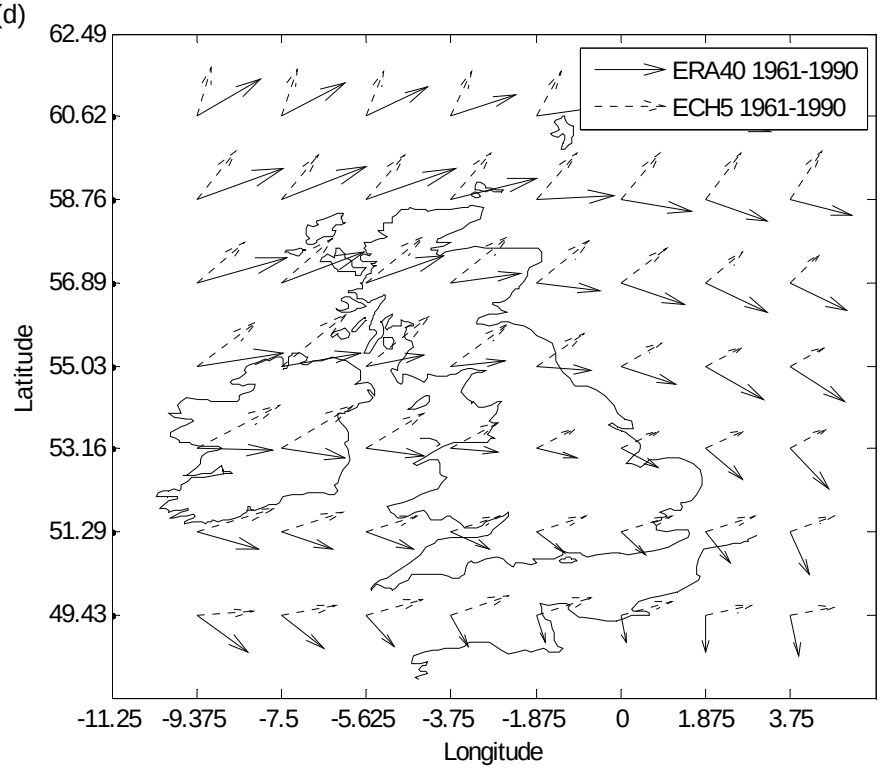

Fig. 5-11 cont. Geostrophic wind vectors ERA40 and ECH5 1961-90

(c) March; (d) April

There is clearly a difference in the underlying pressure pattern in the cases of March and April - as was the case in Chapter 4 with the surface winds. Further investigation of the mean pressure patterns (see Fig. 5-12, a to f) shows that in the ECH5 model, the pressure field pattern for November is similar to that in the ERA40 model. This gives very similar geostrophic wind vectors at all points within the region of interest. However, in March, the low pressure area present in both datasets in the north west of the domain extends further south in the ECH5 model. The high pressure area in the south of the region is confined to eastern points in the ECH5 grid. The resulting pressure pattern creates a local curvature of the geostrophic wind vectors in ECH5 which is not evident in the ERA40 data. A map of the March pressure field for the larger region shows this more clearly: the difference in the location of the low pressure centre causes the variation in wind vectors over the UK.

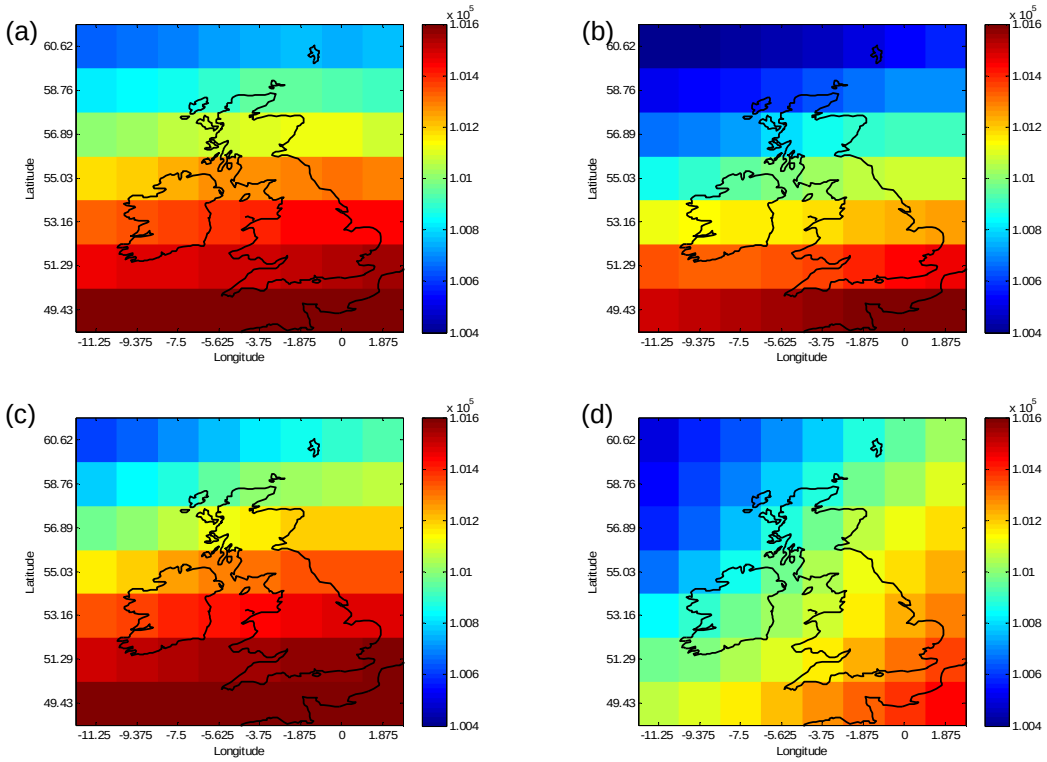

Fig. 5-12 Monthly mean pressure patterns from ERA40 and ECH5 (Pa)

(a) ERA40 November; (b) ECH5 November; (c) ERA40 March; (d) ECH5 March

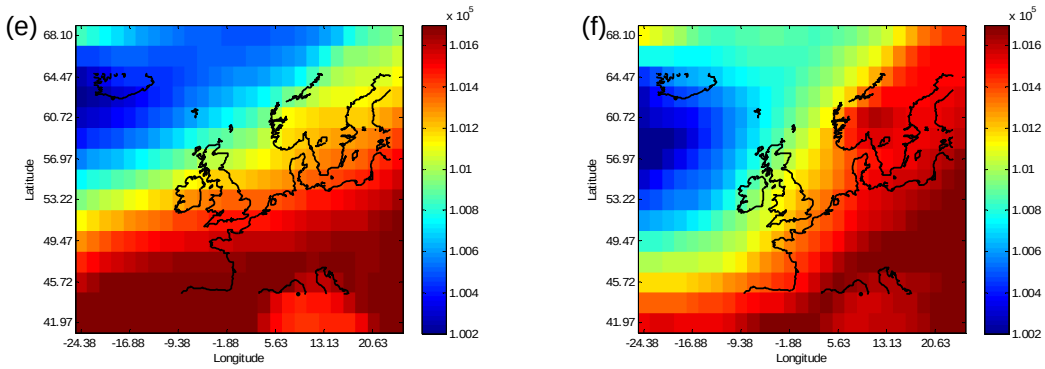

Fig. 5-12 cont. Monthly mean pressure patterns from ERA40 and ECH5 (Pa)

(e) ERA40 March – larger region; (f) ECH5 March – larger region

There is evidence to suggest from all of the analysis that the spring wind climate is not captured satisfactorily within the smaller region of interest. The other seasons would appear, however, to be more successfully represented. These results tally with the results of Demuzere *et al.* (2008), which found "an anomalous low pressure system" to the west of the UK in spring months.

5.3.1.5 Wind roses

Geostrophic wind roses have been drawn for three grid cells identified as 'S Eng' for southern England, 'NE Eng' for north-eastern England and 'Scot' for Scotland (see Fig. 4-8 for locations). As shown in Fig. 5-13, there are some differences in the directional distribution of winds from the two datasets, but they show broadly similar patterns. The ECH5 roses for the Scot and N Eng cells show a small offset relative to the ERA40 roses of around 10˚ for the three most frequent directions, but the NE Eng roses are otherwise very alike. The ECH5 Scot rose shows lower frequencies of winds in the north west quadrant and higher frequencies in the south east quadrant than the ERA Scot rose. The S Eng cell shows some more obvious differences in the two roses, with the ERA40 rose having lower frequencies in the north and south west sectors but higher frequencies in the eastern sector than the ECH5 rose.

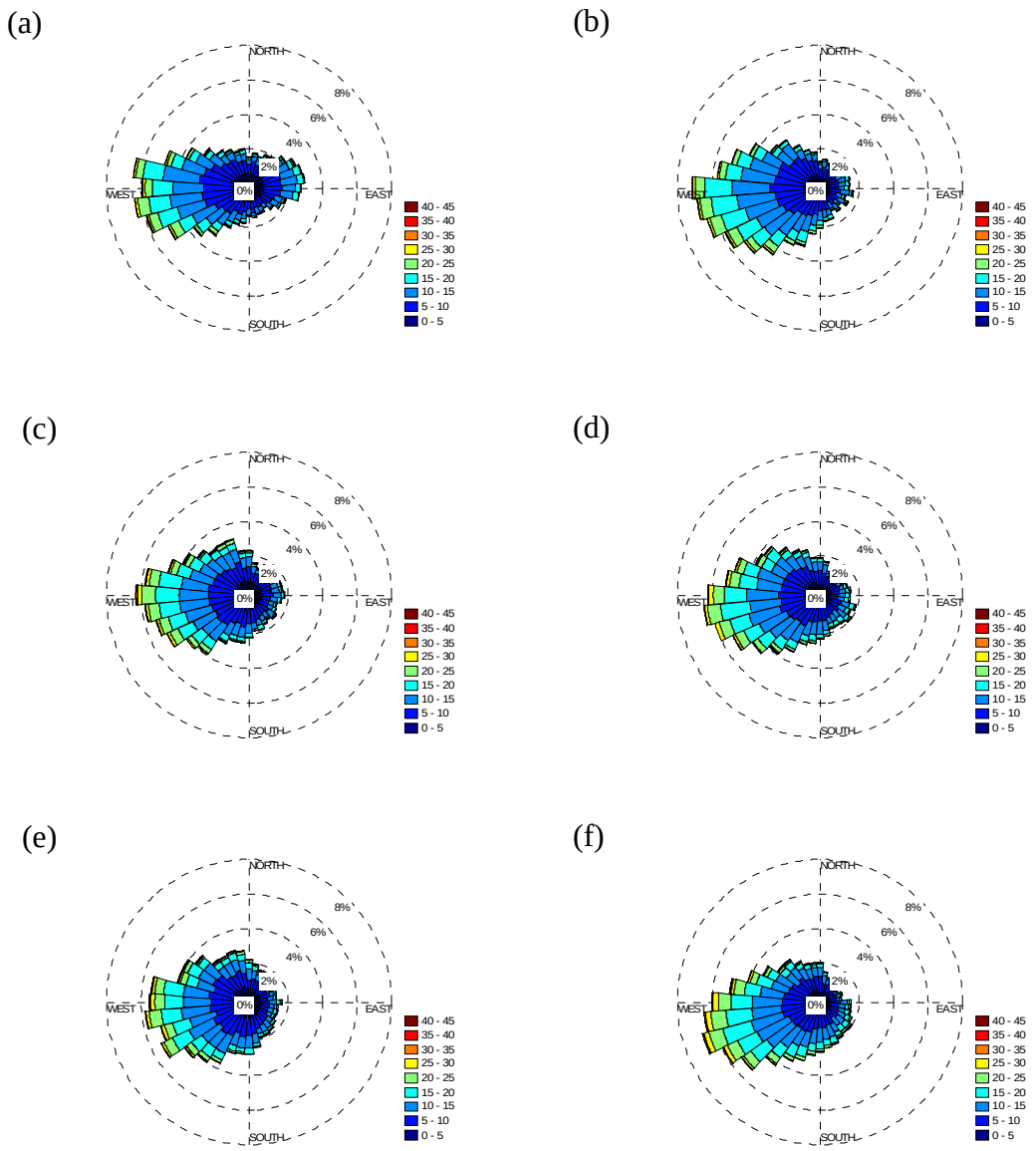

Fig. 5-13 S Eng (a) ERA40 and (b) ECHAM5; NE Eng (c) ERA40 and (d) ECHAM5; Scot (e) ERA40 and (f) ECHAM5

5.3.1.6 Weibull Parameters

An important statistical measure used in the discussion of wind climate, as discussed in Chapter 4, is the wind speed probability distribution. It has been shown that the distribution of the mean wind speed at many sites is well approximated by two-parameter Weibull distribution (Manwell *et al.*, 2002). Calculation of Weibull parameters enables the description of a wind climate without relying on timeseries,

and in the case of winds at turbine hub height, can be used to estimate energy production at a site - as was shown in Chapter 4. Obviously, the distribution of geostrophic winds is not useful for energy production but it does allow a discussion of the variance and spread of the wind speeds at a location.

The four map images in Fig. 5-14 show the spatial characteristics of the Weibull *A* and *k* parameters in the two datasets. The *A* parameter pattern from the ECH5 model closely resembles the pattern from reanalysis, but appears to have generally higher values. The *k* pattern is less well matched between the two models; there is an area of lower value situated over the northern half of the UK in both, and lower values to the northeast and southeast corners, but the pattern to the western half of the region is less similar.

The Weibull parameters calculated from daily mean wind speed values for each grid point show further evidence of the bias towards higher wind speeds in the GCM - as mentioned in 5.3.4. The distributions tend have higher *k* parameter values, which reflects a difference in the frequencies of winds at various speeds. Appendix A.3 demonstrates plots of typical Weibull probability density plots for various values of *k*, with a constant *A* parameter of 5m/s. As can be seen, the distribution becomes more 'normal' as the *k* value increases, and that the mean value tends to be higher whilst the high wind speed frequencies in the 'tail' of the distribution reduce. Physically, this bias toward higher modal and mean geostrophic winds reinforces the theory that ECH5 over-estimates the mean sea-level pressure gradients (from Demuzere *et al.*, (2008), as noted in 5.3.1.2). The higher *k* parameter is also indicative of having lower frequencies in the upper wind speed ranges than those from the ERA40 reanalysis data; this is potentially suggestive of lower spatial and temporal variability and an inability to capture extreme values - something seen in previous parts of the analysis.

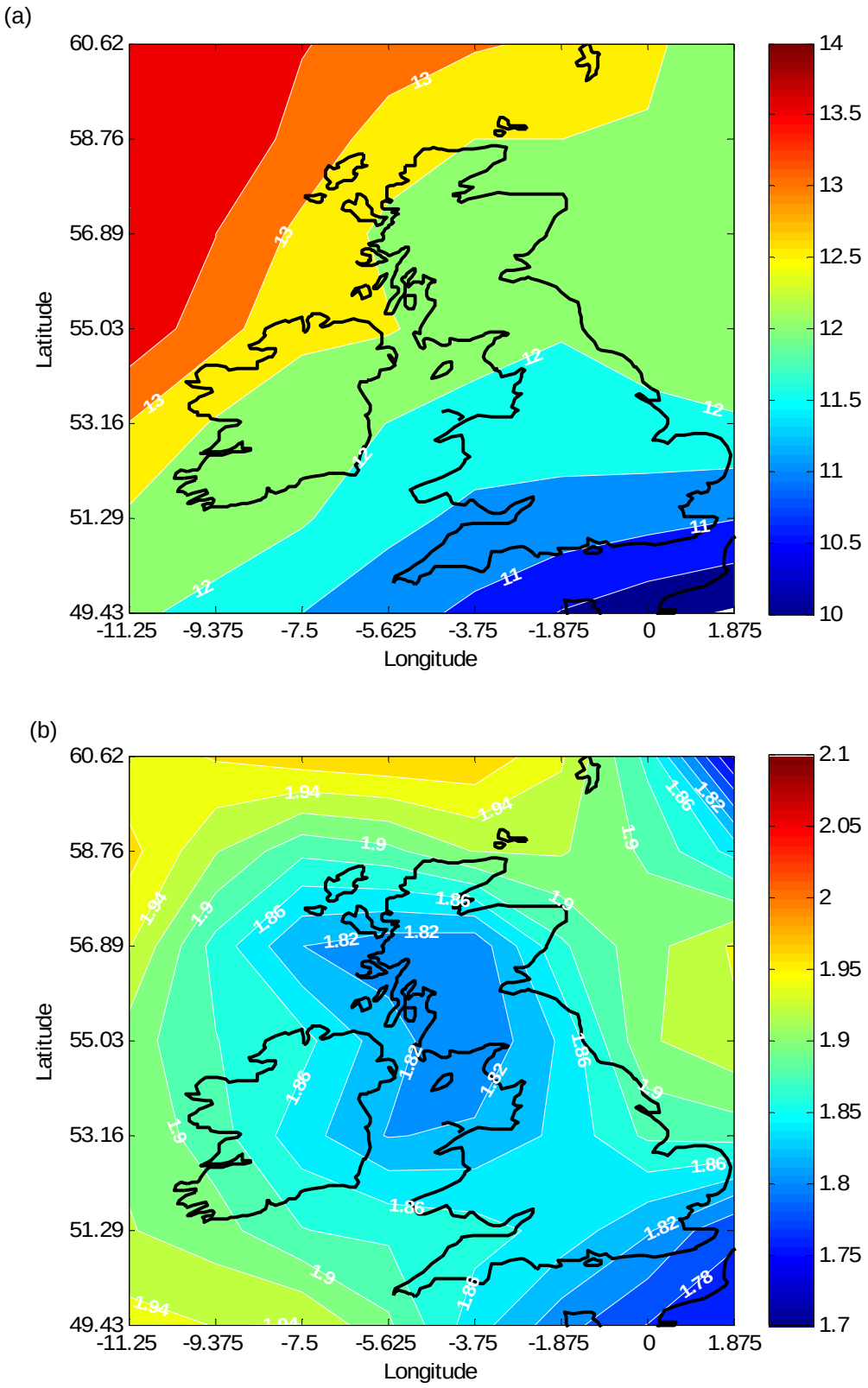

Fig. 5-14 Weibull parameter fields 1961-90

(a) ERA40 *A* parameter (m/s); (b) ERA40 *k* parameter

(c)

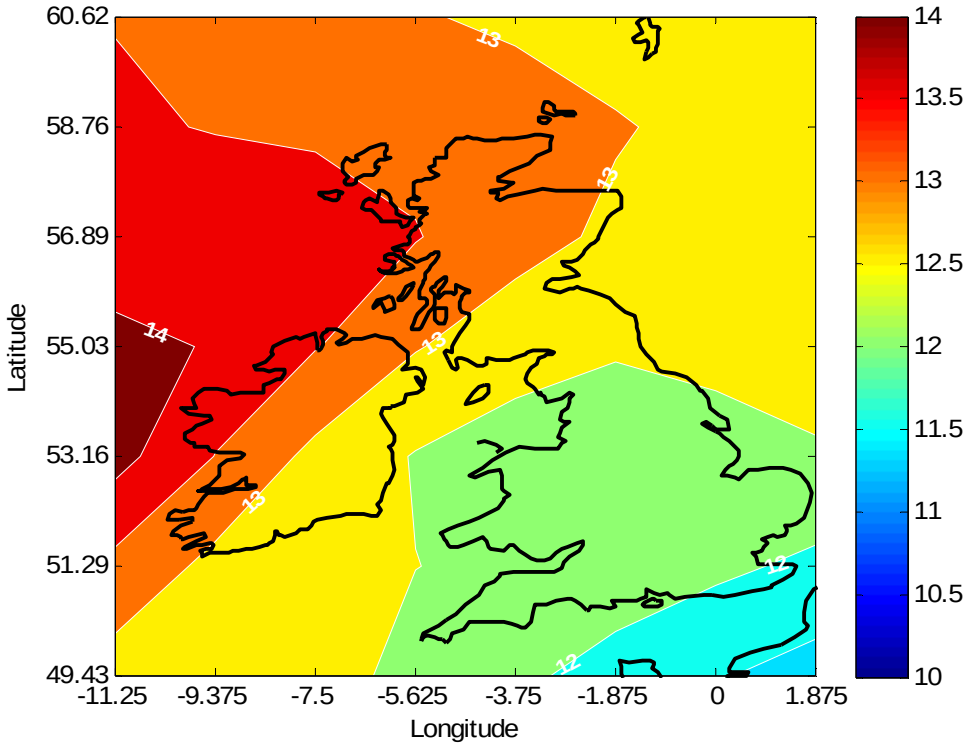

(d)

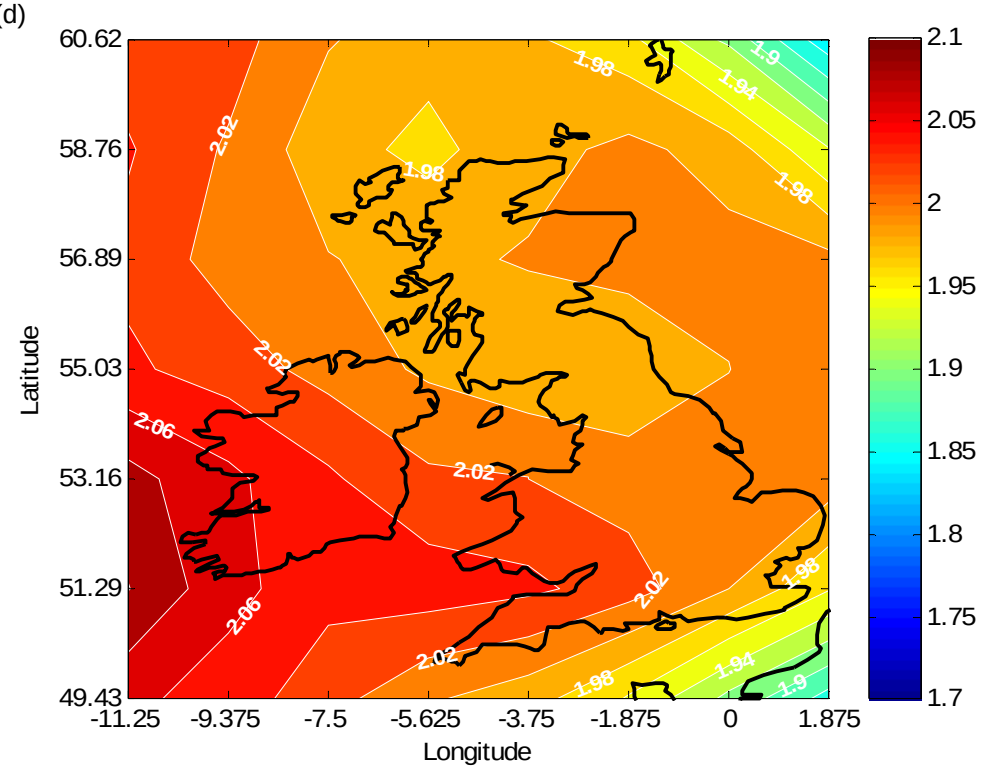

Fig. 5-14 cont. Weibull parameter fields 1961-90

(c) ECH5 *A* parameter (m/s); (d) ECH5 *k* parameter

5.3.1.7 Comparison with other studies

Pryor *et al.* (2005a) carried out a study using a selection of five GCMs, and show using Taylor Diagrams that most capture the mean values of pressure gradient over Scandinavia well, but all show an underestimation of the spatial variability of the pressure gradients when compared to the ERA40 reanalysis data. This might be expected, given their lower spatial resolution, and matches the outcome in the work presented here. In another similar study (Pryor *et al.*, 2005b) the authors found slightly better correspondence in their study between pressure gradients from a different reanalysis dataset, the NCEP-NCAR reanalysis, and those output by the predecessor of the ECH5 model, ECH4 - over a region of size approximately 20˚ latitude and 30˚ longitude around Scandinavia and the Baltic Sea; but they found similar results to those above when comparing various GCMs with the ERA40 reanalysis data. They did, however, calculate the pressure gradient in a slightly different manner to this work, taking the maximum gradient between the adjacent grid point in any of the eight directions from the grid point in question, whereas in this study the calculation was computed in the x and y directions and then the resultant calculated from these two vectors.

Demuzere *et al.* (2008) carried out a comparison of the ECH-5 GCM with the ERA40 reanalysis mean sea-level pressure. They used a slightly longer control period than was applied in this work - 1961-2000 - and a larger but similar spatial domain of 27.5˚W-27.5˚E, 15-85˚N; and they chose the 2.5˚x2.5˚ reanalysis resolution rather than the higher 1˚x1˚ resolution used here. Their main finding with regard to the skill of the GCM was that, for the area in question, only the October-April season was adequately represented with respect to the ERA40 reanalysis; the model output for the summer months did not show sufficient similarity with this baseline. Comparing the results found here directly to those found in Demuzere *et al.* (2008), the autumn and winter months are, on average, better than the spring and summer in both pieces of work. The primary concern in each study is slightly different, and the studies differ in the spatial region under consideration, but given these dissimilarities, the results are compatible.

5.3.1.8 Conclusions on comparison

The analysis in this section has shown that for the area 48˚ to 61˚ north and -12˚ to 3˚ east in particular, the ECH5 GCM replicates some of the main features of the mean monthly geostrophic wind climate as defined by the ERA40 reanalysis for the period 1961-90.

Firstly, the value of the resultant monthly mean wind in the GCM averaged for each month over the thirty-year period matches to within an average of 6% for the autumn and winter months, and an average of 11% for the spring and summer months. The month with the greatest difference was August, and that with the least difference was January. With the exception of January and March, the GCM values are greater than those from the reanalysis data. The interannual variability for each month is less in the results from the GCM than in the reanalysis model, notably in the months of January, February and March.

Considering the relationship spatially, the area showing the lowest correlation in the monthly mean geostrophic wind between the two datasets is the north west, with an R^2 value of 0.89. The R^2 value is highest in the south and east, with values of around 0.95. By taking each monthly field individually and comparing them using Taylor Diagrams, it was shown that when the area under consideration was larger, the spatial patterns were more highly correlated - with similar levels of standard deviation and low RMS error. For the smaller region, directly over the UK, the patterns were not so well correlated in some months, with correlations dropping to less than 0.4 in the months of July and November.

Examining the individual mean monthly fields more closely, the months with the maximum percentage differences between the fields are July and August, with April also showing areas with large differences. The winter months tend to show lower differences over the whole region, with the midlands and south tending to be better than the north. Including direction in the analysis, subjective consideration shows that the vectors for March and April are the months which appear most different in the two datasets over the whole of the smaller region. The other months show differences only in parts of the area, whilst other parts appear fairly similar. When the pressure patterns for March and April are examined, it is clear that the

location of a low pressure area is not the same in the GCM as in the reanalysis data, which results in a different wind vector pattern.

The *A* parameter of the Weibull distribution from both datasets shows a reasonably similar pattern, with the GCM having slightly higher values – as might be expected given its tendency to produce slightly higher mean wind speed values. The *k* parameter field from the GCM, whilst showing some likeness in the spatial pattern, generally has lower values; this indicates a higher mean speed with a smaller range of variability.

Taken all together, the results of the comparison between ECH5 and ERA40 geostrophic wind vectors indicate that whilst the GCM is relatively successful at representing the wind field in the autumn and winter months, it is less so in spring and summer months; this agrees with Demuzere *et al.* (2008). The reason for this may lie in the drivers for UK wind climate, which in winter is strongly related to the large-scale pressure oscillations. Summer wind climate may be more locally driven, and thus ill-captured by the low resolution of the GCM. The wind speeds manifest in the GCM tend to be higher than those from the reanalysis data, and are less variable both temporally and spatially. The tendency towards higher wind speeds is a result of an overestimation in the north-south pressure gradient, whilst the reduced variability could be the consequence of low spatial resolution, or the inability of the model to represent extreme features of the climate.

5.3.2 The Future geostrophic wind patterns

Using geostrophic wind as a qualitative indicator for surface wind, assuming the surface wind will follow similar patterns to the geostrophic wind, the geostrophic wind data from the ECH5 GCM for the future period 2081-2100 (IPCC Data Distribution Centre, 2005b) is analysed for significant changes.

In general, the changes forecast by the GCM for geostrophic winds 2081-2100 show smaller differences than the difference between the GCM 1961-90 hindcast and the ERA40 data for the same period. Pryor *et al.* (2005d) used this to suggest that further analysis of the climate model data was needed, with the clear suggestion that it is not an accurate enough representation of current climate. However, adopting the 'change factor' approach of the IPCC (Wilby *et al.*, 2004)

would suggest considering the projected changes alone - or applied to a more reliable baseline climate - and not the baseline data (1961-90) given by the GCM. In this instance, patterns throughout most of the grid cells suggest a strengthening of the seasonal pattern of wind speeds in the UK, with increases in winter wind speeds and decreases in summer. This is reasonably consistent with what was shown using the change factor method with an RCM in Chapter 4. It is worth recalling that this RCM was unrelated to the GCM used in this section, and so a correspondence of results is of note.

The most basic analysis, given that at this point the main concern is general country-wide trends, is to look at the monthly means averaged over all grid cells. Comparing these side-by-side for the 1961-90 and 2081-2100 periods (Fig. 5-15a and b) the future results are suggestive of very small changes in the average monthly means, with the typical winter/summer pattern being consistent in both periods. In terms of levels of variation with the monthly values for each year, the future data shows an increase in the standard deviation in the months of December and January; this, interestingly, brings it closer to those displayed in the ERA40 data for the 1961-90 control period, as seen in the boxplot of Fig. 5-7b.

(a)

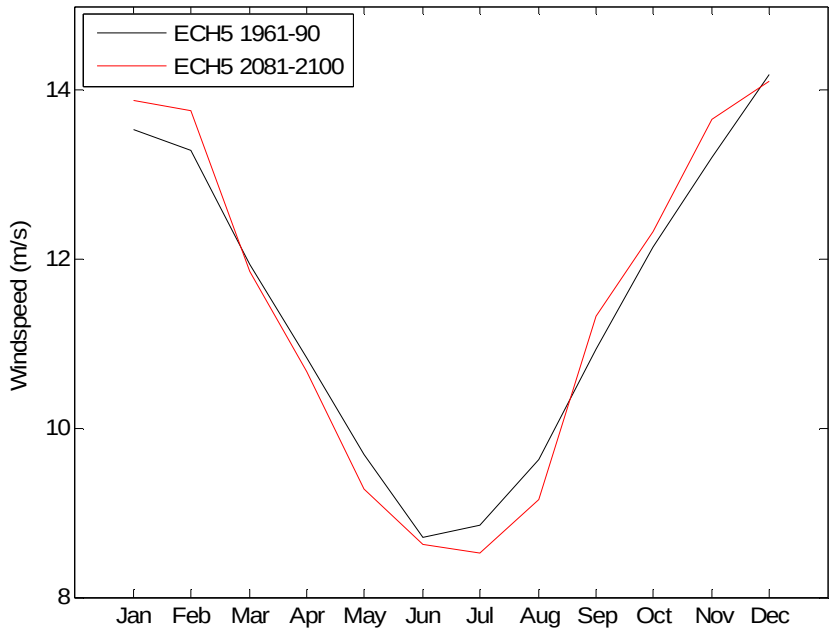

Fig. 5-15 Comparison of ECH5 spatial average monthly means 1961-90 and 2081-2100

(a) 1961-90 monthly means

(b)

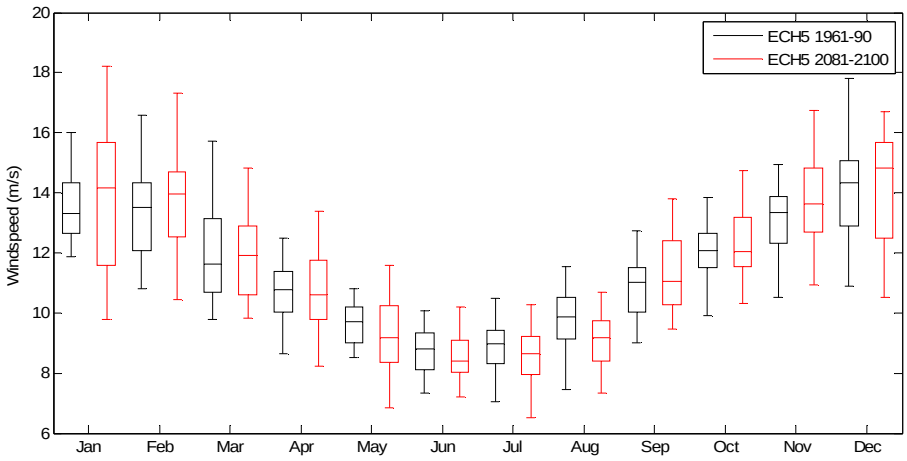

(c)

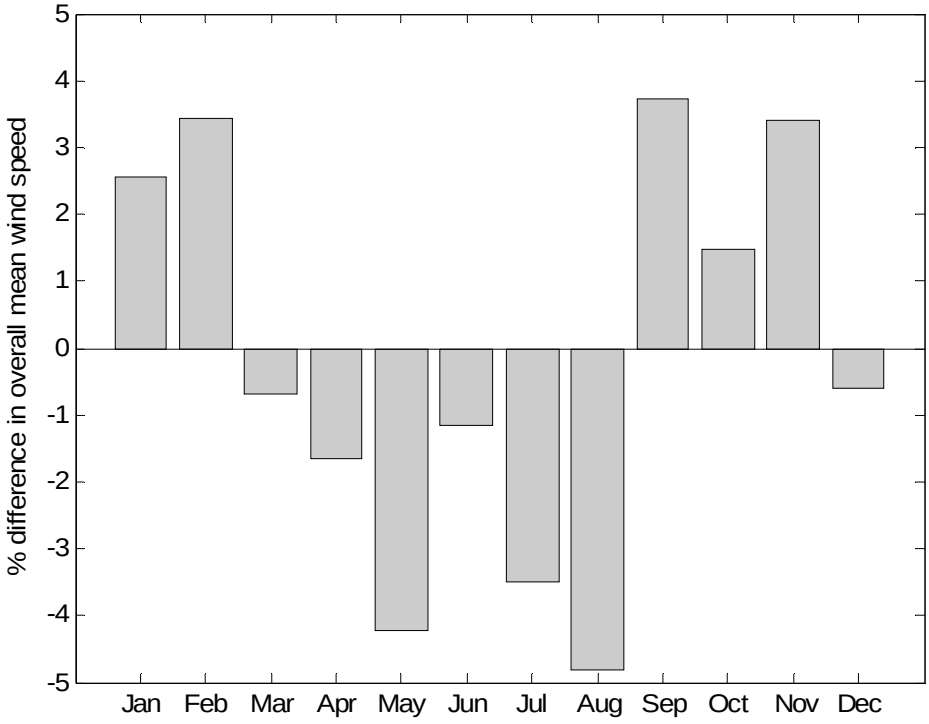

Fig. 5-15 cont. Comparison of ECH5 spatial average monthly means 1961-90 and 2081-2100

(b) 2081-2100 monthly means; (c) Percentage differences in overall monthly means between 1961-90 and 2081-2100

Fig. 5-15c is a chart of the percentage differences in the monthly means. In accord with the general trend found for the surface winds in the RCM as seen in Chapter 4, there is evidence of a strengthening of the seasonal pattern of geostrophic winds.

Decreases of around 1% to 5% in the spring and summer months and increases of 2% to 4% in the autumn and winter months are evident - with the exception of December which shows a small percentage decrease.

The patterns of change within the region for each month of the year show, as for the spatial means, the differences in the future climate are generally smaller in magnitude than the difference between the reanalysis data and the 1961-90 GCM data. The patterns for four of the months (July, August, November and December) are shown in Fig. 5-16. The two summer months show particularly large changes in the mean geostrophic wind speed but these months also showed notably high differences between ECH5 and ERA40 data for the control period, however. The winter months, by contrast, showed more modest percentage changes in the mean speed, whilst also showing correspondingly low differences between ECH5 and ERA40 data for the control period.

- July (Fig. 5-16a) – this month has a particularly large region in the southern half of the domain showing a decrease in the mean geostrophic wind speed of between 8 and 12%, whilst the change shifts to become positive in the northernmost part of Scotland. The offshore region to the north of Scotland undergoes increases in the mean speed of up to 8%.
- August (Fig 5-16b) - the largest decrease in the mean geostrophic wind speed throughout the year of 16% is found in the very south of the domain in August. As with July, the changes become less negative travelling north, and become positive (increasing by 2-4%) for the northernmost part of Scotland.
- November (Fig. 5-16c) – the most notable change in this month occurs offshore to the north east of Scotland, where the mean speed increases by 8-12%. Onshore, the changes are mostly positive over most of the UK, with a maximum increase of 8-10% in the north of Scotland. The south of England experiences small decreases of between 0 and 4%.
- December (Fig. 5-16d) – changes in December are mainly small, ranging from a 4-6% decrease in mean geostrophic wind in the north of Scotland to a 2-6% increase over most of England and Wales.

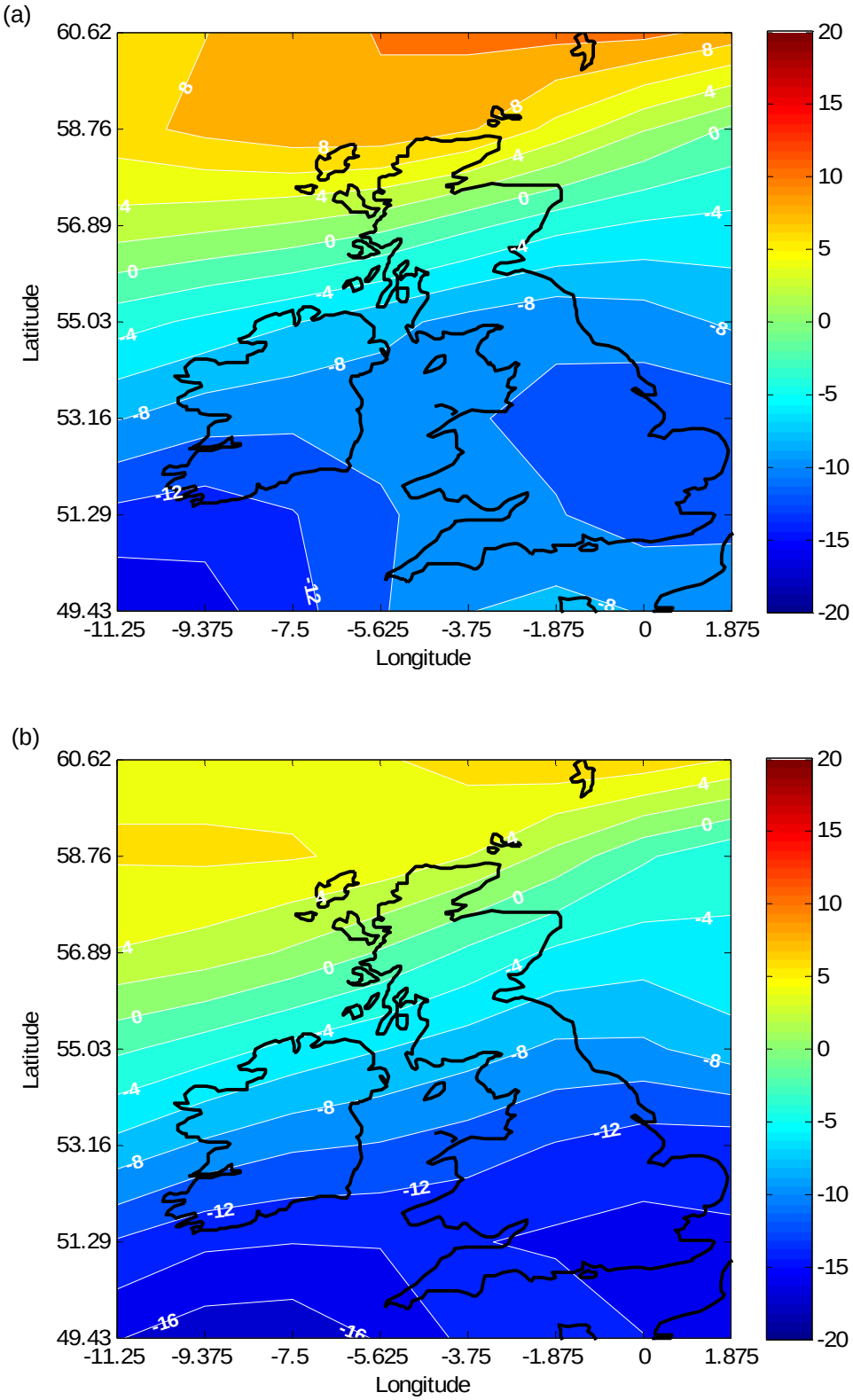

Fig. 5-16 Future percentage differences in monthly mean wind speeds from ECH5 for 2081-2100 vs. 1961-90

(a) July; (b) August

(c)

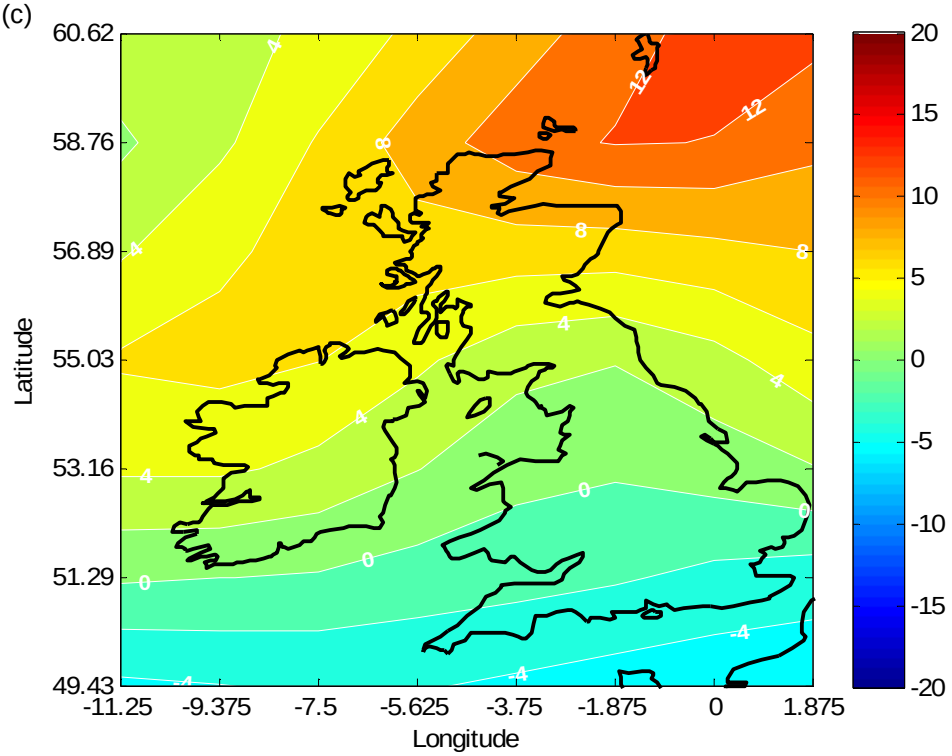

(d)

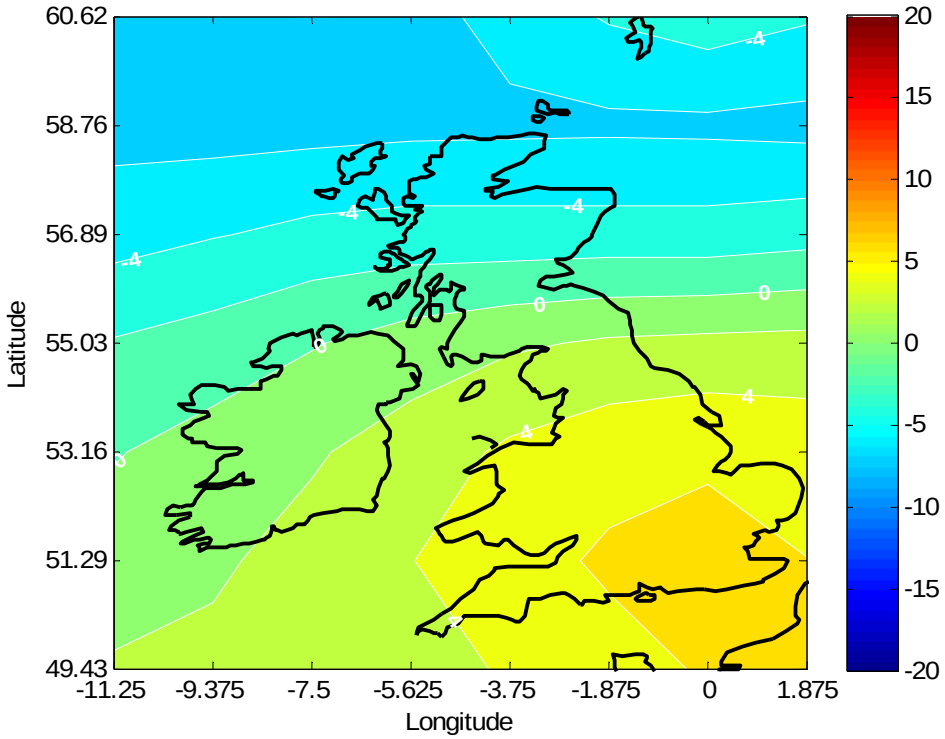

Fig. 5-16 cont. Future percentage differences in monthly mean wind speeds from ECH5 for 2081-2100 vs. 1961-90

(c) November; (d) December

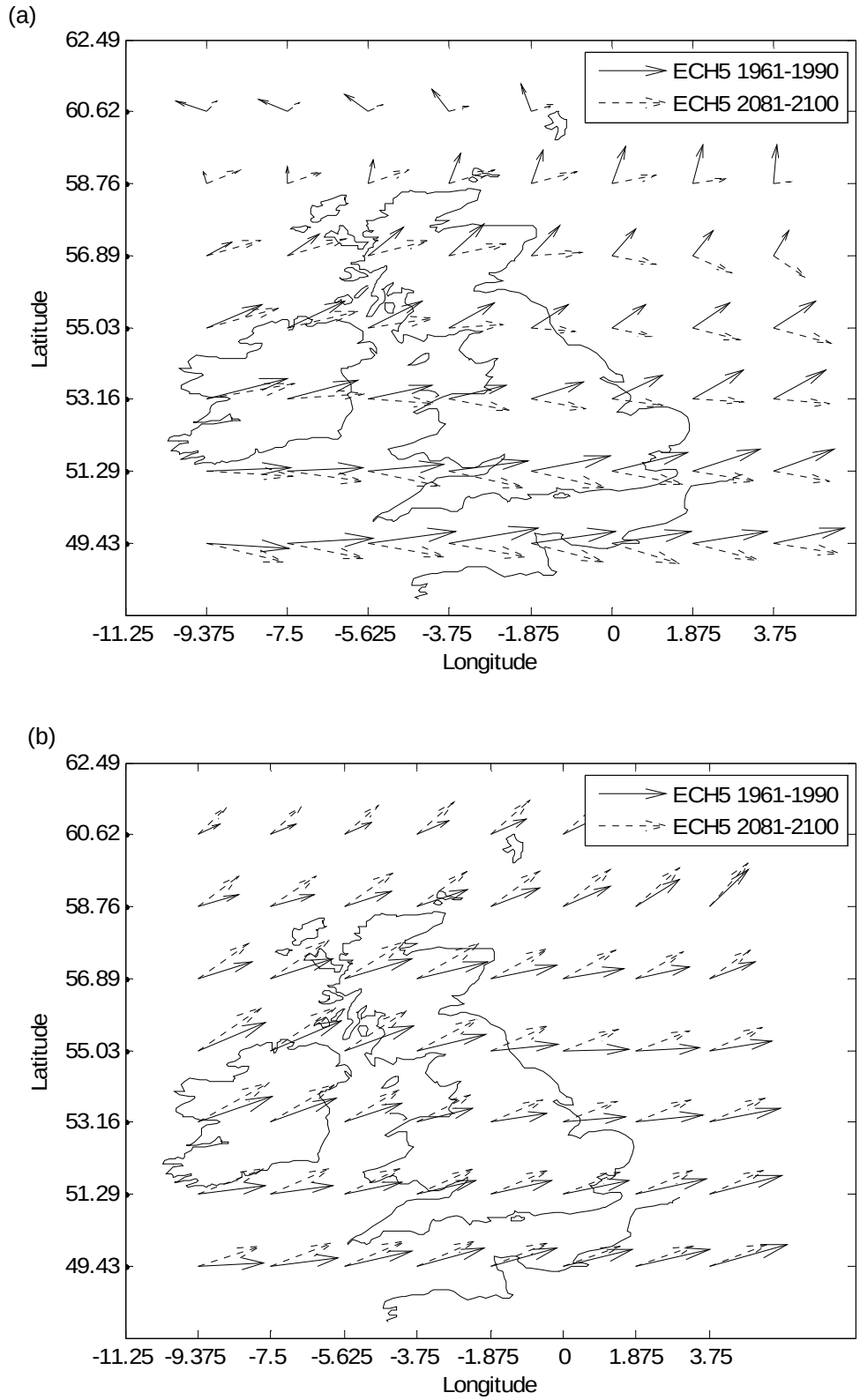

Fig. 5-17 Geostrophic wind vectors ECH5 1961-90 and 2081-2100

(a) May; (b) November

Considering the vector plots of the baseline 1961-90 wind field and the future 2081-2100 as modelled by the ECH5 GCM, two of the months that appear to show the greatest differences between the two periods are shown in Fig. 5-17. For May, there is clearly a change in the mean pressure field such that the cyclone turning the wind anticlockwise in the north west of the region is no longer as strong or there is a change in its location. In November, the wind appears to be turning more anticlockwise in this region and increasing in speed, suggesting the presence of a stronger or more easterly located cyclone in the locality.

The data for the three cells, with locations as described in Fig. 4-8, was processed into wind roses using the control period and future GCM data to highlight any changes in prevailing direction or wind strengths in any particular direction. From Fig. 5-18, there appears only to be very slight changes in the overall annual pattern of wind directions, consistent with the country-wide results presented above. Interestingly, however, an additional small frequency of very high speed winds – between 40 and 45 m/s – appears in the plots for NE Eng and Scot that is not present in the 1961-90 rose. In both cases, this is only present in the sector 255-265˚.

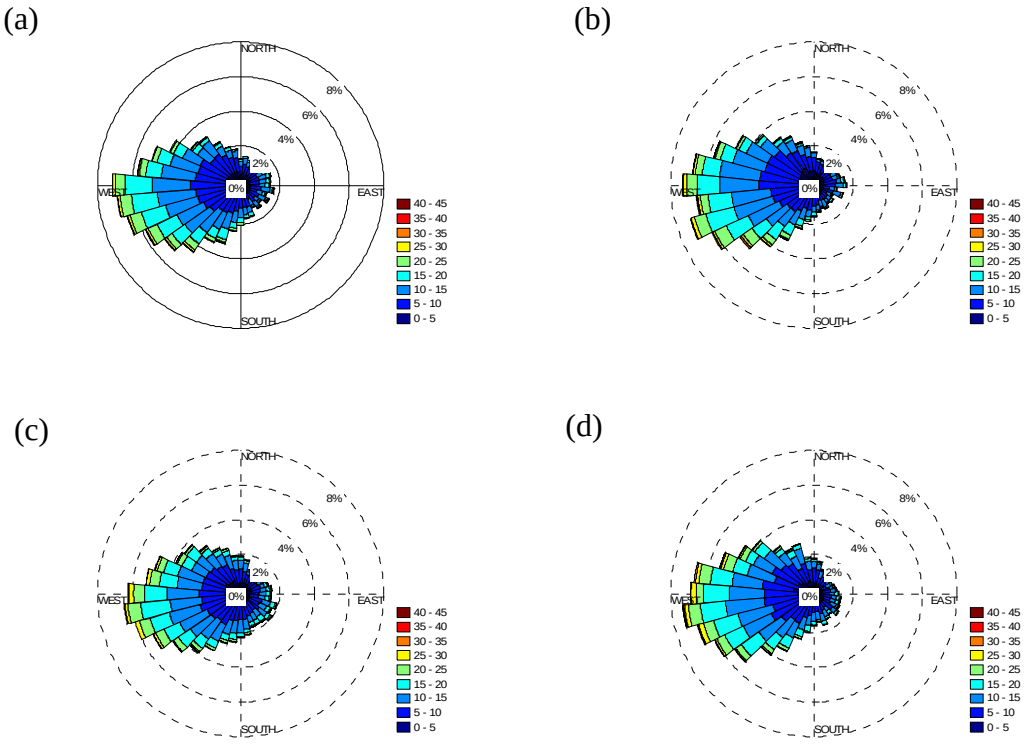

Fig. 5-18 S Eng (a) 1961-90 and (b) 2081-2100; NE Eng (c) 1961-90 and (d) 2081-2100

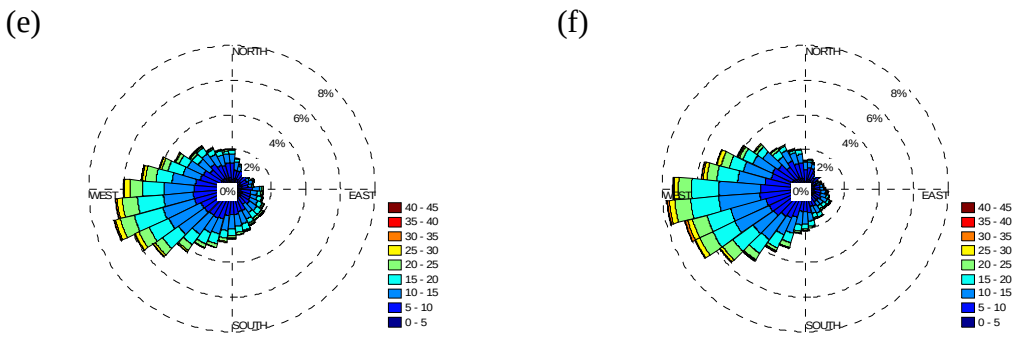

Fig. 5-18 cont. Scot (e) 1961-90 and (f) 2081-2100

The Weibull *A* parameters for the future climate data in Fig. 5-17a look fairly similar in range and spatial pattern to the control period – see Fig. 5-13c. The *k* parameter field (Fig. 5-19b) keeps its general spatial pattern compared with the ECH5 baseline (Fig. 5-14d) but the *k* values are typically lower, particularly in the south east of the domain. The *k* values for the future period are closer to those calculated from the ERA40 reanalysis for the control period, suggesting more skewing of the distribution towards the lower wind speeds and a higher probability of occurrence of extremely high wind speeds.

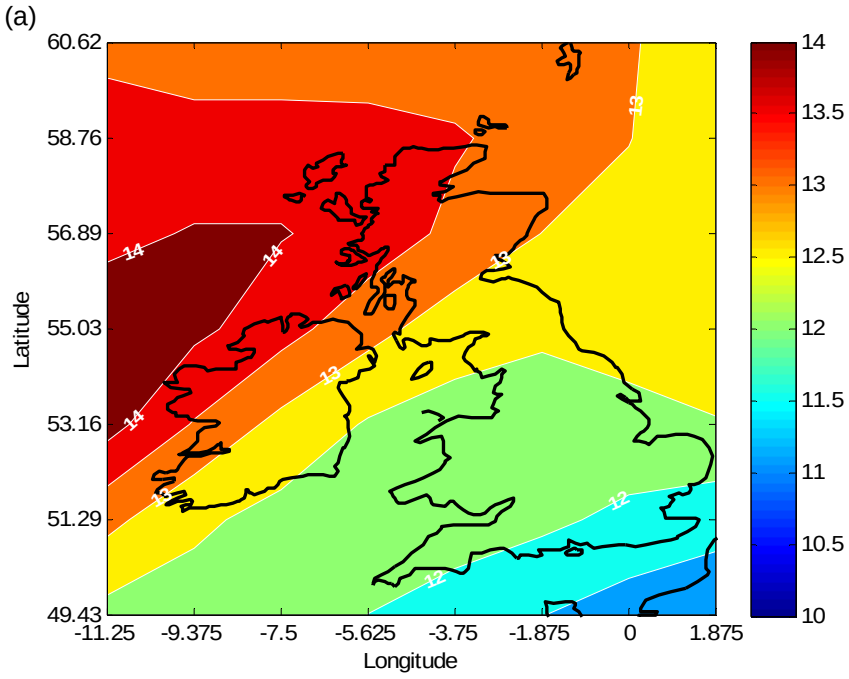

Fig. 5-19 Weibull parameter fields ECH5 2081-2100

(a) *A* parameter (m/s)

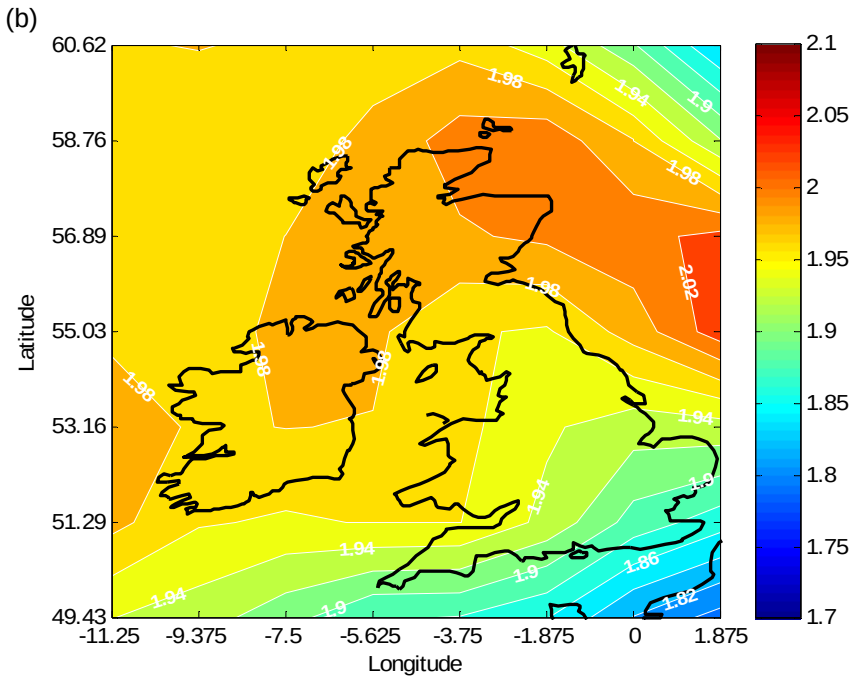

Fig. 5-19 cont. Weibull parameter fields ECH5 2081-2100

(b) *k* parameter

5.3.2.1 Summary

In summary, the future projections for the 2081-2100 period as modelled by the GCM show a slight strengthening of the seasonal wind pattern, with changes for the region as a whole in the range of +5% in the autumn and winter months and -5% in spring and summer. Particular areas within the UK show larger changes than these, however, particularly in the southern UK in the summer months – where a decrease in wind speeds of over 10% is projected – and northern areas in the spring and autumn months. Winter tends to show smaller and more consistent changes over the whole UK. Analysis of the wind vectors shows those months with the most deviation from the baseline climate are May and November. These changes appear to be precipitated by a change in the location of a cyclone to the west of the region.

The Weibull parameters were calculated from both the GCM baseline and future climates. Whilst the *A* (scale) parameter pattern over the country looks very similar for both periods, the *k* (shape) parameter shows a not insignificant decrease in all areas of the UK. This brings the *k* values into a similar range as those from the ERA40 1961-90 data, and is suggestive of a Weibull distribution which is more skewed to the lower wind speeds, but also gives greater frequencies of winds at

higher speeds. This may indicate more extreme conditions; but the result is highly uncertain and needs further investigation.

Considering these results with reference to the wind industry, it is not possible to convert directly from a percentage change in geostrophic wind to a percentage change in surface winds - because it is likely that even a highly simplified linear relationship will not pass through the origin, requiring a constant term in the equation. Even so, a 4-5% change in wind speed could, potentially, result in a 12-15% change in the energy output of a wind turbine over a particular time period. This represents a significant amount of revenue to be either lost or gained. The wind speed changes, averaged over the whole region on an annual basis do not amount to more than around 4%, a figure unlikely to have much bearing on the finances of wind farm operators working in a high wind speed site. Seasonally, wind farms located in the south may suffer from fairly large changes in energy output, particularly summer decreases. The potential strengthening of the seasonal pattern would have the greatest impact not on wind farm owners but on capacity and grid planning. There may also be some indication of a change in the Weibull shape parameter of the wind speed distributions, which could merit further investigation.

In order to assess whether the projected changes in geostrophic wind climate will have a proportionately different impact on surface wind climate, it is necessary to conduct some form of downscaling, and this is dealt with in Chapter 6.

Chapter 6

Downscaling GCM wind climate projections

Chapters 4 and 5 focussed on interpreting projections from climate models in terms of the UK wind climate as a whole, giving some indication of how wind climate in the region may evolve into the next century. It was demonstrated that there is potential for reasonably significant change, particularly at a seasonal level; but due to the low resolution of the models, some form of downscaling is required in order to understand how this would impact at the point where a particular wind farm was located. This chapter aims to address this by using both a physically-based method applied to climate model data, and an empirical method. The analysis is carried out by comparing results for an historical control period with actual observation records from met station sites, and by examining projected future changes for the sites.

6.1 Why is downscaling necessary?

Knowledge of wind climate conditions at individual sites is important at various levels within the wind industry. Developers obviously rely on determining the wind climate at their proposed site in order to secure investment and maintain profitability over its lifetime. Given that the lifetime of a modern wind farm is expected to be in the order of 25 years, climate change is probably not as important a consideration for, for example, project feasibility studies, as it might be for hydropower which has a much longer expected life. It would thus be predominantly large-scale developers, such as the major power generators, who would have an interest in high resolution information from climate change scenarios that run beyond the predicted life of a wind farm. This information could be relevant for development strategies and long-term plans - perhaps for gaining an understanding of whether current sites have potential to be re-developed with updated equipment at the end of their lifetime, or if they ought to be decommissioned and sold on. A similar process of investigation of finances and profitability as that which might be undertaken for a feasibility study might be engaged for this purpose.

Furthermore, site-level wind climate information is of relevance to electricity network companies at both transmission and distribution level. The UK's ageing network infrastructure requires much in the way of investment in the medium-to-long term, especially to provide the greater flexibility needed to enable the connection of renewable sources of generation like wind. Awareness of potential changes in the wind resource at specific locations in the next 50 to 100 years facilitates the making of more sensible decisions for network upgrading and extensions. As an interesting by-product, not specifically related to wind power generation, there are also issues surrounding thermal management of network infrastructure that require site-based knowledge of wind climate since it can act as a cooling system for components. Consideration of thermal management in the context of climate change, with projections of increasing temperatures, will require detailed knowledge of wind climate as an input to thermal models.

Chapter 4 included the results of an investigation into the 10m wind as calculated by the ECHAM5 GCM. The analysis showed that, whilst the GCM successfully matches some of the characteristics of the surface wind climate as manifest in the ERA40 reanalysis - such as the typical seasonal pattern of mean wind speed over the UK – the model generally overestimates the mean wind speed by around 10-20% compared to the ERA40 data. A further issue was that of the resolution of the data; the approximately 2˚ grid squares are far from sufficient to capture the large degree of spatial variability of the surface wind climate in the UK. Compared to the - still fairly coarse - 1˚ resolution of the reanalysis, it was clear that the GCM was unable to distinguish the complex terrain and coastline of the country.

In Chapter 2, some of the current methods for downscaling GCM output were discussed, namely dynamic downscaling in the form of AGCMs or RCMs, and statistical downscaling. Using the output of a regional climate model to dynamically downscale a GCM dramatically improves the resolution, as evident from the second part of Chapter 4; and it is possibly the ideal downscaling method, relying as it does on tangible physics and dynamics rather than empirical methods or statistics. However, the running of the models requires a large input in terms of computer resources, time and climatological expertise. The RCMs are also themselves

currently limited to a resolution which may not itself be sufficient to capture the true wind climate at a specific site.

Chapter 5 showed that, relative to data from the ERA40 reanalysis model, the ECHAM5 GCM is more capable in terms of capturing monthly mean values of geostrophic wind as derived from the large-scale pressure field, as compared to its ability to model surface winds. The relative spatial homogeneity in the geostrophic wind field means the low resolution models can produce more adequate representations, as compared to surface winds with high spatial variability. The geostrophic wind climate is not immediately applicable for wind energy resource applications, as it represents wind speeds far above current turbine hub heights. However, the application of some form of downscaling technique to the GCM geostrophic wind field could provide an acceptable and less resource-intensive alternative to an RCM and, depending on the method developed, could allow detailed analysis at a site level.

6.2 How does geostrophic wind relate to surface wind?

Geostrophic wind, as discussed in Chapter 5, represents wind speeds where friction has little or no influence on the flow, and so is approximated by wind speeds above the planetary boundary layer, some 600-1000m above ground level. The relationship between geostrophic wind speed and surface wind speed is known as the 'geostrophic drag law'. The drag law is a physical relationship, considered to be constant in time, and is defined as:

$$G = \frac{u^*}{\kappa}\sqrt{\left(\ln\left(\frac{u^*}{f \cdot z_0}\right) - A\right)^2 + B^2} \qquad (6.1)$$

where: G is the geostrophic wind speed, u^* is the friction velocity; κ is the von Karman constant with a value of 0.4; z_0 is the surface roughness length; and A and B are dimensionless constants. The parameters A and B within the drag law equation are often empirically derived, and may vary by site. Here they are given values of 1.8 and 4.5 respectively, following the work of Troen & Petersen (1989).

The change in the mean speed from geostrophic to surface level is accounted for in the drag law, but the direction of geostrophic winds are also different to those of surface winds. In theory, the direction of the surface wind and the geostrophic

wind are related by a relationship defined by Ekman - originally for oceanography (Tennekes & Lumley, 1972) - where the offset of the geostrophic wind vector relative to the surface increases exponentially with height. Since the wind in the lower boundary layer is slowed by friction with the surface, its decreasing speed reduces the Coriolis force. The unchanged pressure gradient force is no longer balanced by the weaker Coriolis force and so the surface wind vector tends to the left of the geostrophic wind, as shown in Fig. 3-2b. (Tennekes & Lumley, 1972).

Given a certain geostrophic wind, *G*, using the geostrophic drag law with an iterative function to solve the equation to find the friction velocity, u^*, allows the use of the logarithmic profile to calculate the wind speed at any height above the surface as in eqn. 3.25,

$$U(z) = \frac{u^*}{\kappa} \ln\left(\frac{z}{z_0}\right) \tag{6.2}$$

This relationship assumes neutral atmospheric stability and for unstable or stable atmospheres, must be adjusted as described in appendix A.2.

Analysis of the relationship between geostrophic wind and friction velocity (using a small sample of GCM geostrophic wind data and applying the drag law) shows an almost linear relation, breaking down only at very low geostrophic wind speeds.

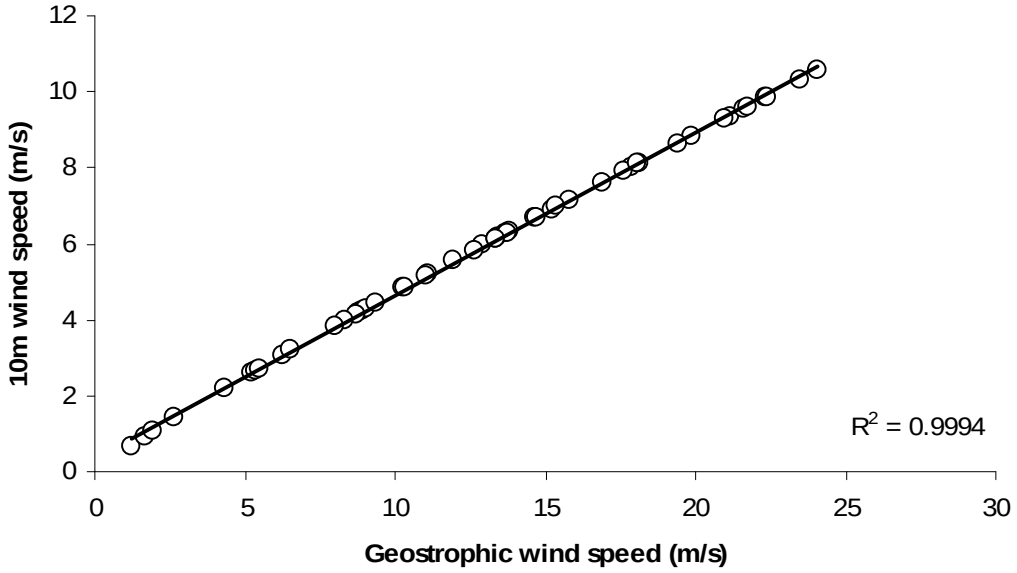

Fig. 6-1 Approximately linear relationship between surface and geostrophic winds using the geostrophic drag law and logarithmic profile

What this means regarding the mathematics, is that the component of the drag law involving the log of u^* is dominant at low speeds, whereas the component involving u^* as a linear coefficient becomes dominant as the speed increases, causing the connection to appear almost linear. The relationship between u^* and U is linear, given a particular height and roughness length, as the log term in the profile equation will be constant for these chosen parameters. These two factors result in the relationship between geostrophic wind and 10m wind at a given constant roughness length being almost linear, except at very low speeds, as shown for a sample of data in Fig. 6-1. This is similar to the relationship found using observations in Hasse (1974).

Further analysis has been conducted to establish the linearity of the relationship between ERA40 geostrophic and surface winds, assuming that because the model has assimilated observations it is a fair approximation to reality. For the grid square with its centre at 53˚ north, 0˚ west, a simple plot of the six-hourly data (Fig. 6-2a) for the first six months of the year 1990 shows a clear connection between variations in the two variables. The scatter of the surface and geostrophic wind data for the period 1981-90 is shown in Fig. 6-2b. A linear regression analysis gives an R^2 correlation coefficient of 0.85, which is acceptably high. A second grid square, centred at 55˚ north, 2˚ west, gives very similar results (Fig. 6-3), with a slightly higher R^2 value of 0.88. Table 6-1 gives the regression coefficients and R^2 values for 1961-70, 1971-80 and 1981-90 for the two sites and confirms a reasonably consistent and strong linear relationship over time.

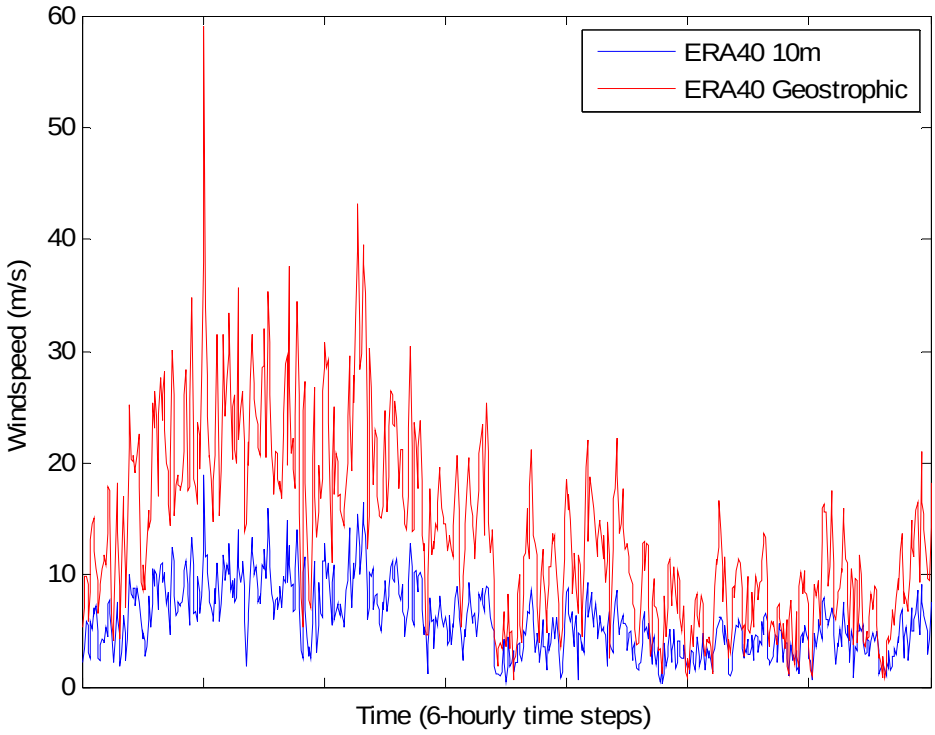

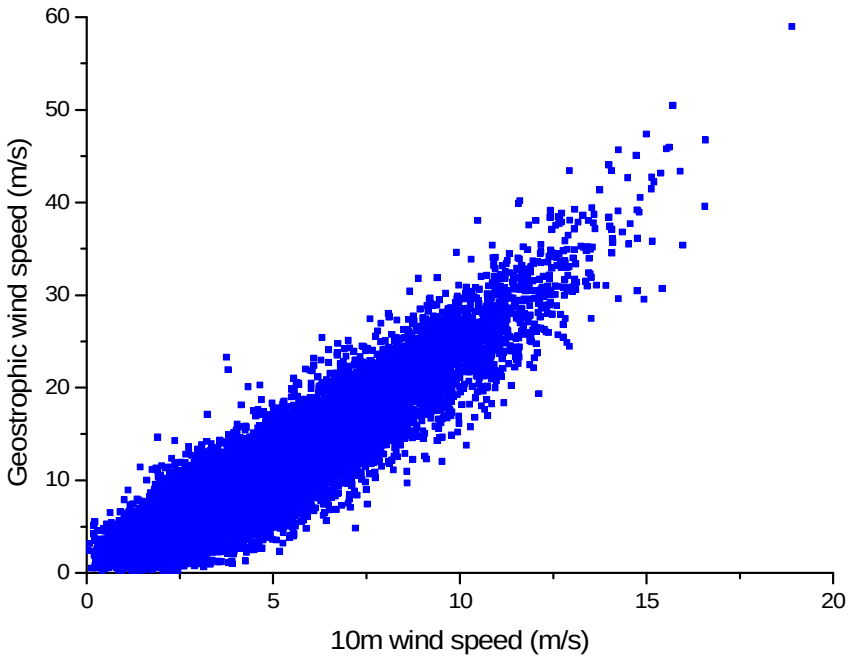

Fig. 6-2 Relationship between surface and geostrophic winds at 53˚ north, 0˚ west

(a) Jan-Jun 1990 6-hourly time series; (b) Scatter plot of 6-hourly values 1981-90

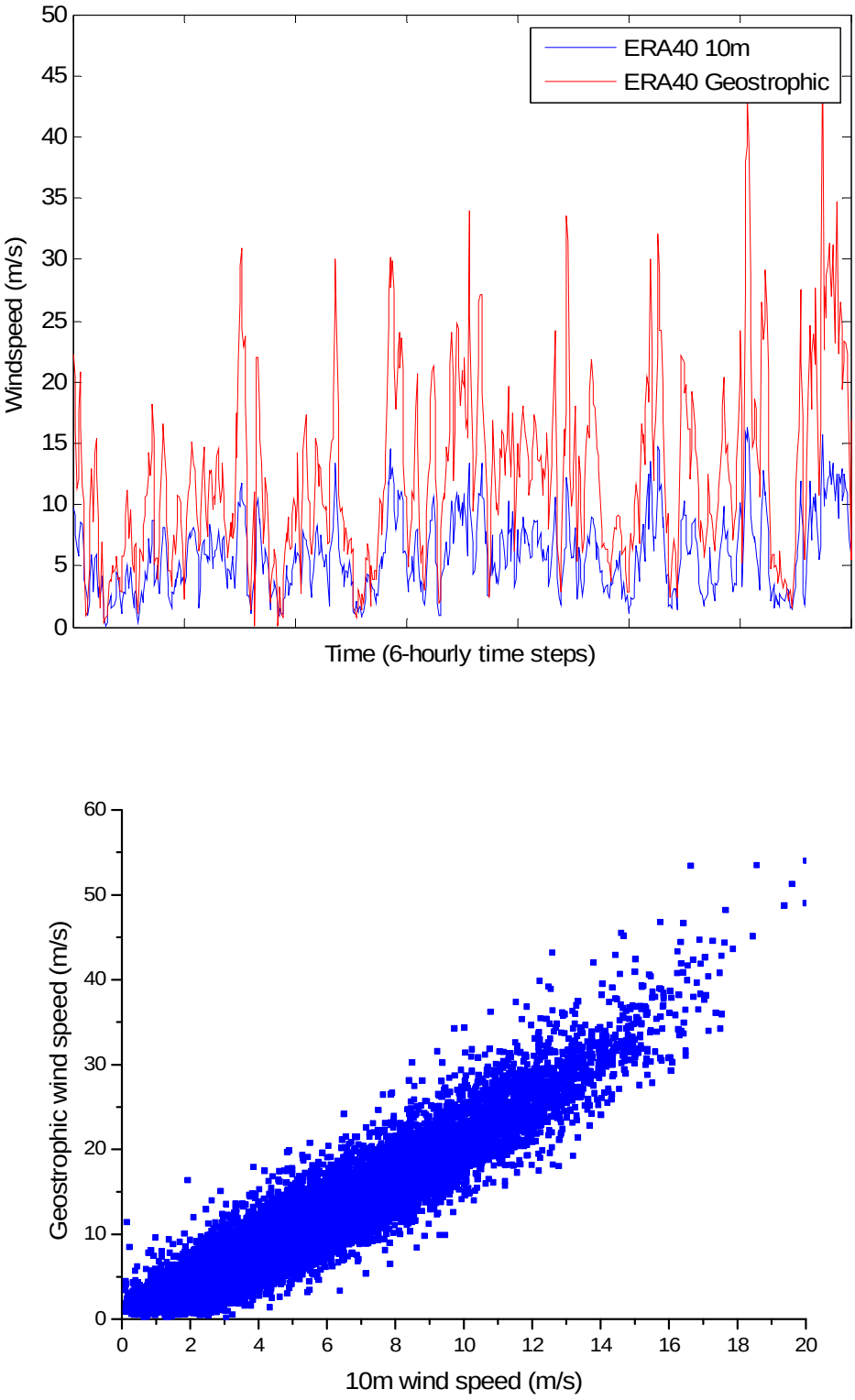

Fig. 6-3 Relationship between surface and geostrophic winds at 55˚ north, 2˚ west

(a) Jan-Jun 1990 6-hourly time series; (b) Scatter plot of 6-hourly values 1981-90

Wittering	R^2	Constant term	Gradient
1961-70	0.82	1.08	0.35
1971-80	0.82	1.03	0.35
1981-90	0.85	1.04	0.35

Boulmer	R^2	Constant term	Gradient
1961-70	0.88	0.96	0.40
1971-80	0.88	0.87	0.41
1981-90	0.89	0.94	0.41

Table 6-1 Relationships between surface and geostrophic winds over time

The table shows for each site: the time period of analysis, the R^2 value for this period, the constant term in the derived linear relationship and the gradient of the line.

6.2.1 Change in Weibull parameters with height

The frequency (or probability) distribution of wind speeds tends to follow a two-parameter Weibull distribution, as discussed in chapters 4 and 5. Some consideration must be given to the frequency (or probability) distribution parameters when carrying out downscaling of geostrophic winds. If the downscaled information is to be used as input to a wind power calculation, it is likely that a Weibull distribution will be assumed. However, although the equations 6.1 and 6.2 describe the relationship between geostrophic wind speed and the surface wind speed, they do not give consideration to the relation between the Weibull parameters of geostrophic and surface winds or any change in the parameters with height.

The scale parameter of the Weibull distribution, *A*, is closely related to the mean wind speed. As the height of interest increases, the mean wind speed will likely increase, and thus *A* is also likely to increase. Justus *et al.* (1978) uses the power law as in eqn. 3.24 to derive the *A* parameter at a height *z* based on the *A* parameter at height z_{ref}, by replacing the mean speed with the *A* parameter as follows,

$$A(z) = A_{ref}\left(\frac{z}{z_{ref}}\right)^{n} \qquad (6.3)$$

where

$$n = \frac{0.37 - 0.088 \ln A_{ref}}{1 - 0.088 \ln\left(\frac{z_{ref}}{10}\right)} \tag{6.4}$$

The shape parameter, *k*, is more closely linked to the variance of the distribution. Increasing height results in an increase in the *k* parameter, up to a certain point (around 100m) when it then begins to decrease again (Justus *et al*., 1978). The relationship derived in Justus *et al.* (1978) to determine the change in *k* with height is given as,

$$k(z) = k_{ref}\left[\frac{1 - 0.088 \ln \frac{z_{ref}}{10}}{1 - 0.088 \ln \frac{z}{10}}\right] \tag{6.5}$$

This, however, is only correct up to a certain height where *k* begins to decrease again. Petersen *et al.* (1998a) depicts the variation of Weibull *A* and *k* parameters of wind speeds with height, with *A* increasing on a log scale (as described above) from 10 to 1000m, whilst *k* forms a curve, increasing from 10m to 100m and then decreasing up to 1000m. Interestingly, the *k* value at 1000m is lower than the value at 10m.

6.3 Downscaling methodologies

In this section, some potential downscaling techniques are investigated with a view to obtaining future changes in site-specific surface wind climate from GCM data. It aims to exploit the relationship between geostrophic and surface winds to establish if it is possible to use the relationship to enhance the accuracy of wind data from a GCM - to make it more applicable on a site-by-site basis. The primary data of interest is the typical monthly mean wind speed at each site over a long period of 20-30 years.

Two routes have been taken, one of which is based on a known physical connection between the variables, and another which relies on developing an empirical statistical relationship between the geostrophic wind and the observed wind climate at the site. The outputs of the downscaling techniques for an historical control period are compared and contrasted against the observational record for

seven sites, and the method considered most appropriate for each site used to create a future profile for the wind climate at that location.

A further downscaling method has been investigated using wind climate analysis software (WAsP) which models the physical relationship described above in a more sophisticated fashion. The results are compared against the other two more simplified techniques to see if any value is added by the enhanced modelling skill of the software.

6.3.1 Site descriptions

To illustrate, seven sites have been identified that have a suitably long time series (at least 15 years) of observed wind climate data at 10m above ground level (a.g.l) within the period 1961 to 1990. See Fig. 6-4 for a UK map showing the locations. The Ordnance Survey maps (Ordnance Survey, 2009) of the regions surrounding each site are in appendix E.

1. Boscombe Down, Wiltshire: Located at 51.161˚ North and 1.753 ˚ West. The site is situated in a region of flat terrain at an elevation of 126m, mainly surrounded by green pasture but quite near to an airfield. The time series of observed data runs for the full control period, from 1961-90.

2. Boulmer, Northumbria: Located at 55.421˚ North and 1.6˚ West. The site is at 23m elevation and situated approximately 2km from the coast, in the vicinity of a helicopter landing pad and quite near to several buildings. The surrounding land is a mixture of grass and arable crops. Data are available from 1975 – 1990, a relatively short period but the closest match to the 1961-90 control period possible.

3. RAF Wittering, Cambridgeshire: Located in an RAF airfield at 52.611˚ North and 0.459˚ West, at an elevation of 73 metres above sea level. It lies in a fairly densely populated area, with a greater proportion of the surroundings covered with buildings than in the previous two examples. There is some grassland and agricultural land in the vicinity, and also a number of banks of trees. The longest period of useable data is from 1969-1990, and thus corresponds slightly better with the 1961-90 control period than the Boulmer station.

4. Fort Augustus, Inverness-shire: Located at 57.138˚ North and 4.719˚ West at an elevation of 42m in the Scottish highlands. It is near an electricity substation, the only building in its immediate vicinity. The surrounding land is largely forested and the station lies around 1.5km from a river and 3km from a large loch. Unlike the previous three sites which were flat, the surrounding terrain in this case is a steep river valley - which could potentially cause problems for wind climate analysis. The period of data used is January 1969 – October 1989.

5. Eskdalemuir, Dumfriesshire: Located at 55.312˚ North and 3.206˚ West at 242m elevation in somewhat undulating terrain in the middle of a fairly dense forest. There are some small buildings nearby and it is just over half a kilometre to a small river. Data used are for the full control period of 1961-1990.

6. Turnhouse, Midlothian: Located at 55.951˚ North and 3.347˚ West at 35m elevation in the middle of a fairly major airport. There are a large number of surrounding buildings and roads, some trees and further beyond this, some agricultural land. The data were available for the entire control period of 1961-1990.

7. Cairngorm, Inverness-shire: Located at 57.124˚ North and 3.644˚ West at the top of a ski run in the Cairngorm mountains, at an elevation of 1090m. There is one small building nearby, and the terrain varies from grass in summer to snow in winter. Data were available from August 1968 – December 1990.

6.3.2 Wind climate data

The ECHAM5 daily mean sea-level pressure data for the period 1961-1990 were extracted at 1.8˚ x 1.8˚ resolution for the UK (IPCC Data Distribution Centre, 2005a). The pressure data were interpolated to a higher spatial resolution of 0.5˚ x 0.5˚ (as with the NCEP-NCAR data used in Watson *et al.* (2001)), using a cubic splining function from the Matlab statistics toolbox. The resulting grid is shown in Fig. 6-4. The interpolated pressure data were then converted to geostrophic u and v wind speeds as with the work in 5.3.1.1. Where GCM 10m data are referred to as

ECH5 hereafter, this is ECHAM5 daily mean wind speed extracted for the period 1961-90 over the UK region at the original 1.8˚ x 1.8˚ resolution with no interpolation.

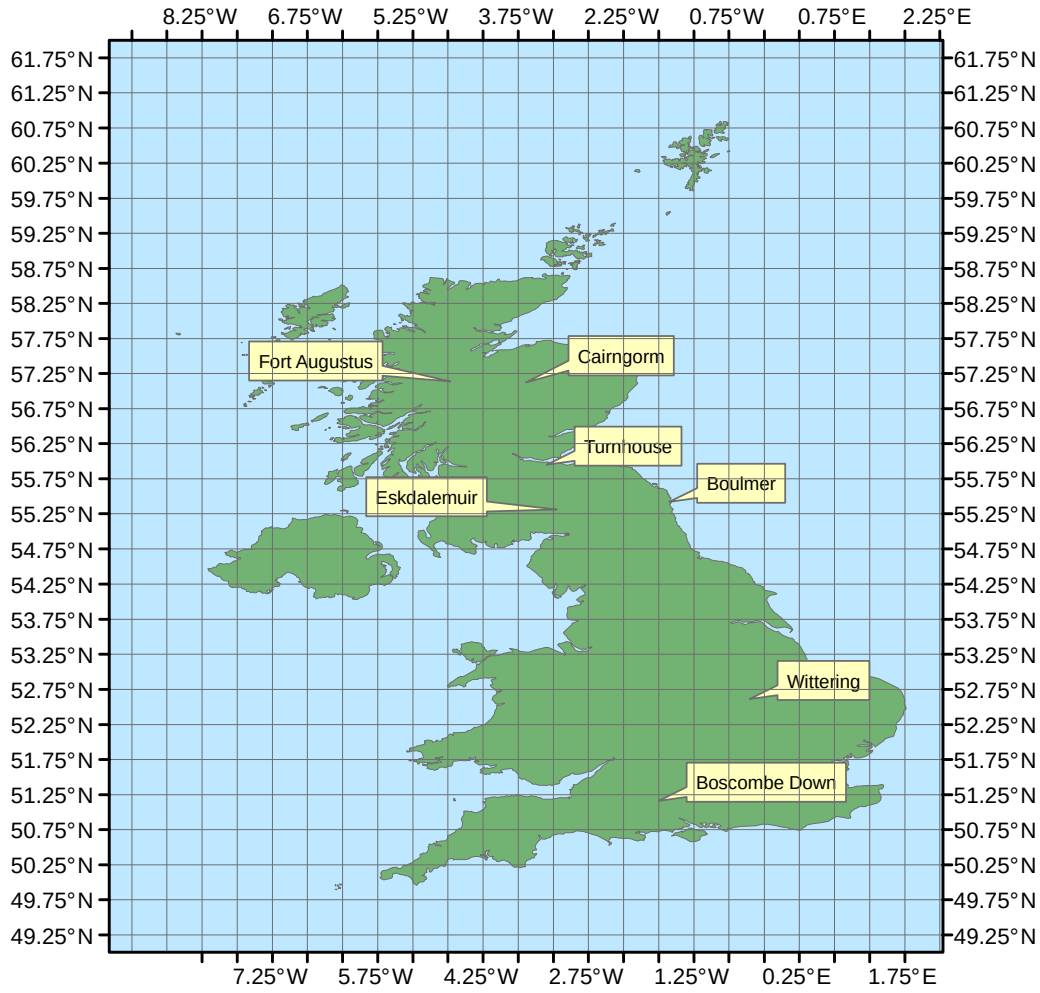

Fig. 6-4 Interpolated 0.5˚ Grid and Met Stations

ERA40 reanalysis six-hourly mean sea-level pressure for 1961-90 has also been used in this chapter for comparison purposes, extracted at 1˚ x 1˚ resolution and interpolated by cubic splines to the same 0.5˚ x 0.5˚ grid as the ECH5 data (European Centre for Medium Range Weather Forecasting, 2006). The six-hourly data were averaged into daily time steps to make it directly comparable to the GCM data, and converted to geostrophic u and v wind speeds as in 5.3.1.1. ERA40 10m mean wind speed data were employed in the work at the original 1˚ x 1˚ resolution, again averaged from six-hourly samples into a daily average value for each grid point over the 1961-90 period.

The observed wind climate data as used in this study were met station data – known as 'MIDAS' data – (UK Meteorological Office, 2006) which, for some of the sites detailed above, were available for the full thirty years of the analysis period, 1961-90. Some stations only had available data for a shorter time within this period; but these were long enough to be considered sufficient to represent the regional wind climate. Mean wind speed and direction information were obtained at hourly resolution for as much of the 1961-90 period as was available for each site. They were processed using a Matlab function which utilised the time stamps in the data files to average the 24 hourly readings for each day into one mean wind speed and direction value. There were unfortunately some missing hourly values in both speed and direction for all the sites; these were ignored in the daily averaging process.

6.3.3 Method 1 - Linear regression

Given the pseudo-linear relationship between geostrophic and surface wind speeds contained within the geostrophic drag law, as demonstrated in section 6.2 above, a simple linear regression between the two variables would be expected to reveal a strong correlation. Using observed surface winds with geostrophic winds from a GCM requires the use of the MOS technique – i.e. deriving a relationship using the output of the model as the predictor and observed variables as their predictand (2.1.8.7) - to compensate for any inherent bias in the model. This ought to give reasonable results for the control period, particularly as the data being considered are twelve month time series of typical monthly means for a defined time period, rather than data with a higher temporal resolution. However, there is a crucial caveat to be borne in mind when carrying out statistical downscaling using future data projected by climate models: that the statistical relationships derived for the control period cannot be certain to apply in the future state. In this case the underlying physical relationship - the geostrophic drag law - is constant and proven. It would be fair, therefore, to expect that the strong relationship would persist in the future - unless winds unrelated to the geostrophic wind, such as those driven by thermal factors, became more common in the UK. This cannot, of course, be ruled out and so caution must be applied when considering any results.

To implement this downscaling method, a typical monthly mean was calculated for each of the twelve months from the even-numbered data points, i.e. every second time step, in the 1961-90 control period from the met station and then from the even-numbered GCM geostrophic wind data points at the 0.5˚ grid square corresponding to the met station site. For a linear regression such that, $y = mx + c$, where y is surface wind and x is the geostrophic wind, the regression coefficients m and c were calculated. The R^2 correlation coefficient was calculated to give an indication of the similarity of the two datasets. The regression coefficients were then applied to the monthly means, calculated from the odd-numbered data points of the GCM geostrophic wind data, to derive a new 10m wind 12-month time series. This was then compared with the 12-month mean time series calculated from odd-numbered data points in the observed time series. These results are denoted 'Lin Reg Geo' in the figures for each site.

There is a possibility that physical modelling within the GCM itself, especially in the case of more homogeneous terrain, may well be better than the simple linear empirical relationships derived between model geostrophic wind and observed surface winds. The derivation of a second linear regression relationship, but this time between GCM 10m winds and observed surface winds may, in fact, give superior results, and this will also be investigated for the case study sites. The method is identical to that described using the geostrophic wind but with GCM 10m wind substituted for geostrophic wind. This relationship obviously does not have the same physical basis as that derived using geostrophic wind, but it compensates empirically for the error involved in the GCM parameterisations. These results are denoted 'Lin Reg 10m' in the figures for each site.

6.3.4 Method 2 - The geostrophic drag law

Applying the established physical relationship between geostrophic and surface winds, i.e. the geostrophic drag law, directly to geostrophic wind speeds should give a good approximation of a site-based wind climate, provided the correct value for surface roughness length is used and that the assumed A and B parameter values are correct; but the relationship does neglect the other topographical features that affect wind climate, such as obstacles and surface elevation.

It would be anticipated that for simple sites, where the surface roughness length is the dominant factor affecting the wind climate and is fairly consistent over the surrounding land, the method will be reasonably successful at capturing the features of the observed wind climate. Further complicating the issue, however, is that rather than using observed geostrophic wind, it would be intended that model data be employed. The method is predicated on the climate model faithfully representing the real geostrophic wind over the time period under consideration. The intrinsic assumption is that the model is capable of representing the large-scale wind climate accurately - so in this section the testing of the model against observed data becomes particularly important. As with the method described in section 6.3.3, the model may actually successfully invoke a number of the surface factors itself in its parameterisation scheme; and the 10m wind might, in fact, represent the site wind climate more successfully than the model geostrophic wind, so an alternative model using GCM 10m winds will also be included.

A typical monthly mean observed wind speed was calculated from met station data for each of the twelve months by grouping the hourly data into monthly datasets, as with method 1 (6.3.3). This was then compared with surface wind datasets generated from the GCM geostrophic wind for the period 1961-90, and the GCM 10m wind climate. These results are shown as 'ECH5 d/s' in the figures for each site. For comparison, the same data were generated for this period from ERA40 geostrophic and 10m winds. For each of these datasets, time series have been extracted for the grid cell in which the observation sites are located, and averaged to give twelve monthly means. These results are shown as 'ERA40 d/s' in the figures for each site.

6.4 Control period results

6.4.1 Boscombe Down

An important note on this site is that it is situated at the very boundary between two of the interpolated 0.5˚ grid squares of the GCM. This may pose a problem whereby the most representative GCM geostrophic wind could actually be from a neighbouring cell, rather than the one in which the met station is specifically located. Since this problem could equally well arise in respect of all sites not precisely in the

centre of a grid square, a rule has been applied that data for each site must be compared with GCM geostrophic wind from the grid box in which it is located, no matter how close to the boundary.

6.4.1.1 Method 1

On an annual basis for Boscombe Down, the geostrophic wind regression ('Lin Reg Geo') performs marginally better than the 10m wind regression ('Lin Reg 10m') in terms of the difference between the actual ('Midas') and derived wind climate. The R^2 result is 0.7945 for the geostrophic regression and a slightly lower 0.7897 for the 10m regression. Fig. 6-5 shows the performance of each model on a monthly basis alongside the original ECH5 10m winds ('10m ECH'), and it is clear that the pattern over the year is very similar using all three datasets - which would be expected, given their close relationship. The maximum differences in the region of 9% are shown in the months of March and April, whilst the best predicted month is August, with a difference of 1% in the geostrophic model and nearly zero in the 10m wind model. The mean absolute percentage error (MAPE) over the year, i.e. averaged so that the negative values do not cancel out the positive or vice versa, is 4.94% for the geostrophic model and 5.1% for the 10m model, suggesting that a slight improvement in the result has been obtained by bypassing the model parameterisations and using the geostrophic wind.

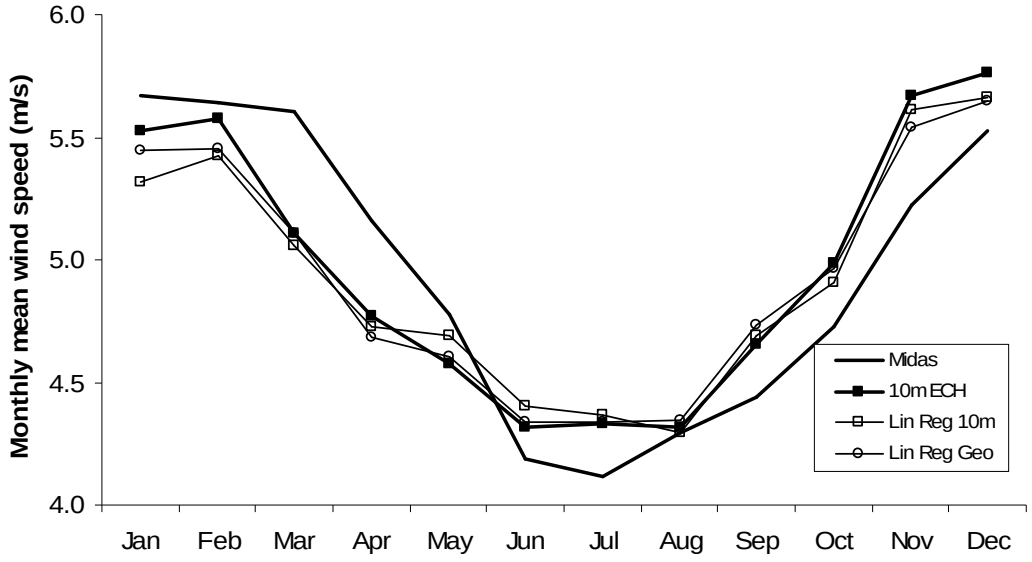

Fig. 6-5 Boscombe Down Method 1 – Linear Regression

6.4.1.2 Method 2

The first attempt at this downscaling technique was carried out using a roughness length of 0.03m, which is slightly higher than for plain grassland - to account for the presence of surrounding roads, buildings and trees; unfortunately this gives a very poor result, with a derived surface wind much higher than the observed wind. The second attempt used a roughness length of 0.1m (Fig. 6-6a, 'ECH5 d/s') - which might be expected for a region surrounded by agricultural land (Boehme, 2006). The second value is more successful in terms of minimising the difference between the downscaled geostrophic wind values and the observed values; but in both cases, the ECH5 10m data ('ECH5 10m') taken directly from the model more closely resembles the observations. Going a step further and using a roughness length of 0.2m to downscale the geostrophic wind data reduces the percentage difference between the downscaled values and the observed values (Fig. 6-6b); however, this is possibly a false improvement as the elevation of the site or the influence of obstacles may impact on the wind speeds as well as the roughness length, and given its situation, a value of 0.2m is probably not realistic. Even at this, the GCM 10m climate is still a better representation of the observed climate, and nothing has been gained by using geostrophic wind.

The original ERA40 10m data ('ERA40 10m') are substantially lower than the observations, indicating perhaps either a systematic low bias in the reanalysis model or simply that the surface parameters assumed in the model are too different compared to the actual values at this specific site. The process of downscaling the ERA40 geostrophic wind data using the drag law with a roughness length of 0.1m ('ERA40 d/s') gives monthly mean values closer to the observations than the original ERA40 10m data. Neither the value of 0.1 or even 0.2 managed to produce a monthly mean wind climate which resembles the observed climate as closely as that developed using a linear regression method.

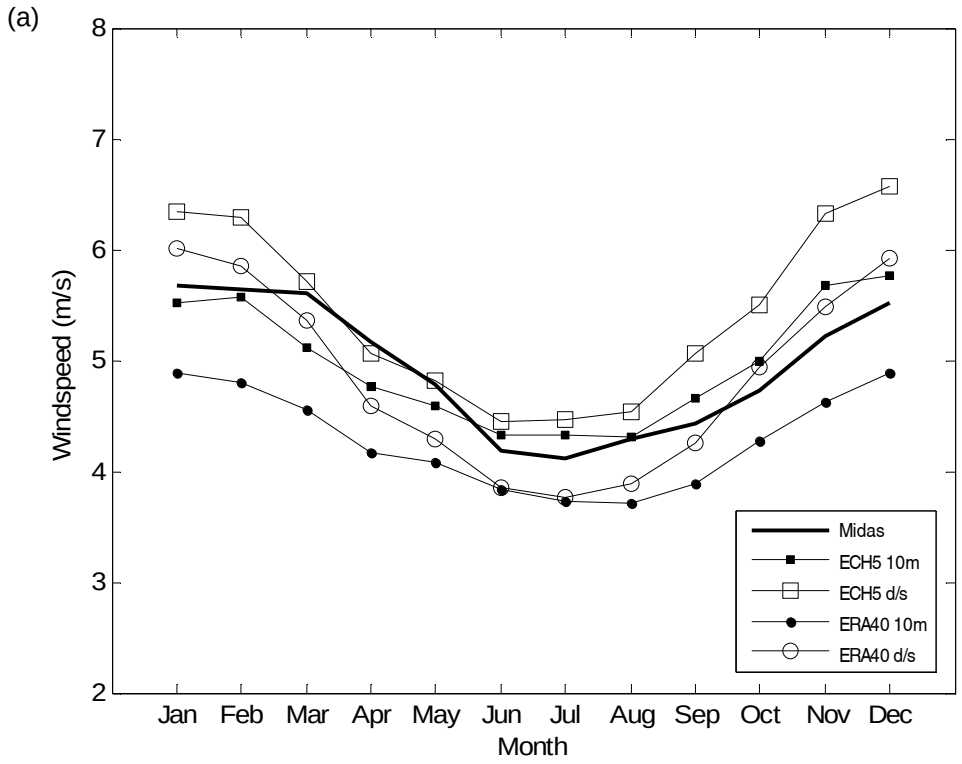

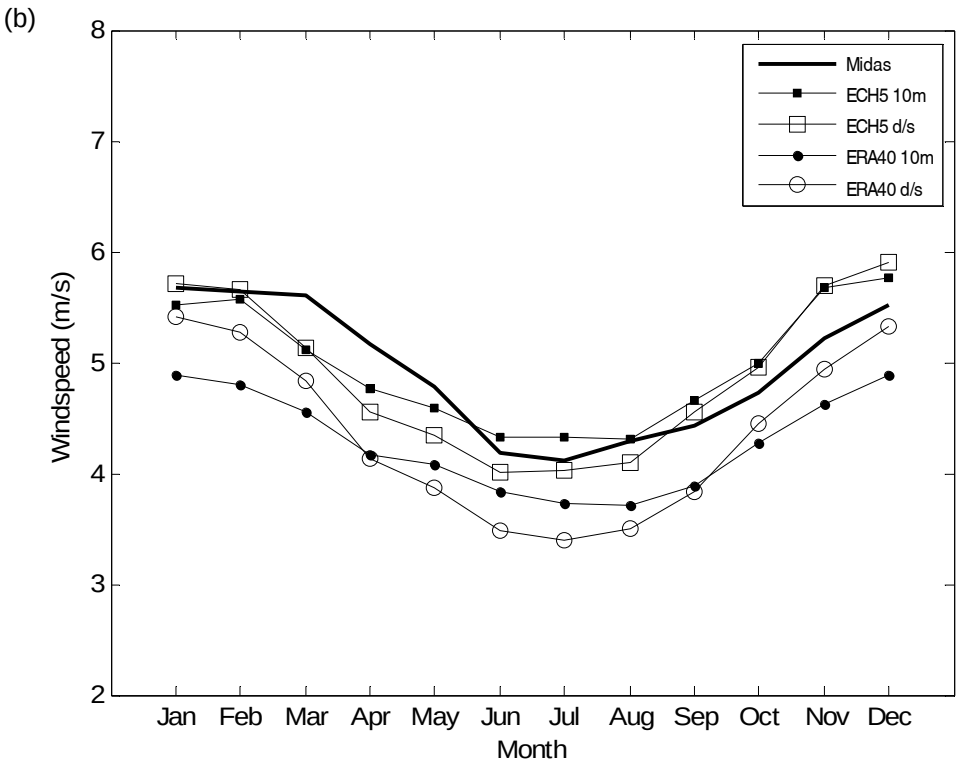

Fig. 6-6 Boscombe Down Method 2 – Drag Law

(a) $z_0 = 0.1$; (b) $z_0 = 0.2$

6.4.1.3 Site summary

The observed data for this site shows mean wind speeds for the months of March and April that are higher than those hindcast by the model. The ERA40 model appears to capture this better than the GCM (Fig. 6-7), presumably due to its assimilation of observed data; but it still shows a slight decrease in March which is not apparent in the station data. The results for March and April for each of the downscaling models are particularly erroneous as a result of this issue. November also shows a consistently large error, with all the models estimating higher winds than observed.

Overall, for the Boscombe Down site there is not much to be gained by using a downscaling technique, as the GCM 10m wind data seems to be just about as accurate. Over a year, the differences in monthly wind speed cancel out to less than 1%, so that an annual energy estimate derived from the GCM data would suffice.

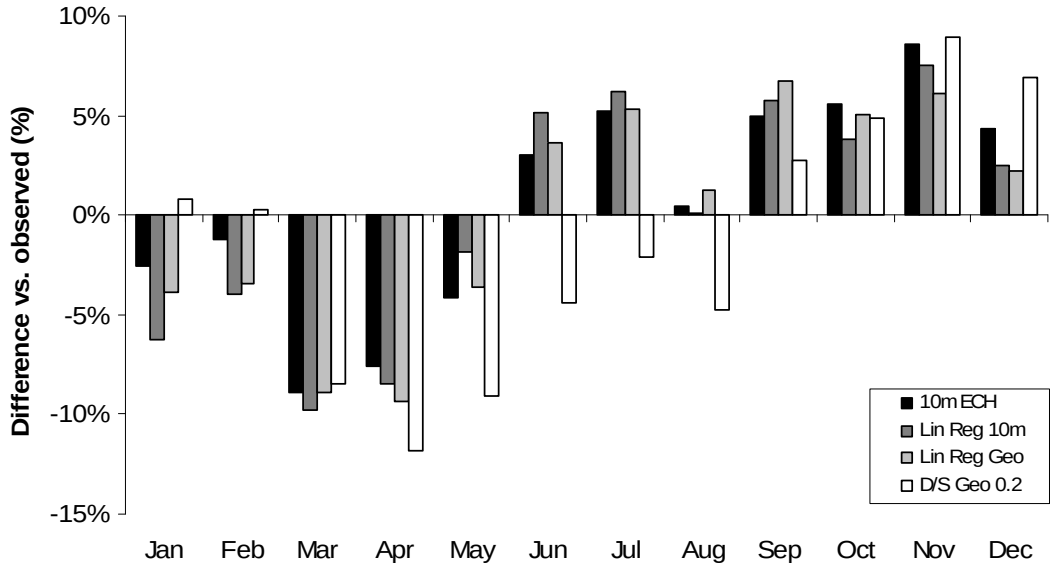

Fig. 6-7 Boscombe Down - Summary of differences in derived and observed datasets

6.4.2 Boulmer

6.4.2.1 Method 1

The regression models at this site appear to perform quite well (Fig. 6-8). The R^2 value for the 10m regression is slightly better at 0.8931, than the geostrophic regression which had an R^2 of 0.8843. The mean absolute percentage difference based on the monthly means gives a very slightly better result for the geostrophic

model, at 4.13%, and the 10m regression coming in at 4.16%. As with the results for Boscombe Down, the pattern of error in the monthly means is similar in both models over the year. The month of maximum error in both cases is March, where the models give an underestimate of approximately 16%; and the most successful months appear to be September and November: the 10m model gives errors of around half a percent and the geostrophic model has an almost zero error for November and 1.2% for September. In the case of the very small errors, there is less consistency between the models in terms of under- or overestimation, but they do show similar directions for the larger differences.

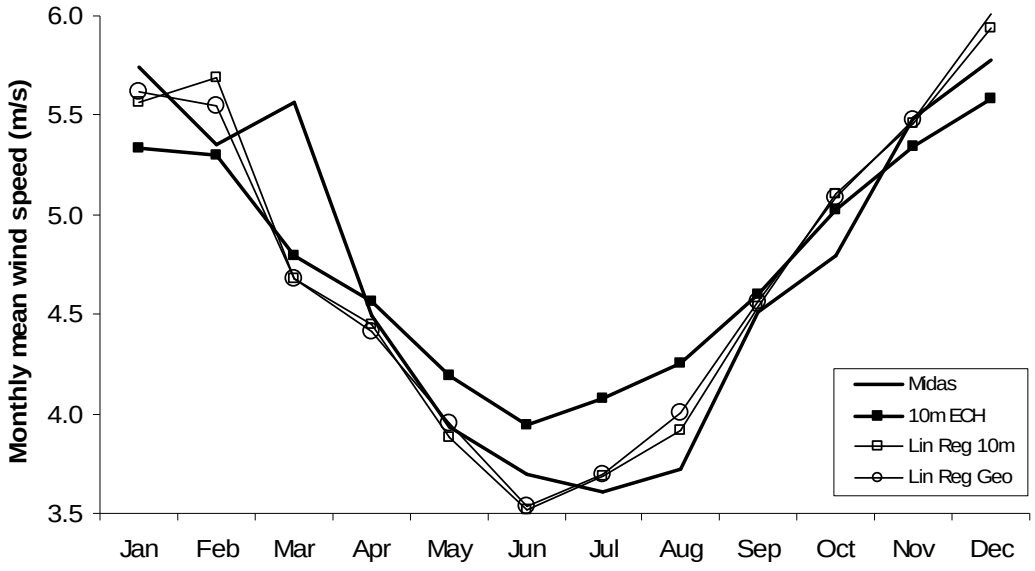

Fig. 6-8 Boulmer Method 1 – Linear regression

6.4.2.2 Method 2

In a similar way to Boscombe Down, the geostrophic wind downscaled using a roughness length of 0.03m is less successful than that using 0.1 (Fig. 6-9a), but both attempts show greater differences than that generated using the original GCM 10m data, despite the lower resolution. As with the Boscombe Down site, increasing the roughness length to 0.2m (Fig. 6-9b) gives a lower percentage difference between the downscaled data and the observed data, but as with Boscombe Down, this is most likely false, as all the characteristics of the site point to a lower roughness value.

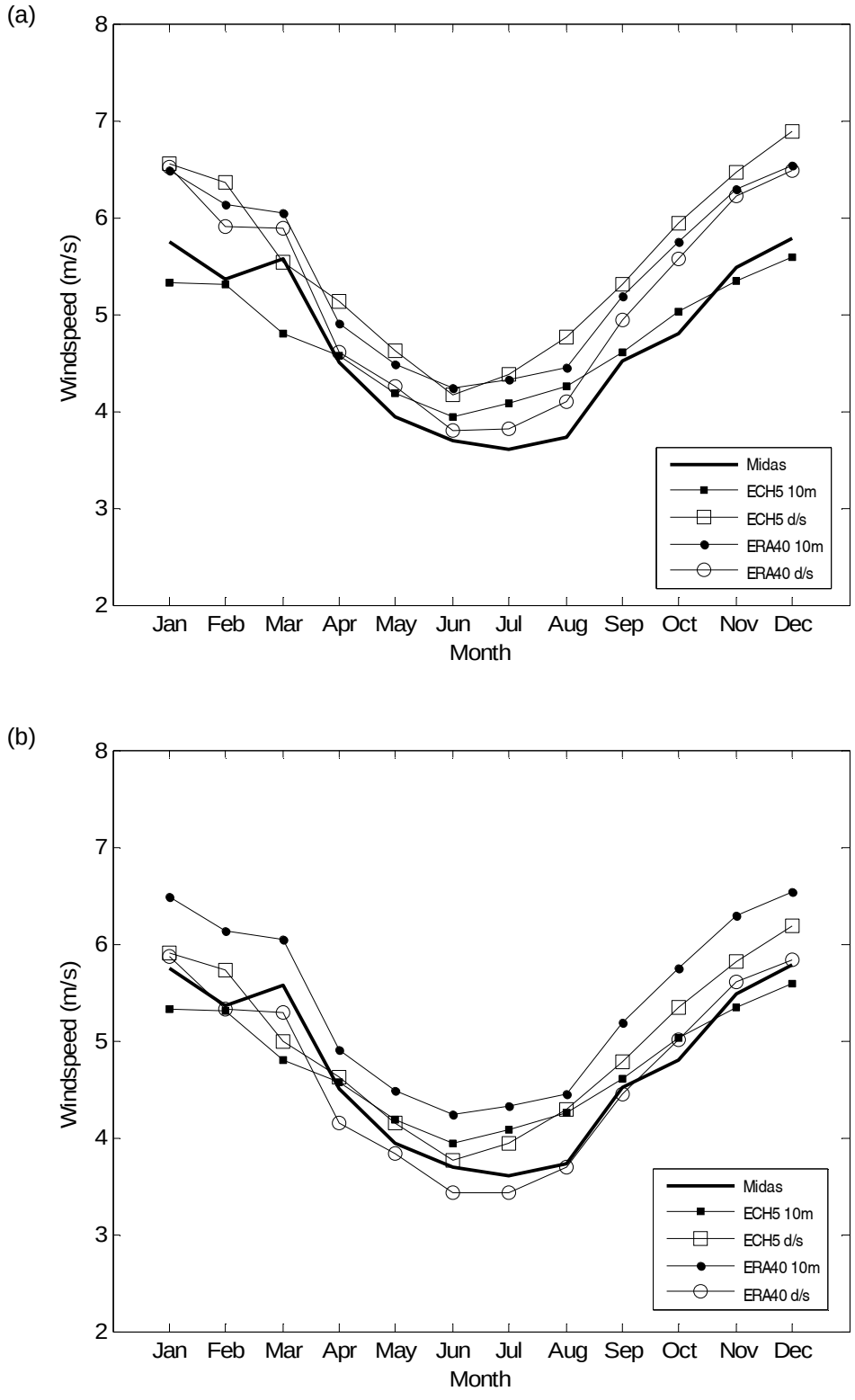

Fig. 6-9 Boulmer Method 2 – Drag Law

(a) $z_0 = 0.1$; (b) $z_0 = 0.2$

The ERA40 data for this region is biased slightly high relative to the raw observed data at the site, and as with Boscombe Down, appears to be more different to the observations than the GCM. Again, downscaling the ERA40 geostrophic wind data using the geostrophic drag law with a roughness length value of 0.1m is an improvement versus the ERA40 10m data.

6.4.2.3 Site summary

For the Boulmer site (Fig. 6-10), there does not seem to be any obvious merit in choosing the geostrophic drag law downscaling option over the GCM 10m winds. The 10m data shows lower percentage errors versus observed in most months - the exceptions being May, June and July, where the downscaling performs better.

Neither the downscaling or the ECH5 10m data taken directly is as good a representation of the observed mean monthly wind climate as that obtained by linear regression. The linear regression with geostrophic winds is, to a very slight extent, better than that with the 10m winds, and both are a small improvement on using the raw GCM 10m data.

In terms of the seasonal pattern, the met station data shows a relative peak in March and lows in August and October. The March peak is better captured by the downscaled geostrophic wind than the ECH5 10m wind, but is still underestimated by 10%. Both the regression models perform worse for the March peak than the GCM 10m wind and the downscaled geostrophic wind, with errors of around 16%.

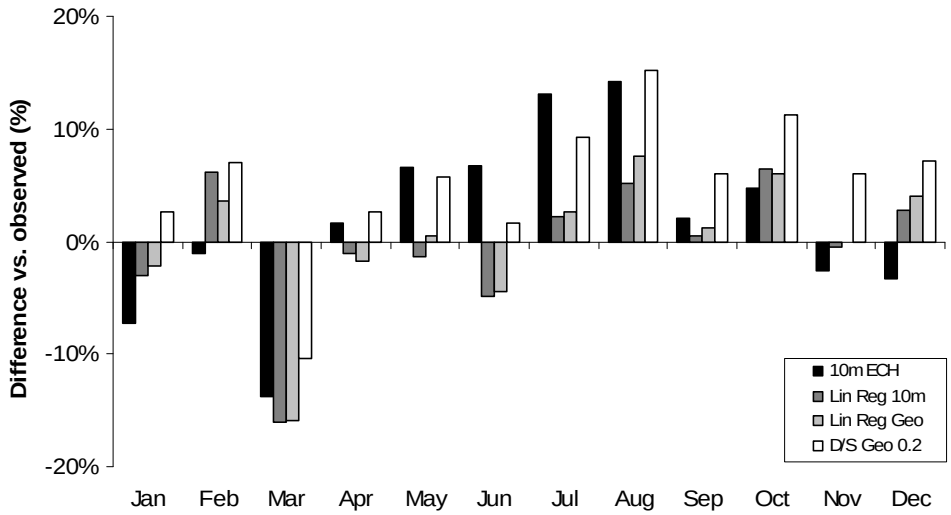

Fig. 6-10 Boulmer - Summary of differences in derived and observed datasets

6.4.3 Wittering

6.4.3.1 Method 1

The results of the linear regressions for Wittering are shown in Fig. 6-11. The R^2 for the geostrophic regression was 0.766, and 0.7251 for the 10m regression, indicating a marginally better result for the geostrophic wind. The percentage difference in the annual average wind was also very slightly better for the geostrophic model, and similarly, in terms of MAPE the geostrophic model did better with 3.56%, as against 4.05% for the 10m model. As anticipated, the pattern of difference over the year is very similar in both models. February, March and April were the worst performing months in terms of matching the observations, with an average absolute percentage difference of 7.37% in the geostrophic regression and 7.88% in the 10m regression. May, June and November were the best predicted months, averaging at 0.53% and 0.47%, for the 10m and geostrophic models respectively.

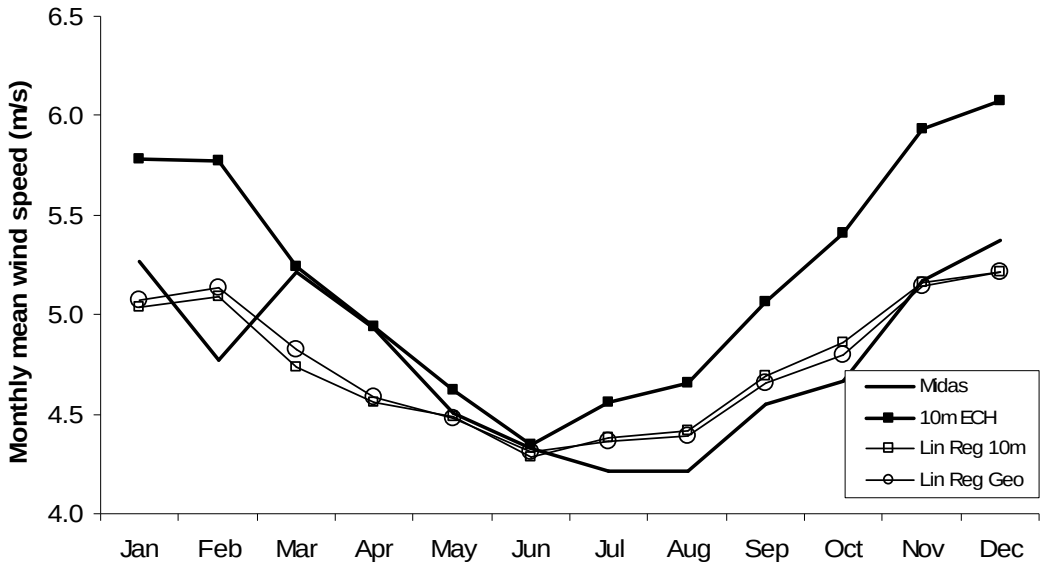

Fig. 6-11 Wittering Method 1 – Linear regression

6.4.3.2 Method 2

As with the previous two sites, the roughness length of 0.03m causes the downscaled geostrophic wind values to be much too great an overestimate of the monthly mean wind speeds, while a value of 0.15m gives a result closer to the observed winds than the original GCM 10m wind climate (see Fig. 6-12).

(a)

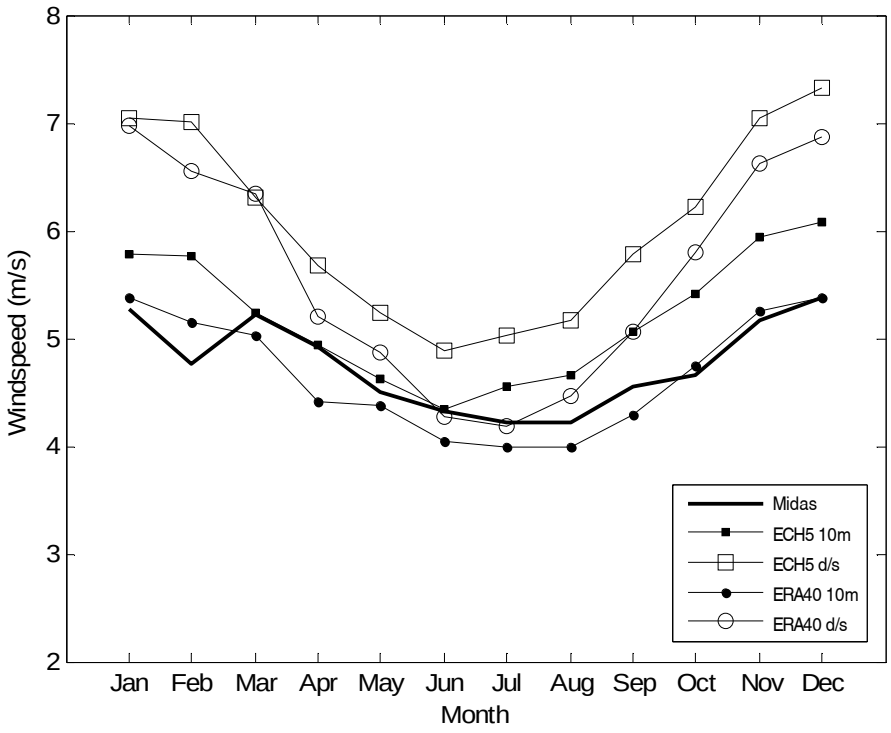

(b)

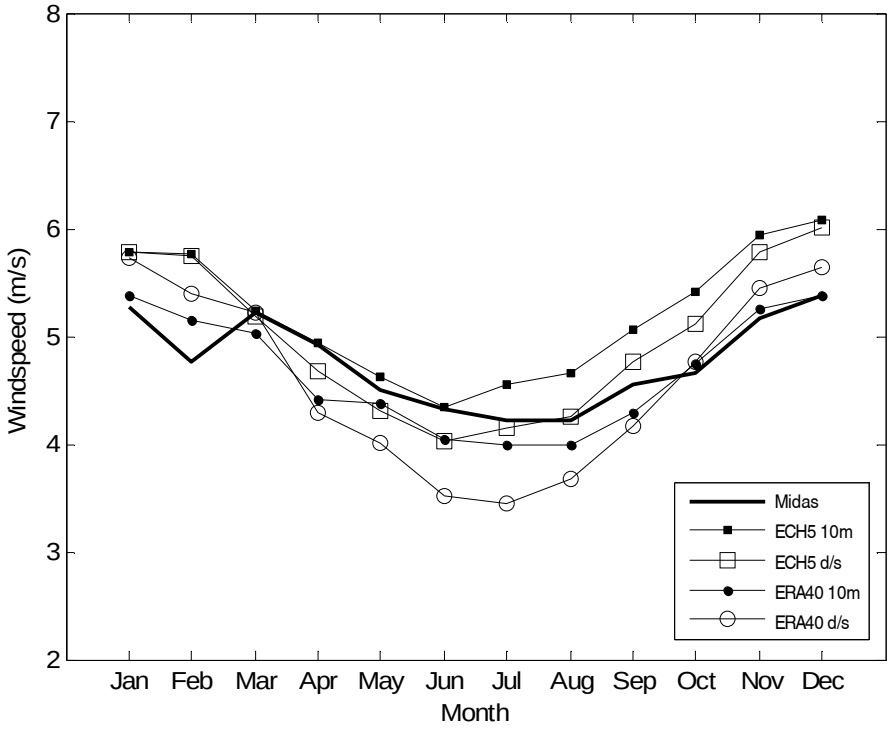

Fig. 6-12 Wittering Method 2 – Drag Law

(a) $z_0 = 0.03$; (b) $z_0 = 0.15$

The downscaled model is very similar to the original 10m GCM data in January, February and March, performs more poorly in April, May and June, but then outperforms it in the later six months of the year.

Ignoring the observed data for a moment, and looking at the downscaled geostrophic and original data from the GCM together, it appears that this roughness length value has resulted in the two values for each month converging, particularly for the spring, summer and autumn months, the values from both datasets are very close. This might suggest that the GCM uses a similar roughness length for this grid square to parameterise the surface wind data from the large-scale variables. The value of 0.15m seems realistic, given the site description. Of all the datasets for this site, the ERA40 10m most closely replicates the observations.

6.4.3.3 Site summary

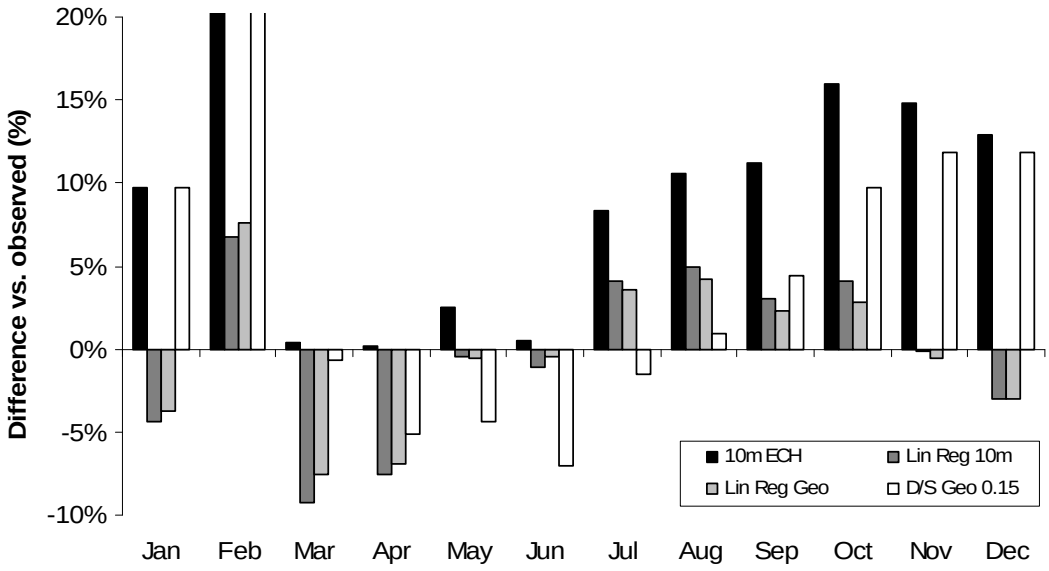

Fig. 6-13 Wittering- Summary of differences in derived and observed datasets

For the Wittering site, all of the downscaling models (see Fig. 6-13) are an improvement over the GCM 10m data, with the linear regressions performing best. The geostrophic linear regression is marginally better than the 10m linear regression, but the differences are quite small.

The observed records indicate a particularly low mean wind speed in February, which rises again in March and April rather than continuing on a downward trend;

this is not apparent in the GCM data, and ERA40 data shows only a very slight rise in March. The annual range over the twelve monthly means is also smaller in the station data than hindcast by the models - as evidenced by the flatter yearly profile. This is more ably represented by the regression models than either the drag-law downscaling or the ECH5 10m data itself.

6.4.4 Fort Augustus

This site is particularly interesting as the observed wind climate is peculiar for two reasons: firstly, because it displays an inverted seasonal pattern, not typical for the UK, and secondly because it has a relatively low mean wind speed. Both factors are likely to be a result of the met station location in a deep valley, surrounded by very mountainous terrain. The sheltering effect of the hills will reduce the mean wind speed significantly; in fact, Troen & Petersen (1989) mention this station in particular as being in a highly sheltered position.

6.4.4.1 Method 1

As with the previous sites analysed, there is very little to separate the results of the two linear regression models (see Fig. 6-14). The R^2 values and MAPEs are 0.5151 and 6.17% for the 10m regression and 0.4838 and 6.18% for the geostrophic regression. The geostrophic model seems to perform very slightly better on the annual average figure. Monthly patterns are, again, very similar in both models. The biggest errors of around 15% are found in August and November, with January and March also poor, with errors in the region of 10%. The most accurately predicted months are February plus the summer months of June and July. Both regression models go some way to re-creating the inverted seasonal pattern of the data, which the raw GCM 10m data clearly does not.

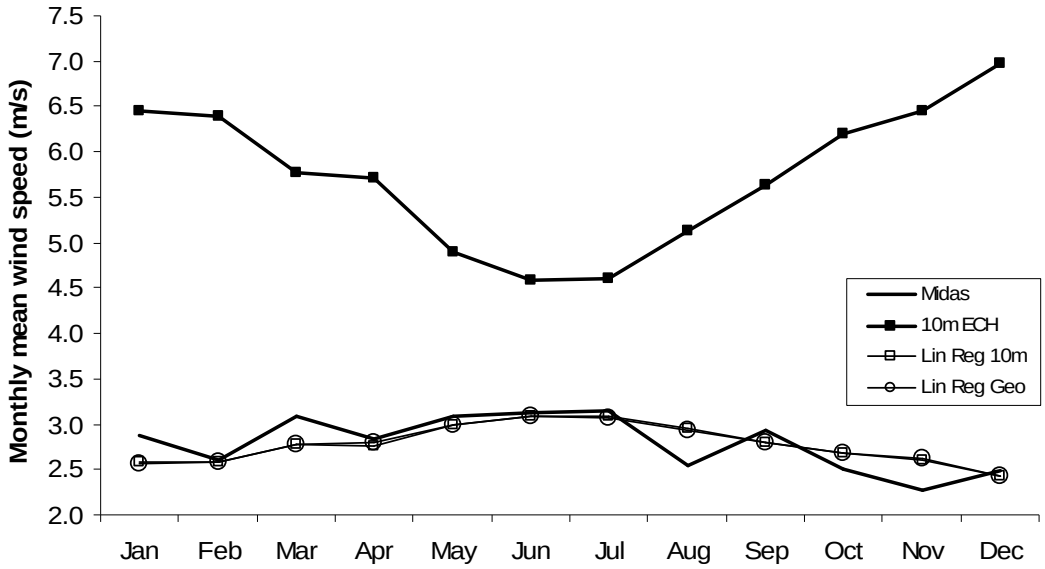

Fig. 6-14 Fort Augustus Method 1 – Linear Regression

6.4.4.2 Method 2

This particular area of the UK has very heterogeneous terrain, varying at some points over scales of metres. Consequently, the parameterisation scheme within a model like the GCM, which is limited to the resolution of the model, is unlikely to represent any of the terrain within the cell due to the averaging process. The slightly higher resolution ERA40 10m wind data does go some way to representing the slightly lower wind speeds in this region, but the GCM 10m data suggests there should be much higher mean winds (see Fig. 6-15). This may be due to the average elevation within the model grid square being set relatively high, whereas this particular met station is positioned in a valley at quite low elevation, in the lee of a westerly hill.

Using a roughness length of 0.1m gives the downscaled GCM geostrophic wind similar values to the model's 10m data, whilst a roughness length of 0.4m makes the downscaled ERA40 geostrophic values closer to the ERA40 10m figures, possibly indicating the particular levels of roughness length set in each model. Applying the roughness length of 0.4m to the GCM downscaled climate brings it nearer to the ERA40 values.

(a)

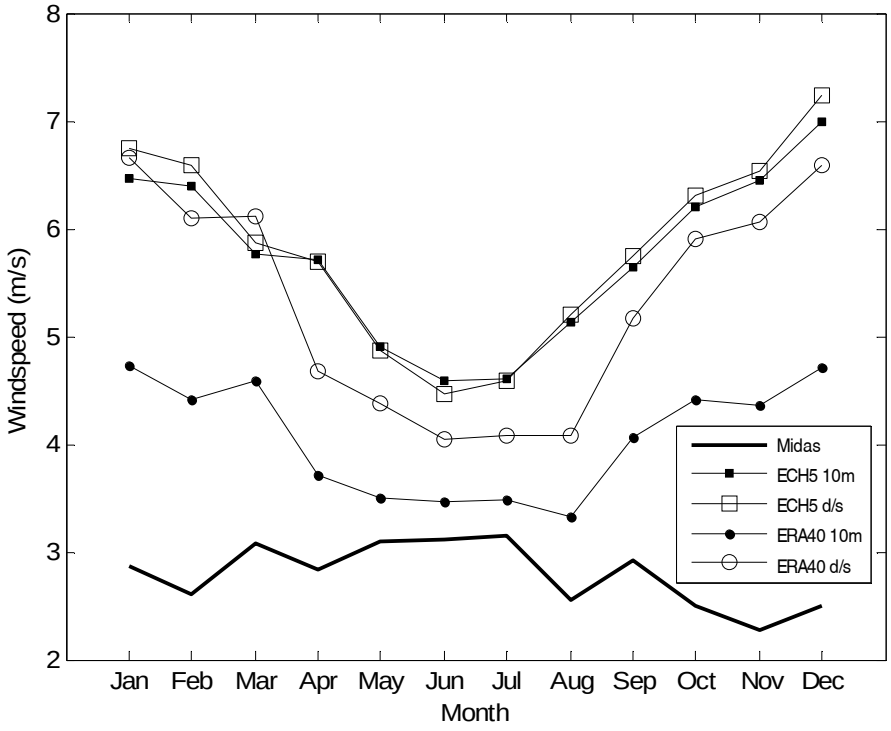

(b)

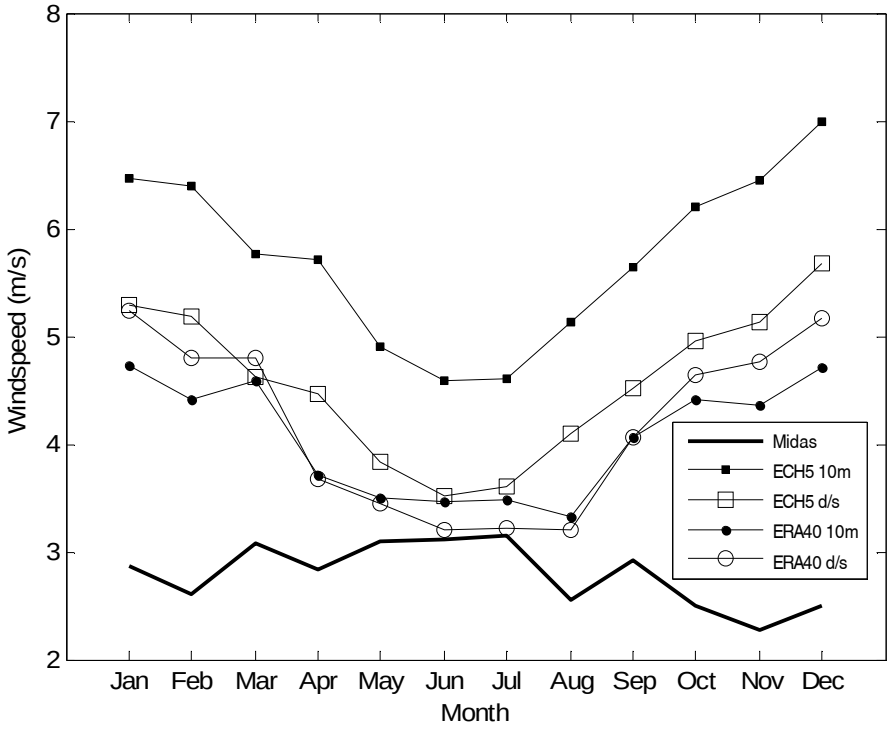

Fig. 6-15 Fort Augustus Method 2 – Drag Law

(a) $z_0 = 0.1$; (b) $z_0 = 0.4$

6.4.4.3 Site summary

What the results in this section show is that there is, indeed, a difficulty both in modelling the wind climate and possibly also with the observed data. The observed wind speed values are low for this region, and show a seasonal pattern inverted from what might be expected for the rest of the country (and what is evident from the analysis of the other sites). A closer inspection of the data shows an unexpectedly high proportion of 'zero' readings - which could be either a quality issue with the data itself, or the result of a sheltering effect or other terrain feature, or both. Either way - and it is impossible to tell which it might be - this suggests further analysis might be required to fully ascertain the reasons.

There does appear to be some advantage in using the downscaled geostrophic wind over the GCM 10m wind, but the linear regression models outperform both by quite a large degree. It is clear, however, that there is still some way to go towards understanding the true wind climate at Fort Augustus.

6.4.5 Eskdalemuir

6.4.5.1 Method 1

The comparison between the two linear regression models for Eskdalemuir is inconclusive (see Fig. 6-16), but both are more successful at representing the observed climate than the GCM 10m model. The R^2 value for the geostrophic model is 0.7134, and a slightly superior 0.741 for the 10m model. The MAPE for the geostrophic model, however, is 4.8%, whilst the 10m model gives a slightly higher error of 4.97%. In terms of the annual average error, the geostrophic model shows a very minor improvement. The months that are least successfully predicted by both models are March and July, with errors of 11%, whilst the best months are April and November, both giving errors of between 0 and 1.2%.

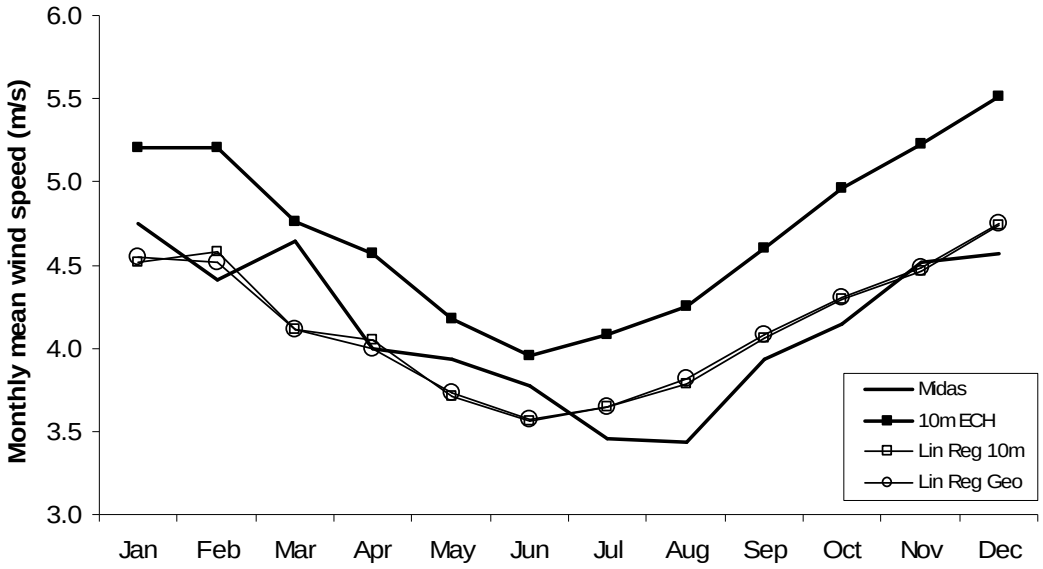

Fig. 6-16 Eskdalemuir Method 1 – Linear regression

6.4.5.2 Method 2

Both the ERA40 and ECH5 10m model results for Eskdalemuir (see Fig. 6-17) produce higher mean wind speeds than the observed, suggesting that they do not account for a high roughness length caused by the presence of the surrounding trees. Using a value of 0.1m for the geostrophic downscaling gives results which, for the ERA40 data are very similar to the model's 10m output. Increasing the roughness length to 0.4m gives better results compared to the observed data; indeed the downscaled GCM data is closer to the observations than the GCM 10m values. In reality, the roughness length should be much higher for heavily forested regions, possibly around 0.8m. This would reduce the modelled wind speeds below the observed, but the elevation of the site is reasonably high, and thus might be expected to undergo a correction for this.

(a)

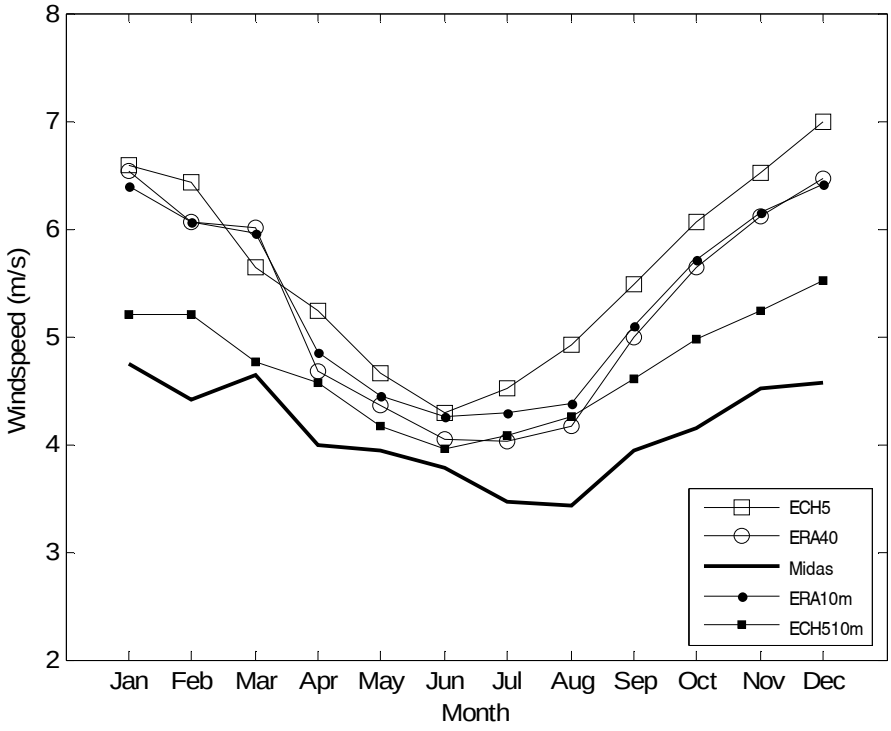

(b)

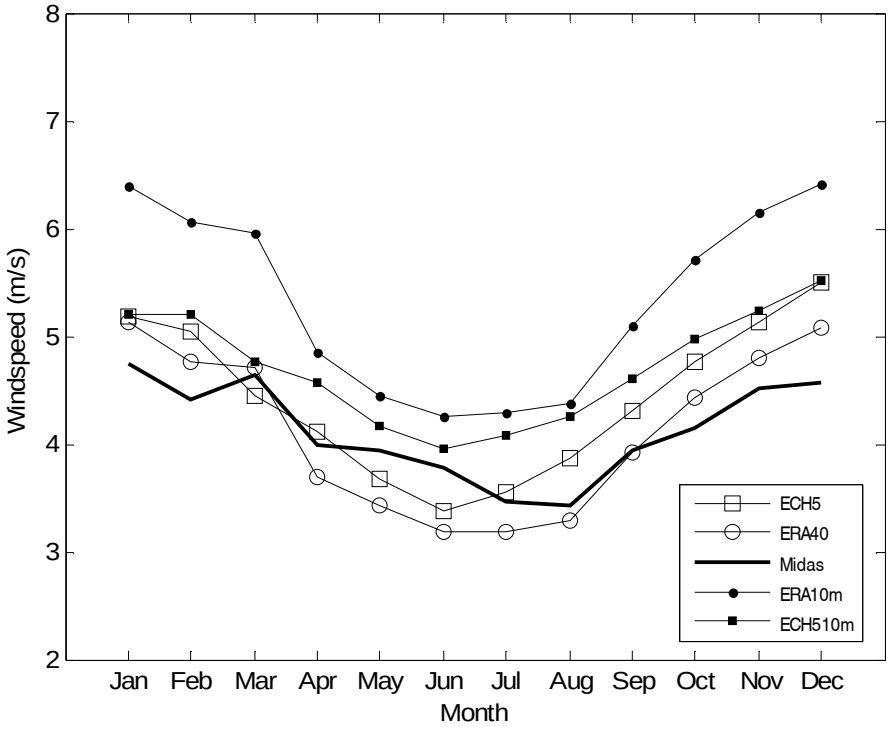

Fig. 6-17 Eskdalemuir Method 2 – Drag Law

(a) $z_0 = 0.1$; (b) $z_0 = 0.4$

6.4.5.3 Site summary

As in the case of Wittering, all of the downscaling models are an improvement here on using the ECH5 10m winds directly, as there seems to be a systematic high bias in the GCM - probably due to the rough forested surface in the vicinity (see Fig. 6-18). As with other sites, a relatively low February and high March wind speed in the observational record is not successfully represented by the models, giving quite significant errors in these months. The observed data implies an annual low in the month of August, whereas the model would suggest June as the low month - which causes a further pattern of error in the downscaling models.

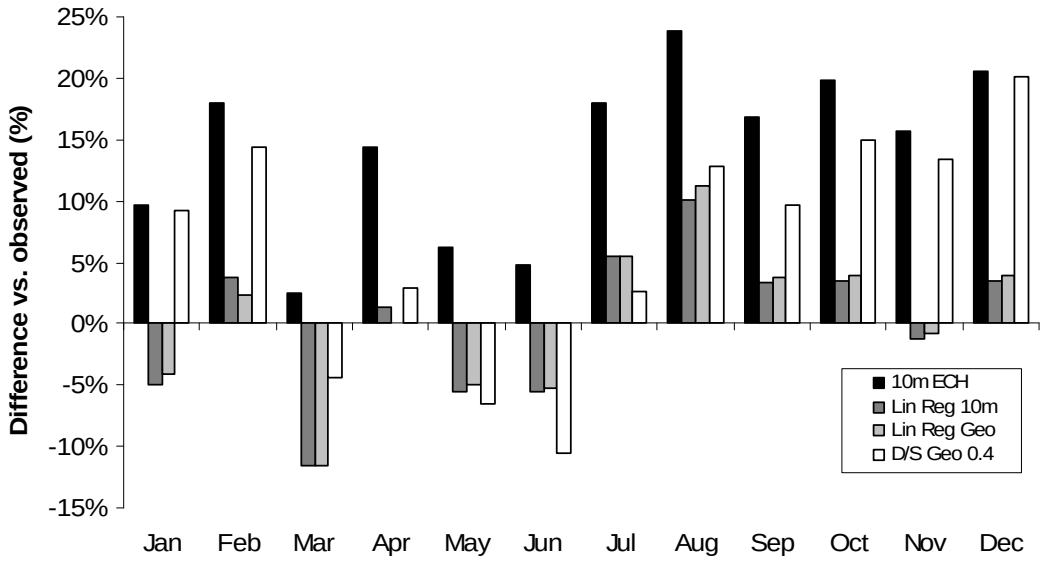

Fig. 6-18 Eskdalemuir - Summary of differences in derived and observed datasets

6.4.6 Turnhouse

6.4.6.1 Method 1

The results for Turnhouse (see Fig. 6-19) are somewhat disappointing, with R^2 values for the even-numbered data of 0.5577 for the geostrophic model, and 0.5953 for the 10m model. However, taking the percentage differences when the model is used to predict the odd-numbered data, the MAPE indicates a fairly good result, with a value of 3.24% for the geostrophic and 3.21% for the 10m winds. The March value is under-predicted by 11% in both models, and August also does badly, with an 8%

overestimate in the geostrophic regression and a 7% overestimate in the 10m regression. The best months were February for the geostrophic model, with an error of close to zero, and September for the 10m model with a 0.39% error. The fact that the equation derived for the even-numbered data points, which appeared to be fairly poor, gives a reasonably good result for the odd-numbered prediction indicates that the relationship is not consistent, and perhaps might be significantly different depending on the data set used to condition it.

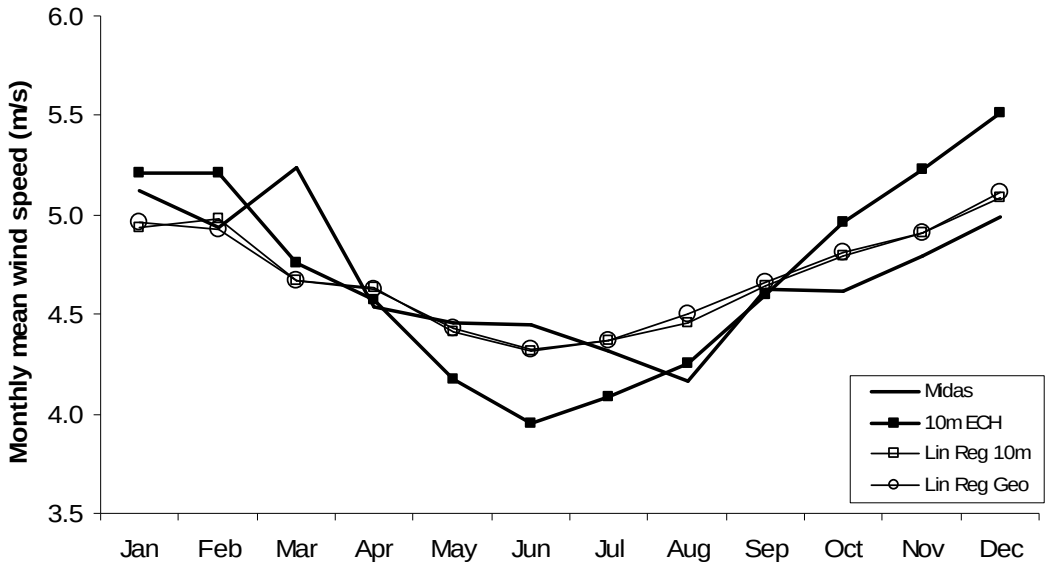

Fig. 6-19 Turnhouse Method 1 – Linear Regression

6.4.6.2 Method 2

Referring to Fig. 6-20, the 10m winds taken directly from the models are a reasonably good representation of the observed data, but the seasonal pattern appears more strong than in the observed data, with higher winter and lower summer winds. A roughness length of 0.3m brings the ECH5 downscaled geostrophic wind to similar values as the model 10m data but this has an even stronger seasonality pattern. The ERA40 data seasonal pattern is stronger again; a roughness of 0.1m gives good summer results but much too high in winter, whilst a roughness of 0.4m makes winter more realistic but the summer values fall too far.

(a)

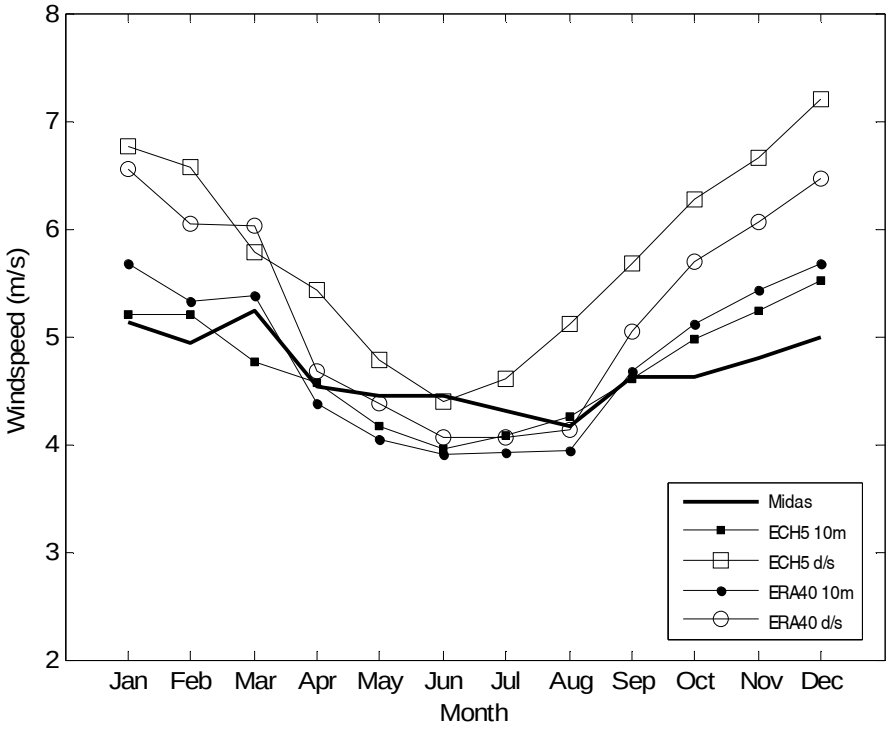

(b)

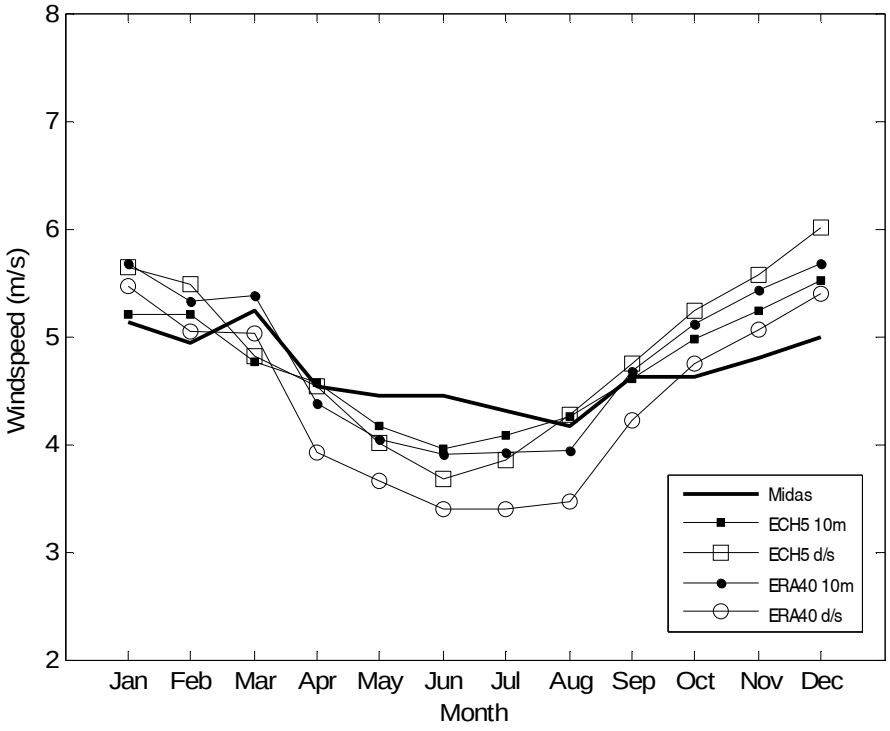

Fig. 6-20 Turnhouse Method 2 – Drag law

(a) $z_0 = 0.1$; (b) $z_0 = 0.3$

6.4.6.3 Site summary

The relatively flat profile of the observed wind speeds at this site is somewhat reflected by the GCM 10m data itself, more so than by the drag law downscaled geostrophic wind which does not present an improvement on the model surface wind. The linear regression models, however, do provide a more adequate representation of the annual profile, minimising the differences quite successfully for most months (Fig. 6-21). March and August display the biggest errors in the regression model, probably for similar reasons to the Eskdalemuir site, where the wind speed has a peak in March and a low in August that are not depicted in the model results.

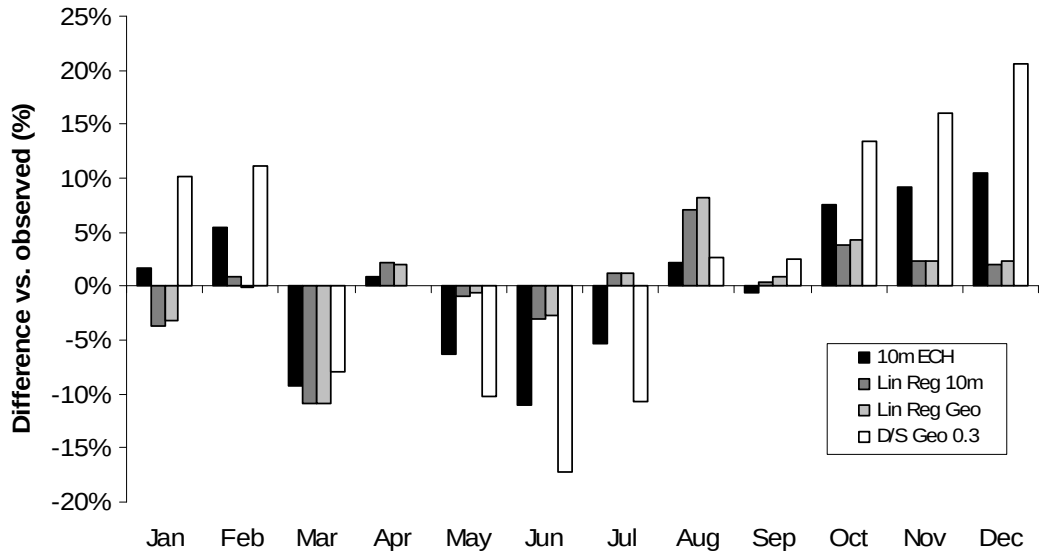

Fig. 6-21 Turnhouse - Summary of differences in derived and observed datasets

6.4.7 Cairngorm

6.4.7.1 Method 1

R^2 values for the two regression models at Cairngorm are calculated at 0.8933 and 0.8889 for the geostrophic and 10m models respectively. As shown in Fig. 6-22, annual average errors are marginally smaller for the geostrophic model, but the geostrophic model MAPE is 6.16% compared to the 10m MAPE of 6.05%. The worst predicted month in both of the models is April - with an 11% error in the geostrophic regression and a 14% error in the 10m regression. Several other months

as generated by the models show errors of around 7-9%, whilst those with common minimum errors are January, and July. The 10m model also shows a minimum error in June, whilst the geostrophic model does not.

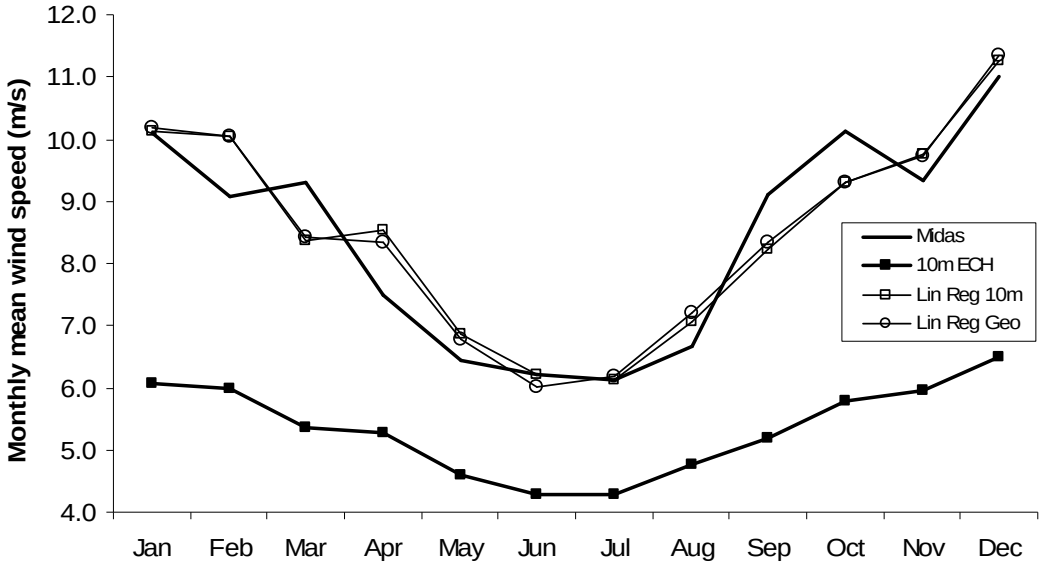

Fig. 6-22 Cairngorm Method 1 – Linear regression

6.4.7.2 Method 2

The extremely high elevation of this observation point would be expected to have a strong bearing on the wind climate by inducing a speed-up effect, resulting in an increase in the mean wind speeds; but this is clearly not captured by the 10m model winds, as the models will have assumed a lower average height for the grid square. The roughness length in the models may also not be representative of the comparatively smooth terrain around the site, with snow present for around four months of the year. A value of 0.01m would be typical for grasslands, but snow would give a lower value due to its relative smoothness (Boehme, 2006). Fig. 6-23 shows results using both these values, and it can be seen that there is not a great deal of difference, but that, particularly for the GCM data, the summer mean speeds are quite close to those observed. In winter, they do not increase by as much as the observed values, however, and so it is likely that the site elevation needs to be accounted for.

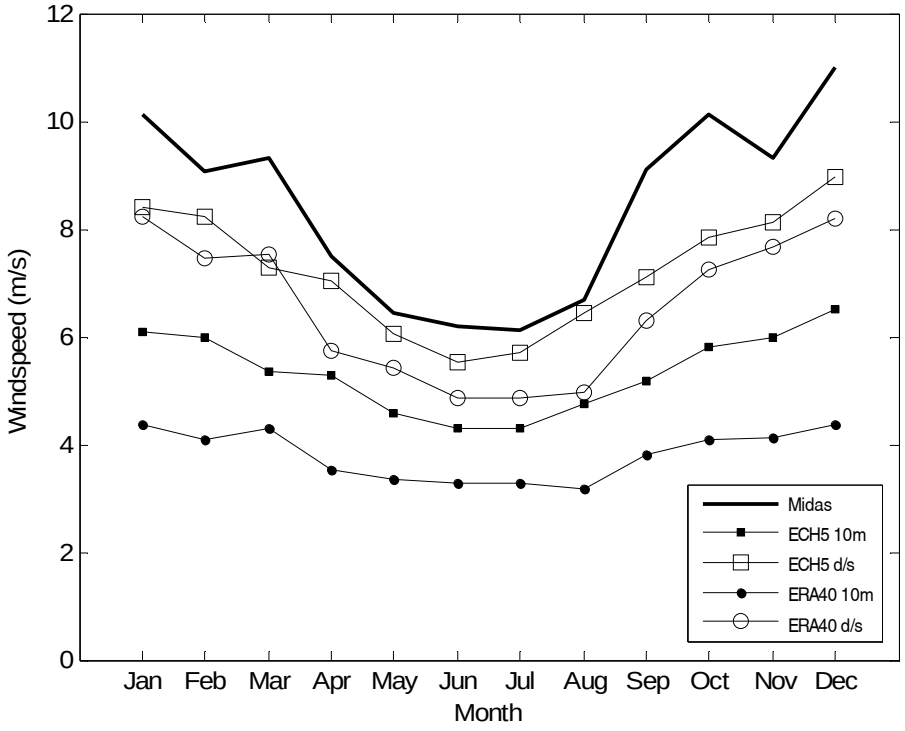

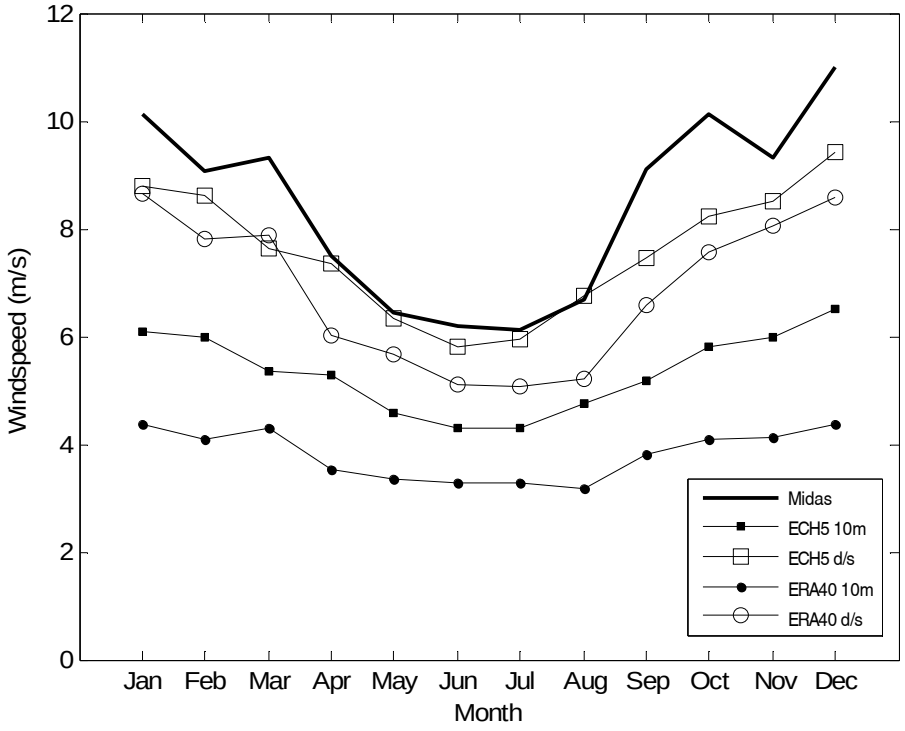

Fig. 6-23 Cairngorm Method 2 – Drag law

(a) $z_0 = 0.01$; (b) $z_0 = 0.005$

6.4.7.3 Site summary

The extreme elevation of this met station site renders it particularly prone to modelling difficulties, particularly at lower resolutions; it would not be expected that the GCM would be representative of wind speeds at the height at which these were recorded. Consequently, all the downscaling methods, as seen in Fig. 6-24, show an improvement in the reproduction of the monthly mean wind speeds compared to the 10m data, as the GCM vastly underestimates the resource available at this level.

One interesting point is that the observed annual range is greater than that modelled, with a tendency towards higher winter peaks. The downscaling methods are all most successful for the May-August period, but fail as the winter extremes are not captured. As with the other sites, the regression models perform best of all the downscaling methods, with the problems being the February-March-April pattern, and some smoothing of an uneven trend in the Autumn months.

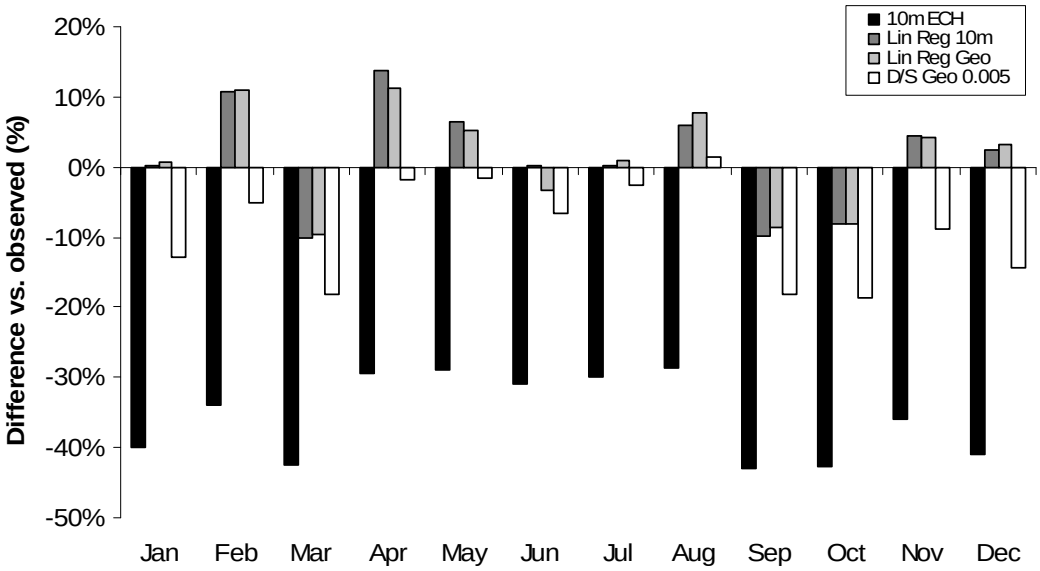

Fig. 6-24 Cairngorm - Summary of differences in derived and observed datasets

6.4.8 Conclusions on downscaling methods

Drawing from this analysis of downscaling methods, the clearest point is that the GCM hindcasting, for March values in particular, is flawed. This may be linked to the discussion in Chapter 5 of the failure to correctly capture the mean pressure pattern for this month, resulting in projections of lower mean wind speeds than

actually observed. However, the observations for most of the sites appear to suggest an unexpected pattern whereby the mean wind speed falls between January and February, and subsequently rises in March. The 10m ERA40 reanalysis data goes some way to capturing the relative gain from February to March at some of the sites, for example, Turnhouse, but the distinctive pattern in the observations is not fully recreated. The origin of this pattern is currently unclear, but it appears not to relate completely to pressure patterns. It is not reflected either in the GCM geostrophic or surface winds.

Site	10m ECH5	Lin Reg 10m	Lin Reg Geo	ECH5 d/s
Boscombe Down	4.71%	5.10%	4.95%	5.43%
Boulmer	6.39%	4.17%	4.14%	7.05%
Wittering	9.02%	4.08%	3.59%	7.33%
Fort Augustus	109.63%	6.20%	6.20%	67.35%
Eskdalemuir	14.20%	4.97%	4.79%	10.13%
Turnhouse	5.83%	3.20%	3.23%	10.20%
Cairngorm	35.57%	6.04%	6.14%	9.19%

Table 6-2 Summary for each site

Table 6-2 shows a summary of the annual mean absolute percentage errors versus MIDAS data using the original GCM 10m data, linear regression with both 10m and geostrophic wind (method 1) and using the drag law (method 2). At some of the sites, the ECH5 10m wind data is relatively successful in representing the monthly mean wind speeds, but in a number of them, such as Boulmer, an improvement is made by using a simple linear regression to empirically correct for differences. In the cases where the GCM 10m winds are not a good depiction of the observed mean monthly wind speeds, downscaling the geostrophic wind using the drag law can enhance the result, but this is generally not as successful as the linear regression model. Downscaling using the drag law alone does not account for factors influencing the wind speeds - such as elevation and atmospheric stability - and by using a regression to build these into the relationship empirically, the result is stronger.

6.4.9 The Wind Atlas Methodology - WAsP

As an extension of the geostrophic drag law method described above, the Wind Atlas methodology attempts to go further, by correcting not only for surface roughness, but also by applying corrections for orographic effects - but in a physically-based manner rather than empirically. This methodology is applied using the Wind Atlas Analysis and Application Program (WAsP). The method invokes the three factors affecting surface wind climate described in 3.3 and shown in Fig.6-25, whereby wind deviates from geostrophic flow due to the influence of surface roughness, the surrounding orography and the presence of obstacles. By removing these influences from observed wind data collected from a typical anemometer at 10m above ground level, a so-called 'regional' wind climate is developed which is strongly related to wind speeds far above ground level. Similarly, a regional wind climate can be applied to develop a site-specific surface wind climate by addition of the three influences (Troen & Petersen, 1989).

WAsP was developed by Risoe National Laboratory in Denmark as a tool for analysis of local wind climate, and is used by many wind farm developers and consultants to assess the wind resource at site level. Given the conditions of relatively homogeneous terrain and topography, WAsP is a useful indicator of the potential wind resource. The idea behind using WAsP as a downscaling tool is that by inputting the geostrophic wind output of a climate model as the 'regional' wind climate or wind atlas, the corresponding surface-level wind climate at a detailed site level can be understood.

The WAsP program takes time series wind data as input and 'cleans' the data to remove the site-specific influences, producing a wind rose and a frequency distribution histogram for each of the sectors in the rose, to which Weibull parameters are fitted. The 'clean' data is presented at a standard range of heights - typically 10m, 25m, 50 m, 100m and 200m - and roughness lengths - typically 0m, 0.03m, 0.1m and 0.4m. WAsP then has the facility to calculate power density from the data, using the frequency distribution; and if it is provided with turbine power curve data, it can generate expected annual energy production figures for a site.

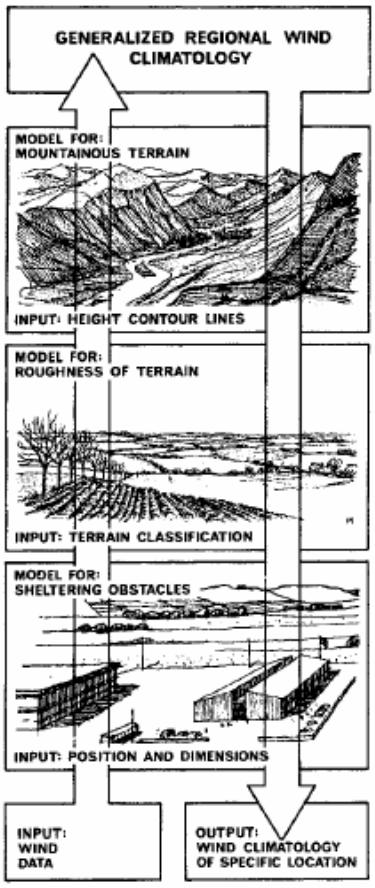

Fig. 6-25 The Wind Atlas Methodology

(Troen & Petersen, 1989)

The advantage of this methodology over the previous ones is that it can account for not only any projected changes in the mean wind speed, but also changes in the Weibull parameters of the distribution. These factors are important for estimating the power output from wind turbines, as described in section 6.2.2.

6.4.9.1 Comparative studies

The WAsP method of downscaling the output of climate models has been employed in a number of other projects, in which the data to be downscaled have either originated from a mesoscale model or from the results of reanalysis models. The outcomes of three such studies are discussed in this section.

KAMM/ WAsP

The Karlsruhe Atmospheric Mesoscale Model (KAMM) was run for this study (Frank *et al.*, 2001) in a statistical-dynamical manner. This means that the surface

climate variables to be modelled by the system were determined in terms of their relationship to the large-scale forcing, plus some surface parameters. Various situations of large-scale climate were run in the model and the surface variables measured. The large-scale climate was then classified into frequencies of occurrence of these various situations and the mesoscale climatology calculated from this. The authors remark that for most wind energy applications in mid-latitude regions, concerned primarily with moderate and high winds, the main parameters required for modelling surface wind are geostrophic wind plus terrain height and surface roughness length; but they refer to other parameters such as temperature and atmospheric stratification as potential inputs.

The modelling process by which the KAMM output was coupled to the WAsP model was numerically and statistically complex, but in simple terms, involved generating a mesoscale wind atlas for a particular region using KAMM, and then inputting this wind atlas to WAsP, which downscaled the output at various locations. This was then compared with data from met stations. They carried out the modelling procedure for four regions: Denmark, Ireland, Northern Portugal and Galicia, and the Faroe Islands. Overall, the conclusion was that the combination of KAMM and WAsP produced more accurate predictions of local wind climate than simple interpolation of the KAMM data.

One particularly interesting issue encountered arose from the choice of map size for input to the WAsP model. Maps with a small diameter, 5-10km, produced errors in the orographic model, where the speed-up effects of hill were underestimated. This impacted on the wind turbine energy calculations, resulting in under-prediction - particularly in areas where the terrain is particularly complex.

POWER

Predicting Offshore Wind Energy Resources (POWER) had the objective of determining the potential offshore wind resources in the seas around the European Union (Watson *et al.*, 2001). They calculated geostrophic wind from a reanalysis mean sea-level pressure dataset, interpolated by bi-cubic splining from 2.5˚x 2.5˚ to 0.5˚x 0.5˚ resolution, and then applied WAsP to the geostrophic wind data to downscale it to surface level. The study found good correspondence between the

downscaled output from WAsP and observational data available for a number of offshore sites.

Aladin/WAsP

This work (Horváth & Horváth, 2006) was similar in theory to the KAMM/ WAsP model coupling, whereby the output from a fairly high resolution mesoscale model was input to the WAsP program in the form of a regional wind atlas, but using a different mesoscale model, Aladin, and considering the region of Croatia. The variable from the model used as input to WAsP was the wind at 850hPa geopotential height, assumed to be geostrophic.

The authors discuss the relationship between geostrophic wind and surface winds in the region, and in particular the effect of Bora winds, common in this area. These winds, which typically occur in the down-slope direction of mountainous regions, are thermally driven, and will not be captured by the geostrophic flow. The observations at surface level, however, will include Bora winds.

They found that using WAsP to downscale mesoscale geostrophic winds resulted in significant differences in mean wind speed compared to actual observations. The study concluded that due to the prevalent effects of Bora winds in this region, the WAsP model with geostrophic winds from a mesoscale model as input was simply not suitable.

Short-term modelling with an NWP

Landberg & Watson (1994) applied WAsP to output from a Numerical Weather Prediction (NWP) model which was forecasting 36 hours ahead for a grid cell of size 50km x 50km. The objective was obtaining a better local short-term wind forecast at a particular site. The NWP model output for geostrophic winds at various heights was trialled and found to give rather poor results when compared with observations, whereas the model wind at a height of 137m seemed to offer the best results, and so it was this wind that was selected to be input to the WAsP model.

The technique was applied over a large section of western Europe, and results indicate that using WAsP was a substantial improvement over some more simplistic methods in most of the locations in the north west of the domain, that is, in the UK and Ireland region. The authors describe a number of sources of error, which fall

into two primary categories: modelling and data. Modelling errors cover factors such as the assumptions in the WAsP and NWP models, like a neutrally stable atmosphere. Another important model issue is that neither WAsP nor the NWP model account for mesoscale winds such as those due to thermal effects. Data problems result from errors or inconsistencies in the observational data, for instance, caused by equipment or by changes at the measurement site. In order to correct this, two empirical-statistical MOS technique have been applied – one a simple linear correlation and the other a neural network. Both performed well but due to the added complexity of the neural network there was found to be no advantage in using it over the simpler linear correlation.

Conclusions from comparative studies

What do these studies suggest about the potential for using WAsP to downscale climate model geostrophic wind data? The most obvious issue is the resolution of the climate model used for input: in both the projects which use mesoscale models as input to WAsP, the resolution of the input data is sub-10m grid squares. The GCM geostrophic wind data is in grid squares of around 200km x 150km, approximately 1.8˚ x 1.8˚, well in excess of the ideal. However, the POWER project used reanalysis data on a 2.5˚ x 2.5˚ grid as input - even lower resolution than the ECH5 GCM - and used a simple bi-cubic interpolation scheme to bring it down to 0.5˚ x 0.5˚ resolution. Their successful results using interpolation suggest that this is, in fact, a reasonable method to use. Geostrophic wind does not show as much variability on a spatial scale as surface wind, driven as it is by the large-scale circulation and is relatively immune to the influence of surface features. The fact that the POWER project was limited to offshore winds might suggest, however, that that the method may be more suited to studies where the surface conditions are more homogeneous, such as over the sea. The possibility of encountering winds which are thermally driven is more likely onshore, and the Aladin/WAsP study found difficulty with this. In the mid-latitudes, i.e. in the UK, winds such as the Bora are less common (with the possible exception of the mountainous Scottish Highlands and around the coasts) and geostrophic flow will account for a great deal of the variability in surface winds.

6.4.9.2 Site Data

Orography and roughness data

For the WAsP process, height, obstacle and roughness length information are required in order to transform the met station data to a regional wind climate, and to downscale the wind atlases to a turbine site within the grid box for each case study. Due to the difficulty in representing obstacles accurately, particularly over such a long time period, this was neglected at all but one site. Height contour data for the region surrounding the location were extracted from digital Ordnance Survey maps (Ordnance Survey, 2009) and was processed using the WAsP map editor to reduce the resolution of the lines to 50m.

Surface classification data were obtained from the CORINE land-surface maps (European Environment Agency, 2007) at 200m resolution in raster files. These were input to the ArcGIS software and converted from raster files to 'polygon' shape files. They had to undergo a further transformation to 'polyline' shape files with each line taking on the surface classification attributes to the left and right of the line as part of its attribute table. The 'polyline' files were converted to WAsP-recognisable roughness lines in ascii format, using an ArcGIS script (Gonzalez, 2008). For each classification value, the corresponding roughness length was identified using the table referred to in Boehme (2006), and the classification values converted to these roughness lengths using the WAsP map editor.

Note on temporal resolution of data

The temporal resolution for modelling wind speed distributions in WAsP is ideally hourly or, if available, sub-hourly. This ensures the best capture of the full range of wind conditions at a site and avoids the 'averaging' of extremes in the full distribution. A reduced temporal resolution where the data are obtained by averaging over periods longer than one hour would be expected to reduce the variance of the data, with corresponding implications for the distribution parameters.

Unfortunately, obtaining climate model information at this level in a useable format is not possible via the current IPCC channels, and daily data is the best available temporal resolution in the binary 'netcdf' format which can be processed relatively straightforwardly in a Matlab function. In order to account for this, and

ensure that the comparison between the GCM output and observed data in the WAsP model is 'like-for-like', the observed hourly data from met stations have been averaged over a 24 hour period.

6.4.9.3 WAsP processing

Due to time and technical constraints in processing the data via the WAsP software, only four out of the seven locations have been analysed as 'case studies'. The advantage of using the wind atlas methodology, which analyses not just the mean wind speed but also the frequency distribution parameters, is that it will take full account of any future changes in wind speed range or variance modelled by the GCM. Ideally, WAsP performs best when the regional wind climate input is over a smaller area; but because geostrophic wind is being used as the 'regional' wind climate, it is expected to vary less and WAsP should, therefore, cope relatively well. Three methods of modelling in WAsP have been tested. Ideally, it would be possible to input the model geostrophic winds into WAsP and have WAsP create a wind atlas applicable to the region of the model grid cell. However, this is not possible with version 9.1 of the software and so some alternatives have been tested and are detailed in this section. The first relies on developing a wind atlas by applying the drag law to the model geostrophic winds independently of WAsP. The second uses the drag law to downscale the model winds to the maximum height above ground level that is acceptable to WAsP and this is then input to WAsP as an observed wind climate. The third method tested takes the GCM 10m wind speeds directly as an observed wind climate for a site within the grid cell concerned.

Pre-prepared regional wind climate – WAsP process 1 (WP1)

WAsP is designed to take time series of wind data at a particular height and location, and, using the location terrain and orography, transform this into generalised frequency distribution and direction information for a range of heights and roughness lengths for the local region. This regional wind information is stored in a format known as a 'wind atlas'. Given that the data from a GCM could be considered to be already generalised for the region of a grid box, an imitation wind atlas can be created directly from the time series of geostrophic wind using the geostrophic drag law (eqn. 6.1) and the logarithmic wind profile (eqn. 6.2) to calculate the time series

of mean wind speed at 10m height with a range of roughness lengths. Using Matlab, Weibull parameters have been fitted to the 10m time series for each roughness length, and then scaled to a range of heights using empirically derived laws from Justus *et al.* (1978) discussed in section 6.2.1.

In Fig. 6-26, the scaling laws are shown to give similar results for *A* and *k* parameters as WAsP itself, for roughness lengths other than the first one in the atlas (because of an assumption that the first value will be over water (Nielsen, 2009)), and for heights up to 100m. Above 100m height, the laws do not hold, and thus the choice of values in the prepared wind atlas is restricted. Given that the purpose of this study is assessing wind energy resources onshore, a roughness length of close to 0m is fairly irrelevant, as are heights over 100m; so ignoring the zero roughness length and not calculating values for heights over 100m is not considered to be a major drawback.

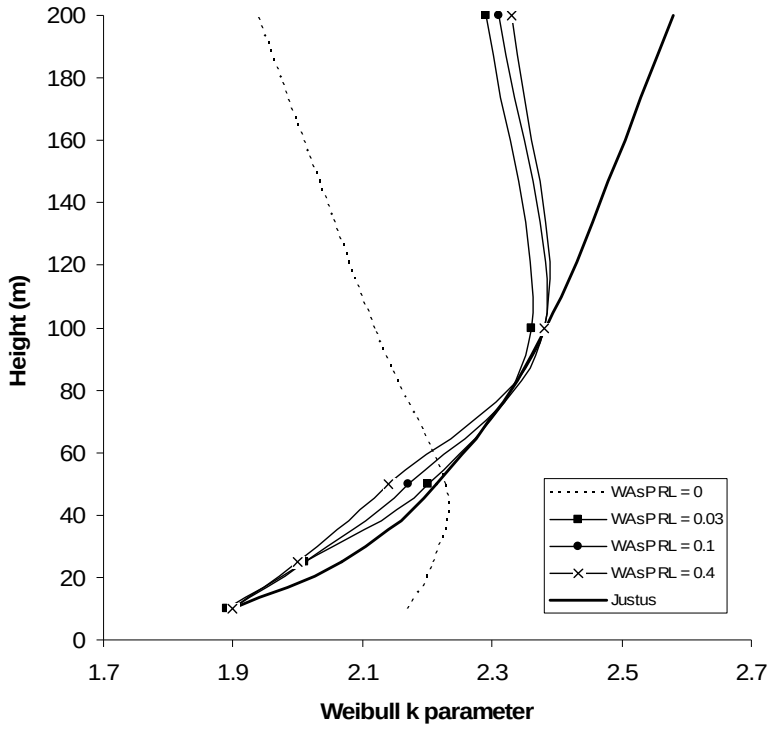

Fig. 6-26 Weibull *k* parameter variation with height

Drag law and logarithmic wind profile time series – WAsP process 2 (WP2)

To use WAsP itself to create a wind atlas using geostrophic wind data is not possible with the current version (9.1) of the software. It will only accept the use of wind speeds input as observed time series at up to 200m height. Given that observed wind approaches geostrophic conditions at heights varying from 600 to 1000m above ground level, inputting a geostrophic wind at 200m would clearly not give good results. The alternative, therefore, is to use the geostrophic drag law and logarithmic profile to scale geostrophic wind to a height somewhere between 10 and 200m using a characteristic surface roughness representative of the region, chosen here to be the roughness length in the prevailing directional sector, and input this to WAsP as observed time series at the site. Using a similar Matlab function as in the previous method this process was carried out for a height of 200m, with a roughness length chosen by considering the roughness rose as presented in WAsP when the roughness map for the region was input.

GCM 10m winds – WAsP process 3 (WP3)

As a point of comparison with methods using the geostrophic wind, the 10m wind data were extracted from the GCM and, in a similar fashion to the previous method, the time series input to WAsP as an observed wind climate, located at the chosen site.

Observed and future wind climates

In order to assess how realistic the wind atlases developed using the three techniques actually are, data from a met station at daily resolution for a similar time period was loaded into the WAsP program for the same location, cleaned by the software to remove any site-specific effects, and used to generate an alternative wind atlas for the region. A third set of wind atlases was then generated for the region using the 2081-2100 time series of daily winds from the interpolated GCM data.

Reference conditions for all wind atlases

The wind atlases contain wind distributions for 4 reference roughness lengths and 5 reference heights above ground level. The pattern of scaling the Weibull *k* parameter

is such that whatever the first roughness length is set to, it does not follow the pattern as described in eqn. 6.3 by Justus *et al*. (1978) as it assumes an offshore profile (Nielsen, 2009). For this reason, it was left as the default value of 0m, and only the results for 0.03m, 0.1m and 0.4m were considered. The heights were chosen as 10m, 25m, 50m, 80m and 100m. The roses of Weibull parameters have 12 sectors each.

6.4.9.4 Boulmer WAsP Method

It was deemed appropriate for Boulmer to carry out an analysis using the WAsP software. WAsP uses a measure called 'ruggedness index', or RIX, to determine how successful its results are likely to be based on the slopes of the terrain within the region being analysed. The presence of slopes greater than 0.3 (height divided by base length) is likely to cause errors in the output, and thus it is advisable to check before carrying out any calculations. The RIX grid for this region shows that most cells fall into an acceptable category, where the amount of terrain with a slope greater than 0.3 is low, and flow separation will not occur. The met station is located in an acceptable cell, so provided the site chosen to predict for is also in a low RIX grid cell, WAsP is believed to give reasonable results in such areas.

Results from the wind atlases derived by the three WAsP processes plus the met station data are shown in Fig. 6-27. WP1 seems to give a consistent difference of around 15% in the mean wind speed and 50% in the power density. Because Boulmer is in close proximity to the sea, it is likely that coastal effects on the stability profile which is not explicitly accounted for by WAsP (Watson *et al.*, 2001), may influence the mean wind speeds; hence this wind atlas will not be representative of observations. The results from WP3 (without interpolation to higher resolution) tend to slightly underestimate the mean winds by around 1-2%. This is less of an underestimate than the geostrophic downscaling in WP2, which gives mean wind speeds of 5-6% less than observations. WP3, however, overestimates the Weibull *k* parameter by 6-8%, whilst WP2 typically underestimates by 3%. The combined effect of these errors results in WP2 giving power densities of around 12-15% lower than observed, whilst WP3 gives slightly better values around 10-13% lower than the observed.

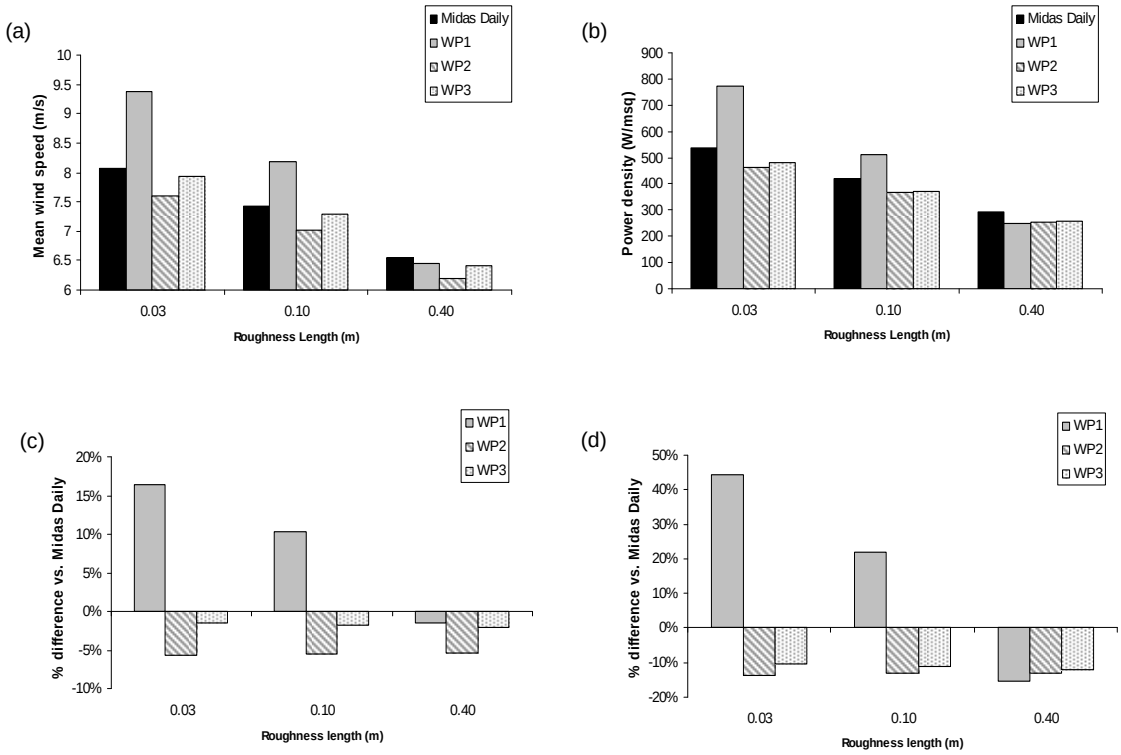

Fig. 6-27 Boulmer WAsP results

(a) Mean speed at 80m; (b) Power density at 80m; % Differences compared to observed data in (c) % mean speed at 80m; (d) power density at 80m

Clearly, at this site, the original GCM 10m wind climate seems - rather unexpectedly - to represent the observed wind climate with reasonable skill. There is a degree of error, amounting to around 10% in the calculation of power density at 80m, but for the purposes of change analysis over long periods, this might not be as big an issue as it would obviously be in a feasibility study for a wind development. The process of downscaling using geostrophic wind and WAsP achieves a somewhat similar degree of accuracy, appearing to perform better at capturing the daily variance, but not quite so well at representing the mean wind speed. In this case, it would probably be advantageous to use both methods in analysis of future data, in order to minimise the error in the overall calculations.

6.4.9.5 Wittering WAsP Method

Like the Boulmer site, the met station for Wittering is located in a cell with an acceptable RIX value and so provided the prediction site is also in a suitable cell, the results can be considered to be free from issues caused by flow separation.

Results for the Wittering site (Fig. 6-28) show that because of discrepancies in the Weibull *k* parameter, there are inconsistencies in the patterns of mean speed differences and power density differences. WP1 performs better than at the other three sites, perhaps due to the location being far from the coast and in a region of fairly homogeneous terrain, so that coastal and thermal effects are minimal. WP1 is, however, still poorer than WP2 and WP3 in terms of error across all heights and roughness lengths, and should probably be discounted.

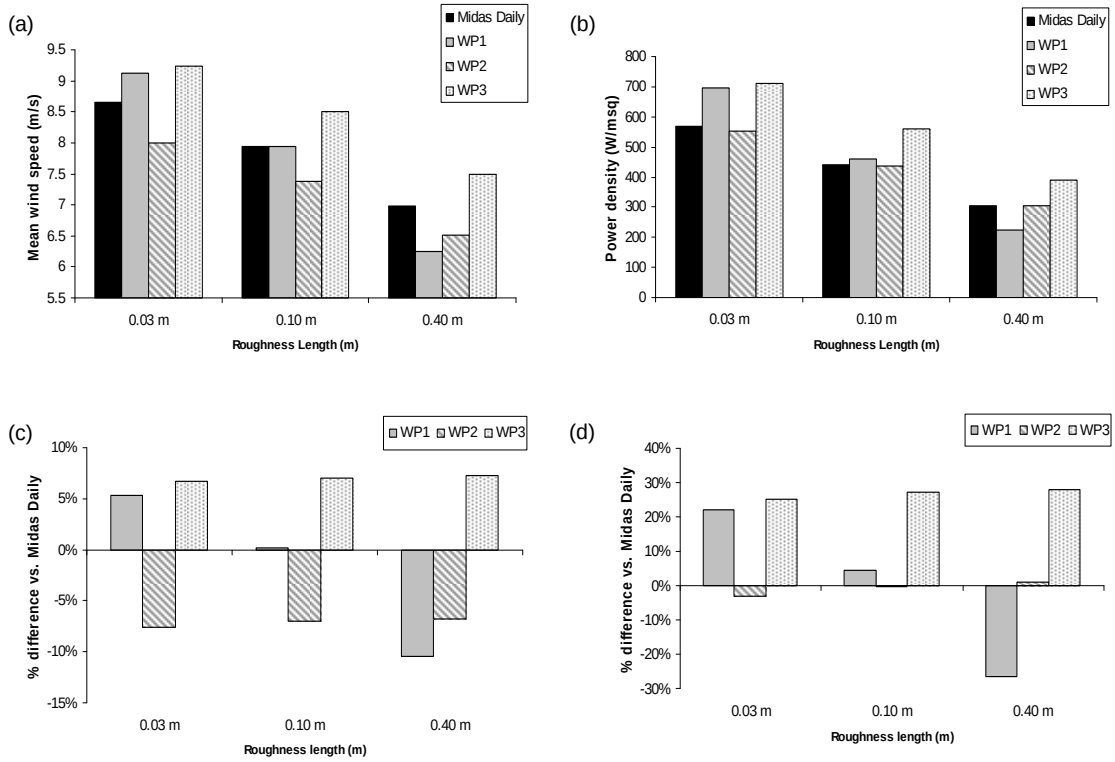

Fig. 6-28 Wittering WAsP results

(a) Mean speed at 80m; (b) Power density at 80m; % Differences compared to observed data in (c) % mean speed at 80m; (d) power density at 80m

WP2 shows a fairly consistent underestimate of the mean wind speed of around 7% at turbine hub height, but very seriously underestimates the Weibull *k* parameter by 25%. This compensates for the mean wind speed error somewhat in the power

density calculation, resulting in figures within 2% of observed at 80m. WP3 overestimates the mean speed by 7%, but performs better with the *k* parameter, coming within 4% of the observed value. However, these small errors are reflected in a difference of over 20% in the calculated power density compared with observed.

6.4.9.6 Eskdalemuir WAsP method

The RIX calculation shows that, like Boulmer and Wittering, the measurement site is in an acceptable cell. It does, however, have a higher value than for the other two sites.

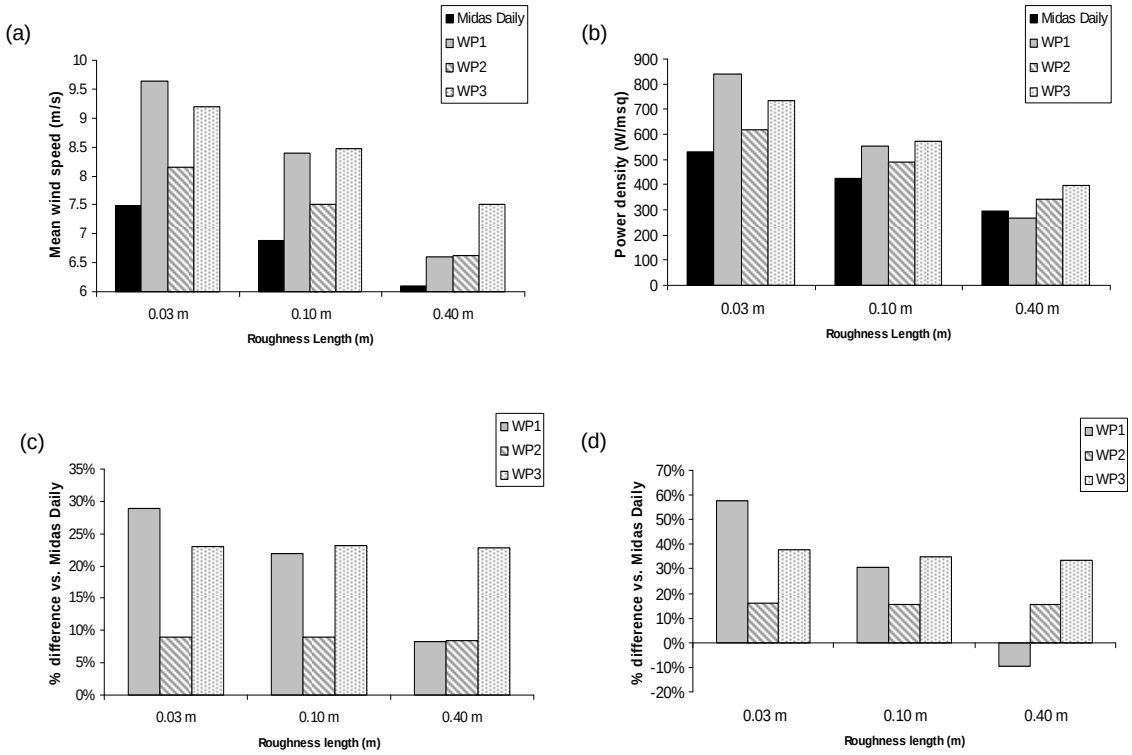

Fig. 6-29 Eskdalemuir WAsP results

(a) Mean speed at 80m; (b) Power density at 80m; % Differences compared to observed data in (c) % mean speed at 80m; (d) power density at 80m

As Fig. 6-29 shows, at Eskdalemuir the downscaling of the geostrophic wind obtains a result for both wind speed and power density much closer to the observed data than the GCM 10m wind climate itself. The imitation wind atlas, as per the other sites, does not perform consistently over all heights and roughness lengths, only giving a result close to the observed data at 0.4m roughness length. The 200m downscaled model wind climate generally overestimates the mean wind speed by 9% at 80m

a.g.l. whilst the 10m climate overestimates by much more - up to 23%. The 200m atlas also only gives an 11% increase in the Weibull k parameter, whilst the 10m atlas has a Weibull k parameter 40% greater than observed. These result in the 200m atlas overestimating power density by 15-16%, while the 10m atlas overestimates by over twice this - between 34 and 38%.

6.4.9.7 Turnhouse WAsP method

This station is located near to Edinburgh and has the longest period of useable data from 1961-1990, so corresponds exactly with the 1961-90 control period extracted from the GCM. The RIX at this site was acceptable. The mast itself is located among several buildings, but only two of these are of significant height - around 7 to 10m. These have been included in the analysis as an obstacle group. The CORINE roughness information suggests a roughness length of 0.02m, chosen as typical for an airport, but due to the presence of several close low-rise buildings, the roughness chosen to downscale the GCM geostrophic wind data to 200m was 0.3m. The remaining downscaling was carried out by WAsP itself, with the obstacles present and the site roughness and elevation contours as provided by the map.

The results, given in Fig. 6-30, are quite similar in terms of percentage error to the results for the Boulmer site. In terms of mean wind speed, WP3 outperforms WP2, but WP2 obtains marginally better results for the Weibull k parameter. The mean wind speed discrepancy for WP2 is around 6%, whilst for WP3 it is just 2%. The differences in Weibull k parameter are larger, with WP2 typically underestimating by 8-10% and WP3 overestimating by 8-14%. The effects on the power density calculation mean that WP2 underestimates the available power by around 10%, while WP3 has a very small error - in the region of 1%.

As with Boulmer, it is probable that coastal effects on the wind climate which are not accounted for by the simplified wind atlas technique employed in WP1 have resulted in the method giving errors of up to 21% in the mean wind speed, and consequent errors of up to 70% in the calculated power density.

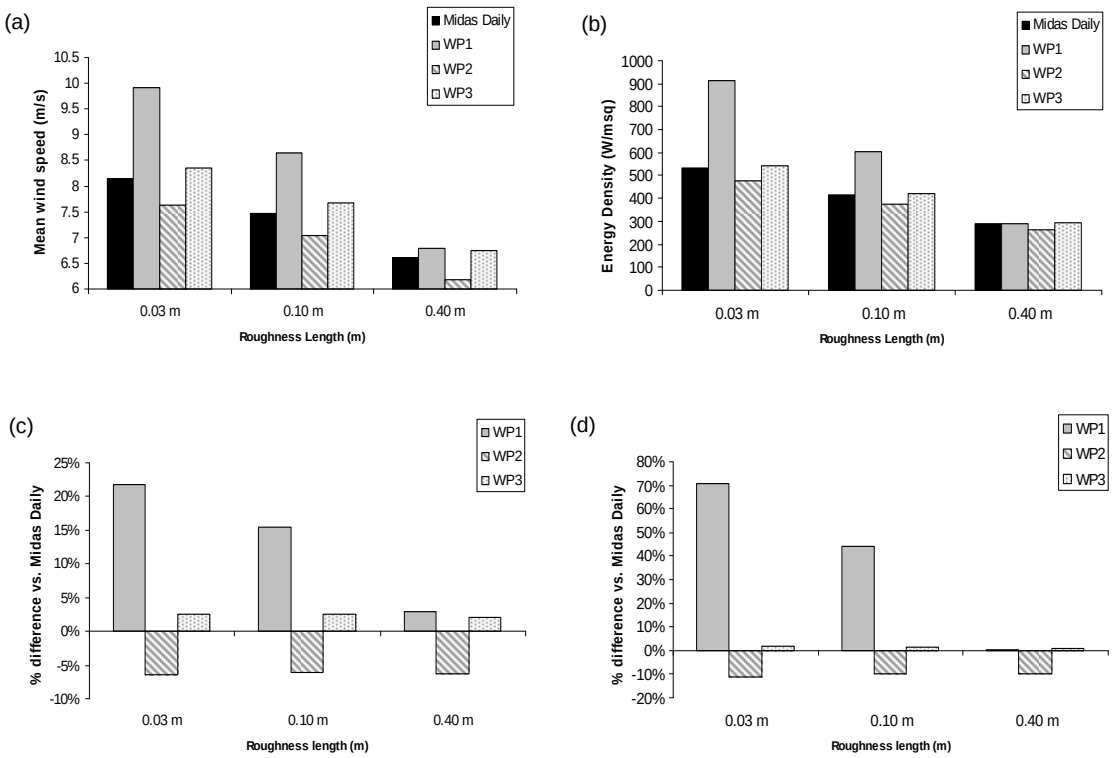

Fig. 6-30 Turnhouse WAsP results

(a) Mean speed at 80m; (b) Power density at 80m; % Differences compared to observed data in (c) % mean speed at 80m; (d) power density at 80m

6.4.10 General conclusions on success of downscaling

The downscaling methods attempt to demonstrate that because a climate model relies on a particular value of a surface parameter such as roughness averaged over a large area to derive a 10m wind climate, the output may not be applicable to every site within the grid square area. The GCM 10m data may, however, be acceptable for sites where the actual conditions match those included in the GCM. The drag-law downscaling method tries to exploit the fact that by taking control of the surface roughness length parameter and deriving a 10m wind climate from the model output of geostrophic wind, the data could be made more applicable to an individual site where the conditions are different. In these cases the data shows relatively good correspondence with observed data for a control period. What the drag-law downscaling process cannot account for, however, is the other local factors that impact on surface wind climate, such as elevation. In order for the model to be more successful, these need to be included.

By carrying out a simple linear regression between the model data and the observed data, many more factors affecting the wind are accounted for - but empirically rather than explicitly - so it is impossible to define the physical nature of the relationship between the two variables. These relationships, whether carried out using 10m model data or geostrophic wind, are much stronger than those developed using the drag law, and are generally also better than using the GCM 10m data directly. The results come tagged with the aforementioned caveat: that these empirical relationships are subject to future change.

Over the four sites analysed using WAsP to evaluate the effects of all the local factors including surface roughness, two of them - Boulmer and Turnhouse - have shown promise with regard to using climate model data to investigate future changes in the wind climate at specific locations. In both these cases, however, it would appear that the GCM 10m wind climate is more successful at representing the observations at a particular site on an annual basis than data generated using geostrophic wind and a downscaling process. This would suggest that the model is capable of capturing climate where the site conditions are similar to those assumed in parameterisation of the model.

The third site, Wittering, is not as well predicted in terms of mean wind speed using the GCM 10m climate, and very badly represented in terms of the Weibull k parameter in the downscaling method. It is clear that the model fails to a degree here. One must be cautious when reapplying this at other sites; a thorough investigation must be completed and the model data compared with observed climate information in order to have any confidence in the projections of future climate obtained.

The final site, Eskdalemuir, is not as well predicted for mean wind speeds as Boulmer and Turnhouse, and the Weibull k parameter is also overestimated to a relatively large degree. This site is interesting, however, because greater success is obtained by using the geostrophic wind, downscaled to 200m and input to WAsP, rather than taking the 10m wind directly. This is probably attributable to the terrain in which the site is located, a heavily forested area, which will not be accounted for by the GCM. By bypassing the GCM parameterisations, the WAsP model using method 2 improves the result.

6.5 Future projected climate

An investigation has been undertaken using the downscaling methods described in 6.3 with future climate projections from the ECH5 GCM. The statistical relationships found using linear regression as in method 1, and the drag law using the most successful roughness length from method 2, were applied to the GCM data for the period 2081-2100. The future projections were compared with the control period (1961-90) data derived by each method and the percentage changes calculated.

In order to understand the potential significance of any changes, the difference between the GCM output for 1961-90 and the observed wind speed was taken as an error bound either side of the predicted value. This error bound is not probabilistic, but merely intended to give an indication of the scale of any future changes in the context of the original model errors. The future changes were considered for the most successful downscaling method at each site in the context of these errors.

6.5.1 Boscombe Down

The pattern of change for the 2081-2100 period across all the downscaling methods and the GCM 10m winds is very consistent for this site, with all methods showing a similar direction of change in each month. The monthly means show a tendency to rise by around 4 to 5% in the winter months and drop by a similar amount in May, June and July. August shows a slightly bigger decrease in the region of 8-10%. Over the period of a year, the changes projected by all models are between -0.4% (10m linear regression) and -2.13% (drag law downscaling), but all are negative.

Because the ECH5 10m was shown to be the most successful representation of the observed climate for this site, Fig. 6-31 shows the original results with the average error bounds (in black) and the future ECH5 10m results with the same error bounds (in red). This shows that the months where the future results fall outside of the error bounds for the control period are July, August and December. In all other cases, the future data is within the control period error and may not be significant.

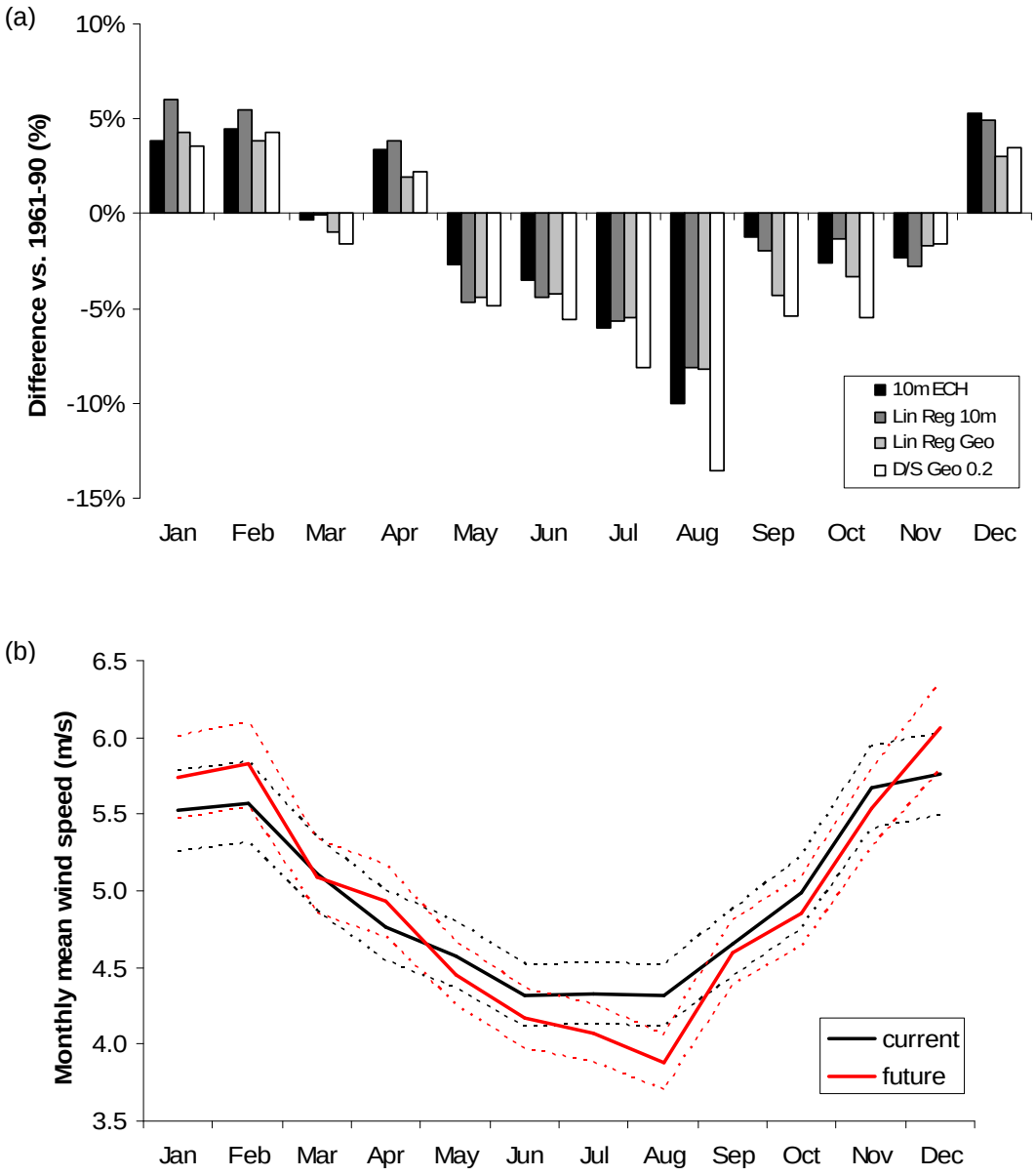

Fig. 6-31 Boscombe Down future projections

(a) % Differences vs. 1961-90 data for each downscaling method; (b) Current and future projections and error bounds using ECH5 10m data

6.5.2 Boulmer

The direction of projected change using the different models is less consistent for Boulmer (see Fig. 6-32) than for the Boscombe Down site. When the changes are small (less than 3%), some models show an increase while others a decrease. This is probably a non-issue, however, due to the small magnitude of the changes involved.

In the case of larger changes, the models show more consistency, with the most significant deviations from the control period results occurring in July, August and September. July and August results show decreases of between 6 and 10% whilst September mean speeds increase by a similar amount. Averaged over the year, the total change is between -0.28% (drag law downscaling) and +0.78% (10m linear regression).

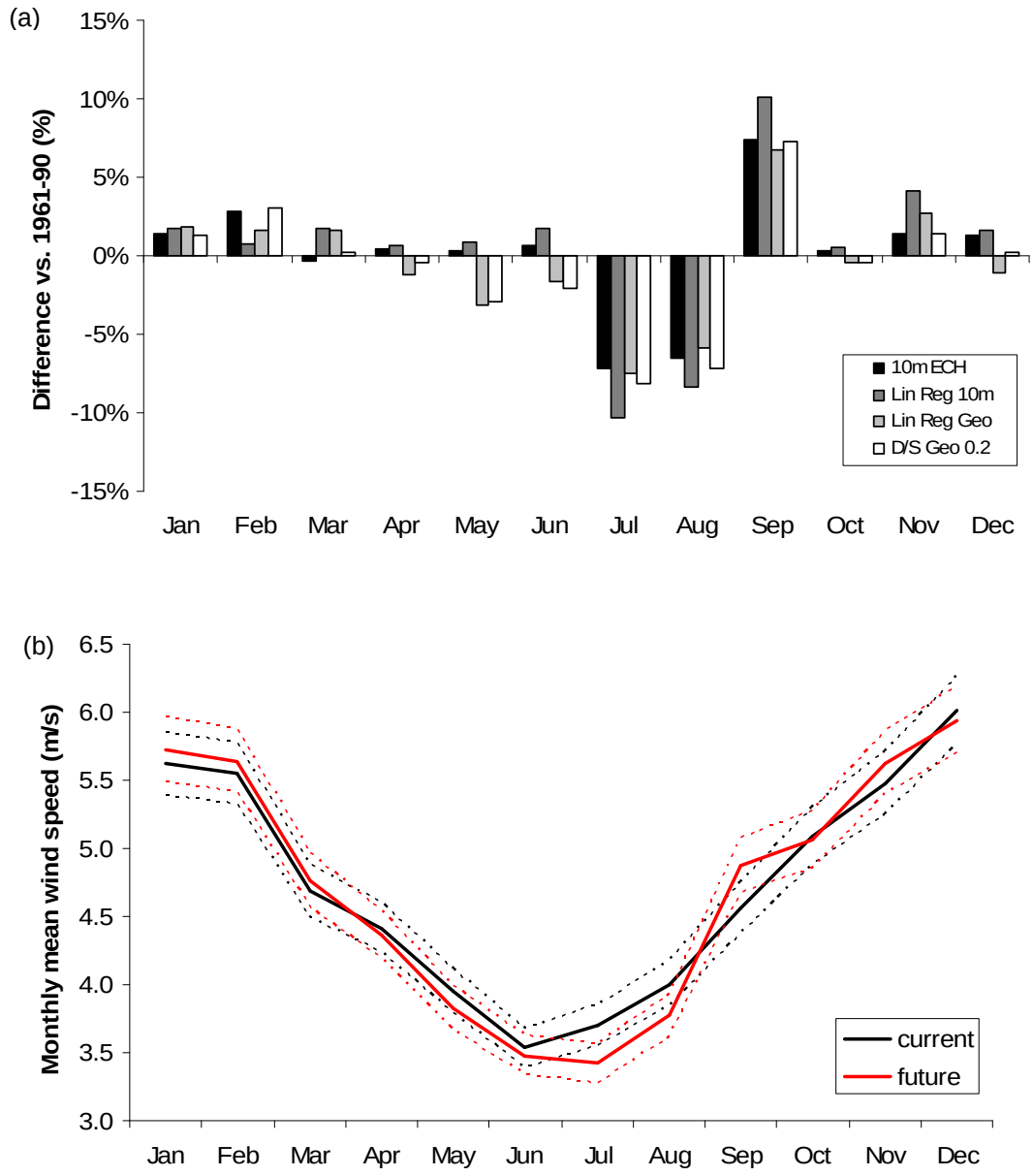

Fig. 6-32 Boulmer future projections

(a) % Differences vs. 1961-90 data for each downscaling method; (b) Current and future projections and error bounds using linear regression of ECH5 geostrophic wind data

Taking the geostrophic linear regression results - which had the lowest error for the control period - and comparing the control period results and their associated mean error (black) with the future results and similar error bounds (red), confirms that the most seriously affected months are July, August and September. The red line falls outside the error bounds of the control period data at these points, suggesting change beyond the error in the original model.

6.5.3 Wittering

The results for the Wittering site show quite a large degree of inconsistency in the direction of change - whether positive or negative - particularly where the change is ±5% or less. The months with consistent change in the mean speed are January, with an increase of 2-3%; December, with an increase of 3-5%; July, with a decrease of 3-8%; and August, with a decrease of 4-12%. Over the year, the changes work out at between -1.28% (drag law downscaling) and +0.42% (geostrophic linear regression).

From the geostrophic linear regression results plotted in Fig. 6-33, the future results (red) reach outside of the error bounds on the control period data (black) in February, March, April and August. There is a replication of the original observed February low/March high pattern in the future data, which was not replicated in the linear regression model data for the control period, but which seems to have been activated here, indicating there is potential for either a significant change, or that the control period showed an anomalous February/March pattern which will not persist in future.

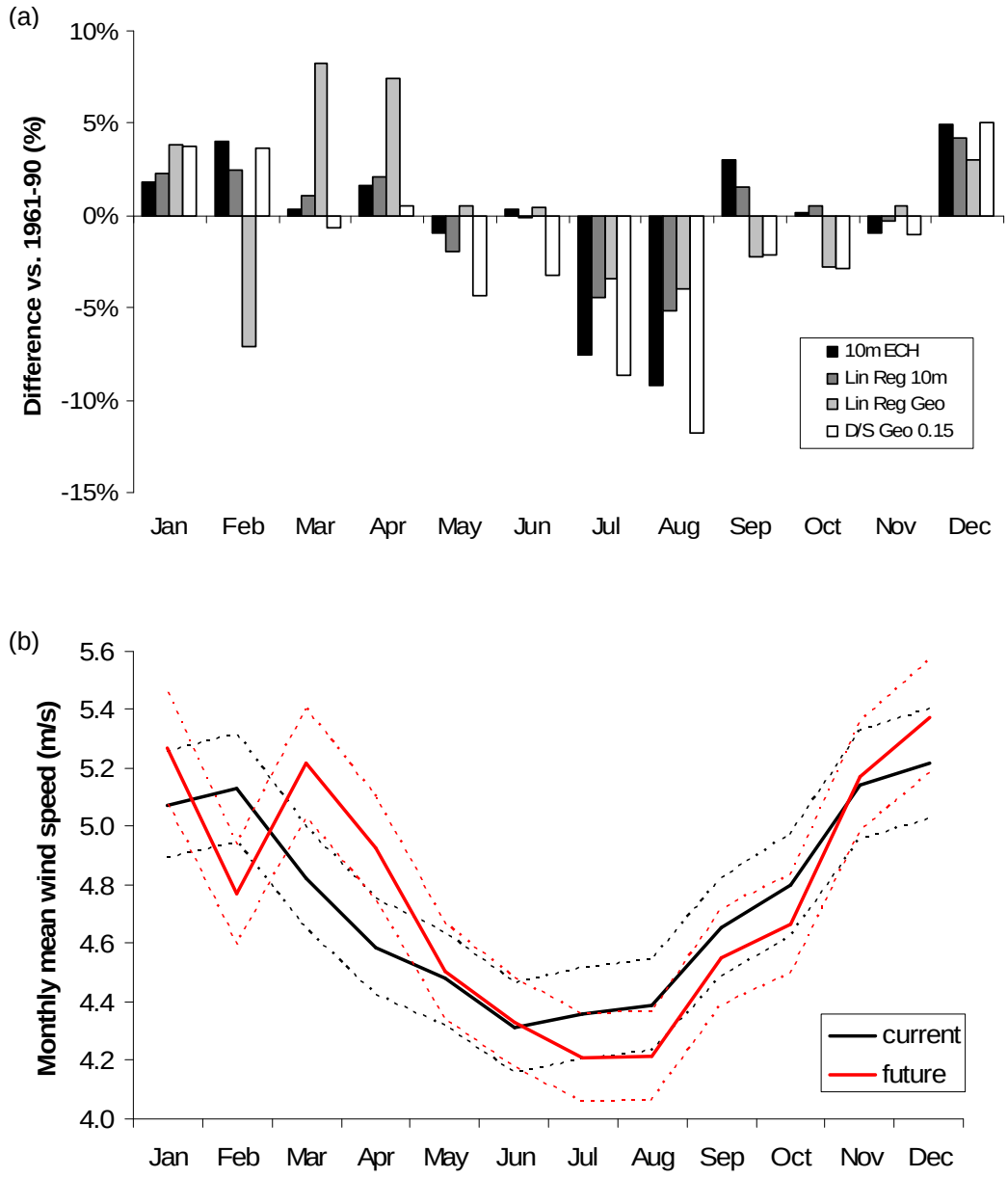

Fig. 6-33 Wittering future projections

(a) % Differences vs. 1961-90 data for each downscaling method; (b) Current and future projections and error bounds using linear regression of ECH5 geostrophic wind data

6.5.4 Fort Augustus

Given the relative lack of success in obtaining useful results from either the GCM 10m data or the drag law downscaling method, it is of little surprise that the future results look very inconsistent. It is probably best in light of this to consider only the linear regression models, as these were much more successful.

All of the monthly changes are within ±4% of the control period results, when the geostrophic linear regression is examined, suggesting very little in the way of significant wind speed changes at Fort Augustus. Looking at Fig. 6-34, the red line showing future data does not ever stray outside the error bounds of the control period data (in black); it is thus fair to suggest that only very minor changes in mean wind speed may be evident in the future. The annual change projected using the regression models is around -0.5%, and so is unlikely to have a discernable impact on wind power production.

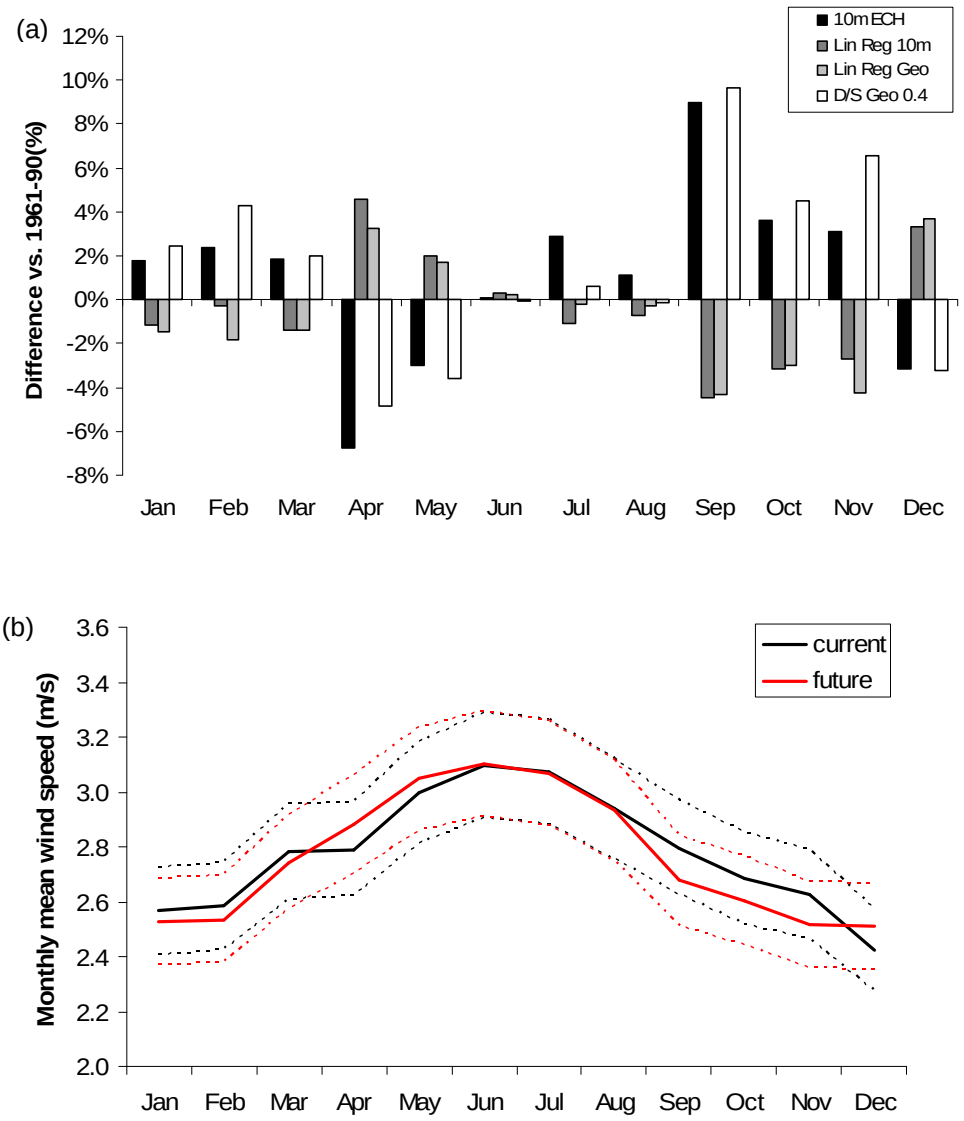

Fig. 6-34 Fort Augutus future projections

(a) % Differences vs. 1961-90 data for each downscaling method; (b) Current and future projections and error bounds using linear regression of ECH5 geostrophic wind data

6.5.5 Eskdalemuir

The results for the Eskdalemuir site (see Fig. 6-35) show some small inconsistencies in the direction of changes, when the changes are in the region of ±1% or less. Otherwise, there is a similar monthly pattern of change to that seen at the Boulmer site.

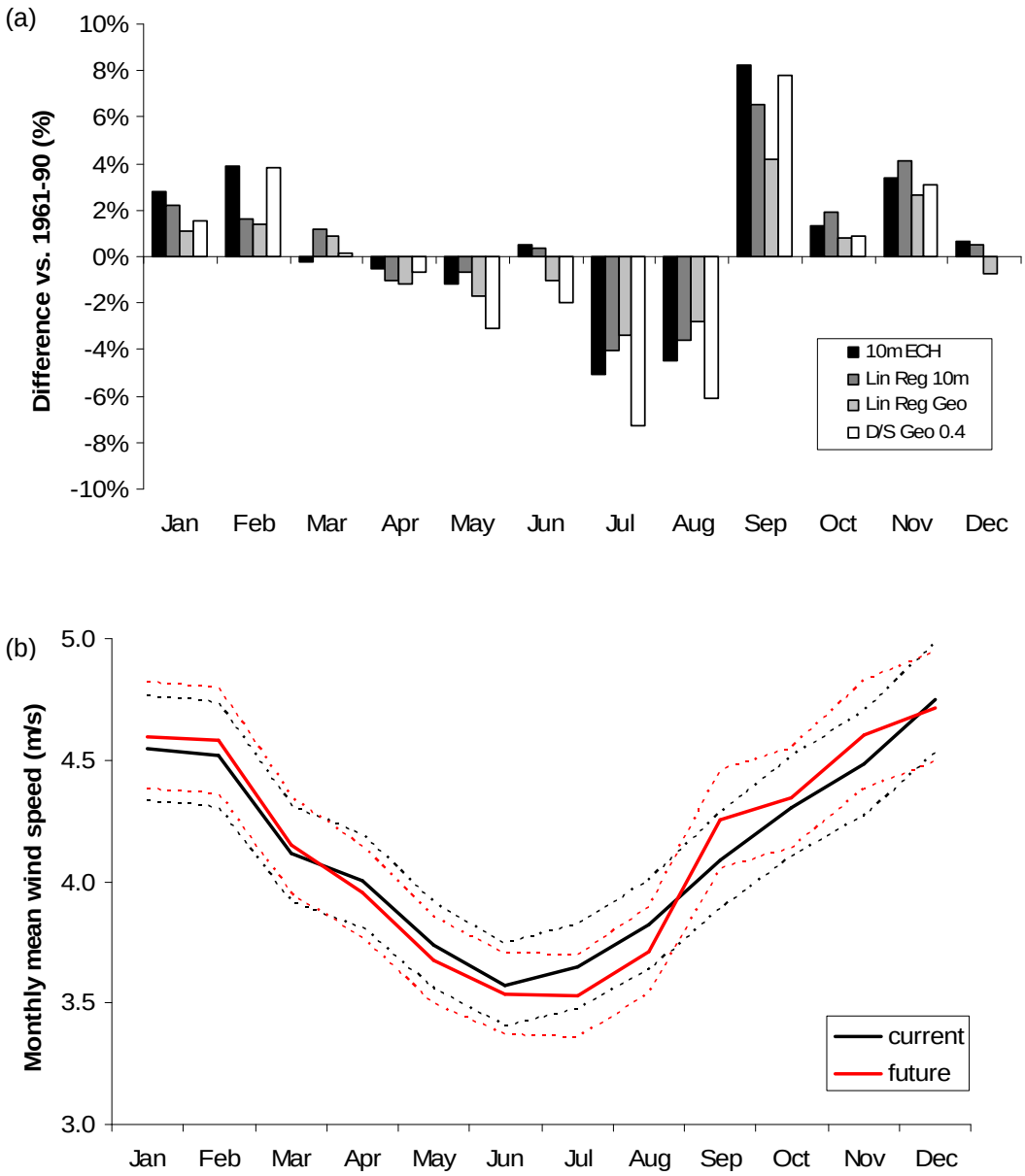

Fig. 6-35 Eskdalemuir future projections

(a) % Differences vs. 1961-90 data for each downscaling method; (b) Current and future projections and error bounds using linear regression of ECH5 geostrophic wind data

January and February show small increases in mean wind speed of around 2% and 2 to 4% respectively, whilst November shows a slightly bigger increase of 3 to 4%. The biggest increase, however, occurs in September, where three of the models project a rise of 6 to 8% in the mean wind speed. The geostrophic linear regression indicates a slightly smaller increase of around 4%. July and August both have decreased mean wind speeds in all the models of between 3 and 7%. The overall changes for the year are less than 1% in all of the models analysed.

The geostrophic linear regression had the smallest control period errors for Eskdalemuir, and its projected changes are the most modest of all the models. The future value never steps outside the error bounds of the control period data, but does come close to doing so in September.

6.5.6 Turnhouse

As for the previous sites, when the projected changes are less than 1% for Turnhouse, the models do not all agree on the direction of change (see Fig. 6-36). There are several months, however, where the changes are larger and more consistent. January, February, October and November all show small increases in mean wind speed of between 1 and 4%. September is projected to increase by a larger degree, around 4 to 8%. April and May show very small decreases of 1 to 2%, and July and August show larger decreases of 2 to 7%. The overall change over the year is small, with all models giving results of less than 1%.

The 10m linear regression shows only one month, September, where the future results fall outside of the control period error bounds, indicating that in most months, it is not possible to be confident about the size of future changes, other than that they are likely to be small.

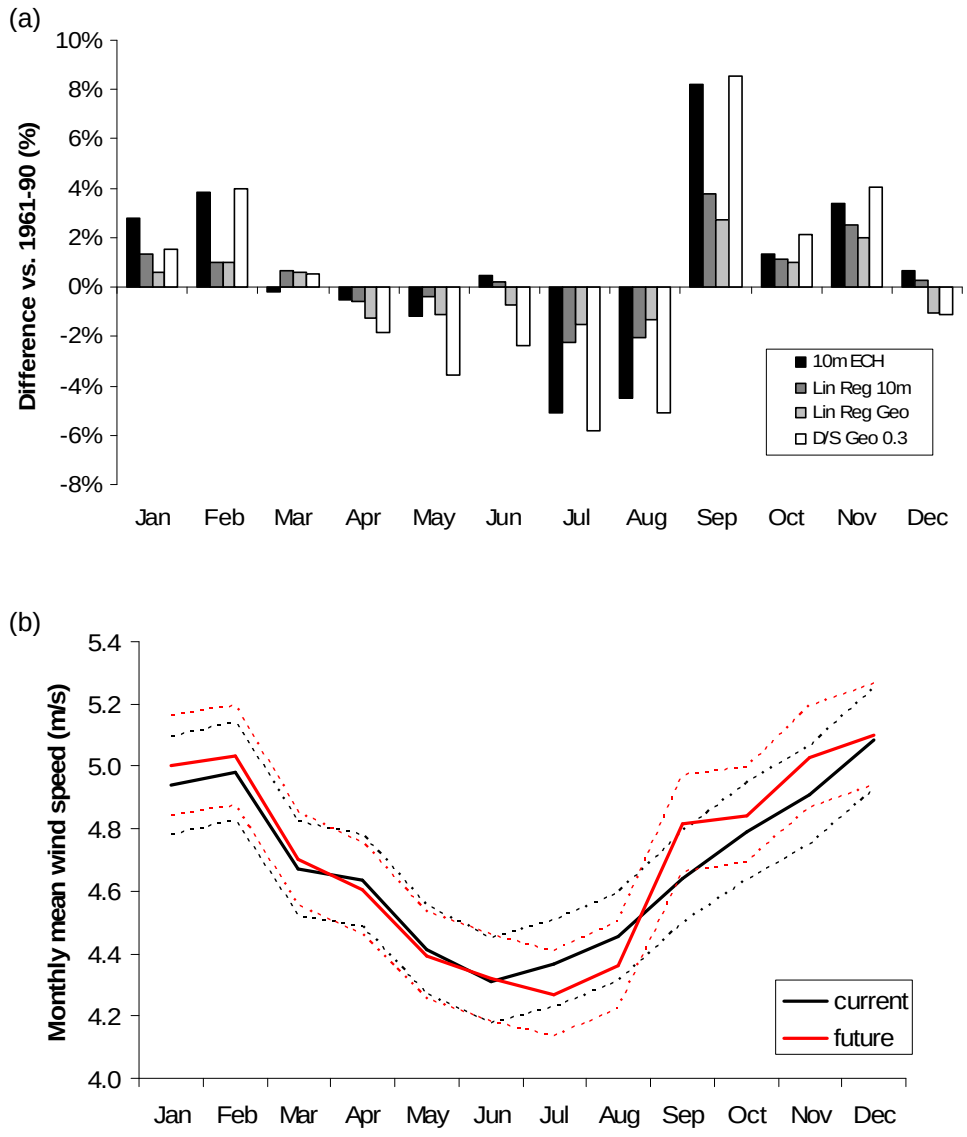

Fig. 6-36 Turnhouse future projections

(a) % Differences vs. 1961-90 data for each downscaling method; (b) Current and future projections and error bounds using linear regression of ECH5 10m data

6.5.7 Cairngorm

The model results for the future period for the Cairngorm site (Fig. 6-37) are broadly consistent in their monthly patterns, except, as before, where the changes are very small. There are three months with relatively large decreases in the mean wind speed – April, 5-9%; May, 3-5%; and December, 3-7%. There are also three months with fairly large increases – September, 10-12%; October, 3-5%; and November, 4-9%.

These serve to produce overall annual changes of 1-1.5%, which are small but greater than at most of the other sites.

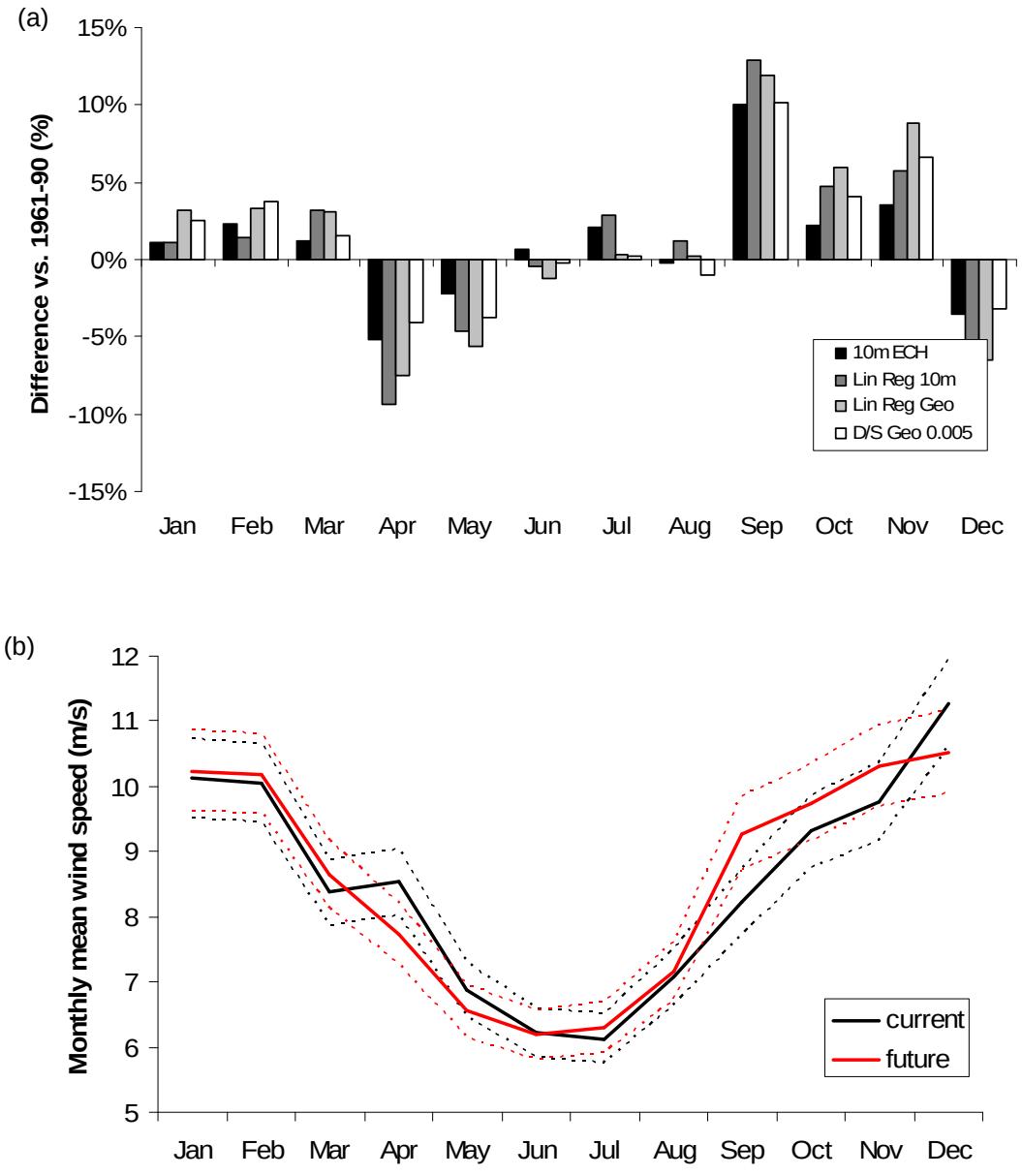

Fig. 6-37 Cairngorm future projections

(a) % Differences vs. 1961-90 data for each downscaling method; (b) Current and future projections and error bounds using linear regression of ECH5 10m data

The 10m linear regression model suggests that in two of the months – April and September – the future results fall outside of the control period error bounds, so that the magnitude of change is greater than the error in the model. This could indicate

some confidence that there will be an impact in these months, albeit reasonably small.

6.5.7.1 Conclusions on futures using simple downscaling

Table 6-3 shows a summary of the annual mean absolute percentage differences (MAPE) for the 2081-2100 period versus the data obtained for the 1961-90 period using the GCM 10m values, linear regression with both 10m and geostrophic wind (method 1) and using the drag law (method 2). The majority of the changes are small, and in all cases, smaller in magnitude than the errors in the models developed for the current period (see Table 6-2).

Site	10m ECH	Lin Reg 10m	Lin Reg Geo	Drag Law
Boscombe Down	3.81%	4.10%	3.81%	4.97%
Boulmer	2.51%	3.54%	2.96%	2.88%
Wittering	2.92%	2.19%	3.63%	3.97%
Fort Augustus	3.24%	2.10%	2.13%	3.48%
Eskdalemuir	2.68%	2.31%	1.83%	3.03%
Turnhouse	2.68%	1.34%	1.23%	3.39%
Cairngorm	2.87%	4.52%	4.80%	3.42%

Table 6-3 Summary for each site

6.5.8 WAsP Case studies (futures)

In order to assess any potential changes in wind climate indicated by the GCM, the same three WAsP methods as above have been carried out for the two more successful sites, Boulmer and Turnhouse, using ECH5 data for the period 2081-2100.

6.5.8.1 Boulmer, Northumberland

The results for the WAsP processing of data from 2081-2100 for all of the methods when compared with data from 1961-90 show very little in the way of significant change for this site (see Fig. 6-38). Considering the results at 80m height and 0.1m roughness length, i.e. which would apply to a turbine placed in this region, there is a very slight increase in the mean speed of under 1% using the GCM 10m climate

directly. The method which uses derived 200m observed wind climates results in a even more slight change, this time a decrease, in mean wind speed.

Both WP2 and WP3 show a small decrease in the Weibull k parameter of just less than 1% for WP3 but a rather more significant 4-5% for WP2. The combined effects of these changes give a fairly consistent projected increase in power density at the site of between 3 and 4% versus the methods' baselines.

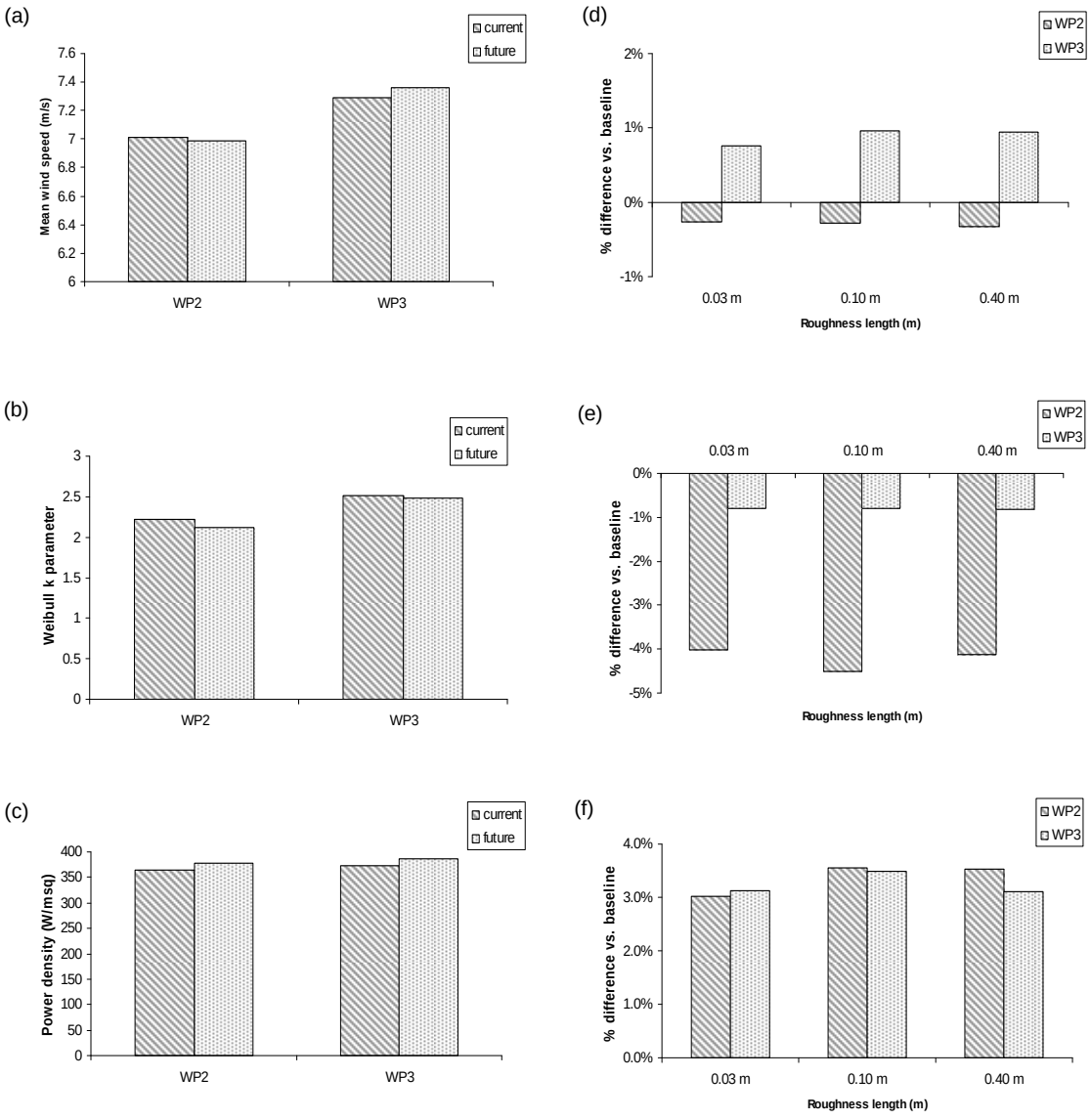

Fig. 6-38 Boulmer Future WAsP results

(a) Mean speed at 80m; (b) Weibull k parameter at 80m; (c) Power density at 80m; % Differences compared to observed data in (d) % mean speed at 80m; (e) Weibull k parameter; (f) power density at 80m

The changes projected here are, in both cases, lower than the differences between the modelled and observed climate. Pryor *et al.* (2005d) suggest that it is difficult to use results like this with any confidence, given that the magnitude of the error is greater.

6.5.8.2 Turnhouse, Midlothian

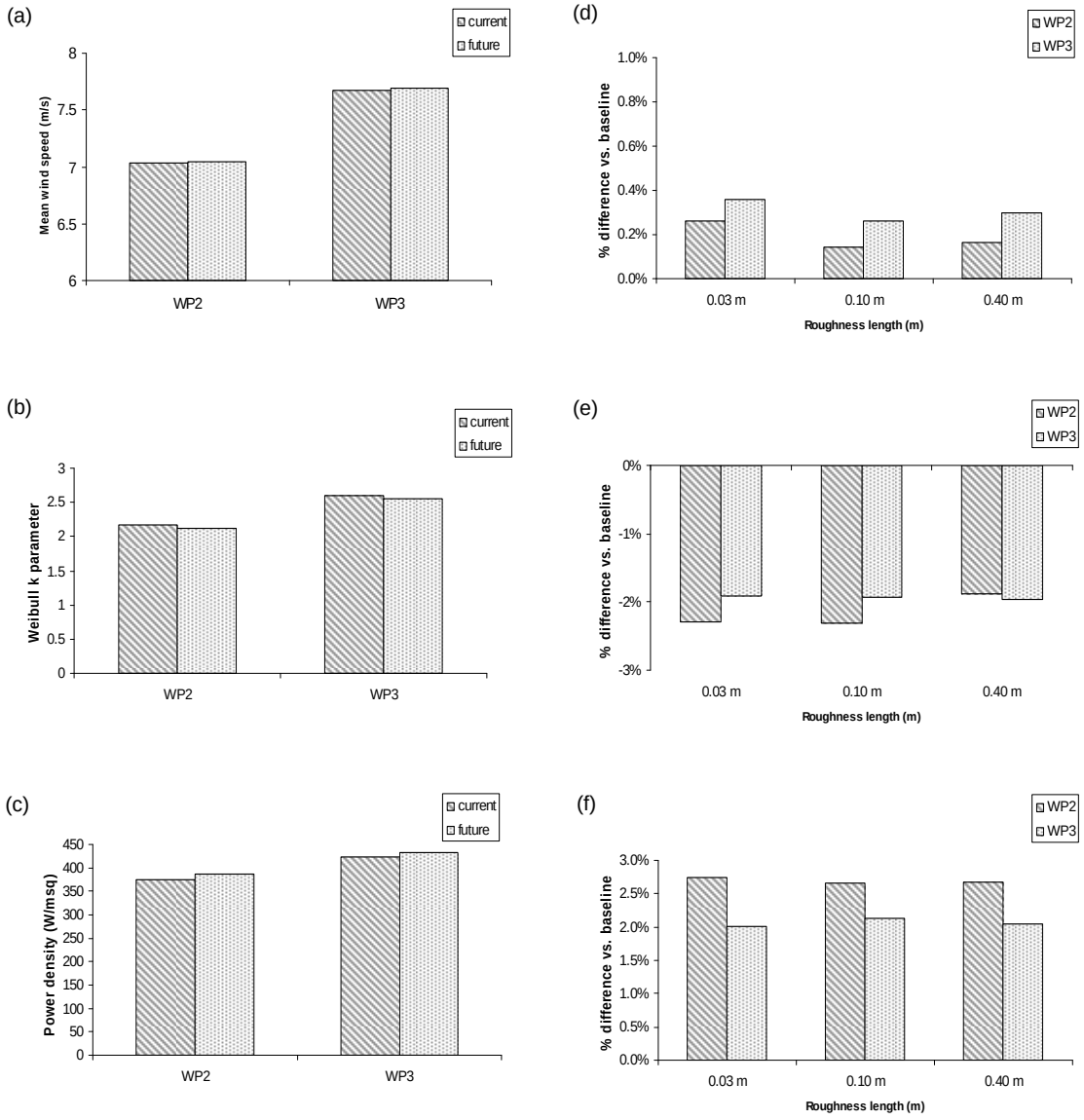

Fig. 6-39 Turnhouse Future WAsP results

(a) Mean speed at 80m; (b) Weibull k parameter at 80m; (c) Power density at 80m; Differences compared to observed data in (d) % mean speed at 80m; (e) Weibull k parameter; (f) power density at 80m

Both sets of projected wind data for the site at Turnhouse, using WP2 and WP3, show only very minor changes (see Fig. 6-39). WP2 calculates a projected increase in the mean wind speed at 80m of around 0.1-0.2%, whilst WP3 gives an increase of 0.2-0.4%. The change in Weibull k parameter in this region given by both WP2 and WP3 is around -2%. The consequent increase in power density in the region is approximately 2% calculated using WP2 and 2.6% using WP3. Neither sets of projections are potentially significant, and, are well within the error in the model calculated for the control period.

Conclusion on WAsP futures

Of the locations analysed for future changes, neither show any large degree of change on an annual basis; without doing the WAsP analysis on a monthly basis it is not possible to tell whether the monthly changes are consistent, or if the annual change is the compound effect of some positive and some negative changes.

Trying to identify precisely why the differences exist between method 2 and method 3 is difficult without access to the underlying model - so as to carry out controlled experiments. It is clear, firstly, that there are factors employed in the ECH5 climate model that are not accounted for by the simple use of the drag law; and, secondly, that the use of WAsP introduces further factors that may or may not be more accurate.

6.6 Conclusions

The methods detailed in section 6.3 for obtaining typical monthly mean wind speeds from a GCM at site level proved to be fairly reasonable for most of the sites tested. Errors were generally around ±5% per month, but tended to average out over the year to give much smaller errors. Some months showed larger errors, particularly March, which seems to be poorly represented by the GCM - as demonstrated in previous chapters. In general, the linear regression models performed more successfully than the drag-law downscaling and the GCM 10m data taken directly from the model, but in some cases the GCM itself was a better representation.

Examining the future projections from the GCM using the downscaling models highlighted in most cases a pattern of change consistent with that found in the RCM in Chapter 4, with winter mean speeds increasing and summer mean speeds

decreasing. At a number of the sites, however, the changes were relatively small compared to the error calculated in the models for the control period; so it is not possible to be confident about these changes.

The main deficiency in these models is their failure to take account of the wind speed distribution. They only provide an analysis of the mean wind speed, rather than the variability, and so it was not possible to examine the changes to this aspect of the wind climate projected by the GCM. To give some insight into variability, the WAsP software was used to investigate some of the test sites. It was established that the linear regression models were more successful than the use of the geostrophic drag law, as they may empirically account for more influencing factors than the drag law. WAsP was chosen for its ability to include some of these other factors in the analysis, alongside surface roughness.

The WAsP analysis provided, in the form of a 'wind atlas', the annual mean wind speeds, Weibull k parameters and power density at a selection of standardised roughness lengths and heights. Compared to the wind atlas generated from the MIDAS station data, the mean wind speeds found using the derived GCM 200m wind climate tended to be within ±10% of observed. The mean wind speeds found using the GCM 10m winds varied more, from -2 to +25%. This, of course, is only representative of the four sites tested, but indicates that more research is necessary to establish if using the GCM 200m winds could give more consistent results. It was shown that there was quite a large discrepancy in the Weibull k parameters in respect of all the datasets, which - combined with the wind speed errors - gave significant differences in the power density calculations.

In terms of future results, the Boulmer study appears to provide similar results to the other downscaling methods, with very minor changes anticipated for the future period. Analysis of the data for Turnhouse showed similarly slight changes in future conditions. Whilst the use of WAsP is interesting in this situation, and could potentially give benefits above the use of regression of monthly mean wind speeds - such as estimates of variability - it is unclear at the moment whether or not the results are any more successful than the statistical downscaling methods. It is possible that using WAsP in conjunction with time series from a higher resolution RCM may be more appropriate, and further research in this area would be worthwhile. Meanwhile,

it has been shown that the linear regression of monthly mean wind speeds gives credible enough hindcasts, rendering them in the same order of usefulness as the regional climate modelling results discussed in Chapter 4.

Chapter 7

Conclusions

This chapter summarises the findings of this thesis and discusses the implications of these findings for the generation of wind power in the UK, both in terms of long-term financial viability and of the potential impact on the management of the electricity system. Some suggestions are made as to possible strategies for dealing with the repercussions of climate change on wind power generation; and plans for further work are outlined.

7.1 Discussion of results

7.1.1 Sensitivity of wind to changes in wind climate

The sensitivity of the financing of wind power to possible changes in the wind climate was discussed in section 3.8. It was found that, in comparison to three other factors - capital cost, operations and maintenance (O&M) costs and electricity export price - the net present value (NPV) of a wind power project was more sensitive to variations in the mean wind speed. Considering an example site where the wind speed is relatively low, perhaps on the threshold of what might be considered viable, a 10% drop in wind speeds will result in a drop of approximately 20% in energy output. In the circumstances of the particular project modelled, this forces the NPV into the negative region, and hence renders it completely untenable. For a site with probably one of the highest potential mean wind speeds expected in the UK, a 10% fall in the mean wind speed would result in a 20% reduction in NPV which, whilst not undermining the feasibility of the project, would obviously reduce profits. By the same token, a similar rise in the mean wind speed would generate a similarly proportionate increase in profits.

Looking to the wider issue of actual energy cost, sites with both relatively high and low mean wind speeds show greater cost sensitivity to decreases in the mean wind than to increases; thus a 10% reduction in mean wind speed will result in an increase in energy cost of between 10 and 30%, whereas a 10% increase in the mean wind speed will decrease energy costs by approximately 5 to 15%. In a

situation where wind power is expensive compared to conventional thermal or nuclear power, either of these scenarios would have a significant impact on a number of aspects of the industry, from individual project finances to public acceptance.

When considering wind energy outputs it is necessary to take account not only of mean wind speeds, but also of the variability of the wind - that is, its frequency distribution parameters. Based on the typical Weibull distribution (as described in Chapter 4), the A parameter is strongly related to the mean wind speed, whilst the k parameter is more related to the standard deviation. A lower k parameter will result from a distribution more skewed towards lower wind speeds and which extends further, giving low frequencies of higher wind speeds. Changes in the k parameter also have the potential to affect energy output. As shown in section 3.8.2, however, varying the value of k between 1.8 and 2.2 only changes the energy output over a year by ± 1.7%. This suggests that unless any future variation is greater than 10%, it is unlikely to cause any major problems in project finance. However, this does not take account of other factors that may be influenced by a change in k parameter. Although the Weibull k parameter is not the preferred indicator for extreme conditions, a change in the k value at a site might loosely indicate an impact on parameters sensitive to changes in extreme wind conditions - like maintenance costs for example.

Another issue meriting attention is that of the capacity factors of wind power developments. The government's aim of increasing the percentage of electricity generated from wind power has knock-on implications for the design and management of the entire power system. Wind is obviously not given full capacity credit for the installed power, but is instead 'counted' as a percentage of this, which will be related to its likely capacity factor (see 3.5). The capacity factor of a development is a major contributor to development decisions. Significant changes to capacity factor figures as a result of changes in the mean wind speed, must be accounted for in capacity planning.

7.1.2 Direct use of GCM surface wind projections

Using a General Circulation Model (GCM) to analyse changes in surface wind climate is unlikely – at the current stage of model evolution – to give the optimum

results due to their poor spatial resolution compared with the spatially inhomogeneous nature of wind climate. Until the resolution markedly improves, it is difficult to verify the accuracy of the models compared with observed data. However, it is worth investigating how realistic or otherwise the hindcast results of a GCM are when compared with observed or validated model data, in order to understand if any useful information can be gleaned from the future projections thus generated.

An analysis of the 10m wind climate from the ECHAM5 GCM for the period 1961-90 alongside 10m winds from the ERA40 reanalysis for the same period showed that the GCM captures some - but not all - of the general characteristics of the typical monthly mean wind climate in the UK. The large-scale spatial pattern is represented, but the low resolution of the model is clearly incapable of capturing the coastline with acceptable precision. The GCM has a tendency to over-estimate the mean wind speed when compared with the ERA40 reanalysis; this is potentially indicative of either having chosen different surface parameter values in the parameterisation scheme to obtain the wind speeds from large-scale climate features, or from a difference in the pressure gradients used to calculate the geostrophic wind speeds. Seasonally, the model appears to overestimate the mean wind speeds most severely in summer, and least in the winter months. A reason for this may be that the large-scale climate factors used in the parameterisation scheme are perhaps less dominant in summer months, when thermally-driven winds not included or not modelled sufficiently in the scheme may play a greater role. The annual temporal variability is thus underestimated, as shown by the Weibull k parameters calculated from the daily time series; these are consistently higher than those calculated from comparable daily averaged time series from the ERA40 reanalysis data. The results from two runs of the GCM for the control period were compared as part of the analysis in Chapter 4, and these both showed a fairly similar pattern in the hindcast - with just a few exceptions.

Based on the hindcast analysis, it is clear that any future projections from the model can, at best, be interpreted as a qualitative suggestion of what may occur in future, but possibly would not be good enough for a detailed study - such as a resource assessment. The indications for future mean wind speeds are that there will

be little in the way of perceptible change by the 2081-2100 period. The spatial pattern remains fairly consistent and most of the average monthly changes are within ±5% of the control period mean, with a tendency to increase in winter months and decrease in summer. Looking at the changes in the typical monthly patterns over the UK shows that most activity appears in the north west, over Scotland and its Atlantic coast, where some of the increases and decreases are rather more significant than the regional average. There is no indication of changes in the annual Weibull parameters from the model, except for a very slight decrease in the south west of the region.

7.1.3 Regional climate model surface wind projections

Dynamic downscaling of GCM output using a Regional Climate Model (RCM) increases the resolution of the results, and thus should make the surface wind climate results more applicable at a given location. There is a reasonable degree of correspondence between the output for the future period (2081-2100) from the RCM analysed in section 4.4 and the results from the ECHAM5 GCM, with an emphasis on seasonal changes – increasing mean speeds in winter and decreases in summer. It is possible to make more confident inferences about spatial changes using the RCM data than from the GCM output due to its higher resolution. The very north and west of Scotland are again shown to be most likely to undergo significant change, but with the two regions showing contradictory changes. It is difficult to determine whether these changes are an artefact of the model, or are due to alterations in the pattern of large-scale influences.

Because of the increased resolution of the results, it was considered reasonable to use the changes in projected future mean wind speed to calculate the potential changes in seasonal energy outputs. From this it is clear that even small changes in mean wind speeds can affect the output of a wind turbine; and although these results are perhaps still not of a high enough resolution to be directly applicable to a particular site within one of the grid cells, they suggest modelling at higher resolution may be prudent given the magnitude of the calculated effects.

7.1.4 Using large-scale climate as a proxy for surface wind

The parameterisation of surface wind climate from larger-scale climate features as part of the GCM modelling process means that there has been an intrinsic averaging

process carried out, particularly relating to surface elevation and roughness. Without access to the background detail of the model, it is difficult both to define its limitations and consequently to apply any sort of corrections. It was considered, therefore, that going back to the large-scale climate features - particularly mean sea-level pressure - may also provide more insight than the GCM calculated surface winds as to the driving forces behind any changes in wind climate, and be more indicative of the shape of these future changes. Using the large-scale climate as a proxy for the surface wind would begin a downscaling process whereby a lesser degree of averaging could be applied.

7.1.5 The North Atlantic Oscillation

The North Atlantic Oscillation (NAO) was considered as a possible proxy, representing the variation in the large-scale climate known to affect the UK area. However, there are two problems with the use of the NAO to explain UK wind speeds, as identified in Chapter 5. Firstly, the phenomenon really only influences climate in the winter months - perhaps extending to cover November and March - thus leaving no way of analysing the summer months. The second problem is that the analysis shows that the NAO only explains 50% of the variance in winter wind speeds. This leaves half of the variance unexplained, and when analysing the effects of climate change, would be unaccounted for if the NAO were used as the only proxy.

The NAO is commonly derived from a station based index, or in the case of a model, an index obtained from two grid squares in the vicinity of the stations. However, there is some evidence to suggest that some GCMs project a movement in the centres of action of the NAO. This would not be accounted for if a station-type NAO index was being extracted from the model, as the stations are at fixed locations. Deriving an NAO index using a statistical method is possible, but given the two issues highlighted above, this was not believed to be a credible route on which to continue. It may, however, be useful to investigate other large-scale pressure patterns and oscillations which may be more strongly related and which may act in all seasons.

7.1.6 Geostrophic wind

With the NAO only explaining some of the variance in UK wind climate, it is possible that the local, regional pressure fields may provide more reliable insight. The geostrophic wind is derived from the mean sea-level pressure gradients over a defined distance of latitude and longitude. When compared to the geostrophic wind derived from ERA40 reanalysis, the ECHAM5 geostrophic wind climate showed more similarity than the similar comparison of surface winds carried out in chapter 4. In terms of typical monthly means averaged over the region, the GCM showed a slight overestimation relative to ERA40, with the largest discrepancies being in the summer months. This is presumably when the geostrophic influence on surface winds becomes relatively less dominant. The similarity in spatial patterns of mean speeds over a fairly large region was very high, reducing in likeness as the region was shrunk and focussed towards the UK landmass. It was shown in section 5.3.1.4 that this is due to a mismatch in the location of a region of low pressure to the north and west of the UK. The variation in geostrophic wind speeds in the GCM is lower than that manifest in the reanalysis winds, indicating a possible failure to capture the extremes of climate.

In terms of what geostrophic wind projections suggest for the future of the UK wind climate, there is a similar indication of summer decreases and winter increases as was evident in the surface wind projections - with most regionally averaged changes in the region of ±5%. The spatial patterns of change show slightly fewer examples of extremes than those of the surface wind. The Weibull k parameter shows a more spatially consistent decrease than was projected using the surface wind data.

Overall, this part of the investigation has confirmed that the surface wind climate is strongly linked in the GCM to the geostrophic wind, and that the future changes calculated from the surface wind projections indicate a ‘trickle-down’ effect from the large-scale wind climate. This provides a good basis for using geostrophic wind for downscaling, bypassing the GCM’s attempts to parameterise surface wind speeds within a low resolution grid.

7.1.7 Site-level results – control period

It is difficult to make the assumption that, under conditions of change, any empirical or statistical relationship established for the current period will endure in the same manner into the future. It may be 'safer', at least within the large uncertainties already present in climate modelling, to base the downscaling technique on physical relationships determined from established laws; this suggests that a form of 'dynamic downscaling' might be preferable. In practice, dynamic downscaling is more difficult than statistical downscaling in terms of requirements for computing power and expertise; and so using a linear flow model like WAsP may be a good compromise - it is not dynamic, but nor is it strictly empirical since it is based on physical relationships between upper-boundary layer flow and surface wind. Unfortunately, it is limited in its capability in areas of very heterogeneous terrain, particularly with large variations in elevation and in forested regions.

Two other simple techniques were applied to GCM wind data to begin with: one which developed an empirical relationship between monthly mean observed surface winds and the GCM data; and one which used the geostrophic drag law applied to geostrophic wind - calculated from GCM pressure fields - to derive monthly mean surface winds. Both new datasets were compared with observed data. The drag law model corrects geostrophic wind for surface roughness effects, but neglects other influencing factors such as atmospheric stability and elevation. The results from this downscaling method are also influenced by an inherent error within the model itself, as a result of which it does not correctly estimate the true mean geostrophic wind climate. The empirical regression model corrects, by means of a 'black box', for all the factors that influence surface wind and any implicit model error, and thereby gives smaller errors when compared to the observations for the control period. In all but one of the cases analysed, the regression models were superior to using the GCM 10m winds directly, whereas the drag law methods were only better for three out of the seven sites - those with particularly complex site locations.

Using WAsP to model the 'regional wind climate' using site data and comparing this to a regional wind climate created in WAsP from both the GCM 10m data and GCM geostrophic wind downscaled to 200m by the drag law, it was found

that at only two sites did the mean wind speeds from the GCM data come within ±5% of those from observed data. The rest showed larger discrepancies, suggesting that either:

- the sites were not well modelled in WAsP - particularly for the heavily forested area in Eskdalemuir (see 6.4.9.6);
- or that the GCM did not present a good representation of the site conditions within its parameterisations, and so WAsP will have corrected for a different set of site parameters;
- or, finally, that the GCM climate was too far removed from reality.

7.1.8 Site level results – future periods

The results of the analysis using all of the techniques employed reinforce the findings of the previous chapters. Because the work is based on annual rather than seasonal data, the changes projected in mean regional surface wind speeds are generally small, and consequently the annual energy output changes likely for wind farms are minimal. On a seasonal basis, drops in summer monthly means and increases in winter monthly means could have significant implications for the management of electricity supply.

The change in the Weibull k parameter is highlighted at the sites where WAsP analysis was carried out as a potential point for future change. It may tentatively suggest an increase in the frequency of extreme winds, but analysis of mean wind speed frequency distributions is not the most reliable means of investigating this aspect.

7.2 Financial implications of results

From the sensitivity analysis carried out in Chapter 3, it was clear that the project economics of wind power generation are susceptible to changes in wind climate. However, the changes in wind speed at various sites around the country, as analysed in Chapter 6, are quite small on an annual basis, and would create only a small change in overall energy output at a wind farm situated in these locations. To show this, the mean annual energy output for a single turbine at each site has been calculated for the control period, and for the future period, and the percentage change derived.

Taking the model for each site in which the smallest error was present (as more confidence is attached to the calculations of future change using these results), only three of the seven sites, Boscombe Down, Turnhouse and Cairngorm, show future energy outputs that are beyond the error bars on the control period data.

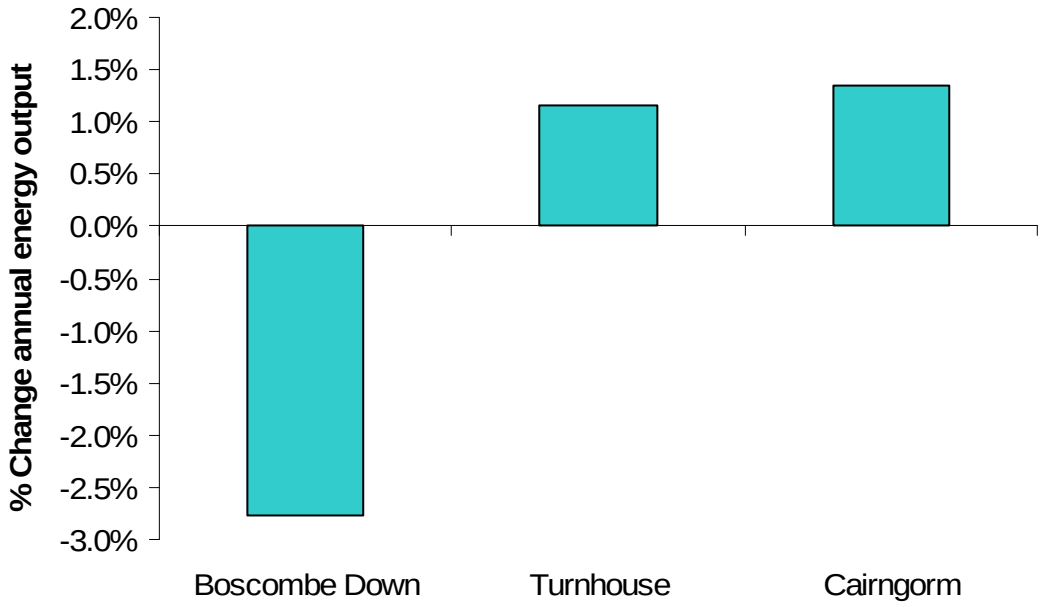

Fig. 7-1: Future change in energy outputs at three sites based on change in annual mean wind speed

Even then, the percentage changes are small, ranging from -2.75% at Boscombe Down to +1.5% at Cairngorm. Using these changes, the same RETScreen[1] model with the same parameters as used in Chapter 3 has been applied for a wind farm of ten turbines at each of these three sites, for present and future conditions. This model assumes a constant average sales price for electricity over the year - including the value of Renewables Obligation Certificates (ROCs). The two main points of comparison used in Chapter 3 were the project NPV and the cost of energy.

One of the three sites, Turnhouse, which has a relatively low mean wind speed, has a project NPV in current conditions that is, in fact, negative, with the cost of energy production higher than the export cost. With a small rise in the future mean wind speed, the NPV rises to a positive figure, and the cost of energy falls by about the same percentage as the energy rise, around 1.15%. However, the proximity

[1] [1] RETScreen is a registered trademark of Natural Resources Canada, © 1997-2009

of the figures to the breakeven point means doubt must be cast on the viability of this particular site for a wind farm development.

The Boscombe Down site showed the largest potential change in energy output - a fall of 2.76%. The cost of energy production rises by a similar percentage in response. In terms of the project NPV, it appears to affect the more sensitive area of the curve, with the NPV falling by over 27%. It still remains feasible, but the equity payback time increases from 9 years to 9.5 years.

The third site, at Cairngorm, is a rather obscure choice of location for a wind farm - very remote, at high altitude, limited infrastructure - but is interesting due to its very high mean wind speed. If it were possible to locate a development in the area, a small increase in energy output by the end of the 21st Century of 1.35% would make a relatively minor change to the project NPV of 2.27% and no difference to the equity payback period which stays at a very low 2.3 years. The cost of energy would fall by 1.13%, similar to the percentage increase in energy output. Because the site would be so highly profitable anyway, it is much less vulnerable to small changes in the mean wind speed.

If we were to model the changes from the RCM data used in Chapter 4 for the grid boxes in which these sites are located, only the results for Boscombe Down fall outwith the error bounds on the model calculated when compared with met station data - some of these errors are, incidentally, very large. The Boscombe Down results project an increase in energy output of 3.78%, similar in magnitude but opposite in direction to the empirical downscaling result. This results in an increase in the future NPV of over 30% and a reduction in the cost of energy generation of 3.6%.

Using the WAsP model of the Boulmer and Turnhouse sites, a turbine has been added to the model at the location of the met station and the mean wind speed at the site calculated. WAsP calculates the annual energy production (AEP) as well as the mean wind climate; but there is a slight discrepancy between this and the energy output calculated by RETScreen (due to a difference in the assumed power curve), so for consistency, the RETScreen values of energy have been used. The variations in Weibull k parameters have been included in the analysis. There are some differences between the results as calculated using the two different WAsP methods, but in

general, none of the future changes using either method are as large as the differences between the model climates and the original met station data. The changes in financial parameters for the future period versus the control period are small for both sites, with the largest change being a drop in the NPV of around 6% at Boulmer using WAsP method 2, caused by a fall in annual energy output of around 1.6%.

The conclusion based on this kind of limited 'feasibility' study for a potential wind project is that very little can be expected to change in the parameters considered at the sites investigated here in the next 50-100 years. Of course, this kind of analysis neglects the dynamic nature of electricity prices in the UK and their relationship to demand. Prices tend to be highest at times of peak demand, and currently that means the winter months, when ambient temperatures are lowest and daylight is at its minimum. An increase in winter mean wind speeds could increase revenue for wind generators during this period. The potential shortfall in summer revenue due to dropping wind speeds would probably be relatively less than the winter gain, due to the lower sales price during this period, creating an overall positive situation for the wind operators. However, some other factors must be accounted for in considering these scenarios: firstly, the implications of changes in wind generation capacity at peak times for fossil-fuel generators are not clear, and this could further affect prices; secondly, with ambient temperatures projected to rise, it is possible that the current winter peak in demand could become smaller, or at some point could even move to a summer peak as demand for space cooling grows; thirdly, the current system of financial support in the form of ROCs contains a certain degree of variability in the price obtained per certificate, and the system itself may also be subject to alteration. Without a dynamic market model, it is not possible to arrive at firm conclusions about the seasonal pricing effects, but the possibilities certainly merit further investigation.

The simple feasibility study described here does not account for any interannual variations in income, which may be of some importance. There have been some fairly major fluctuations in oil prices in recent years, resulting from political and economic instabilities, and these directly affected gas and oil prices in the UK. As a portion of the electricity supply system depends on oil and gas, the

costs of traditional generation must rise with oil prices. If oil - and natural gas - reserves are indeed in decline, it might be expected that the price would tend to increase further in the coming decades. This would put generators of renewable power in a much more competitive position, and the sale price of a unit of electricity would rise year-on-year, potentially combating any losses resulting from small changes in the resources.

7.3 Implications of results for the electricity industry

7.3.1 Wind power generation

The results outlined here show that on an annual basis, the models indicate no certain discernable change in the energy output from a wind power production site over the next 100 years. In terms of the implications for the finances of an individual wind farm operator, there is probably little concern in terms of overall viability of a project, particularly as climate assessment is ongoing, and projections are really only necessary within the lifetime of a development, generally put at 20-25 years.

Most of the analyses, whilst not returning identical values, showed a typical pattern where mean wind speeds are projected to fall in summer and rise in winter (although some anomalies to this trend were found, particularly in the RCM results). As discussed in section 7.2, this pattern could have an interesting effect on the pricing mechanisms for wind, but establishing the response of the market to these changes would require in-depth economic modelling. Changes in the demand pattern with a rise in ambient temperature would introduce further complexity to the modelling problem.

In terms of changes in the optimum locations for wind farms, these are also likely to see little in the way of perceptible change. Troen & Petersen (1989) suggests that current mean wind speeds are higher in the northern half of the UK; this is already reflected in the higher installed capacity of wind generation in Scotland compared to England (BWEA, 2009). The analysis of surface mean wind speeds over the whole UK area using the GCM and the RCM showed similar annual patterns for the future period as for the control period, and so it is likely that the north-south difference will persist.

7.3.2 Network operators

The network operators in the UK are already under some degree of pressure with regards to wind power development. Connections of new wind farms to the distribution network, in particular, are difficult to manage with variations in power flows already causing difficulties. In a situation where the variability of the resource may be increasing, as with a decreasing k value, there may be even more management difficulties arising. Reliability of the network could potentially be affected due to more frequent occurrences of high wind speeds, causing greater fault levels and higher maintenance requirements.

One point that requires further modelling is the increase in winter wind speeds and how that might impact on the ability of network operators to manage large power flows - especially those on the distribution network, with an increasing number of wind farms, all with high energy output for a number of months. Curtailing generation from wind farms is sometimes part of distribution network management strategy, albeit fairly rare. It is an expensive option, as the operators will still require payment for 'non-produced' electricity; and so an increase in the potential for this situation to occur may require a different management method.

7.3.3 Wind power strategy and targets

The UK intends to meet a large proportion of its electricity demand using wind power, the incentive being the meeting of emissions reduction targets. Currently, demand is highest in winter, and a rising mean winter wind speed would be beneficial in meeting the higher demand in these periods, thus assisting in the reduction of the country's carbon emissions levels. On an annual basis, it does not appear that it will be any more or less feasible to meet the wind power production targets in future.

The current winter peak/summer trough electricity demand pattern may itself be altered by rising ambient temperature arising from climate change. The present requirements for space heating in winter may reduce and, coupled with increasing prosperity, the desire for summer space cooling may begin to smooth the winter peak/summer trough pattern. Whilst a falling winter demand coupled with greater wind supply could ultimately drive down the price of electricity, an increasing

summer demand would be particularly problematic, with a smaller wind power contribution. It would lead to greater requirements for despatchable balancing plant, such as gas or coal, and drive up costs - not to mention carbon emissions.

7.4 Strategies for dealing with changes

The primary strategy at this stage for those both interested and concerned must be further investigation of climate impacts on renewable energy resources together with additional research into the other potential climate change impacts on the electricity system, predominantly demand changes. Sophisticated modelling of the wholesale electricity market under conditions of increased seasonal variability is necessary to understand the impact on revenue streams for wind farm operators. Since the impact is unlikely to aggregate into a serious change in lifetime revenue, the strategies required will be focussed on gaining understanding of the fluctuations and management of the finances, with the expectation that these will 'iron out' over the longer term.

Ever-increasing accuracy in forecasting techniques, both on a relatively long time-scale - of, say, a week - and hour-by-hour predicted data for demand and weather conditions will assist in the operation of the electricity network in periods of high stress. Long-term, network managers may need to analyse 'worst-case' scenarios in order to forecast the potential for network problems. With regard to these longer-term analyses, it is likely that the skill of climate models will increase in the future, making these impact assessments more accurate and potentially more straightforward.

The obvious answer in terms of maintaining the most economic electricity supply is 'storage', whereby high wind conditions are exploited to produce excess electricity which is then put aside for use during low wind periods. The UK currently employs two pumped hydro storage facilities but Boehme (2006) found that even under current conditions, further capacity would enable greater exploitation of non-despatchable renewable electricity sources. Clearly then, an increase in disparity between wind generation in different seasons would enhance the case for developing more storage capacity. The development of additional grid

interconnectors between the UK and countries in northern Europe could also act as a balancing system as a result of the diversity of wind climates across the continent.

It will be the combination and interaction of the changes in both energy supply and demand that the industry will, directly or indirectly, be burdened with. It is important that there be a full understanding of how the interaction will occur before mitigating strategies can be developed and deployed. There is of course a danger that the risk could be over- or underestimated if the individual effects are considered in isolation from each other.

7.5 Limitations of the work

7.5.1 Resolution

This work has considered two main sources of climate change information: the ECHAM 5 GCM and the UKCIP02 RCM. In both cases, the resolution of the gridded data is low for wind resource analysis purposes, given the high spatial heterogeneity of wind climate. Whilst the gridded data gives an indication of the average conditions across the area enclosed within the cell, it is not necessarily representative of any particular site as the local surroundings contain so many other influencing factors. This was seen when looking at site data and comparing with the grid box data directly derived from the GCM in Chapter 6. The RCM goes some way to increasing the resolution of its driving GCM, but is still limited to 50km grid squares.

The downscaling methods applied in Chapter 6 were designed to analyse the wind resource at specific sites rather than on a grid basis. The sites were chosen to represent as diverse a range of wind conditions and surrounding terrain as possible, but do not all lend themselves to being potential wind farm sites for various reasons. The conclusions are very specific to these individual sites and it is not possible to confidently state that other sites in their vicinities would undergo similar future changes; and thereby they are only a hypothetical ‘snapshot’ of the projected UK-wide impacts of climate variation on wind power.

7.5.2 Models

There are a growing number of GCMs and RCMs being developed by different organisations globally and it would be interesting to look at the range of different results produced by more than one model. Current best practice for climate change analysis and impacts studies is to employ the ensemble modelling technique, using a large number of runs of each model, and to analyse the results from more than one climate model. The results are processed to assign a probability distribution over a range of values for the output parameters, rather than a single deterministic value. Unfortunately, limited access to multiple model runs and time restrictions have prevented this work from using ensemble output and further climate models; and so it is not possible to assign probabilities to the results of this work.

7.5.3 Variability

There may be some significant changes to the interannual variability of energy output over time. This would be important to developers and financiers, as the income of a site will fluctuate year by year; whilst not a problem in the long-term this could cause financial pressure in the short-term. Most of the downscaling work in this thesis has focused on monthly, seasonal and annual mean wind speeds over 20-30 year periods, but there is a requirement to understand the variability within these figures between different years. Analysis of the Weibull distribution parameters give some insight into intra-annual variability, but the analysis was limited due to large differences in model and site results, and also by the lower temporal resolution of model output compared to observed data.

7.6 Further work

This study has uncovered a number of interesting results that could be pursued in further work.

7.6.1 Probabilistic modelling

Over the last number of years, the probabilistic method of climate modelling has begun to emerge as ‘best practice’ when carrying out impact assessment. Using a number of runs, preferably from several independent climate models, would allow the projections of future change to be expressed probabilistically, depending on the

outcome of the various model runs. Applying this technique to the work contained in this thesis would no doubt increase the reliability of the results, and possibly introduce a number of different future scenarios for consideration.

7.6.2 Weather typing

Experience of the many techniques of climate downscaling has led to the conclusion that 'weather typing' perhaps offers the most advantageous approach. Classification of the large-scale circulation patterns and identifying the surface-level climate features that correspond to these would provide very flexible data that could be applied in many different climate impact investigations, not just to wind power resources. It would also enable a more scenario-based approach to be adopted, where different outcomes are studied alongside their potential.

7.6.3 More site analyses/seasonal analyses

The site downscaling technique was applied in this work to only a limited number of sites, so it was not possible to develop from these a representative view of the entire country. Potentially, more sites could be included using the method for different types of region, in order to understand the broader impacts across the country.

7.6.4 Extremes analysis

Given the decreases identified in the Weibull k parameter values across the country, an analysis of the extreme wind speed distributions may also be merited. Alternatively, an analysis of long return-period winds may provide similar information on the change in extreme wind climates in the future.

7.6.5 Combined renewable supply and demand modelling

The electricity supply system is very dynamic with varying levels of feedback in operation, and the ability to model the impacts of increasing renewables penetration in the system, coupled with a changing demand profile is thus required. Under climate change conditions, it is likely that all renewable resources will be vulnerable to alterations in output; this needs to be captured in order to plan effectively. Further to this, consideration must be given to the economic effects of the combined potential changes and interactions.

7.7 Overall conclusions

Wind power is a fast-growing contributor to the generation of electricity in the UK, and due to the relatively plentiful supply of wind, should be a financially sound investment at many locations around the country. The dilemma over choosing suitable datasets for wind resource analysis is a feature of any current development project, as there are a limited number of suitable sources, particularly at high resolution. This problem can be circumvented somewhat by using techniques such as measure-correlate-predict and the wind atlas methodology; but these rely heavily on good quality observations, which are not easy to obtain. Introducing climate change into the discussion involves further data dilemmas, as even the most recent generation of climate models are limited to a spatial resolution far from ideal for wind analysis. Downscaling techniques all come with caveats and inherent difficulties, and so the uncertainties in all analyses are high. It may be that best- and worst-case scenario analysis could be more beneficial for an integrated study than relying on model results. In this way, precise climate data is not required but rather some limits on the range and distribution of variables which can be used to derive the worst outcome possible and model the electricity system's response to this. Knowledge of probabilities of various outcomes would be a useful extension to this, in order to conduct risk-impact studies.

The initial parts of this work focussed very much on investigating the information available from climate models at a general UK-wide level. The first step was to examine how alike or otherwise the model data is compared to other datasets for a 30 year historical control period; secondly, the magnitude and range of potential future changes was established from the model data for the end of the 21st Century. Using a GCM 10m dataset, 10m data from an RCM, and derived GCM geostrophic winds, all the models tended to show only small changes in annual mean wind speed over the whole country - in the region of ±5% below the 10% threshold defined in the sensitivity study as critical. This would result in fairly small changes in energy output from wind farms if it were to be the actual outcome.

To try and gain more insight into effects at individual sites around the UK, two very simple techniques were applied, one involving a physical relationship between geostrophic and surface winds, and the other a derived empirical transfer

function between model and observed data. The GCM parameterisations themselves - i.e. the GCM 10m winds - were found to be superior in most cases to the simplified physical relationship, except in regions where the terrain was very complex. In general, the empirical model was superior to both the GCM 10m data and the physical relationship, as it compensates for both the large-scale model error and the failure to parameterise the wind successfully; but there is no guarantee that the same empirical relationship will persist into the future. Looking at the projected future changes with the empirical models showed only very minor changes in mean wind speeds, again unlikely to have much impact on an individual wind farm operator.

A third downscaling method was introduced for site-level analysis, which is an extended version of the physical relationship, using the wind atlas methodology in the form of WAsP software. This type of analysis was carried out for four sites, and was shown to give reasonable results for only two of these. Under future conditions, results showed very modest changes, in a similar range to the more simple downscaling methods.

The results from the downscaling were used to carry out a 'before and after' project financial analysis, to establish whether any critical changes would occur in the parameters necessary for project viability. Only one of the sites experienced a change that could be described as 'critical', where a small drop in energy output placed the site on the borderline of feasibility. For that one site, it is not feasible under current conditions to locate a wind development there; but with a small change in future energy output, it may turn out to be more productive. Wind project economics is clearly sensitive to what might seem like minor changes in the wind climate, but in the majority of cases, the impacts derived from the modelling carried out here are not large.

Other impacts at a seasonal level may cause more of an issue under future conditions. A tendency for the mean wind speed to rise further in winter and fall further in summer - that is, an exacerbation of the recognised seasonal pattern - is a feature of most of the analyses in the majority of locations. This may have implications for electricity network management in terms of, for example, dealing with large power flows in winter on the distribution network. If the temperature rises

in line with model projections it could also combine with changes in seasonal demand pattern to create a capacity gap in the summer months.

What is most important to understand about the impact of climate change on wind power is the combined effect of a number of changing conditions, rather than looking at individual changes in isolation. Wind generation has such different characteristics to energy supplied by traditional centralised fossil fuel or nuclear plant that there is at this stage a great need for change to manage the intended increase in its contribution. Climate change adds a layer of further uncertainty to this already precarious system, and it would be a mistake when developing a long-term strategy, if no consideration were given to the possibility of different conditions in the future.

The original hypothesis of the work was that climate change impacts on wind resources would necessitate a change of strategy in the wind power industry. From the results of a limited analysis of climate modelling data and a discussion of economic effects it appears that the magnitude of any such change is likely to be relatively small, and be unlikely - as the sole impacting factor - to require any strategic adjustments to maintain the economic viability of the industry. The potential changes to average capacity factors for UK wind power would be expected on the basis of the results found here to be minimal. Some issues surrounding seasonal pricing may require adjustments by individual operators, and in combination with other impacts caused by a changing climate, could result in a need for mitigating strategies. Further work is required to ascertain how the impacts would interact and to develop actions needed to address potential problems.

References

Adam, D. (2007). *US answer to global warming: smoke and giant space mirrors.* The Guardian Retrieved November 2008, from http://www.guardian.co.uk/environment/2007/jan/27/usnews.frontpagenews.

AMS – *See American Meteorology Society*

American Meteorology Society (2009). *Glossary of Meteorology (online).* Retrieved November 2008, from http://amsglossary.allenpress.com/glossary.

Aubrey, C. (2007). *Supply Chain: The race to meet demand.* EWEA Retrieved July 2009, from http://www.ewea.org/fileadmin/ewea_documents/documents/publications/WD/2007_january/0701-WD26-focus.pdf.

BADC – *see British Atmospheric Data Centre*

Barry, R. G., Chorley, R.J. (1998). *Atmosphere, weather and climate*. Routledge, London,

BBC News (2009). *Russia to cut Ukraine gas supply.* Retrieved June 2009, from http://news.bbc.co.uk/1/hi/world/europe/7812368.stm.

Beniston, M. (1998). *From turbulence to climate: Numerical investigations of the atmosphere with a hierarchy of models*. Springer-Verlag, Berlin,

BERR – *see Department of Business, Enterprise and Regulatory Reform*

Boehme, T. (2006). Matching renewable electricity generation with demand in Scotland. Institute for Energy Systems, School of Engineering. University of Edinburgh. *PhD Thesis.*

Boehme, T., Wallace, A.R. (2008). *Hindcasting Hourly Wind Power across Scotland Based on Met Station Data*. Wind Energy **11**: 233-244.

Breslow, P. B., Sailor, D.J. (2002). *Vulnerability of wind power resources to climate change in the continental United States*. Renewable Energy **27**: 585-598.

British Atmospheric Data Centre (2009a). *Met Office - Global Radiosonde Data (1997-present).* Retrieved May 2009, from http://badc.nerc.ac.uk/data/radiosglobe/.

British Atmospheric Data Centre (2009b). *Met Office Wind Profilers.* Retrieved May 2009, from http://badc.nerc.ac.uk/data/ukmo-wind-prof/.

British Atmospheric Data Centre (2009c). *MIDAS Land Surface Stations data (1853-current).* Retrieved January 2008, from http://badc.nerc.ac.uk/data/surface/.

British Wind Energy Association (2007). *Wind energy technology.* Retrieved July 2009, from http://www.bwea.com/ref/tech.html.

British Wind Energy Association (2009a). *The British Wind Energy Association.* Retrieved July 2009, from http://www.bwea.com/.

British Wind Energy Association (2009b). *Wind power statistics.* Retrieved July 2009, from http://www.bwea.com/statistics/.

Burch S.F., N. M., Ravenscroft, F. and Whittaker J. (1992). Computer Modelling of the UK Wind Resource; Final Overview Report. ETSU Report WN7055. Energy Technology Support Unit, Harwell, UK.

Burton, T., Sharpe, D., Jenkins, N., Bossanyi, E. (2001). *Wind Energy Handbook*. J. Wiley & Sons, Chichester.

Busuioc, A., Chen, D., Hellstrom, C. (2001). *Performance of statistical downscaling models in GCM validation and regional climate change estimates: Application for Swedish precipitation.* International Journal of Climatology **21**: 557-578.

BWEA – *see British Wind Energy Association*

Cook, E. R., D'Arrigo, R.D. (2002). *A Well-Verified, Multiproxy Reconstruction of the Winter North Atlantic Oscillation Index since a.d. 1400*. Journal of Climate **15**(13): 1754–1764.

Corbel G., Allen, J. T., Woolf D.K. and Gibb S (2007). *Wind trends in the Highlands and Islands of Scotland 1960 - 2004 and their relation to the North Atlantic Oscillation*. AMS 87th Annual Meeting, 19th Conference on Climate Variability and Change, Texas, USA.

Danish Wind Industry Association (2009). *The Global Market.* Retrieved November 2009, from http://www.windpower.org/en/knowledge/statistics/the_global_market.html.

DECC –*See Department for Energy and Climate Change*

Demuzere, M., Werner, M., van Lipzig, N.P.M., Roeckner, E. (2008). *An analysis of present and future ECHAM5 pressure fields using a classification of circulation patterns*. International Journal of Climatology (In press).

Department for Energy and Climate Change (2009a). *EU Emissions Trading System (EU ETS)* Retrieved January 2009, from http://www.decc.gov.uk/en/content/cms/what_we_do/change_energy/tackling_clima/emissions/eu_ets/eu_ets.aspx.

Department for Energy and Climate Change (2009b). *International energy policy.* Retrieved January 2009, from http://www.decc.gov.uk/en/content/cms/what_we_do/change_energy/int_energy/policy/policy.aspx.

Department for Energy and Climate Change (2009c). *Kyoto and the European Union.* Retrieved January 2009, from http://www.defra.gov.uk/environment/climatechange/internat/un-kyoto/.

Department for Energy and Climate Change (2009d). *The UK Renewable Energy Strategy 2009.* Retrieved July 2009, from http://www.decc.gov.uk/en/content/cms/what_we_do/uk_supply/energy_mix/ren

ewable/res/res.aspx.

Department of Business, Enterprise and Regulatory Reform (2001). *Wind energy fact sheet 11: Wind energy and the electricity network.* Retrieved June 2009, from http://www.berr.gov.uk/files/file17809.pdf.

Department of Business, Enterprise and Regulatory Reform (2008) *Energy Statistics: Electricity*. Retrieved November 2008,from http://www.berr.gov.uk/energy/statistics/source/electricity/page18527.html

Department of Business, Enterprise and Regulatory Reform (2009a). *UK Wind speed database.* Retrieved January 2009, from http://www.berr.gov.uk/energy/sources/renewables/explained/wind/windspeed-database/page27708.html.

Department of Business, Enterprise and Regulatory Reform. (2009b). *What is the renewables obligation?* Retrieved July 2009, from http://www.berr.gov.uk/energy/sources/renewables/policy/renewables-obligation/what-is-renewables-obligation/page15633.html.

Department of Trade and Industry (2007a). Meeting the Energy Challenge: A White Paper on Energy. Department of Trade and Industry.

Department of Trade and Industry (2007b). Reform of the renewables obligation. Department of Trade and Industry.

DTI – *See Department of Trade and Industry*

Dutton, J. A. (1976). *The ceaseless wind - an introduction to the theory of atmospheric motion*. McGraw-Hill.

EIA – *See Energy Information Administration*

EMEC (2009). *The European Marine Energy Centre Ltd.* Retrieved May 2009, from http://www.emec.org.uk/.

Enercon. (2009). *Enercon Storm Control.* Retrieved January 2009, from http://www.enercon.de/en/enerconsturmregelung.htm.

Energy Information Administratiom (2006). *International Energy Statistics: Total Primary Energy Consumption.* Retrieved December 2008, from http://tonto.eia.doe.gov/cfapps/ipdbproject/IEDIndex3.cfm?tid=44&pid=44&aid=2.

EU Commission. (2009). *EU ETS post 2012.* Retrieved January 2009, from http://ec.europa.eu/environment/climat/emission/ets_post2012_en.htm.

European Centre for Medium-Range Weather Forecasts (2006). ECMWF ERA-40 Re-Analysis data. British Atmospheric Data Centre. Retrieved March 2008, from http://badc.nerc.ac.uk/data/ecmwf-e40/

European Environment Agency (2007). Corine land cover 2000 (CLC2000) seamless vector database. (c)EEA, Copenhagen. Retrieved January 2008, from http://dataservice.eea.europa.eu/dataservice/metadetails.asp?id=950

Folland, C.K., Karl, T. R., Christy, J.R., Clarke, R.A., Gruza, G.V., Jouzel, J., Mann, M.E., Oerlemans, J., Salinger, M.J., Wang, S.-W. (2001). Observed Climate Variability and Change. *Climate Change 2001: The Scientific Basis. Contribution of Working Group I to the Third Assessment Report of the Intergovernmental Panel on Climate Change.* [J. T. Houghton, Y. Ding, D.J. Griggs, M. Noguer, P.J. van der Linden, X. Dai, K. Maskell, and C.A. Johnson (eds.)] Cambridge University Press, Cambridge, United Kingdom and New York, NY, USA.

Forster, P., V. Ramaswamy, P. Artaxo, T. Berntsen, R. Betts, D.W. Fahey, J. Haywood, J. Lean, D.C. Lowe, G. Myhre, J. Nganga, R. Prinn, G. Raga, M. Schulz and R. Van Dorland (2007). Changes in Atmospheric Constituents and in Radiative Forcing. *Climate Change 2007: The Physical Science Basis. Contribution of Working Group I to the Fourth Assessment Report of the Intergovernmental Panel on Climate Change*. [S. Solomon, D. Qin, M. Manning, Z. Chen, M. Marquis, K.B. Averyt, M. Tignor and H.L. Miller. (eds)] Cambridge University Press, Cambridge, United Kingdom and New York, NY, USA.

Frank, H. P., Rathmann, O., Mortensen, N.G., Landberg, L. (2001). *The NumericalWind Atlas - the KAMM/WAsP Method* (Risø–R–1252(EN). Risoe National Laboratory, Roskilde, Denmark.

G8 (2005). Gleneagles Plan of Action: *Climate change, clean energy and sustainable development*.

G8 Information Centre (2005). *What is the G8?* Retrieved November 2008, from http://www.g7.utoronto.ca/what_is_g8.html.

Gillet, N. P., Allen, M.R., McDonald, R.E., Senior, C.A., Shindell, D.T., Schmidt, G.A. (2002). *How linear is the Arctic Oscillation response to greenhouse gases?* Journal of Geophysical Research **107**(D3).

Gillet, N. P., Graf, H.F., Osborn, T.J. (2003). Climate Change and the North Atlantic Oscillation. *The North Atlantic Oscillation: Climate Significance and Environmental Impact*. J. W. Hurrell, Kushnir, Y. ,Ottersen, G.,Visbeck, M., Geophysical Monograph Series **134**.

Giorgi, F., Christensen, B. H., J., Hulme, M., Von Storch, H., Whetton, P., Jones, R., Mearns, L., Fu,C. (2001). Regional Climate Information – Evaluation and Projections. *Climate Change 2001: The Scientific Basis. Contribution of Working Group I to the Third Assessment Report of the Intergovernmental Panel on Climate Change*. [J. T. Houghton, Y. Ding, D.J. Griggs, M. Noguer, P.J. van der Linden, X. Dai, K. Maskell, and C.A. Johnson (eds)] Cambridge University Press, Cambridge, United Kingdom and New York, NY, USA.

Gonzalez, J. (2008). *Export level contours to wasp*. Retrieved January 2009, from http://arcscripts.esri.com/details.asp?dbid=13950

Google. (2009). *Google Earth.* Retrieved June 2009, from http://earth.google.co.uk/.

Gordon, A., Grace, W., Schwerdtfeger, P., Byron-Scott, R. (1998). *Dynamic meteorology: A basic course*. Arnold, London.

Guggenheim, D. (2006). *An Inconvenient Truth*.

Halliday J, A. M., Palutikof J, Watson S, Dunbabin P, Bunn J, Dukes M, Surguy I. (1995). *Assessment of the Accuracy of the DTI's Database of UK Wind Speeds*. ETSU W/11/00401/REP.

Harrison, G. P., Kiprakis, A.E., Wallace, A.R. (2002). *A new era for mini-hydro*. International Water Power and Dam Construction **54**(11): 20-24.

Harrison, G. P., Whittington, H.W., Wallace, A.R. (2003). *Climate change impacts on financial risk in hydropower projects*. IEEE Trans. Power Systems **18**(4): 1324-1330.

Harrison, G. P., Wallace, A.R. (2005). *Climate sensitivity of marine energy*. Renewable Energy **30**(12): 1801-1817

Harrison, G. P., Cradden, L.C., Chick,J. P. (2008). *Preliminary assessment of climate change impacts on the UK onshore wind energy resource*. Energy Sources **30**(14): 1286-1299.

Hasse, L. (1974). *Note on the surface-to-geostrophic wind relationship from observations in the German Bight*. Boundary-Layer Meteorology **6**: 197-201.

Hess, P., Brezowsky, H. (1977). Katalog der Grosswetterlagen Europas 1881–1976. Berichte des Deutschen Wetterdienstes 113. Offenbach am Main.

Horváth, L., Horváth, K. (2006). *Validation of the wind resource prediction for coupled ALADIN/WAsP modelling system in complex terrain*. European Wind Energy Conference 2006, Athens, Greece.

Horváth, L., Panza,T., Karadža, N. (2007). *The influence of high wind hysteresis effect on wind turbine power production at Bura-dominated site*. EWEC 2007, Milan.

Hulme, M., Jenkins, G.J., Lu, X., Turnpenny, J.R., Mitchell, T.D., Jones, R.G., Lowe, J., Murphy, J.M., Hassell, D., Boorman, P., McDonald, R., Hill, S. (2002). Climate Change Scenarios for the United Kingdom: The UKCIP02 Scientific Report. Norwich, Tyndall Centre for Climate Change Research, University of East Anglia**:** 120pp.

Hurrell, J. (1995). *NAO Index Data provided by the Climate Analysis Section, NCAR, Boulder, USA* .

Hurrell, J. W., Kushnir, Y., Visbeck, M. (2001). *The North Atlantic Oscillation*. Science **291**(5504): 603-605.

Hurrell, J. W., Kushnir, Y. ,Visbeck, M., Ottersen, G. (2003). An Overview of the North

Atlantic Oscillation. *The North Atlantic Oscillation: Climate Significance and Environmental Impact*. J. W. Hurrell, Kushnir, Y. ,Ottersen, G.,Visbeck, M., Geophysical Monograph Series **134**.

Huth, R., Pokorna, L. (2005). *Simultaneous analysis of climatic trends in multiple variables: An example of application of multivariate statistical methods*. International Journal of Climatology **25**: 469-484.

Idso, C., Singer, S.F. (2009). Climate Change Reconsidered: 2009 Report of the Nongovernmental Panel on Climate Change (NIPCC). Chicago, IL, The Heartland Institute.

International Energy Agency (2007). State of the art of Remote Wind Speed Sensing Techniques using Sodar, Lidar and Satellites. Risoe National Laboratory.

Intergovernmental Panel on Climate Change (2007a). Annex 1: Glossary. *Climate Change 2007: The Physical Science Basis. Contribution of Working Group I to the Fourth Assessment Report of the Intergovernmental Panel on Climate Change*. [S. Solomon, D. Qin, M. Manning, Z. Chen, M. Marquis, K.B. Averyt, M. Tignor and H.L. Miller. (eds)] Cambridge University Press, Cambridge, United Kingdom and New York, NY, USA.

Intergovernmental Panel on Climate Change (2007b). Summary for policymakers. *Climate Change 2007: The Physical Science Basis. Contribution of Working Group I to the Fourth Assessment Report of the Intergovernmental Panel on Climate Change*. [S. Solomon, D. Qin, M. Manning, Z. Chen, M. Marquis, K.B. Averyt, M. Tignor and H.L. Miller. (eds)] Cambridge University Press, Cambridge, United Kingdom and New York, NY, USA.

Intergovernmental Panel on Climate Change (2009). *Organization.* Retrieved February 2009, from http://www.ipcc.ch/organization/organization.htm.

IPCC – *See Intergovernmental Panel on Climate Change*

IPCC Data Distribution Centre (2005a) *IPCC DDC AR4 ECHAM5/MPI-OM 20C3M*.World Climate Research Program. Retrieved March 2008, from https://esg.llnl.gov:8443/home/publicHomePage.do

IPCC Data Distribution Centre (2005b) *IPCC DDC AR4 ECHAM5/MPI-OM SRESA2*.World Climate Research Program. Retrieved March 2008, from https://esg.llnl.gov:8443/home/publicHomePage.do

James, P. M. (2007). *An objective classification method for Hess and Brezowsky Grosswetterlagen over Europe*. Theoretical and Applied Climatology **88**: 17-42.

Jenkins, N., Allan, R., Crossley, P., Kirschen, D., Strbac, G. (2000). *Embedded Generation*. The Institution of Electrical Engineers. London,

Jenkinson, A. F., Collison, F.P. (1977). *An initial climatology of gales over the North Sea Synoptic Climatology, Branch Memorandum No 62*., Meteorological Office, Bracknell.

Jha, A. (2008). UK overtakes Denmark as world's biggest offshore wind generator. The Guardian. London.

Jones, P. D., Jonsson, T., Wheeler, D. (1997). *Extension to the North Atlantic oscillation using early instrumental pressure observations from Gibraltar and south-west Iceland*. International Journal of Climatology **17**(13): 1433 - 1450.

Justus, C. G., Hargraves, W.R., Mikhail, A., Graber, D. (1978). *Methods for estimating wind speed frequency distribution*. Journal of Applied Meteorology **17**: 350-353.

Kalnay, E., Kanamitsu, M., Kistler, R., Collins, W., Deaven, D., Gandin, L., Iredell, M., Saha, S., White, G., Woollen, J., Zhu, Y., Chelliah, M., Brisuzaki, W., Higgins, W., Janowiak, J., Mo, K.C., Ropelewski, C., Wang, J., Leetmaa, A.., Reynolds, R., Jenne, R., Joseph, D. (1996). *The NCEP/NCAR 40 reanalysis project*. Bulletin of the American Meteorological Society **77**: 437-471.

Kidson, J. W., Thompson, C.S. (1998). *A comparison of statistical and model-based downscaling techniques for local climate variations*. Journal of Climate **11**(4): 735–753.

Lamb, H. H. (1950). *Types and spells of weather around the year in the British Isles: Annual trends, seasonal structure of the year, singularities*. Quarterly Journal of the Royal Meteorological Society **76**(330): 393-429.

Lamb, H. H. (1972). *British Isles weather types and a register of the daily sequence of circulation patterns 1861-1971*. Geophysical Memoirs **16**.

Landberg, L., Watson, S.J. (1994). *Short-term prediction of local wind conditions* Boundary-Layer Meteorology **70**: 171-195.

Le Treut, H., R. Somerville, U. Cubasch, Y. Ding, C. Mauritzen, A. Mokssit, T. Peterson and M. Prather (2007). Historical Overview of Climate Change. *Climate Change 2007: The Physical Science Basis. Contribution of Working Group I to the Fourth Assessment Report of the Intergovernmental Panel on Climate Change*. [S. Solomon, D. Qin, M. Manning, Z. Chen, M. Marquis, K.B. Averyt, M. Tignor and H.L. Miller. (eds)] Cambridge University Press, Cambridge, United Kingdom and New York, NY, USA.

Leggett, J. (2005). *Half gone*. Portobello Books Ltd., London.

Li, X., Sailor, D.J. (2000). *Application of Tree-Structured Regression for Regional Precipitation Prediction Using General Circulation Model Output*. Climate Research **16**(1): 17-30.

Löschel, A., Moslener, U., Rübbelke, D.T.G (2009). *Indicators of energy security in industrialised countries*. Energy Policy (In Press, corrected proof).

Lynch, P. (2008). *The origins of computer weather prediction and climate modeling*. Journal of Computational Physics **227**: 3431-3444.

Mann, M. E., R. S. Bradley, and M. K. Hughes (1999). *Northern hemisphere temperatures during the past millennium: Inferences, uncertainties, and*

limitations. Geophysical Research Letters **26**(6): 759–762.

Manwell, J. F., McGowan, J. G., Rogers, A. L. (2002). *Wind Energy Explained: Theory, Design and Application*. J. Wiley & Sons. Chichester,

McGuffie, K., Henderson-Sellers, A. (1997). *A climate modelling primer*. John Wiley & Sons Ltd. Chichester, UK,

McQueen, D., Watson, S. (2006). *Validation of wind speed prediction methods at offshore sites*. Wind Energy **9**: 75-85.

MCT. (2009). *Marine Current Turbines.* Retrieved May 2009, from http://www.marineturbines.com/.

Mearns, L. O., Bogardi, I., Giorgi, F., Matyasovsky, I., Palecki, M. (1999). *Comparison of climate change scenarios generated from regional climate model experiments and statistical downscaling*. Journal of Geophysical Research **104**(D6): 6603-6621.

Mearns, L. O., Giorgi, F., Whetton, P., Pabon, D., Hulme, M., Lal, M (2003). Guidelines for the Use of Climate Scenarios Developed from Regional Climate Models. IPCC Supporting Material.

Meehl, G. A., T.F. Stocker, W.D. Collins, P. Friedlingstein, A.T. Gaye, J.M. Gregory, A. Kitoh, R. Knutti, J.M. Murphy, A. Noda, S.C.B. Raper, I.G. Watterson, A.J. Weaver and Z.-C. Zhao (2007). Global Climate Projections. *Climate Change 2007: The Physical Science Basis. Contribution of Working Group I to the Fourth Assessment Report of the Intergovernmental Panel on Climate Change*. [S. Solomon, D. Qin, M. Manning, Z. Chen, M. Marquis, K.B. Averyt, M. Tignor and H.L. Miller. (eds)] Cambridge University Press, Cambridge, United Kingdom and New York, NY, USA.

Microsoft (2009). *Bing (Beta).* Retrieved June 2009, from http://www.bing.com/

Mortensen, N. G., Heathfield, D.N., Myllerup, L., Landberg, L., Rathmann, O. (2009). Wind Atlas Analysis and Application Program (version 9.1). Risø National Laboratory, Roskilde, Denmark

Murphy, J. (1999). *An evaluation of statistical and dynamical techniques for downscaling local climate*. Journal of Climate **12**(8): 2256-2284.

Murphy, J. (2000). *Predictions of climate change over Europe using statistical and dynamical downscaling techniques*. International Journal of Climatology **20**: 489-501.

Natural Resources Canada (2005). *Clean Energy Project Analysis Third Edition: RETScreen® Engineering & Cases Textbook.* Natural Resources Canada.

Natural Resources Canada (2009). RETscreen (version 4). Natural Resources Canada. RETSCREEN is a registered trademark of Natural Resources Canada, © 1997-2009.

Nebojsa Nakicenovic, J. A., Gerald Davis, Bert de Vries, Joergen Fenhann, Stuart Gaffin, Kenneth Gregory, Arnulf Grübler, Tae Yong Jung, Tom Kram, Emilio Lebre La Rovere, Laurie Michaelis, Shunsuke Mori, Tsuneyuki Morita, William Pepper, Hugh Pitcher, Lynn Price, Keywan Riahi, Alexander Roehrl, Hans-Holger Rogner, Alexei Sankovski, Michael Schlesinger, Priyadarshi Shukla, Steven Smith, Robert Swart, Sascha van Rooijen, Nadejda Victor, Zhou Dadi (2000). *Emissions Scenarios*. Cambridge University Press. Cambridge, UK.

Nielsen, M. (2009). Default roughness over water. Personal Correspondence from WA^{S}P support team.

NIPCC – *See Non-governmental International Panel on Climate Change*

Non-governmental International Panel on Climate Change (2009). *About the NIPCC*. Retrieved July 2009, from http://www.nipccreport.org/.

Ordnance Survey (2009) Ordnance Survey Maps of Great Britain. Edina Digimap. Retrieved April 2009, from http://edina.ac.uk/digimap/

Osborn, T. (2000). *North Atlantic Oscillation.* CRU Information Sheets Retrieved July 2007, from http://www.cru.uea.ac.uk/cru/info/nao/.

Osborn, T. J., Briffa, K.R., Tett, S. F. B., Jones, P.D., Trigo, R.M. (1999). *Evaluation of the North Atlantic Oscillation as simulated by a coupled climate model*. Climate Dynamics **15**: 685-702.

Pan, Z., Christensen, J.H., Arritt, R.W., Gutowski Jr, W.J., Takle, E.S., Otieno, F. (2001). *Evaluation of uncertainties in regional climate change simulations*. Journal of Geophysical Research **106**(D16): 17735-17751.

Pearce, F. (2002). *Top climate scientist ousted.* New Scientist Retrieved November 2008, from http://www.newscientist.com/article/dn2191-top-climate-scientist-ousted.html.

Pearce, F. (2006). *Climate change special: State of denial*. New Scientist **2576**: 18-21.

Pelamis. (2007). *UK's first wave farm announced.* Retrieved July 2009, from http://www.pelamiswave.com/news_archive.php?offset=18.

Pelamis. (2009). *The Pelamis wave energy converter.* Retrieved May 2009, from http://www.pelamiswave.com/content.php?id=161.

Perry, M., Hollis, D. (2005). *The generation of monthly gridded datasets for a range of climatic variables over the United Kingdom*. International Journal of Climatology **25**: 1,041-1,054.

Petersen, E. L., Mortensen, N. G., Landberg, L., Hojstrup, J., Frank, H. P. (1998a). *Wind Power Meteorology. Part I: Climate and Turbulence*. Wind Energy **1**: 2-22.

Petersen, E. L., Mortensen, N. G., Landberg, L., Hojstrup, J., Frank, H. P. (1998b). *Wind Power Meteorology. Part II: Siting and Models.* . Wind Energy **1**: 55-72.

Phillips, T. (2009). *Deep solar minimum.* Science@Nasa Retrieved July 2009, from

http://science.nasa.gov/headlines/y2009/01apr_deepsolarminimum.htm.

Pinto, J. G., Zacharias, S., Fink, A.H., Leckebusch, G.C., Ulbrich, U. (2009). *Factors contributing to the development of extreme North Atlantic cyclones and their relationship with the NAO* Climate Dynamics **32**(5): 711-737.

Post, W. M., Peng, T.H., Emanuel, W.R., King, A.W., Dale, V.H., DeAngelis, D.L. (1990). *The global carbon cycle*. American Scientist **78**: 310-326.

Pryor, S. C., Barthelmie, R.J. (2003). *Long-term trends in near-surface flow over the Baltic*. International Journal of Climatology **23**: 271-289.

Pryor, S. C., Barthelmie, R.J., Schoof, J.T. (2004). *How coherent is inter-annual variability of wind indices across Europe and what are the implications for large scale penetration by wind energy of electricity markets?* European Wind Energy Conference, London, UK.

Pryor, S. C., Schoof, J.T., Barthelmie, R.J. (2005a). *Climate change impacts on wind speeds and wind energy density in northern Europe: Empirical downscaling of multiple AOGCMs*. Climate Research **29**: 183-198.

Pryor, S. C., Schoof, J.T., Barthelmie, R.J. (2005b). *Empirical downscaling of wind speed probability distribution*. Journal of Geophysical Research **110**.

Pryor, S. C., Barthelmie, R.J., Schoof, J.T. (2005c). *The impact of non-stationarities in the climate system on the definition of 'a normal wind year': A case study from the Baltic*. International Journal of Climatology **25**: 735-752.

Pryor, S. C., Barthelmie, R.J., Kjellstrom, E. (2005d). *Potential climate change impact on wind energy resources in northern Europe: analyses using a regional climate model*. Climate Dynamics **25**: 815-835.

Raisanen, J., Hansson, U., Ullerstig, A., Doscher, R., Graham, L.P., Jones, C., Meier, H.E.M., Samuelsson, P., Willen, U. (2004). *European climate in the late twenty-first century: Regional simulations with two driving global models and two forcing scenarios*. Climate Dynamics **22**: 13-31.

Roeckner, E., Bäuml, G., Bonaventura, L., Brokopf, R., Esch, M., Giorgetta, M., Hagemann, S., Kirchner, I., Kornblueh,L., Manzini, E., Rhodin, A., Schlese,U., Schulzweida, U., Tompkins, A. (2003). The atmospheric general circulation model ECHAM5: Part 1: Model Description. Hamburg, Germany, Max Planck Institute for Meteorology.

Sailor, D. J., Hu, T., Li,X., Rosen, J.N. (2000). *A Neural Network Approach to Local Downscaling of GCM Wind Statistics for Assessment of Wind Power Implications of Climate Variability and Climatic Change*. Renewable Energy **19**: 359-378.

Sailor, D.J., Smith, M., Hart, M. (2008). *Climate change implications for wind power resources in the Northwest United States*. Renewable Energy **33**: 2393-2406.

Salmon, M. (2004). *North Atlantic Oscillation.* Retrieved July 2007, from

http://www.cru.uea.ac.uk/cru/data/nao.htm.

Scottish and Southern Electricity. (2009). *Beauly-Denny Public Enquiry.* Retrieved July 2009, from http://www.beaulydenny.co.uk/.

Segal, M., Pan, Z., Arritt, R.W., Takle, E.S. (2001). *On the potential change in wind power over the US due to increases of atmospheric greenhouse gases*. Renewable Energy **24**: 235-243.

Siegismund, F., Schrum, C. (2001). *Decadal changes in the wind forcing over the North Sea*. Climate Research **18**: 39-45.

Sinden, G. (2007). *Characteristics of the UK wind resource: Long-term patterns and relationship to electricity demand* Energy Policy **35**(1): 112-127.

Skjærseth, J. B., Wettestad, J. (2008). *Implementing EU emissions trading: success or failure?* . International Environmental Agreements: Politics, Law and Economics **8**: 275-290.

Solman, S. A., Nunez, M. N. (1999). *Local estimates of global climate change: A statistical downscaling approach*. International Journal of Climatology **19**: 835-861.

Steffen, W. (2008). *Working Group 1 report of the IPCC Fourth Assessment—An editorial* Global Environmental Change **18**(1): 1-3.

Stern, N. (2006). The economics of climate change - Executive Summary. HM Treasury.

Strbac, G., Shakoor, A., Black, M., Pudjianto, D., Bopp, T. (2007). *Impact of wind generation on the operation and development of the UK electricity sytems*. Electric Power Systems Research **77**: 1214-1227.

Stull, R. B. (1993). *An introduction to boundary layer meteorology*. Kluwer Academic Publishers, Dordrecht, The Netherlands.

Taylor, K. E. (2001). *Summarizing multiple aspects of model performance in a single diagram*. Journal of Geophysical Research **106**: 7183-7192.

Taylor, K. E. (2005). Taylor diagram primer, PCMDI.

Tennekes, H., Lumley, J.L. (1972). *A first course in turbulence*. The Massachusetts Institute of Technology. Cambridge, USA,

Trigo, R., Palutifok, J.P. (2001). *Precipitation scenarios over Iberia: A comparison between direct GCM output and different downscaling techniques*. Journal of Climate **14**: 4422-4446.

Troen, I., Petersen, E.L. (1989). *European Wind Atlas*. Riso National Laboratory. Roskilde,

U. Dusek, G. P. F., L. Hildebrandt, J. Curtius, J. Schneider, S. Walter, D. Chand, and F. Drewnick, S. H., D. Jung, S. Borrmann, M. O. Andreae (2006). *Size matters more than chemistry for cloud-nucleating ability of aerosol particles*. Science **312**: 1375-1378.

UK Meteorological Office (2008). *Fact sheet No. 13 – Upper air observations and the tephigram.* Retrieved November 2008, from http://www.metoffice.gov.uk/corporate/library/factsheets/factsheet13.pdf.

UK Meteorological Office (2006). MIDAS Land Surface Stations data (1853-current). British Atmospheric Data Centre. Retrieved April 2009, from http://badc.nerc.ac.uk/data/ukmo-midas

Ulbrich, U., Christoph, M. (1999). *A shift of the NAO and increasing storm track activity over Europe due to anthropogenic greenhouse gas forcing* Climate Dynamics **15**(7): 551-559.

UNFCCC – *See United Nations Framework Convention on Climate Change*

United Nations Framework Convention on Climate Change (2009a). *Clean Development Mechanism.* Retrieved January 2009, from http://unfccc.int/kyoto_protocol/mechanisms/clean_development_mechanism/items/2718.php.

United Nations Framework Convention on Climate Change (2009b). *Definition of climate change.* Retrieved July 2009, from http://unfccc.int/files/documentation/text/html/list_search.php?what=keywords&val=&valan=g&anf=0&id=10.

United Nations Framework Convention on Climate Change (2009c). *Kyoto Protocol.* Retrieved January 2009, from http://unfccc.int/kyoto_protocol/items/2830.php.

Uppala, S. M., Kållberg, P.W., Simmons, A.J., Andrae, U., da Costa Bechtold, V., Fiorino, M., Gibson, J.K., Haseler, J., Hernandez, A., Kelly, G.A., Li, X., Onogi, K., Saarinen, S., Sokka, N., Allan, R.P., Andersson, E., Arpe, K., Balmaseda, M.A., Beljaars, A.C.M., van de Berg, L., Bidlot, J., Bormann, N., Caires, S., Chevallier, F., Dethof, A., Dragosavac, M., Fisher, M., Fuentes, M., Hagemann, S., Hólm, E., Hoskins, B.J., Isaksen, L., Janssen, P.A.E.M., Jenne, R., McNally, A.P., Mahfouf, J.-F., Morcrette, J.-J., Rayner, N.A., Saunders, R.W., Simon, P., Sterl, A., Trenberth, K.E., Untch, A., Vasiljevic, D., Viterbo, P., and Woollen, J. (2005). *The ERA-40 re-analysis*. Quarterly Journal of the Royal Meteorological Society **131**: 2961-3012.

Vestas. (2004). *V90-3.0 MW Product Brochure.* Retrieved June 2007, from http://www.vestas.com/en/wind-power-solutions/wind-turbines/3.0-mw.aspx.

Voith Hydro Wavegen Limited (2009). *Limpet.* Retrieved May 2009, from http://www.wavegen.co.uk/what_we_offer_limpet.htm.

Wallace, A. R., Kiprakis, A.E. (2002). *Reduction of voltage violations from embedded generators connected to the distribution network by intelligent reactive power control*. Fifth International Conference on Power System Management and Control, Institution of Electrical Engineers, London.

Watson, G. M., Halliday, J.A., Brownsword, R.A., Palutikof, J.P., Holt, T., Barthelmie, R.J., Coelingh, J.P., van Zuylen, E.J., Cleijne, J.W. (2001). Predicting offshore

wind energy resources (POWER). Rutherford Appleton Laboratory.

Wilby, R. L., Wigley, T. M. L., Conway, D., Jones, P. D., Hewitson, B. C., Main, J., Wilks, D. S. (1998). *Statistical downscaling of general circulation model output: A comparison of methods.* Water Resources Research **34**(11): 2995-3008.

Wilby, R. L., Wigley, T.M.L. (2000). *Precipitation predictors for downscaling: Observed and general circulation model relationships.* International Journal of Climatology **20**: 641-661.

Wilby, R. L., Charles, S.P., Zorita, E., Timbal, B., Whetton, P., Mearns, L.O. (2004). Guidelines for the use of climate scenarios developed from statistical downscaling methods. IPCC Supporting Material.

Woolf, D. K., Challenor, P.G., Cotton, P.D (2002). *Variability and predictability of the North Atlantic wave climate*. Journal of Geophysical Research **107**: 3145.

Zorita, E., von Storch, H. (1998). *The analog method as a simple statistical downscaling technique: Comparison with more complicated methods*. Journal of Climate **12**: 2474-2489.

Appendix A

A.1 Wind Turbine Power Extraction – Actuator disc model

The following derivation of the key equations is adapted from Burton *et al* (2001).

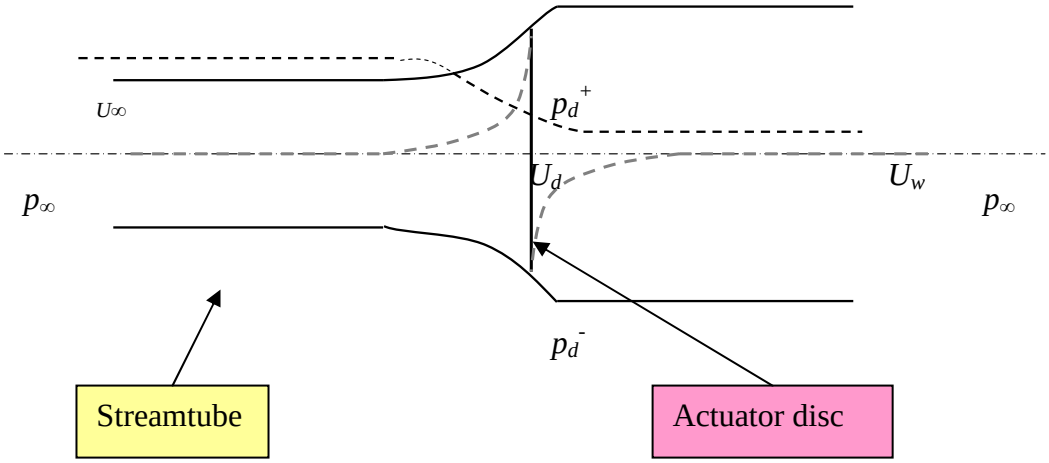

Fig. A-1 Actuator disc model

(Burton *et al*, 2001)

Mass flowrate within an air flow is a function of the air density (ρ), the cross-sectional area of the streamtube (A_x) and the flow velocity (U) such that,

$$\dot{m} = \rho A_x U \tag{A.1}$$

The concept of continuity states that mass flowrate is constant throughout the streamtube, and thus,

$$\rho A_\infty U_\infty = \rho A_d U_d = \rho A_w U_w \tag{A.2}$$

The velocity change induced by the actuator disc is superimposed on the free-stream velocity as a proportion of the incoming velocity (U_∞), using the term, a, the axial flow induction factor: the extra velocity change is equal to $-a\,U_\infty$. This gives the velocity at the disc,

$$U_d = U_\infty - U_\infty a = U_\infty (1-a) \tag{A.3}$$

There is no net force acting on the system as it is surrounded by air at constant atmospheric pressure, therefore the force causing a rate of change in momentum of the air is entirely due to the pressure drop over the disc, so the momentum equation

$$F_P = \dot{m}(U_\infty - U_w) \tag{A.4}$$

can be written as:

$$(p_d^+ - p_d^-)A_d = (U_\infty - U_w)\rho A_d U_\infty (1-a) \tag{A.5}$$

Bernoulli's equation states that, under a steady state, for any two points within a fluid where there is no work done on or by that fluid, the energy in the flow is constant. Hence, the sum of the kinetic energy, the static pressure and gravitational potential energy is constant,

$$\frac{1}{2}\rho U^2 + p + \rho g h = const \tag{A.6}$$

Applying Bernoulli's equation to the upstream-disc section and again to the disc-downstream sections of the streamtube gives,

$$\frac{1}{2}\rho_\infty U_\infty{}^2 + p_\infty + \rho_\infty g h_\infty = \frac{1}{2}\rho_d U_d{}^2 + p_d^+ + \rho_d g h_d \tag{A.7}$$

and

$$\frac{1}{2}\rho_d U_d{}^2 + p_d^- + \rho_d g h_d = \frac{1}{2}\rho_w U_w{}^2 + p_\infty + \rho_w g h_w \tag{A.8}$$

We can assume constant density and no change in the height of the system, so that $\rho_\infty = \rho_d = \rho_w$, and $h_\infty = h_d = h_w$,

$$\frac{1}{2}\rho U_\infty{}^2 + p_\infty = \frac{1}{2}\rho U_d{}^2 + p_d^+ \tag{A.9}$$

$$\frac{1}{2}\rho U_w{}^2 + p_\infty = \frac{1}{2}\rho U_d{}^2 + p_d^- \tag{A.10}$$

Subtracting 3.9 and 3.10 gives,

$$p_d^+ - p_d^- = \frac{1}{2}\rho(U_\infty^2 - U_w^2) \tag{A.11}$$

Substituting back in for the pressure drop in equation 3.5,

$$\left(\frac{1}{2}\rho(U_\infty^2 - U_w^2)\right)A_d = (U_\infty - U_w)\rho A_d U_\infty (1-a) \tag{A.12}$$

Therefore,

$$U_w = (1-2a)U_\infty \tag{A.13}$$

Rearranging 3.5 to show the force on the air caused by the actuator disc in terms of U_w, gives:

$$(p_d^+ - p_d^-)A_d = 2\rho A_d U_\infty^2 a(1-a) \quad \text{(A.14)}$$

Power is the rate of work done by the force, i.e. the force times the velocity at the disc,

$$P = F_d U_d = 2\rho A_d U_\infty^3 a(1-a) \quad \text{(A.15)}$$

In a situation with no actuator disc (i.e. wind turbine) the power available in the air can be found by considering the kinetic energy, where

$$KE = \frac{1}{2} m U^2 \quad \text{(A.15)}$$

Power can be expressed as kinetic energy per unit time, such that

$$P = \frac{1}{2}\dot{m}U^2 = \frac{1}{2}\rho A U^3 \quad \text{(A.16)}$$

where $\dot{m}$ is the mass flow rate as given in 3.1. We define a power coefficient, C_p, as the ratio of power extracted by the disc to the power available in the air,

$$C_p = \frac{2\rho A_d U_\infty^3 a(1-a)}{\frac{1}{2}\rho U_\infty^3 A_d} = 4a(1-a)^2 \quad \text{(A.17)}$$

The maximum C_p occurs when $\frac{dC_p}{da} = 0 = 4(1-a)(1-3a)$ which gives $a = \frac{1}{3}$, thus

$$C_{p,\max} = \frac{16}{27} = 0.593 \quad \text{(A.18)}$$

This is known as the Betz limit, and infers that a maximum of 59% of the energy in the air can be extracted by a wind turbine.

A.2 Atmospheric stability

The temperature of air in the boundary layer changes with increasing height from the earth's surface, with the rate of change often described as the 'lapse rate'. For an individual air parcel within the boundary later, its vertical motion depends on its particular temperature. A parcel warmer than the surrounding air will have a lower density and will move upwards, whilst a parcel cooler than its surroundings and consequently a higher density will move downwards. When the parcel has the same temperature as the surrounding air, no vertical motion is observed. The thermal effects on wind speeds in the boundary layer are described by defining the stratification of the atmosphere as stable, unstable or neutral as given in Burton *et al*, 2001:

Unstable

A large degree of surface heating, for example during daytime, results in a more rapid temperature decrease with height. High temperatures near the ground can cause an air parcel to increase in temperature, and hence it will rise. It undergoes adiabatic cooling as it rises, i.e. the pressure decreases and the volume increases but there is no heat energy added or subtracted from the system. If the parcel does not reach equilibrium temperature with the surrounding air, it will continue to rise. These updrafts lead to large-scale turbulent eddies and there is a relatively small change in the mean wind speed with height.

Stable

When the rising air undergoing adiabatic cooling drops to a lower temperature than the surrounding air, its upward motion will be curtailed and it will fall again. This will tend to occur when the temperature profile with height is more vertical, i.e. a less rapid decrease with height. The change in mean wind speed with height is often large in these cases, where the turbulent motion is dominated by surface friction effects.

Neutral

In a neutral situation, as the air cools adiabatically as it rises, it attains similar temperatures to the surrounding air and an equilibrium is reached. The dominant effects on the wind are the surface friction and the Coriolis force.

Wind shear profile

In the neutral case, the wind shear profile is given by the logarithmic relation as in 3.11. In unstable or stable atmospheres, the logarithmic profile must be adjusted by a factor to account for stability effects such that,

$$U(z) = \frac{u^*}{\kappa}\left[\ln\left(\frac{z}{z_0}\right) - \psi\left(\frac{z}{L}\right)\right] \qquad \text{(A.19)}$$

where ψ is an empirical function and L is the Monin-Obukhov length, related to surface temperature and heat flux (Troen & Petersen, 1989). Petersen *et al* (1998a) shows how the wind speed profile with height changes with atmospheric stability (Fig. A-1); stable conditions give a more constant slope than the unstable conditions, which show a much greater change in the first few metres followed by a much slower change from 10m to 60m. The neutral profile fits in between the two conditions.

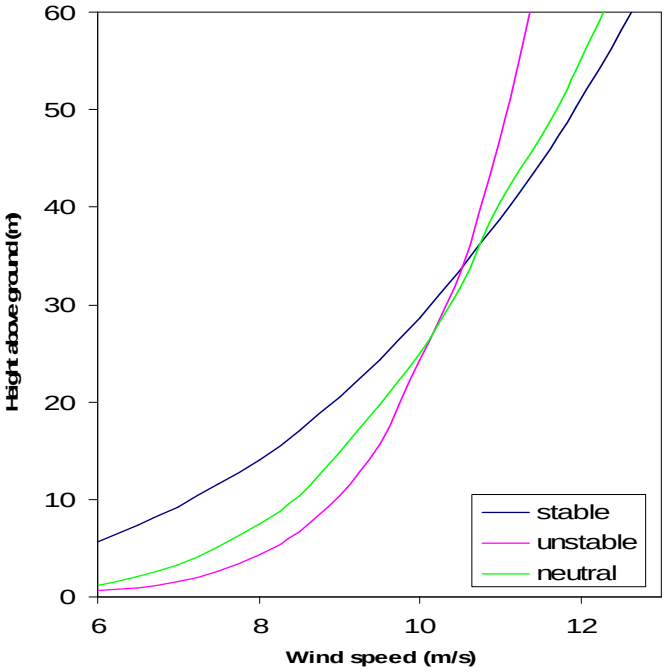

Fig. A-2 Wind speed profiles at varying height

(Petersen *et al*, 1998a)

A.3 Weibull distribution parameters

The Weibull distribution parameters – *A*, the scale parameter and *k*, the shape parameter – combine to produce differently shaped probability density functions. For a distribution with a constant *k* parameter of 2, Fig. B-2 shows the result of varying *A* between 3 m/s and 10 m/s. The larger the *A* value, the higher the modal value of wind speed in the distribution. *A* is very closely related to the mean wind speeds, so a site with a high mean wind speed will have a high value of *A*.

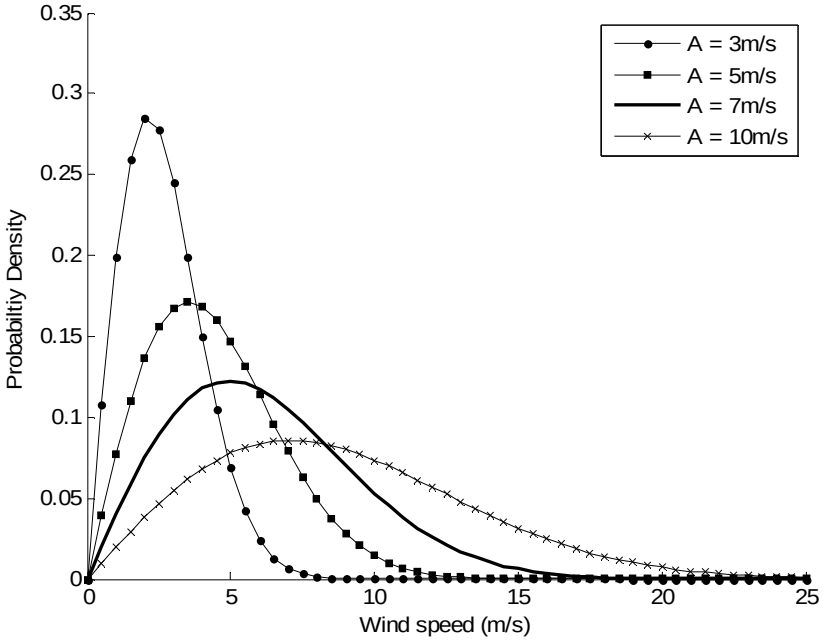

Fig. A-3 Weibull distribution with constant *k* = 2

(Adapted from Manwell *et al*, 2002)

A similar exercise, but this time keeping the *A* parameter constant at 5m/s and varying the value of *k* between 1.25 and 3, is shown in Fig. B-3. Lower *k* values tend to result in distributions that are 'skewed' to the lower wind speed region of the graph but which have 'tails' that extend further giving low frequencies of extreme wind speeds. Higher *k* values give distributions that appear more like a typical normal distribution with less skewing and shorter tails.

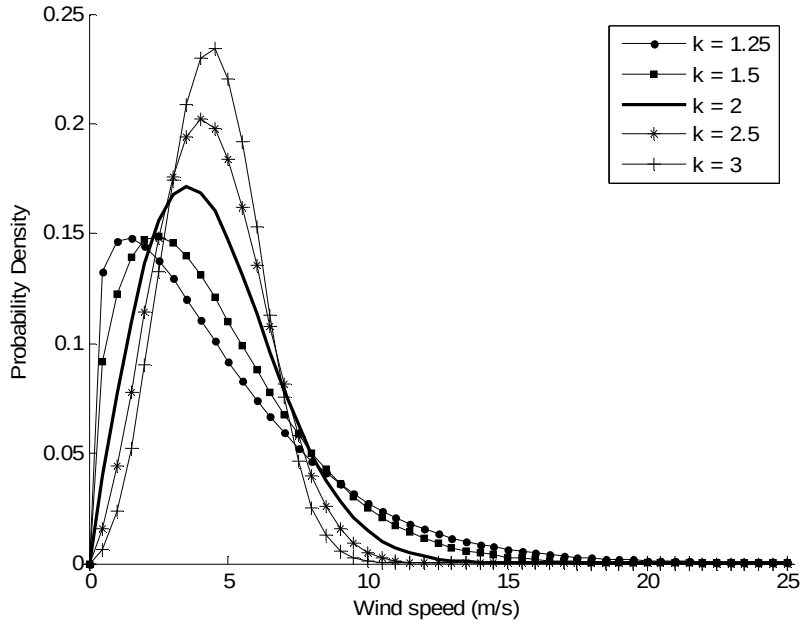

Fig. A-4 Weibull distribution with constant *A* = 5m/s

(Adapted from Manwell *et al*, 2002)

Various combinations of *A* and *k* are presented in Fig. B-4. It is clear that there is a wide range of possible Weibull distribution shapes that result from the typical wind climates found in the UK.

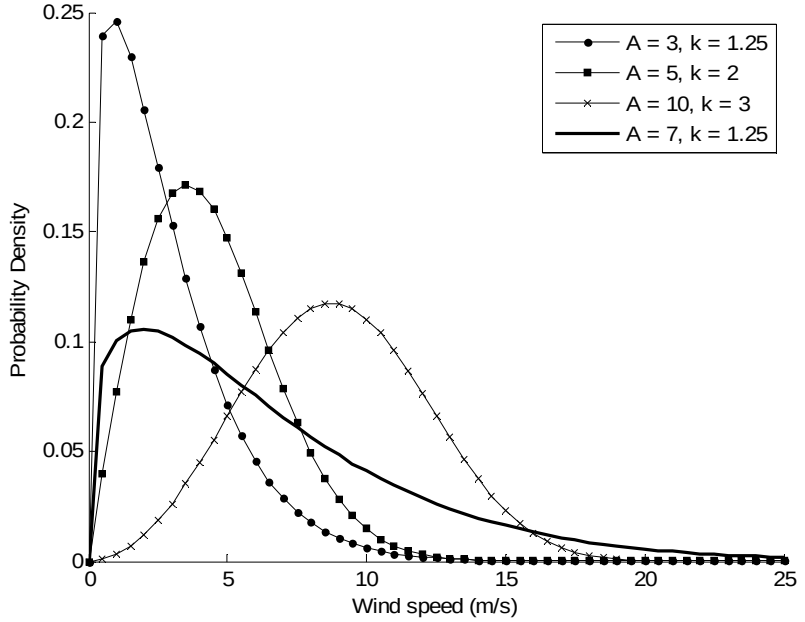

Fig. A-5 Weibull distribution with varying *A* and *k* parameters

(Adapted from Manwell *et al*, 2002)

Appendix B

B.1 Taylor diagrams

The Taylor Diagram was devised by Karl Taylor (Taylor, 2001) as a means of graphically comparing climate datasets. It can be used with model output and/or observations and allows quick analysis of how well two datasets correspond with each other. In Taylor (2005) the author describes how, given two variables, f_n and r_n, defined at N points in time or space, i.e. either in time series or a spatial field, three statistical measures of correspondence can be calculated – correlation coefficient, root mean square difference and standard deviation – and the results displayed in a Taylor Diagram.

Correlation coefficient, R:

$$R = \frac{\frac{1}{N}\sum_{n=1}^{N}(f_n - \overline{f})(r_n - \overline{r})}{\sigma_f \sigma_r} \tag{B.1}$$

where $\overline{f}$, $\overline{r}$ and σ_f , σ_r are the means and standard deviations of f_n and r_n respectively.

Centred pattern root mean square (RMS) difference, E':

$$E' = \left[\frac{1}{N}\sum_{n=1}^{N}\left[\left(f_n - \overline{f}\right) - \left(r_n - \overline{r}\right)\right]^2\right]^{\frac{1}{2}} \tag{B.2}$$

The three statistics are related such that,

$$E'^2 = \sigma_f^2 + \sigma_r^2 - 2\sigma_f \sigma_r R \tag{B.3}$$

which follows the cosine rule where,

$$c^2 = a^2 + b^2 - 2ab\cos\theta \tag{B.4}$$

This allows the three statistics to be represented geometrically as in Fig. B-1. When comparing the ECHAM5 GCM ('test field') and the ERA40 data ('reference field'),

the standard deviations are normalised by the standard deviation of each month of ERA40 data, so that the ERA40 data points are always at the red circle point on the x axis having a normalised value of one. The centralised pattern RMS errors are also normalised.

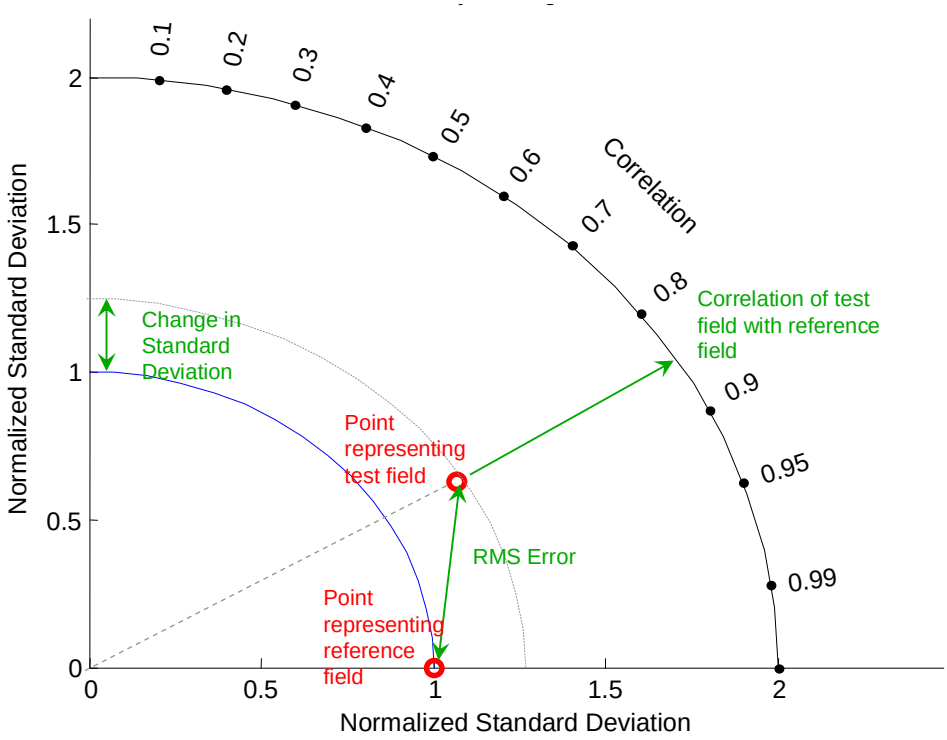

Fig. B-1 Example Taylor Diagram

A Matlab function was written to create bespoke Taylor Diagrams for this application.

Appendix C – Surface Winds

C.1 Comparison of ECHAM5 with ERA40 1961-90

Fig. C-1: Run 1, percentage differences in monthly mean wind speed

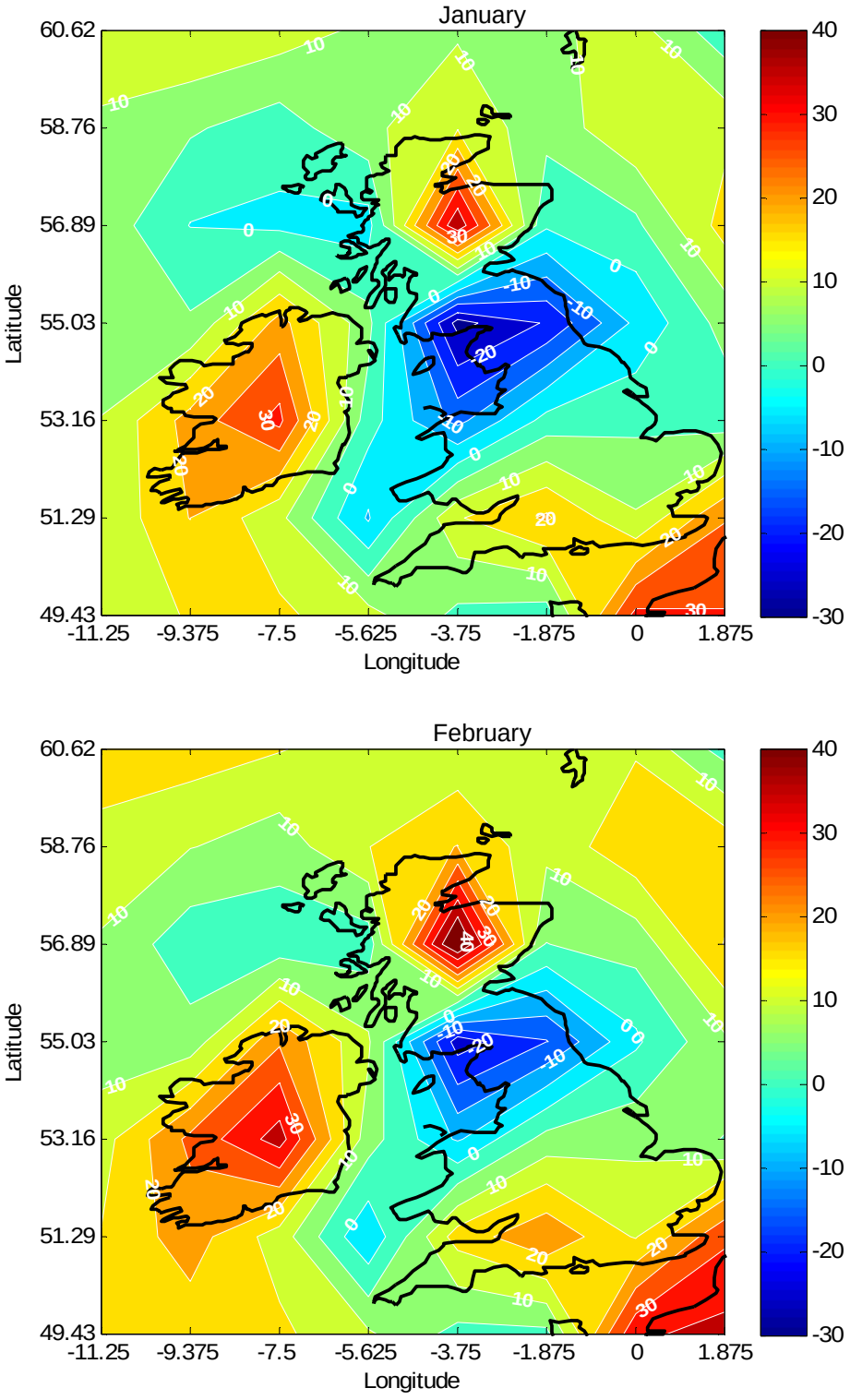

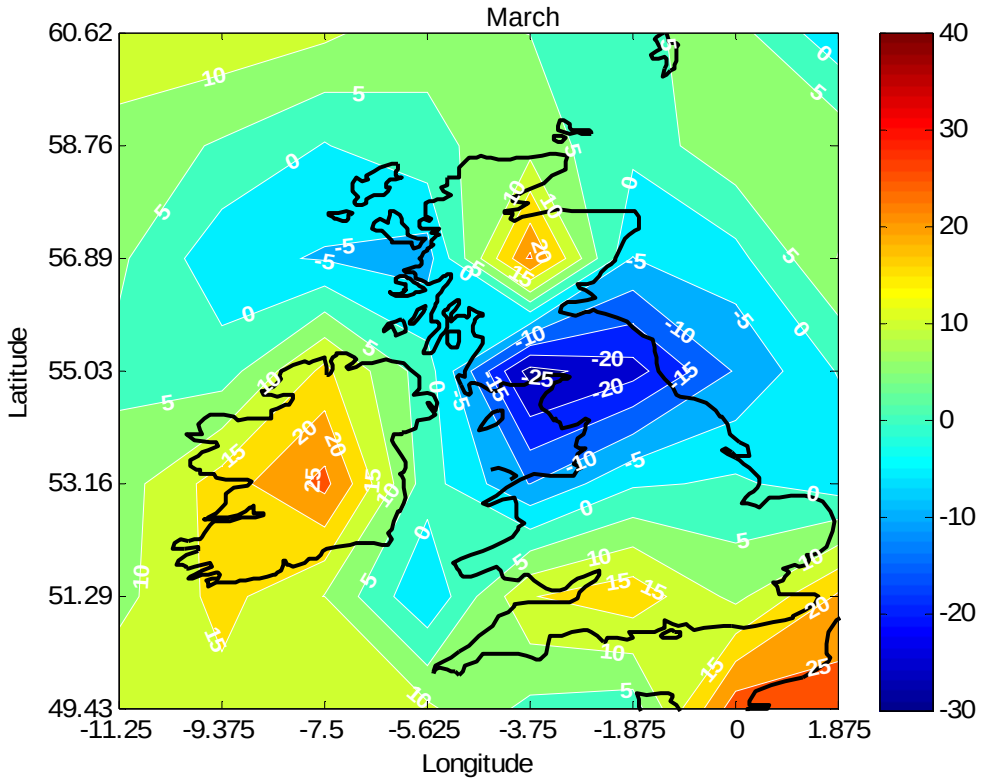
March
60.62
58.76
56.89
55.03
53.16
51.29
49.43
Latitude
-11.25
-9.375
-7.5
-5.625
-3.75
-1.875
0
1.875
Longitude
40
30
20
10
0
-10
-20
-30

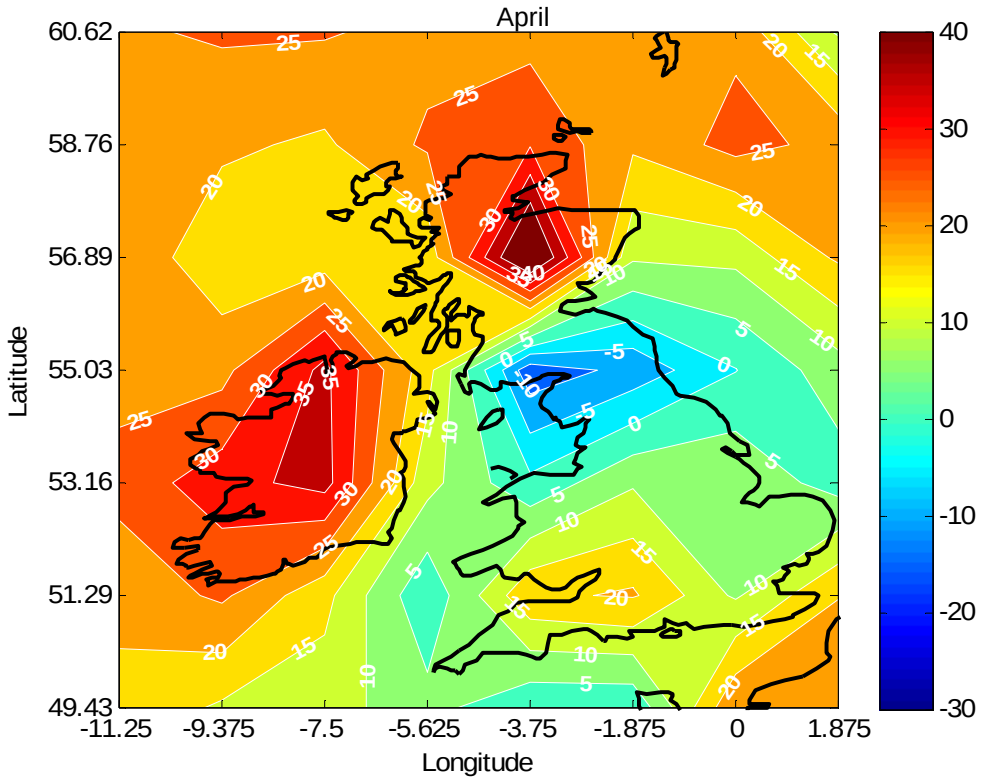
April
60.62
58.76
56.89
55.03
53.16
51.29
49.43
Latitude
-11.25
-9.375
-7.5
-5.625
-3.75
-1.875
0
1.875
Longitude
40
30
20
10
0
-10
-20
-30

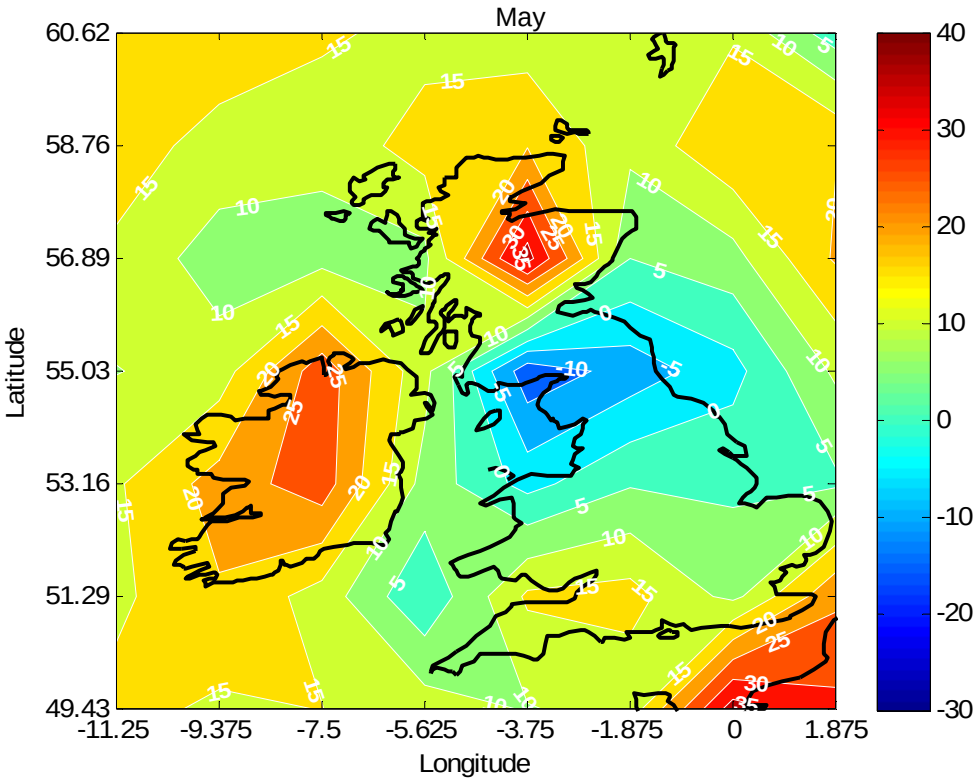
May
60.62
58.76
56.89
55.03
53.16
51.29
49.43
Latitude
-11.25
-9.375
-7.5
-5.625
-3.75
-1.875
0
1.875
Longitude
40
30
20
10
0
-10
-20
-30

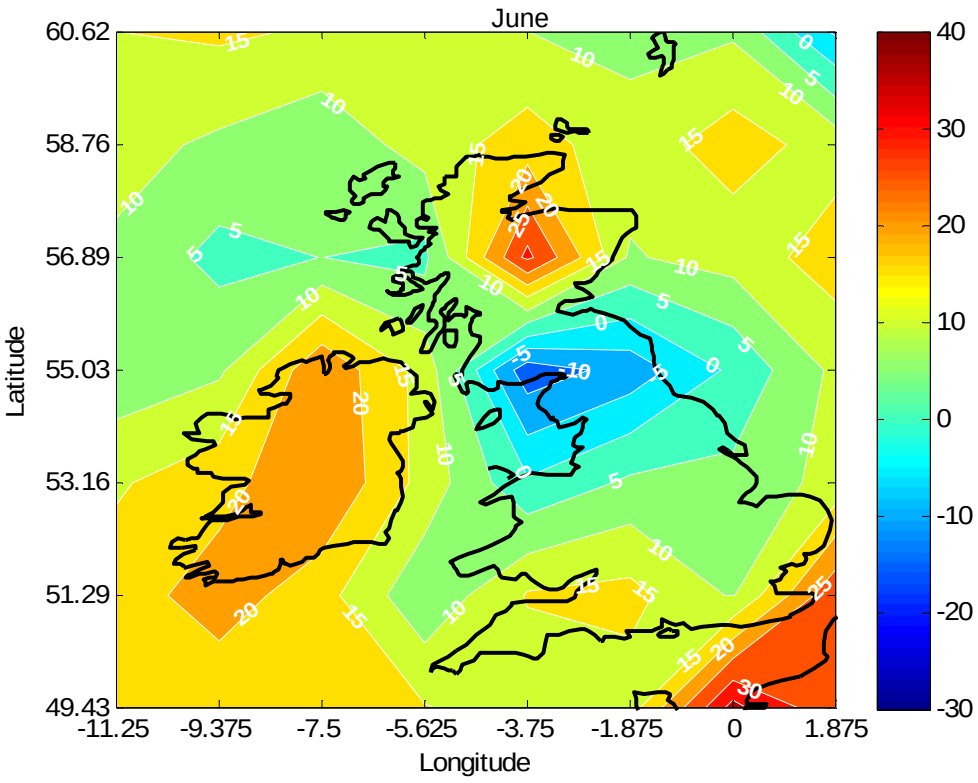
June
60.62
58.76
56.89
55.03
53.16
51.29
49.43
Latitude
-11.25
-9.375
-7.5
-5.625
-3.75
-1.875
0
1.875
Longitude
40
30
20
10
0
-10
-20
-30

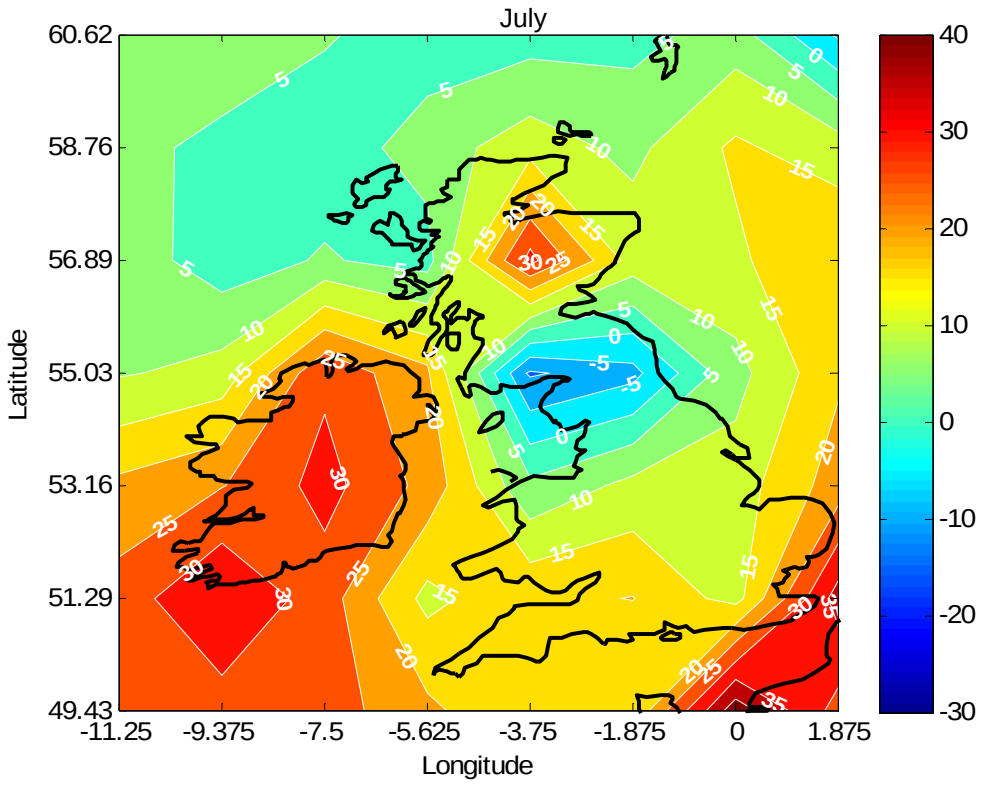
July
60.62
58.76
56.89
55.03
53.16
51.29
49.43
Latitude
-11.25
-9.375
-7.5
-5.625
-3.75
-1.875
0
1.875
Longitude
40
30
20
10
0
-10
-20
-30

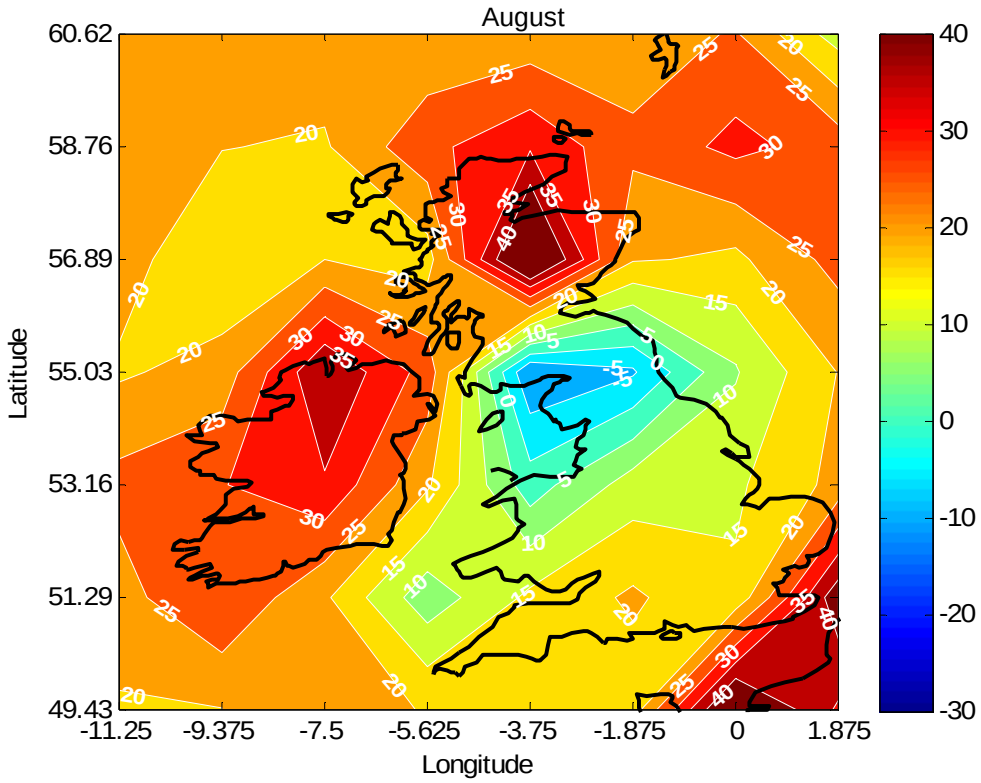
August
60.62
58.76
56.89
55.03
53.16
51.29
49.43
Latitude
-11.25
-9.375
-7.5
-5.625
-3.75
-1.875
0
1.875
Longitude
40
30
20
10
0
-10
-20
-30

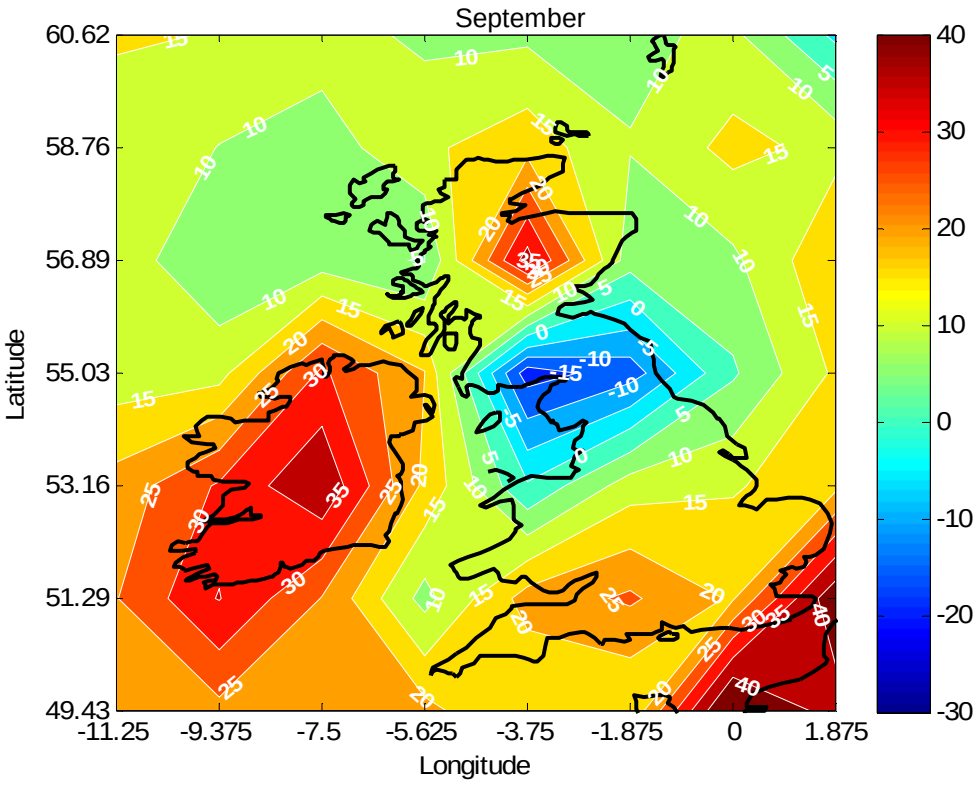
September
60.62
58.76
56.89
55.03
53.16
51.29
49.43
Latitude
-11.25
-9.375
-7.5
-5.625
-3.75
-1.875
0
1.875
Longitude
40
30
20
10
0
-10
-20
-30

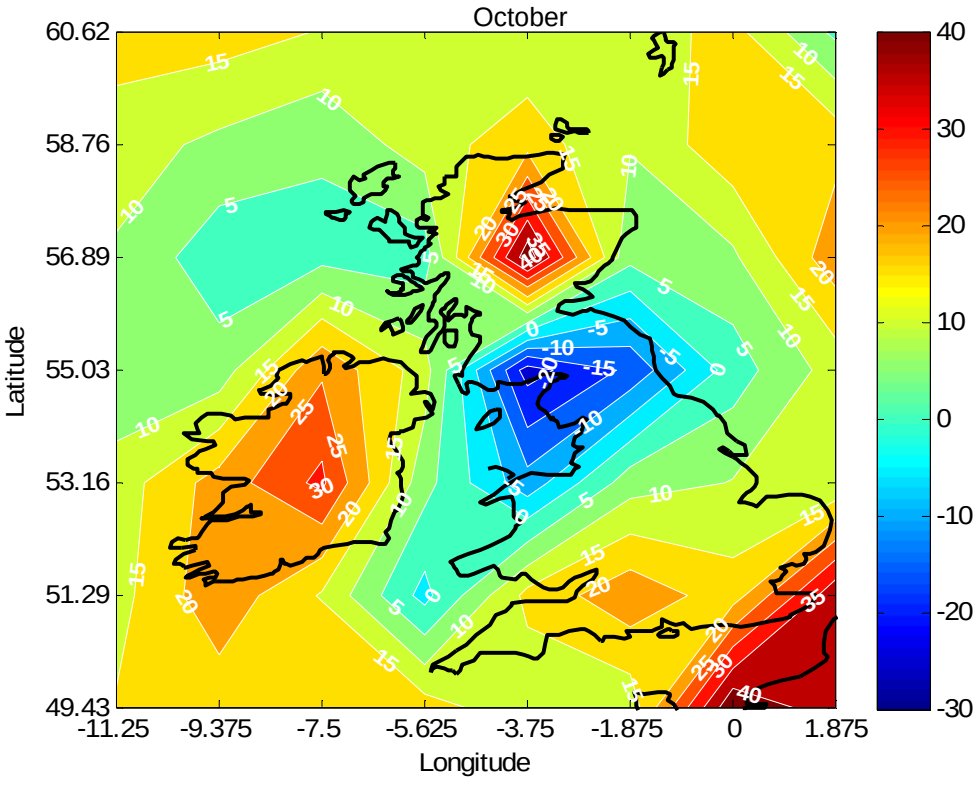
October
60.62
58.76
56.89
55.03
53.16
51.29
49.43
Latitude
-11.25
-9.375
-7.5
-5.625
-3.75
-1.875
0
1.875
Longitude
40
30
20
10
0
-10
-20
-30

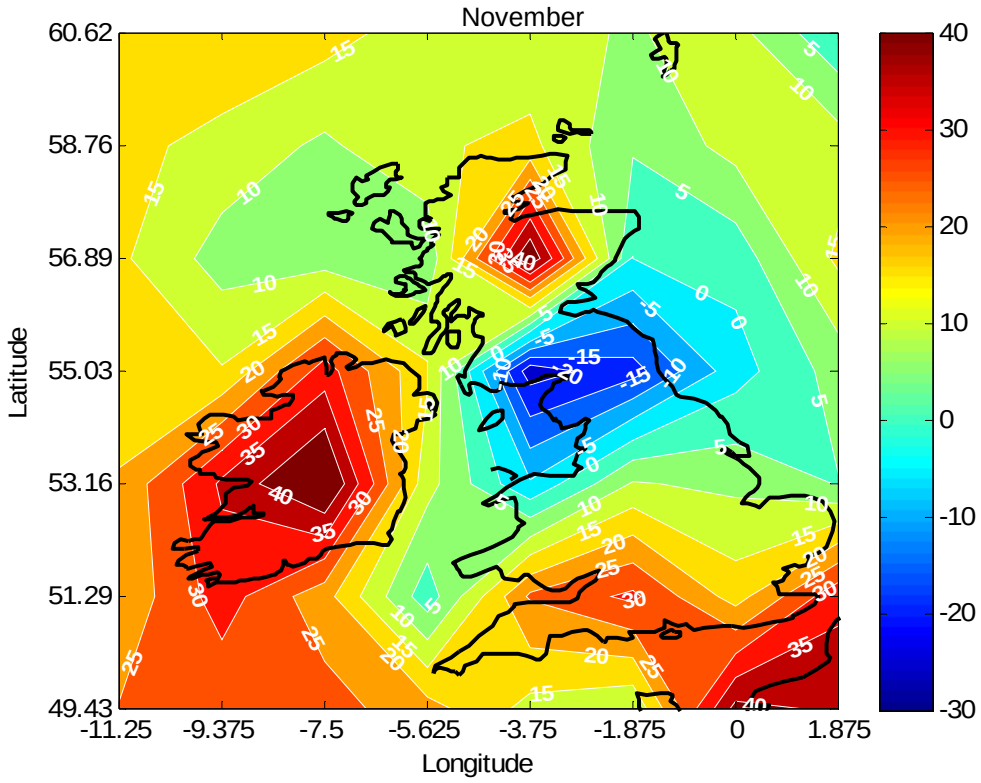
November
60.62
58.76
56.89
55.03
53.16
51.29
49.43
Latitude
-11.25
-9.375
-7.5
-5.625
-3.75
-1.875
0
1.875
Longitude
40
30
20
10
0
-10
-20
-30

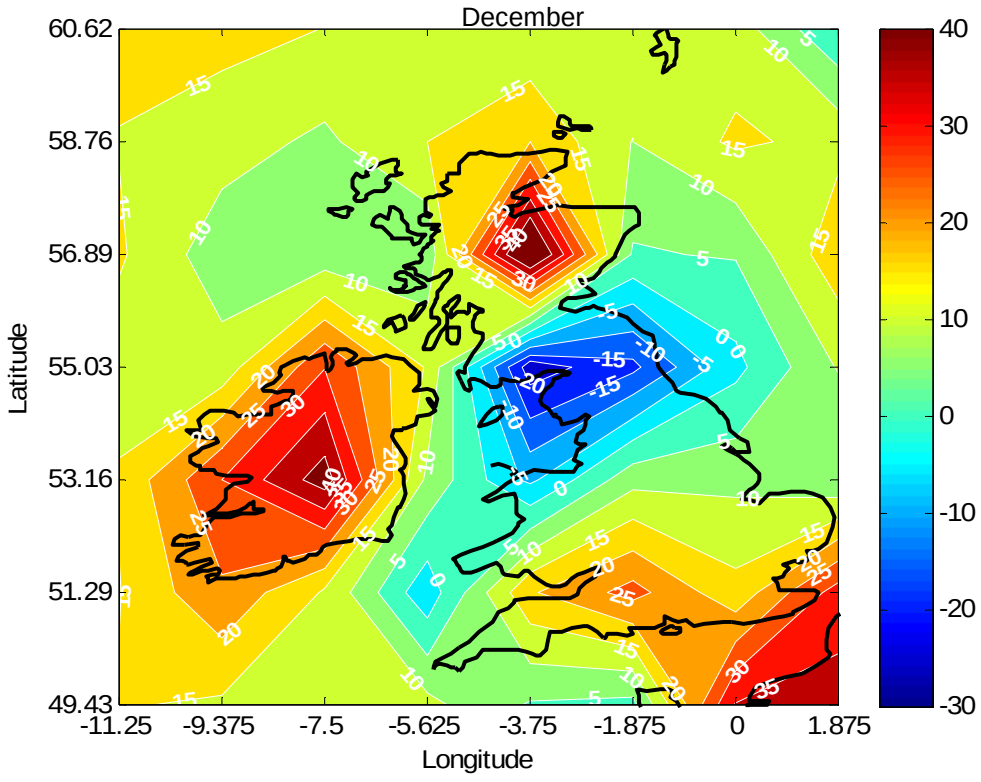
December
60.62
58.76
56.89
55.03
53.16
51.29
49.43
Latitude
-11.25
-9.375
-7.5
-5.625
-3.75
-1.875
0
1.875
Longitude
40
30
20
10
0
-10
-20
-30

Fig. C-2: Run 2, percentage differences in monthly mean wind speed

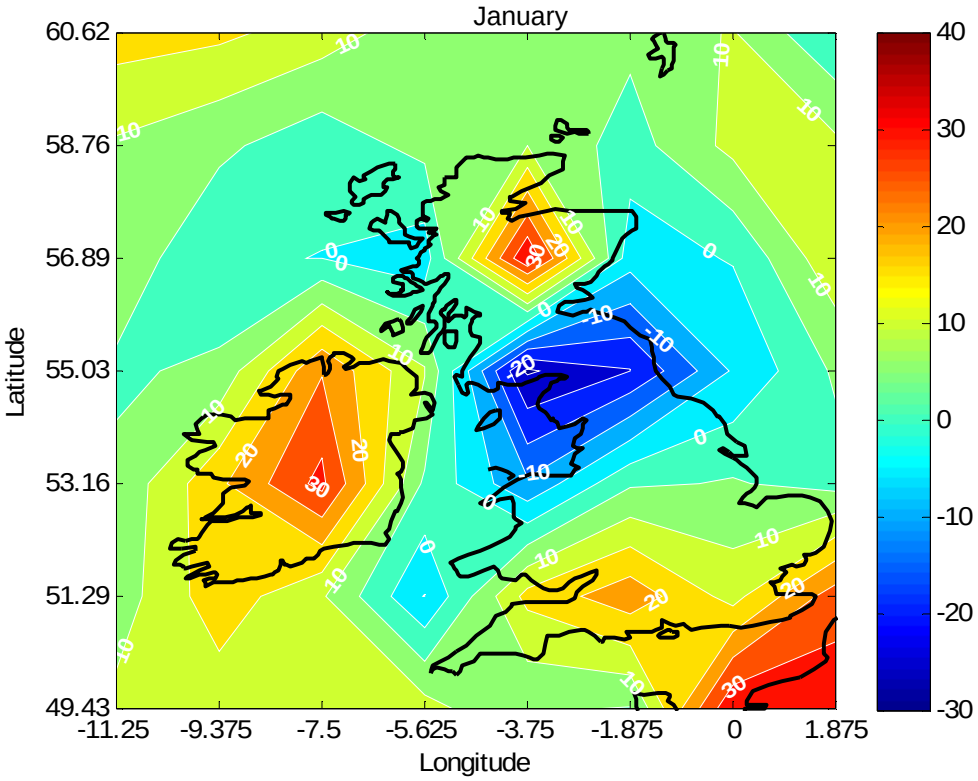

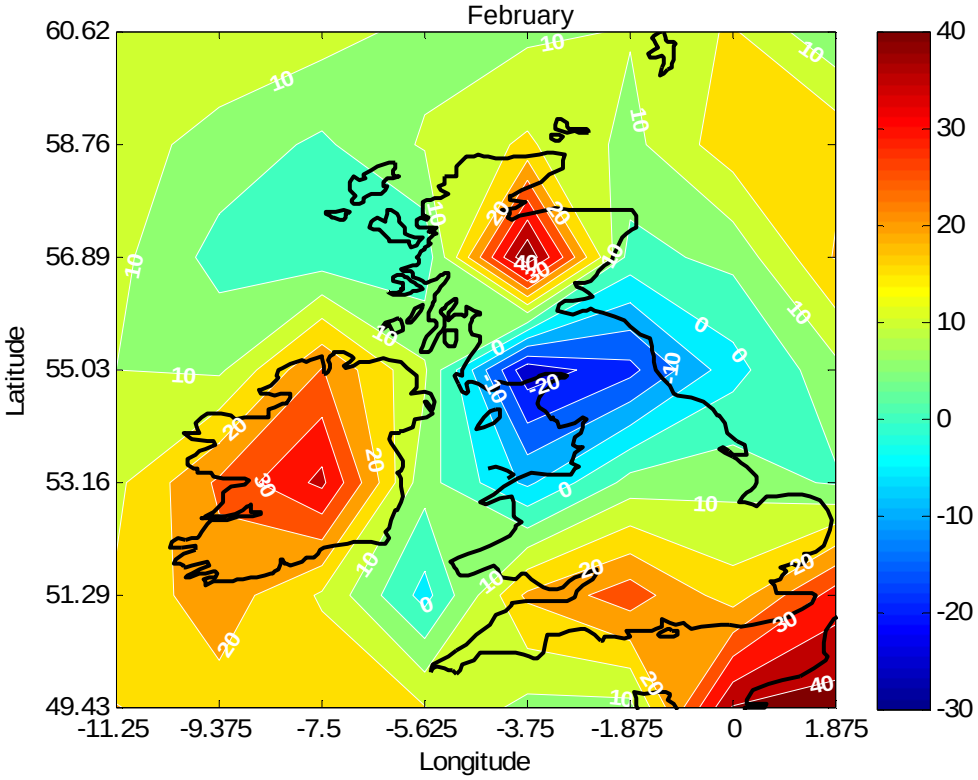

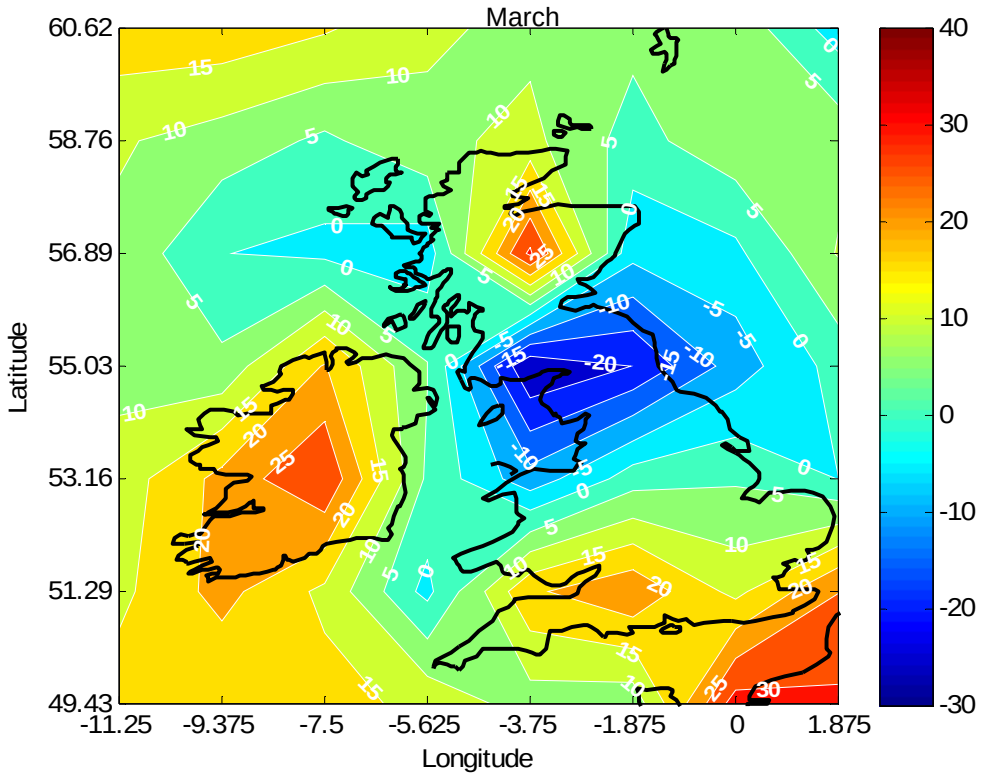
March
60.62
58.76
56.89
55.03
53.16
51.29
49.43
Latitude
-11.25
-9.375
-7.5
-5.625
-3.75
-1.875
0
1.875
Longitude
40
30
20
10
0
-10
-20
-30

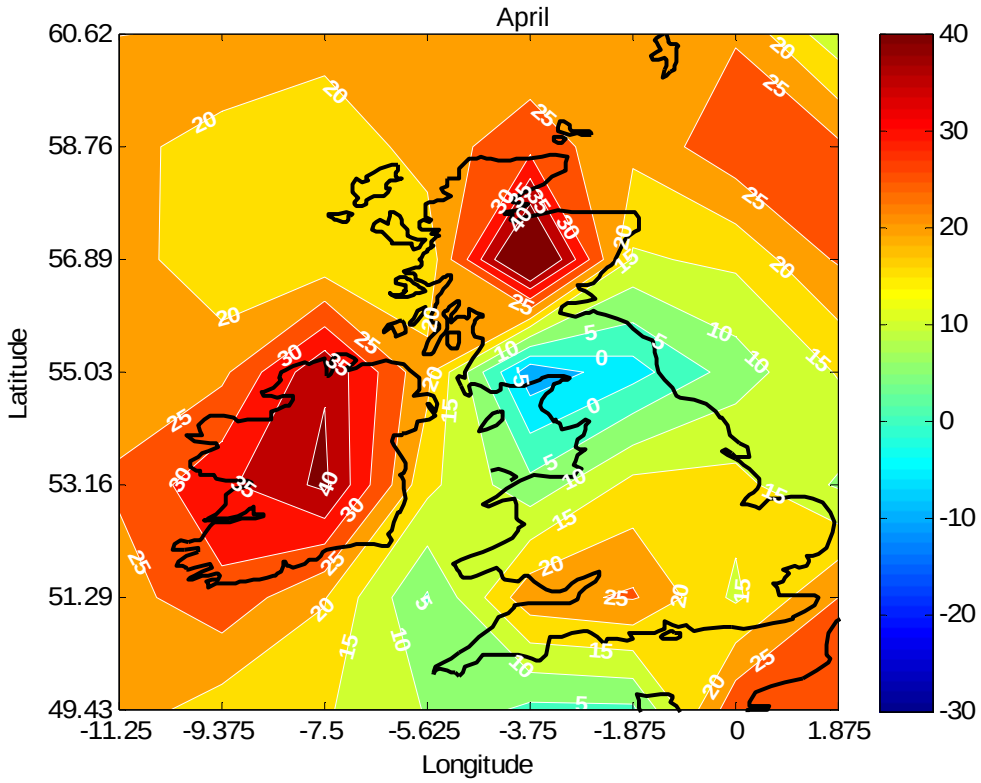
April
60.62
58.76
56.89
55.03
53.16
51.29
49.43
Latitude
-11.25
-9.375
-7.5
-5.625
-3.75
-1.875
0
1.875
Longitude
40
30
20
10
0
-10
-20
-30

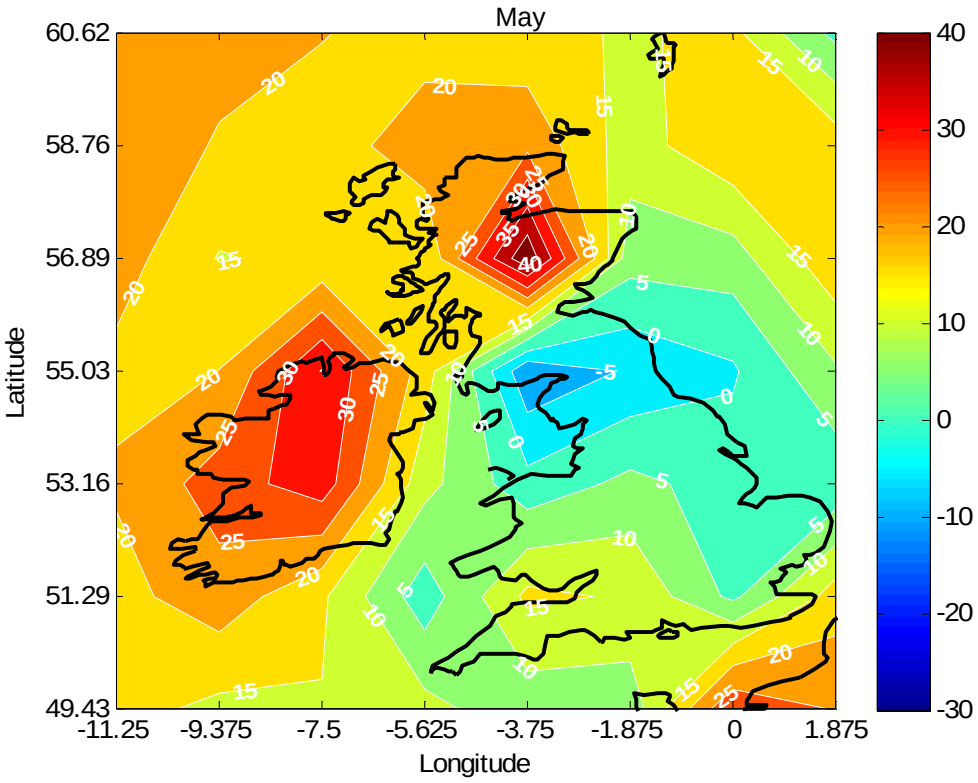
May
60.62
58.76
56.89
55.03
53.16
51.29
49.43
Latitude
-11.25
-9.375
-7.5
-5.625
-3.75
-1.875
0
1.875
Longitude
40
30
20
10
0
-10
-20
-30

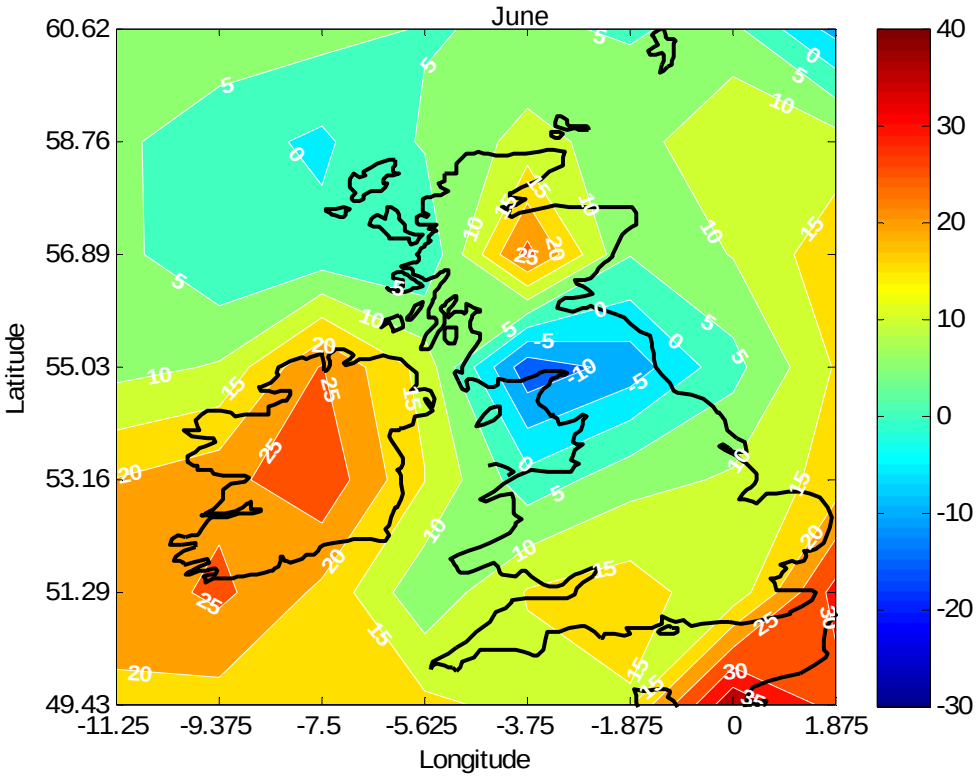
June
60.62
58.76
56.89
55.03
53.16
51.29
49.43
Latitude
-11.25
-9.375
-7.5
-5.625
-3.75
-1.875
0
1.875
Longitude
40
30
20
10
0
-10
-20
-30

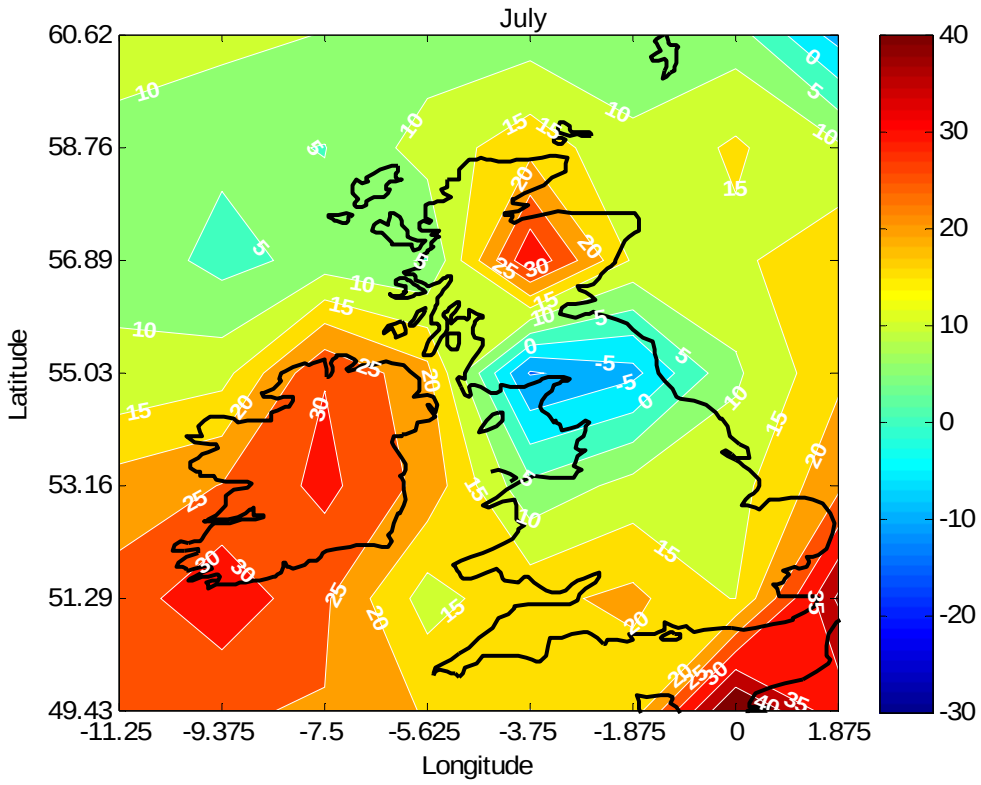
July
60.62
58.76
56.89
55.03
53.16
51.29
49.43
Latitude
-11.25
-9.375
-7.5
-5.625
-3.75
-1.875
0
1.875
Longitude
40
30
20
10
0
-10
-20
-30

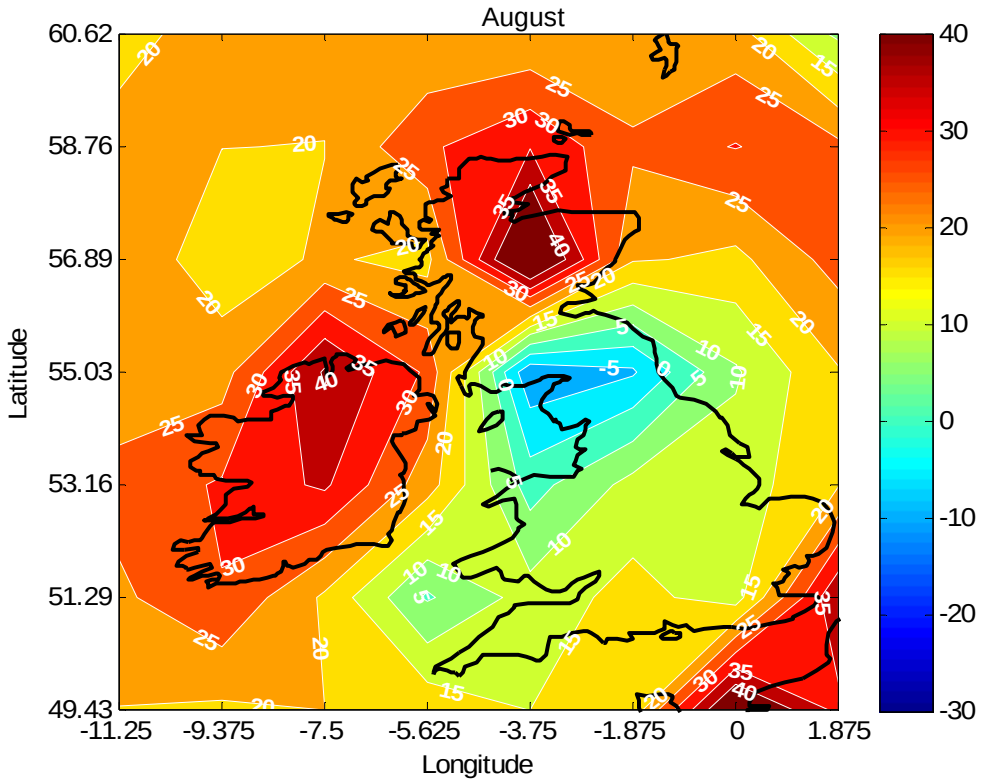
August
60.62
58.76
56.89
55.03
53.16
51.29
49.43
Latitude
-11.25
-9.375
-7.5
-5.625
-3.75
-1.875
0
1.875
Longitude
40
30
20
10
0
-10
-20
-30

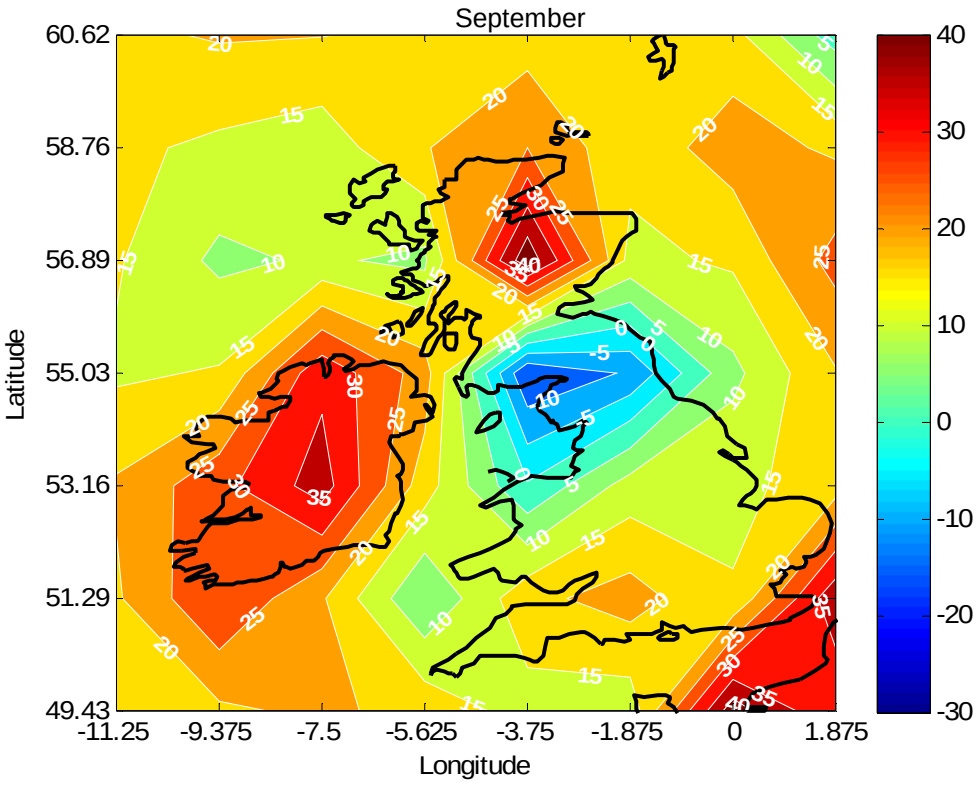
September
60.62
58.76
56.89
55.03
53.16
51.29
49.43
Latitude
-11.25
-9.375
-7.5
-5.625
-3.75
-1.875
0
1.875
Longitude
40
30
20
10
0
-10
-20
-30

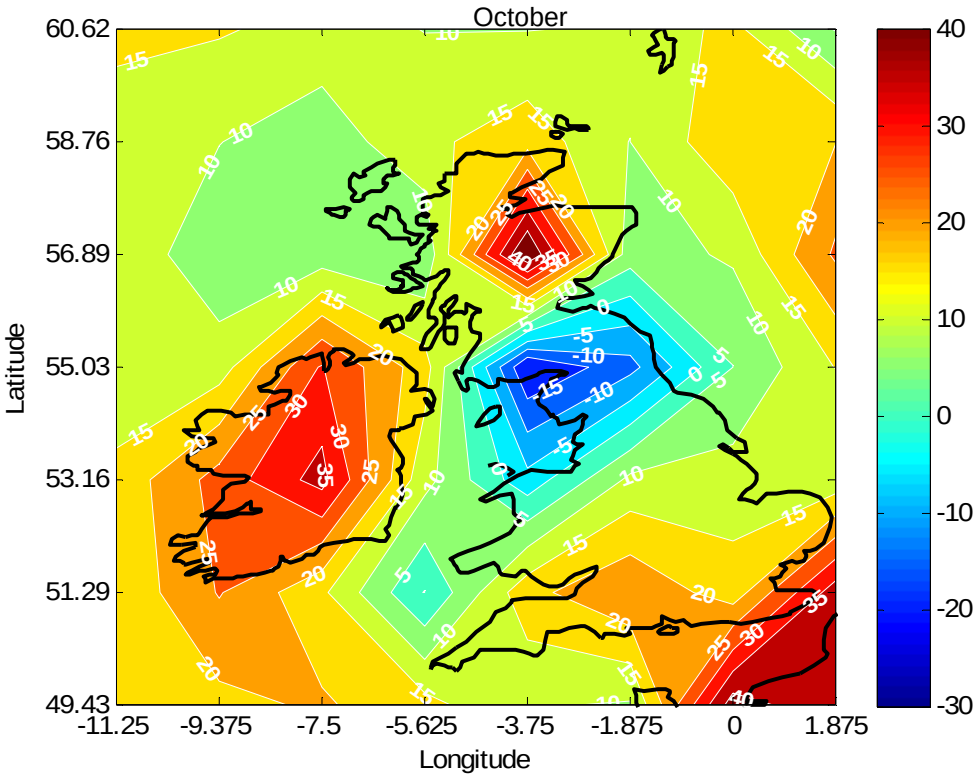
October
60.62
58.76
56.89
55.03
53.16
51.29
49.43
Latitude
-11.25
-9.375
-7.5
-5.625
-3.75
-1.875
0
1.875
Longitude
40
30
20
10
0
-10
-20
-30

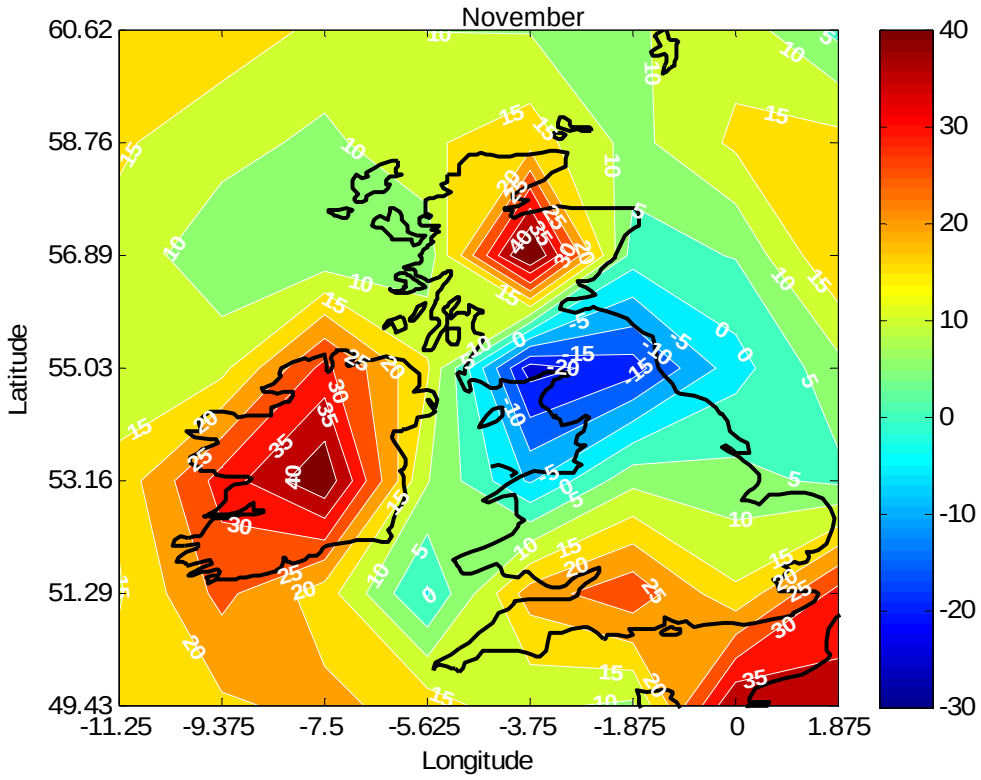
November
60.62
58.76
56.89
55.03
53.16
51.29
49.43
Latitude
-11.25
-9.375
-7.5
-5.625
-3.75
-1.875
0
1.875
Longitude
40
30
20
10
0
-10
-20
-30

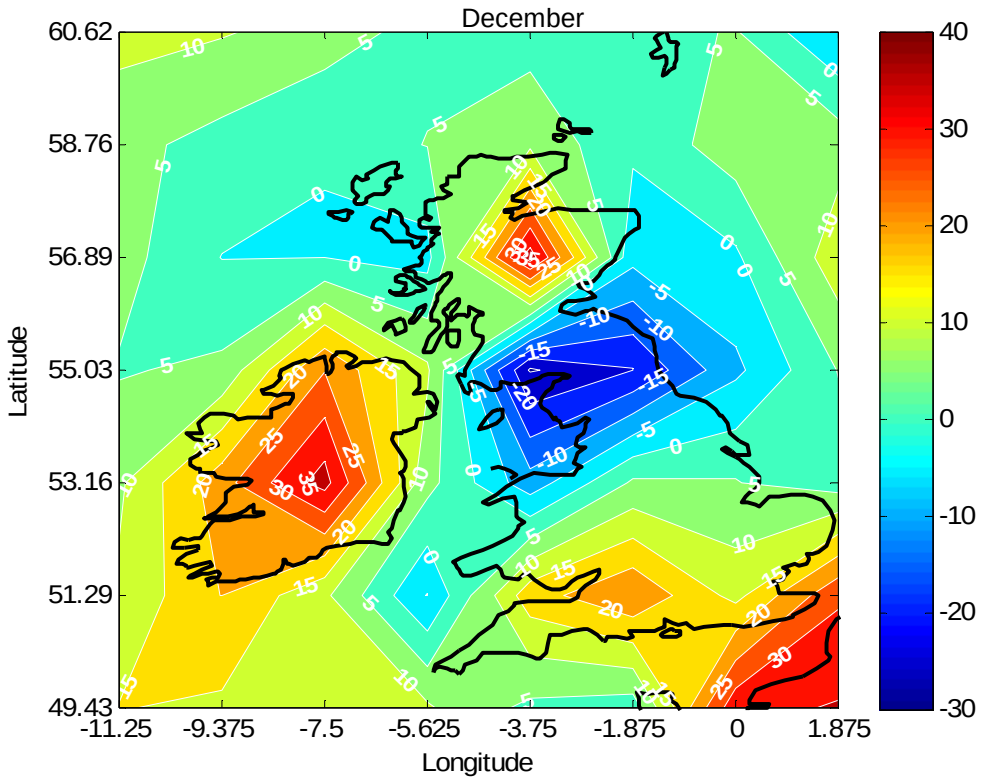
December
60.62
58.76
56.89
55.03
53.16
51.29
49.43
Latitude
-11.25
-9.375
-7.5
-5.625
-3.75
-1.875
0
1.875
Longitude
40
30
20
10
0
-10
-20
-30

Fig. C-3: Run 1, monthly mean wind speed vectors

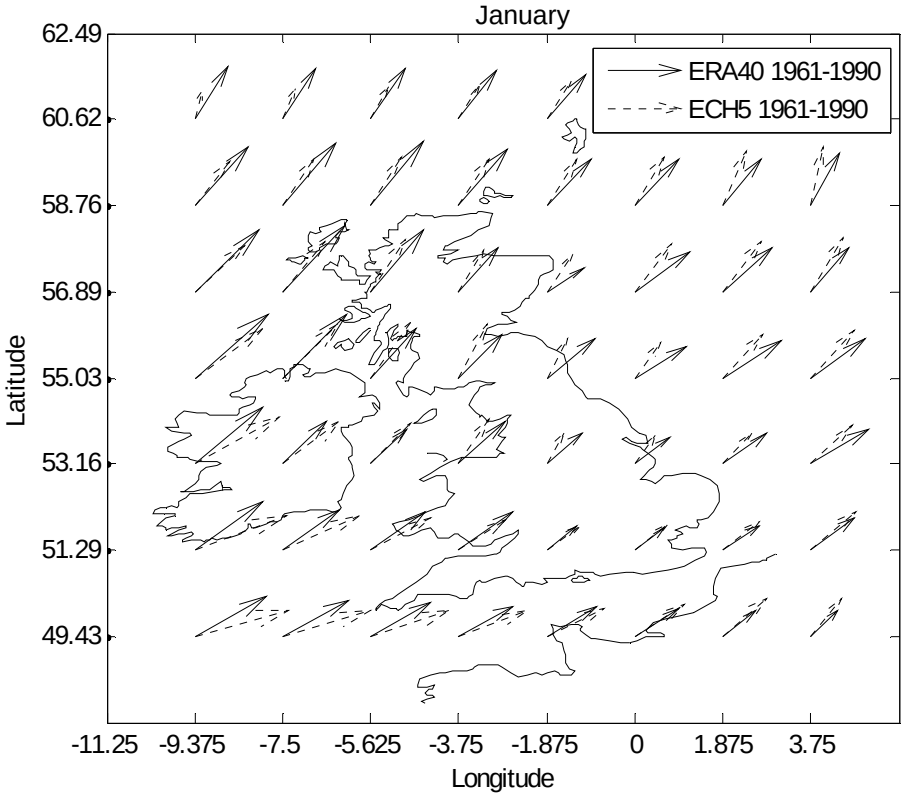

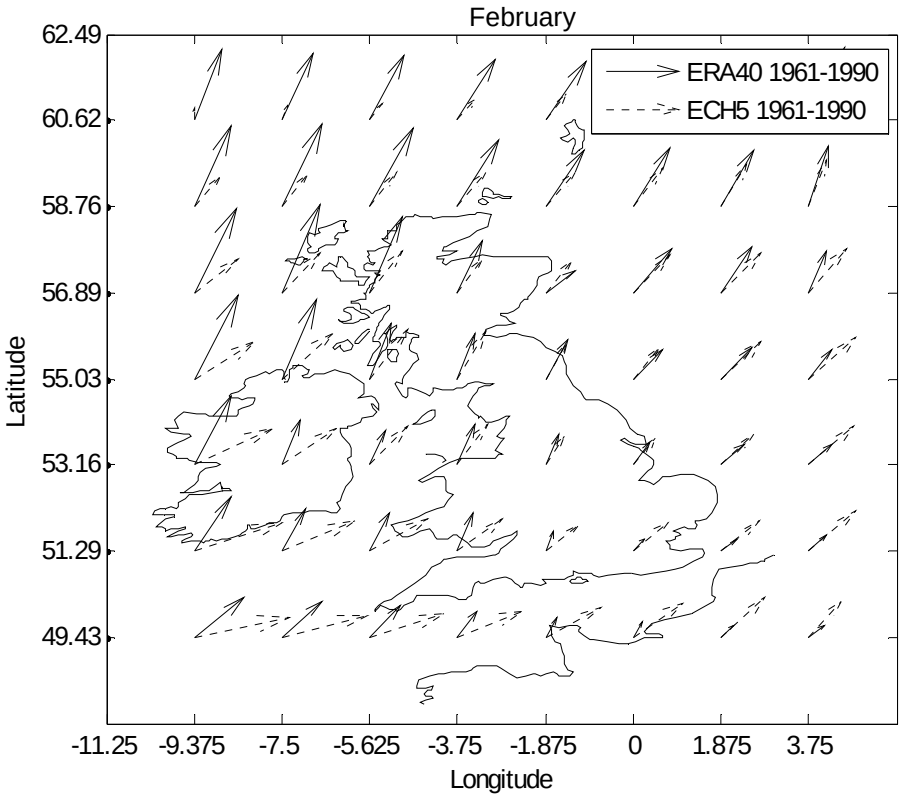

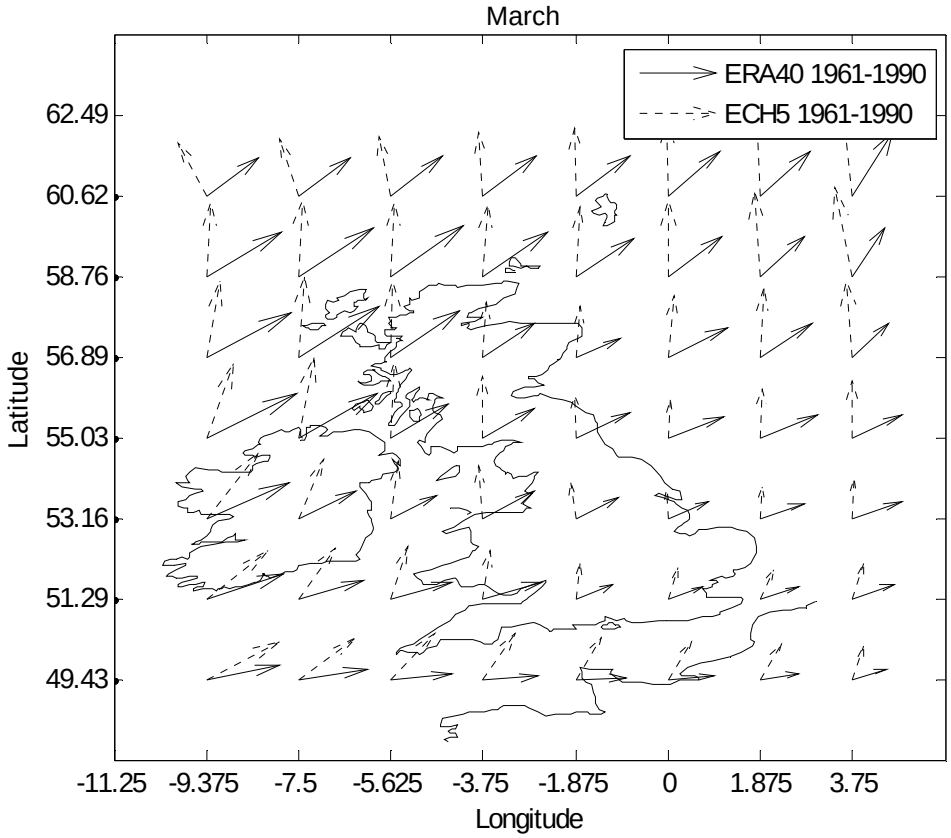
March
ERA40 1961-1990
ECH5 1961-1990
62.49
60.62
58.76
56.89
55.03
53.16
51.29
49.43
Latitude
-11.25
-9.375
-7.5
-5.625
-3.75
-1.875
0
1.875
3.75
Longitude

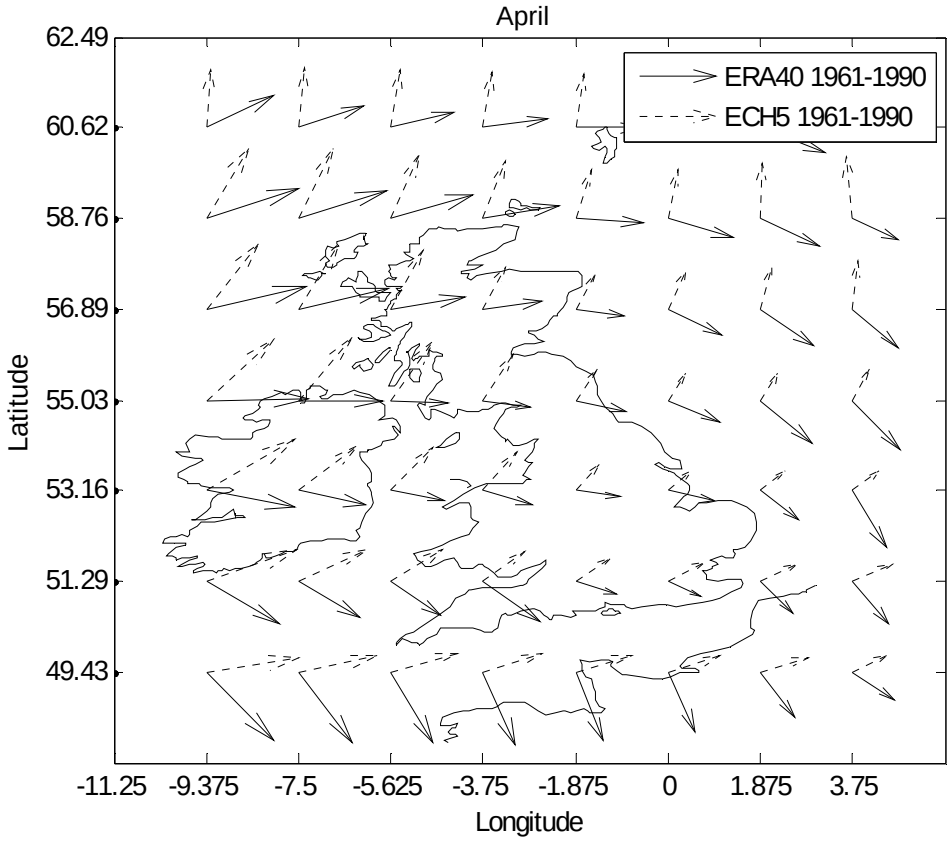
April
ERA40 1961-1990
ECH5 1961-1990
62.49
60.62
58.76
56.89
55.03
53.16
51.29
49.43
Latitude
-11.25
-9.375
-7.5
-5.625
-3.75
-1.875
0
1.875
3.75
Longitude

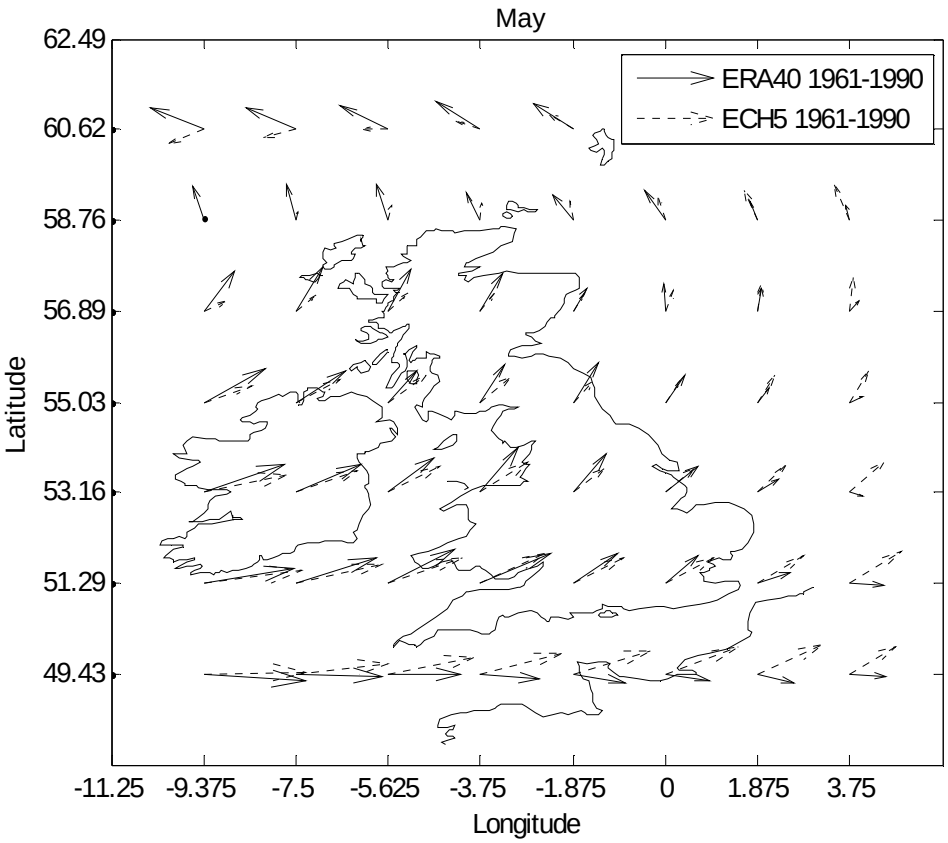
May
ERA40 1961-1990
ECH5 1961-1990
62.49
60.62
58.76
56.89
55.03
53.16
51.29
49.43
Latitude
-11.25
-9.375
-7.5
-5.625
-3.75
-1.875
0
1.875
3.75
Longitude

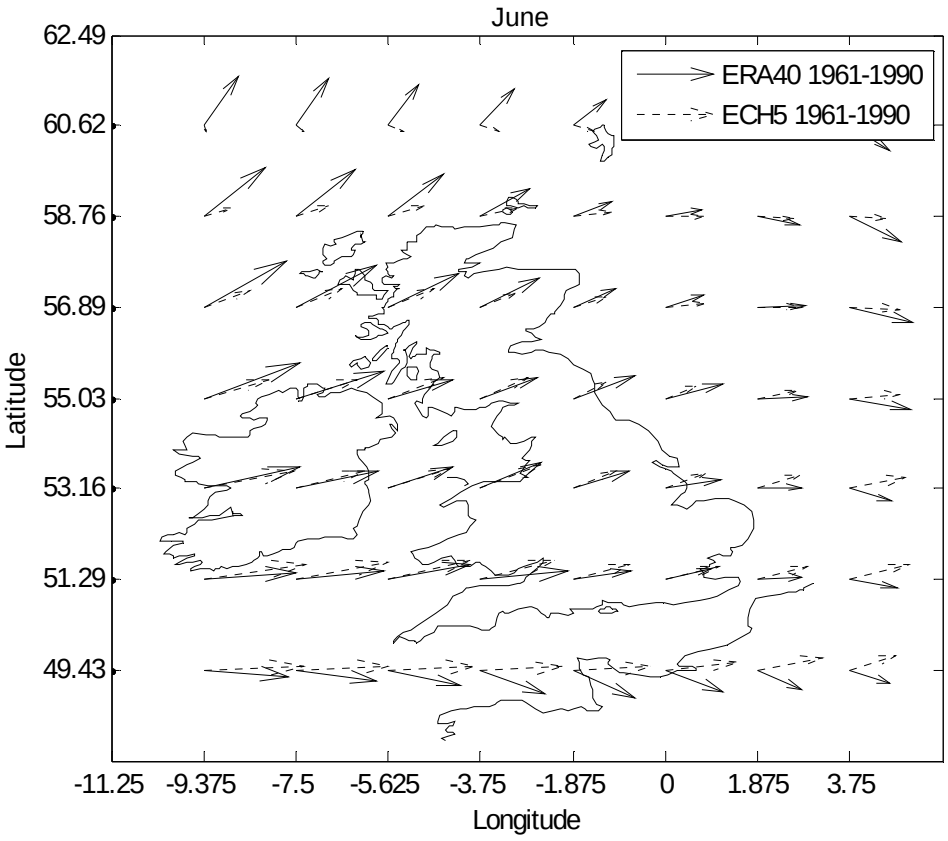
June
ERA40 1961-1990
ECH5 1961-1990
62.49
60.62
58.76
56.89
55.03
53.16
51.29
49.43
Latitude
-11.25
-9.375
-7.5
-5.625
-3.75
-1.875
0
1.875
3.75
Longitude

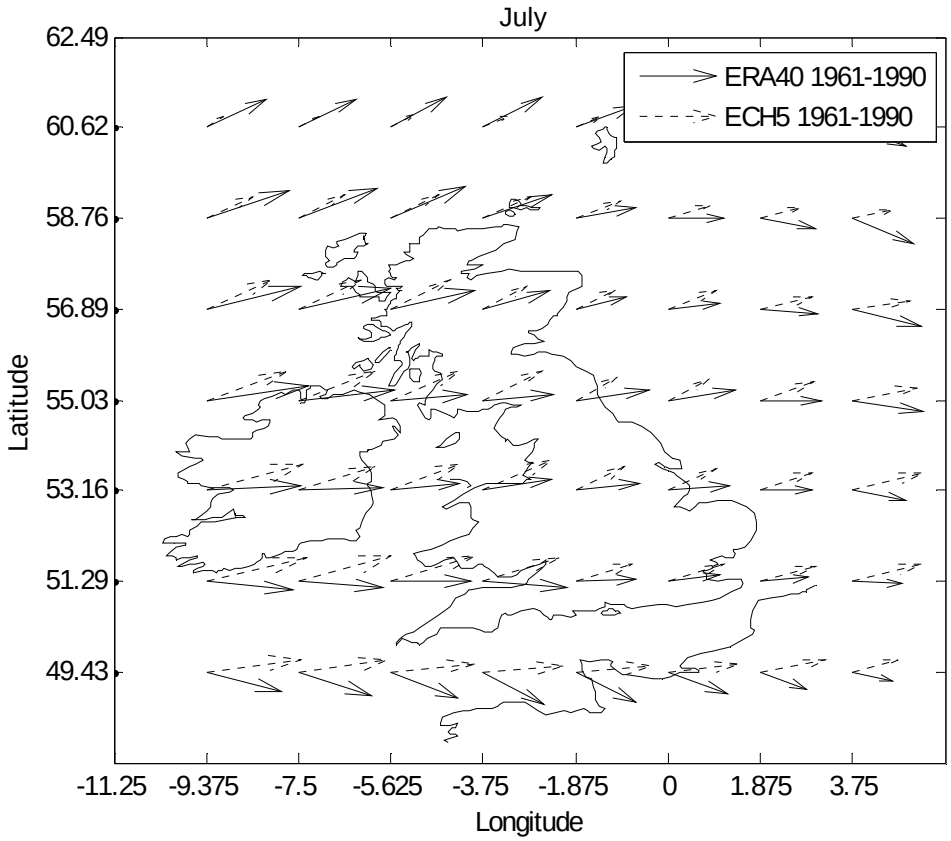
July
ERA40 1961-1990
ECH5 1961-1990
62.49
60.62
58.76
56.89
55.03
53.16
51.29
49.43
Latitude
-11.25
-9.375
-7.5
-5.625
-3.75
-1.875
0
1.875
3.75
Longitude

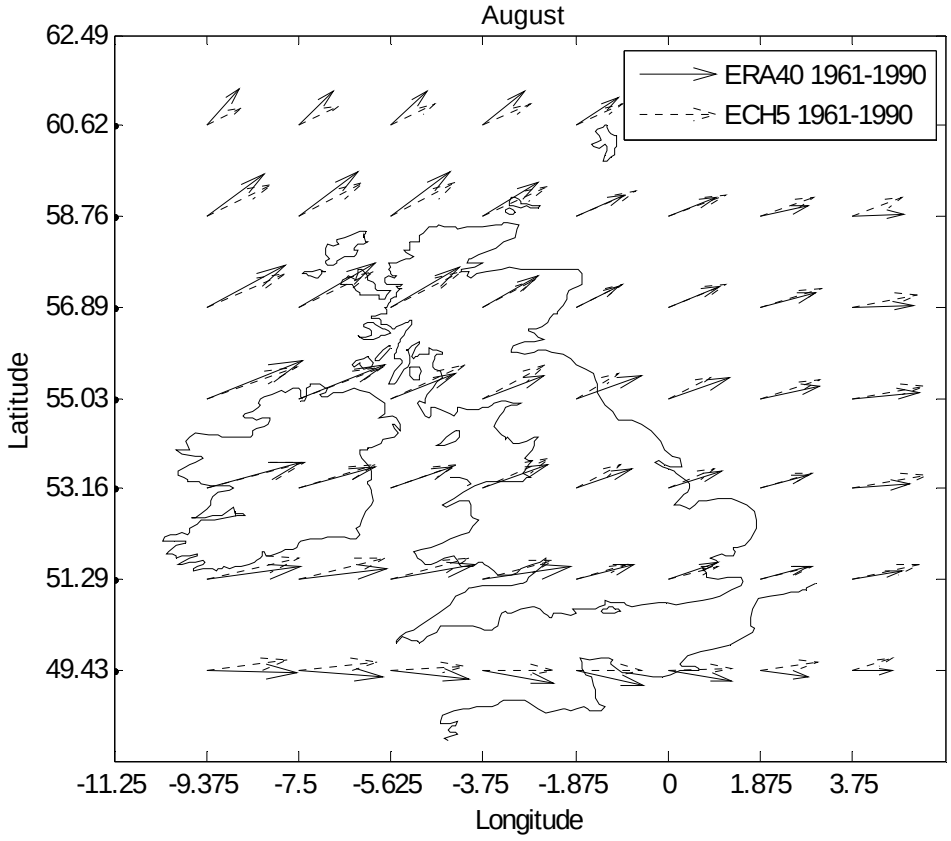
August
ERA40 1961-1990
ECH5 1961-1990
62.49
60.62
58.76
56.89
55.03
53.16
51.29
49.43
Latitude
-11.25
-9.375
-7.5
-5.625
-3.75
-1.875
0
1.875
3.75
Longitude

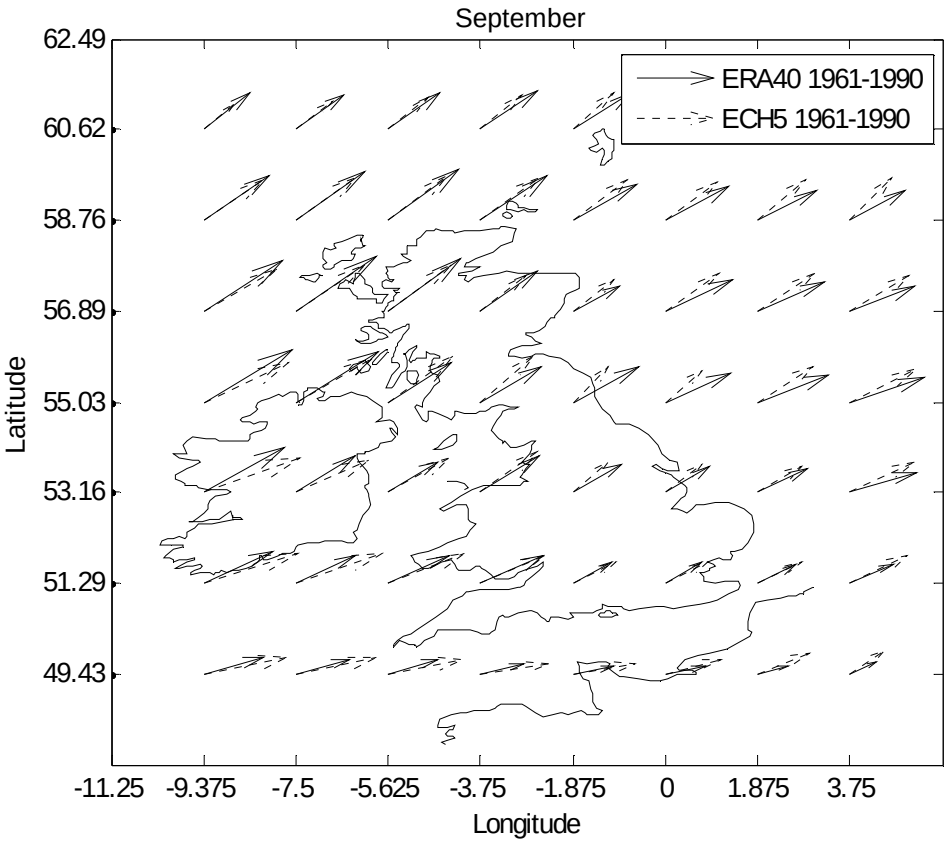
September
ERA40 1961-1990
ECH5 1961-1990
62.49
60.62
58.76
56.89
55.03
53.16
51.29
49.43
Latitude
-11.25
-9.375
-7.5
-5.625
-3.75
-1.875
0
1.875
3.75
Longitude

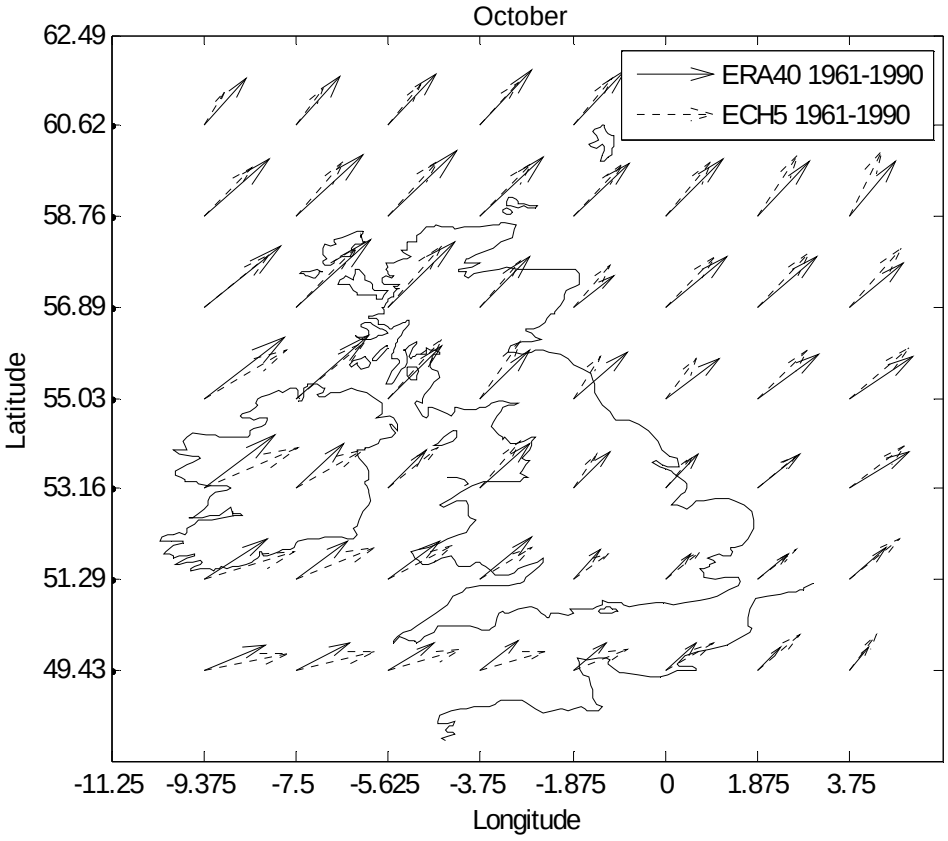
October
ERA40 1961-1990
ECH5 1961-1990
62.49
60.62
58.76
56.89
55.03
53.16
51.29
49.43
Latitude
-11.25
-9.375
-7.5
-5.625
-3.75
-1.875
0
1.875
3.75
Longitude

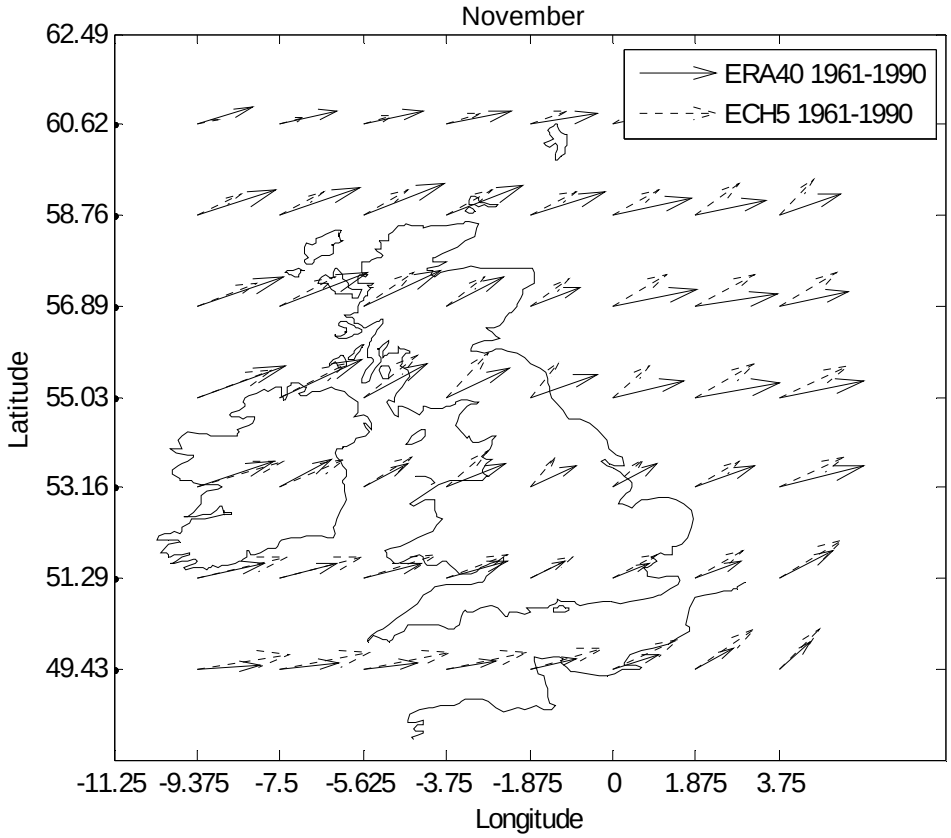
November
ERA40 1961-1990
ECH5 1961-1990
62.49
60.62
58.76
56.89
55.03
53.16
51.29
49.43
Latitude
-11.25 -9.375 -7.5 -5.625 -3.75 -1.875 0 1.875 3.75
Longitude

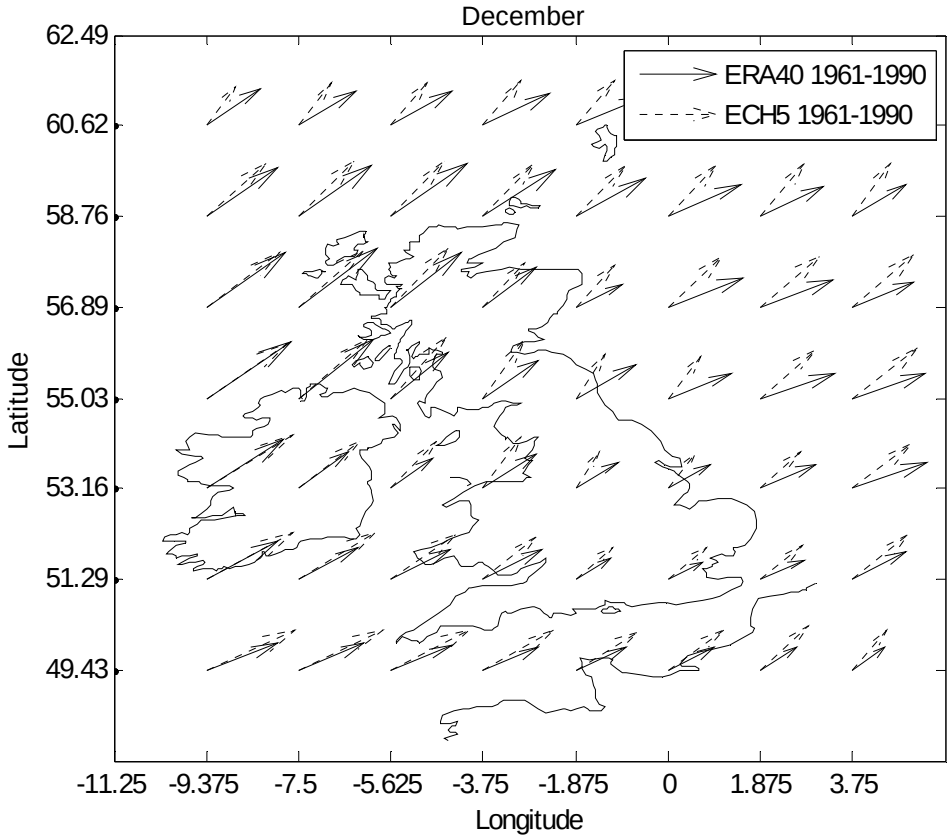
December
ERA40 1961-1990
ECH5 1961-1990
62.49
60.62
58.76
56.89
55.03
53.16
51.29
49.43
Latitude
-11.25 -9.375 -7.5 -5.625 -3.75 -1.875 0 1.875 3.75
Longitude

Fig. C-4: Run 4, monthly mean wind speed vectors

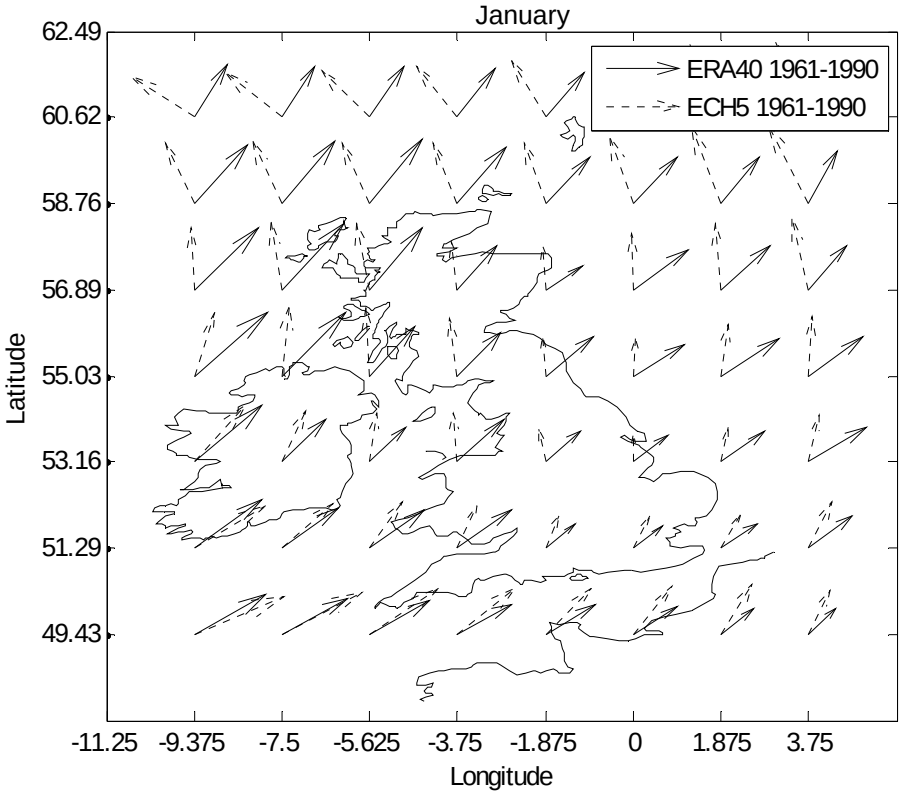

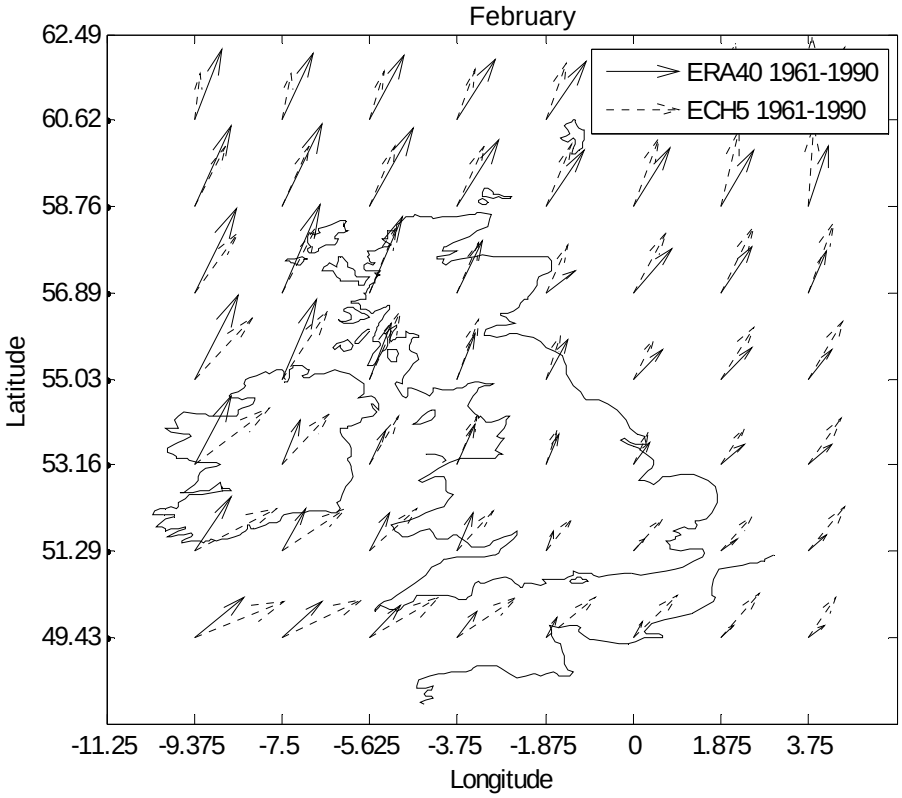

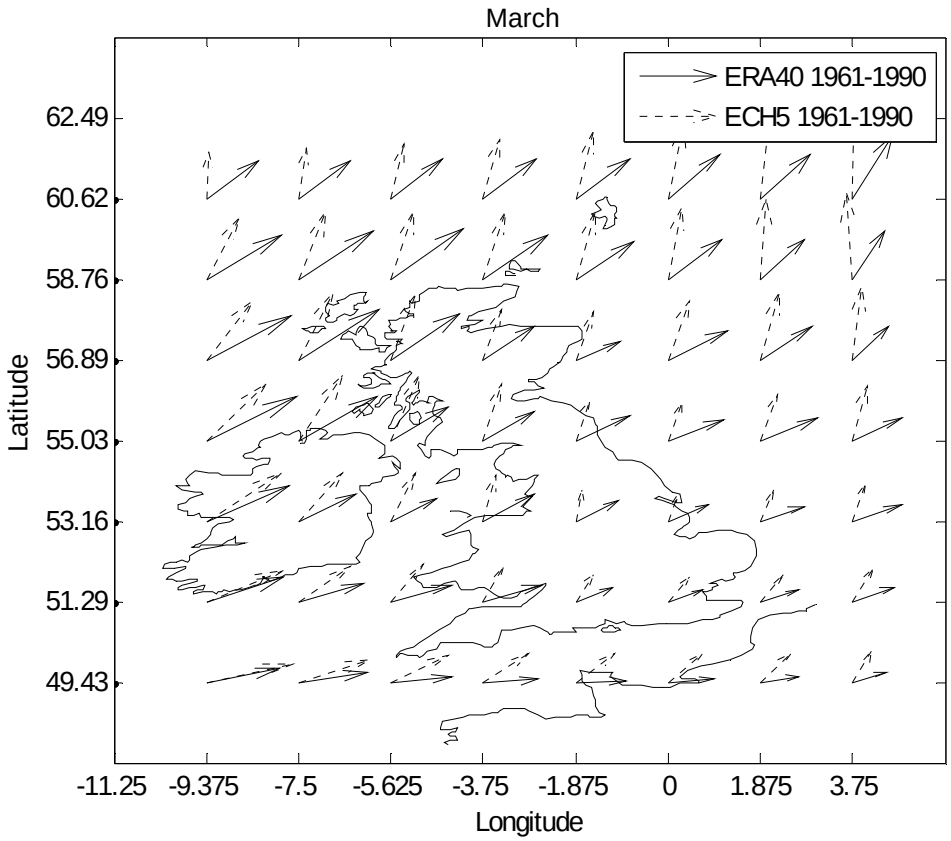
March
ERA40 1961-1990
ECH5 1961-1990
62.49
60.62
58.76
56.89
55.03
53.16
51.29
49.43
Latitude
-11.25
-9.375
-7.5
-5.625
-3.75
-1.875
0
1.875
3.75
Longitude

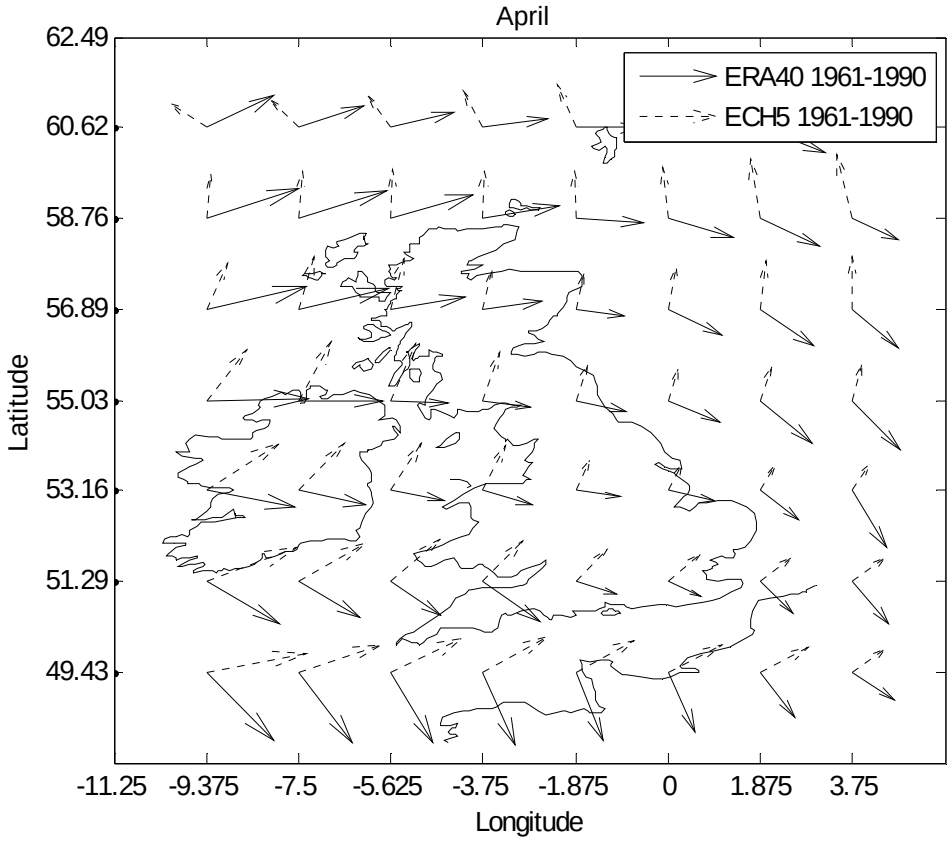
April
ERA40 1961-1990
ECH5 1961-1990
62.49
60.62
58.76
56.89
55.03
53.16
51.29
49.43
Latitude
-11.25
-9.375
-7.5
-5.625
-3.75
-1.875
0
1.875
3.75
Longitude

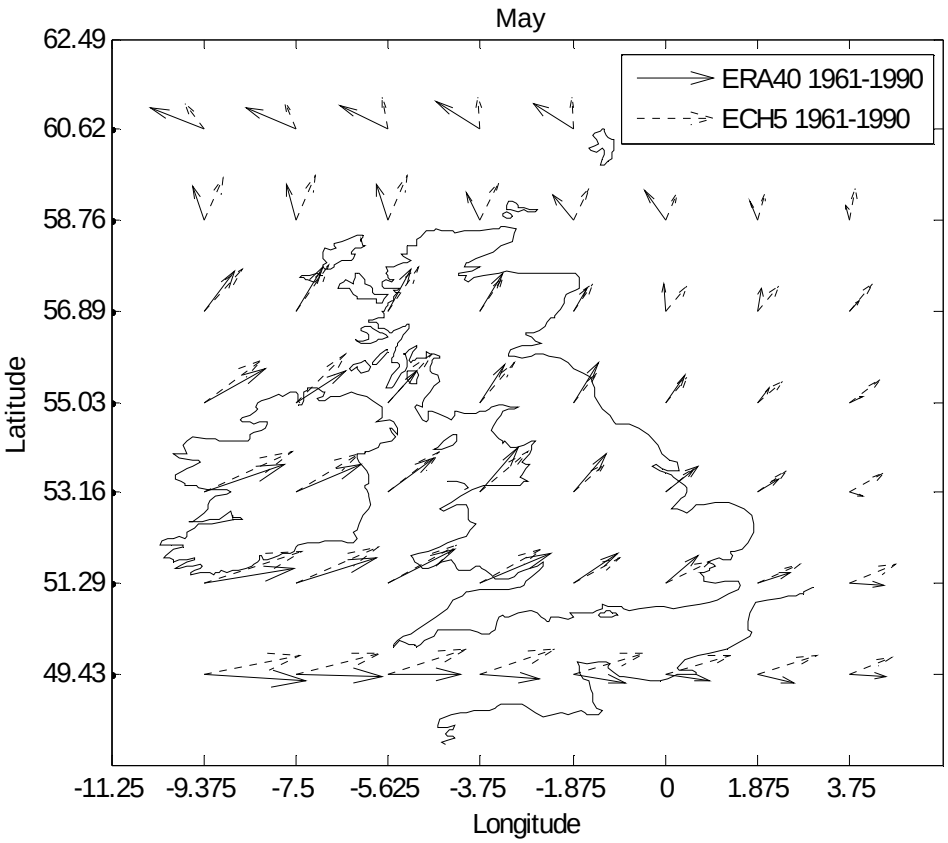
May
ERA40 1961-1990
ECH5 1961-1990
62.49
60.62
58.76
56.89
55.03
53.16
51.29
49.43
Latitude
-11.25
-9.375
-7.5
-5.625
-3.75
-1.875
0
1.875
3.75
Longitude

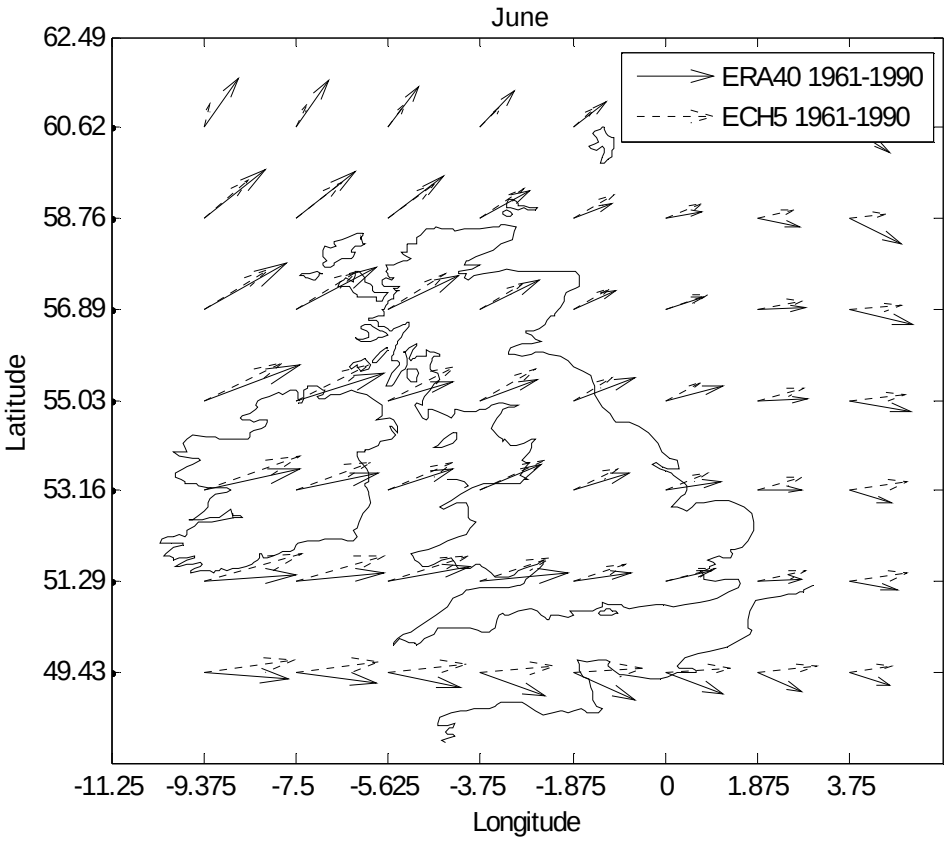
June
ERA40 1961-1990
ECH5 1961-1990
62.49
60.62
58.76
56.89
55.03
53.16
51.29
49.43
Latitude
-11.25
-9.375
-7.5
-5.625
-3.75
-1.875
0
1.875
3.75
Longitude

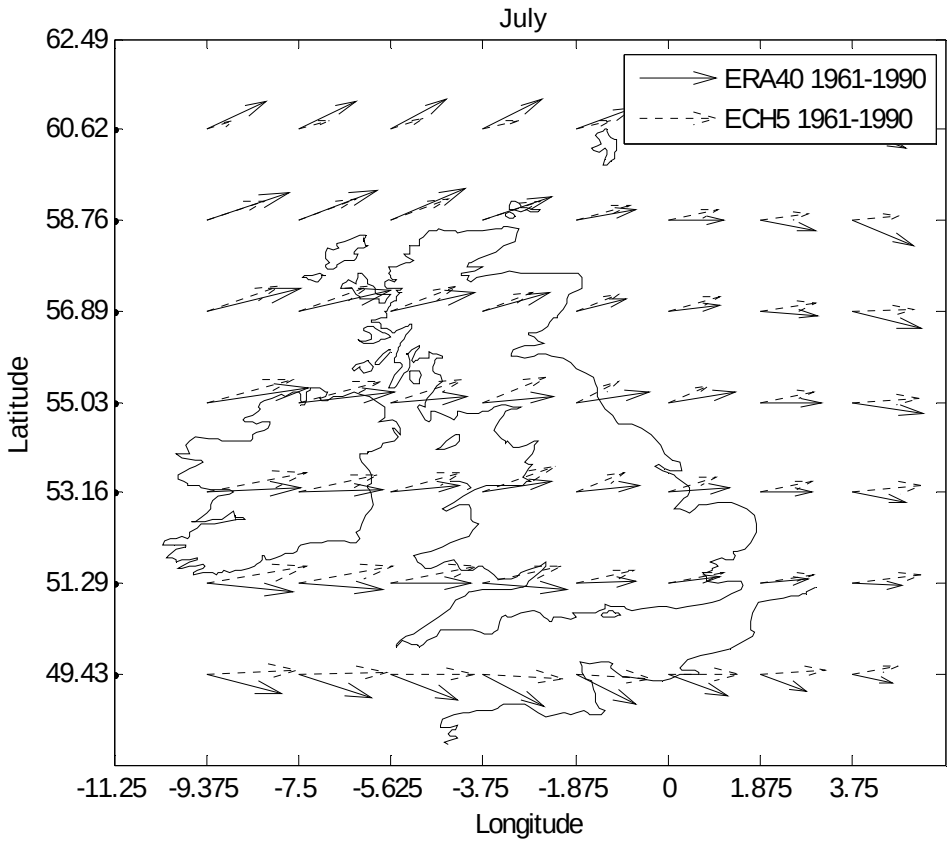
July
ERA40 1961-1990
ECH5 1961-1990
62.49
60.62
58.76
56.89
55.03
53.16
51.29
49.43
Latitude
-11.25
-9.375
-7.5
-5.625
-3.75
-1.875
0
1.875
3.75
Longitude

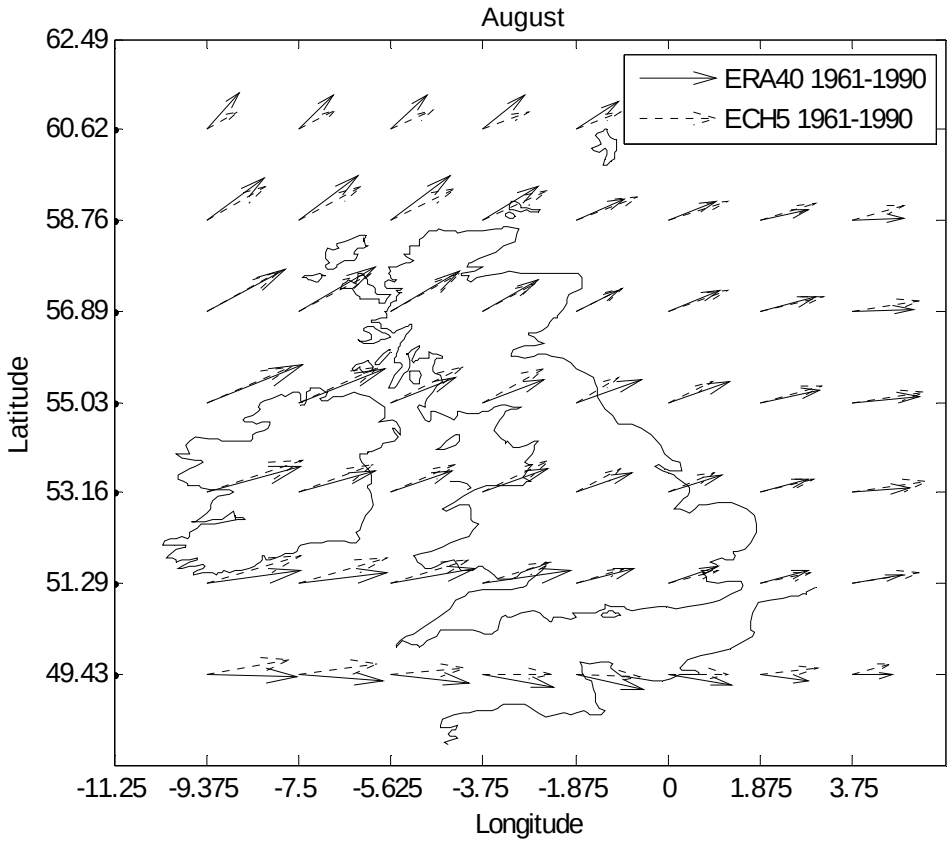
August
ERA40 1961-1990
ECH5 1961-1990
62.49
60.62
58.76
56.89
55.03
53.16
51.29
49.43
Latitude
-11.25
-9.375
-7.5
-5.625
-3.75
-1.875
0
1.875
3.75
Longitude

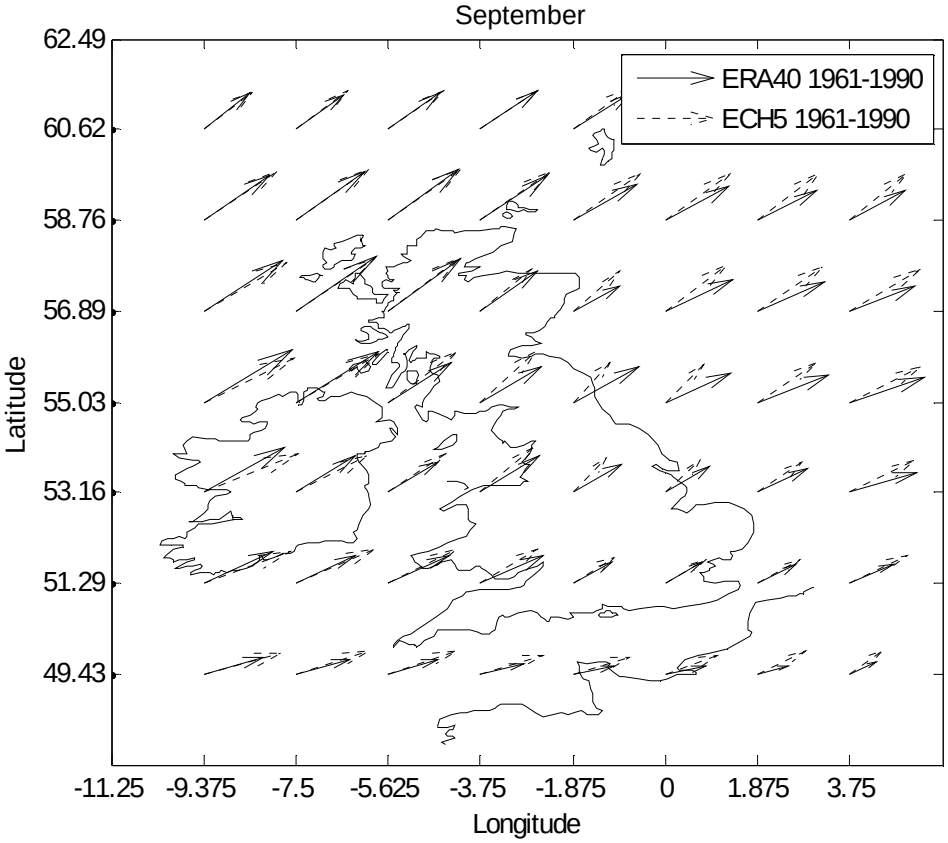
September
ERA40 1961-1990
ECH5 1961-1990
62.49
60.62
58.76
56.89
55.03
53.16
51.29
49.43
Latitude
-11.25
-9.375
-7.5
-5.625
-3.75
-1.875
0
1.875
3.75
Longitude

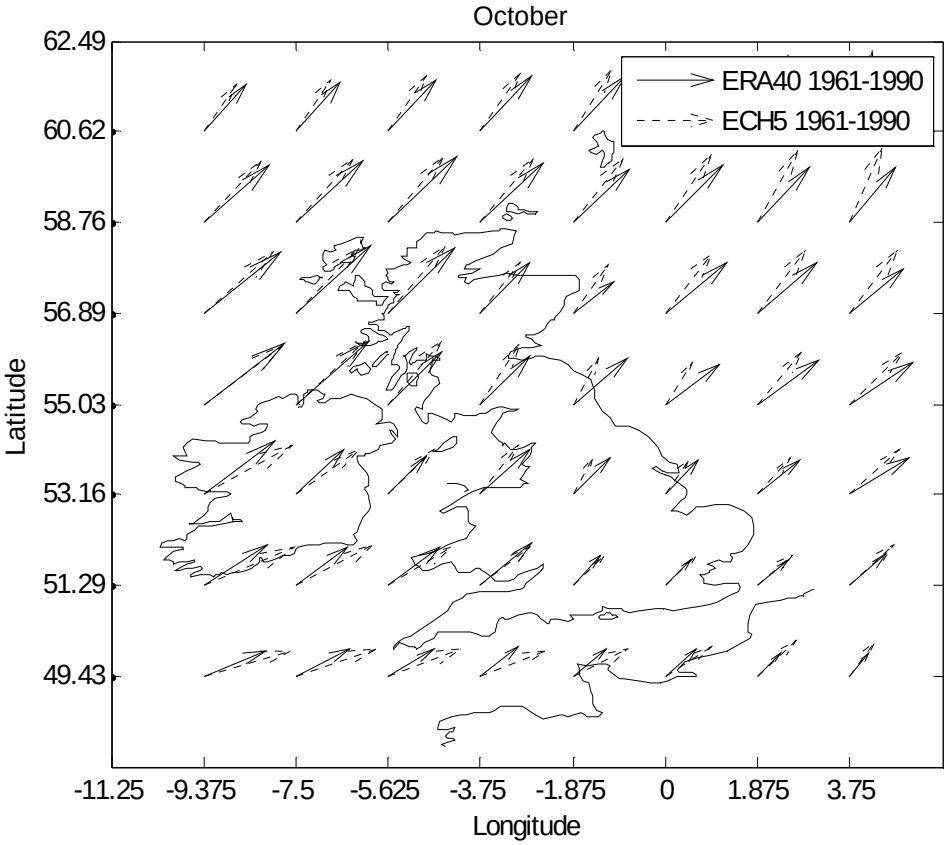
October
ERA40 1961-1990
ECH5 1961-1990
62.49
60.62
58.76
56.89
55.03
53.16
51.29
49.43
Latitude
-11.25
-9.375
-7.5
-5.625
-3.75
-1.875
0
1.875
3.75
Longitude

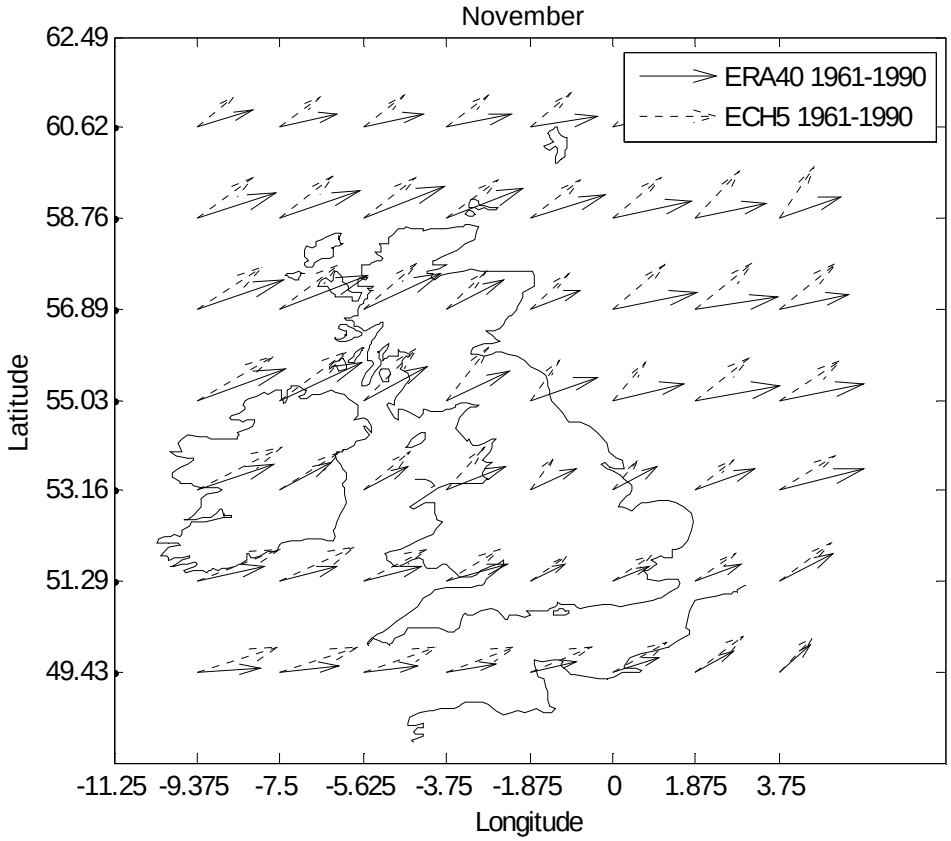
November
ERA40 1961-1990
ECH5 1961-1990
62.49
60.62
58.76
56.89
55.03
53.16
51.29
49.43
Latitude
-11.25 -9.375 -7.5 -5.625 -3.75 -1.875 0 1.875 3.75
Longitude

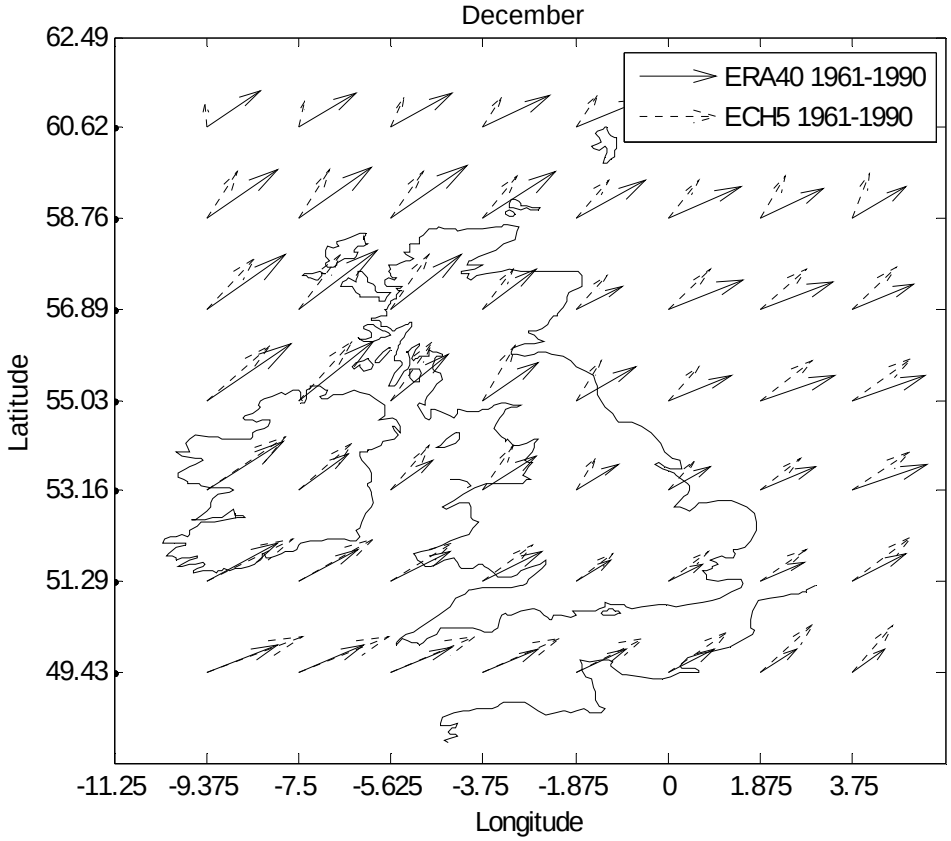
December
ERA40 1961-1990
ECH5 1961-1990
62.49
60.62
58.76
56.89
55.03
53.16
51.29
49.43
Latitude
-11.25 -9.375 -7.5 -5.625 -3.75 -1.875 0 1.875 3.75
Longitude

C.2 Comparison of 2081-2100 with 1961-90 for ECHAM5

Fig. C-5: Future percentage differences in monthly mean wind speed (Run 1 baseline)

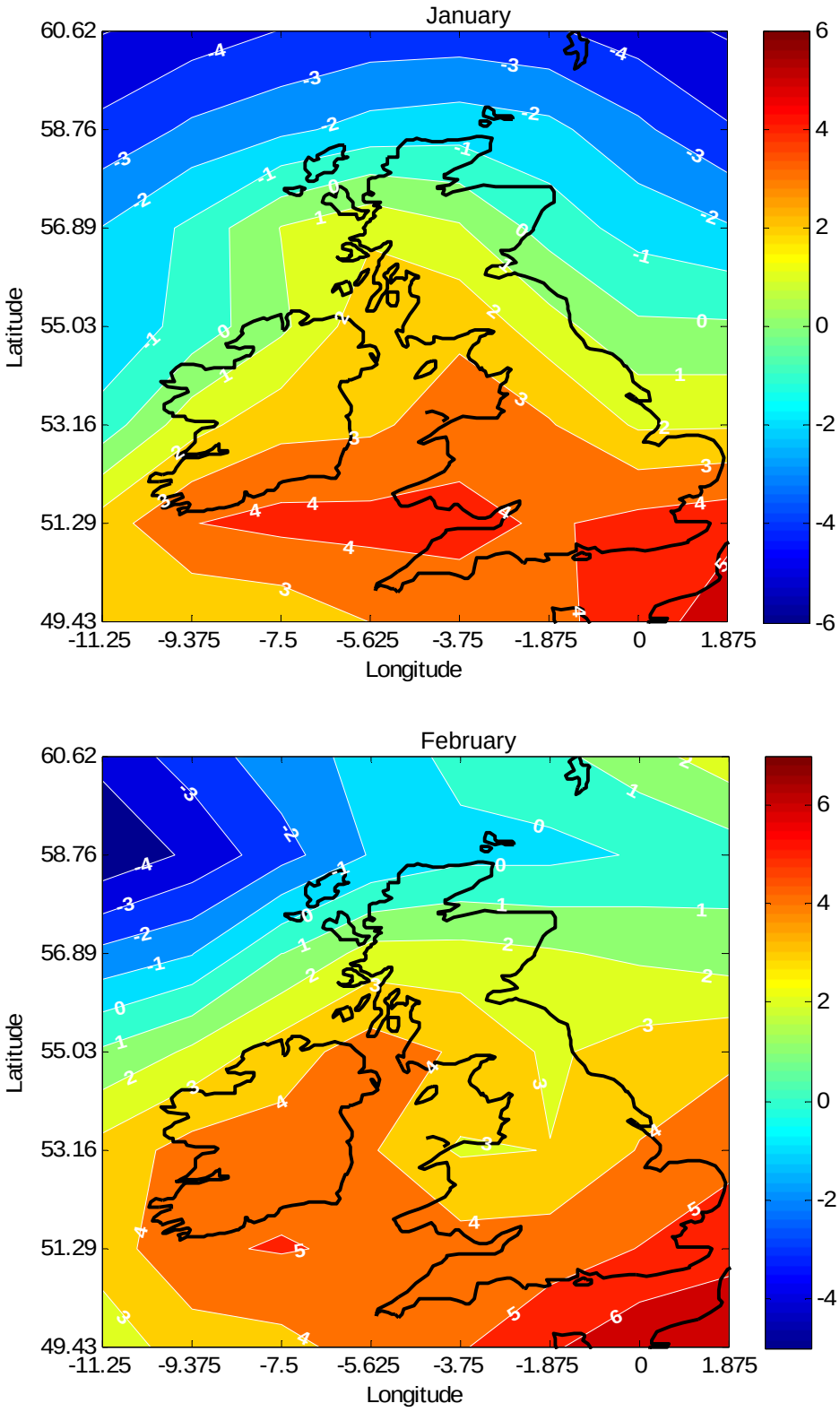

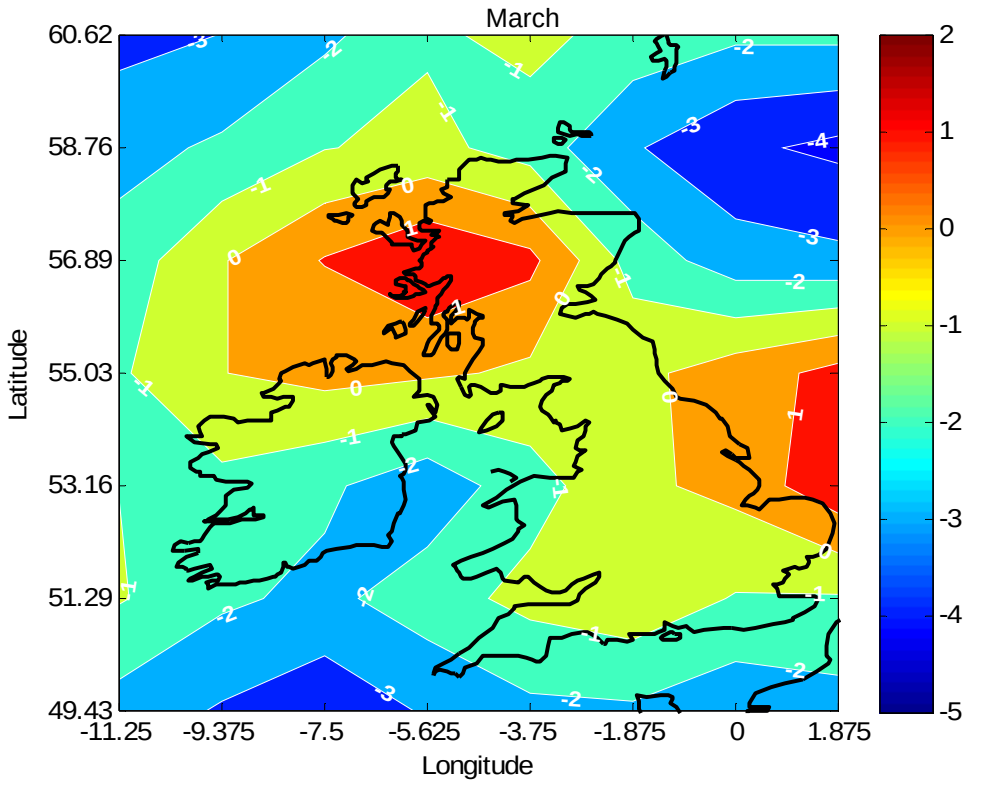
March
60.62
58.76
56.89
55.03
53.16
51.29
49.43
Latitude
-11.25
-9.375
-7.5
-5.625
-3.75
-1.875
0
1.875
Longitude
2
1
0
-1
-2
-3
-4
-5

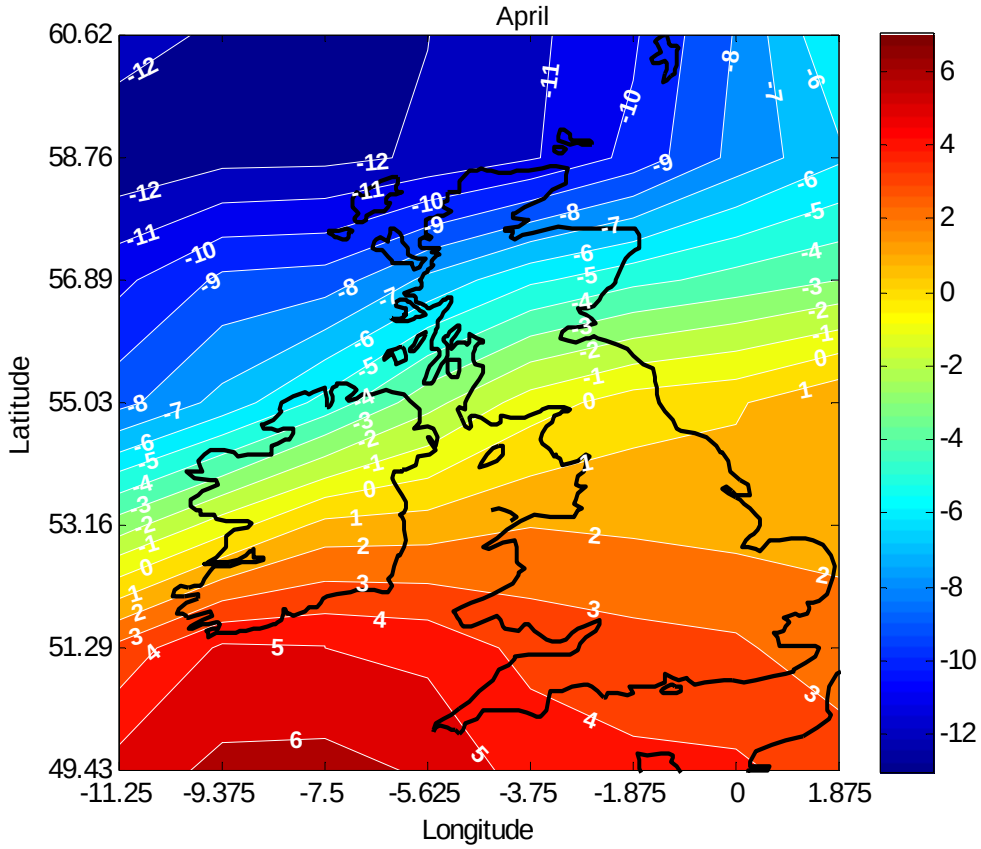
April
60.62
58.76
56.89
55.03
53.16
51.29
49.43
Latitude
-11.25
-9.375
-7.5
-5.625
-3.75
-1.875
0
1.875
Longitude
6
4
2
0
-2
-4
-6
-8
-10
-12

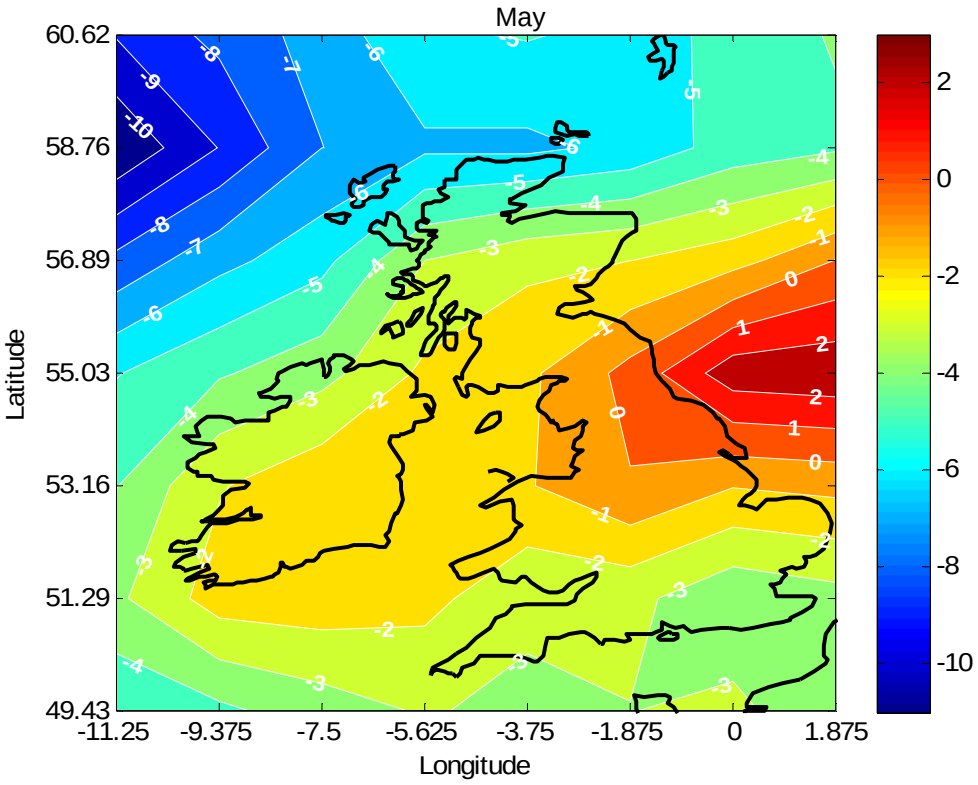
May
60.62
58.76
56.89
55.03
53.16
51.29
49.43
Latitude
-11.25
-9.375
-7.5
-5.625
-3.75
-1.875
0
1.875
Longitude
2
0
-2
-4
-6
-8
-10

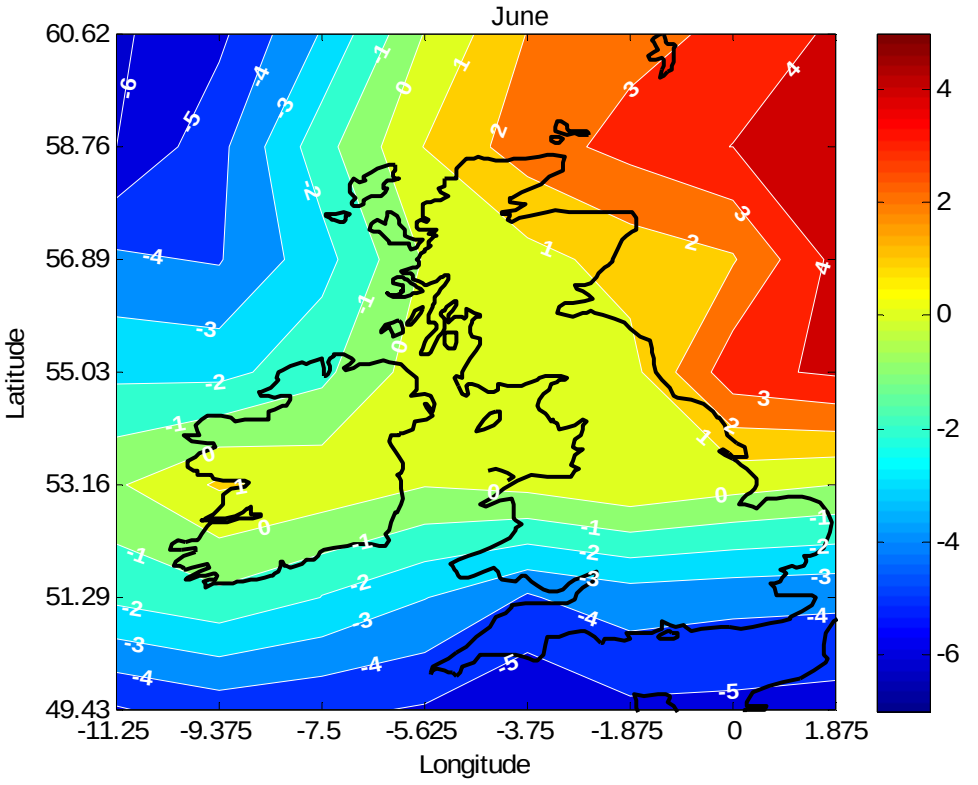
June
60.62
58.76
56.89
55.03
53.16
51.29
49.43
Latitude
-11.25
-9.375
-7.5
-5.625
-3.75
-1.875
0
1.875
Longitude
4
2
0
-2
-4
-6

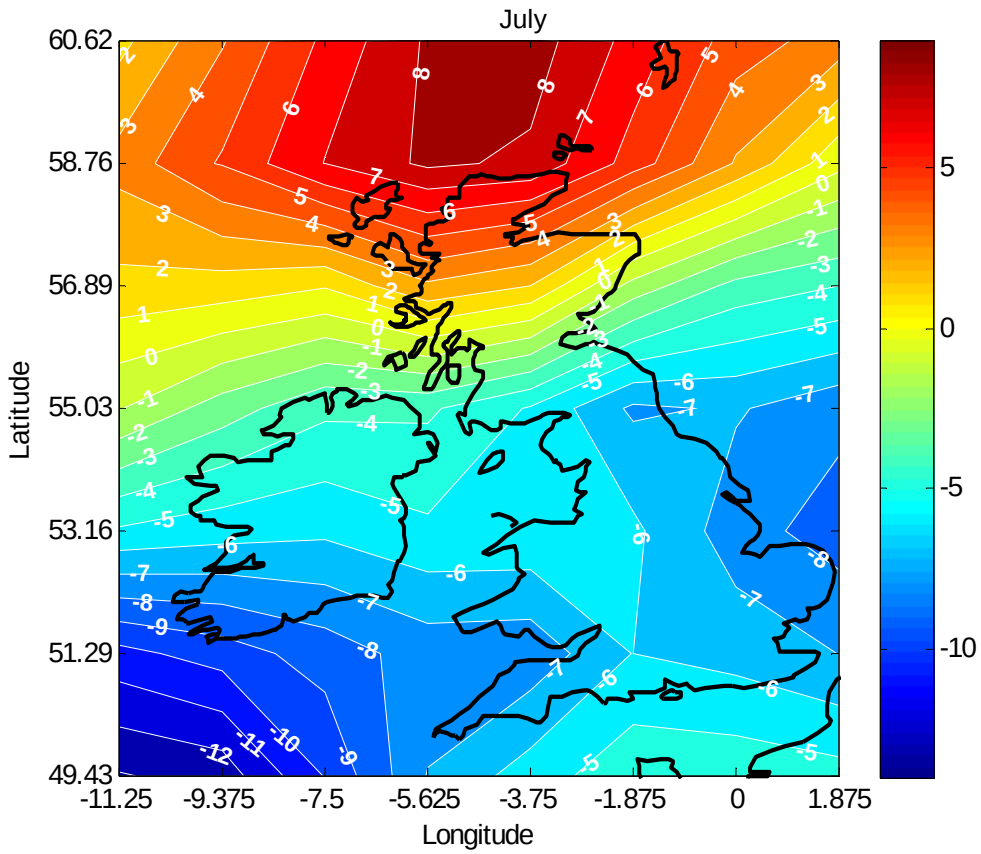
July
60.62
58.76
56.89
55.03
53.16
51.29
49.43
Latitude
-11.25
-9.375
-7.5
-5.625
-3.75
-1.875
0
1.875
Longitude
5
0
-5
-10

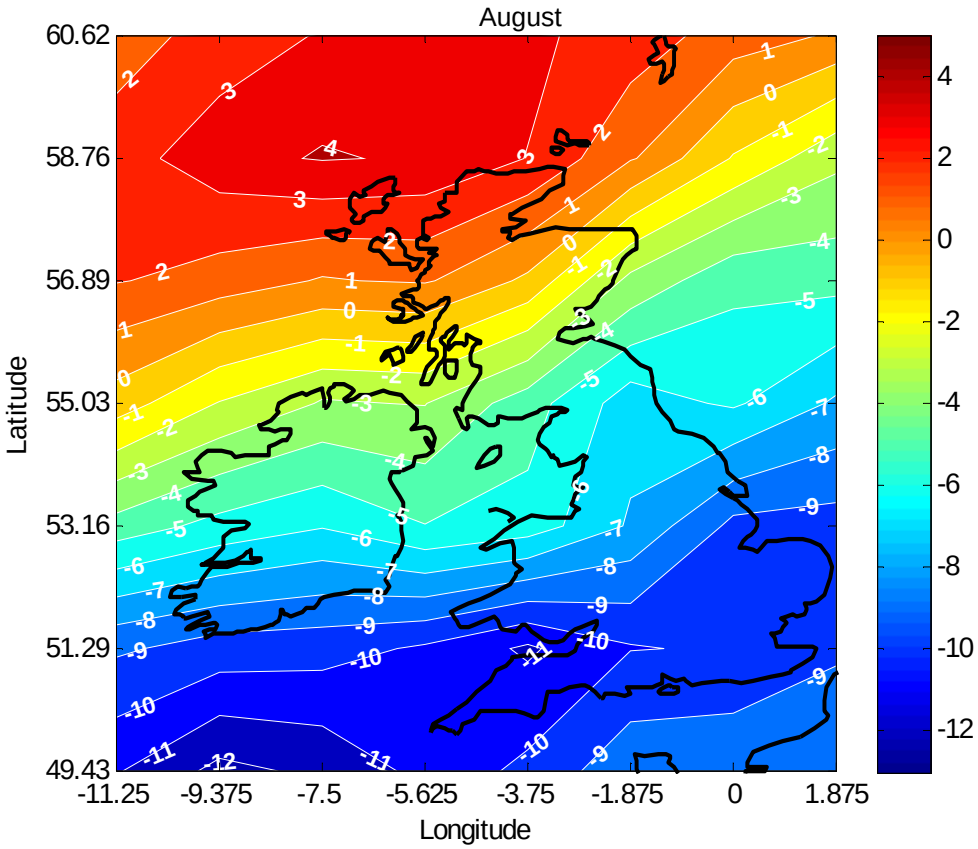
August
60.62
58.76
56.89
55.03
53.16
51.29
49.43
Latitude
-11.25
-9.375
-7.5
-5.625
-3.75
-1.875
0
1.875
Longitude
4
2
0
-2
-4
-6
-8
-10
-12

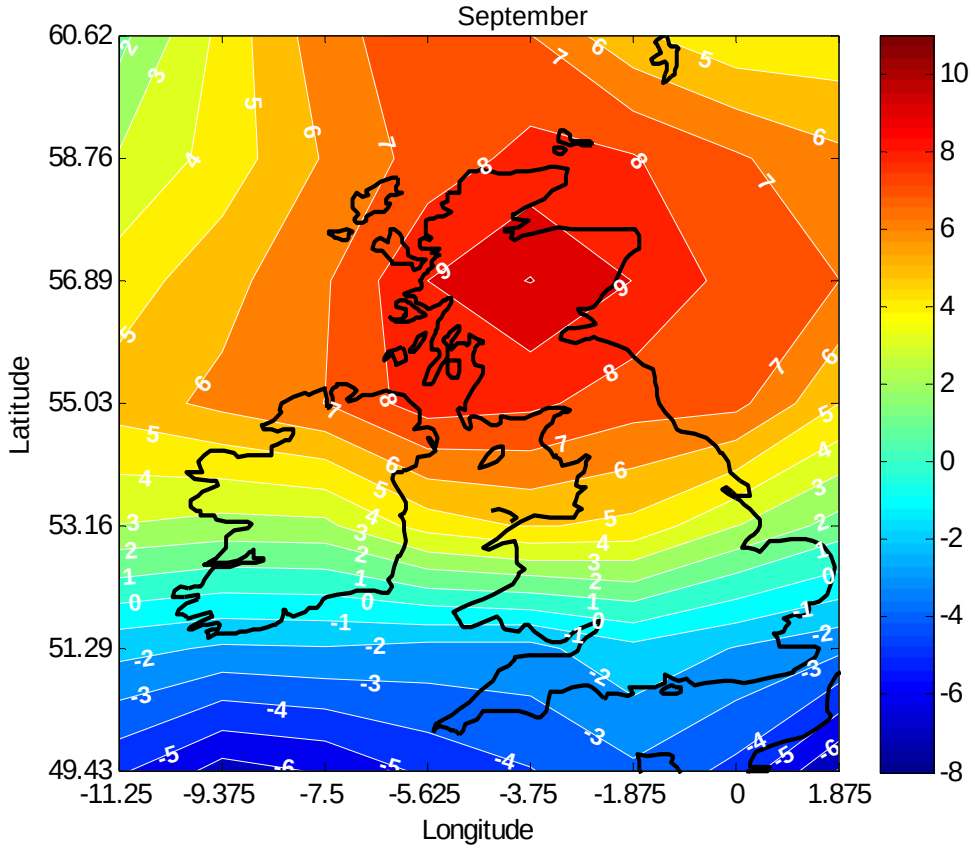
September
60.62
58.76
56.89
55.03
53.16
51.29
49.43
Latitude
-11.25
-9.375
-7.5
-5.625
-3.75
-1.875
0
1.875
Longitude
10
8
6
4
2
0
-2
-4
-6
-8

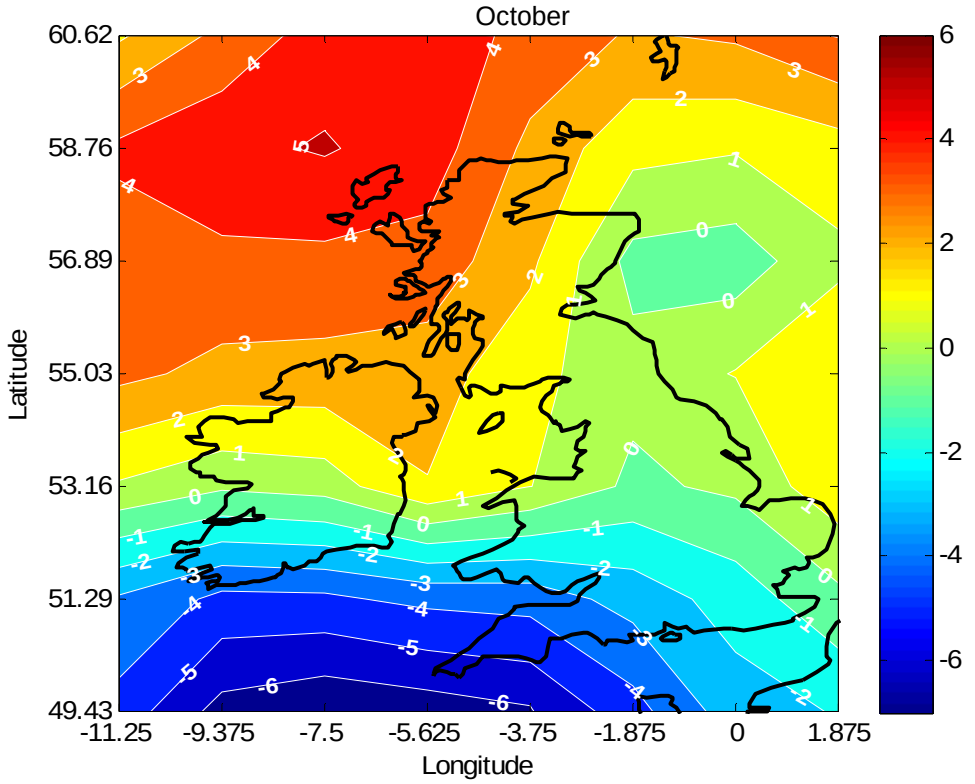
October
60.62
58.76
56.89
55.03
53.16
51.29
49.43
Latitude
-11.25
-9.375
-7.5
-5.625
-3.75
-1.875
0
1.875
Longitude
6
4
2
0
-2
-4
-6

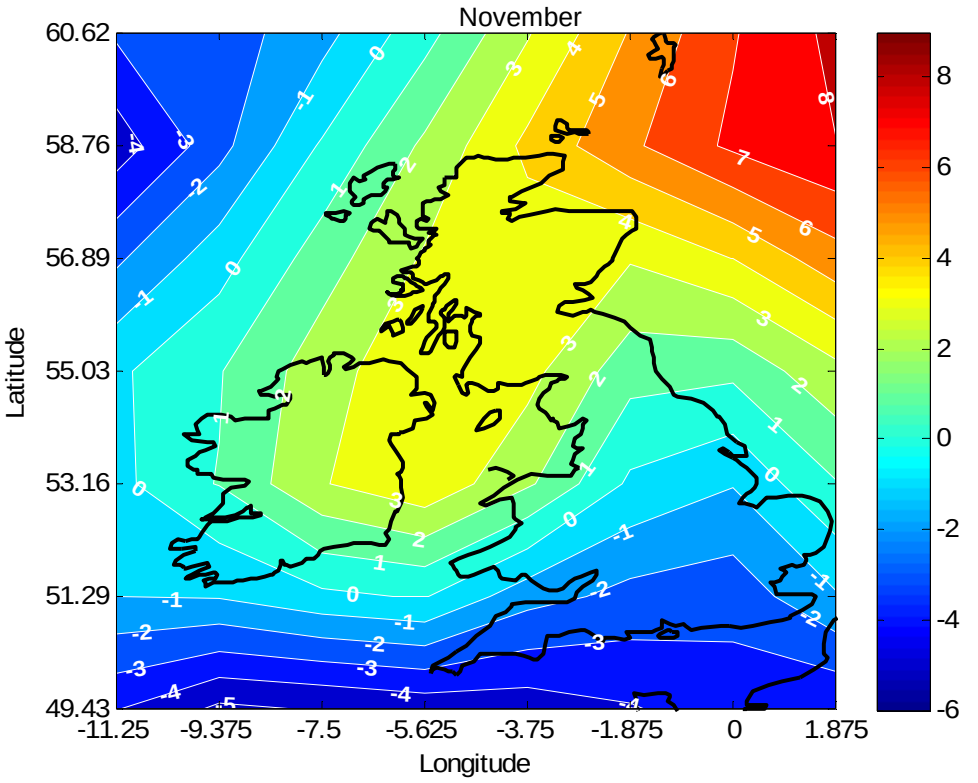
November
60.62
58.76
56.89
55.03
53.16
51.29
49.43
Latitude
-11.25
-9.375
-7.5
-5.625
-3.75
-1.875
0
1.875
Longitude
8
6
4
2
0
-2
-4
-6

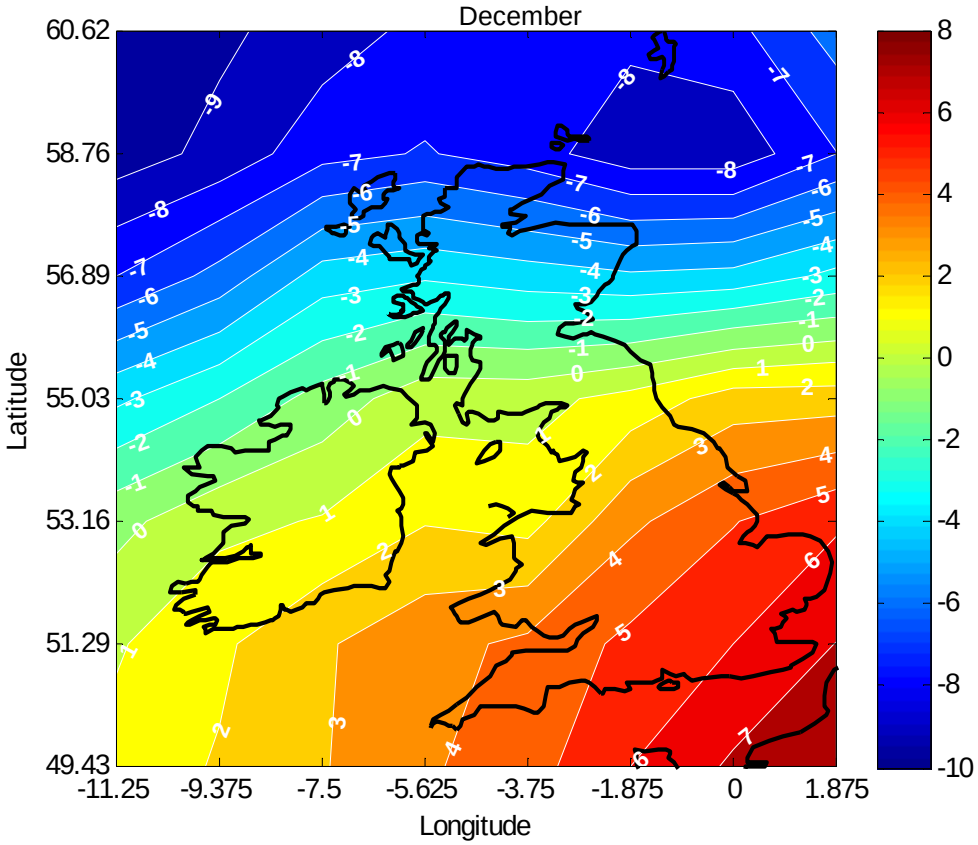
December
60.62
58.76
56.89
55.03
53.16
51.29
49.43
Latitude
-11.25
-9.375
-7.5
-5.625
-3.75
-1.875
0
1.875
Longitude
8
6
4
2
0
-2
-4
-6
-8
-10

Fig. C-6: Future, percentage differences in monthly mean wind speed (Run 4 baseline)

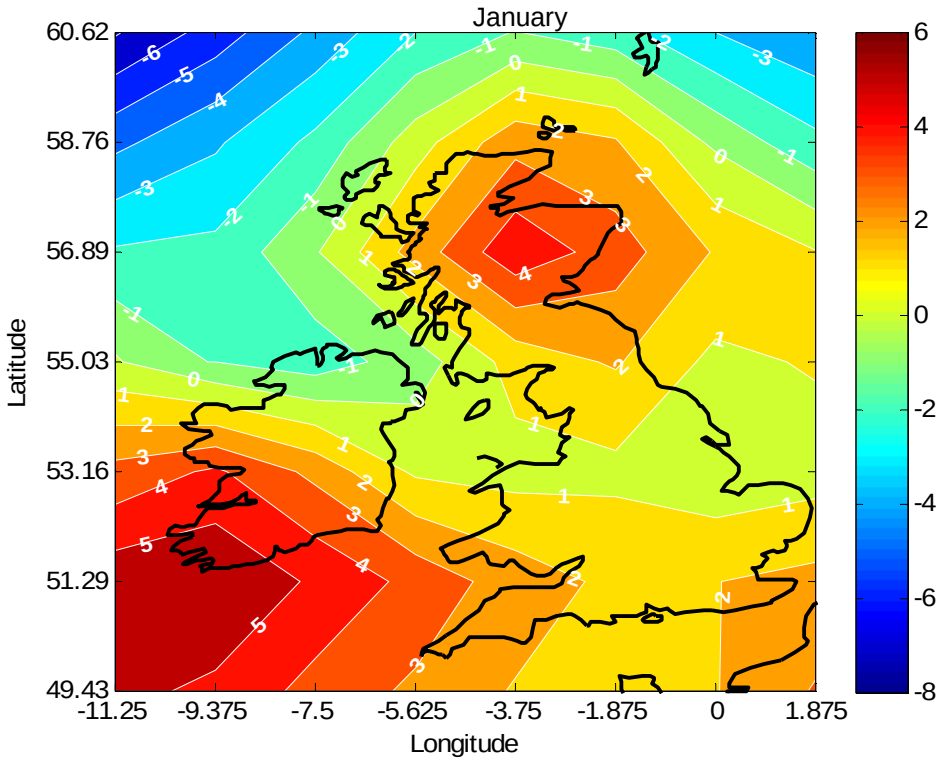

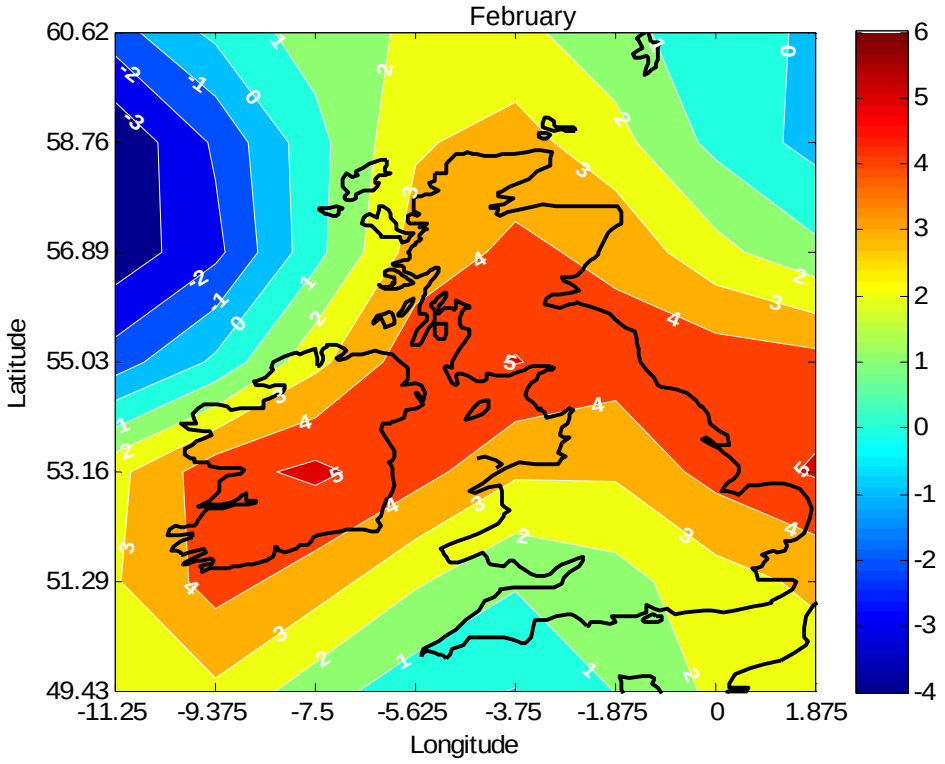

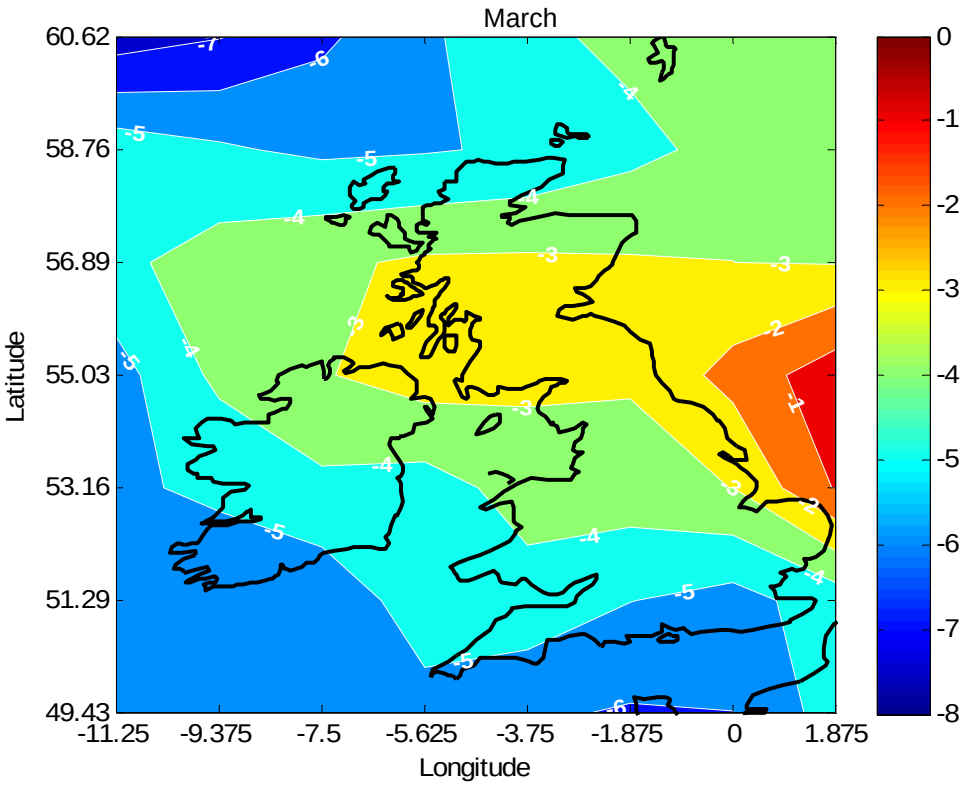
March
60.62
58.76
56.89
55.03
53.16
51.29
49.43
Latitude
-11.25
-9.375
-7.5
-5.625
-3.75
-1.875
0
1.875
Longitude
0
-1
-2
-3
-4
-5
-6
-7
-8

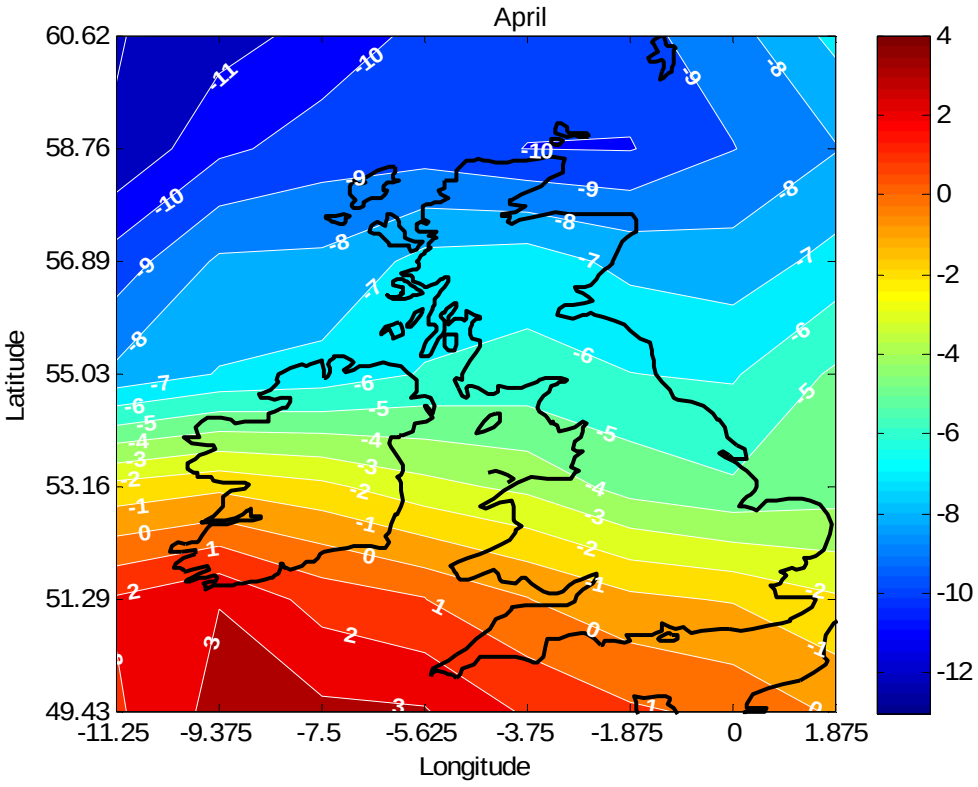
April
60.62
58.76
56.89
55.03
53.16
51.29
49.43
Latitude
-11.25
-9.375
-7.5
-5.625
-3.75
-1.875
0
1.875
Longitude
4
2
0
-2
-4
-6
-8
-10
-12

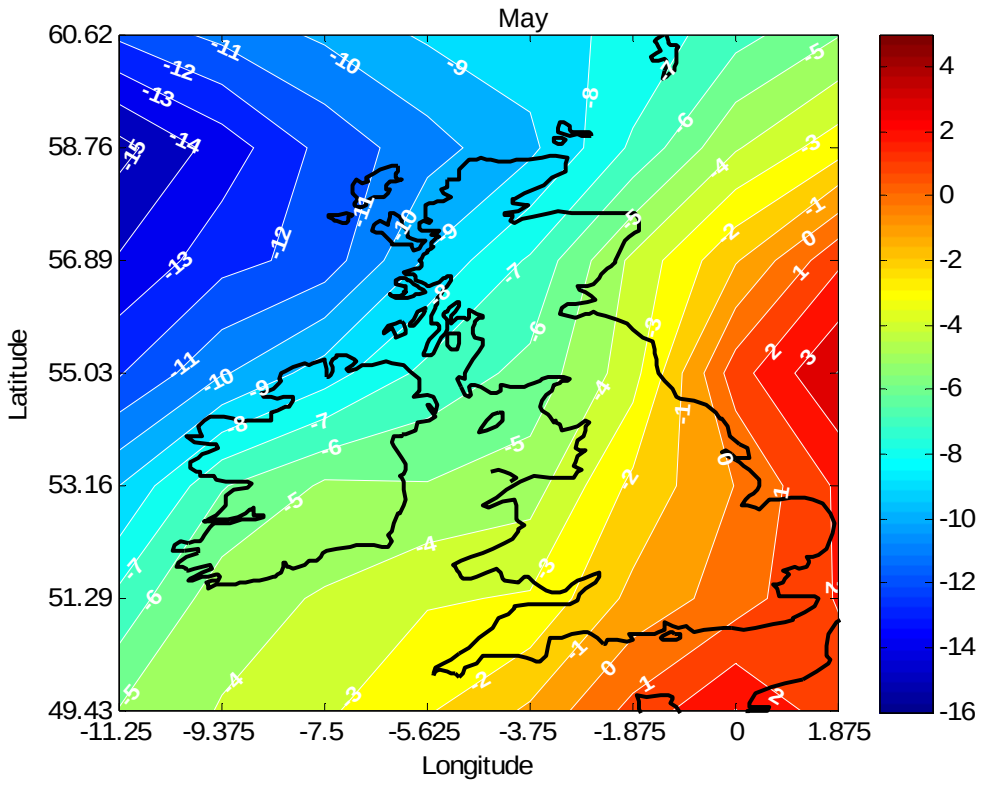
May
60.62
58.76
56.89
55.03
53.16
51.29
49.43
Latitude
-11.25
-9.375
-7.5
-5.625
-3.75
-1.875
0
1.875
Longitude
4
2
0
-2
-4
-6
-8
-10
-12
-14
-16

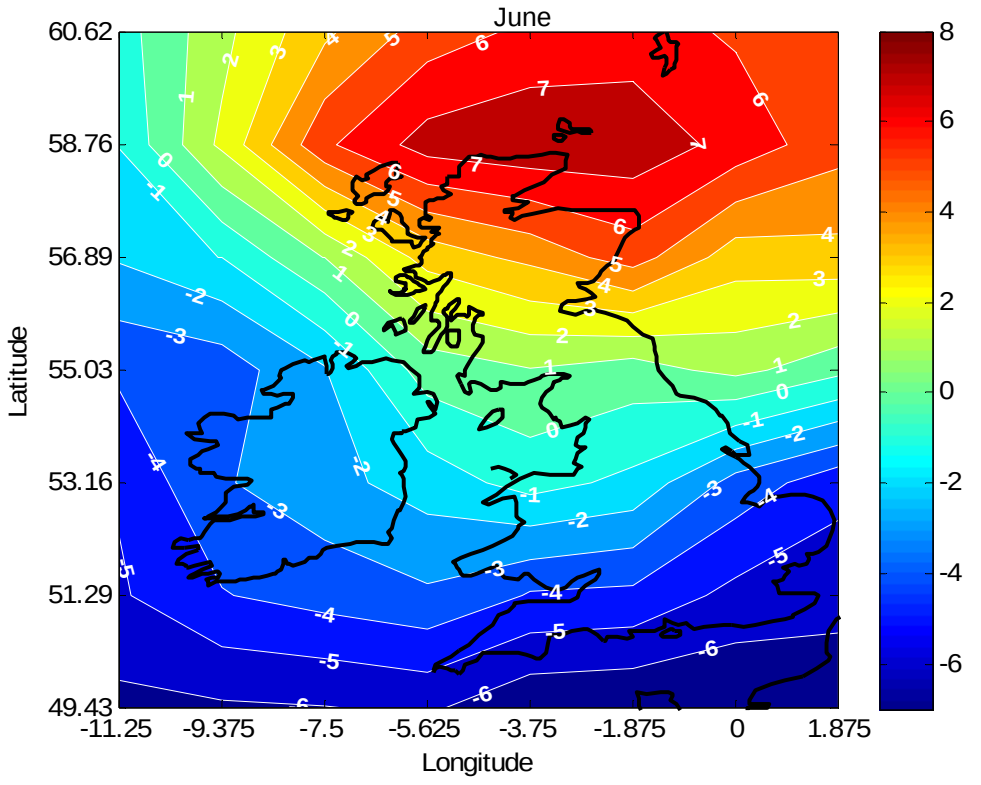
June
60.62
58.76
56.89
55.03
53.16
51.29
49.43
Latitude
-11.25
-9.375
-7.5
-5.625
-3.75
-1.875
0
1.875
Longitude
8
6
4
2
0
-2
-4
-6

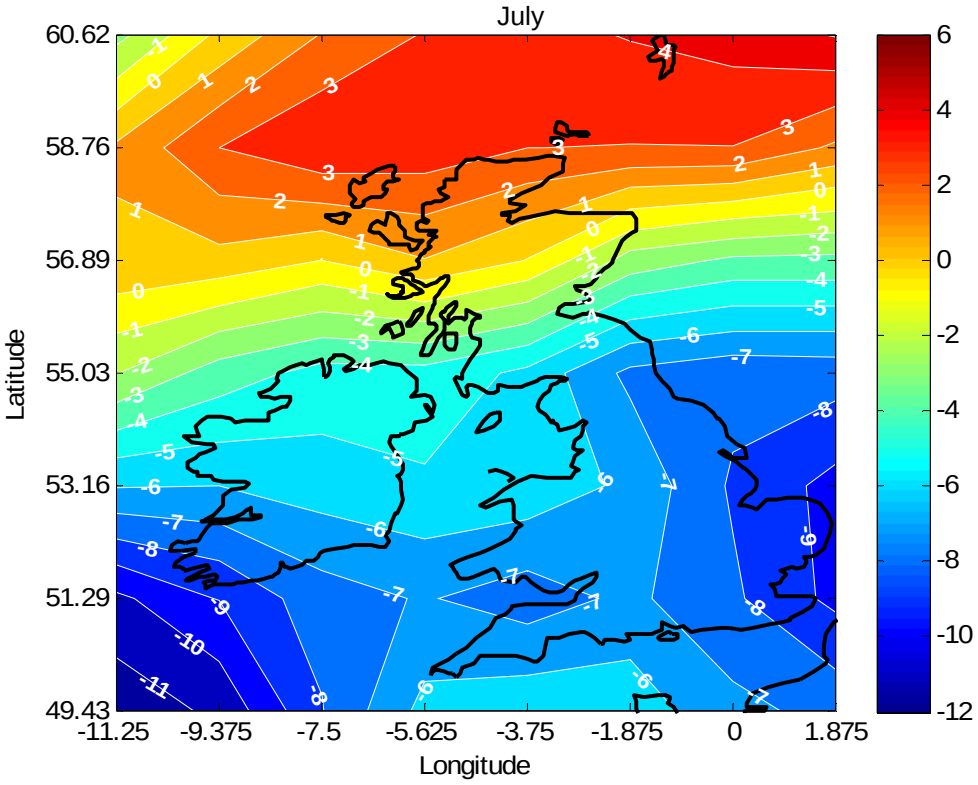
July
60.62
58.76
56.89
55.03
53.16
51.29
49.43
Latitude
-11.25
-9.375
-7.5
-5.625
-3.75
-1.875
0
1.875
Longitude
6
4
2
0
-2
-4
-6
-8
-10
-12

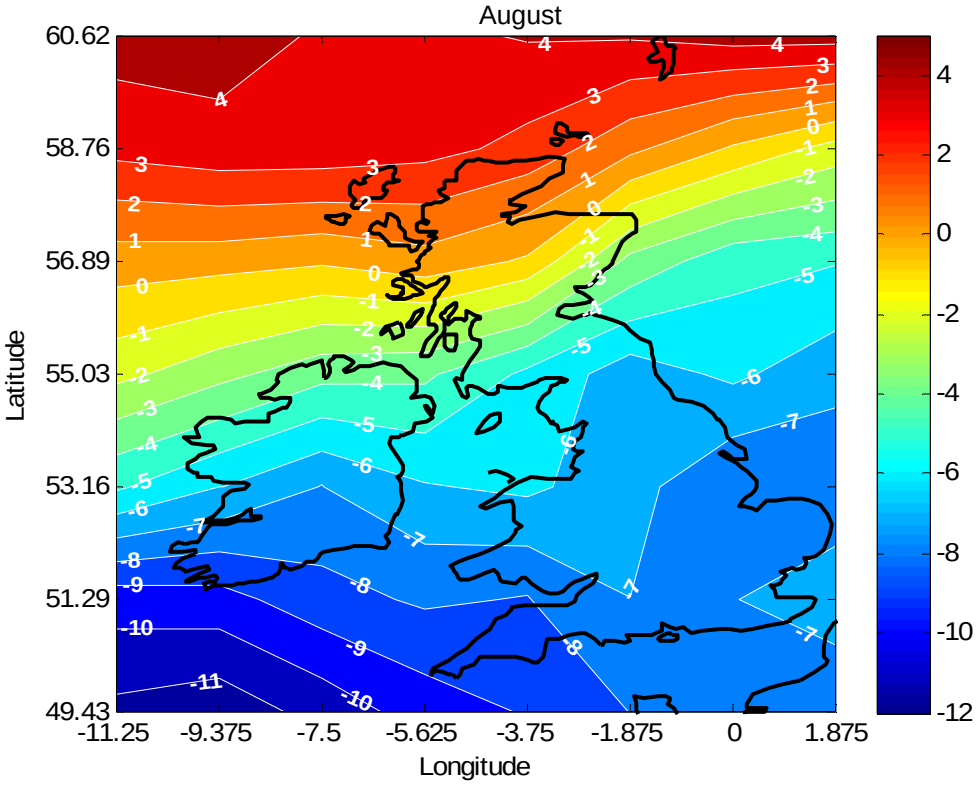
August
60.62
58.76
56.89
55.03
53.16
51.29
49.43
Latitude
-11.25
-9.375
-7.5
-5.625
-3.75
-1.875
0
1.875
Longitude
4
2
0
-2
-4
-6
-8
-10
-12

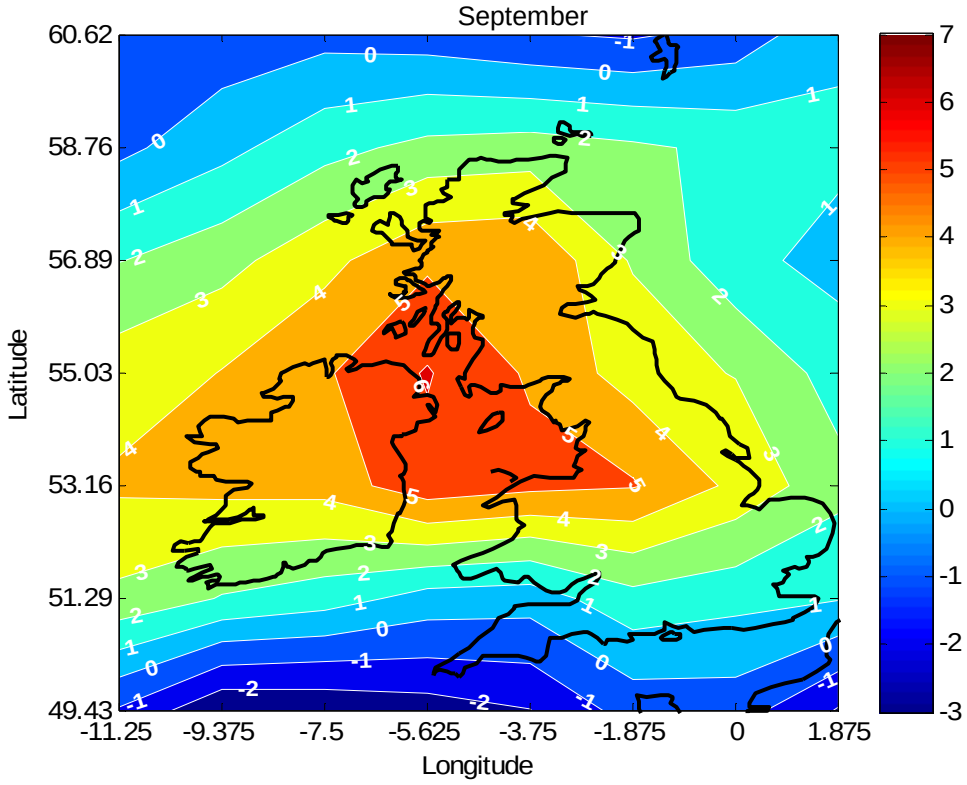
September
60.62
58.76
56.89
55.03
53.16
51.29
49.43
Latitude
-11.25
-9.375
-7.5
-5.625
-3.75
-1.875
0
1.875
Longitude
7
6
5
4
3
2
1
0
-1
-2
-3

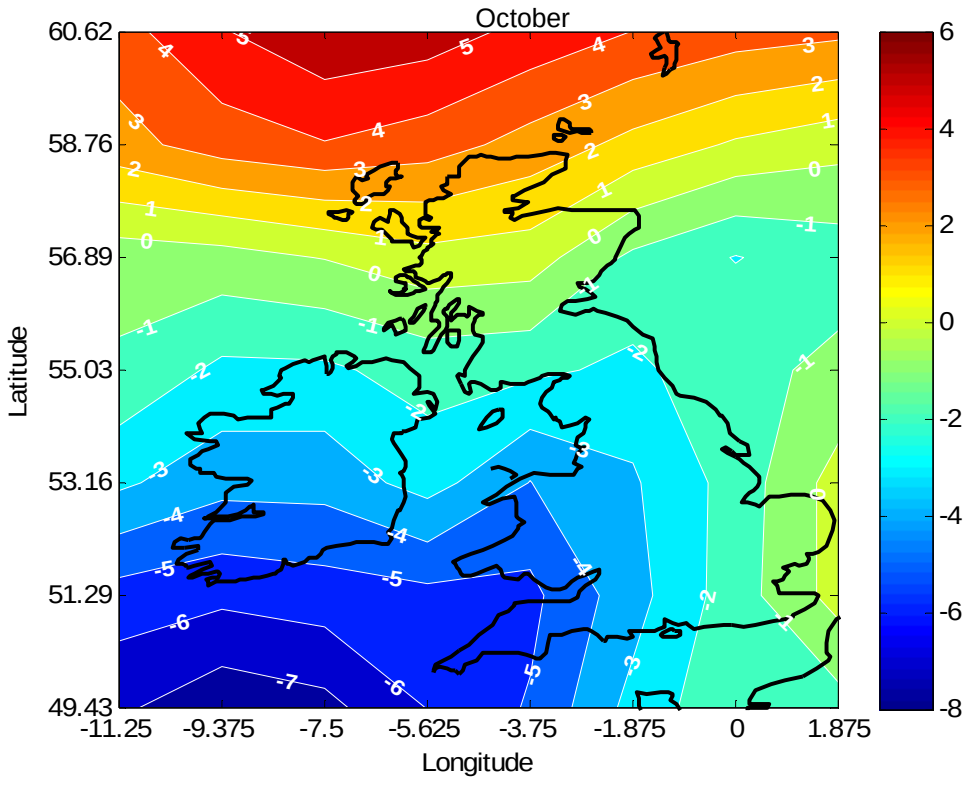
October
60.62
58.76
56.89
55.03
53.16
51.29
49.43
Latitude
-11.25
-9.375
-7.5
-5.625
-3.75
-1.875
0
1.875
Longitude
6
4
2
0
-2
-4
-6
-8

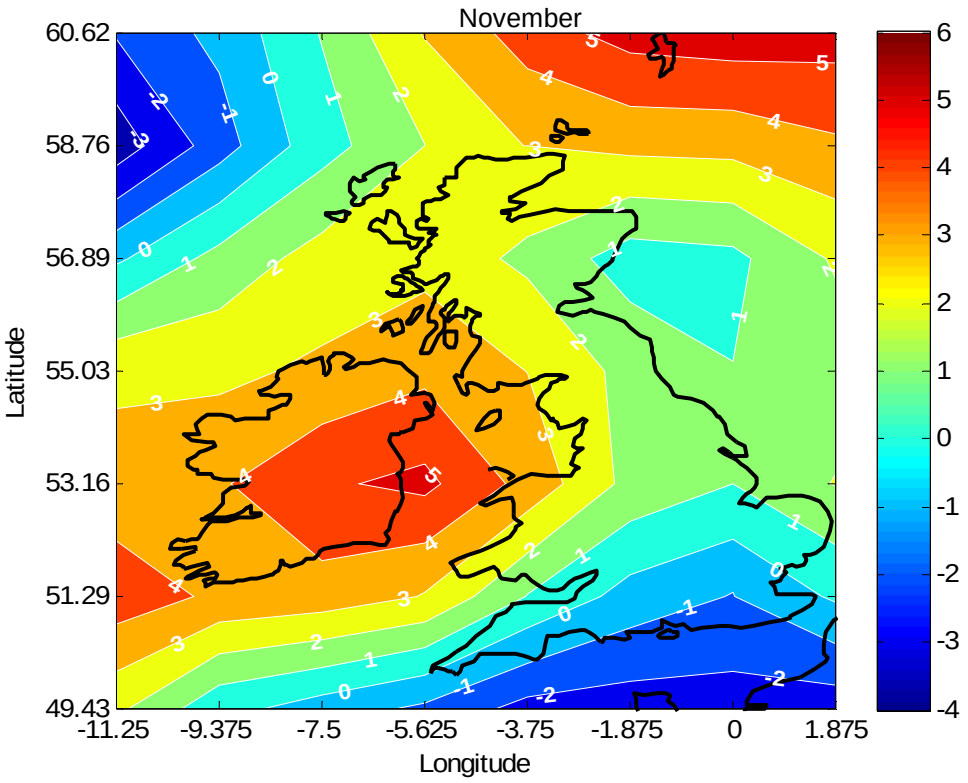
November
60.62
58.76
56.89
55.03
53.16
51.29
49.43
Latitude
-11.25
-9.375
-7.5
-5.625
-3.75
-1.875
0
1.875
Longitude
6
5
4
3
2
1
0
-1
-2
-3
-4

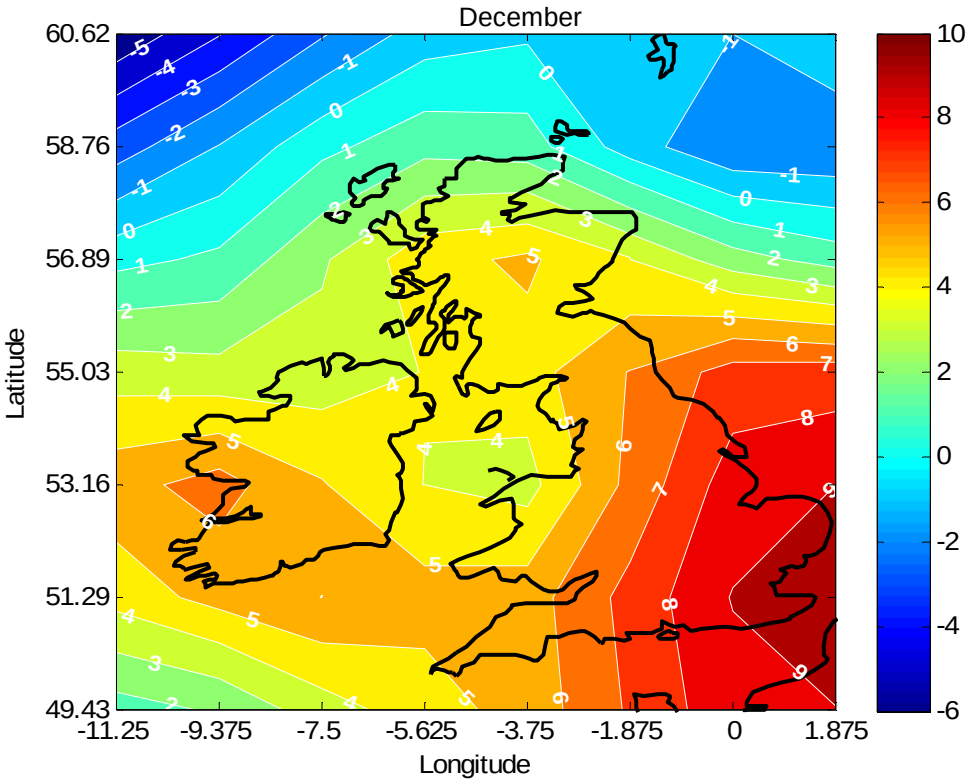
December
60.62
58.76
56.89
55.03
53.16
51.29
49.43
Latitude
-11.25
-9.375
-7.5
-5.625
-3.75
-1.875
0
1.875
Longitude
10
8
6
4
2
0
-2
-4
-6

Fig. C-7: Future, monthly mean wind speed vectors (Run 1 baseline)

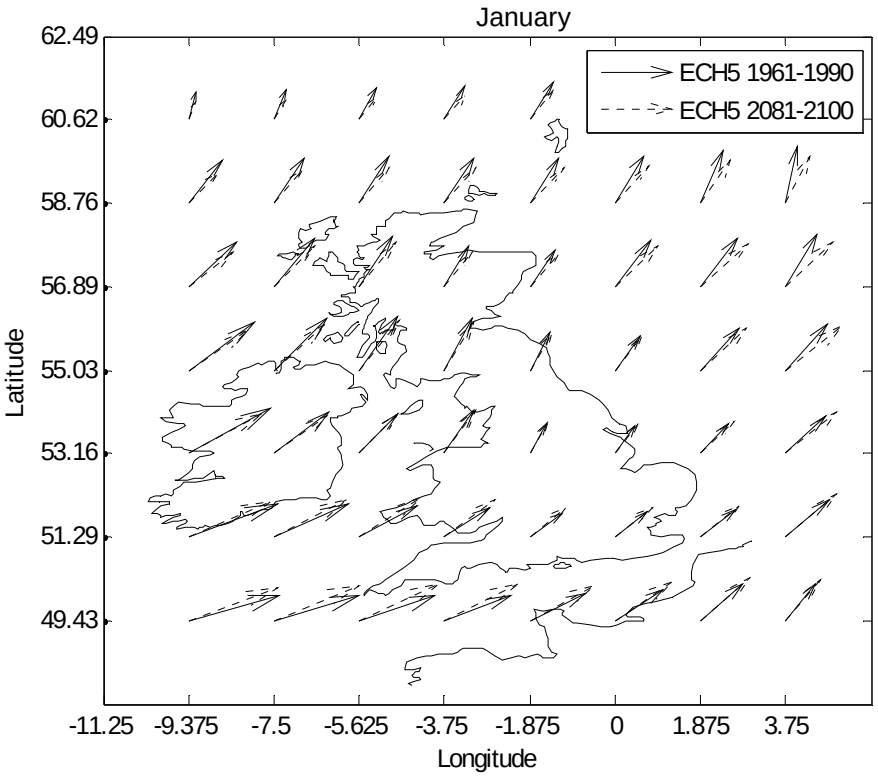

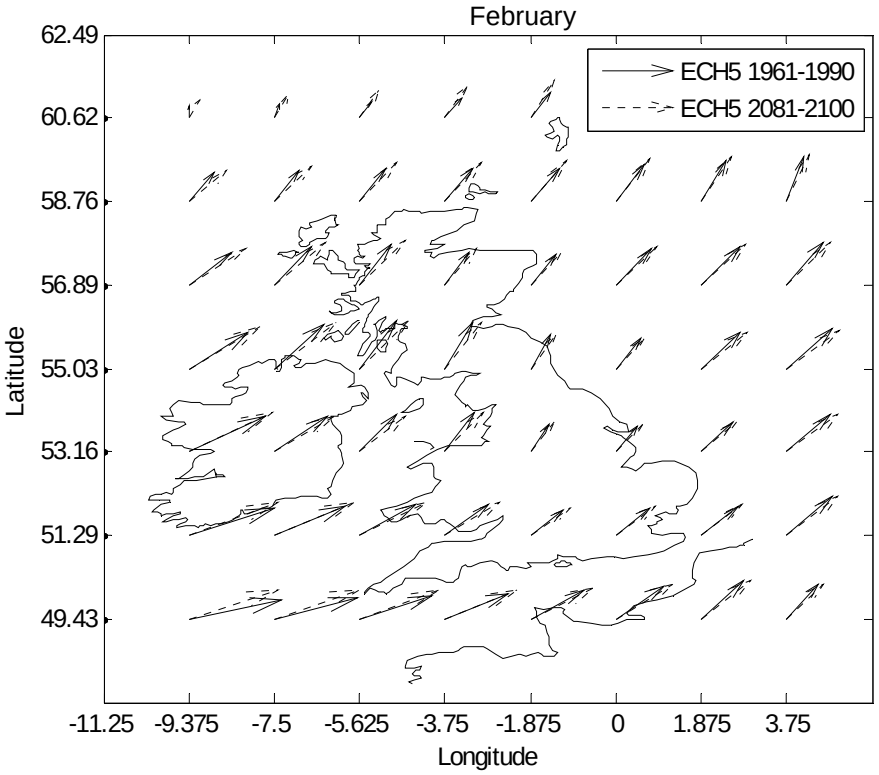

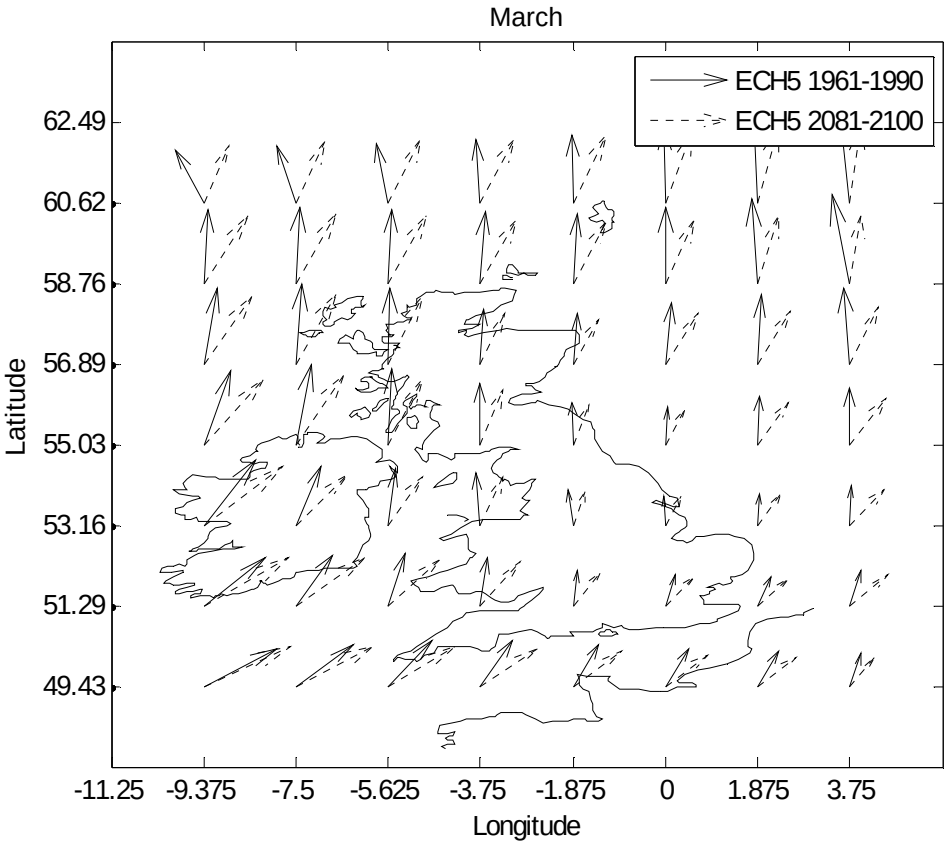
March
ECH5 1961-1990
ECH5 2081-2100
62.49
60.62
58.76
56.89
55.03
53.16
51.29
49.43
Latitude
-11.25
-9.375
-7.5
-5.625
-3.75
-1.875
0
1.875
3.75
Longitude

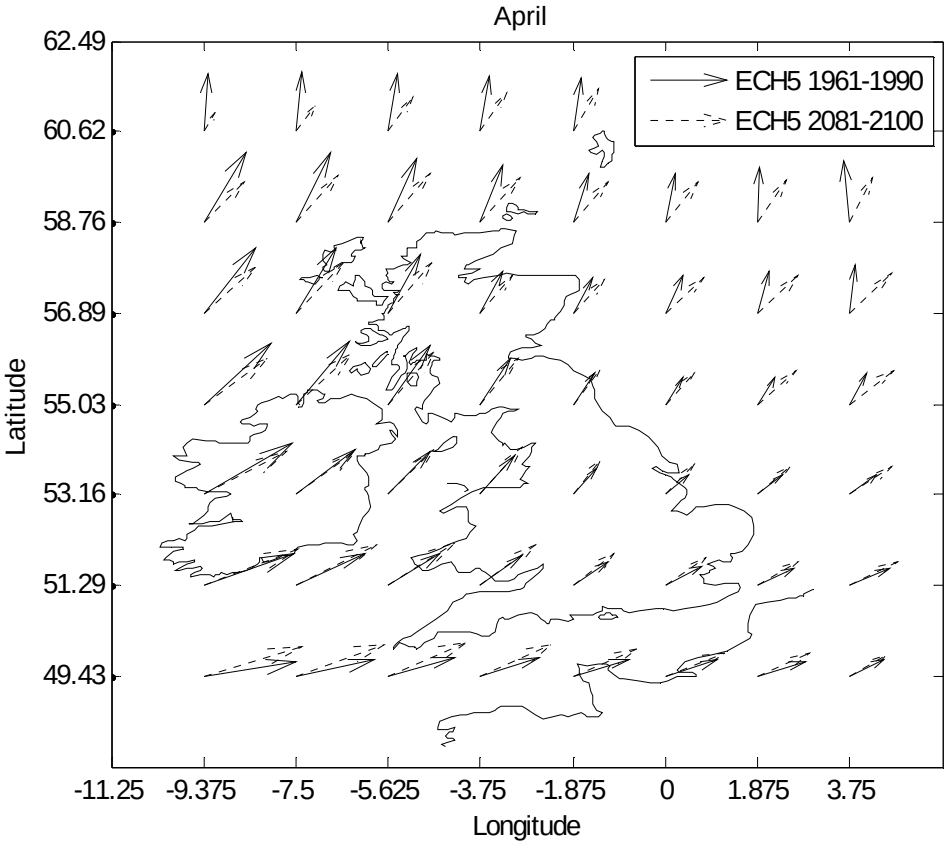
April
ECH5 1961-1990
ECH5 2081-2100
62.49
60.62
58.76
56.89
55.03
53.16
51.29
49.43
Latitude
-11.25
-9.375
-7.5
-5.625
-3.75
-1.875
0
1.875
3.75
Longitude

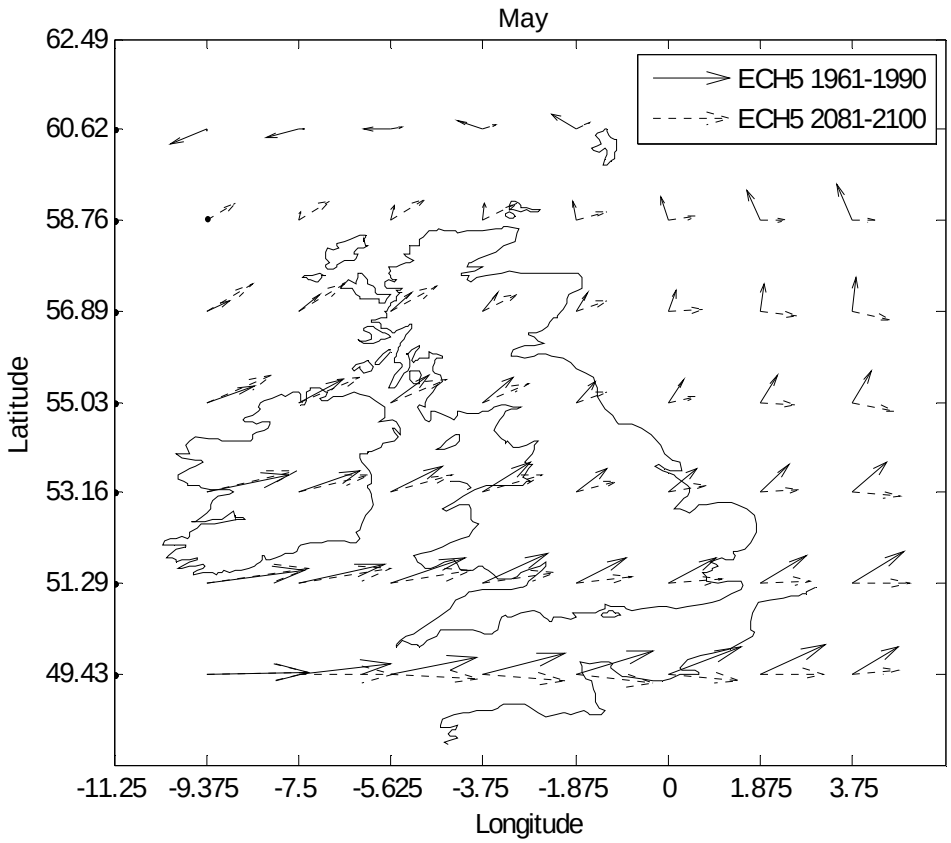
May
ECH5 1961-1990
ECH5 2081-2100
62.49
60.62
58.76
56.89
55.03
53.16
51.29
49.43
Latitude
-11.25
-9.375
-7.5
-5.625
-3.75
-1.875
0
1.875
3.75
Longitude

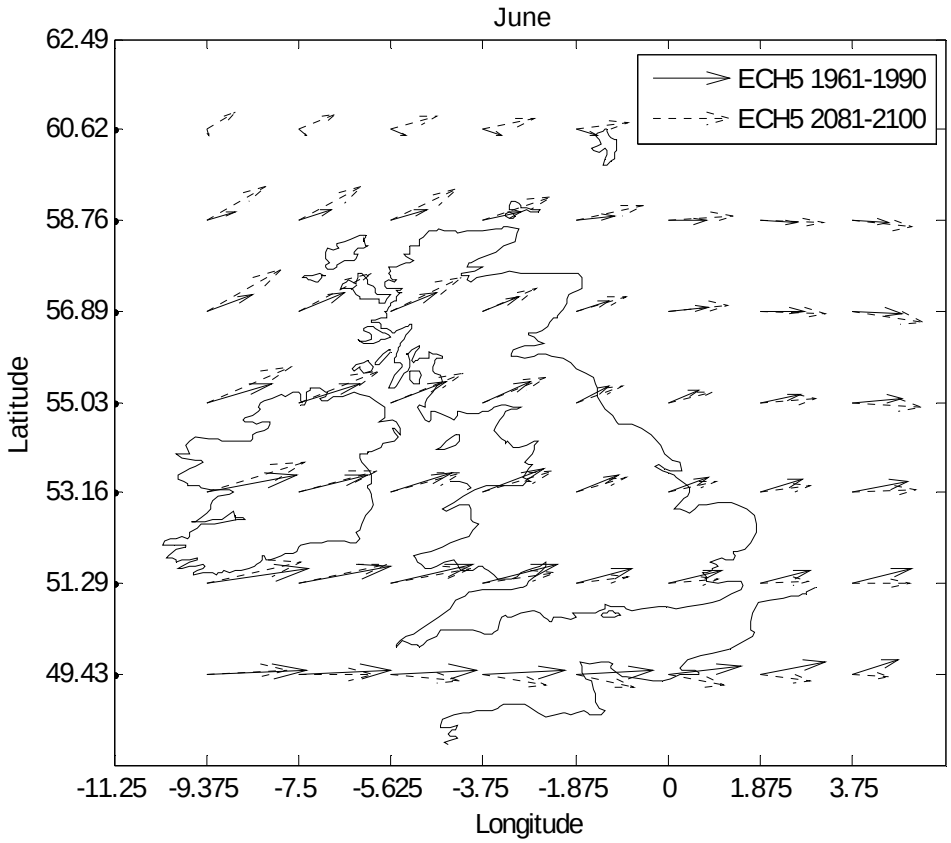
June
ECH5 1961-1990
ECH5 2081-2100
62.49
60.62
58.76
56.89
55.03
53.16
51.29
49.43
Latitude
-11.25
-9.375
-7.5
-5.625
-3.75
-1.875
0
1.875
3.75
Longitude

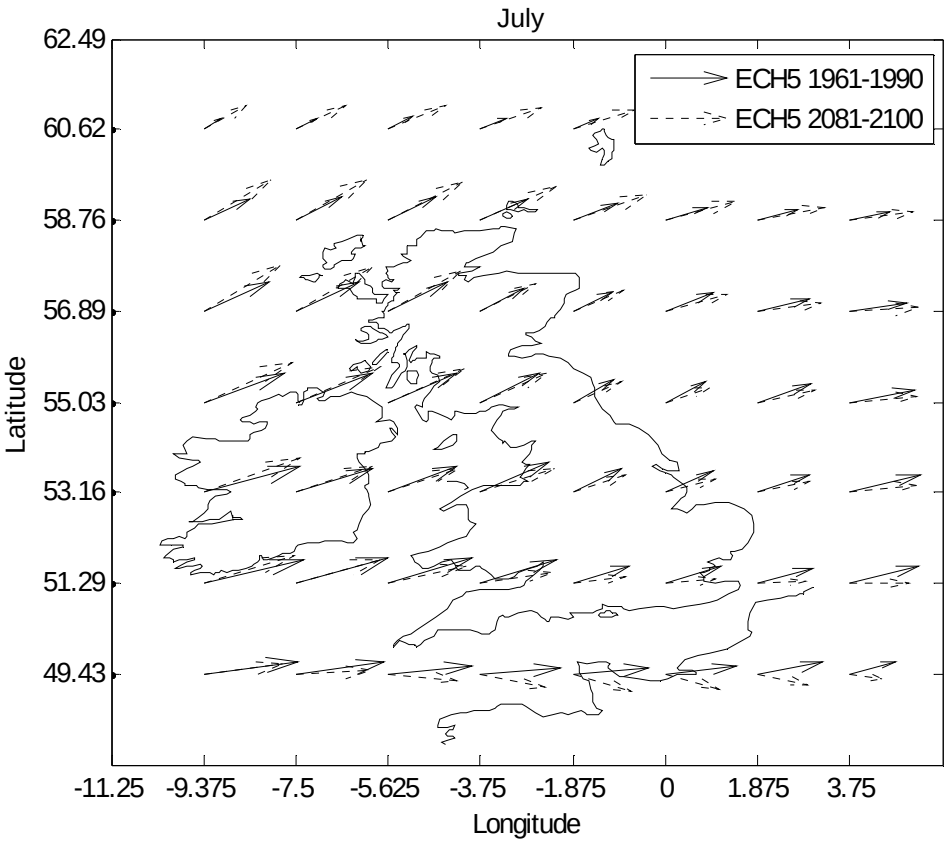
July
ECH5 1961-1990
ECH5 2081-2100
62.49
60.62
58.76
56.89
55.03
53.16
51.29
49.43
Latitude
-11.25
-9.375
-7.5
-5.625
-3.75
-1.875
0
1.875
3.75
Longitude

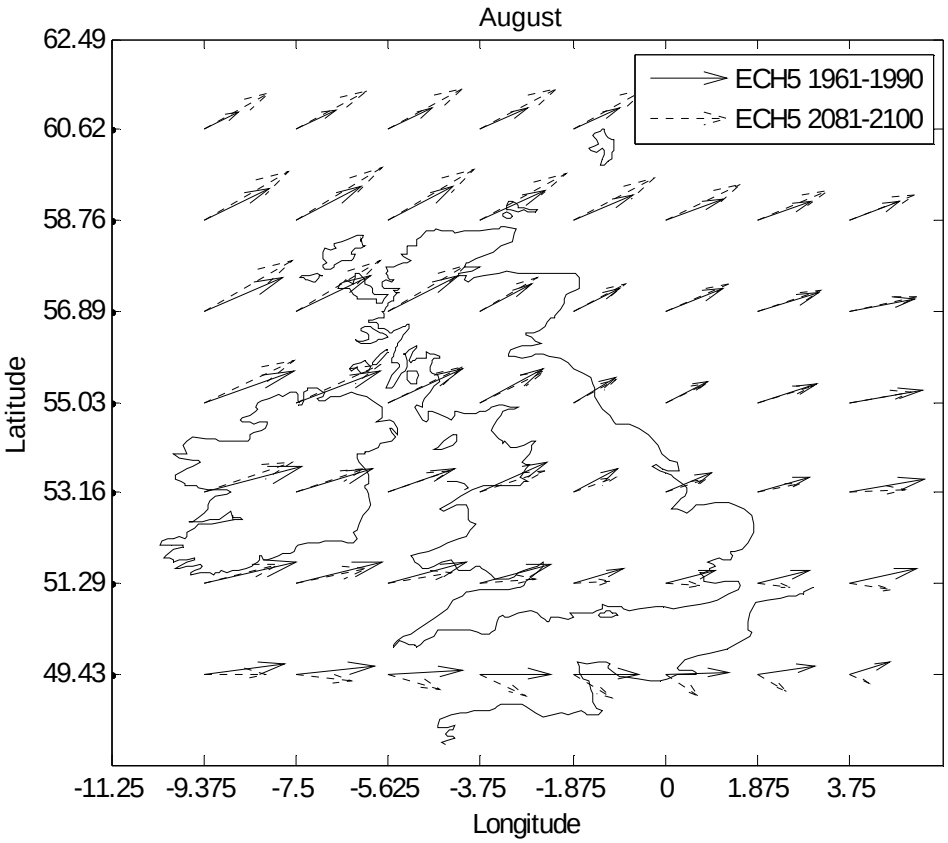
August
ECH5 1961-1990
ECH5 2081-2100
62.49
60.62
58.76
56.89
55.03
53.16
51.29
49.43
Latitude
-11.25
-9.375
-7.5
-5.625
-3.75
-1.875
0
1.875
3.75
Longitude

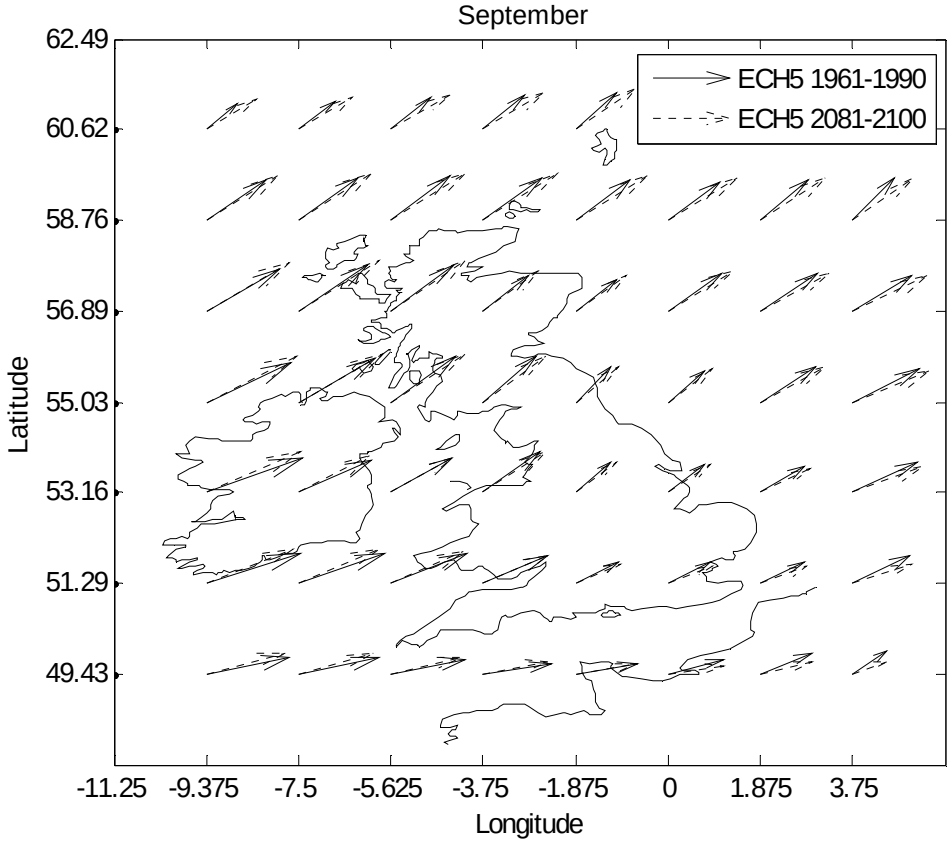
September
ECH5 1961-1990
ECH5 2081-2100
62.49
60.62
58.76
56.89
55.03
53.16
51.29
49.43
Latitude
-11.25
-9.375
-7.5
-5.625
-3.75
-1.875
0
1.875
3.75
Longitude

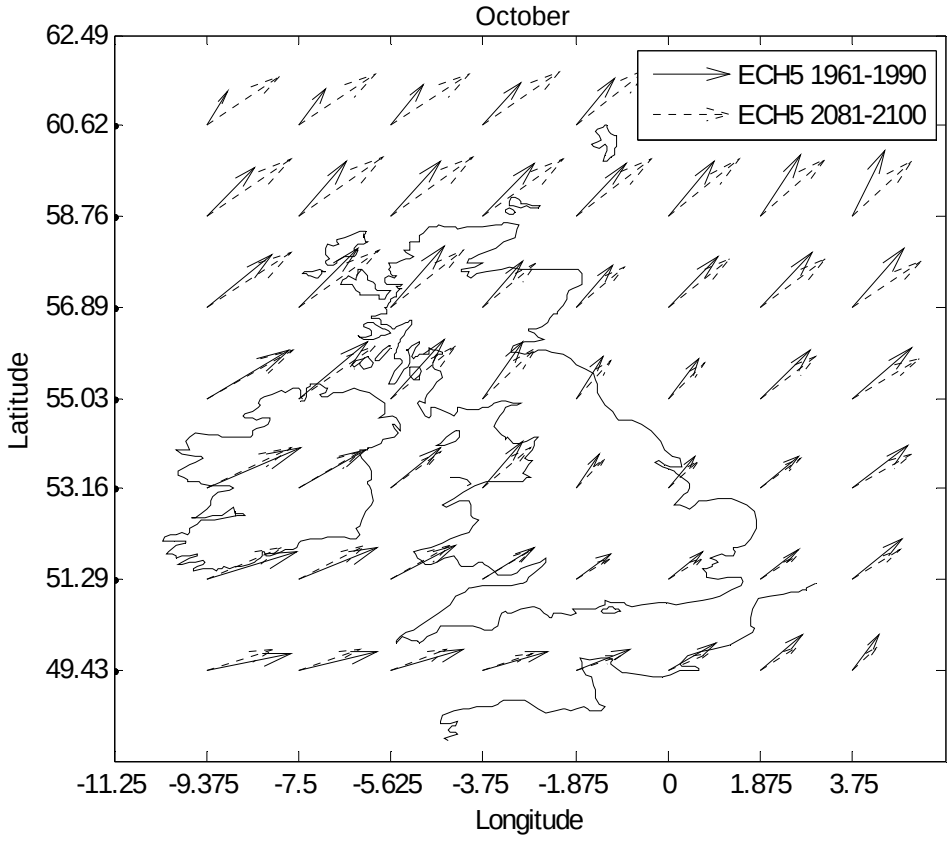
October
ECH5 1961-1990
ECH5 2081-2100
62.49
60.62
58.76
56.89
55.03
53.16
51.29
49.43
Latitude
-11.25
-9.375
-7.5
-5.625
-3.75
-1.875
0
1.875
3.75
Longitude

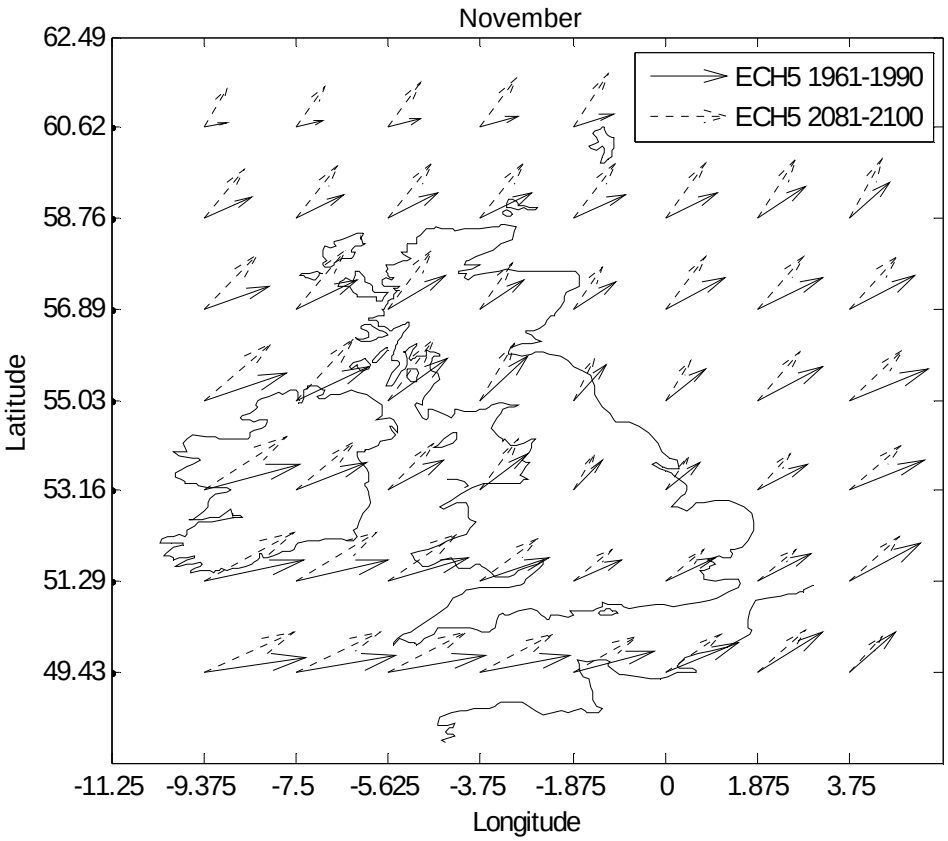
November
ECH5 1961-1990
ECH5 2081-2100
62.49
60.62
58.76
56.89
55.03
53.16
51.29
49.43
Latitude
-11.25
-9.375
-7.5
-5.625
-3.75
-1.875
0
1.875
3.75
Longitude

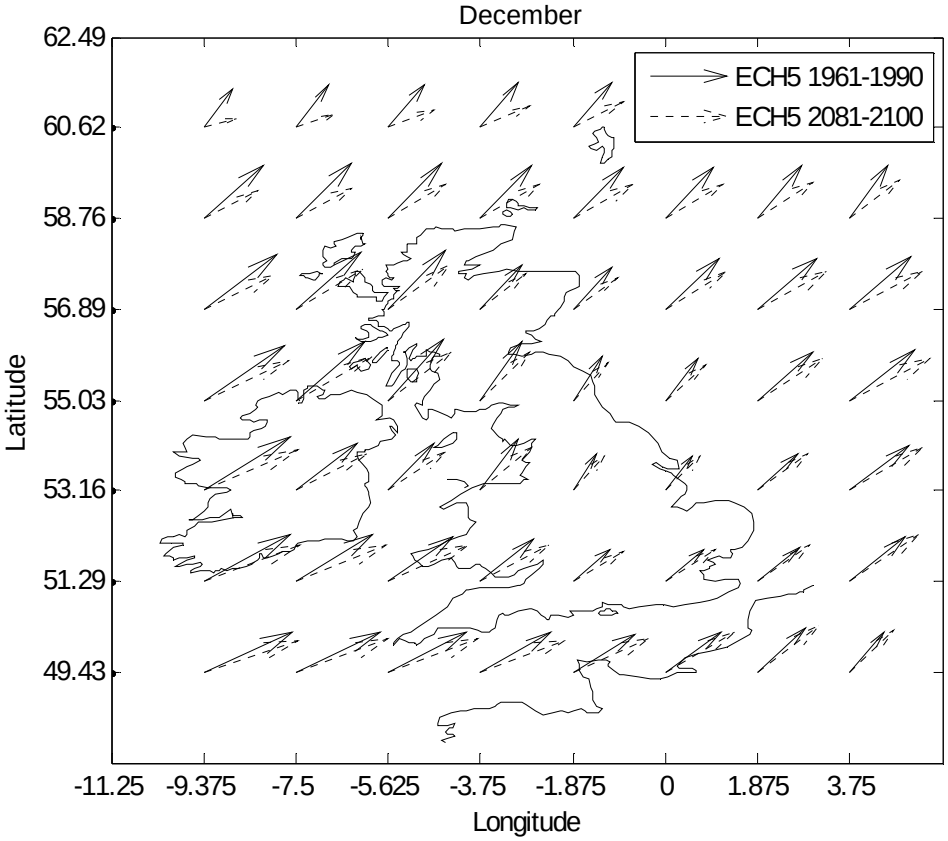
December
ECH5 1961-1990
ECH5 2081-2100
62.49
60.62
58.76
56.89
55.03
53.16
51.29
49.43
Latitude
-11.25
-9.375
-7.5
-5.625
-3.75
-1.875
0
1.875
3.75
Longitude

Fig. C-8: Future, monthly mean wind speed vectors (Run 4 baseline)

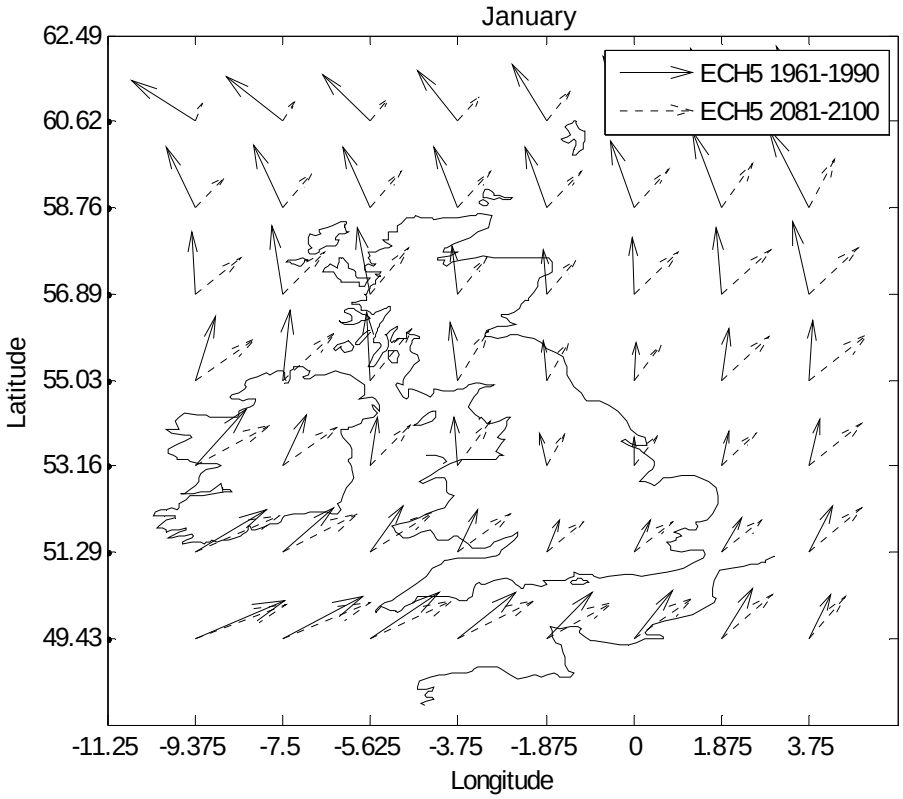

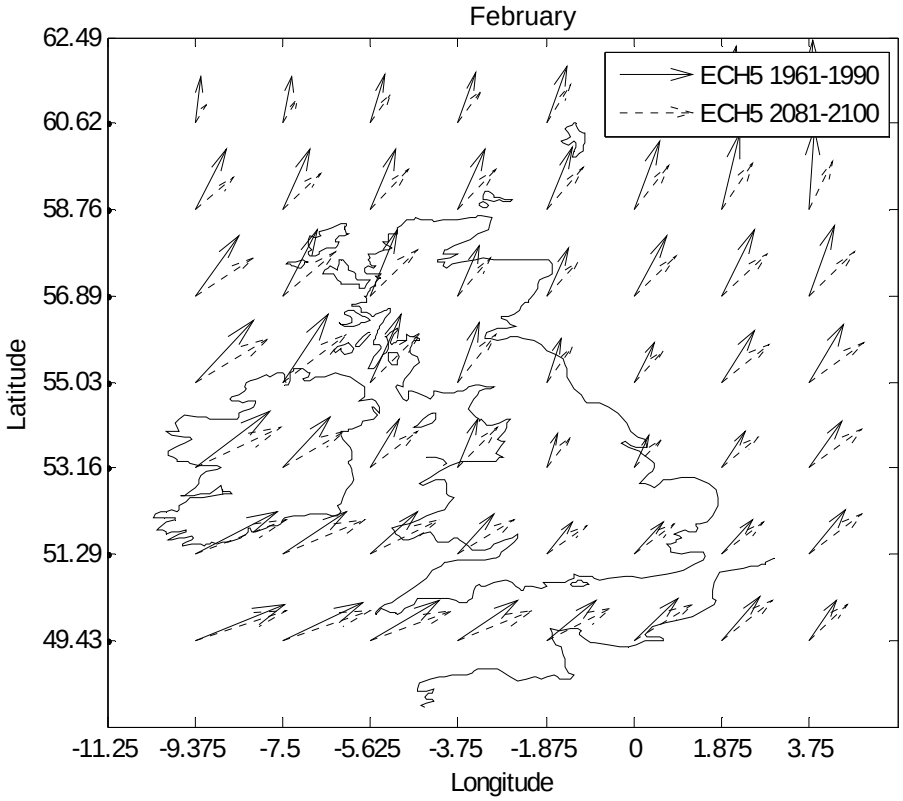

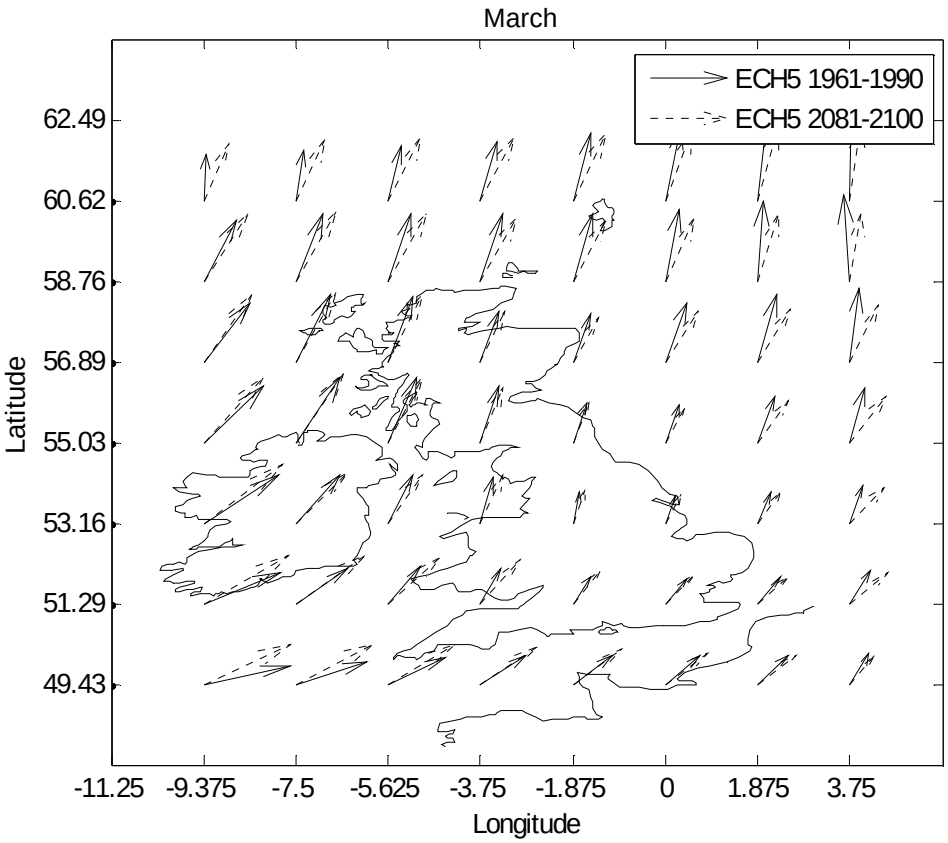
March
ECH5 1961-1990
ECH5 2081-2100
62.49
60.62
58.76
56.89
55.03
53.16
51.29
49.43
Latitude
-11.25
-9.375
-7.5
-5.625
-3.75
-1.875
0
1.875
3.75
Longitude

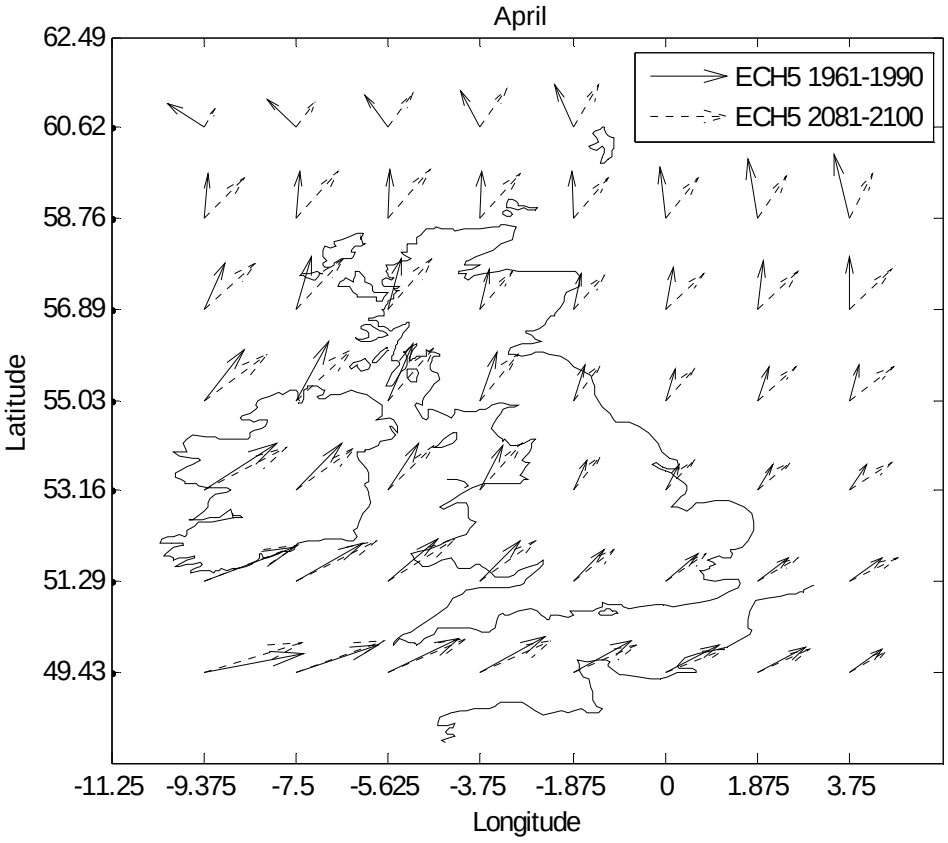
April
ECH5 1961-1990
ECH5 2081-2100
62.49
60.62
58.76
56.89
55.03
53.16
51.29
49.43
Latitude
-11.25
-9.375
-7.5
-5.625
-3.75
-1.875
0
1.875
3.75
Longitude

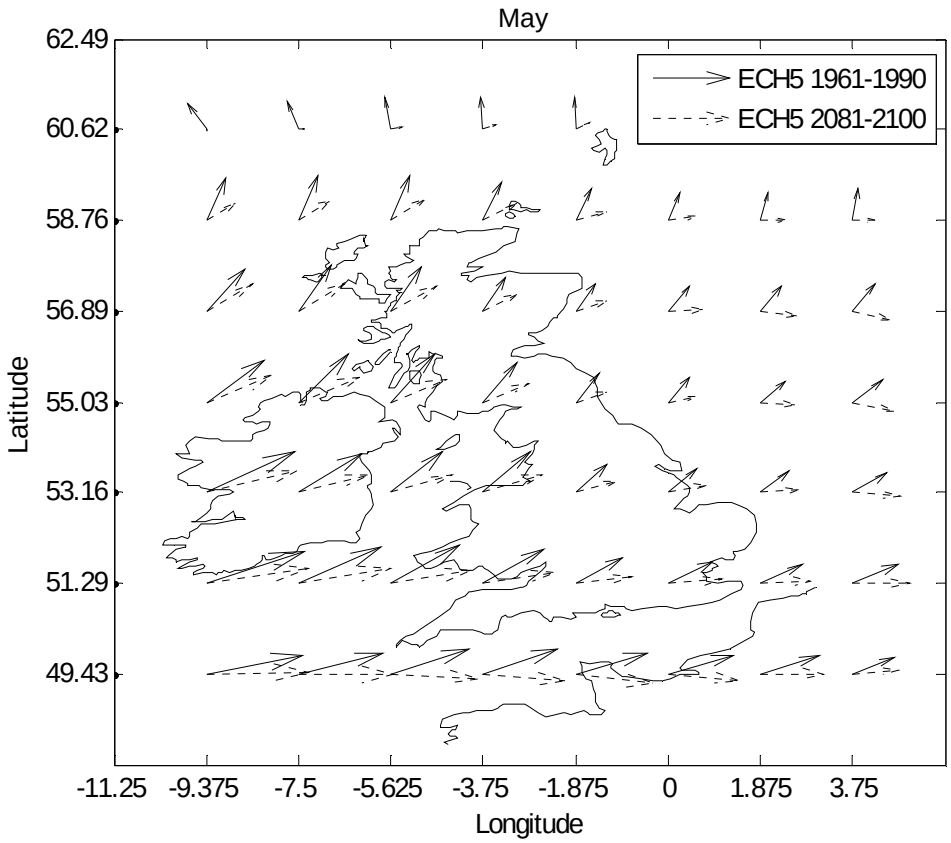
May
ECH5 1961-1990
ECH5 2081-2100
62.49
60.62
58.76
56.89
55.03
53.16
51.29
49.43
Latitude
-11.25
-9.375
-7.5
-5.625
-3.75
-1.875
0
1.875
3.75
Longitude

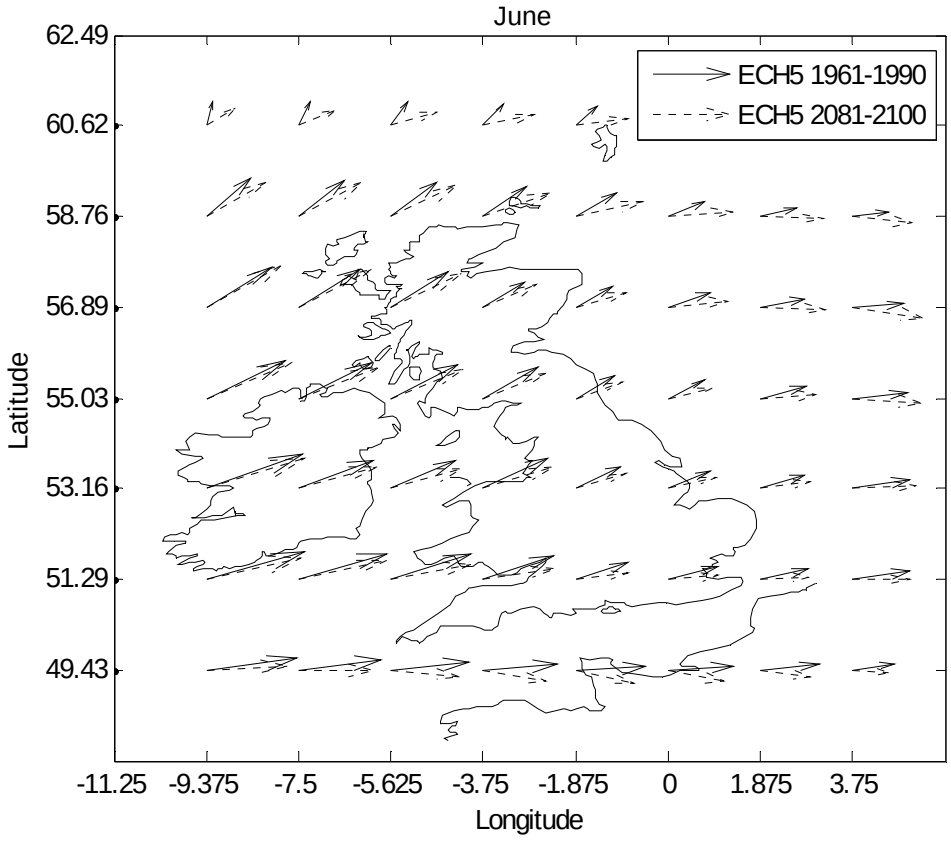
June
ECH5 1961-1990
ECH5 2081-2100
62.49
60.62
58.76
56.89
55.03
53.16
51.29
49.43
Latitude
-11.25
-9.375
-7.5
-5.625
-3.75
-1.875
0
1.875
3.75
Longitude

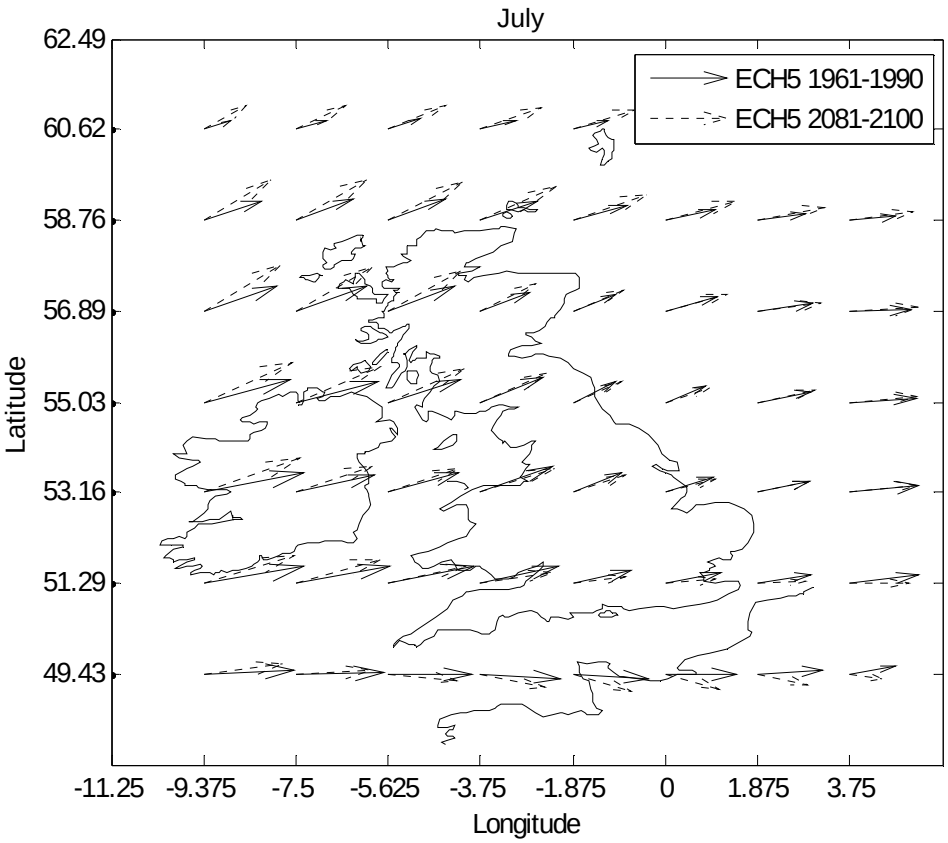
July
ECH5 1961-1990
ECH5 2081-2100
62.49
60.62
58.76
56.89
55.03
53.16
51.29
49.43
Latitude
-11.25
-9.375
-7.5
-5.625
-3.75
-1.875
0
1.875
3.75
Longitude

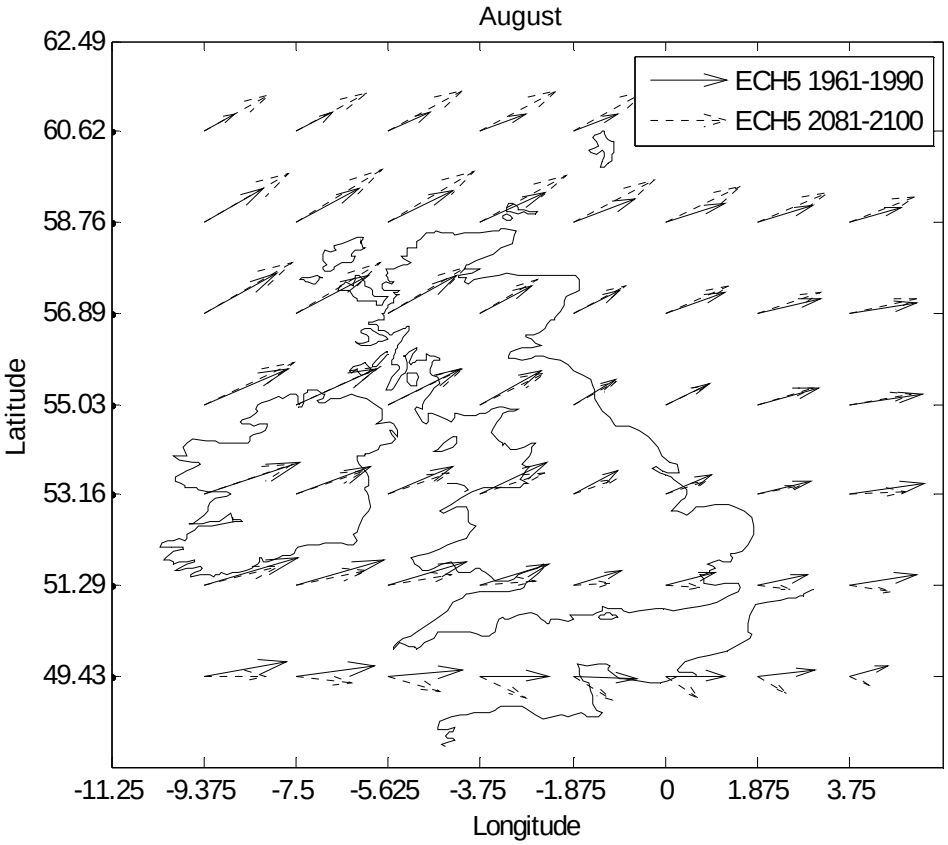
August
ECH5 1961-1990
ECH5 2081-2100
62.49
60.62
58.76
56.89
55.03
53.16
51.29
49.43
Latitude
-11.25
-9.375
-7.5
-5.625
-3.75
-1.875
0
1.875
3.75
Longitude

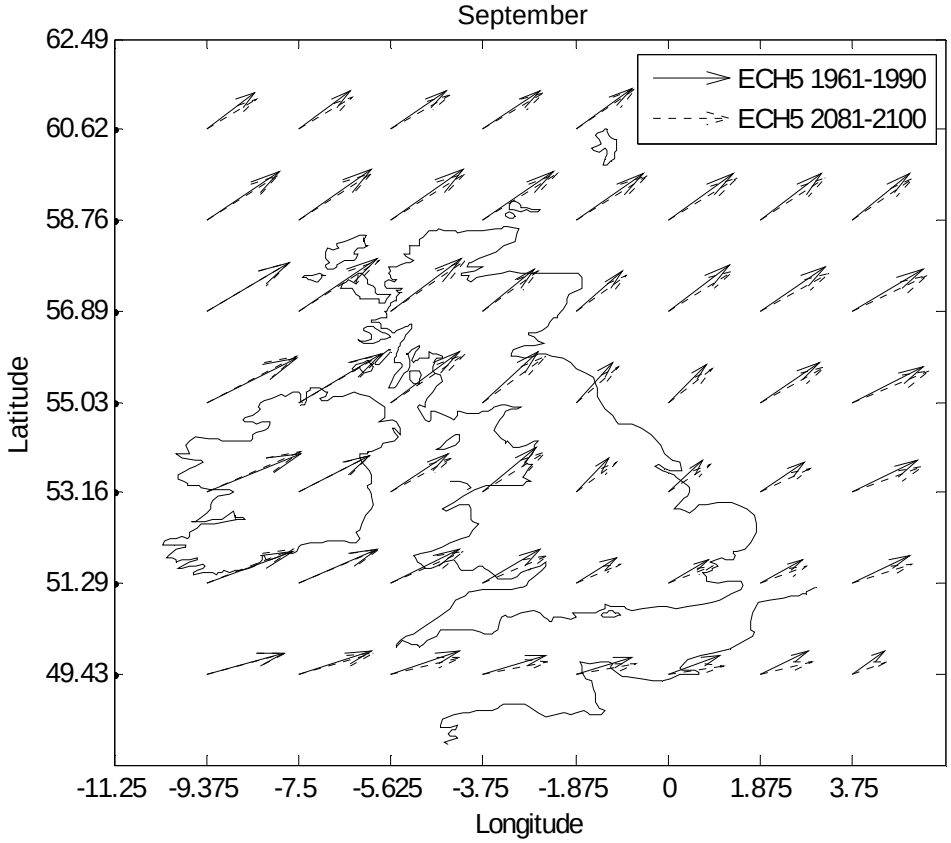
September
ECH5 1961-1990
ECH5 2081-2100
62.49
60.62
58.76
56.89
55.03
53.16
51.29
49.43
Latitude
-11.25
-9.375
-7.5
-5.625
-3.75
-1.875
0
1.875
3.75
Longitude

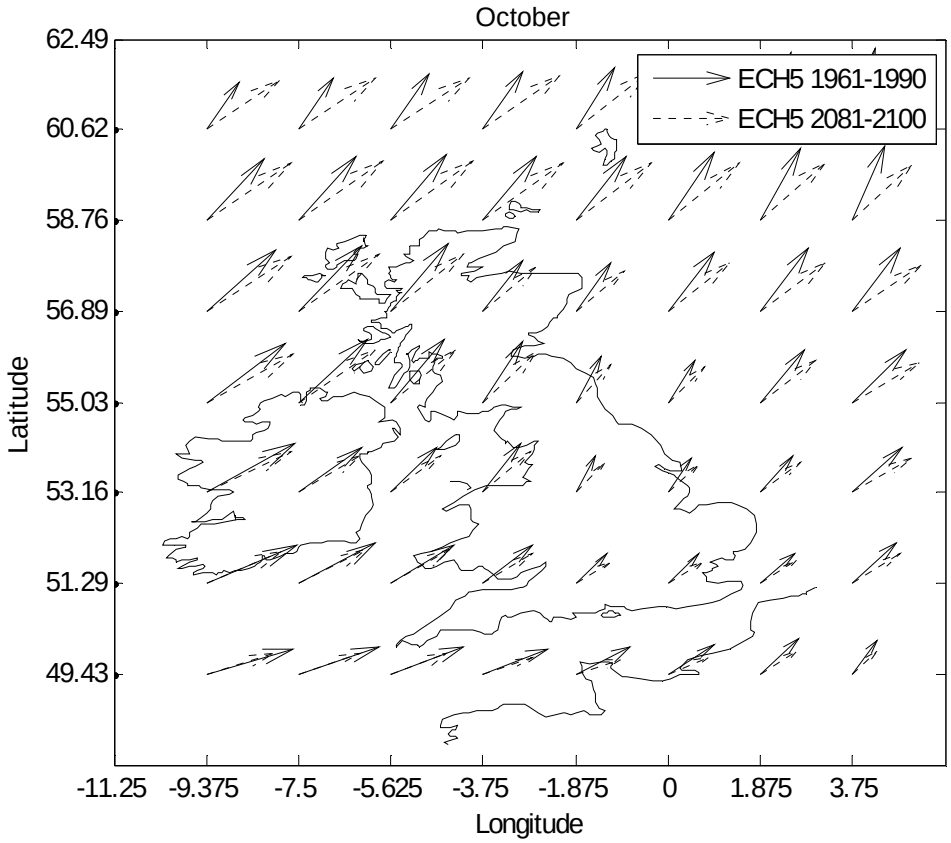
October
ECH5 1961-1990
ECH5 2081-2100
62.49
60.62
58.76
56.89
55.03
53.16
51.29
49.43
Latitude
-11.25
-9.375
-7.5
-5.625
-3.75
-1.875
0
1.875
3.75
Longitude

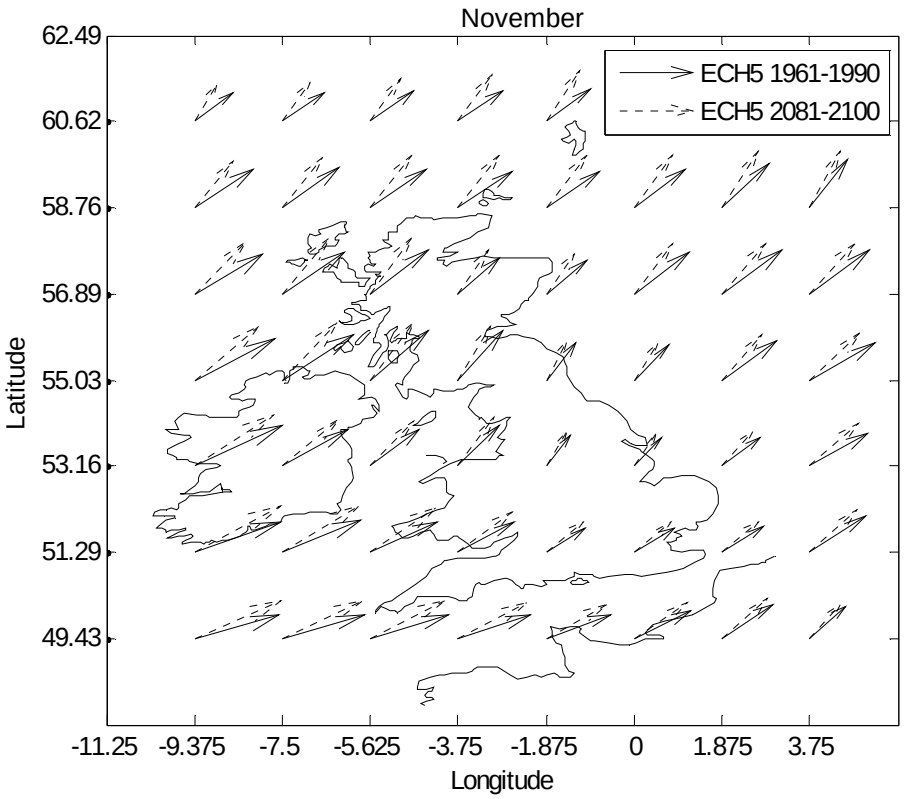
November
ECH5 1961-1990
ECH5 2081-2100
62.49
60.62
58.76
56.89
55.03
53.16
51.29
49.43
Latitude
-11.25
-9.375
-7.5
-5.625
-3.75
-1.875
0
1.875
3.75
Longitude

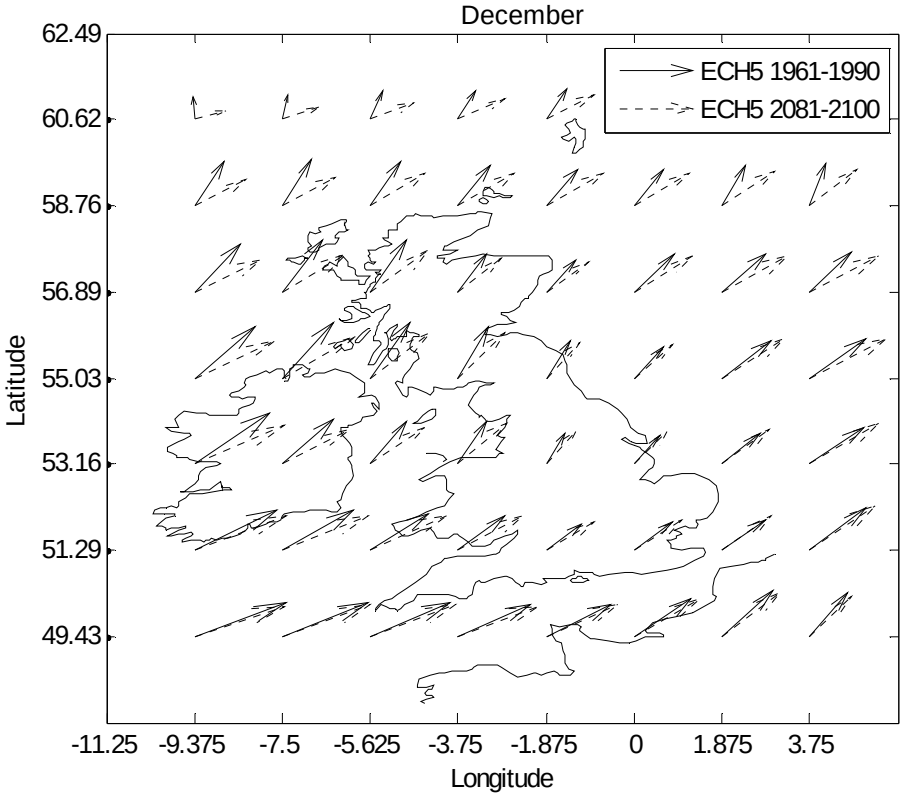
December
ECH5 1961-1990
ECH5 2081-2100
62.49
60.62
58.76
56.89
55.03
53.16
51.29
49.43
Latitude
-11.25
-9.375
-7.5
-5.625
-3.75
-1.875
0
1.875
3.75
Longitude

Appendix D – Geostrophic winds

D.1 Comparison of ECHAM5 with ERA40 1961-90

Fig. D-1: Percentage differences in monthly mean wind speed

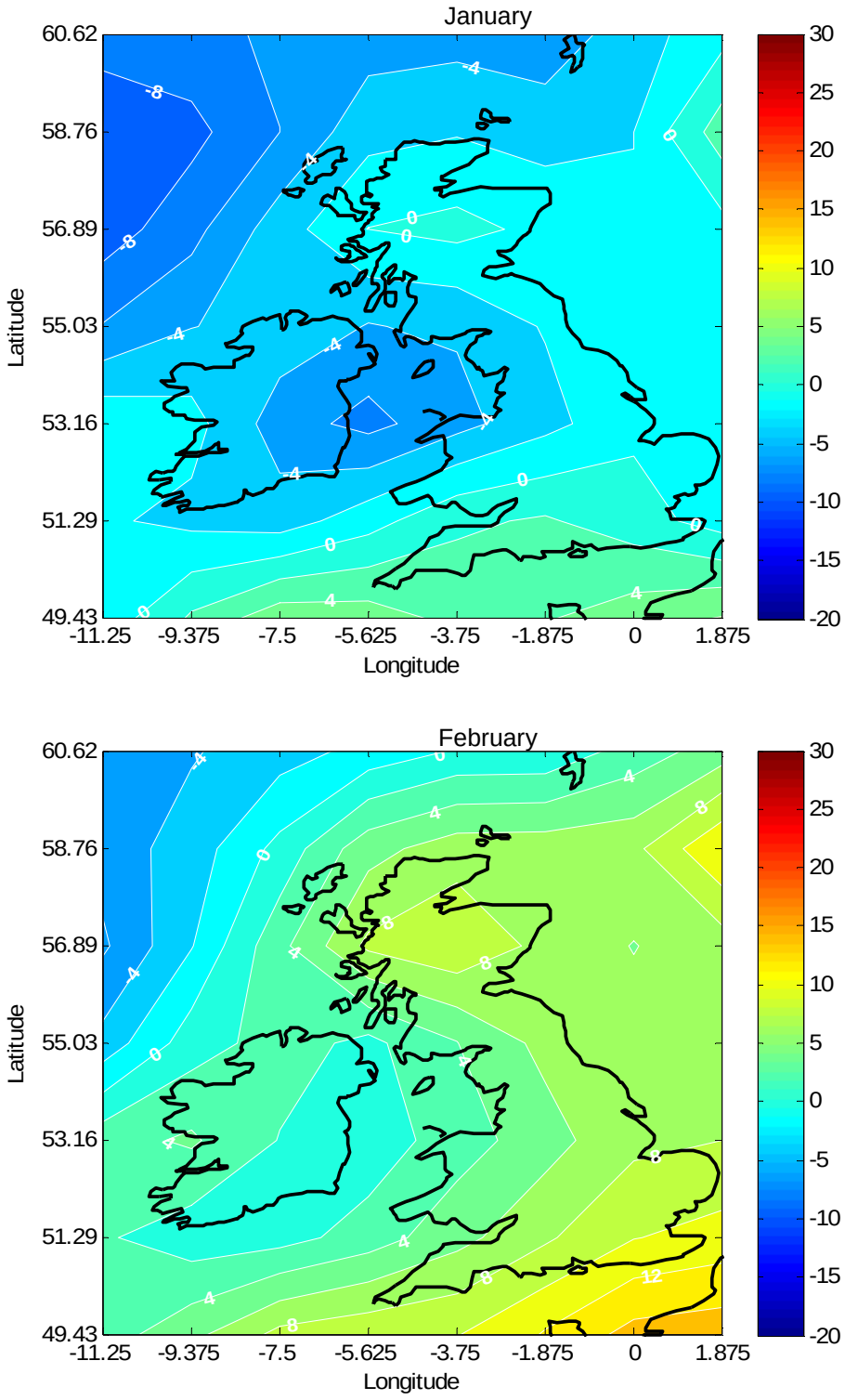

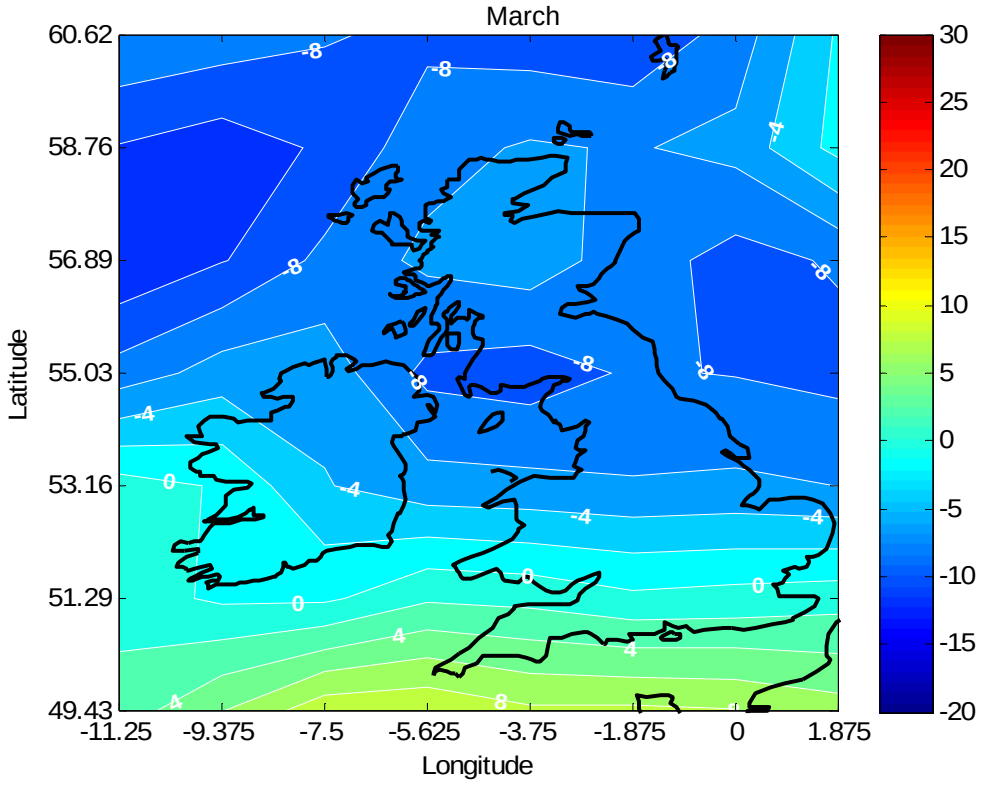
March
60.62
58.76
56.89
55.03
53.16
51.29
49.43
Latitude
-11.25
-9.375
-7.5
-5.625
-3.75
-1.875
0
1.875
Longitude
30
25
20
15
10
5
0
-5
-10
-15
-20

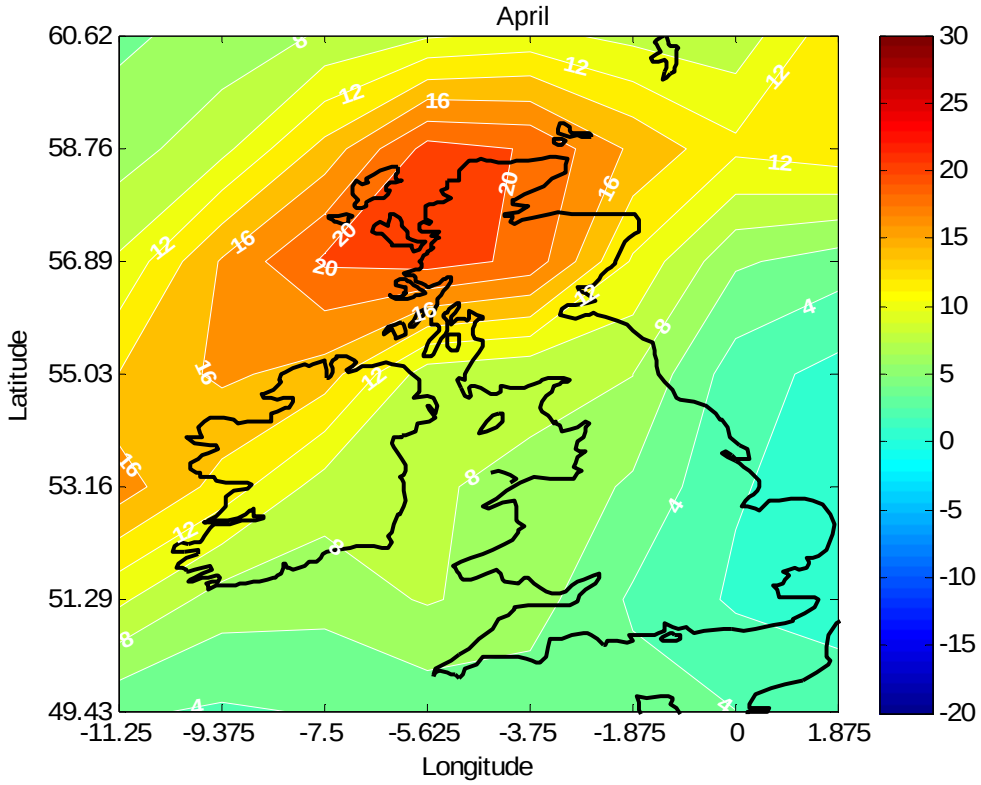
April
60.62
58.76
56.89
55.03
53.16
51.29
49.43
Latitude
-11.25
-9.375
-7.5
-5.625
-3.75
-1.875
0
1.875
Longitude
30
25
20
15
10
5
0
-5
-10
-15
-20

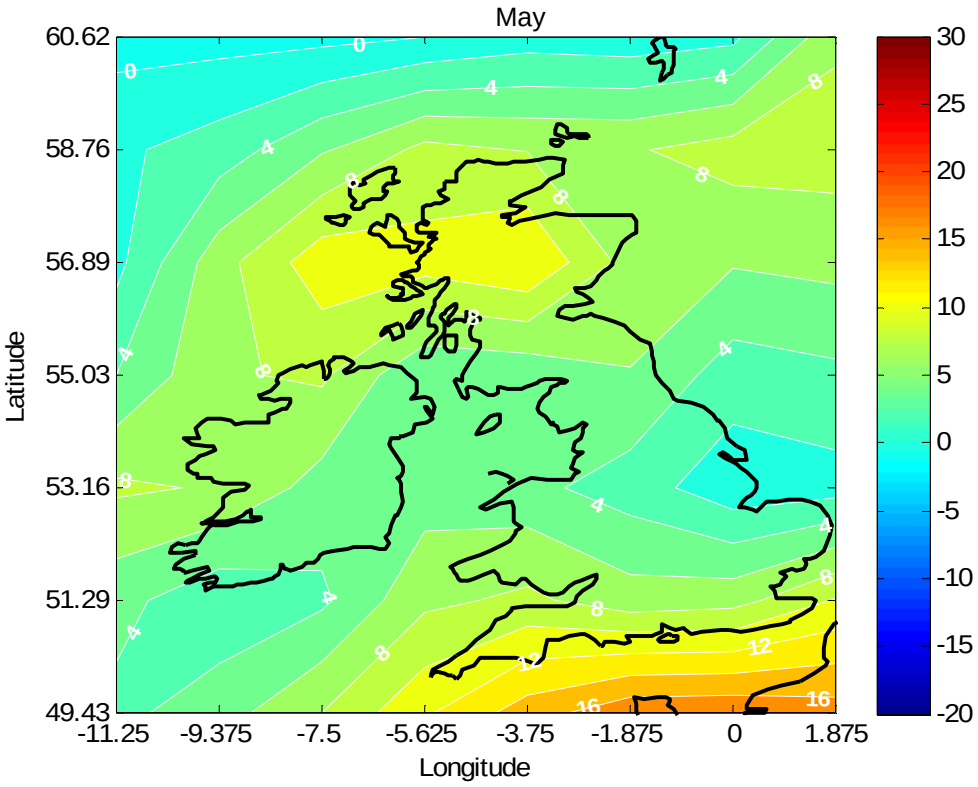
May
60.62
58.76
56.89
55.03
53.16
51.29
49.43
Latitude
-11.25
-9.375
-7.5
-5.625
-3.75
-1.875
0
1.875
Longitude
30
25
20
15
10
5
0
-5
-10
-15
-20

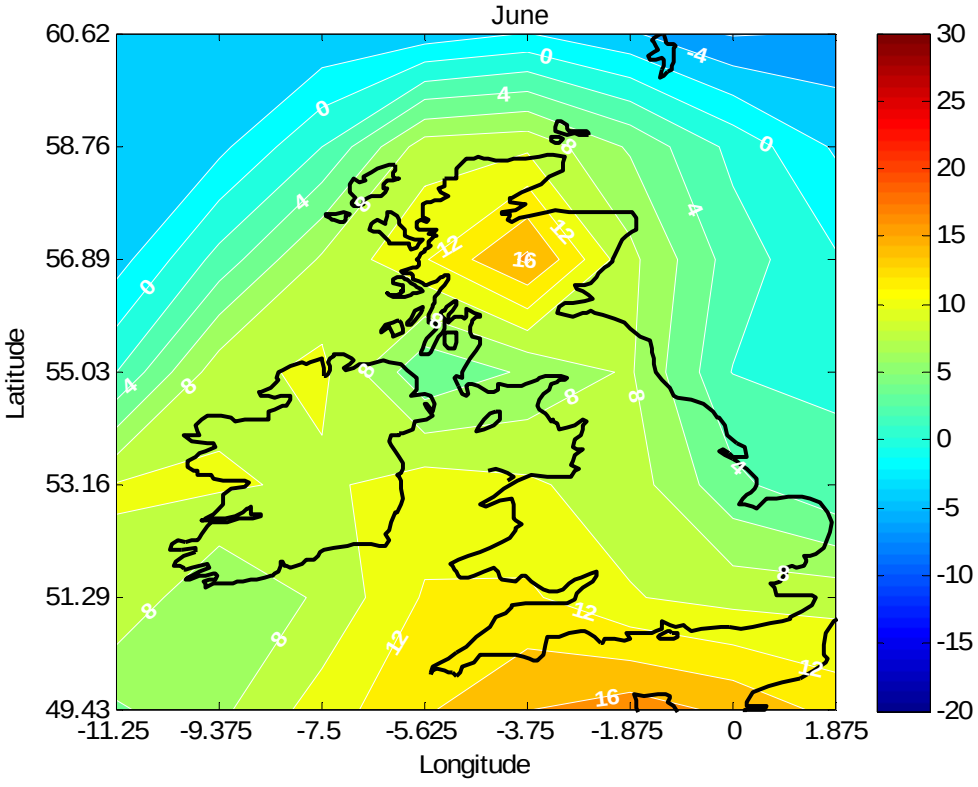
June
60.62
58.76
56.89
55.03
53.16
51.29
49.43
Latitude
-11.25
-9.375
-7.5
-5.625
-3.75
-1.875
0
1.875
Longitude
30
25
20
15
10
5
0
-5
-10
-15
-20

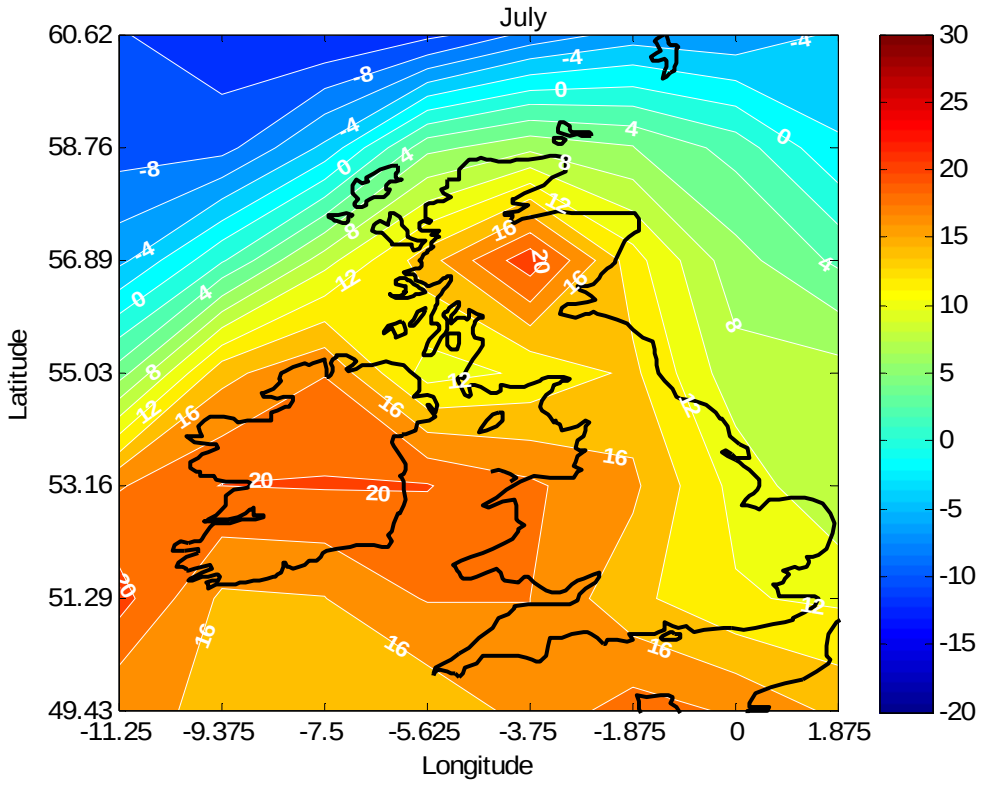
July
60.62
58.76
56.89
55.03
53.16
51.29
49.43
Latitude
-11.25
-9.375
-7.5
-5.625
-3.75
-1.875
0
1.875
Longitude
30
25
20
15
10
5
0
-5
-10
-15
-20

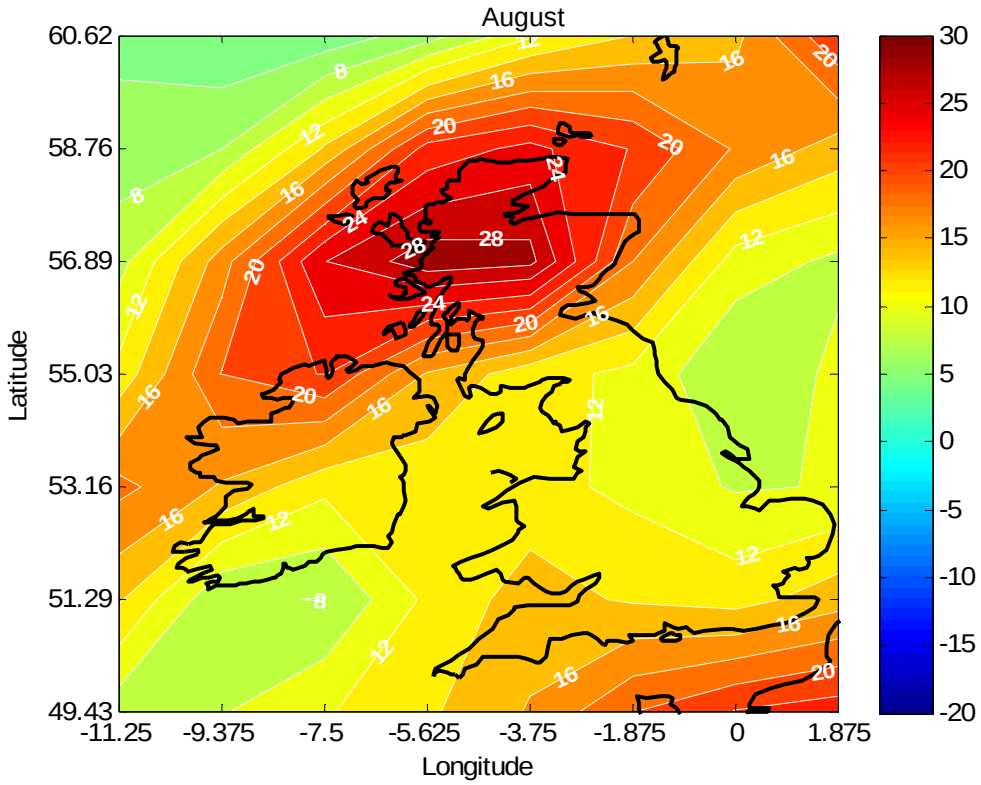
August
60.62
58.76
56.89
55.03
53.16
51.29
49.43
Latitude
-11.25
-9.375
-7.5
-5.625
-3.75
-1.875
0
1.875
Longitude
30
25
20
15
10
5
0
-5
-10
-15
-20

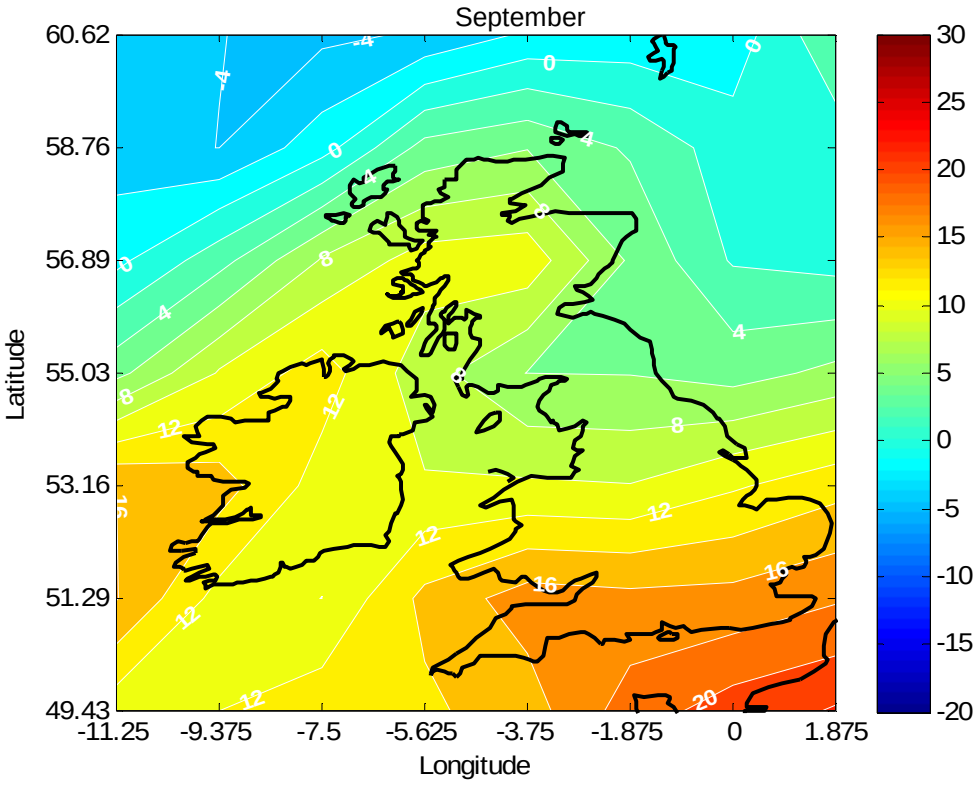
September
60.62
58.76
56.89
55.03
53.16
51.29
49.43
Latitude
-11.25
-9.375
-7.5
-5.625
-3.75
-1.875
0
1.875
Longitude
30
25
20
15
10
5
0
-5
-10
-15
-20

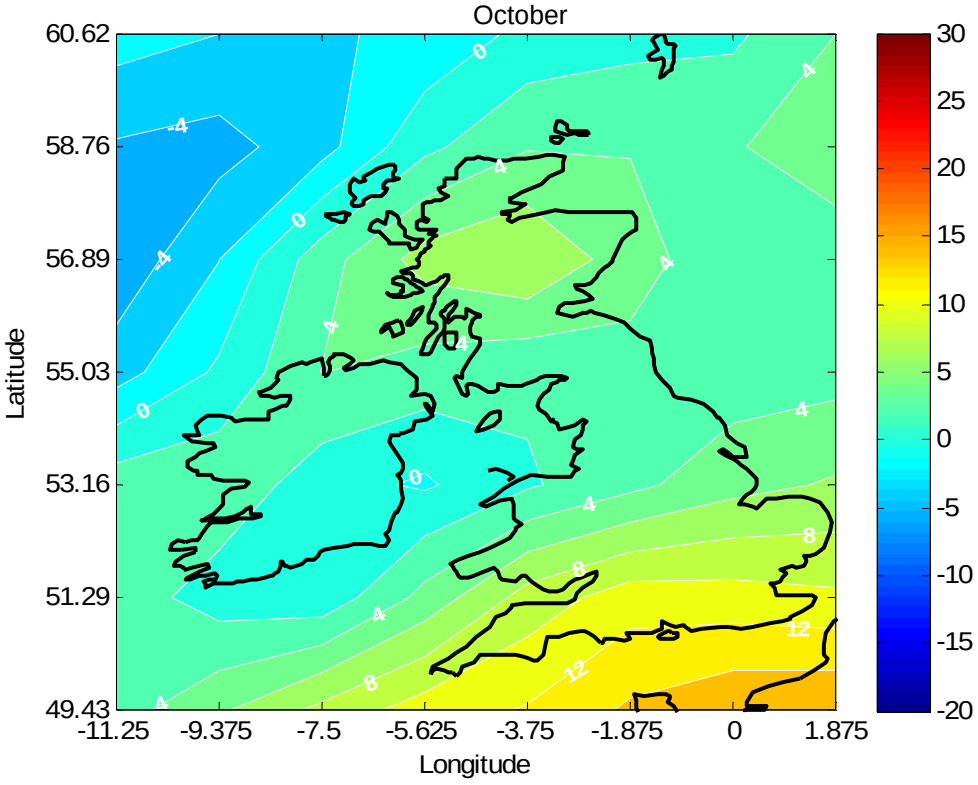
October
60.62
58.76
56.89
55.03
53.16
51.29
49.43
Latitude
-11.25
-9.375
-7.5
-5.625
-3.75
-1.875
0
1.875
Longitude
30
25
20
15
10
5
0
-5
-10
-15
-20

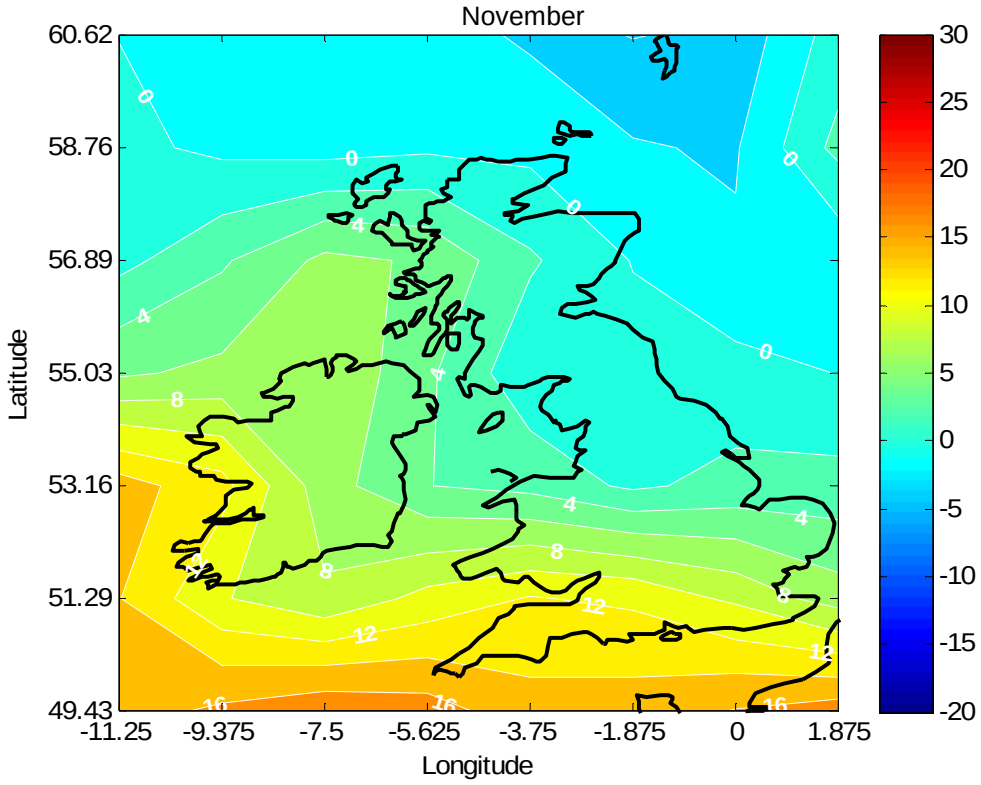
November
60.62
58.76
56.89
55.03
53.16
51.29
49.43
Latitude
-11.25
-9.375
-7.5
-5.625
-3.75
-1.875
0
1.875
Longitude
30
25
20
15
10
5
0
-5
-10
-15
-20

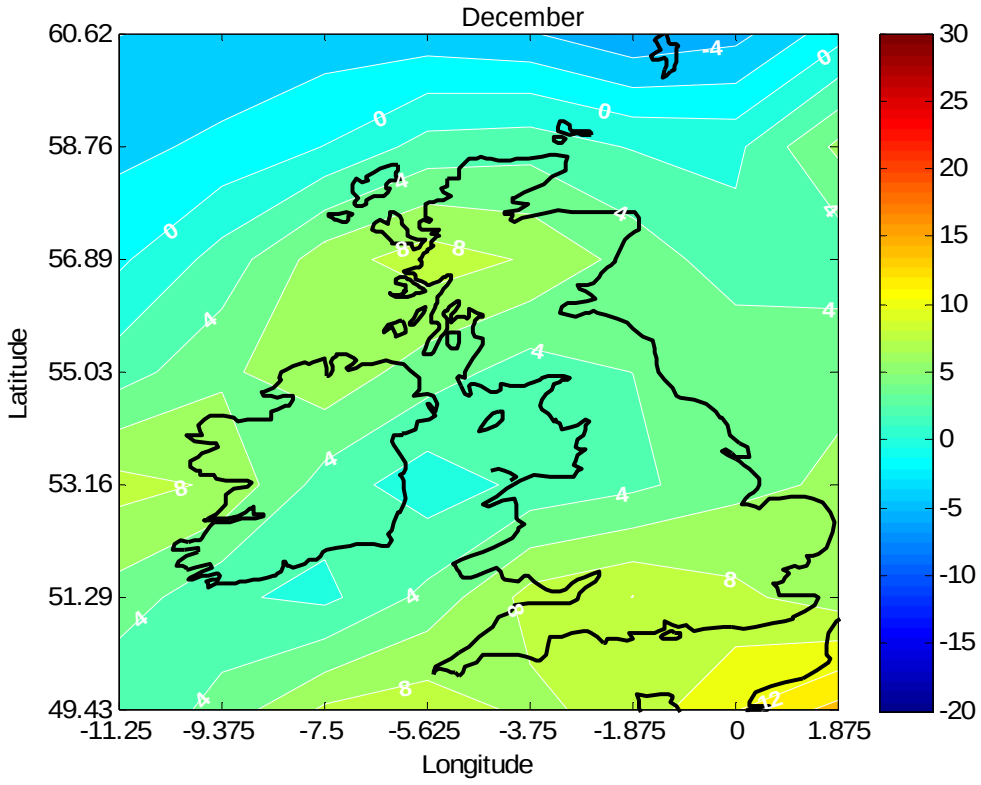
December
60.62
58.76
56.89
55.03
53.16
51.29
49.43
Latitude
-11.25
-9.375
-7.5
-5.625
-3.75
-1.875
0
1.875
Longitude
30
25
20
15
10
5
0
-5
-10
-15
-20

Fig. D-2: monthly mean wind speed vectors

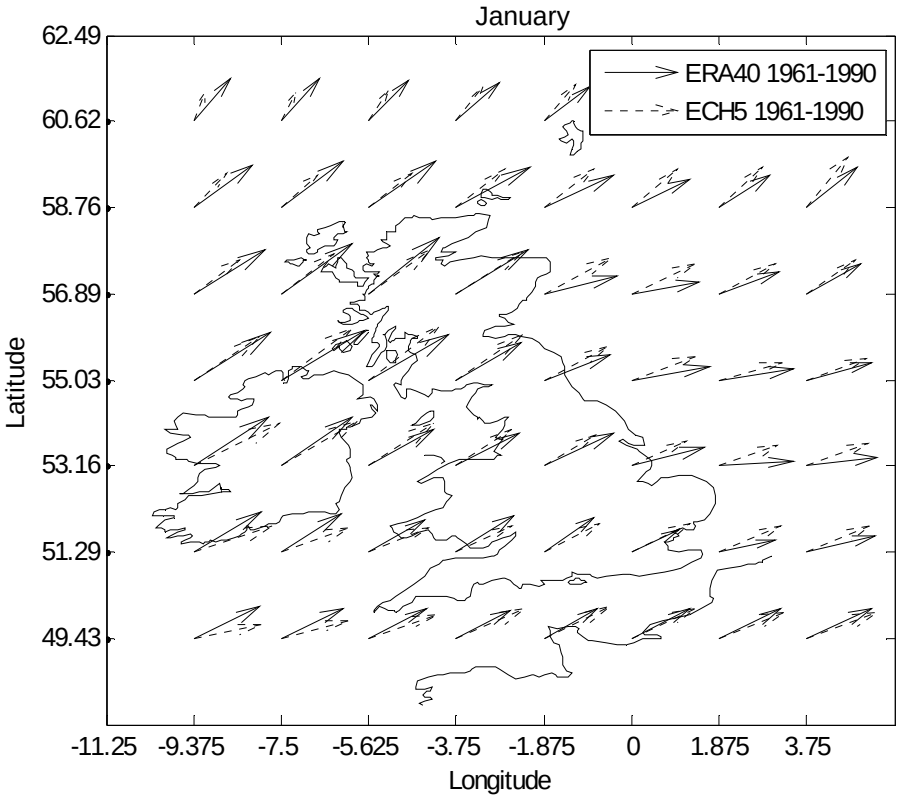

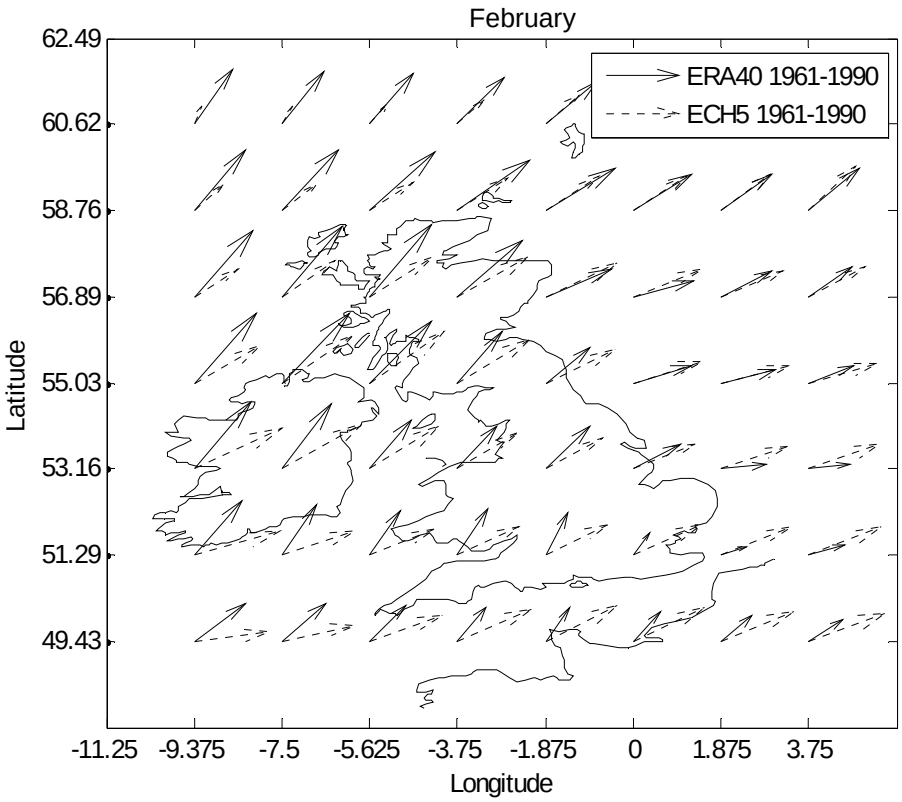

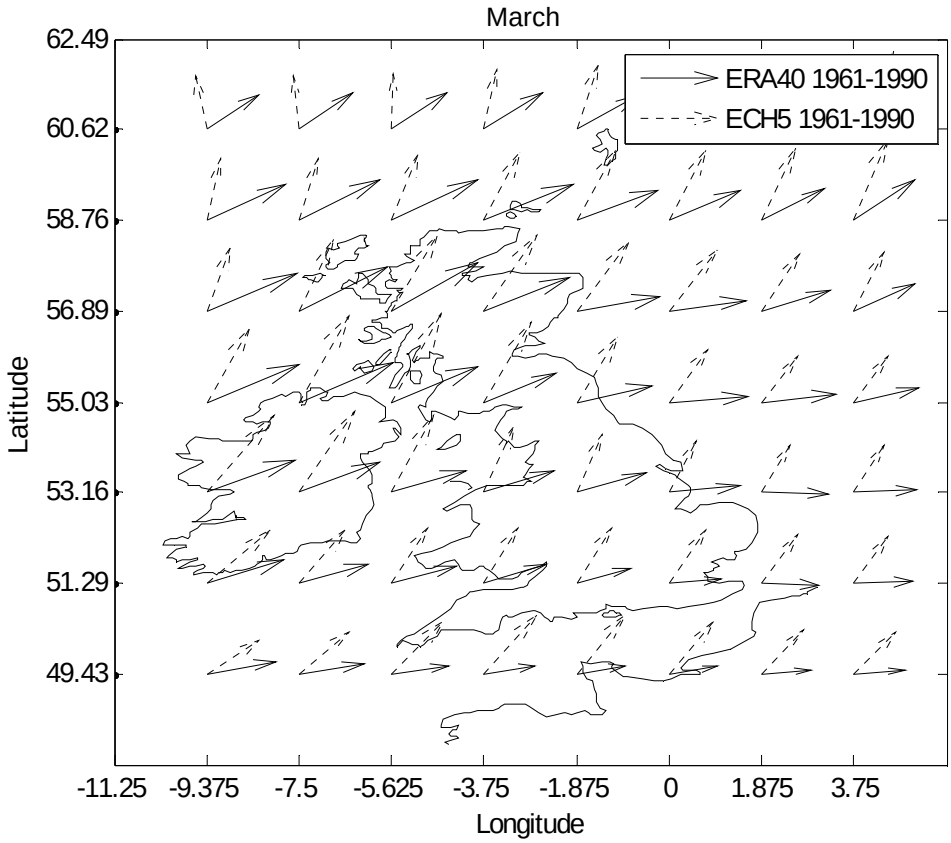
March
ERA40 1961-1990
ECH5 1961-1990
62.49
60.62
58.76
56.89
55.03
53.16
51.29
49.43
Latitude
-11.25
-9.375
-7.5
-5.625
-3.75
-1.875
0
1.875
3.75
Longitude

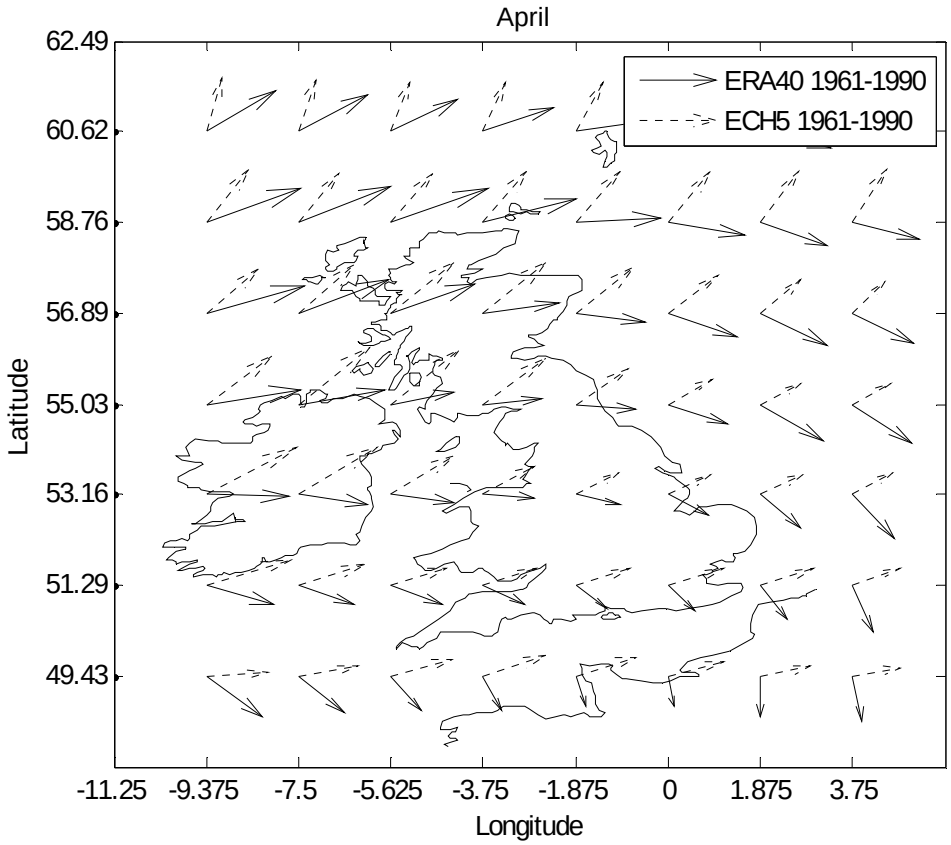
April
ERA40 1961-1990
ECH5 1961-1990
62.49
60.62
58.76
56.89
55.03
53.16
51.29
49.43
Latitude
-11.25
-9.375
-7.5
-5.625
-3.75
-1.875
0
1.875
3.75
Longitude

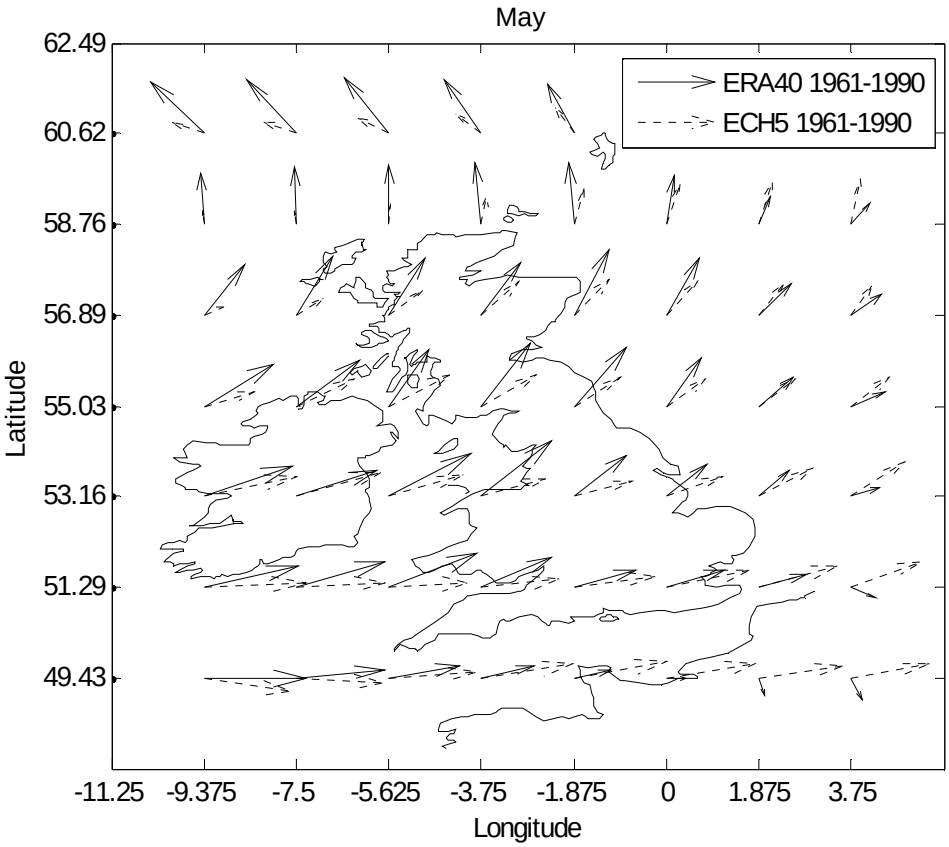
May
ERA40 1961-1990
ECH5 1961-1990
62.49
60.62
58.76
56.89
55.03
53.16
51.29
49.43
Latitude
-11.25
-9.375
-7.5
-5.625
-3.75
-1.875
0
1.875
3.75
Longitude

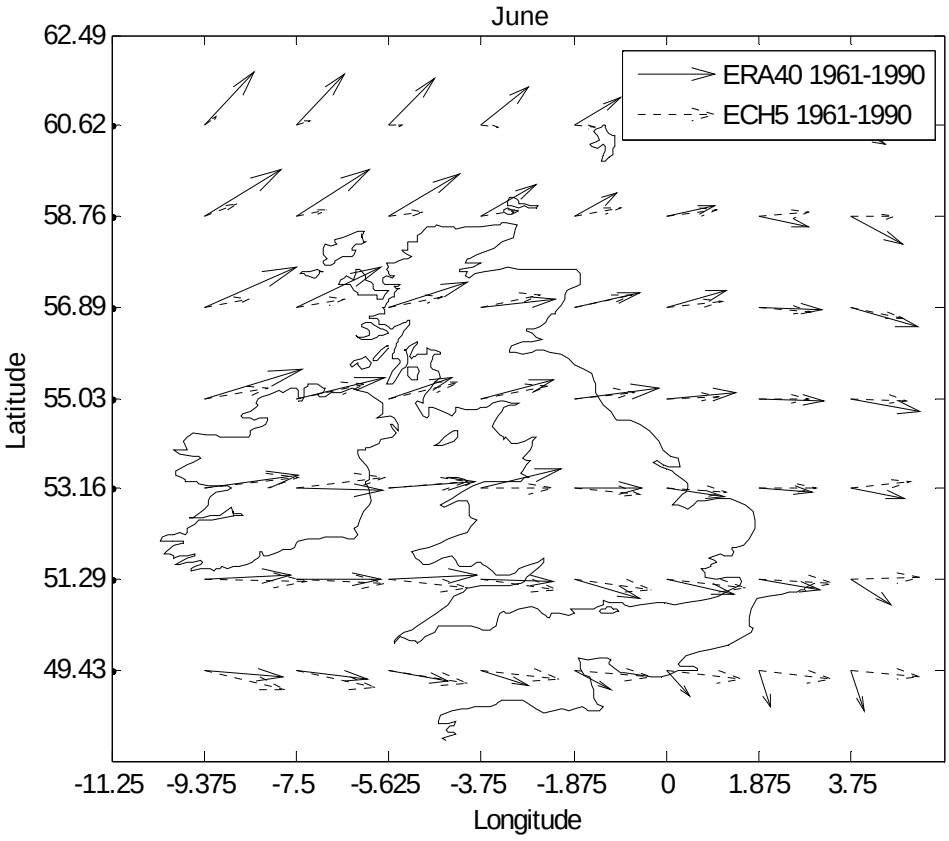
June
ERA40 1961-1990
ECH5 1961-1990
62.49
60.62
58.76
56.89
55.03
53.16
51.29
49.43
Latitude
-11.25
-9.375
-7.5
-5.625
-3.75
-1.875
0
1.875
3.75
Longitude

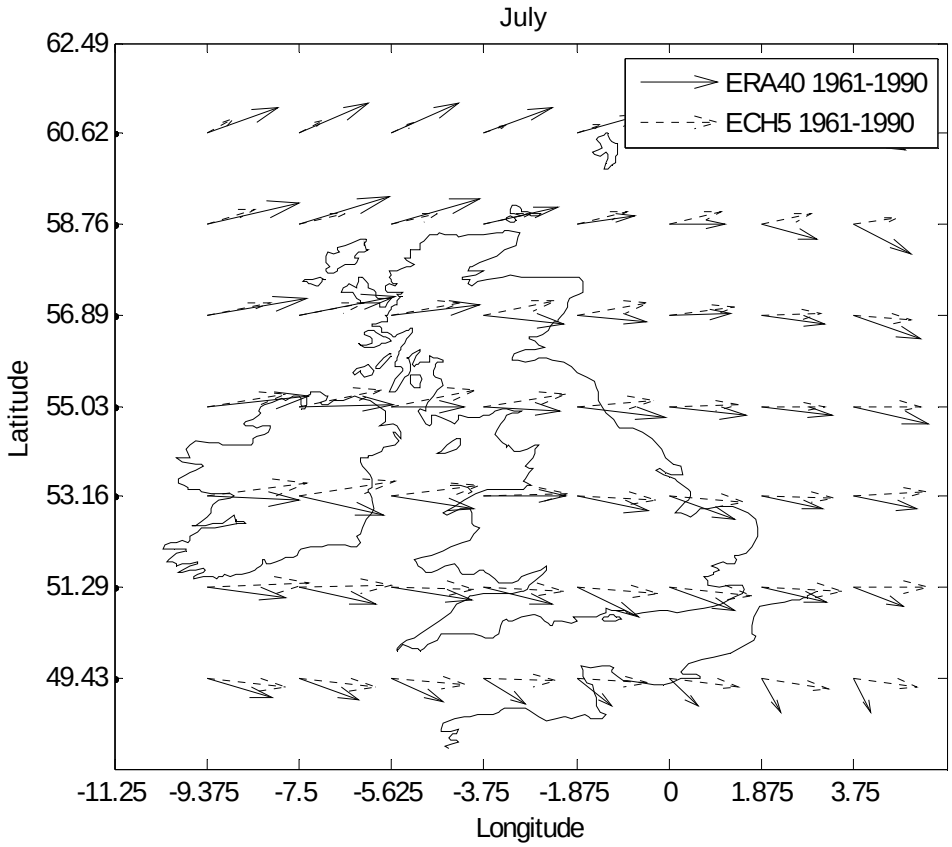
July
ERA40 1961-1990
ECH5 1961-1990
62.49
60.62
58.76
56.89
55.03
53.16
51.29
49.43
Latitude
-11.25
-9.375
-7.5
-5.625
-3.75
-1.875
0
1.875
3.75
Longitude

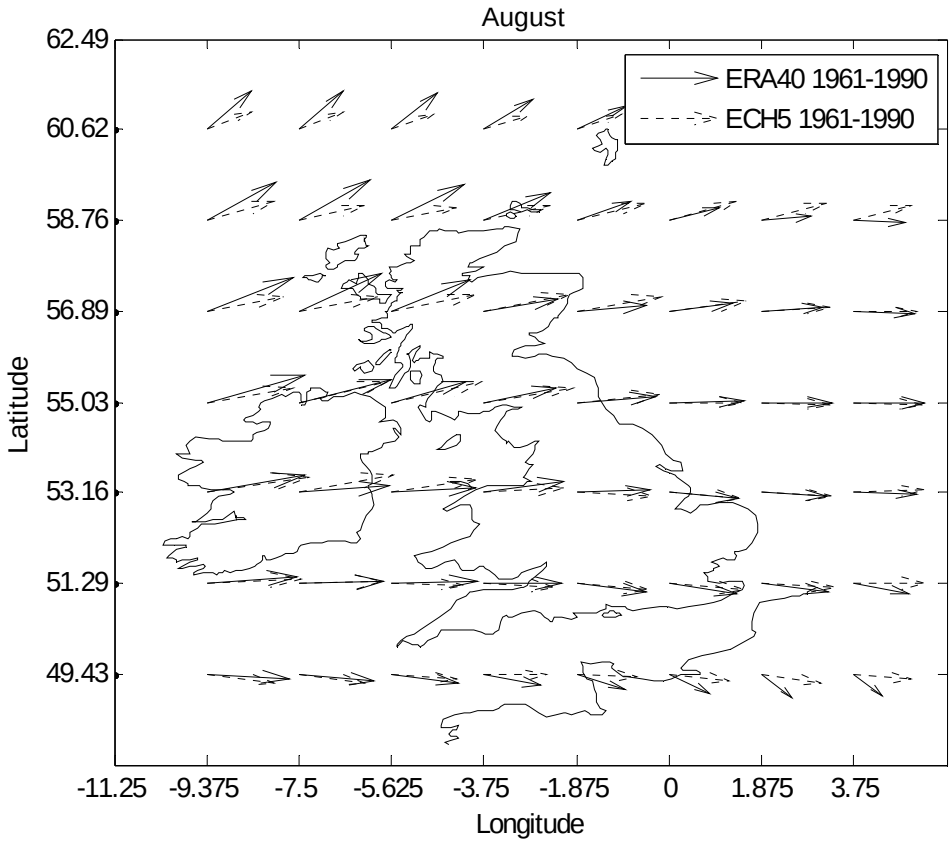
August
ERA40 1961-1990
ECH5 1961-1990
62.49
60.62
58.76
56.89
55.03
53.16
51.29
49.43
Latitude
-11.25
-9.375
-7.5
-5.625
-3.75
-1.875
0
1.875
3.75
Longitude

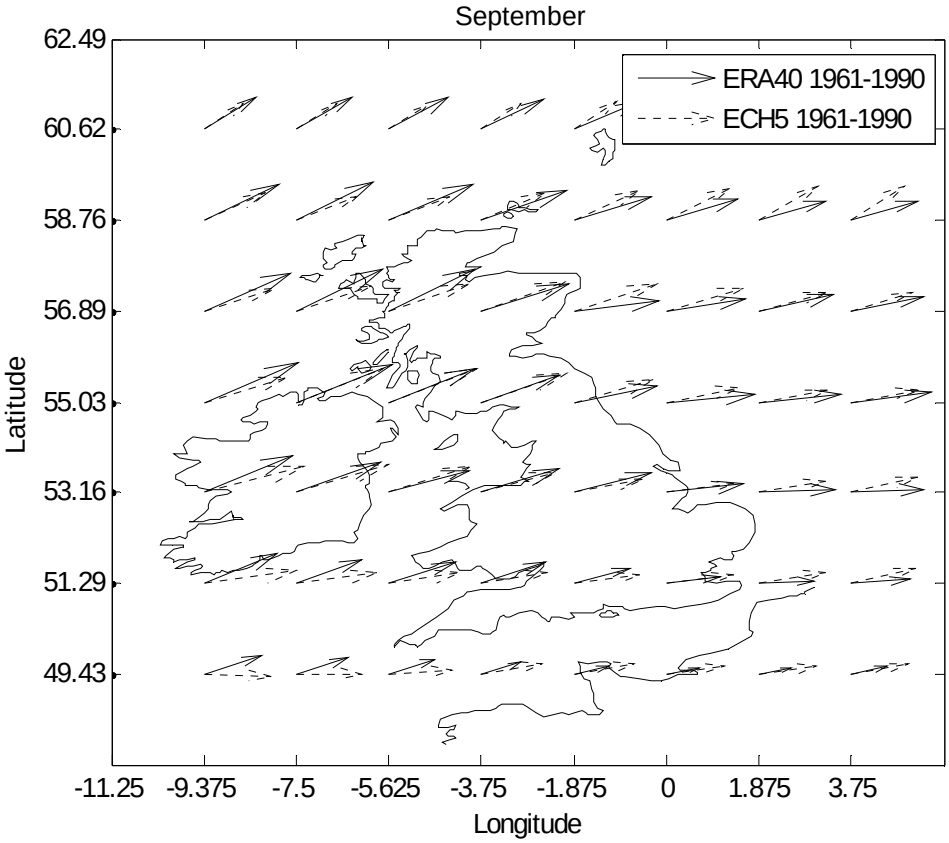
September
ERA40 1961-1990
ECH5 1961-1990
62.49
60.62
58.76
56.89
55.03
53.16
51.29
49.43
Latitude
-11.25
-9.375
-7.5
-5.625
-3.75
-1.875
0
1.875
3.75
Longitude

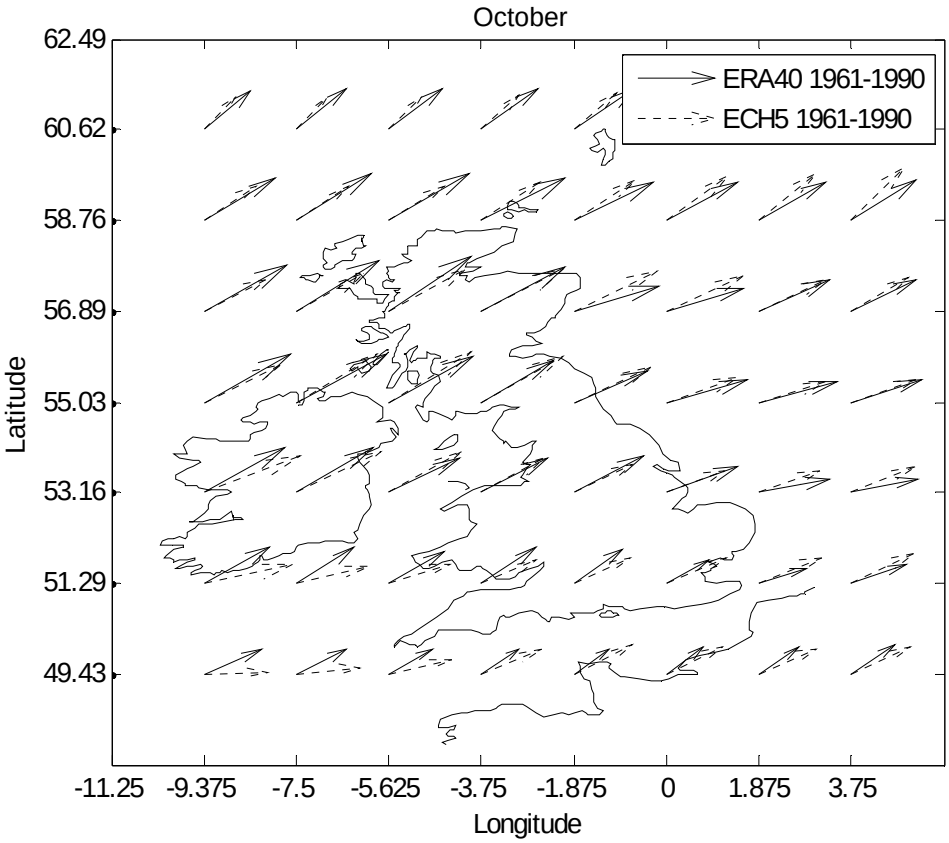
October
ERA40 1961-1990
ECH5 1961-1990
62.49
60.62
58.76
56.89
55.03
53.16
51.29
49.43
Latitude
-11.25
-9.375
-7.5
-5.625
-3.75
-1.875
0
1.875
3.75
Longitude

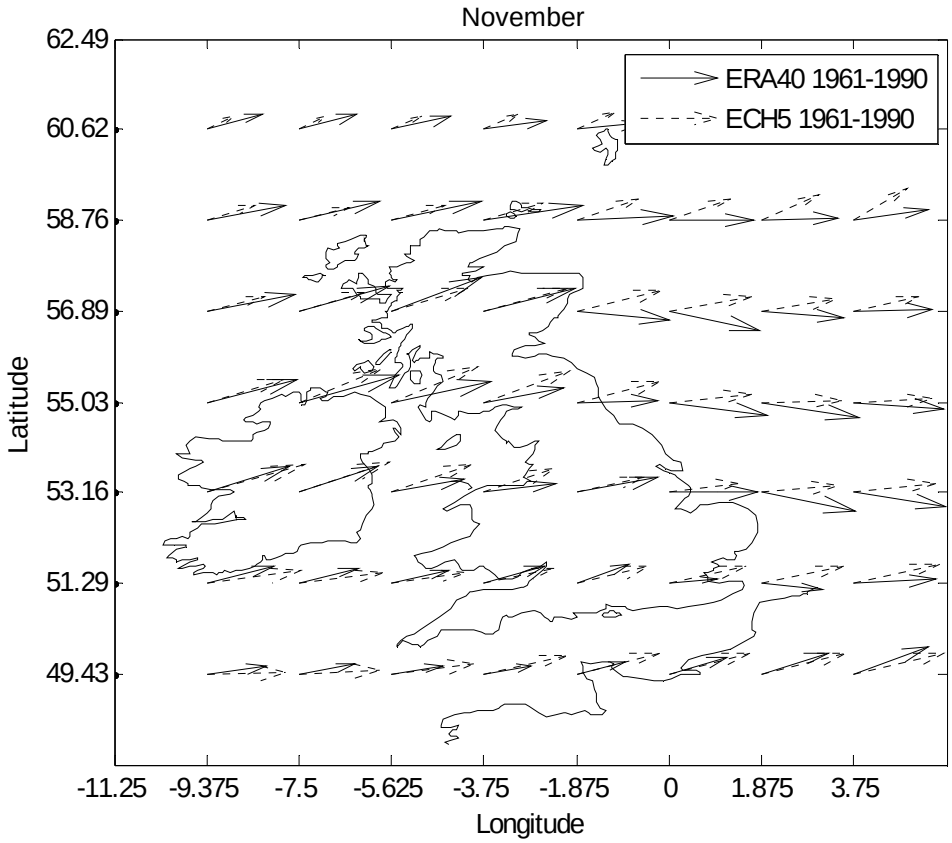
November
ERA40 1961-1990
ECH5 1961-1990
62.49
60.62
58.76
56.89
55.03
53.16
51.29
49.43
Latitude
-11.25
-9.375
-7.5
-5.625
-3.75
-1.875
0
1.875
3.75
Longitude

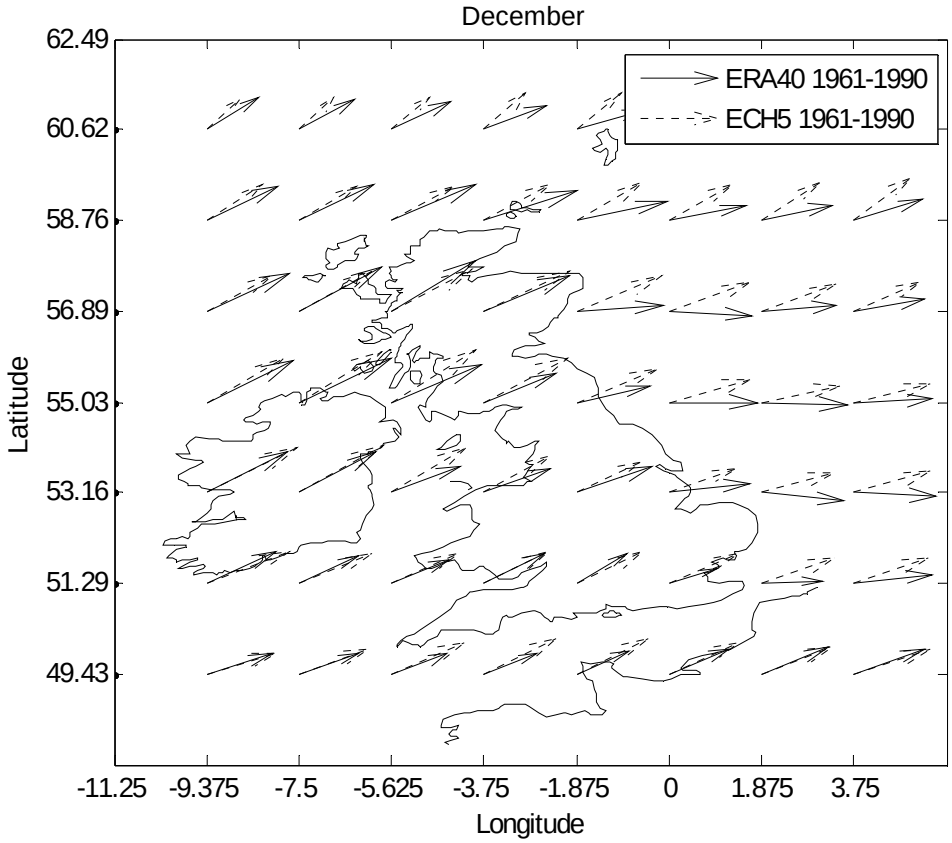
December
ERA40 1961-1990
ECH5 1961-1990
62.49
60.62
58.76
56.89
55.03
53.16
51.29
49.43
Latitude
-11.25
-9.375
-7.5
-5.625
-3.75
-1.875
0
1.875
3.75
Longitude

D.2 Comparison of 2081-2100 with 1961-90 for ECHAM5

Fig. D-3: Future, percentage differences in monthly mean wind speed

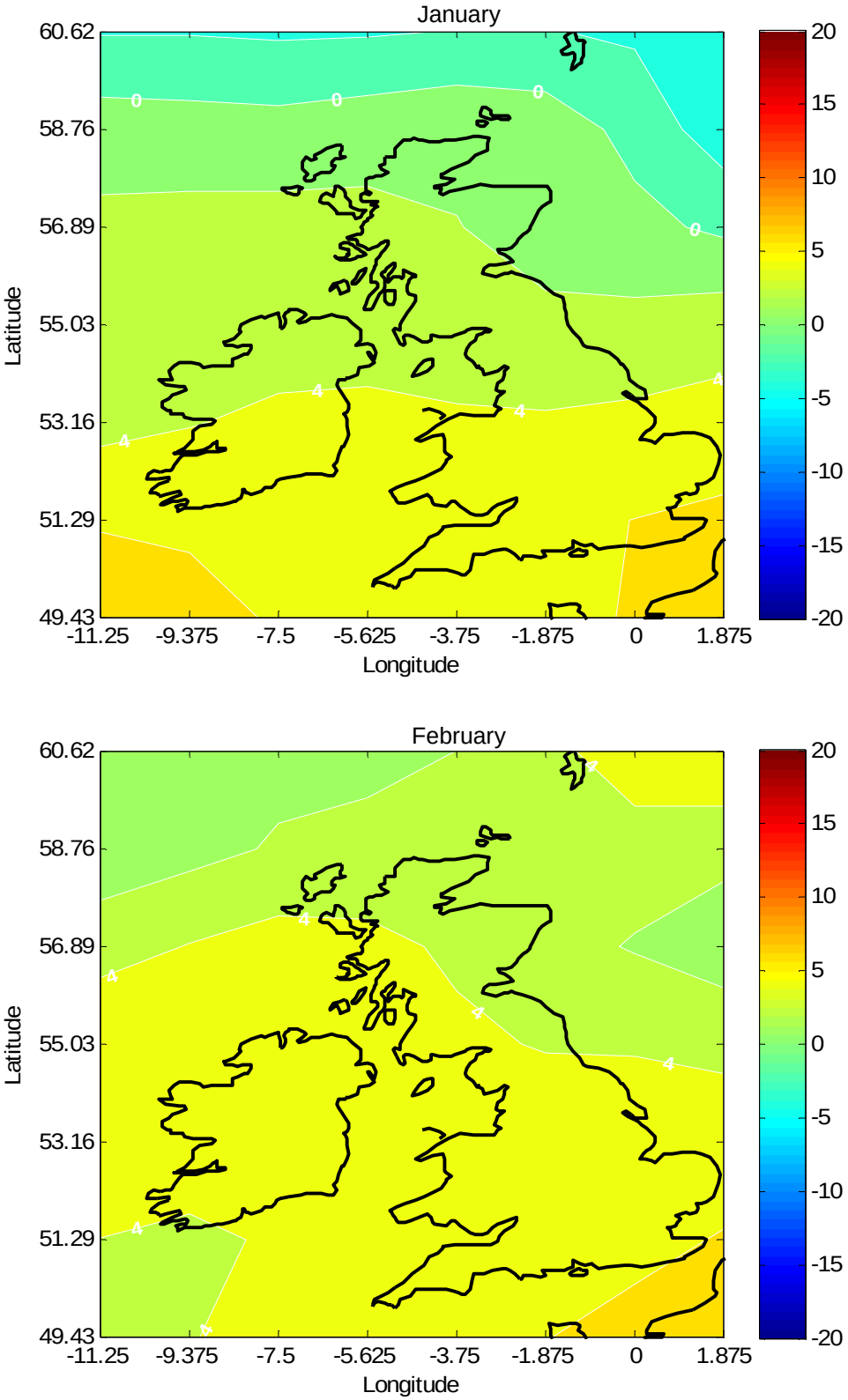

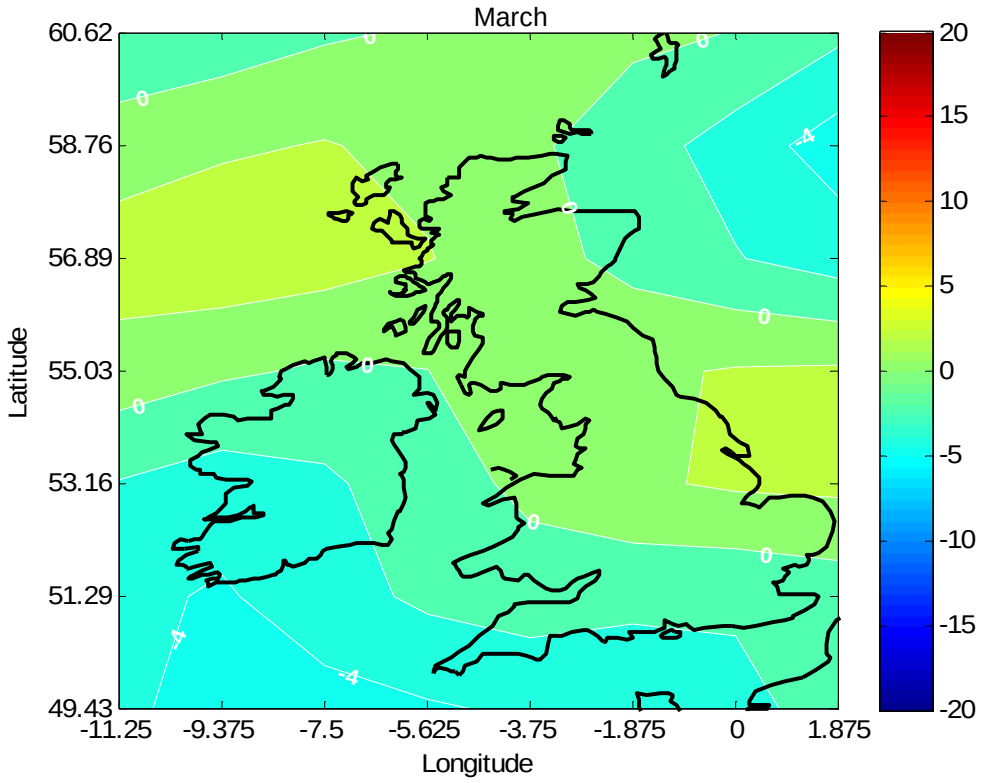
March
60.62
58.76
56.89
55.03
53.16
51.29
49.43
Latitude
-11.25
-9.375
-7.5
-5.625
-3.75
-1.875
0
1.875
Longitude
20
15
10
5
0
-5
-10
-15
-20

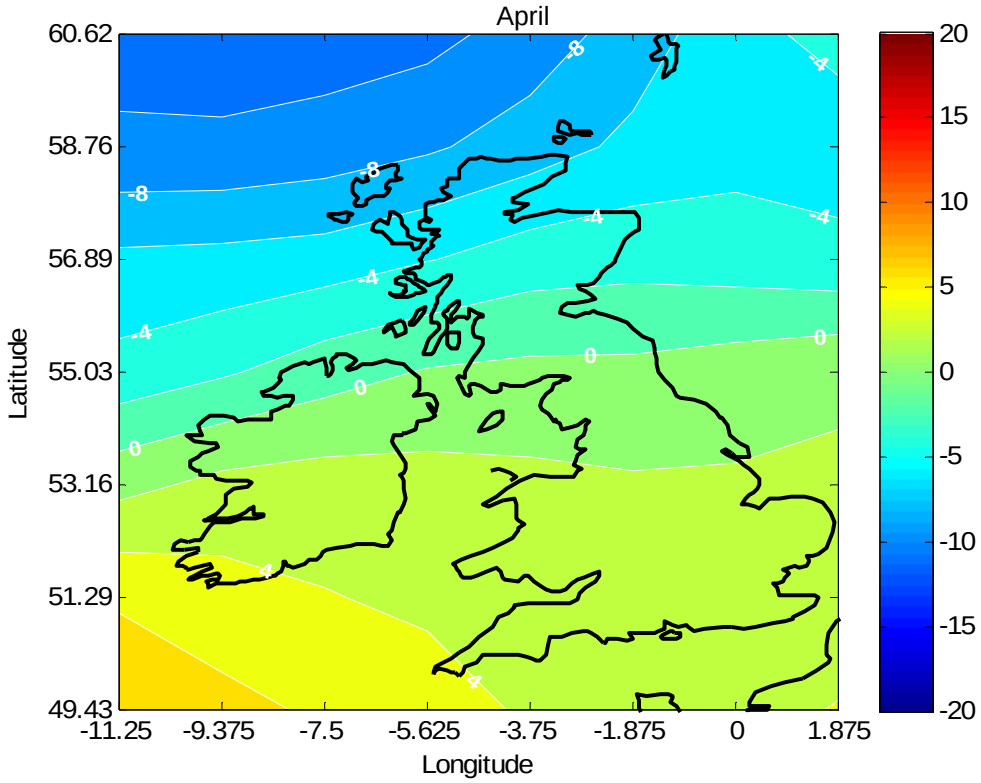
April
60.62
58.76
56.89
55.03
53.16
51.29
49.43
Latitude
-11.25
-9.375
-7.5
-5.625
-3.75
-1.875
0
1.875
Longitude
20
15
10
5
0
-5
-10
-15
-20

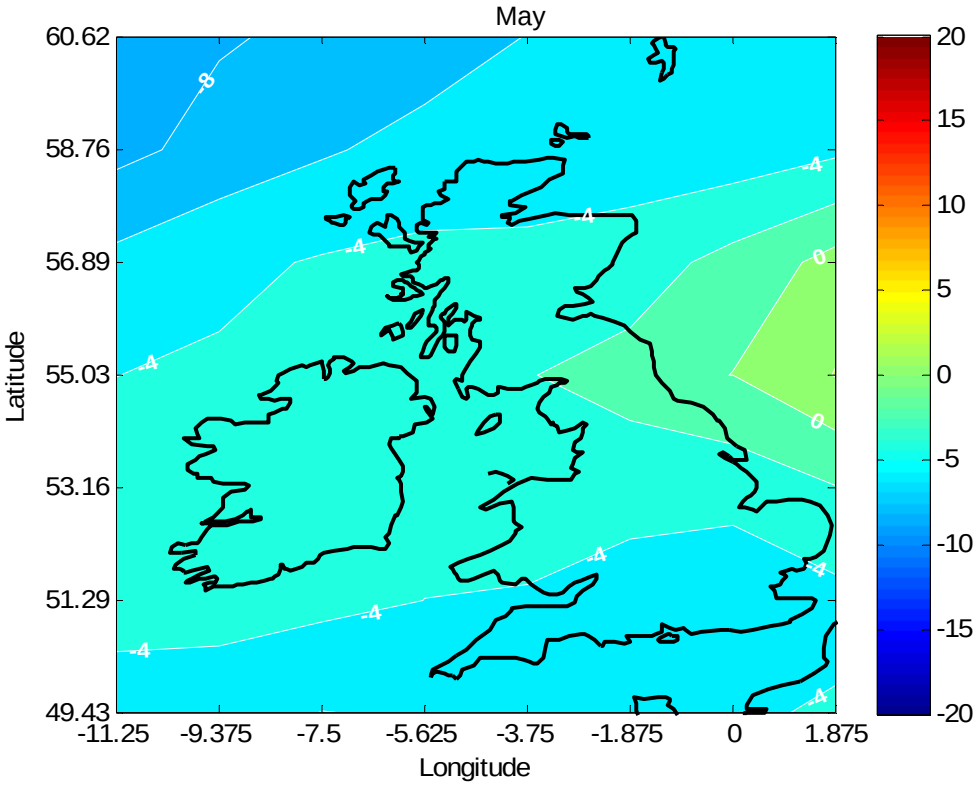
May
60.62
58.76
56.89
55.03
53.16
51.29
49.43
Latitude
-11.25
-9.375
-7.5
-5.625
-3.75
-1.875
0
1.875
Longitude
20
15
10
5
0
-5
-10
-15
-20

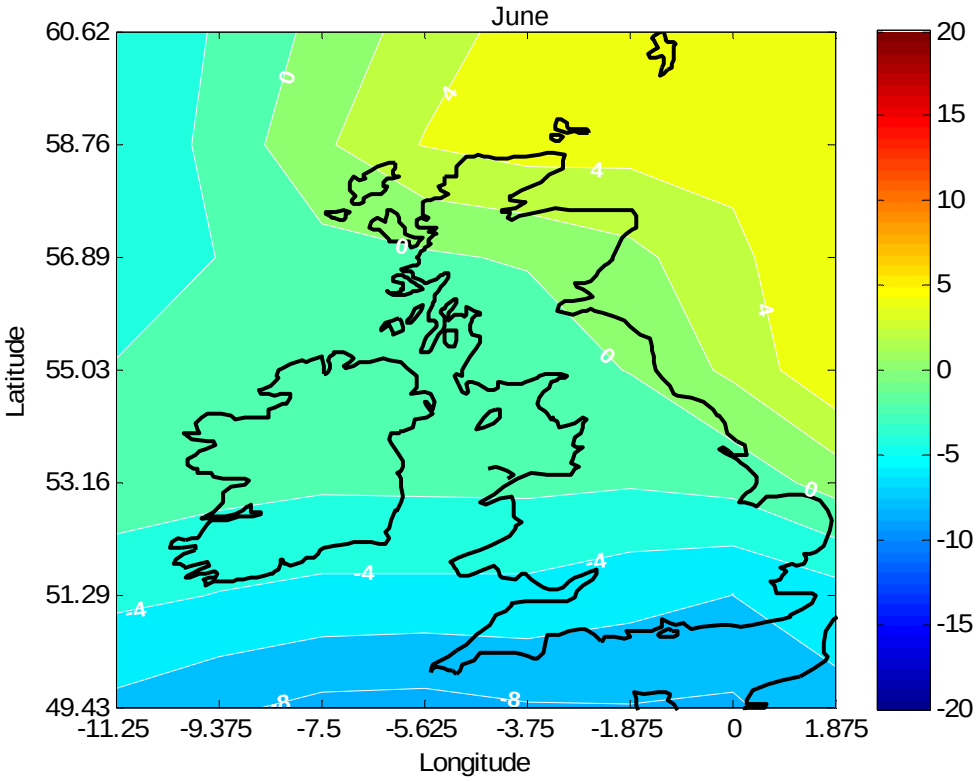
June
60.62
58.76
56.89
55.03
53.16
51.29
49.43
Latitude
-11.25
-9.375
-7.5
-5.625
-3.75
-1.875
0
1.875
Longitude
20
15
10
5
0
-5
-10
-15
-20

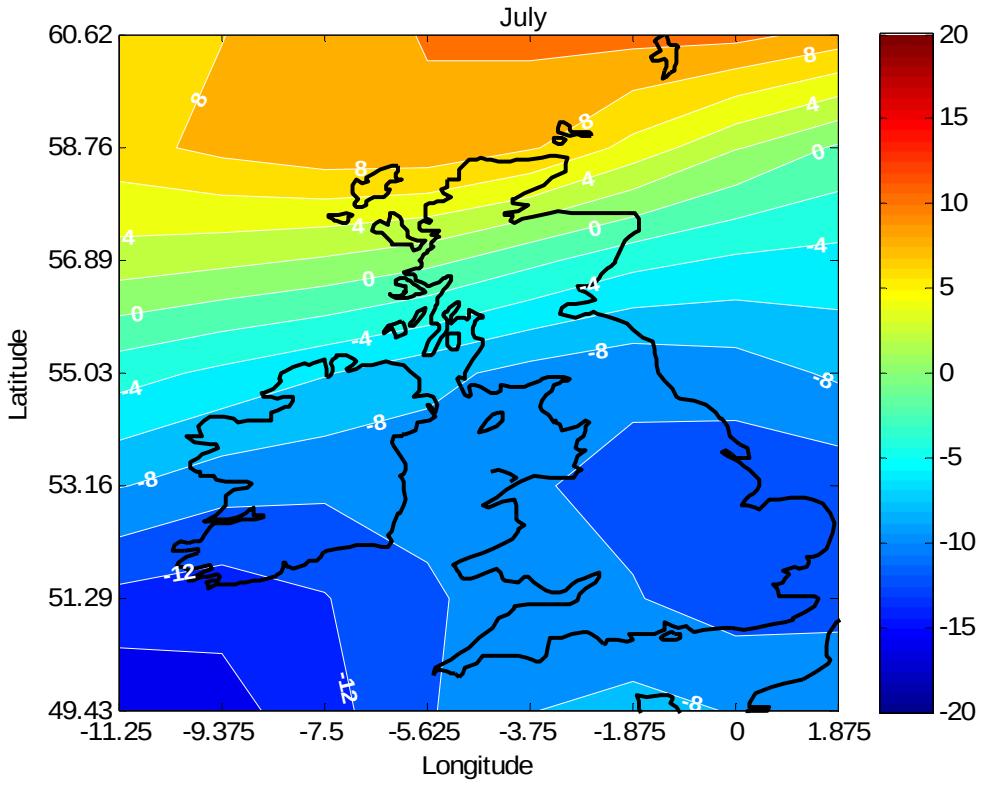
July
60.62
58.76
56.89
55.03
53.16
51.29
49.43
Latitude
-11.25
-9.375
-7.5
-5.625
-3.75
-1.875
0
1.875
Longitude
20
15
10
5
0
-5
-10
-15
-20

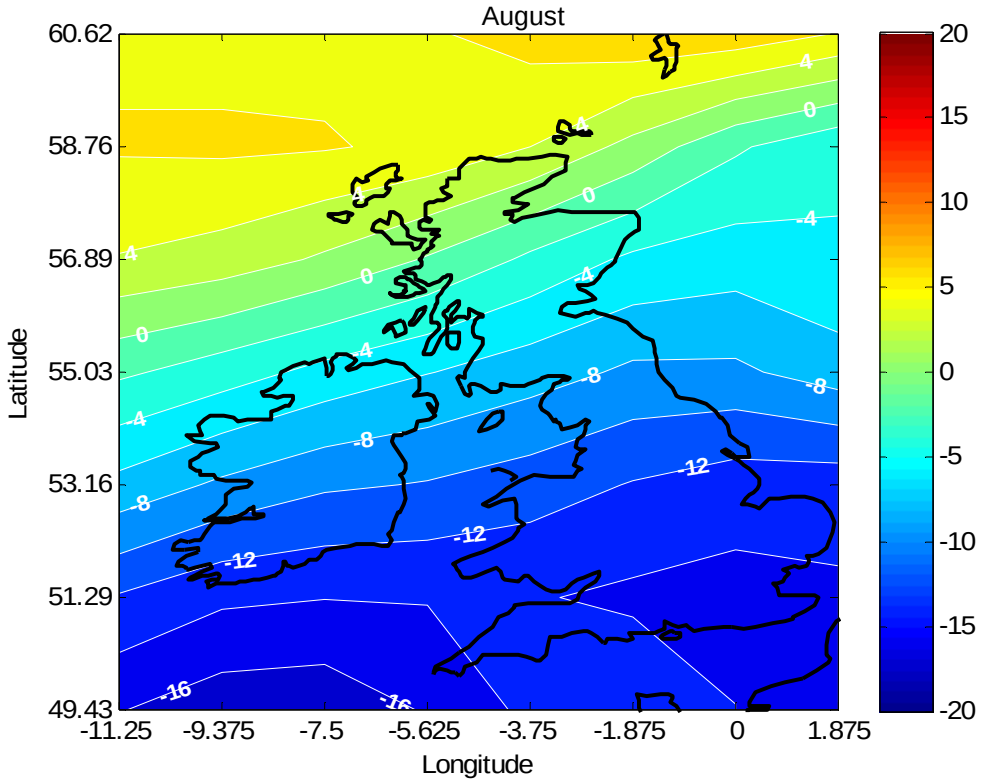
August
60.62
58.76
56.89
55.03
53.16
51.29
49.43
Latitude
-11.25
-9.375
-7.5
-5.625
-3.75
-1.875
0
1.875
Longitude
20
15
10
5
0
-5
-10
-15
-20

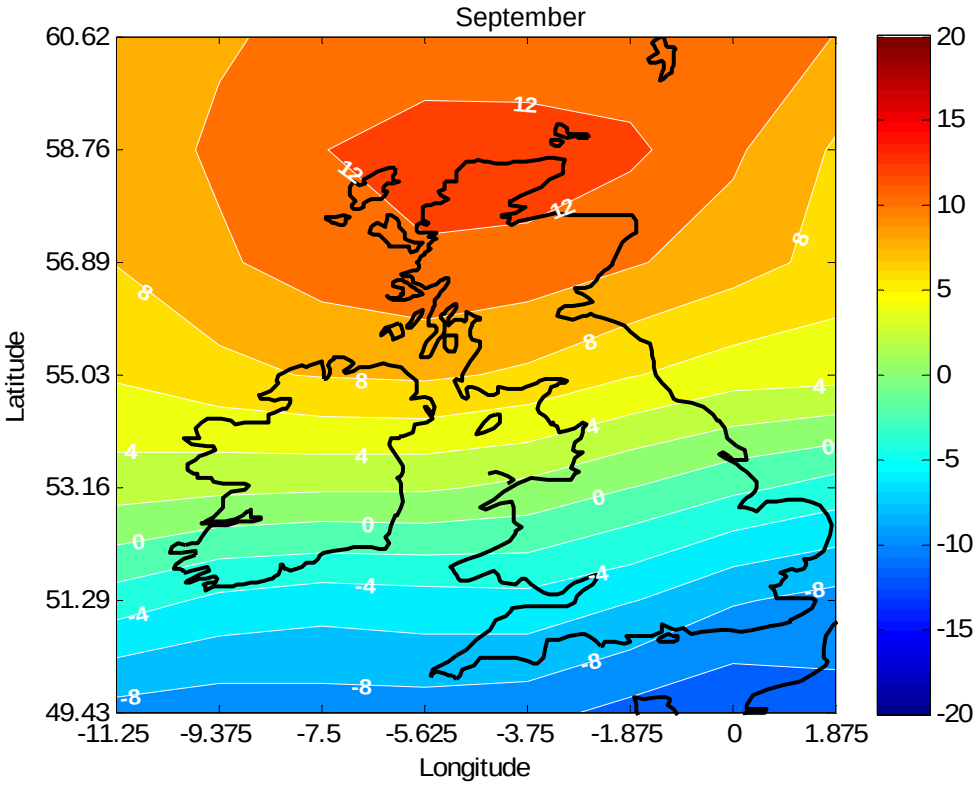
September
60.62
58.76
56.89
55.03
53.16
51.29
49.43
Latitude
-11.25
-9.375
-7.5
-5.625
-3.75
-1.875
0
1.875
Longitude
20
15
10
5
0
-5
-10
-15
-20

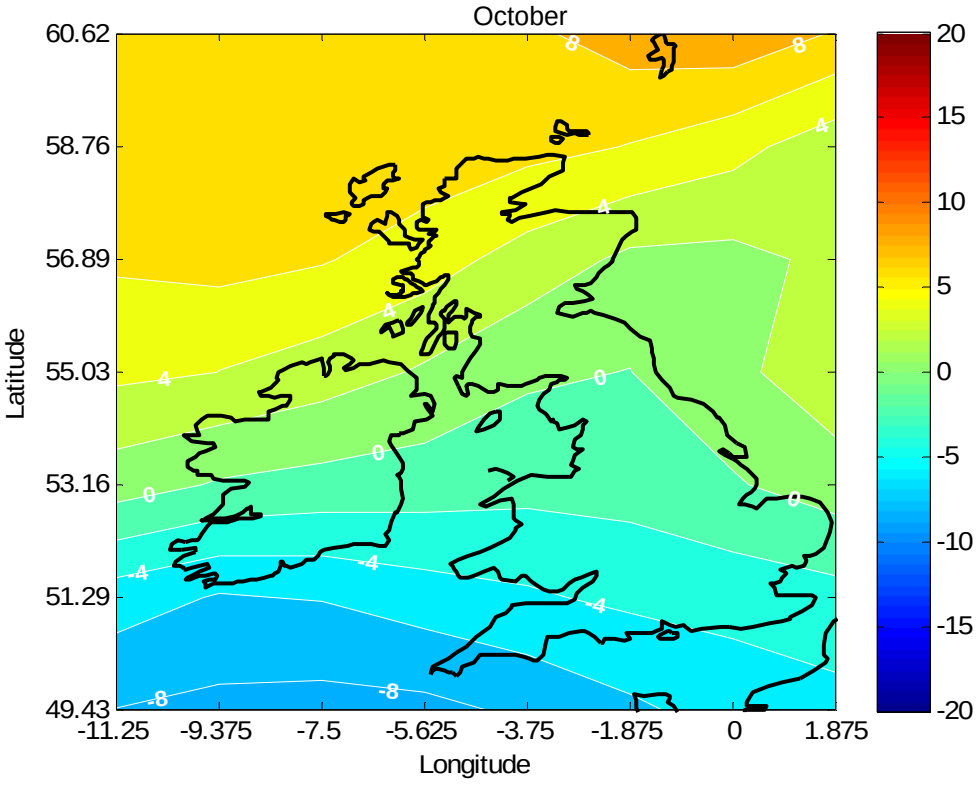
October
60.62
58.76
56.89
55.03
53.16
51.29
49.43
Latitude
-11.25
-9.375
-7.5
-5.625
-3.75
-1.875
0
1.875
Longitude
20
15
10
5
0
-5
-10
-15
-20

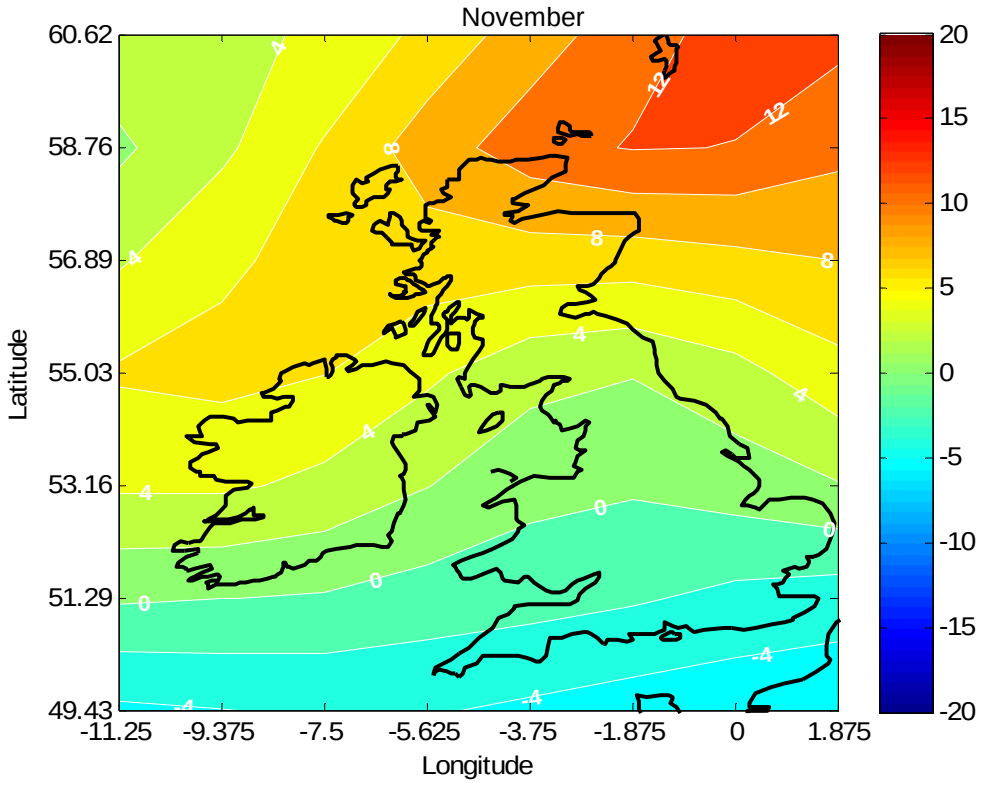
November
60.62
58.76
56.89
55.03
53.16
51.29
49.43
Latitude
-11.25
-9.375
-7.5
-5.625
-3.75
-1.875
0
1.875
Longitude
20
15
10
5
0
-5
-10
-15
-20

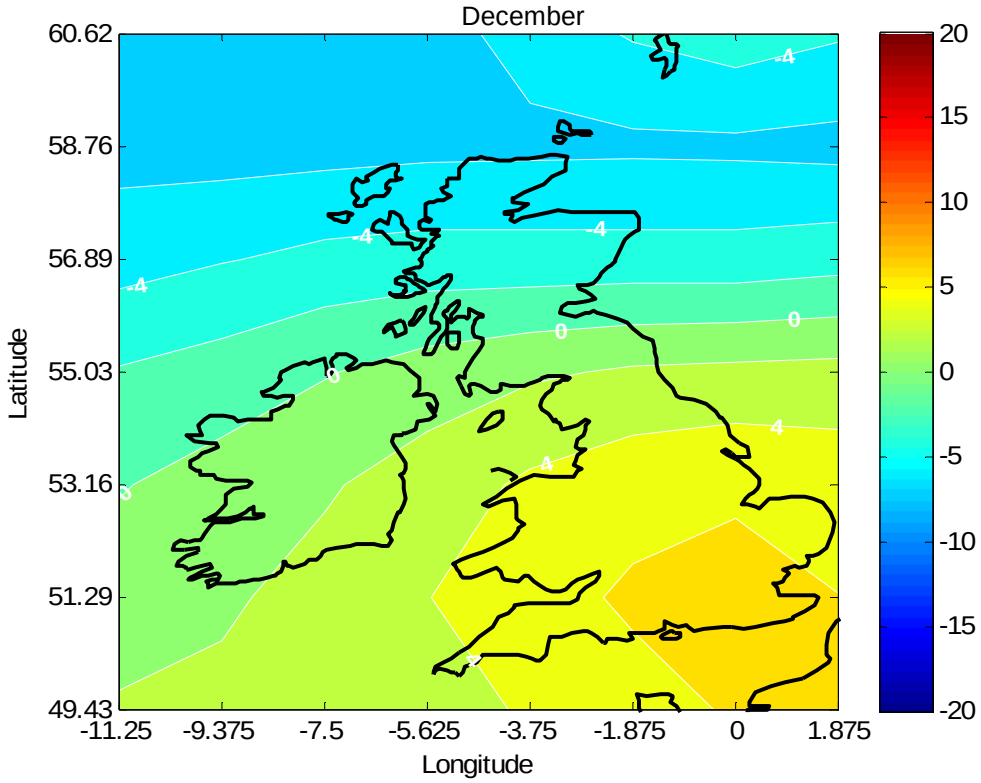
December
60.62
58.76
56.89
55.03
53.16
51.29
49.43
Latitude
-11.25
-9.375
-7.5
-5.625
-3.75
-1.875
0
1.875
Longitude
20
15
10
5
0
-5
-10
-15
-20

Fig. D-4: Future, monthly mean wind speed vectors

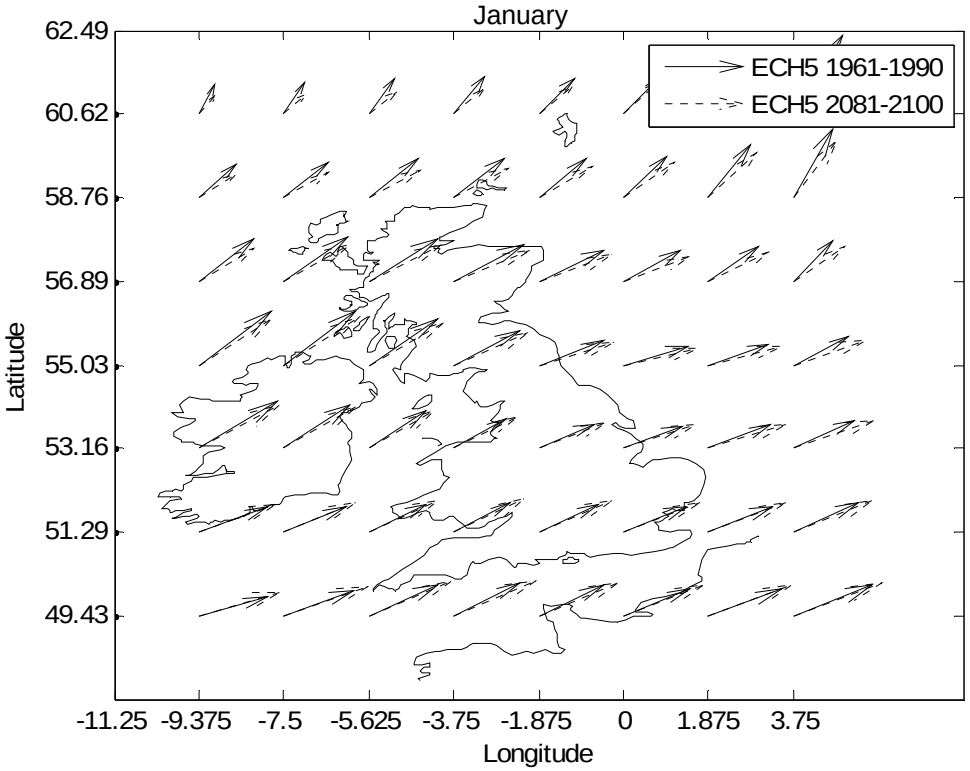

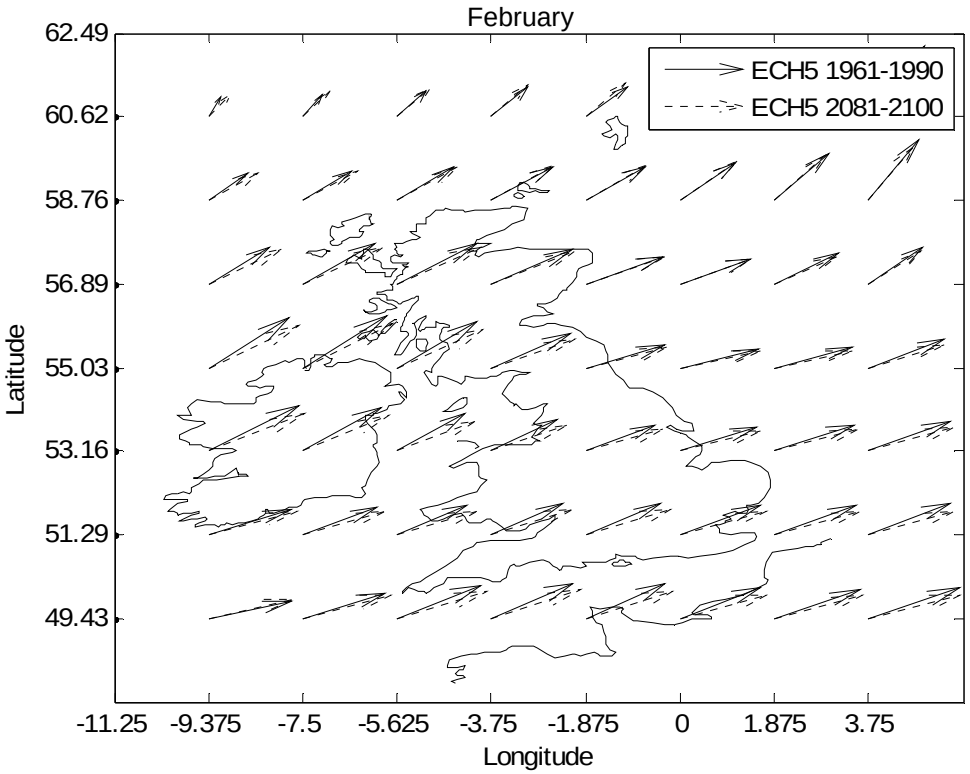

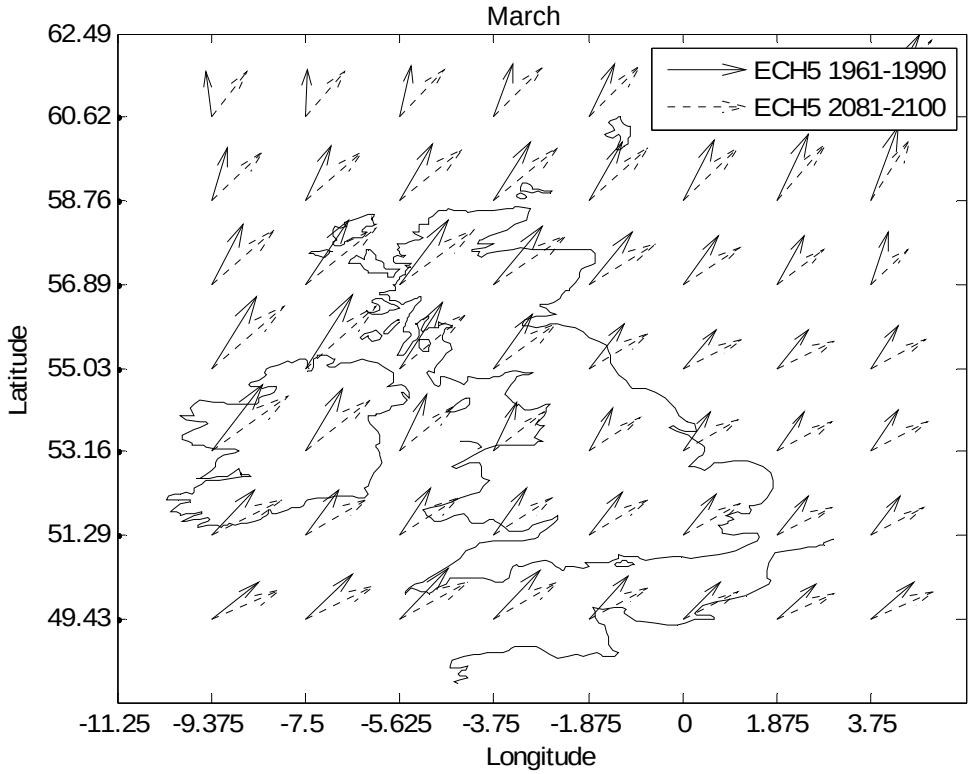
March
ECH5 1961-1990
ECH5 2081-2100
62.49
60.62
58.76
56.89
55.03
53.16
51.29
49.43
Latitude
-11.25
-9.375
-7.5
-5.625
-3.75
-1.875
0
1.875
3.75
Longitude

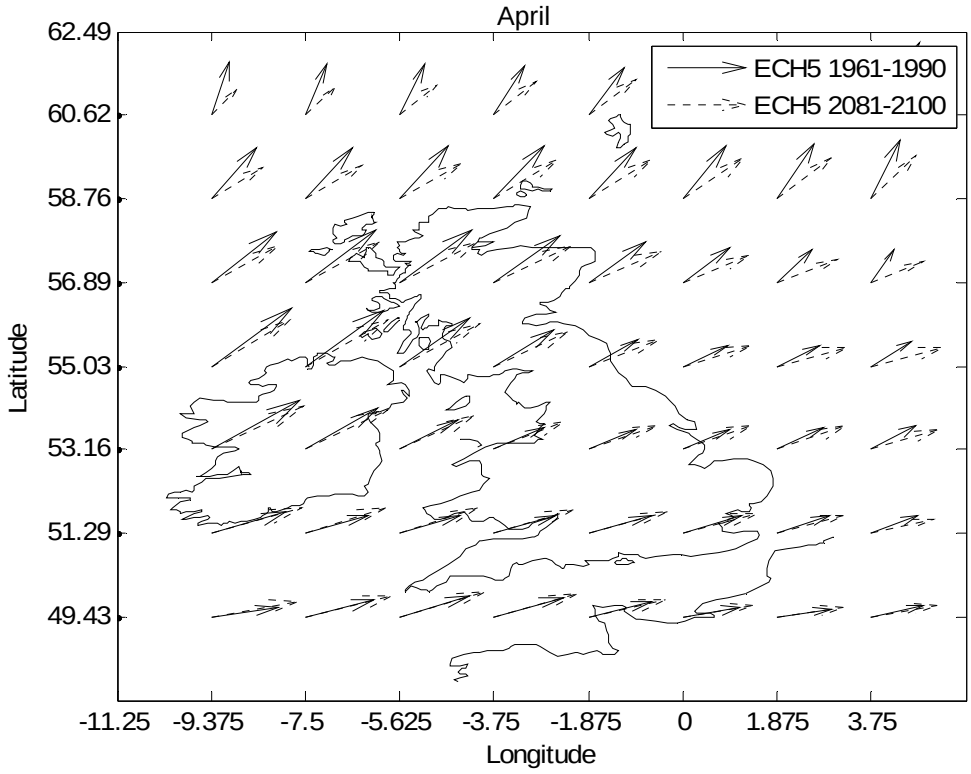
April
ECH5 1961-1990
ECH5 2081-2100
62.49
60.62
58.76
56.89
55.03
53.16
51.29
49.43
Latitude
-11.25
-9.375
-7.5
-5.625
-3.75
-1.875
0
1.875
3.75
Longitude

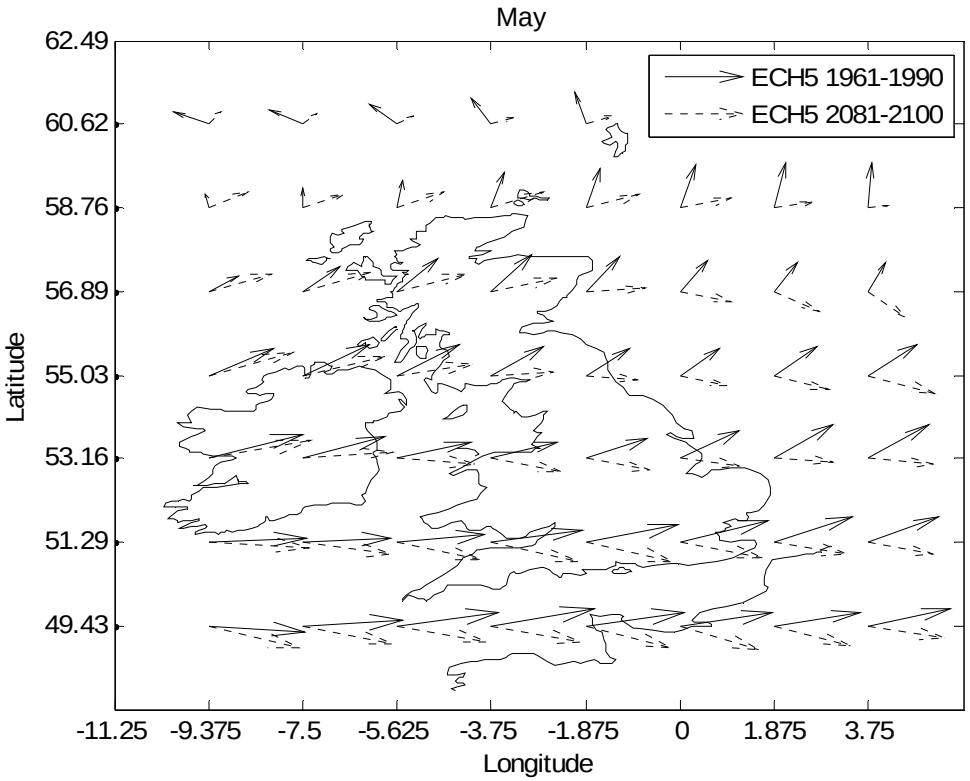
May
ECH5 1961-1990
ECH5 2081-2100
62.49
60.62
58.76
56.89
55.03
53.16
51.29
49.43
Latitude
-11.25
-9.375
-7.5
-5.625
-3.75
-1.875
0
1.875
3.75
Longitude

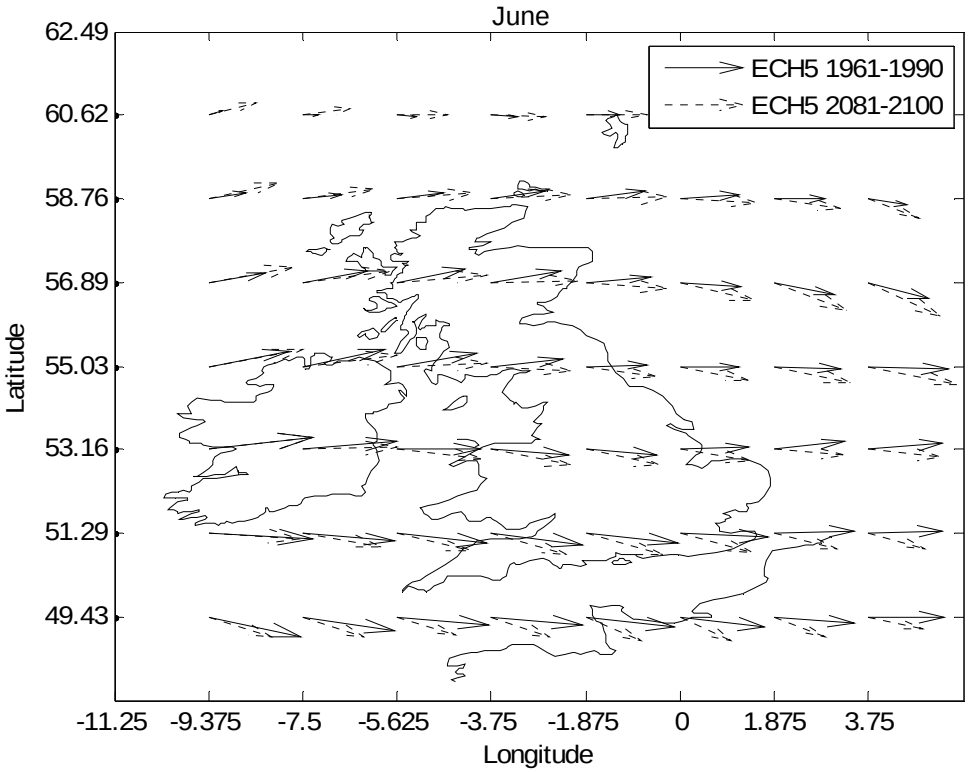
June
ECH5 1961-1990
ECH5 2081-2100
62.49
60.62
58.76
56.89
55.03
53.16
51.29
49.43
Latitude
-11.25
-9.375
-7.5
-5.625
-3.75
-1.875
0
1.875
3.75
Longitude

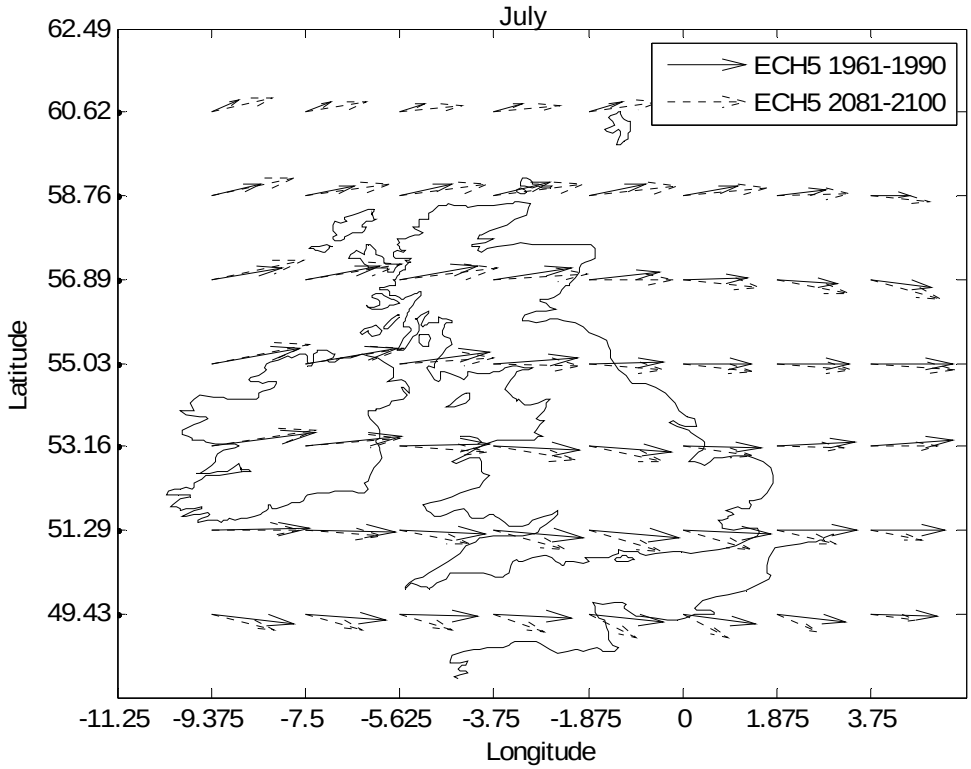
July
ECH5 1961-1990
ECH5 2081-2100
62.49
60.62
58.76
56.89
55.03
53.16
51.29
49.43
Latitude
-11.25
-9.375
-7.5
-5.625
-3.75
-1.875
0
1.875
3.75
Longitude

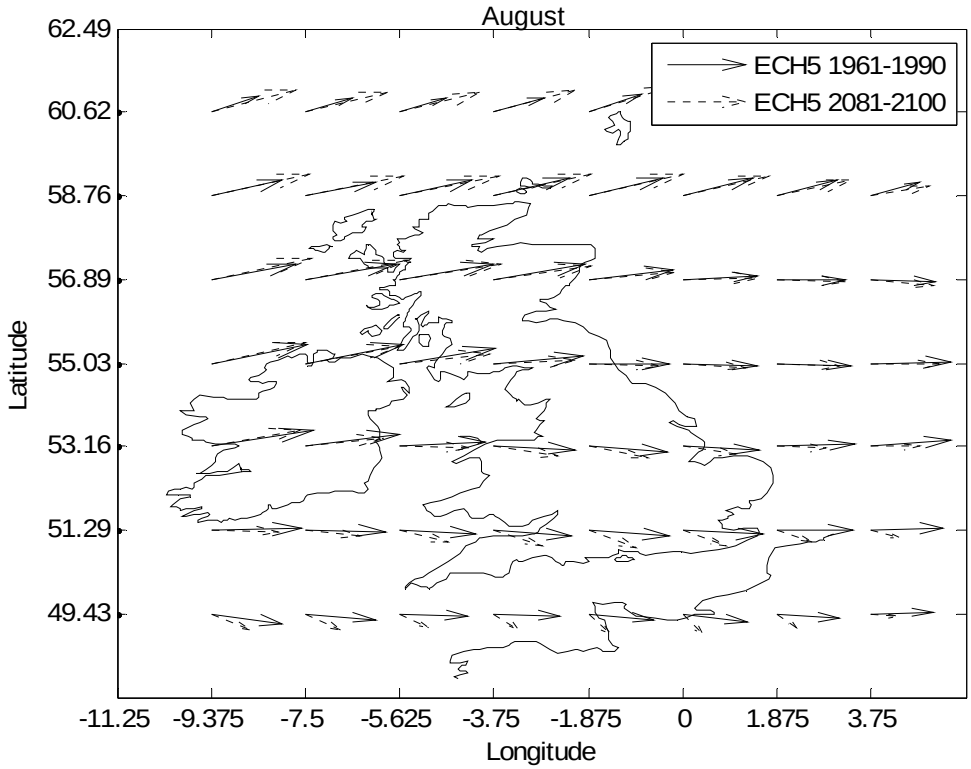
August
ECH5 1961-1990
ECH5 2081-2100
62.49
60.62
58.76
56.89
55.03
53.16
51.29
49.43
Latitude
-11.25
-9.375
-7.5
-5.625
-3.75
-1.875
0
1.875
3.75
Longitude

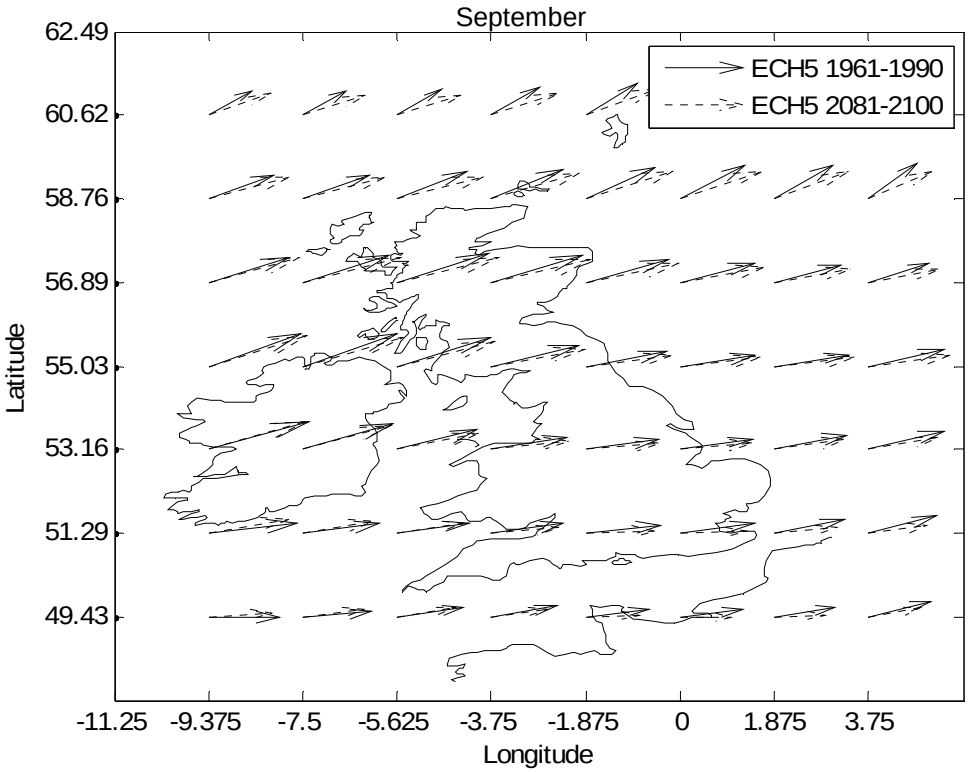
September
ECH5 1961-1990
ECH5 2081-2100
62.49
60.62
58.76
56.89
55.03
53.16
51.29
49.43
Latitude
-11.25
-9.375
-7.5
-5.625
-3.75
-1.875
0
1.875
3.75
Longitude

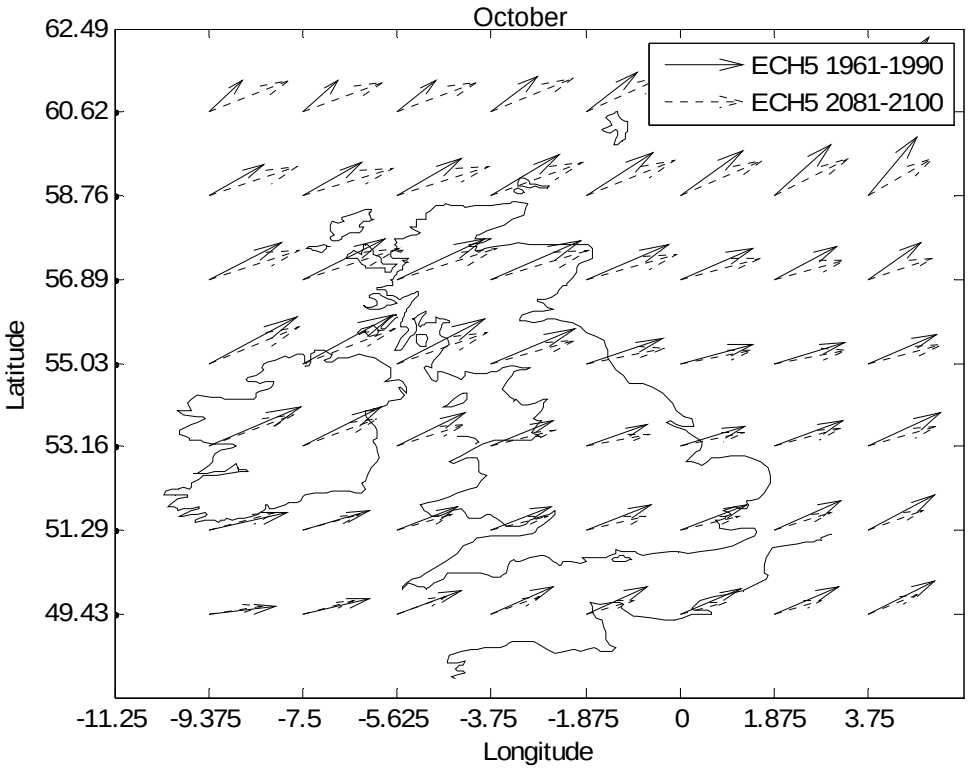
October
ECH5 1961-1990
ECH5 2081-2100
62.49
60.62
58.76
56.89
55.03
53.16
51.29
49.43
Latitude
-11.25
-9.375
-7.5
-5.625
-3.75
-1.875
0
1.875
3.75
Longitude

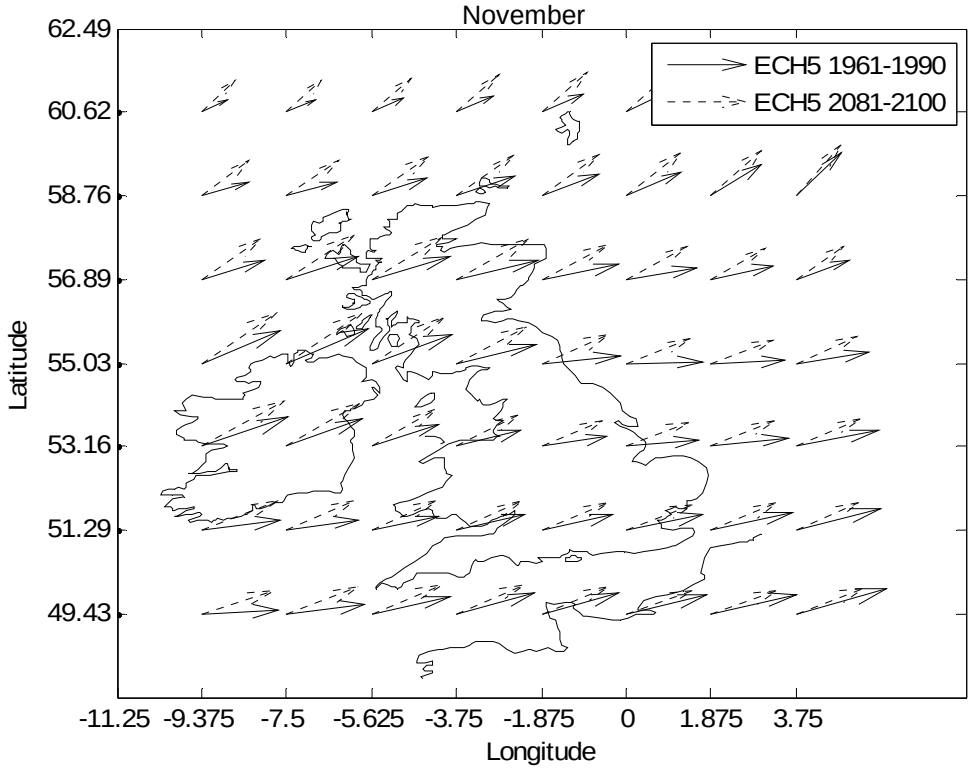
November
ECH5 1961-1990
ECH5 2081-2100
62.49
60.62
58.76
56.89
55.03
53.16
51.29
49.43
Latitude
-11.25 -9.375 -7.5 -5.625 -3.75 -1.875 0 1.875 3.75
Longitude

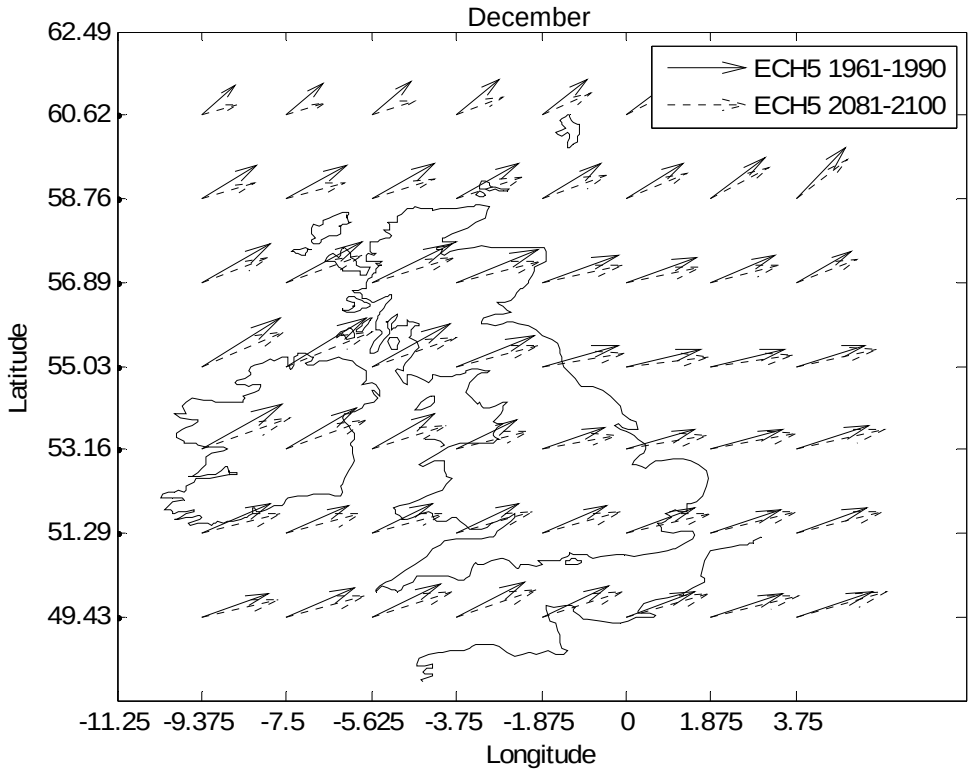
December
ECH5 1961-1990
ECH5 2081-2100
62.49
60.62
58.76
56.89
55.03
53.16
51.29
49.43
Latitude
-11.25 -9.375 -7.5 -5.625 -3.75 -1.875 0 1.875 3.75
Longitude

Appendix E

Fig. E-1: Boulmer

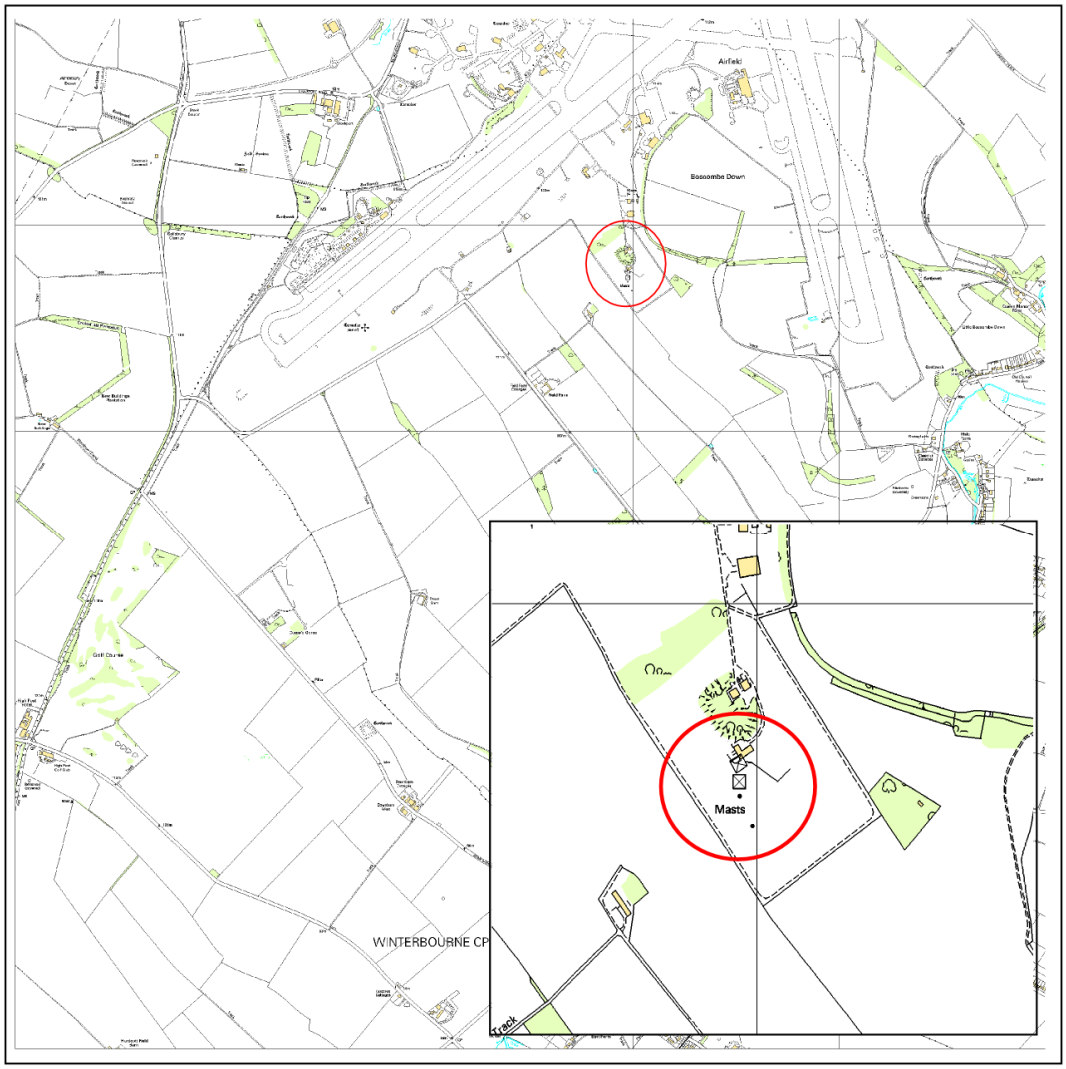

Fig. E-2: Boscombe Down

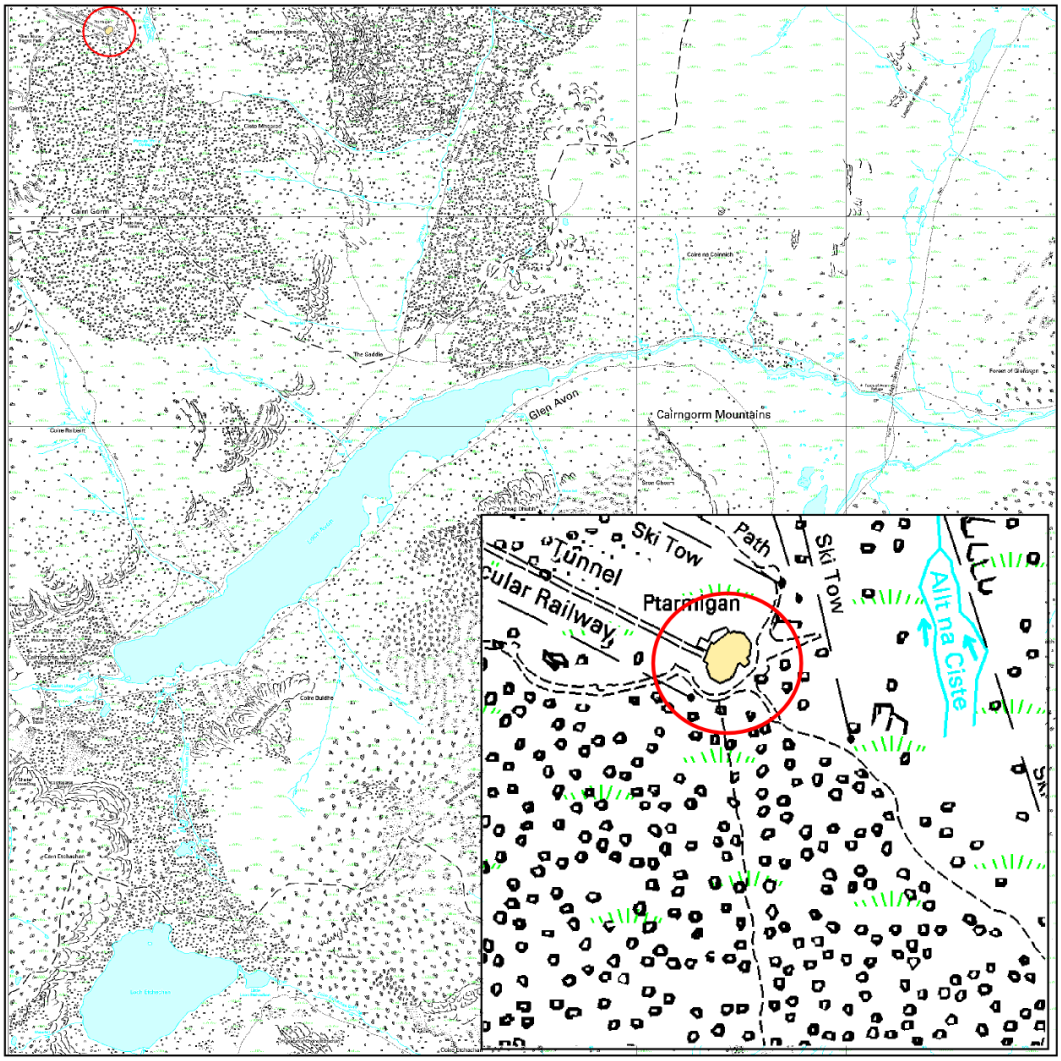

Fig. E-3: Cairngorm

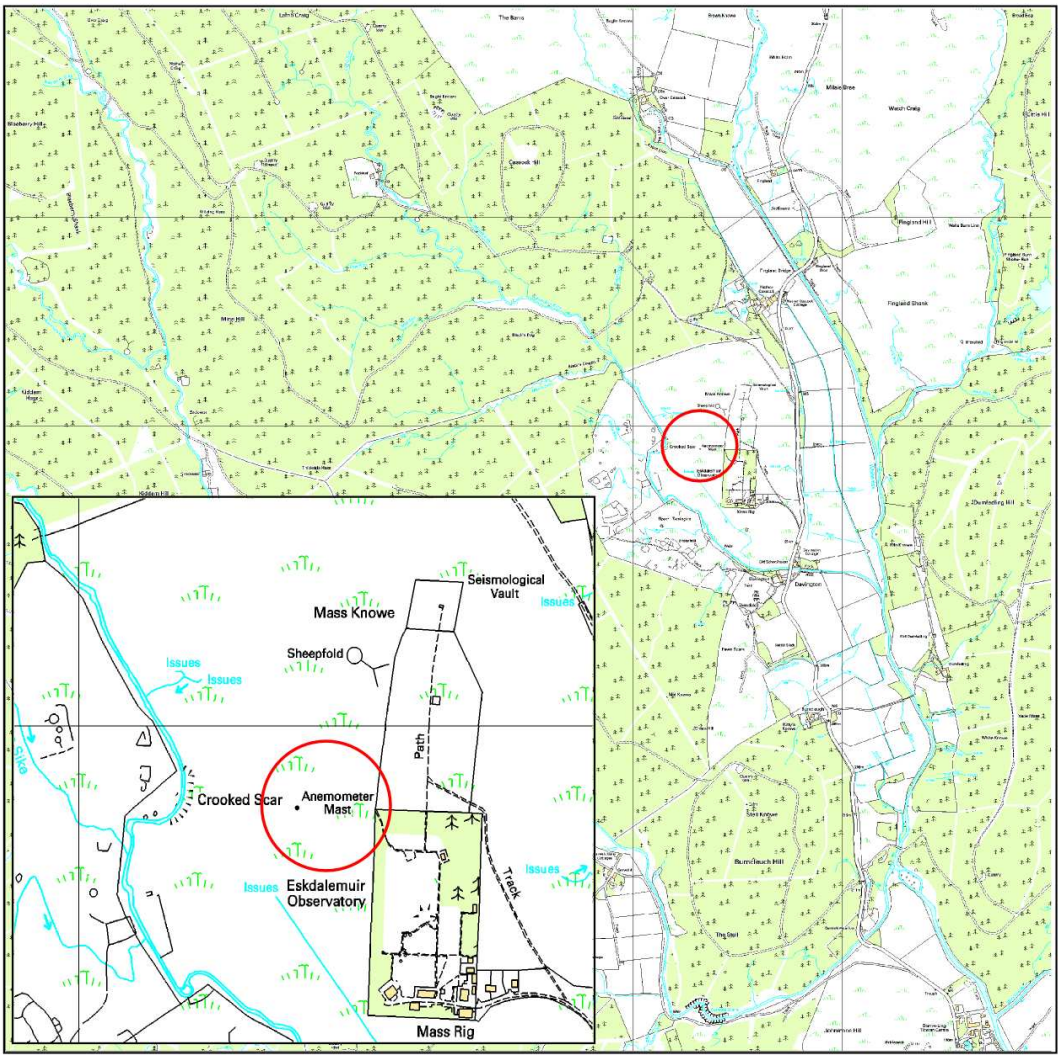

Fig. E-4: Eskdalemuir

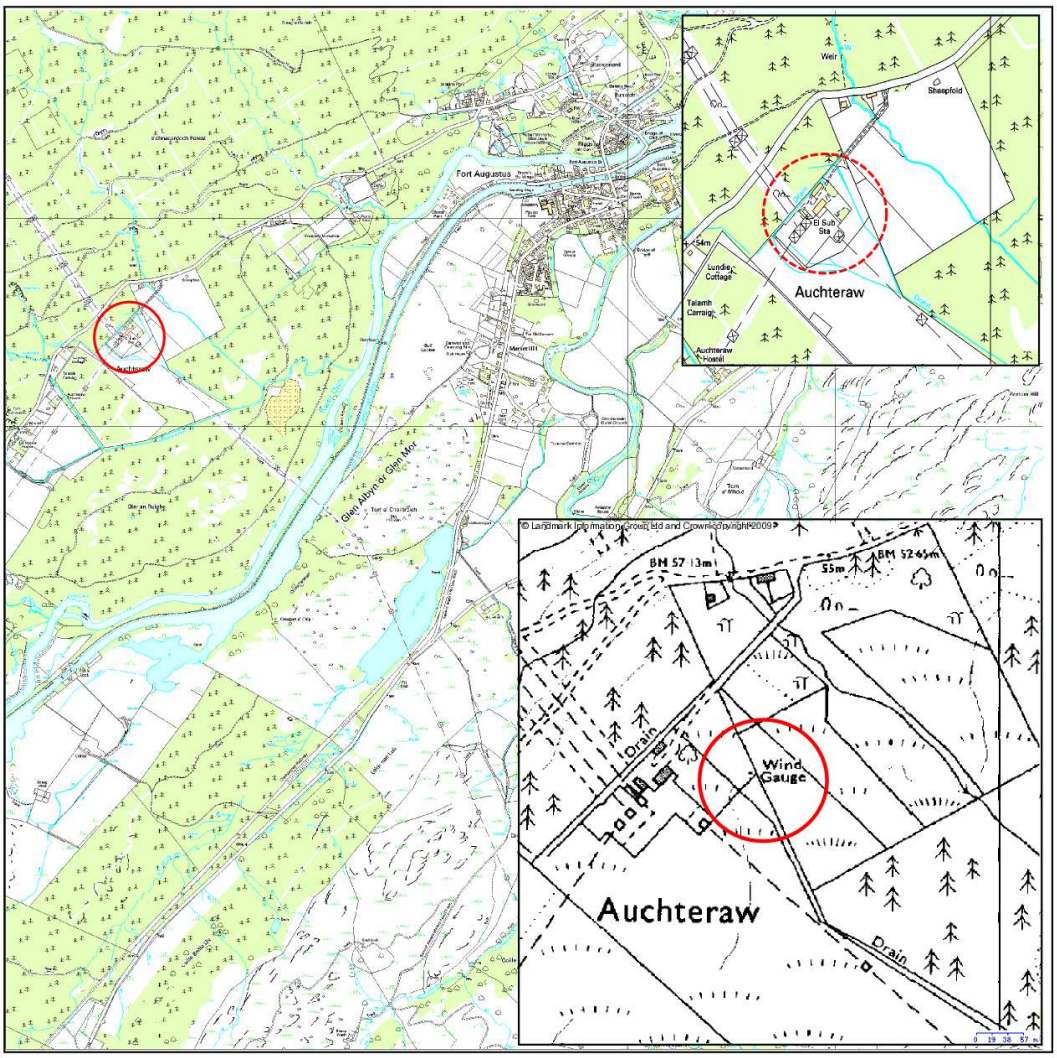

Fig. E-5: Fort Augustus

Note: The wind monitoring station at the Fort Augustus site no longer exists (current view shown zoomed-in in the top right); however, an older version of the Ordnance Survey map for the region shows the location of the anemometer during the years for which measurements were obtained (bottom right).

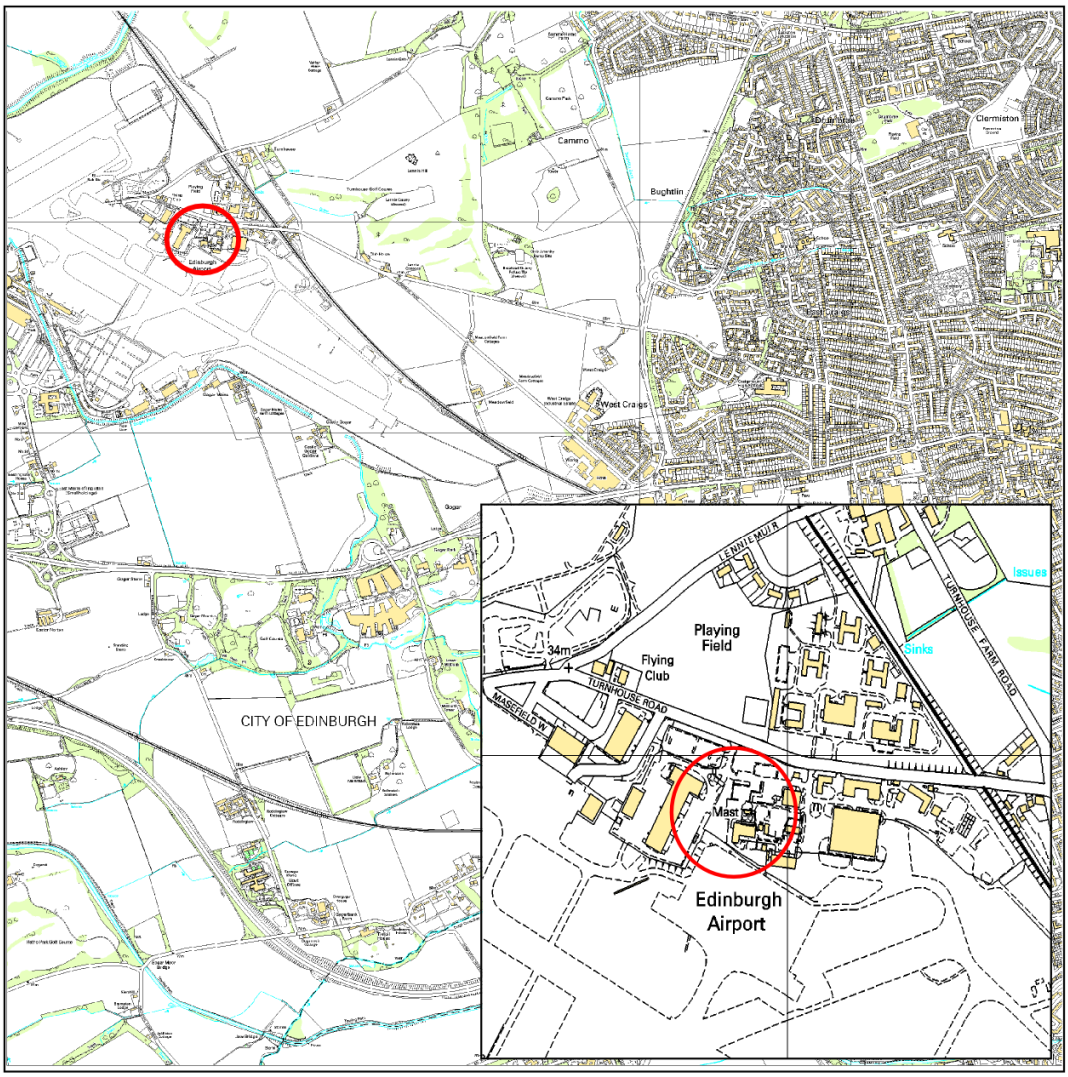

Fig. E-6: Turnhouse

Fig. E-7: Wittering